SRR-CWDA-2014-00060
Revision 2

Updates to the H-Area Tank Farm Stochastic Fate and Transport Model

July 2016

Prepared by: Savannah River Remediation LLC
Waste Disposal Authority
Aiken, SC 29808

Savannah River Remediation
AECOM | BECHTEL | CH2M | BWXT

Prepared for U.S. Department of Energy Under Contract No. DE-AC09-09SR22505

APPROVALS

Author:

Barry Lester
Savannah River Remediation LLC
Waste Disposal Authority

7/5/2016
Date

Technical Review (per ENG.51):

Steven Hommel
Savannah River Remediation LLC
Waste Disposal Authority

7/5/2016
Date

Management Review:

Kent Rosenberger
Savannah River Remediation LLC
Waste Disposal Authority

7/5/2016
Date

REVISION SUMMARY

REV. #	DESCRIPTION	DATE OF ISSUE
0	Initial issue. Prepared in support of the Tank 16 Special Analysis.	January 2015
1	Revision to support the Tank 12 Special Analysis.	August 2015
2	Revision to support of the Type I and II Tanks Special Analysis.	July 2016

EXECUTIVE SUMMARY

This report describes changes to the Savannah River Site's *H-Area Tank Farm Stochastic Fate and Transport Model* (SRR-CWDA-2014-00060, Rev. 1), which was originally developed for the H-Area Tank Farm (HTF) Performance Assessment (PA) report using GoldSim. GoldSim is a graphical, object-oriented computer program, designed to implement dynamic, probabilistic simulation capability to support decision-making. In preparation for use in the Types I and II Tanks Special Analysis (SA), several updates to the GoldSim model were implemented and are documented herein.

The HTF model uses a GoldSim-based contaminant transport module in deterministic or probabilistic mode to simulate the release of radionuclides from grouted engineered storage tanks and from ancillary equipment, and the subsequent migration of the released constituents through the natural system to the accessible environment. For each realization of a Monte Carlo or Latin Hypercube Sampling (LHS) of data, the HTF Stochastic Fate and Transport Model calculates radionuclide/chemical concentrations along a 100-meter and 1-meter boundary surrounding the HTF. Based on these concentrations the model then calculates doses along the 100-meter boundary for use in the Member of Public (MOP) dose analysis and at the 1-meter boundary for use in the Inadvertent Human Intruder (IHI) analysis. In addition, the model can calculate doses from contact with drill cuttings for an Acute Intruder analysis.

Note that an earlier versions of this report (SRR-CWDA-2014-00060, Rev. 0) described the bifurcation of the GoldSim model into two individual GoldSim models. One model (HTF_Transport_Model_v3.000_Rad) was designed to evaluate the dose impacts associated with radionuclide migration from the tanks and ancillary structures at the HTF and the other (HTF_Transport_Model_v3.000_NonRad) was designed to evaluate the impacts associated with non-radioactive chemical migration from the tanks and ancillary structures. This document pertains to updates to and results from an updated version of the RAD version only.

This document describes updates to the HTF Stochastic Fate and Transport Model including updates to: 1) the inventory values for Tanks 9, 10, 11, 13, 14, and 15; 2) stochastic distributions used for inventories for Tanks 13, 14, and 15; 3) iodine K_d's and strontium K_d distributions; 4) the points of assessment (POAs) along the 1-meter facility boundary to more adequately represent the advective transport processes simulated in the HTF PORFLOW model; 5) the annulus contamination zone structure, reflecting changes in the PORFLOW model and the set of PORFLOW generated diffusion coefficient input files; 6) the set of PORFLOW generated flow input files reflecting the changes to the annulus contamination zone, the added scenario calculations, and the addition of parameters to allow simulation of Configurations B-E; 7) the alternate scenarios available in the model, with the addition of a set of scenarios to evaluate the sensitivity of the modeled system to different quality grouts; and 8) the distributions for source specific saturated zone Darcy velocities.

Section 1.0 of this report is an introduction to the model and its purpose. Section 2.0 documents the changes to the model and Section 3.0 documents the benchmark testing performed to show that these GoldSim models represent an abstraction that is a valid surrogate for the three-dimensional HTF PORFLOW Model, and is amenable for use in Monte Carlo/LHS mode to perform uncertainty and sensitivity analyses. During the testing, results from the GoldSim and the PORFLOW models were compared to show that the GoldSim abstraction adequately and

efficiently approximates the trends and results produced by the more computationally rigorous HTF PORFLOW Model.

TABLE OF CONTENTS

LIST OF FIGURES

LIST OF TABLES

ACRONYMS

CPU	Central Processing Unit
CZ	Contamination Zone
DLL	Dynamic Link Library
GTG	GoldSim Technology Group LLC
HTF	H-Area Tank Farm
IHI	Inadvertent Human Intruder
LHS	Latin Hypercube Sampling
MCL	Maximum Contaminant Level
MDC	Minimum Detectable Concentration
MOP	Member of Public
NRC	U.S. Nuclear Regulatory Commission
PA	Performance Assessment
POA	Point of Assessment
SA	Special Analysis
SRS	Savannah River Site
SZ	Saturated Zone
UZ	Unsaturated Zone

1 INTRODUCTION

The H-Area Tank Farm (HTF) Stochastic Fate and Transport Models are object-oriented probabilistic models designed to simulate the advective-dispersive transport of dissolved radiological (RAD) and chemical (NONRAD) waste constituents in groundwater and the risk posed by the dissolved wastes to Members of the Public (MOP). The models are GoldSim based, allowing the user to evaluate the modeled systems sensitivity to inputted parameters and the influence of parameter uncertainty on the model results. An updated version of the radiological (RAD) waste transport model, version HTF_Transport_Model_v4.000_Rad has been developed for use in sensitivity and uncertainty studies that will be part of the basis of the Tank Types I and II Special Analysis (SA). The GoldSim based model is used to quantify the likely range of radionuclide releases from the grouted H-Area Tanks and the potential dose impacts to members of the public (MOP) associated with the migration of waste to the accessible environment, after HTF facility closure. The accessible environment (for the purpose of compliance) is the area outside of a 100-meter perimeter surrounding the HTF waste tanks and ancillary equipment. In addition, the model evaluates an Inadvertent Human Intruder (IHI) scenario that assumes that the intruder drills a well within one meter of the facility boundary.

The HTF Stochastic Fate and Transport Models were developed as a series of abstractions that simulate the same processes as the HTF PORFLOW Model. These abstractions approximate the processes of radionuclide/chemical transport from waste tanks and ancillary equipment sources in a simplified manner that effectively allows sensitivity and uncertainty analyses to be performed in a time-efficient manner, while still allowing the influence of parameters on the transport processes to be examined. The RAD model also includes a dose calculator, which evaluates dose at points of compliance, based on the concentrations generated by the self-contained transport abstraction module or generated by the HTF PORFLOW Model. The two HTF Stochastic Fate and Transport Models were constructed using GoldSim software (Version 10.5) (see GTG-2010c and GTG-2010d for further software details).

1.1 Radionuclide Transport Module

The radionuclide module of the HTF Stochastic Fate and Transport Model can be conceptualized as a set of coupled engineered-barrier/natural-barrier abstractions run in sequence. The engineered barrier abstractions include the 29 HTF waste tanks listed in Table 1-1 and the 18 ancillary structures listed in Table 1-2 (see Figure 1-1). As noted in Table 1-2, the 18 ancillary structures are comprised of nine pump tanks (HPT 2 through 10), three evaporators (E242_H, E242_16H, and E242_25H), two CTS pump pits, and four areas of transfer line pipes (HTF_T_Line1, HTF_T_Line2, HTF_T_Line3, and HTF_T_Line4). The natural barrier abstractions include the unsaturated zone (UZ) abstractions and saturated zone (SZ) abstractions. A UZ abstraction is run simultaneously with each engineered–barrier abstraction that lies above the SZ and the radionuclide releases from the UZ (or SZ if any part of the engineered barrier resides in the SZ) become a source term for each engineered-barrier specific SZ abstraction.

Table 1-1: Simulated HTF Tanks

Tank (See Figure 1-1)	Model Source Index
Tank 9	1
Tank 10	2
Tank 11	3
Tank 12	4
Tank 13	5
Tank 14	6
Tank 15	7
Tank 16	8
Tank 21	9
Tank 22	10
Tank 23	11
Tank 24	12
Tank 29	13
Tank 30	14
Tank 31	15
Tank 32	16
Tank 35	17
Tank 36	18
Tank 37	19
Tank 38	20
Tank 39	21
Tank 40	22
Tank 41	23
Tank 42	24
Tank 43	25
Tank 48	26
Tank 49	27
Tank 50	28
Tank 51	29

Table 1-2: Simulated HTF Ancillary Equipment

Ancillary Equipment (See Figure 1-1)	Model Source Index
HPT2	30
HPT3	31
HPT4	32
HPT5	33
HPT6	34
HPT7	35
HPT8	36
HPT9	37
HPT10	38
E242_H	39
E242_16H	40
E242_25H	41
HTF_T_Line1	42
HTF_T_Line2	43
HTF_T_Line3	44
HTF_T_Line4	45
CTSO	46
CTSN	47

Figure 1-1: Layout of HTF Including Ancillary Equipment

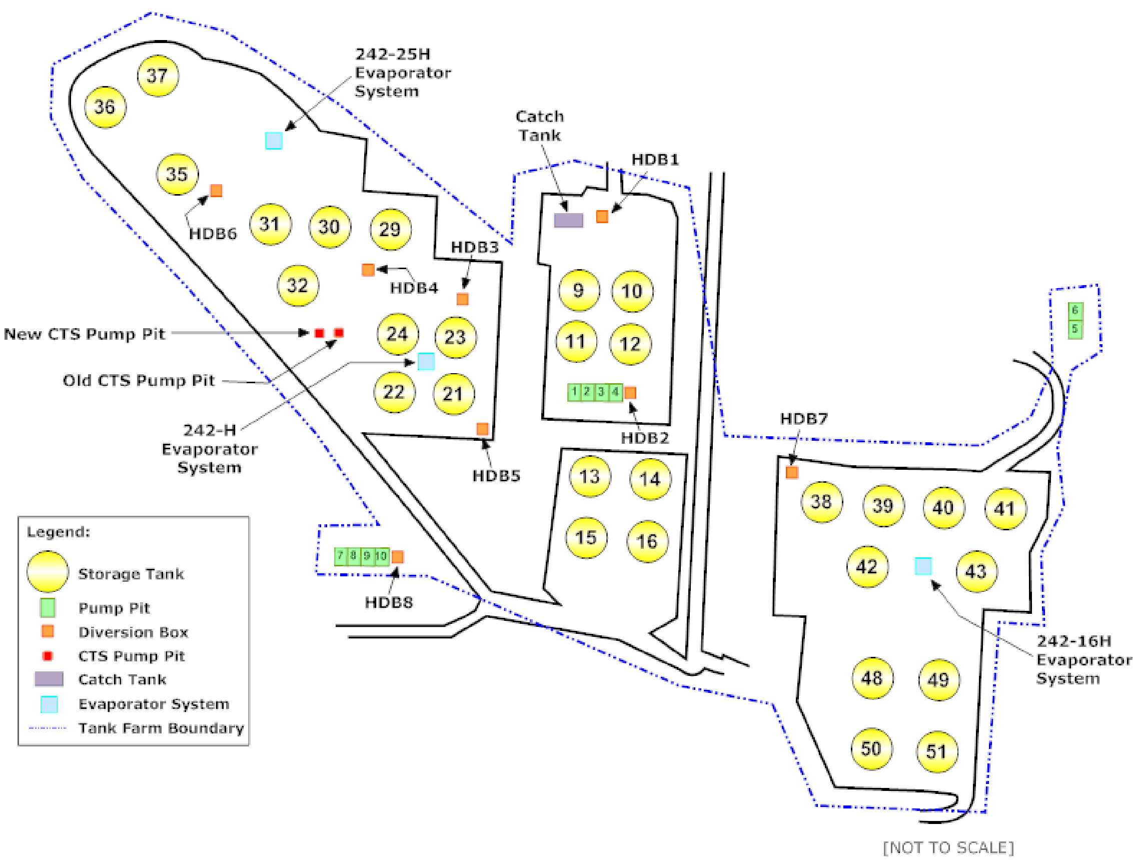

For convenience, the UZ is numerically handled as extensions of the individual engineered barriers (i.e., a string of mixing cells connecting the engineered barrier with the SZ). The engineered barrier and underlying UZ are sometimes referred together as the vadose zone. Within the HTF PORFLOW Model, this vadose zone is modeled as quasi three-dimensional (radial) waste tanks. The GoldSim abstraction is based on compartmentalization of the engineered barrier into simplified one-dimensional segments comprised of GoldSim Cell Pathway elements (i.e., mixing cells). Each segment is comprised of one or more mixing cells linked in series. The waste tank/UZ abstraction (vadose zone) is comprised of several segments or strings of mixing cells. All tank types include linked mixing cells representing the reducing grout, the contamination zone (CZ), the liners, and the concrete basemat. In addition, tanks containing an initial inventory in the annulus and/or sand layers include mixing cells representing the grouted annulus (Type I and Type II tanks), the wall (Type I and Type II tanks), and the sand pads (Type II tanks only).

The UZ is explicitly modeled using mixing cells for all but the Type I and Type II tanks. Note that certain design elements, such as the concrete roof, and wall and annulus above the grout, are not represented in the HTF Stochastic Fate and Transport Models but are represented in the HTF PORFLOW Model. These design elements are important for generating flow fields used to simulate solute transport within and release from the tanks, but are not major pathways for contaminant release from the engineered structures.

A flow chart depicting the structure of the submodel used to evaluate the submerged Type I tanks and the partially submerged Type II tanks is presented in Figure 1-2. A flow chart depicting the structure of the model used to evaluate Type III, IIIA, and IV tanks is presented in Figure 1-3.

Figure 1-2: Flow Chart Depicting Type I and II Tanks

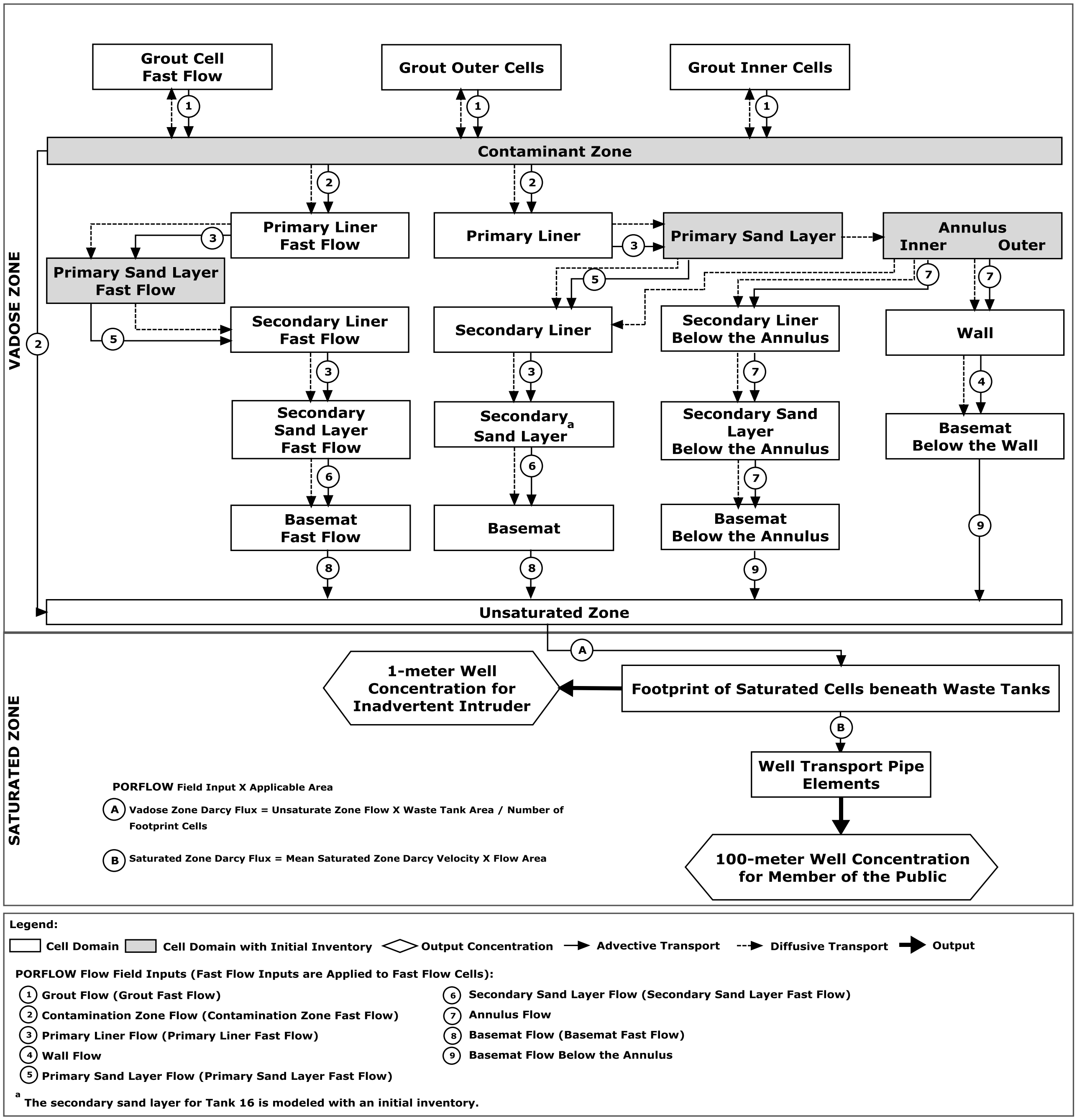

Figure 1-3: Flow Chart Depicting Type III, IIIA, and IV Tanks

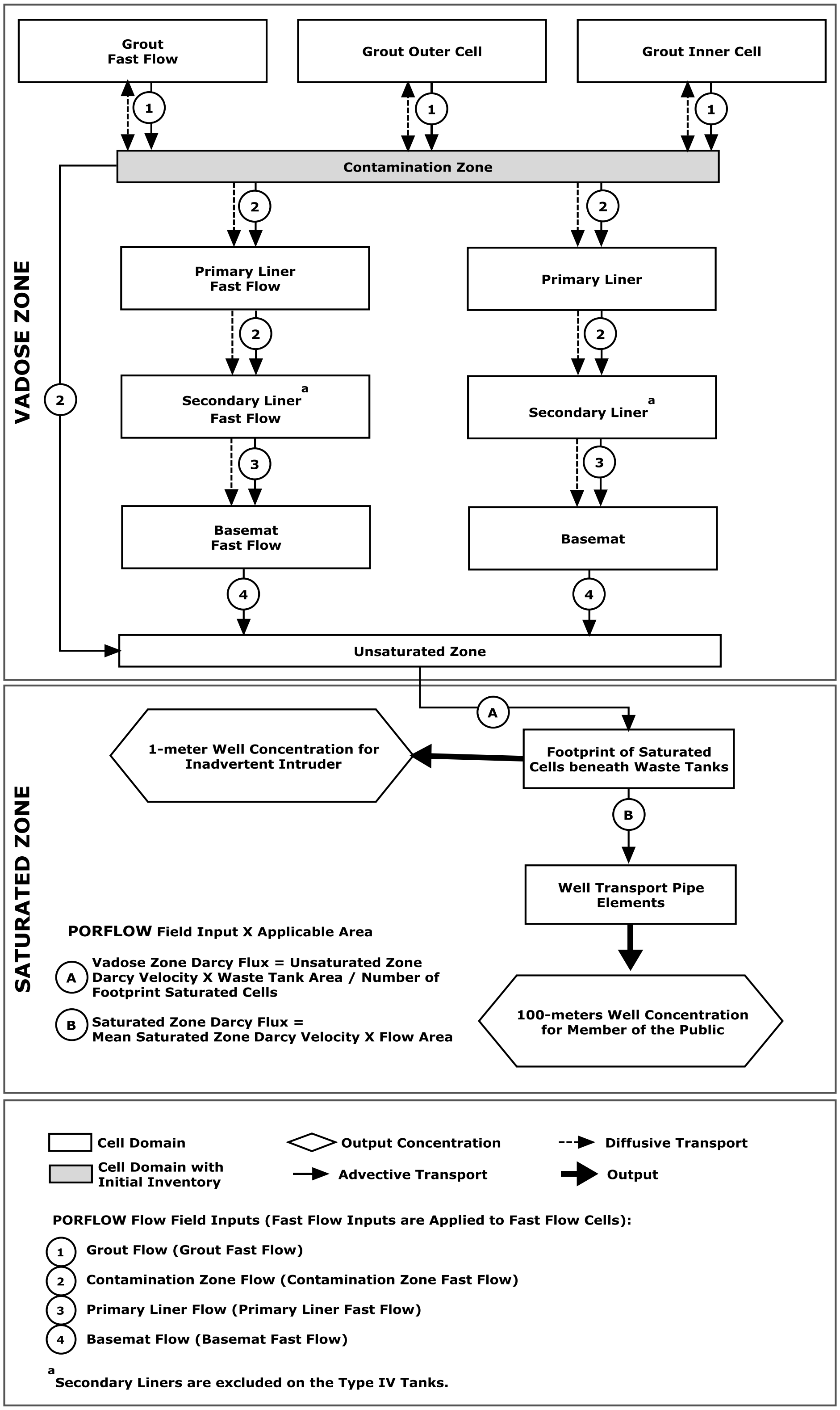

In a more general sense, the HTF Stochastic Fate and Transport Model solves the equations for transport of dissolved radionuclides within the engineered barrier system (the waste tank and ancillary structures) and the natural barrier system (the UZ and SZ). Note that the tank source releases are defined by explicitly evaluating dissolved solute transport through the structure and the ancillary equipment sources are defined by evaluating dissolved solute transport of an instantaneous emplacement of the inventory into the backfill surrounding the structure. Within each engineered barrier (tank or type of ancillary equipment) and the UZ directly beneath the engineered barrier, transport migration is described by advective-diffusive transport within one-dimensional vertical segments comprised of mixing cells. Horizontal advective and diffusive links between the annulus and wall at the top of the secondary liner, for the Type I and Type II tanks (see Figure 1-4 and Figure 1-5) and between the primary-sand layer and annulus for Type II tanks (see Figure 1-5), are implemented in the model. The implementation of horizontal links in the Type I/Type II tank models, reflects the importance of evaluating the release of inventory initially found in the annuli of these two tank types.

Figure 1-4: Typical Type I Tank Modeling Dimensions

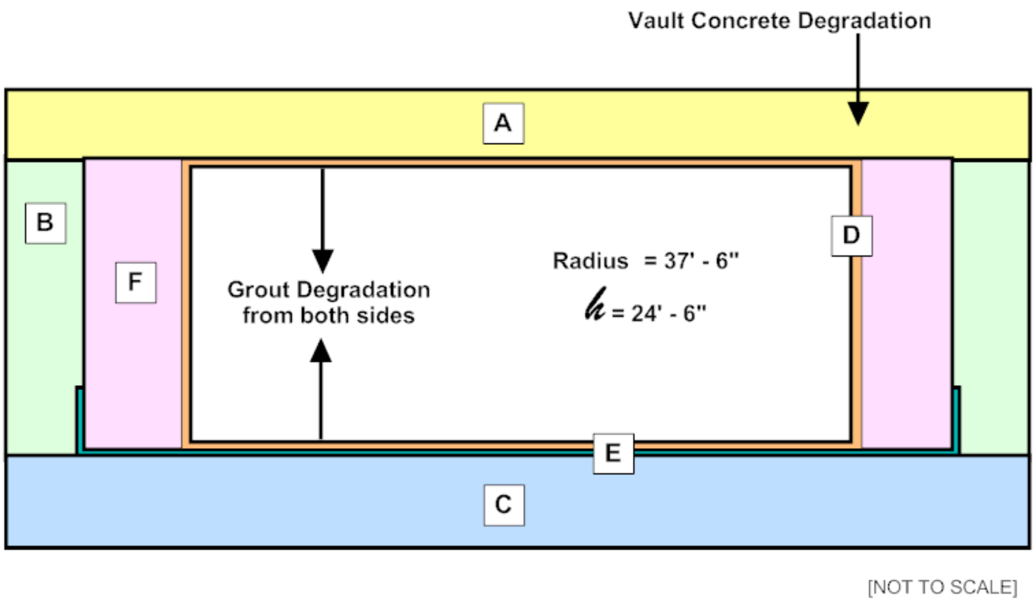

LABEL	THICKNESS
A Concrete Roof	22"
B Concrete Wall	22"
C Concrete Basemat	30"
D Primary Liner	0.5"
E Secondary Liner	5' high and 0.5" thick
F Grouted Annulus	30"

[SRR-CWDA-2010-00128]

Figure 1-5: Typical Type II Tank Modeling Dimensions

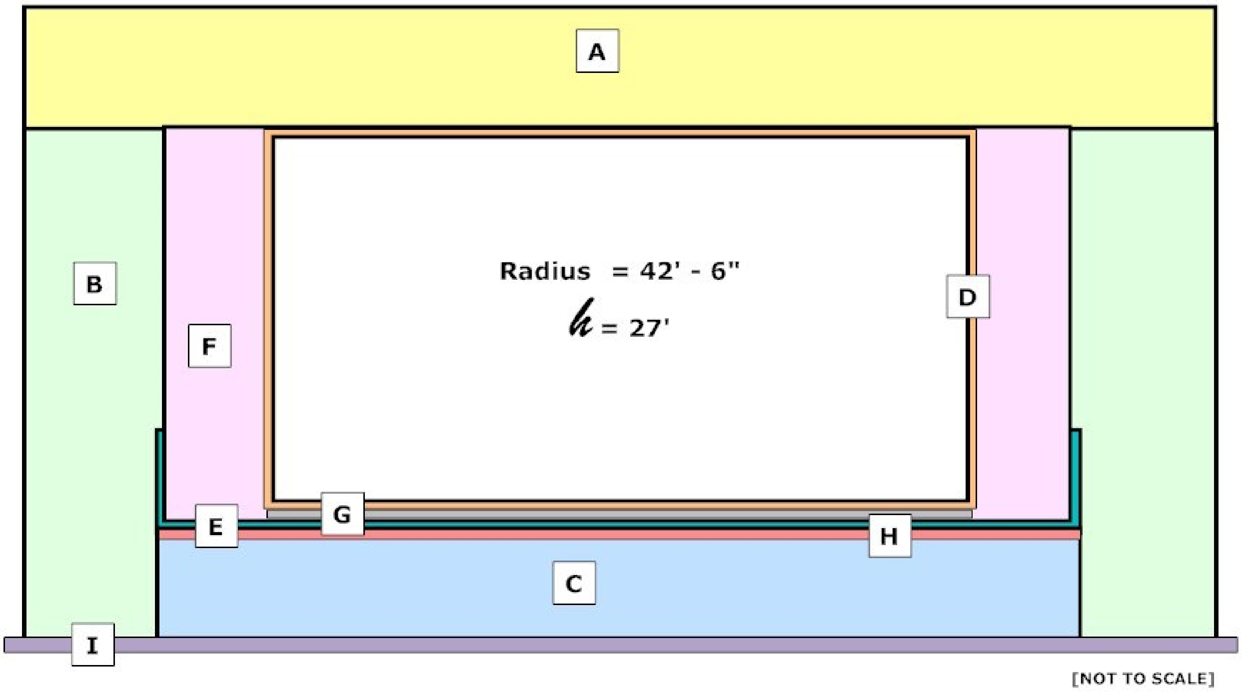

LABEL	THICKNESS
A Roof	45"
B Wall	33"
C Basemat	42"
D Primary Liner	0.5"
E Secondary Liner	5' high and 0.5" thick
F Grouted Annulus	30.625"
G Primary Sand Pad	1"
H Secondary Sand Pad	1"
I Working Slab	6"

[SRR-CWDA-2010-00128]

The transport module of the HTF Stochastic Fate and Transport Models simulate the transport of dissolved species subject to sorption. The models also take into consideration the influence of solubility control within the CZ, located beneath the grout immediately above the primary liner. In addition, the RAD model simulates decay and ingrowth along decay chains. Other processes controlling the mass release from the waste tank structures include time-dependent physical and chemical degradation of concrete zones and steel liner failure. These material breakdown processes are implicitly considered in the HTF Stochastic Fate and Transport Models through the use of spatially-averaged, component-specific (e.g., grout, annulus, wall, etc.), PORFLOW-generated time histories of Darcy velocities which control the advective transport. Additionally, effective diffusion coefficients used in the tank abstractions are time-dependent, following the PORFLOW model effective diffusion coefficient time histories.

The releases from ancillary equipment sources are approximated by releasing the inventory directly into the backfill at a specified time (510 years). The influence of dispersion is not explicitly considered in the waste tank structure or UZ. Numerical dispersion associated with mixing cell discretization, as discussed in the *GoldSim User's Guide* (GTG-2010c), does influence the releases from the tank and UZ. In the SZ, dispersion is explicitly simulated.

The governing equation that is used to evaluate radionuclide migration through the vadose zone, describing one-dimensional advective-diffusive transport through the individual strings of mixing cells connected in series, is given as follows (**Equation 1-1**):

Equation 1-1

$$\frac{\partial(\varphi RC)}{\partial t} = D_{eff}\frac{\partial^2 C}{\partial l^2} - v\frac{\partial C}{\partial l} - \varphi R\lambda C + \sum_{i=1}^{Np}\varphi R\lambda_{pi}C_{pi}$$

where:

C	=	solute concentration (m/L^3)
R	=	retardation coefficient
φ	=	effective porosity
t	=	time (T)
D_{eff}	=	effective diffusion coefficient τD (L^2/T)
v	=	Darcy velocity (L/T)
α	=	dispersivity (L)
λ	=	decay coefficient (T^{-1})
λ_{pi}	=	ingrowth coefficient of the i^{th} parent (T^{-1})
Np	=	number of parent species
l	=	transport pathway coordinate (L)

With respect to radionuclide migration of the releases from the tanks and ancillary equipment through the SZ, a two-step procedure is used to evaluate the dissolved species transport process. The two-step procedure begins by evaluating the solution for one-dimensional advective-dispersive transport along a particle pathway emanating from the engineered barrier center. The one-dimensional advective-dispersive transport equation is solved using the GoldSim software's "pipe-pathway elements". The "pipe-pathway elements" use a one-dimensional advective-dispersive analytical solution solved in the Laplace domain and numerically inverted using the de Hoog algorithm (GTG-2010e).

The one-dimensional solution is then enhanced to approximate the influence of horizontal- and vertical-transverse dispersion using the GoldSim software's "plume function". The "plume function" approximates the influence of transverse dispersion on the transported mass by generating a scaling factor based on the vertical and horizontal extent of the release volume, the distance from the source release area to the points of interest, and the magnitude of the horizontal- and vertical- transverse dispersivities used in the calculations. The concentrations at the compliance points used in the dose analysis are derived from the product of the scaling factor and the one-dimensional "pipe-pathway" solution for species concentrations.

The governing equation describing the combined three-dimensional advective-dispersive transport along a flow pathline, can be described as follows (Equation 1-2):

Equation 1-2

$$\frac{\partial(\varphi RC)}{\partial t} = D_L \frac{\partial^2 C}{\partial l^2} + D_{Th} \frac{\partial^2 C}{\partial w^2} + D_{Tv} \frac{\partial^2 C}{\partial h^2} - v_l \frac{\partial C}{\partial l} - \varphi R \lambda C + \sum_{i=1}^{Np} \varphi R \lambda_{pi} C_{pi}$$

where:

C	=	solute concentration (m/L^3)
R	=	retardation coefficient
φ	=	effective porosity
t	=	time (T)
D_L	=	longitudinal dispersion coefficient $v\alpha_L$ (L^2/T)
D_{Th}	=	horizontal transverse dispersion coefficient $v\alpha_{Th}$ (L^2/T)
D_{Tv}	=	vertical transverse dispersion coefficient $v\alpha_{Tv}$ (L^2/T)
v	=	Darcy velocity along particle pathline (L/T)
α	=	dispersivity (L)
λ	=	decay coefficient (T^{-1})
λ_{pi}	=	ingrowth coefficient of the ith parent (T^{-1})
Np	=	number of parent species
l	=	transport pathway coordinate (L)

In addition, note that within the CZ, the concentration C in a mixing cell becomes nonlinear for any solubility-controlled species, i, and is defined as:

Equation 1-3

$$C = \min\left\{C_i, S_{limit}\frac{M_i}{\sum_{j=1}^{j=N_{iso}} M_j}\right\}$$

where:

S_{limit}	=	solubility limit (m/L^3)
M_j	=	mass of isotope j in the cell (m)
N_{iso}	=	number of isotopes of species i element

1.2 Dose Calculator Module

In addition to simulating radionuclide transport, the RAD HTF Stochastic Fate and Transport Model contains a second module, designed to calculate receptor doses to the MOP or the IHI. The doses are evaluated at specified points of compliance including sectors along the 100-meter boundary and the 1-meter boundary. Concentrations used in the dose calculations can be from 1) the results generated by the transport abstraction module, 2) results imported directly from output generated by the HTF PORFLOW Model, and/or 3) concentrations based on exposure to contaminated drill cuttings. The dose calculations are abstracted from conceptualizations of possible exposure pathways. A complete description of the Dose Calculator and its latest updates, can be found in SRR-CWDA-2013-00058, Rev. 1.

1.3 Previous Model Updates

Previous updates to the HTF Stochastic Fate and Transport Models are documented in Revision 0 of this report (SRR-CWDA-2014-00060, Rev. 0), in Revision 1 of this report (SRR-CWDA-2014-00060, Rev. 1) and in *H-Area Tank Farm Stochastic Fate and Transport Model* (SRR-CWDA-2010-00093, Rev. 2).

2 MODEL UPDATES

This section describes the updates to HTF Stochastic Fate and Transport Model that differentiates the model described herein from the models described in SRR-CWDA-2014-00060, Rev. 0, SRR-CWDA-2014-00060, Rev. 1, and in SRR-CWDA-2010-00093, Rev. 2.

As noted in the Executive Summary, 1-meter points of assessment (POAs) were specifically added to the RAD model for use in the Special Analysis (SA). This SA is being used to evaluate the influence of changes to the expected inventories on radionuclide and chemical releases from waste tanks. This major revision will form the basis of any further updates to the model. In addition to incorporating the 1-meter POAs in the HTF Stochastic Fate and Transport Models, the inventory values associated with Tank 12 have also been updated to reflect characterization data.

As noted in the Executive Summary, a set of updates were implemented in the GoldSim model for use in the Types I and II Tanks SA. This section (Section 2) describes the updates to the HTF Stochastic Fate and Transport Model including changes to: 1) the inventory values for Tanks 9, 10, 11, 13, 14, and 15 (Section 2.1.1); 2) stochastic distributions used for inventories in for Tanks 13, 14, and 15 (Section 2.1.2); 3) the iodine K_d's and strontium K_d distributions (Section 2.2); 4) the points of assessment (POAs) along the 1-meter facility boundary to more adequately represent the advective transport processes simulated in the HTF PORFLOW model (Section 2.3); 5) the annulus contamination zone structure, reflecting changes in the PORFLOW model and the set of PORFLOW generated diffusion coefficient input files (Section 2.4); 6) the set of PORFLOW generated flow input files reflecting the changes to the annulus contamination zone, the added scenario calculations, and the addition of parameters to allow simulation of Configurations B through E (Section 2.5); 7) the alternate scenarios available in the model, with the addition of a set of scenarios to evaluate the sensitivity of the modeled system to different quality grouts (Section 2.6) and 8) the source specific saturated zone Darcy velocities (Section 2.7).

2.1 Types I and II Tanks SA Inventory Values and Distributions

2.1.1 Inventory Values

The HTF Radionuclide Stochastic Fate and Transport Model (HTF_Transport_Model_v4.000_Rad) was updated to reflect the latest changes in the HTF closure inventory. Prior to the final changes implemented in HTF_Transport_Model_v4.000_Rad, Tank 16 inventory values based on final characterization data and the Tank 12 inventory assignments based on sample results taken during Tank 12 waste removal and tank cleaning efforts were updated and documented in Revision 5 of SRR-CWDA-2010-00023. Since the approval of SRR-CWDA-2010-00023, the Tank 12 final characterization and inventory determination was completed and documented in the *Tank 12 Inventory Determination,* SRR-CWDA-2015-00075. Using the Tank 12 final characterization data and the final characterization of other Type I and II tanks, additional adjustments were made to the assigned residual inventories for the following HTF Type I and II tanks: Tanks 9, 10, 11, 13, 14 and 15. Revision 6 of *H-Tank Farm Closure Inventory for Use in Performance Assessment Modeling*, (SRR-CWDA-2010-00023) presents updated assigned radionuclide and chemical inventory values for Tanks 9, 10, 11, 13, 14 and 15 for use in fate and transport modeling. These assigned inventory values were updated in order to incorporate lessons learned from the Type I and Type II tanks that have completed final characterization to date. This inventory applies to both Tank 12 Special Analysis modeling, as presented in *Tank 12 Inventory Determination* (SRR-CWDA-2015-00075), and Performance Assessment modeling, as presented in *H-Tank Farm Waste Tank Closure Inventory for Use in Performance Assessment Modeling.* [SRR-CWDA-2010-00023] Revision 4 of SRR-CWDA-2010-00023 incorporates changes to the waste tank closure inventory approach with respect to the Savannah River Site (SRS) *Liquid Waste Tank Residuals Sampling and Analysis Program Plan* (LWTRSAPP) and the *Liquid Waste Tank Residuals Sampling-Quality Assurance Program Plan* (LWTRS-QAPP). [SRR-CWDA-2011-00050, SRR-CWDA-2011-00117]

For use in upcoming uncertainty and sensitivity studies in the Types I and II Tanks SA, the radionuclide inventory values for Tank 9, Tank 10, Tank 11, Tank 13, Tank 14, and Tank 15 have been updated in HTF_Transport_Model_v4.000_Rad. These updated radionuclide inventory values have replaced their previous values found in the GoldSim data elements used in the HTF Stochastic Fate and Transport Model. The updated values along with the remaining values used in the Tank 12 SA (SRR-CWDA-2015-00073, Rev. 0), are presented in Table 2-1 through Table 2-7. The values presented in Table 2-1 through Table 2-4 represent the inventories found in the CZ at the bottom of the tank. The values presented in Table 2-5 represent the inventories found at the floor of the annulus in each of the Type I Tanks. The values presented in Table 2-6 and Table 2-7, represent the inventories found at the primary and secondary sand layers as well as the floor of the annulus for Type II Tanks. A full description of the approach used to estimate this inventory is provided in SRR-CWDA-2010-00023, Rev. 6.

Table 2-1: HTF Inventory Estimates in Curies for Use in Modeling (Tanks 9 to 16)

Radionuclide	Tank 9	Tank 10	Tank 11	Tank 12	Tank 13	Tank 14	Tank 15	Tank 16
Ac-227	1.0E+00	1.0E+00	1.0E+00	0	1.0E+00	1.0E+00	1.0E+00	0
Al-26	1.0E+00	1.0E+00	1.0E+00	0	1.0E+00	1.0E+00	1.0E+00	0
Am-241	1.3E+03	1.3E+03	1.3E+03	1.32E+02	1.3E+03	1.3E+03	1.3E+03	1.6E+00
Am-242m	2.7E+00	2.7E+00	2.7E+00	2.96E-02	2.7E+00	2.7E+00	2.7E+00	2.5E-05
Am-243	3.0E+01	3.0E+01	3.0E+01	1.63E-01	3.0E+01	3.0E+01	3.0E+01	2.1E-04
C-14	1.0E+00	1.0E+00	1.0E+00	3.16E-03	1.0E+00	1.0E+00	1.0E+00	1.6E-03
Cf-249	1.0E+00	1.0E+00	1.0E+00	0	1.0E+00	1.0E+00	1.0E+00	5.0E-05
Cf-251	1.0E+00	1.0E+00	1.0E+00	0	1.0E+00	1.0E+00	1.0E+00	1.3E-04
Cl-36	1.0E-03	1.0E-03	1.0E-03	0	1.0E-03	1.0E-03	1.0E-03	4.7E-06
Cm-243	6.2E+00	6.2E+00	6.2E+00	5.06E-02	6.2E+00	6.2E+00	6.2E+00	9.9E-05
Cm-244	7.3E+02	7.3E+02	7.3E+02	1.08E+00	7.3E+02	7.3E+02	7.3E+02	4.3E-03
Cm-245	7.5E-01	7.5E-01	7.5E-01	3.02E-04	7.5E-01	7.5E-01	7.5E-01	6.2E-06
Cm-246	0	0	0	0	0	0	0	0
Cm-247	1.0E+00	1.0E+00	1.0E+00	0	1.0E+00	1.0E+00	1.0E+00	3.0E-09
Cm-248	1.0E+00	1.0E+00	1.0E+00	0	1.0E+00	1.0E+00	1.0E+00	1.4E-07
Co-60	5.0E+01	5.0E+01	5.0E+01	0	5.0E+01	5.0E+01	5.0E+01	8.8E-05
Cs-135	4.2E-02	4.2E-02	4.2E-02	6.27E-05	4.2E-02	4.2E-02	4.2E-02	5.3E-05
Cs-137	6.7E+03	6.7E+03	6.7E+03	6.1E+01	6.7E+03	6.7E+03	6.7E+03	1.5E-02
Eu-152	2.0E+01	2.0E+01	2.0E+01	0	2.0E+01	2.0E+01	2.0E+01	0
Eu-154	3.0E+02	3.0E+02	3.0E+02	0	3.0E+02	3.0E+02	3.0E+02	0
Eu-155	0	0	0	0	0	0	0	0
Gd-152	0	0	0	0	0	0	0	0
H-3	1.0E+00	1.0E+00	1.0E+00	0	1.0E+00	1.0E+00	1.0E+00	0
I-129	3.0E-02	3.0E-02	3.0E-02	3.76E-02	3.0E-02	3.0E-02	3.0E-02	1.3E-03
K-40	1.2E-02	1.2E-02	1.2E-02	0	1.2E-02	1.2E-02	1.2E-02	4.1E-05
Nb-93m	0.0E+00	0.0E+00	0.0E+00	0	0.0E+00	0.0E+00	0.0E+00	0
Nb-94	1.1E-01	1.1E-01	1.1E-01	2.73E-03	1.1E-01	1.1E-01	1.1E-01	8.9E-03
Ni-59	9.5E+01	9.5E+01	9.5E+01	1.96E+00	9.5E+01	9.5E+01	9.5E+01	1.3E-03
Ni-63	5.2E+03	5.2E+03	5.2E+03	1.68E+02	5.2E+03	5.2E+03	5.2E+03	1.5E-03
Np-237	4.7E-01	4.7E-01	4.7E-01	1.58E-01	4.7E-01	4.7E-01	4.7E-01	1.5E-03
Pa-231	3.1E-02	3.1E-02	3.1E-02	1.53E-02	3.1E-02	3.1E-02	3.1E-02	6.2E-03
Pb-210	0	0	0	0	0	0	0	0
Pd-107	1.0E-01	1.0E-01	1.0E-01	0	1.0E-01	1.0E-01	1.0E-01	0
Pt-193	1.0E-01	1.0E-01	1.0E-01	0	1.0E-01	1.0E-01	1.0E-01	0
Pu-238	3.0E+03	3.0E+03	3.0E+03	8.75E+02	3.0E+03	3.0E+03	3.0E+03	4.6E+00
Pu-239	1.3E+02	1.3E+02	1.3E+02	4.27E+01	1.3E+02	1.3E+02	1.3E+02	2.2E-01
Pu-240	3.8E+01	3.8E+01	3.8E+01	1.63E+01	3.8E+01	3.8E+01	3.8E+01	9.5E-02
Pu-241	5.7E+02	5.7E+02	5.7E+02	1.01E+02	5.7E+02	5.7E+02	5.7E+02	3.5E-02
Pu-242	1.0E+00	1.0E+00	1.0E+00	0	1.0E+00	1.0E+00	1.0E+00	2.0E-05
Pu-244	1.0E+00	1.0E+00	1.0E+00	0	1.0E+00	1.0E+00	1.0E+00	2.1E-07
Ra-226	3.8E-02	3.8E-02	3.8E-02	2.91E-03	3.8E-02	3.8E-02	3.8E-02	7.3E-04
Ra-228	2.1E+00	2.1E+00	2.1E+00	6.06E-03	2.1E+00	2.1E+00	2.1E+00	0

Table 2-1: HTF Inventory Estimates in Curies for Use in Modeling (Tanks 9 to 16) (Continued)

Radionuclide	Tank 9	Tank 10	Tank 11	Tank 12	Tank 13	Tank 14	Tank 15	Tank 16
Se-79	1.0E+00	1.0E+00	1.0E+00	0	1.0E+00	1.0E+00	1.0E+00	0
Sm-147	0	0	0	0	0	0	0	0
Sm-151	1.1E+04	1.1E+04	1.1E+04	0	1.1E+04	1.1E+04	1.1E+04	0
Sn-126	1.2E+01	1.2E+01	1.2E+01	1.39E-01	1.2E+01	1.2E+01	1.2E+01	0
Sr-90	2.0E+05	2.0E+05	2.0E+05	8.08E+04	2.0E+05	2.0E+05	2.0E+05	9.4E+03
Tc-99	3.0E+00	3.0E+00	3.0E+00	7.24E-02	3.0E+00	3.0E+00	3.0E+00	1.7E+00
Th-229	2.6E-03	2.6E-03	2.6E-03	1.28E-03	2.6E-03	2.6E-03	2.6E-03	0
Th-230	3.5E-02	3.5E-02	3.5E-02	2.21E-03	3.5E-02	3.5E-02	3.5E-02	2.4E-04
Th-232	2.9E-02	2.9E-02	2.9E-02	6.63E-02	2.9E-02	2.9E-02	2.9E-02	0
U-232	2.1E-03	2.1E-03	2.1E-03	2.15E-02	2.1E-03	2.1E-03	2.1E-03	0
U-233	4.4E-01	4.4E-01	4.4E-01	2.03E-01	4.4E-01	4.4E-01	4.4E-01	1.9E-02
U-234	1.5E-01	1.5E-01	1.5E-01	5.47E-02	1.5E-01	1.5E-01	1.5E-01	1.2E-02
U-235	1.6E-02	1.6E-02	1.6E-02	3.42E-04	1.6E-02	1.6E-02	1.6E-02	3.3E-06
U-236	2.1E-02	2.1E-02	2.1E-02	0	2.1E-02	2.1E-02	2.1E-02	0
U-238	2.5E-01	2.5E-01	2.5E-01	5.88E-03	2.5E-01	2.5E-01	2.5E-01	1.2E-05
Zr-93	4.7E+01	4.7E+01	4.7E+01	3.98E+00	4.7E+01	4.7E+01	4.7E+01	7.1E-03

[SRR-CWDA-2010-00023, Rev. 6; SRR-CWDA-2015-00075, Rev. 1]

Table 2-2: HTF Inventory Estimates in Curies for Use in Modeling (Tanks 21 to 32)

Radionuclide	Tank 21	Tank 22	Tank 23	Tank 24	Tank 29	Tank 30	Tank 31	Tank 32
Ac-227	1.0E+00	1.0E+00	1.0E+00	1.0E+00	1.0E+00	1.0E+00	1.0E+00	1.0E+00
Al-26	1.0E+00	1.0E+00	1.0E+00	1.0E+00	1.0E+00	1.0E+00	1.0E+00	1.0E+00
Am-241	5.0E+00	5.0E+00	5.0E+00	5.0E+00	1.1E+03	1.1E+03	1.1E+03	1.1E+03
Am-242m	1.0E+00	1.0E+00	1.0E+00	1.0E+00	1.0E+00	1.0E+00	1.0E+00	1.0E+00
Am-243	1.0E+00	1.0E+00	1.0E+00	1.0E+00	1.0E+00	1.0E+00	1.0E+00	1.0E+00
C-14	1.0E+00	1.0E+00	1.0E+00	1.0E+00	1.0E+00	1.0E+00	1.0E+00	1.0E+00
Cf-249	1.0E+00	1.0E+00	1.0E+00	1.0E+00	1.0E+00	1.0E+00	1.0E+00	1.0E+00
Cf-251	1.0E+00	1.0E+00	1.0E+00	1.0E+00	1.0E+00	1.0E+00	1.0E+00	1.0E+00
Cl-36	2.1E-03	2.1E-03	2.1E-03	2.1E-03	2.1E-03	2.1E-03	2.1E-03	2.1E-03
Cm-243	1.0E+00	1.0E+00	1.0E+00	1.0E+00	1.0E+00	1.0E+00	1.0E+00	1.0E+00
Cm-244	4.6E+00	4.6E+00	4.6E+00	4.6E+00	2.2E+03	2.2E+03	2.2E+03	2.2E+03
Cm-245	1.0E+00	1.0E+00	1.0E+00	1.0E+00	1.0E+00	1.0E+00	1.0E+00	1.0E+00
Cm-246	0	0	0	0	0	0	0	0
Cm-247	1.0E+00	1.0E+00	1.0E+00	1.0E+00	1.0E+00	1.0E+00	1.0E+00	1.0E+00
Cm-248	1.0E+00	1.0E+00	1.0E+00	1.0E+00	1.0E+00	1.0E+00	1.0E+00	1.0E+00
Co-60	1.0E+00	1.0E+00	1.0E+00	1.0E+00	1.0E+00	1.0E+00	1.0E+00	1.0E+00
Cs-135	2.3E-02	2.3E-02	2.3E-02	2.3E-02	7.1E-03	7.1E-03	7.1E-03	7.1E-03
Cs-137	2.4E+03	2.4E+03	2.4E+03	2.4E+03	5.5E+03	5.5E+03	5.5E+03	5.5E+03
Eu-152	1.0E+00	1.0E+00	1.0E+00	1.0E+00	3.8E+01	3.8E+01	3.8E+01	3.8E+01
Eu-154	8.3E+00	8.3E+00	8.3E+00	8.3E+00	9.2E+02	9.2E+02	9.2E+02	9.2E+02
Eu-155	0	0	0	0	0	0	0	0
Gd-152	0	0	0	0	0	0	0	0
H-3	1.0E+00	1.0E+00	1.0E+00	1.0E+00	1.0E+00	1.0E+00	1.0E+00	1.0E+00
I-129	2.1E-04	2.1E-04	2.1E-04	2.1E-04	6.7E-03	6.7E-03	6.7E-03	6.7E-03
K-40	1.1E-03	1.1E-03	1.1E-03	1.1E-03	1.1E-03	1.1E-03	1.1E-03	1.1E-03
Nb-93m	0	0	0	0	0	0	0	0
Nb-94	1.1E-01	1.1E-01	1.1E-01	1.1E-01	1.1E-01	1.1E-01	1.1E-01	1.1E-01
Ni-59	1.0E+00	1.0E+00	1.0E+00	1.0E+00	1.0E+00	1.0E+00	1.0E+00	1.0E+00
Ni-63	9.1E+00	9.1E+00	9.1E+00	9.1E+00	7.9E+02	7.9E+02	7.9E+02	7.9E+02
Np-237	1.3E-02	1.3E-02	1.3E-02	1.3E-02	4.0E-01	4.0E-01	4.0E-01	4.0E-01
Pa-231	2.1E-03	2.1E-03	2.1E-03	2.1E-03	2.1E-03	2.1E-03	2.1E-03	2.1E-03
Pb-210	0	0	0	0	0	0	0	0
Pd-107	2.1E-01	2.1E-01	2.1E-01	2.1E-01	2.1E-01	2.1E-01	2.1E-01	2.1E-01
Pt-193	2.1E-01	2.1E-01	2.1E-01	2.1E-01	2.1E-01	2.1E-01	2.1E-01	2.1E-01
Pu-238	7.2E+01	7.2E+01	7.2E+01	7.2E+01	2.8E+03	2.8E+03	2.8E+03	1.5E+04
Pu-239	1.0E+00	1.0E+00	1.0E+00	1.0E+00	2.4E+02	2.4E+02	2.4E+02	2.4E+02
Pu-240	3.6E-01	3.6E-01	3.6E-01	3.6E-01	1.5E+02	1.5E+02	1.5E+02	1.5E+02
Pu-241	2.1E+00	2.1E+00	2.1E+00	2.1E+00	4.6E+03	4.6E+03	4.6E+03	4.6E+03
Pu-242	1.0E+00	1.0E+00	1.0E+00	1.0E+00	1.0E+00	1.0E+00	1.0E+00	1.0E+00
Pu-244	1.0E+00	1.0E+00	1.0E+00	1.0E+00	1.0E+00	1.0E+00	1.0E+00	1.0E+00
Ra-226	2.1E-02	2.1E-02	2.1E-02	2.1E-02	2.1E-02	2.1E-02	2.1E-02	2.1E-02
Ra-228	2.1E+00	2.1E+00	2.1E+00	2.1E+00	2.1E+00	2.1E+00	2.1E+00	2.1E+00

Table 2-2: HTF Inventory Estimates in Curies for Use in Modeling (Tanks 21 to 32) (Continued)

Radionuclide	Tank 21	Tank 22	Tank 23	Tank 24	Tank 29	Tank 30	Tank 31	Tank 32
Se-79	1.0E+00	1.0E+00	1.0E+00	1.0E+00	1.0E+00	1.0E+00	1.0E+00	1.0E+00
Sm-147	0	0	0	0	0	0	0	0
Sm-151	2.4E+02	2.4E+02	2.4E+02	2.4E+02	7.7E+04	7.7E+04	7.7E+04	7.7E+04
Sn-126	1.0E+00	1.0E+00	1.0E+00	1.0E+00	1.0E+00	1.0E+00	1.0E+00	1.0E+00
Sr-90	3.1E+02	3.1E+02	3.1E+02	3.1E+02	2.0E+04	2.0E+04	2.0E+04	2.0E+04
Tc-99	1.6E-01	1.6E-01	1.6E-01	1.6E-01	9.7E+00	9.7E+00	9.7E+00	9.7E+00
Th-229	2.1E-03	2.1E-03	2.1E-03	2.1E-03	2.1E-03	2.1E-03	2.1E-03	2.1E-03
Th-230	2.1E-02	2.1E-02	2.1E-02	2.1E-02	2.1E-02	2.1E-02	2.1E-02	2.1E-02
Th-232	2.1E-02	2.1E-02	2.1E-02	2.1E-02	2.7E-02	2.7E-02	2.7E-02	2.7E-02
U-232	2.1E-03	2.1E-03	2.1E-03	2.1E-03	2.1E-03	2.1E-03	2.1E-03	2.1E-03
U-233	6.0E-02	6.0E-02	6.0E-02	6.0E-02	1.3E+00	1.3E+00	1.3E+00	1.3E+00
U-234	2.2E-02	2.2E-02	2.2E-02	2.2E-02	6.6E-01	6.6E-01	6.6E-01	6.6E-01
U-235	2.1E-02	2.1E-02	2.1E-02	2.1E-02	2.1E-02	2.1E-02	2.1E-02	2.1E-02
U-236	2.1E-02	2.1E-02	2.1E-02	2.1E-02	1.1E-01	1.1E-01	1.1E-01	1.1E-01
U-238	7.4E-03	7.4E-03	7.4E-03	7.4E-03	8.4E-02	8.4E-02	8.4E-02	8.4E-02
Zr-93	8.8E-03	8.8E-03	8.8E-03	8.8E-03	5.7E-01	5.7E-01	5.7E-01	5.7E-01

[SRR-CWDA-2010-00023, Rev. 6]

Table 2-3: HTF Inventory Estimates in Curies for Use in Modeling (Tanks 35 to 42)

Radionuclide	Tank 35	Tank 36	Tank 37	Tank 38	Tank 39	Tank 40	Tank 41	Tank 42
Ac-227	1.0E+00	1.0E+00	1.0E+00	1.0E+00	1.0E+00	1.0E+00	1.0E+00	1.0E+00
Al-26	1.0E+00	1.0E+00	1.0E+00	1.0E+00	1.0E+00	1.0E+00	1.0E+00	1.0E+00
Am-241	1.1E+03	1.1E+03	1.1E+03	1.1E+03	1.1E+03	1.1E+03	1.1E+03	1.1E+03
Am-242m	1.0E+00	1.0E+00	1.0E+00	1.0E+00	1.0E+00	1.0E+00	1.0E+00	1.0E+00
Am-243	1.0E+00	1.0E+00	1.0E+00	1.0E+00	1.0E+00	1.0E+00	1.0E+00	1.0E+00
C-14	1.0E+00	1.0E+00	1.0E+00	1.0E+00	1.0E+00	1.0E+00	1.0E+00	1.0E+00
Cf-249	1.0E+00	1.0E+00	1.0E+00	1.0E+00	1.0E+00	1.0E+00	1.0E+00	1.0E+00
Cf-251	1.0E+00	1.0E+00	1.0E+00	1.0E+00	1.0E+00	1.0E+00	1.0E+00	1.0E+00
Cl-36	2.1E-03	2.1E-03	2.1E-03	2.1E-03	2.1E-03	2.1E-03	2.1E-03	2.1E-03
Cm-243	1.0E+00	1.0E+00	1.0E+00	1.0E+00	1.0E+00	1.0E+00	1.0E+00	1.0E+00
Cm-244	2.2E+03	2.2E+03	2.2E+03	2.2E+03	2.2E+03	2.2E+03	2.2E+03	2.2E+03
Cm-245	1.0E+00	1.0E+00	1.0E+00	1.0E+00	1.0E+00	1.0E+00	1.0E+00	1.0E+00
Cm-246	0	0	0	0	0	0	0	0
Cm-247	1.0E+00	1.0E+00	1.0E+00	1.0E+00	1.0E+00	1.0E+00	1.0E+00	1.0E+00
Cm-248	1.0E+00	1.0E+00	1.0E+00	1.0E+00	1.0E+00	1.0E+00	1.0E+00	1.0E+00
Co-60	1.0E+00	1.0E+00	1.0E+00	1.0E+00	1.0E+00	1.0E+00	1.0E+00	1.0E+00
Cs-135	7.1E-03	7.1E-03	7.1E-03	7.1E-03	7.1E-03	7.1E-03	7.1E-03	7.1E-03
Cs-137	5.5E+03	5.5E+03	5.5E+03	5.5E+03	5.5E+03	5.5E+03	5.5E+03	5.5E+03
Eu-152	3.8E+01	3.8E+01	3.8E+01	3.8E+01	3.8E+01	3.8E+01	3.8E+01	3.8E+01
Eu-154	9.2E+02	9.2E+02	9.2E+02	9.2E+02	9.2E+02	9.2E+02	9.2E+02	9.2E+02
Eu-155	0	0	0	0	0	0	0	0
Gd-152	0	0	0	0	0	0	0	0
H-3	1.0E+00	1.0E+00	1.0E+00	1.0E+00	1.0E+00	1.0E+00	1.0E+00	1.0E+00
I-129	6.7E-03	6.7E-03	6.7E-03	6.7E-03	6.7E-03	6.7E-03	6.7E-03	6.7E-03
K-40	1.1E-03	1.1E-03	1.1E-03	1.1E-03	1.1E-03	1.1E-03	1.1E-03	1.1E-03
Nb-93m	0	0	0	0	0	0	0	0
Nb-94	1.1E-01	1.1E-01	1.1E-01	1.1E-01	1.1E-01	1.1E-01	1.1E-01	1.1E-01
Ni-59	1.0E+00	1.0E+00	1.0E+00	1.0E+00	1.0E+00	1.0E+00	1.0E+00	1.0E+00
Ni-63	7.9E+02	7.9E+02	7.9E+02	7.9E+02	7.9E+02	7.9E+02	7.9E+02	7.9E+02
Np-237	4.0E-01	4.0E-01	4.0E-01	4.0E-01	4.0E-01	4.0E-01	4.0E-01	4.0E-01
Pa-231	2.1E-03	2.1E-03	2.1E-03	2.1E-03	2.1E-03	2.1E-03	2.1E-03	2.1E-03
Pb-210	0	0	0	0	0	0	0	0
Pd-107	2.1E-01	2.1E-01	2.1E-01	2.1E-01	2.1E-01	2.1E-01	2.1E-01	2.1E-01
Pt-193	2.1E-01	2.1E-01	2.1E-01	2.1E-01	2.1E-01	2.1E-01	2.1E-01	2.1E-01
Pu-238	1.5E+04	2.8E+03	2.8E+03	2.8E+03	1.5E+04	1.5E+04	2.8E+03	1.5E+04
Pu-239	2.4E+02	2.4E+02	2.4E+02	2.4E+02	2.4E+02	2.4E+02	2.4E+02	2.4E+02
Pu-240	1.5E+02	1.5E+02	1.5E+02	1.5E+02	1.5E+02	1.5E+02	1.5E+02	1.5E+02
Pu-241	4.6E+03	4.6E+03	4.6E+03	4.6E+03	4.6E+03	4.6E+03	4.6E+03	4.6E+03
Pu-242	1.0E+00	1.0E+00	1.0E+00	1.0E+00	1.0E+00	1.0E+00	1.0E+00	1.0E+00
Pu-244	1.0E+00	1.0E+00	1.0E+00	1.0E+00	1.0E+00	1.0E+00	1.0E+00	1.0E+00
Ra-226	2.1E-02	2.1E-02	2.1E-02	2.1E-02	2.1E-02	2.1E-02	2.1E-02	2.1E-02
Ra-228	2.1E+00	2.1E+00	2.1E+00	2.1E+00	2.1E+00	2.1E+00	2.1E+00	2.1E+00

Table 2-3: HTF Inventory Estimates in Curies for Use in Modeling (Tanks 35 to 42) (Continued)

Radionuclide	Tank 35	Tank 36	Tank 37	Tank 38	Tank 39	Tank 40	Tank 41	Tank 42
Se-79	1.0E+00	1.0E+00	1.0E+00	1.0E+00	1.0E+00	1.0E+00	1.0E+00	1.0E+00
Sm-147	0	0	0	0	0	0	0	0
Sm-151	7.7E+04	7.7E+04	7.7E+04	7.7E+04	7.7E+04	7.7E+04	7.7E+04	7.7E+04
Sn-126	1.0E+00	1.0E+00	1.0E+00	1.0E+00	1.0E+00	1.0E+00	1.0E+00	1.0E+00
Sr-90	2.0E+04	2.0E+04	2.0E+04	2.0E+04	2.0E+04	2.0E+04	2.0E+04	2.0E+04
Tc-99	9.7E+00	9.7E+00	9.7E+00	9.7E+00	9.7E+00	9.7E+00	9.7E+00	9.7E+00
Th-229	2.1E-03	2.1E-03	2.1E-03	2.1E-03	2.1E-03	2.1E-03	2.1E-03	2.1E-03
Th-230	2.1E-02	2.1E-02	2.1E-02	2.1E-02	2.1E-02	2.1E-02	2.1E-02	2.1E-02
Th-232	2.7E-02	2.7E-02	2.7E-02	2.7E-02	2.7E-02	2.7E-02	2.7E-02	2.7E-02
U-232	2.1E-03	2.1E-03	2.1E-03	2.1E-03	2.1E-03	2.1E-03	2.1E-03	2.1E-03
U-233	1.3E+00	1.3E+00	1.3E+00	1.3E+00	1.3E+00	1.3E+00	1.3E+00	1.3E+00
U-234	6.6E-01	6.6E-01	6.6E-01	6.6E-01	6.6E-01	6.6E-01	6.6E-01	6.6E-01
U-235	2.1E-02	2.1E-02	2.1E-02	2.1E-02	2.1E-02	2.1E-02	2.1E-02	2.1E-02
U-236	1.1E-01	1.1E-01	1.1E-01	1.1E-01	1.1E-01	1.1E-01	1.1E-01	1.1E-01
U-238	8.4E-02	8.4E-02	8.4E-02	8.4E-02	8.4E-02	8.4E-02	8.4E-02	8.4E-02
Zr-93	5.7E-01	5.7E-01	5.7E-01	5.7E-01	5.7E-01	5.7E-01	5.7E-01	5.7E-01

[SRR-CWDA-2010-00023, Rev. 6]

Table 2-4: HTF Inventory Estimates in Curies for Use in Modeling (Tanks 43 to 51)

Radionuclide	Tank 43	Tank 48	Tank 49	Tank 50	Tank 51
Ac-227	1.0E+00	1.0E+00	1.0E+00	1.0E+00	1.0E+00
Al-26	1.0E+00	1.0E+00	1.0E+00	1.0E+00	1.0E+00
Am-241	1.1E+03	1.1E+03	1.1E+03	1.1E+03	1.1E+03
Am-242m	1.0E+00	1.0E+00	1.0E+00	1.0E+00	1.0E+00
Am-243	1.0E+00	1.0E+00	1.0E+00	1.0E+00	1.0E+00
C-14	1.0E+00	1.0E+00	1.0E+00	1.0E+00	1.0E+00
Cf-249	1.0E+00	1.0E+00	1.0E+00	1.0E+00	1.0E+00
Cf-251	1.0E+00	1.0E+00	1.0E+00	1.0E+00	1.0E+00
Cl-36	2.1E-03	2.1E-03	2.1E-03	2.1E-03	2.1E-03
Cm-243	1.0E+00	1.0E+00	1.0E+00	1.0E+00	1.0E+00
Cm-244	2.2E+03	2.2E+03	2.2E+03	2.2E+03	2.2E+03
Cm-245	1.0E+00	1.0E+00	1.0E+00	1.0E+00	1.0E+00
Cm-246	0	0	0	0	0
Cm-247	1.0E+00	1.0E+00	1.0E+00	1.0E+00	1.0E+00
Cm-248	1.0E+00	1.0E+00	1.0E+00	1.0E+00	1.0E+00
Co-60	1.0E+00	1.0E+00	1.0E+00	1.0E+00	1.0E+00
Cs-135	7.1E-03	7.1E-03	7.1E-03	7.1E-03	7.1E-03
Cs-137	5.5E+03	5.5E+03	5.5E+03	5.5E+03	5.5E+03
Eu-152	3.8E+01	3.8E+01	3.8E+01	3.8E+01	3.8E+01
Eu-154	9.2E+02	9.2E+02	9.2E+02	9.2E+02	9.2E+02
Eu-155	0	0	0	0	0
Gd-152	0	0	0	0	0
H-3	1.0E+00	1.0E+00	1.0E+00	1.0E+00	1.0E+00
I-129	6.7E-03	6.7E-03	6.7E-03	6.7E-03	6.7E-03
K-40	1.1E-03	1.1E-03	1.1E-03	1.1E-03	1.1E-03
Nb-93m	0	0	0	0	0
Nb-94	1.1E-01	1.1E-01	1.1E-01	1.1E-01	1.1E-01
Ni-59	1.0E+00	1.0E+00	1.0E+00	1.0E+00	1.0E+00
Ni-63	7.9E+02	7.9E+02	7.9E+02	7.9E+02	7.9E+02
Np-237	4.0E-01	4.0E-01	4.0E-01	4.0E-01	4.0E-01
Pa-231	2.1E-03	2.1E-03	2.1E-03	2.1E-03	2.1E-03
Pb-210	0	0	0	0	0
Pd-107	2.1E-01	2.1E-01	2.1E-01	2.1E-01	2.1E-01
Pt-193	2.1E-01	2.1E-01	2.1E-01	2.1E-01	2.1E-01
Pu-238	1.5E+04	2.8E+03	2.8E+03	1.5E+04	1.5E+04
Pu-239	2.4E+02	2.4E+02	2.4E+02	2.4E+02	2.4E+02
Pu-240	1.5E+02	1.5E+02	1.5E+02	1.5E+02	1.5E+02
Pu-241	4.6E+03	4.6E+03	4.6E+03	4.6E+03	4.6E+03
Pu-242	1.0E+00	1.0E+00	1.0E+00	1.0E+00	1.0E+00
Pu-244	1.0E+00	1.0E+00	1.0E+00	1.0E+00	1.0E+00
Ra-226	2.1E-02	2.1E-02	2.1E-02	2.1E-02	2.1E-02
Ra-228	2.1E+00	2.1E+00	2.1E+00	2.1E+00	2.1E+00

Table 2-4: HTF Inventory Estimates in Curies for Use in Modeling (Tanks 43 to 51) (Continued)

Radionuclide	Tank 43	Tank 48	Tank 49	Tank 50	Tank 51
Se-79	1.0E+00	1.0E+00	1.0E+00	1.0E+00	1.0E+00
Sm-147	0	0	0	0	0
Sm-151	7.7E+04	7.7E+04	7.7E+04	7.7E+04	7.7E+04
Sn-126	1.0E+00	1.0E+00	1.0E+00	1.0E+00	1.0E+00
Sr-90	2.0E+04	2.0E+04	2.0E+04	2.0E+04	2.0E+04
Tc-99	9.7E+00	9.7E+00	9.7E+00	9.7E+00	9.7E+00
Th-229	2.1E-03	2.1E-03	2.1E-03	2.1E-03	2.1E-03
Th-230	2.1E-02	2.1E-02	2.1E-02	2.1E-02	2.1E-02
Th-232	2.7E-02	2.7E-02	2.7E-02	2.7E-02	2.7E-02
U-232	2.1E-03	2.1E-03	2.1E-03	2.1E-03	2.1E-03
U-233	1.3E+00	1.3E+00	1.3E+00	1.3E+00	1.3E+00
U-234	6.6E-01	6.6E-01	6.6E-01	6.6E-01	6.6E-01
U-235	2.1E-02	2.1E-02	2.1E-02	2.1E-02	2.1E-02
U-236	1.1E-01	1.1E-01	1.1E-01	1.1E-01	1.1E-01
U-238	8.4E-02	8.4E-02	8.4E-02	8.4E-02	8.4E-02
Zr-93	5.7E-01	5.7E-01	5.7E-01	5.7E-01	5.7E-01

[SRR-CWDA-2010-00023, Rev. 6]

Table 2-5: HTF Annulus Floor Inventory Estimates in Curies for Use in Modeling Type I Tanks

Radionuclide	Tank 9	Tank 10	Tank 11	Tank 12
Ac-227	1.0E+00	1.0E+00	1.0E+00	0
Al-26	1.0E+00	1.0E+00	1.0E+00	0
Am-241	3.9E-01	3.9E-01	3.9E-01	9.8E-02
Am-242m	2.0E-04	2.0E-04	2.0E-04	4.9E-05
Am-243	4.2E-04	4.2E-04	4.2E-04	1.0E-04
C-14	2.6E-04	2.6E-04	2.6E-04	6.4E-05
Cf-249	3.3E-04	3.3E-04	3.3E-04	0
Cf-251	8.9E-04	8.9E-04	8.9E-04	0
Cl-36	1.6E-04	1.6E-04	1.6E-04	0
Cm-243	7.2E-04	7.2E-04	7.2E-04	1.8E-04
Cm-244	2.0E-02	2.0E-02	2.0E-02	5.1E-03
Cm-245	3.9E-06	3.9E-06	3.9E-06	9.7E-07
Cm-246	0	0	0	0
Cm-247	2.5E-10	2.5E-10	2.5E-10	0
Cm-248	2.8E-07	2.8E-07	2.8E-07	0
Co-60	9.8E-05	9.8E-05	9.8E-05	0
Cs-135	1.0E-03	1.0E-03	1.0E-03	2.6E-04
Cs-137	2.0E+02	2.0E+02	2.0E+02	4.9E+01
Eu-152	2.1E+01	2.1E+01	2.1E+01	0
Eu-154	8.8E-02	8.8E-02	8.8E-02	0
Eu-155	0	0	0	0
Gd-152	0	0	0	0
H-3	1.0E+00	1.0E+00	1.0E+00	0
I-129	4.1E-04	4.1E-04	4.1E-04	1.0E-04
K-40	8.9E-06	8.9E-06	8.9E-06	0
Nb-93m	0	0	0	0
Nb-94	1.4E-04	1.4E-04	1.4E-04	3.4E-05
Ni-59	4.9E-04	4.9E-04	4.9E-04	1.2E-04
Ni-63	1.9E-02	1.9E-02	1.9E-02	4.7E-03
Np-237	1.1E-03	1.1E-03	1.1E-03	2.7E-04
Pa-231	8.2E-05	8.2E-05	8.2E-05	2.0E-05
Pb-210	0	0	0	0
Pd-107	5.3E-03	5.3E-03	5.3E-03	0
Pt-193	5.3E-03	5.3E-03	5.3E-03	0
Pu-238	1.6E+00	1.6E+00	1.6E+00	3.9E-01
Pu-239	2.5E-01	2.5E-01	2.5E-01	6.2E-02
Pu-240	1.1E-01	1.1E-01	1.1E-01	2.8E-02
Pu-241	3.0E-01	3.0E-01	3.0E-01	7.6E-02
Pu-242	4.4E-05	4.4E-05	4.4E-05	0
Pu-244	3.7E-08	3.7E-08	3.7E-08	0
Ra-226	5.5E-05	5.5E-05	5.5E-05	1.4E-05
Ra-228	5.3E-02	5.3E-02	5.3E-02	5.3E-02

Table 2-5: HTF Annulus Floor Inventory Estimates in Curies for Use in Modeling Type I Tanks (Continued)

Radionuclide	Tank 9	Tank 10	Tank 11	Tank 12
Se-79	4.8E+00	4.8E+00	4.8E+00	0
Sm-147	0	0	0	0
Sm-151	4.7E+00	4.7E+00	4.7E+00	0
Sn-126	4.6E+00	4.6E+00	4.6E+00	4.6E+00
Sr-90	5.3E+02	5.3E+02	5.3E+02	1.3E+02
Tc-99	1.0E-01	1.0E-01	1.0E-01	2.5E-02
Th-229	5.3E-05	5.3E-05	5.3E-05	5.3E-05
Th-230	1.9E-05	1.9E-05	1.9E-05	4.8E-06
Th-232	7.1E-04	7.1E-04	7.1E-04	7.1E-04
U-232	5.3E-05	5.3E-05	5.3E-05	5.3E-05
U-233	5.9E-04	5.9E-04	5.9E-04	1.5E-04
U-234	6.5E-04	6.5E-04	6.5E-04	1.6E-04
U-235	9.2E-06	9.2E-06	9.2E-06	2.3E-06
U-236	3.6E-05	3.6E-05	3.6E-05	0
U-238	4.1E-05	4.1E-05	4.1E-05	1.0E-05
Zr-93	4.5E-02	4.5E-02	4.5E-02	1.1E-02

[SRR-CWDA-2010-00023, Rev. 6; SRR-CWDA-2015-00075, Rev. 1]

Table 2-6: HTF Annulus and Sand Layers Inventory Estimates in Curies for Use in Modeling (Type II Tanks 13 and 14)

Radionuclide	Tank 13 Primary Sand	Tank 13 Annulus Floor	Tank 13 Secondary Sand	Tank 14 Primary Sand	Tank 14 Annulus Floor	Tank 14 Secondary Sand
Ac-227	1.0E+00	1.0E+00	0	1.0E+00	1.0E+00	0
Al-26	1.0E+00	1.0E+00	0	1.0E+00	1.0E+00	0
Am-241	3.9E-01	3.9E-01	0	5.1E+00	3.9E-01	0
Am-242m	2.0E-04	2.0E-04	0	2.6E-03	2.0E-04	0
Am-243	4.2E-04	4.2E-04	0	5.4E-03	4.2E-04	0
C-14	2.6E-04	2.6E-04	0	3.3E-03	2.6E-04	0
Cf-249	3.3E-04	3.3E-04	0	4.3E-03	3.3E-04	0
Cf-251	8.9E-04	8.9E-04	0	1.2E-02	8.9E-04	0
Cl-36	1.6E-04	1.6E-04	0	2.1E-03	1.6E-04	0
Cm-243	7.2E-04	7.2E-04	0	9.4E-03	7.2E-04	0
Cm-244	2.0E-02	2.0E-02	0	2.6E-01	2.0E-02	0
Cm-245	3.9E-06	3.9E-06	0	5.0E-05	3.9E-06	0
Cm-246	0	0	0	0	0	0
Cm-247	2.5E-10	2.5E-10	0	3.2E-09	2.5E-10	0
Cm-248	2.8E-07	2.8E-07	0	3.7E-06	2.8E-07	0
Co-60	9.8E-05	9.8E-05	0	1.3E-03	9.8E-05	0
Cs-135	1.0E-03	1.0E-03	0	1.3E-02	1.0E-03	0
Cs-137	2.0E+02	2.0E+02	0	2.5E+03	2.0E+02	0
Eu-152	2.1E+01	2.1E+01	0	2.1E+01	2.1E+01	0
Eu-154	8.8E-02	8.8E-02	0	1.1E+00	8.8E-02	0
Eu-155	0	0	0	0	0	0
Gd-152	0	0	0	0	0	0
H-3	1.0E+00	1.0E+00	0	1.0E+00	1.0E+00	0
I-129	4.1E-04	4.1E-04	0	5.4E-03	4.1E-04	0
K-40	8.9E-06	8.9E-06	0	1.2E-04	8.9E-06	0
Nb-93m	0	0	0	0	0	0
Nb-94	1.4E-04	1.4E-04	0	1.8E-03	1.4E-04	0
Ni-59	4.9E-04	4.9E-04	0	6.3E-03	4.9E-04	0
Ni-63	1.9E-02	1.9E-02	0	2.4E-01	1.9E-02	0
Np-237	1.1E-03	1.1E-03	0	1.4E-02	1.1E-03	0
Pa-231	8.2E-05	8.2E-05	0	1.1E-03	8.2E-05	0
Pb-210	0	0	0	0	0	0
Pd-107	5.3E-03	5.3E-03	0	6.9E-02	5.3E-03	0
Pt-193	5.3E-03	5.3E-03	0	6.9E-02	5.3E-03	0
Pu-238	1.6E+00	1.6E+00	0	2.0E+01	1.6E+00	0
Pu-239	2.5E-01	2.5E-01	0	3.2E+00	2.5E-01	0
Pu-240	1.1E-01	1.1E-01	0	1.5E+00	1.1E-01	0
Pu-241	3.0E-01	3.0E-01	0	4.0E+00	3.0E-01	0
Pu-242	4.4E-05	4.4E-05	0	5.7E-04	4.4E-05	0
Pu-244	3.7E-08	3.7E-08	0	4.8E-07	3.7E-08	0
Ra-226	5.5E-05	5.5E-05	0	7.1E-04	5.5E-05	0
Ra-228	5.3E-02	5.3E-02	0	6.9E-01	5.3E-02	0

Table 2-6: HTF Annulus and Sand Layers Inventory Estimates in Curies for Use in Modeling (Type II Tanks 13 and 14) (Continued)

Radionuclide	Tank 13 Primary Sand	Tank 13 Annulus Floor	Tank 13 Secondary Sand	Tank 14 Primary Sand	Tank 14 Annulus Floor	Tank 14 Secondary Sand
Se-79	4.8E+00	4.8E+00	0	4.8E+00	4.8E+00	0
Sm-147	0	0	0	0	0	0
Sm-151	4.7E+00	4.7E+00	0	6.1E+01	4.7E+00	0
Sn-126	4.6E+00	4.6E+00	0	4.6E+00	4.6E+00	0
Sr-90	5.3E+02	5.3E+02	0	6.9E+03	5.3E+02	0
Tc-99	1.0E-01	1.0E-01	0	1.3E+00	1.0E-01	0
Th-229	5.3E-05	5.3E-05	0	6.9E-04	5.3E-05	0
Th-230	1.9E-05	1.9E-05	0	2.5E-04	1.9E-05	0
Th-232	7.1E-04	7.1E-04	0	9.3E-03	7.1E-04	0
U-232	5.3E-05	5.3E-05	0	6.9E-04	5.3E-05	0
U-233	5.9E-04	5.9E-04	0	7.7E-03	5.9E-04	0
U-234	6.5E-04	6.5E-04	0	8.5E-03	6.5E-04	0
U-235	9.2E-06	9.2E-06	0	1.2E-04	9.2E-06	0
U-236	3.6E-05	3.6E-05	0	4.7E-04	3.6E-05	0
U-238	4.1E-05	4.1E-05	0	5.4E-04	4.1E-05	0
Zr-93	4.5E-02	4.5E-02	0	5.9E-01	4.5E-02	0

[SRR-CWDA-2010-00023, Rev. 6]

Table 2-7: HTF Annulus and Sand Layers Inventory Estimates in Curies for Use in Modeling (Type II Tanks 15 and 16)

Radionuclide	Tank 15 Primary Sand	Tank 15 Annulus Floor	Tank 15 Secondary Sand	Tank 16 Primary Sand	Tank 16 Annulus Floor	Tank 16 Secondary Sand
Ac-227	1.0E+00	1.0E+00	0	0	0	0
Al-26	1.0E+00	1.0E+00	0	0	0	0
Am-241	3.9E-01	3.9E-01	0	5.1E+00	7.5E+00	1.0E-01
Am-242m	2.0E-04	2.0E-04	0	2.6E-03	3.8E-03	5.1E-05
Am-243	4.2E-04	4.2E-04	0	5.4E-03	8.0E-03	1.1E-04
C-14	2.6E-04	2.6E-04	0	3.3E-03	4.9E-03	6.6E-05
Cf-249	3.3E-04	3.3E-04	0	4.3E-03	6.3E-03	8.6E-05
Cf-251	8.9E-04	8.9E-04	0	1.2E-02	1.7E-02	2.3E-04
Cl-36	1.6E-04	1.6E-04	0	2.1E-03	3.1E-03	4.2E-05
Cm-243	7.2E-04	7.2E-04	0	9.4E-03	1.4E-02	1.9E-04
Cm-244	2.0E-02	2.0E-02	0	2.6E-01	3.9E-01	5.3E-03
Cm-245	3.9E-06	3.9E-06	0	5.0E-05	7.4E-05	1.0E-06
Cm-246	0	0	0	0	0	0
Cm-247	2.5E-10	2.5E-10	0	3.2E-09	4.8E-09	6.5E-11
Cm-248	2.8E-07	2.8E-07	0	3.7E-06	5.4E-06	7.3E-08
Co-60	9.8E-05	9.8E-05	0	1.3E-03	1.9E-03	2.6E-05
Cs-135	1.0E-03	1.0E-03	0	1.3E-02	2.0E-02	2.7E-04
Cs-137	2.0E+02	2.0E+02	0	2.5E+03	3.7E+03	5.1E+01
Eu-152	2.1E+01	2.1E+01	0	0	0	0
Eu-154	8.8E-02	8.8E-02	0	0	0	0
Eu-155	0	0	0	0	0	0
Gd-152	0	0	0	0	0	0
H-3	1.0E+00	1.0E+00	0	0	0	0
I-129	4.1E-04	4.1E-04	0	5.4E-03	7.9E-03	1.1E-04
K-40	8.9E-06	8.9E-06	0	1.2E-04	1.7E-04	2.3E-06
Nb-93m	0	0	0	0	0	0
Nb-94	1.4E-04	1.4E-04	0	1.8E-03	2.6E-03	3.5E-05
Ni-59	4.9E-04	4.9E-04	0	6.3E-03	9.3E-03	1.3E-04
Ni-63	1.9E-02	1.9E-02	0	2.4E-01	3.6E-01	4.9E-03
Np-237	1.1E-03	1.1E-03	0	1.4E-02	2.0E-02	2.8E-04
Pa-231	8.2E-05	8.2E-05	0	1.1E-03	1.6E-03	2.1E-05
Pb-210	0	0	0	0	0	0
Pd-107	5.3E-03	5.3E-03	0	0	0	0
Pt-193	5.3E-03	5.3E-03	0	0	0	0
Pu-238	1.6E+00	1.6E+00	0	2.0E+01	3.0E+01	4.1E-01
Pu-239	2.5E-01	2.5E-01	0	3.2E+00	4.7E+00	6.4E-02
Pu-240	1.1E-01	1.1E-01	0	1.5E+00	2.1E+00	2.9E-02
Pu-241	3.0E-01	3.0E-01	0	4.0E+00	5.8E+00	7.9E-02
Pu-242	4.4E-05	4.4E-05	0	5.7E-04	8.4E-04	1.1E-05
Pu-244	3.7E-08	3.7E-08	0	4.8E-07	7.0E-07	9.5E-09
Ra-226	5.5E-05	5.5E-05	0	7.1E-04	1.0E-03	1.4E-05
Ra-228	5.3E-02	5.3E-02	0	0	0	0

Table 2-7: HTF Annulus and Sand Layers Inventory Estimates in Curies for Use in Modeling (Type II Tanks 15 and 16) (Continued)

Radionuclide	Tank 15 Primary Sand	Tank 15 Annulus Floor	Tank 15 Secondary Sand	Tank 16 Primary Sand	Tank 16 Annulus Floor	Tank 16 Secondary Sand
Se-79	4.8E+00	4.8E+00	0	0	0	0
Sm-147	0	0	0	0	0	0
Sm-151	4.7E+00	4.7E+00	0	0	0	0
Sn-126	4.6E+00	4.6E+00	0	0	0	0
Sr-90	5.3E+02	5.3E+02	0	6.9E+03	1.0E+04	1.4E+02
Tc-99	1.0E-01	1.0E-01	0	1.3E+00	1.9E+00	2.6E-02
Th-229	5.3E-05	5.3E-05	0	0	0	0
Th-230	1.9E-05	1.9E-05	0	2.5E-04	3.7E-04	5.0E-06
Th-232	7.1E-04	7.1E-04	0	0	0	0
U-232	5.3E-05	5.3E-05	0	0	0	0
U-233	5.9E-04	5.9E-04	0	7.7E-03	1.1E-02	1.5E-04
U-234	6.5E-04	6.5E-04	0	8.5E-03	1.2E-02	1.7E-04
U-235	9.2E-06	9.2E-06	0	1.2E-04	1.8E-04	2.4E-06
U-236	3.6E-05	3.6E-05	0	0	0	0
U-238	4.1E-05	4.1E-05	0	5.4E-04	7.9E-04	1.1E-05
Zr-93	4.5E-02	4.5E-02	0	5.9E-01	8.7E-01	1.2E-02

[SRR-CWDA-2010-00023, Rev. 6]

2.1.2 Inventory Distributions

In the HTF Stochastic Fate and Transport Model for radionuclides, uncertainty in the CZ inventory values is considered by species- and tank-dependent distributions of inventory multipliers. Uncertainties in all tanks, except Tanks 12 and 16, are described by log uniform inventory multiplier distributions. The minimum and maximum values of these log uniform distributions are presented in Table 2-8.

For all species in Tank 12 and most species in Tank 16, uncertainty in the CZ inventory multipliers is described by normal distributions, with the means and standard deviations of the distributions presented in Table 2-9 and Table 2-10, respectively. The inventory multiplier values for Tanks 12 and 16 are calculated by dividing residual inventory mean and standard deviation probability distribution values by the actual inventory values.

The residual inventory distributions are generated for each constituent with an analysis that uses an inventory formula with input values of the concentration mean and standard deviation for each radionuclide, along with the residual material density, solids content, and residual material volume. Probabilistic distributions (usually a normal distribution) are assigned to each of these input values. An example of the inventory formula can be found in SRR-CWDA-2015-00075, *Tank 12 Inventory Determination*, Section 3.4 Final Inventory Determination. The analysis uses 10,000 realizations to develop the probability distributions for mean inventory and standard deviation for each radionuclide. Those radionuclides with only Minimum Detectable Concentrations (MDCs) are not included in the development of inventory distributions but have an assigned maximum inventory multiplier mean value of 1.0 and a standard deviation of 0.5.

For Tank 16, uncertainties for I-129 and Tc-99 are described using log-normal multiplier distributions with their true means and standard deviations also listed in Table 2-10.

Note that with the exception of Tank 16, uncertainty is not considered in the sand layer and annulus floor inventories due to the absence of sampling data. For most species in Tank 16, uncertainty in the annulus inventories is described by a normal distribution, with the means and standard deviations values of the distributions also presented in Table 2-10. Uncertainty for the I-129 annulus inventory is described using a gamma distribution with the mean and standard deviation listed in Table 2-10. For all species in Tank 16, uncertainty in the sand layer inventory multipliers is described by normal distributions, with the means and standard deviation values of the distributions presented in Table 2-10. Note that the sand layer multipliers are the same for both sand layers.

For the Types I and II Tanks SA, the maximum value for log uniform distributions for the Sr-90 inventory multiplier for Tanks 13 through 15, has been reduced to 2 and the minimum increased to 0.25 (see shaded values in Table 2-8). The basis for this change is documented in SRR-CWDA-2016-00062, Rev.0.

Table 2-8: Inventory Multipliers

	Type I (Tanks 9-11)		Type II (Tanks 13-15)		Tank IV (Tanks 21-24)		Tank III (Tanks 29-32)		Type III A (Tanks 35-51)	
Distribution	**LogUniform**		**LogUniform**		**LogUniform**		**LogUniform**		**LogUniform**	
Isotope	**Min**	**Min**	**Min**	**Max**	**Min**	**Max**	**Min**	**Max**	**Min**	**Max**
Ac-227	0.01	1	0.01	1	0.01	1	0.01	1	0.01	1
Al-26	0.01	1	0.01	1	0.01	1	0.01	1	0.01	1
Am-241	0.01	10	0.01	10	0.01	10	0.1	10	0.1	10
Am-242m	0.01	1	0.01	1	0.01	1	0.01	1	0.01	1
Am-243	0.01	1	0.01	1	0.01	1	0.01	1	0.01	1
C-14	0.01	1	0.01	1	0.01	1	0.01	1	0.01	1
Cf-249	0.01	1	0.01	1	0.01	1	0.01	1	0.01	1
Cf-251	0	1	0	1	0	1	0	1	0	1
Cl-36	0.01	1	0.01	1	0.01	1	0.01	1	0.01	1
Cm-243	0.01	1	0.01	1	0.01	1	0.01	1	0.01	1
Cm-244	0.01	10	0.01	10	0.01	10	0.1	10	0.1	10
Cm-245	0.01	1	0.01	1	0.01	1	0.01	1	0.01	1
Cm246	0	0	0	0	0	0	0	0	0	0
Cm-247	0.01	1	0.01	1	0.01	1	0.01	1	0.01	1
Cm-248	0.01	1	0.01	1	0.01	1	0.01	1	0.01	1
Co-60	0.01	1	0.01	1	0.01	1	0.01	1	0.01	1
Cs-135	0.01	10	0.01	10	0.01	10	0.1	10	0.1	10
Cs-137	0.01	10	0.01	10	0.01	10	0.1	10	0.1	10
Eu-152	0.01	10	0.01	10	0.01	1	0.01	1	0.01	1
Eu-154	0.01	10	0.01	10	0.01	10	0.1	10	0.1	10
Eu-155	0	0	0	0	0	0	0	0	0	0
Gd-152	0	0	0	0	0	0	0	0	0	0
H-3	0.01	1	0.01	1	0.01	1	0.01	1	0.01	1
I-129	0.01	1	0.01	1	0.01	1	0.01	1	0.01	1
K-40	0.01	1	0.01	1	0.01	1	0.01	1	0.01	1
Nb-93m	0.01	1	0.01	1	0.01	1	0.01	1	0.01	1
Nb-94	0.01	1	0.01	1	0.01	1	0.01	1	0.01	1
Ni-59	0.01	10	0.01	10	0.01	1	0.01	1	0.01	1
Ni-63	0.01	10	0.01	10	0.01	10	0.1	10	0.1	10
Np-237	0.01	10	0.01	10	0.01	10	0.1	10	0.1	10
Pa-231	0.01	1	0.01	1	0.01	1	0.01	1	0.01	1
Pb-210	0	0	0	0	0	0	0	0	0	0
Pd-107	0.01	1	0.01	1	0.01	1	0.01	1	0.01	1
Pt-193	0.01	1	0.01	1	0.01	1	0.01	1	0.01	1
Pu-238	0.01	10	0.01	10	0.01	10	0.1	10	0.1	10
Pu-239	0.01	10	0.01	10	0.01	10	0.1	10	0.1	10
Pu-240	0.01	10	0.01	10	0.01	10	0.1	10	0.1	10
Pu-241	0.01	10	0.01	10	0.01	10	0.1	10	0.1	10

Table 2-8: Inventory Multipliers (Continued)

	Type I (Tanks 9-11)		Type II (Tanks 13-15)		Tank IV (Tanks 21-24)		Tank III (Tanks 29-32)		Type III A (Tanks 35-51)	
Distribution	**LogUniform**		**LogUniform**		**LogUniform**		**LogUniform**		**LogUniform**	
Isotope	**Min**	**Min**	**Min**	**Max**	**Min**	**Max**	**Min**	**Max**	**Min**	**Max**
Pu-242	0.01	1	0.01	1	0.01	1	0.01	1	0.01	1
Pu-244	0.01	1	0.01	1	0.01	1	0.01	1	0.01	1
Ra-226	0.01	1	0.01	1	0.01	1	0.01	1	0.01	1
Ra-228	0.01	1	0.01	1	0.01	1	0.01	1	0.01	1
Se-79	0.01	10	0.01	10	0.01	1	0.01	1	0.01	1
Sm-147	0	0	0	0	0	0	0	0	0	0
Sm-151	0.01	10	0.01	10	0.01	10	0.1	10	0.1	10
Sn-126	0.01	10	0.01	10	0.01	10	0.1	10	0.1	10
Sr-90	0.01	10	0.25	2	0.01	10	0.1	10	0.1	10
Tc-99	0.01	10	0.01	10	0.01	10	0.1	10	0.1	10
Th-229	0.01	1	0.01	1	0.01	1	0.01	1	0.01	1
Th-230	0.01	1	0.01	1	0.01	1	0.01	1	0.01	1
Th-232	0.01	1	0.01	1	0.01	1	0.01	1	0.01	1
U-232	0.01	1	0.01	1	0.01	1	0.01	1	0.01	1
U-233	0.01	10	0.01	10	0.01	10	0.1	10	0.1	10
U-234	0.01	10	0.01	10	0.01	10	0.1	10	0.1	10
U-235	0.01	1	0.01	1	0.01	1	0.1	1	0.1	10
U-236	0.01	1	0.01	1	0.01	1	0.01	1	0.01	1
U-238	0.01	10	0.01	10	0.01	10	0.1	10	0.1	10
Zr-93	0.01	10	0.01	10	0.01	10	0.1	10	0.1	10

[SRR-CWDA-2010-00023, Rev. 6]

Table 2-9: Tank 12 Inventory Multipliers

	Tank 12	
Location	CZ	
Isotope	Mean	Standard Deviation
Ac-227	1	0.5
Al-26	1	0.5
Am-241	0.71	0.33
Am-242m	0.73	0.36
Am-243	0.85	0.30
C-14	1	0.5
Cf-249	1	0.5
Cf-251	1	0.5
Cl-36	1	0.5
Cm-243	1	0.5
Cm-244	1	0.5
Cm-245	1	0.5
Cm246	1	0.5
Cm-247	1	0.5
Cm-248	1	0.5
Co-60	1	0.5
Cs-135	1	0.5
Cs-137	0.80	0.31
Eu-152	1	0.5
Eu-154	1	0.5
Eu-155	1	0.5
Gd-152	1	0.5
H-3	1	0.5
I-129	1.09	0.31
K-40	1	0.5
Nb-93m	1	0.5
Nb-94	1	0.5
Ni-59	0.73	0.33
Ni-63	0.78	0.31
Np-237	0.63	0.36
Pa-231	0.66	0.35
Pb-210	1	0.5
Pd-107	1	0.5
Pt-193	1	0.5
Pu-238	0.70	0.34
Pu-239	0.70	0.34
Pu-240	0.68	0.34
Pu-241	0.68	0.35
Pu-242	1	0.5
Pu-244	1	0.5
Ra-226	1	0.5
Ra-228	0.73	0.34
Se-79	1	0.5
Sm-147	1	0.5
Sm-151	1	0.5

Table 2-9: Tank 12 Inventory Multipliers (continued)

	Tank 12	
Location	**CZ**	
Isotope	**Mean**	**Standard Deviation**
Sn-126	0.94	0.27
Sr-90	0.95	0.27
Tc-99	1.11	0.29
Th-229	1	0.5
Th-230	1	0.5
Th-232	0.65	0.36
U-232	0.99	0.40
U-233	1	0.5
U-234	0.79	0.31
U-235	0.66	0.35
U-236	1	0.5
U-238	0.62	0.37
Zr-93	0.86	0.28

Table 2-10: Tank 16 Inventory Multipliers

	Tank 16					
Location	**CZ**		**Annulus**		**Sand Layers**	
Isotope	**Mean**	**Standard Deviation**	**Mean**	**Standard Deviation**	**Mean**	**Standard Deviation**
Ac-227	1	0.5	1	0.5	1	0.5
Al-26	1	0.5	1	0.5	1	0.5
Am-241	0.50	0.31	0.64	0.18	0.61	0.17
Am-242m	1	0.5	1	0.5	1	0.5
Am-243	1	0.5	1	0.5	1	0.5
C-14	1	0.5	1	0.5	1	0.5
Cf-249	1	0.5	1	0.5	1	0.5
Cf-251	1	0.5	1	0.5	1	0.5
Cl-36	1	0.5	1	0.5	1	0.5
Cm-243	1	0.5	1	0.5	1	0.5
Cm-244	1	0.5	1	0.5	1	0.5
Cm-245	1	0.5	1	0.5	1	0.5
Cm246	1	0.5	1	0.5	1	0.5
Cm-247	1	0.5	1	0.5	1	0.5
Cm-248	1	0.5	1	0.5	1	0.5
Co-60	1	0.5	0.65	0.17	0.61	0.17
Cs-135	1	0.5	0.81	0.10	0.77	0.09
Cs-137	1	0.5	0.78	0.11	0.74	0.10
Eu-152	1	0.5	1	0.5	1	0.5
Eu-154	1	0.5	1	0.5	1	0.5
Eu-155	1	0.5	1	0.5	1	0.5
Gd-152	1	0.5	1	0.5	1	0.5
H-3	1	0.5	1	0.5	1	0.5
I-129	0.41[1]	0.37[1]	0.70[2]	0.26[2]	0.67	0.25
K-40	1	0.5	1	0.5	1	0.5
Nb-93m	1	0.5	1	0.5	1	0.5
Nb-94	1	0.5	1	0.5	1	0.5
Ni-59	1	0.5	1	0.5	1	0.5
Ni-63	1	0.5	1	0.5	1	0.5
Np-237	1	0.5	0.62	0.18	0.59	0.17
Pa-231	1	0.5	1	0.5	1	0.5
Pb-210	1	0.5	1	0.5	1	0.5
Pd-107	1	0.5	1	0.5	1	0.5
Pt-193	1	0.5	1	0.5	1	0.5
Pu-238	0.50	0.31	0.65	0.17	0.61	0.16
Pu-239	0.50	0.31	0.62	0.18	0.59	0.17
Pu-240	0.50	0.31	0.62	0.18	0.59	0.17
Pu-241	1	0.5	0.59	0.20	0.56	0.18
Pu-242	0.5	1	0.67	0.16	0.63	0.15
Pu-244	0.5	1	1	0.5	1	0.5
Ra-226	0.5	1	1	0.5	1	0.5
Ra-228	0.5	1	1	0.5	1	0.5
Se-79	0.5	10	1	0.5	1	0.5
Sm-147	0.5	0	1	0.5	1	0.5
Sm-151	0.5	10	1	0.5	1	0.5

Table 2-10: Tank 16 Inventory Multipliers (continued)

	Tank 16					
Location	**CZ**		**Annulus**		**Sand Layers**	
Isotope	**Mean**	**Standard Deviation**	**Mean**	**Standard Deviation**	**Mean**	**Standard Deviation**
Sn-126	1	0.5	1	0.5	1	0.5
Sr-90	0.50	0.32	0.63	0.18	0.60	0.17
Tc-99	0.15[1]	0.14	0.83	0.16	0.79	0.15
Th-229	1	0.5	1	0.5	1	0.5
Th-230	1	0.5	1	0.5	1	0.5
Th-232	1	0.5	1	0.5	1	0.5
U-232	1	0.5	1	0.5	1	0.5
U-233	0.45	0.32	1	0.5	1	0.5
U-234	0.45	0.31	0.81	0.10	0.77	0.09
U-235	0.50	0.32	0.88	0.10	0.84	0.09
U-236	1	0.5	1	0.5	1	0.5
U-238	0.5	0.32	0.81	0.10	0.77	0.088
Zr-93	1	0.5	1	0.5	1	0.5

[SRR-CWDA-2014-00060, Rev. 1]
[1] Log Normal Distribution
[2] Gamma Distribution with a minimum of 0 and a maximum of 10

2.2 Iodine K_d Values and Strontium K_d Distributions

The primary change in the Case A partitioning coefficient (K_d) values implemented in HTF_Transport_Model_v4.000_Rad for the Types I and II Tanks SA is the updating of the Reduced Region II cement K_d values for iodine. An iodine K_d value of 2 mL/g replaced the previous value of 9 mL/g for Reduced Region II cement. This change is based on preliminary information provided by SRNL and is conservative in that it allows for more rapid transport of iodine through cementitious materials. This change addresses, in part, an NRC concern regarding uncertainty surrounding the iodine K_d values used in the HTF PA [ML15301A710].

In addition, based on a review of available literature, the probabilistic distribution for strontium's partitioning coefficient in the saturated zone (SZ) sandy soil was changed from a log-normal distribution to a triangular distribution with a minimum, most likely, and maximum value of 4, 5, and 6 mL/g, respectively as shown in Figure 2-1. The justification for this change can be found in SRR-CWDA-2016-00061, Rev. 0.

Figure 2-1: GoldSim Stochastic Element for Strontium Sandy-Soil K_d Distribution

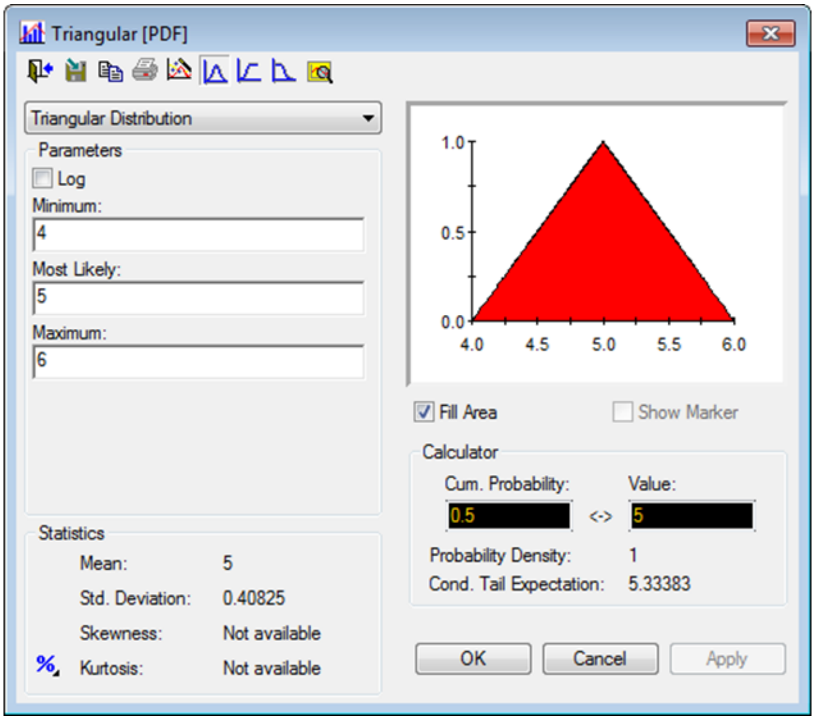

2.3 Updating of 1-Meter IHI Wells and Associated Data

For the IHI scenario, the HTF PORFLOW Model calculates IHI dose along a 1-meter facility boundary whereas prior to HTF_Transport_Model_v4.000_Rad, the HTF Stochastic Fate and Transport Models calculated IHI dose by means of seven hypothetical IHI wells postulated to be directly adjacent to specific waste tanks within the boundary of the tank farm. As a modeling improvement in HTF_Transport_Model_v3.000_Rad (see SRR-CWDA-2014-00060 Rev. 1), additional POAs were incorporated into the HTF Stochastic Fate and Transport Models along a 1-meter facility boundary to better replicate equivalent IHI dose calculations as found in the HTF PORFLOW Model. In HTF_Transport_Model_v4.000_Rad these POA locations were updated to include more well locations and centerlines and offsets based on particle tracks from the centers of the tanks were remeasured (see Figure 2-2).

For establishing the spatial data for transport distances and GoldSim plume Function application at the 1-meter POAs in HTF_Transport_Model_v3.000_Rad, a qualitative approach was applied in which specific model values (i.e., buffer distance, centerline distance, offset distance, and a flow rate multiplier) were modified for each waste tank until a relatively close match (or calibration) was achieved between GoldSim's 1-meter dose results and PORFLOW's 1-meter dose results. In HTF_Transport_Model_v4.000_Rad this approach was modified to allow only vertical mixing and plume divergence to be used as a calibration tool to account for differences in the PORFLOW and GoldSim models. This limitation reflects the major differences in the rigor of the two models where the fully three-dimensional aspects of the PORFLOW model include vertical components of flow (which influence mixing of plumes from different sources) and the influence of a flow divide which causes divergence of releases from specific tanks in two directions. The divergence of plumes is especially prominent in the Type II tanks as can be seen in releases from Tanks 13, 14, 15, and 16 as shown in Figures 2-3, 2-4, 2-5, and 2-6, respectively.

Figure 2-2: IHI POAs for HTF

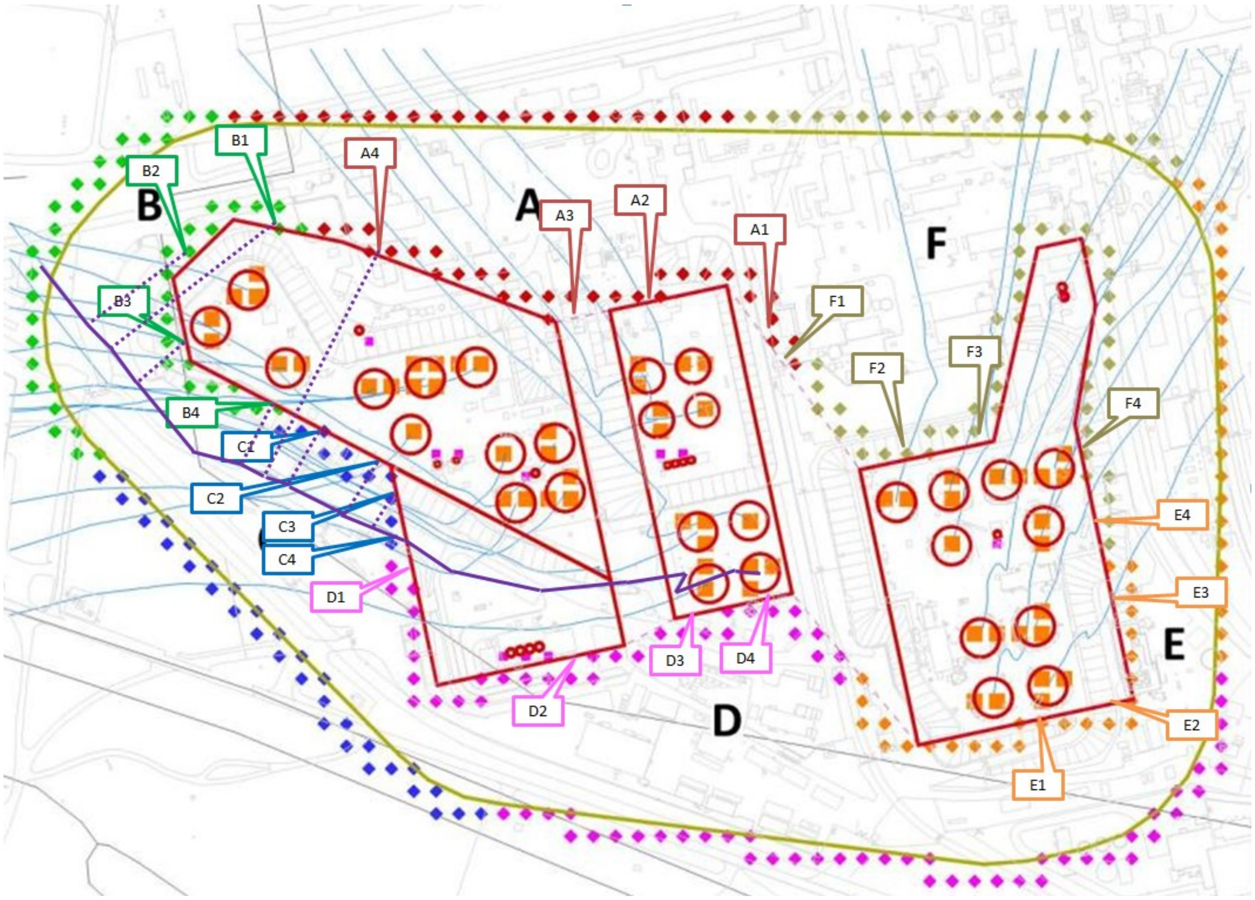

Figure 2-3: Plume Divergence in Release from Tank 13

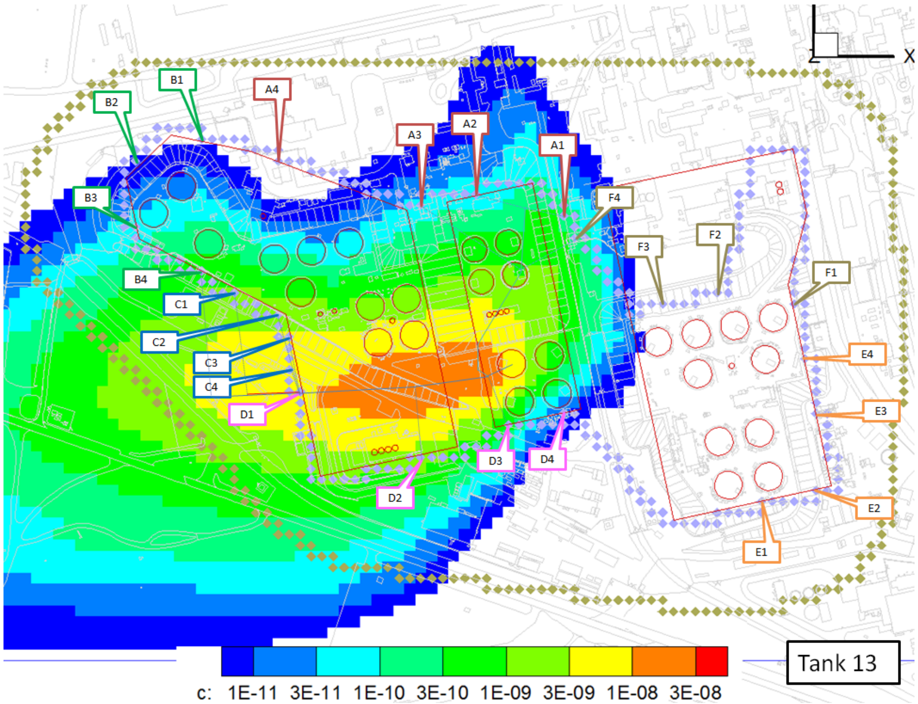

Figure 2-4: Plume Divergence in Release from Tank 14

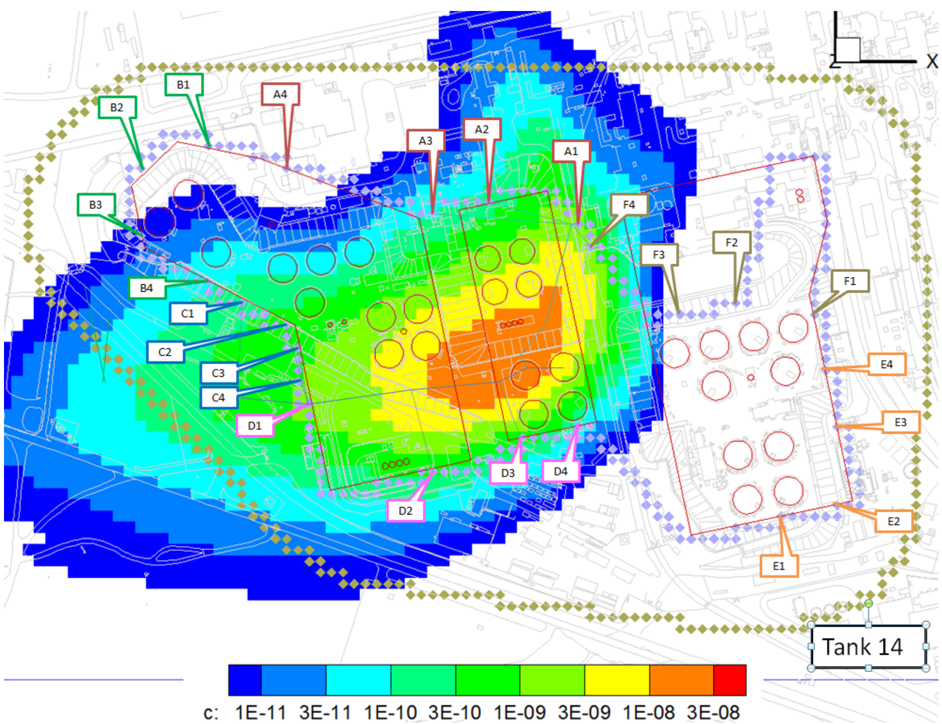

Figure 2-5: Plume Divergence in Release from Tank 15

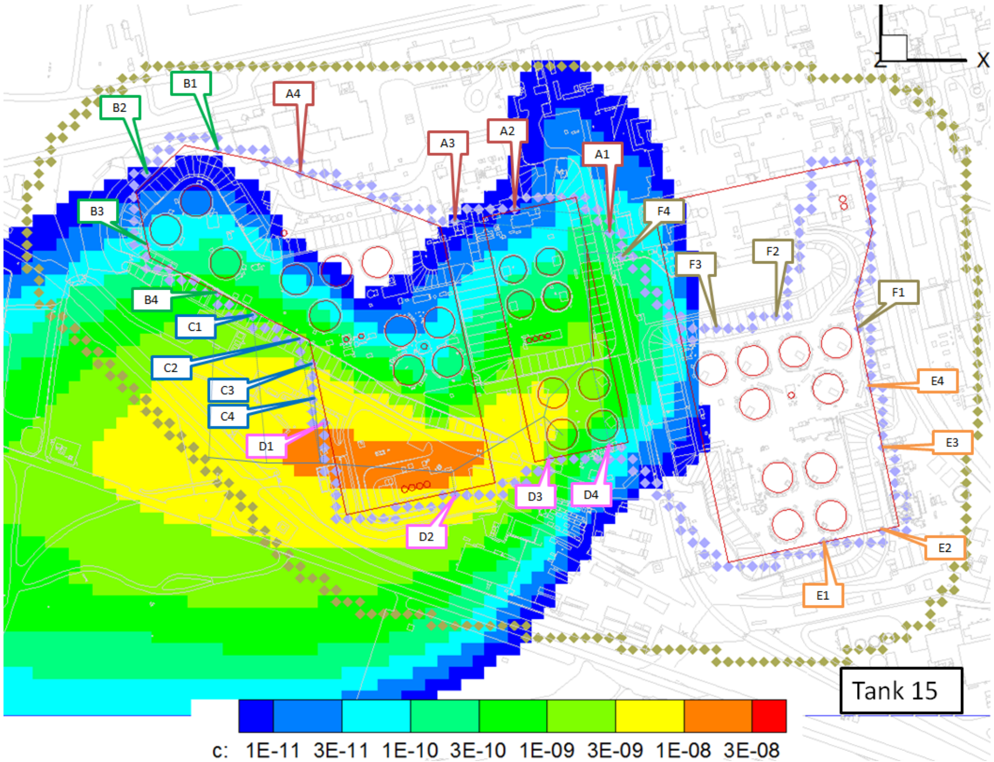

Figure 2-6: Plume Divergence in Release from Tank 16

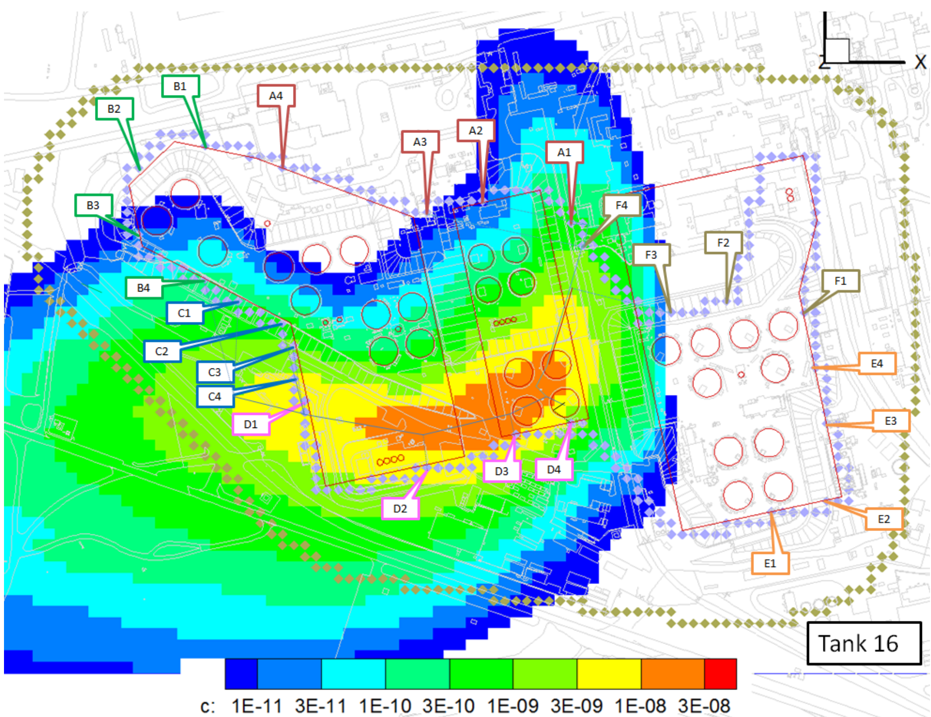

2.4 Annulus Contamination Zone

In the latest PORFLOW model being used for the Types I and II Tanks SA, the residual radionuclides residing in the annulus are initially placed in a thin contaminated zone CZ at the bottom of the annulus. This zone is 0.5 inches thick in the Type I tank models and 1.0 inches thick in the Type II tank models. This thin layer has been added to the string of mixing cells representing the annulus in HTF_Transport_Model_v4.000_Rad. In addition, an extra mixing cell of the same thickness was added above the annulus CZ to limit the degree of numerical dispersion in the upward direction. For Case A, the time-dependent effective diffusion coefficient annulus CZ remains the same as that of the rest of the annulus so the GoldSim model continues to read the PORFLOW model-generated time series for the annulus values, but for alternative configurations (Case B through Case E), the PORFLOW model-generated time series files have been expanded to include the values for the annulus contaminant zone. Note that because of the effort involved generating new time-dependent effective diffusion coefficient files for the stochastic model the model GoldSim model was updated to use 9.42E-06 cm^2/s for the Case C and Case E realizations.

Note that while the deterministic settings of the GoldSim model can support all five flow configurations (i.e., Cases A through E), when the model is run in a probabilistic mode, Cases B and D are actually modeled as variations on Cases C and E, respectively. In other words, when Case B is randomly selected, the configurations for Case C are used, and when Case D is randomly selected, the configurations for Case E are used. The primary difference between Case B versus Case C (and likewise Case D versus Case E) is that in Case C and Case E, the reducing capacity of the full volume of reducing grout is not available to influence the infiltrating water and thus the water chemistry is driven by the number of pore volumes that have passed through the CZ as opposed to the reducing grout. Another difference_is that in Case C and Case E, degradation is based on a degradation curve (see SRR-CWDA-2010-00128, Rev 1, Table 4.2-30), and in Case B and Case D, degradation is assumed to be a step change at year 501.

2.5 PORFLOW Generated Flow Fields

The previously PORFLOW output-generated flow-field files for the Case A and stochastic simulations were updated to include horizontal flow data for the CZ to allow the GoldSim model the flexibility to be used to evaluate the implications of not considering the horizontal flow in the simplified abstraction. In addition PORFLOW output-generated flow-field files for alternate configurations Case B, Case C, Case D, and Case E, were generated to allow for benchmarking these alternate fast zone cases (see Appendix A). The flow-field files for Cases B through E, also included the CZ horizontal flow data. [SRNL-STI-2016-00224]

2.6 Types I and II Tanks Special Analysis Hydraulic Conductivity Sensitivity Study

In addition to the aforementioned GoldSim model updates, HTF_Transport_Model_v4.000_Rad was updated to allow for a set of seven flow sensitivity radionuclide transport runs to be simulated, based on a new set of PORFLOW flow runs and their exported flow-field data files. The specifics of the sensitivity runs are presented in Table 2-11 . These flow sensitivities were run for all tank types, Case A, 20,000 years. The exception is Study 7 where TypeI_noliner and TypeII_noliner are the same as Case A so have not been rerun. [SRNL-STI-2016-00224]

Table 2-11: Cementitious Materials Hydraulic Performance Scenarios

Sensitivity Study	Liner	Tank Concrete *K* (cm/s)	Tank Primary Grout *K* (cm/s)	Tank Annulus Grout *K* (cm/s)
Study 1 – average grout	Per PA	3.5E-08	3.5E-08	3.5E-08
Study 2 – below average grout	Per PA	3.5E-08	1.0E-07	1.0E-07
Study 3 – poor grout	Per PA	3.5E-08	3.2E-07	3.2E-07
Study 4 – backfill grout	Per PA	3.5E-08	4.1E-05	4.1E-05
Study 5 – backfill vault	Per PA	4.1E-05	3.5E-08	3.5E-08
Study 6 – all backfill	Per PA	4.1E-05	4.1E-05	4.1E-05
Study 7 – no liner	Failed at t = 0	3.5E-08	3.5E-08	3.5E-08

[SRNL-STI-2016-00224]

2.7 Saturated Zone Darcy Velocity Stochastic Distribution

The saturated zone Darcy velocities used in the HTF Stochastic Fate and Transport Model are source-specific values based on PORFLOW model transport simulations where the center of mass of a pulse released in the area of the source is tracked until it crosses the 100-meter boundary. The Darcy velocities are in turn calculated from the time it takes for the center of mass to reach the 100-meter boundary, the distance traveled, and the porosity used in the analysis. The deterministic values used in the GoldSim model have not been updated, but the stochastic distribution used in in sensitivity and uncertainty analyses have been. The previous versions of the HTF Stochastic Fate and Transport Model used a uniform distribution with the minimum value set to 0.5 times the source-specific Darcy velocity and the maximum value set to 1.5 times the source-specific Darcy velocity. In Version 4.000 of the HTF Radionuclide Stochastic Fate and Transport Model (HTF_Transport_Model_v4.000_Rad), the distribution has been switched to a truncated normal distribution. In the new distribution, the mean is set to the tank-specific deterministic value, the standard deviation to 0.25 times the mean value, and the minimum and maximum values are set to 0.5 and 1.5 times the source-specific Darcy velocities, respectively. This change in Darcy velocity distributions is implemented for both the tanks and the ancillary equipment.

3 MODEL BENCHMARKING RESULTS

3.1 Benchmarking Overview

The HTF Stochastic Radionuclide Fate and Transport Model is a probabilistic model designed to perform parameter uncertainty and parameter sensitivity analyses used to help evaluate the potential for radionuclide migration from the tanks and ancillary structures in the HTF to the accessible environment. The probabilistic model to be used for future analyses was constructed using the GoldSim software and represents an enhancement to previous modeling versions. The HTF Stochastic Radionuclide Fate and Transport Models represents an abstraction of the HTF PORFLOW Model (SRR-CWDA-2010-00128, SRNL-STI-2014-00612, and SRNL-STI-2016-00224) used to perform radionuclide transport simulations. Dose calculations for both GoldSim and PORFLOW simulations are performed using the same dose calculator (SRR-CWDA-2013-00058).

Use of the abstraction model reduces the analysis time needed for multi-realization processes, such as Monte Carlo sampling or Latin Hypercube Sampling (LHS). In order for the probabilistic model abstraction to be used, in lieu of the HTF PORFLOW Model, its validity must first be tested by comparing the abstraction model results with HTF PORFLOW Model results for a representative case. A reasonable degree of agreement between the two models is necessary to give confidence that the trends produced in the probabilistic analysis reflect the trends that would occur if the HTF PORFLOW Model is run repeatedly in Monte Carlo (or LHS) probabilistic mode.

Because of the simplifications associated with the abstractions used in the HTF radionuclide Stochastic Fate and Transport Model (i.e., reduction in dimensionality, coarser spatial and temporal discretization, abstractions of nonlinear processes, etc.), a perfect match between GoldSim and PORFLOW results is not expected. However, basic features of breakthrough curves reflecting processes such as material degradation and changes in chemical environments should be similar.

The benchmarking analysis for the radionuclide transport model is comprised of four phases. The first phase focuses on how well the abstraction model can approximate the H-Tank Farm PORFLOW model-generated radionuclide releases from the waste tanks using the Case A flow configuration. In this initial phase of the study, GoldSim model-generated breakthrough curves of radionuclide releases (mass fluxes) to the SZ are compared to PORFLOW model-generated breakthrough curves. Note that although, in general, the PORFLOW model represents a more rigorous approximation of the modeled system, the GoldSim model approximates the dissolution/precipitation process in a more rigorous manner, taking into account all isotopes of all species in a fully coupled analysis. The second phase focuses on how well the abstraction model approximates the migration of dissolved radionuclides released from the tanks and ancillary equipment as the radionuclides are transported to the 100-meter boundary (see Figure 3-1). Similarly, the third phase focuses on how well the abstraction model approximates the migration of dissolved radionuclides released from the tanks and ancillary equipment as the radionuclides are transported to the nearby 1-meter boundary (see Figure 2-2). GoldSim-to-PORFLOW model comparisons of doses at the 100-meter and 1-meter boundaries for Phases 2 and 3, form the basis of how well the abstraction model approximates the dilution/attenuation processes in the SZ. In particular, breakthrough curves representing the radionuclide dose contributions over time for individual sectors (Sectors A through F) and the maximum values reached when considering all sectors are evaluated. The final phase of the benchmarking effort compares GoldSim abstraction releases from tanks to the SZ with PORFLOW generated results for the alternate flow configurations (Cases B through E). The final phase results are presented in Appendix A.

Figure 3-1: Particle Tracking Pathlines from the Center of Each Tank

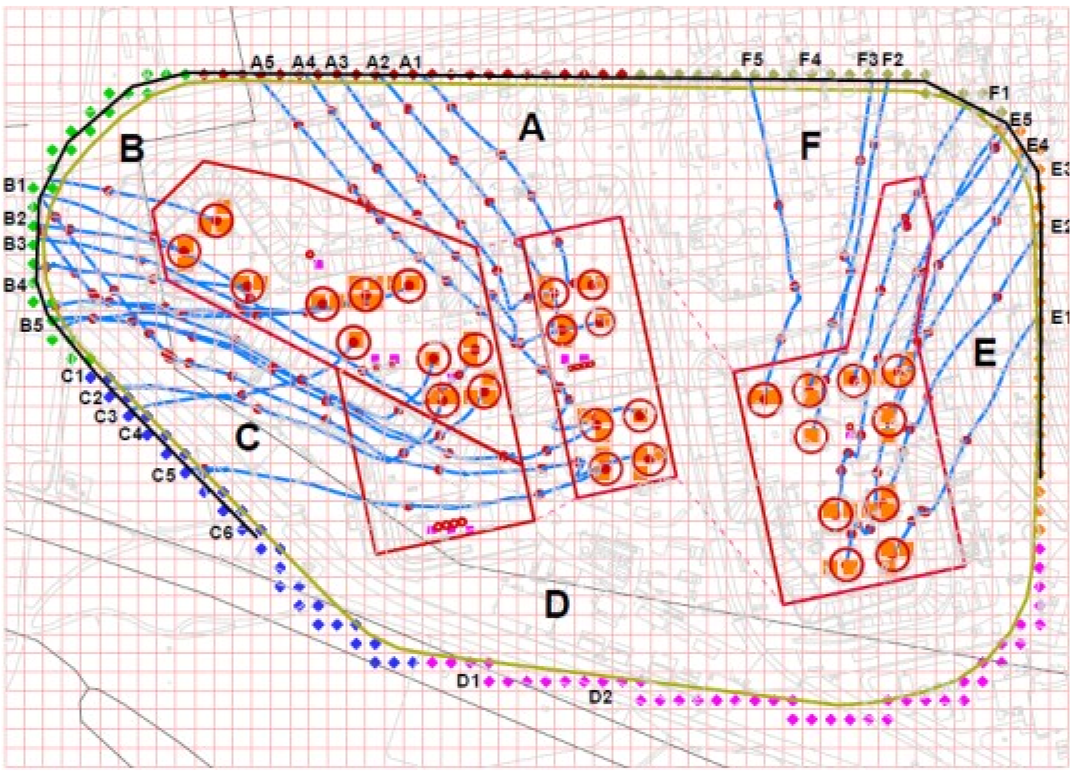

The following sections describe the approach used to benchmark the HTF Stochastic Fate and Transport Model to the HTF PORFLOW Model and the results of that benchmarking.

3.2 Benchmarking Results for the Radionuclide Transport Model

As described above, the benchmarking analysis for the HTF radionuclide transport model was comprised of four phases. The first phase focuses on how well the abstraction model (i.e., the HTF Stochastic Fate and Transport Models) can approximate the PORFLOW-generated radionuclide releases from different tank types using the Case A flow configuration. The second and third phases focus on how well the abstraction model approximates the radionuclide transport behavior in the SZ. The final phase (presented in Appendix A) evaluates how well the GoldSim abstraction approximates alternate flow configurations (Cases B through E) that include fast pathways that can enhance the release of residual radionuclides from grouted tanks.

3.2.1 Phase 1: Mass Releases to the Saturated Zone

The species evaluated during this benchmarking effort represent major dose contributors and parent species for major dose contributors that are part of decay chains. In addition, species chosen for the model comparison exhibit a wide range sorptive properties and solubility limits. Two independent species are used in the benchmarking including I-129 and Tc-99. The other species are members of the decay chains (or partial decay chains): 1) Am-241→ Np-237, 2) Am-243→Pu-239, and 3) Pu-238→U-234→Th-230→Ra-226. To limit the effort involved in assembling this document, breakthrough curves for the radionuclides Pu-238 and Th-230 are not presented with the results although their inventories are included in the ingrowth calculations.

During benchmarking, variances of ~50% or less for peak release-rates, were considered acceptable, as long as the general trends matched well. Note that for some tanks, greater latitude in peak release comparisons was considered acceptable for releases. For example, where an event (such as Eh transition) associated with a many order of magnitude change in K_d or solubility (i.e. Tc-99), the one-day time steps used in the PORFLOW model may generate a breakthrough peak release of greater magnitude but narrower width. In general, the GoldSim abstractions for all tanks accurately calculate Tc-99 releases from the CZ. They also accurately calculate the annulus releases over a long period prior to the Eh transition to Oxidized Region II. When most of the Tc-99 from the annulus has been released from the system, the remaining mass, which will be released in the Eh transition-induced surge, may be spatially distributed in a manner that may result in differences between GoldSim and PORFLOW breakthrough curve peaks. This distribution of mass associated with three-dimensional aspects of plume formation may not be fully captured by the GoldSim model. In addition, since the chemical region transition induced mass release peaks may occur over a short period of time relative to time step lengths, differences between GoldSim and PORFLOW model peaks may be enhanced.

Also, for strongly sorbing radionuclides such as Np-237, early releases, which are dominated by diffusion may differ radically between the two models. The strongly sorptive nature of neptunium is reflected in a K_d of around 10,000 ml/g in concrete. The strongly sorptive nature of a dissolve species in conjunction with differences in discretization between the two models may reflect large differences in numerical diffusion controlling the early shape of the breakthrough curve.

Note that all benchmark simulations used to compare tank releases were performed without using more than one isotope of any species. This circumvented differences between how the PORFLOW model and the GoldSim model are structured to handle the combined influence of isotopes on solubility calculations. The GoldSim model solves for elemental based concentrations and then apportions the dissolved mass among all species being modeled. The PORFLOW model does not simulate all species in the same tank release run, allowing greater concentrations of specific radionuclides to occur simultaneously. Further discussion on the differences between how the GoldSim model and the PORFLOW model evaluate solubility, and examples showing comparisons of results of this report, can be found in Revision 1 of this report.

3.2.1.1 Type I Tank with Intact Liner (Tank 9)

A comparison of the PORFLOW HTF Model and the GoldSim HTF RAD Model mass releases of I-129, Tc-99, Am-243, Pu-239, U-234, Ra-226, Am-241, and Np-237, as presented in Figure 3-2 through Figure 3-9, indicate that the GoldSim model produces a good approximation of the releases from Tank 9 generated by the PORFLOW model. Note that

Figure 3-9 contains two breakthough curves describing the release of Np-237. The GoldSim model is constructed to allow the user to choose between 5, 10, 15, 20, 25, or 30 mixing cells linked in series to represent the basemat. The GoldSim model chooses the number of mixing cells that is equal to or just above the number of elements PORFLOW uses to vertically discretize the basemat, given this limitation. In normal mode, the GoldSim model is set to use 15 mixing cells to represent the basemat for Type I tanks, but in PORFLOW the basemat is vertically discretized into only 12 elements. The two GoldSim model breakthrough curves in Figure 3-8 (based on using 10 or 15 mixing cells) show how much difference numerical dispersion can influence the results. Note that since using 15 mixing cells introduces less numerical dispersion it is the default choice in the model.

Table 3-1 summarizes the peak values for these releases. Variances of ~50% or less for peak releases, as seen in the I-129, Tc-99, Am-243, Pu-239, U-234, Ra-226, Am-241, and Np-237 results, were considered acceptable.

Table 3-1: GoldSim and PORFLOW Model Peak Release from the UZ to the SZ Comparisons for Tank 9 within 20,000 years

Radionuclide	PORFLOW Peak Release (mol/yr)	PORFLOW Time of Peak Release (yr)	GoldSim Peak Release (mol/yr)	GoldSim Time of Peak Release (yr)	Peak Release Percent Difference GoldSim vs PORFLOW
I-129	6.1E-02	11,418	4.9E-02	11,420	-20%
Tc-99	4.7E-05	8,521	4.6E-05	9,010	-2%
Am-243	8.4E-05	13,793	9.2E-05	13,850	10%
Pu-239	9.6E-06	15,851	9.7E-06	16,010	1%
U-234	1.9E-03	12,116	2.2E-3	12,130	16%
Ra-226	2.2E-06	11,692	2.3E-06	11,700	5%
Am-241	2.6E-013	13,293	2.5E-13	13,420	-4%
Np-237	2.4E-05	20,000	1.2E-05	20,000	-50%
Np-237[1]	2.4E-05	20,000	3.3E-05	20,000	38%

[1] Used coarser discretization of basemat cells.

Figure 3-2: Tank 9 I-129 Release to the Saturated Zone

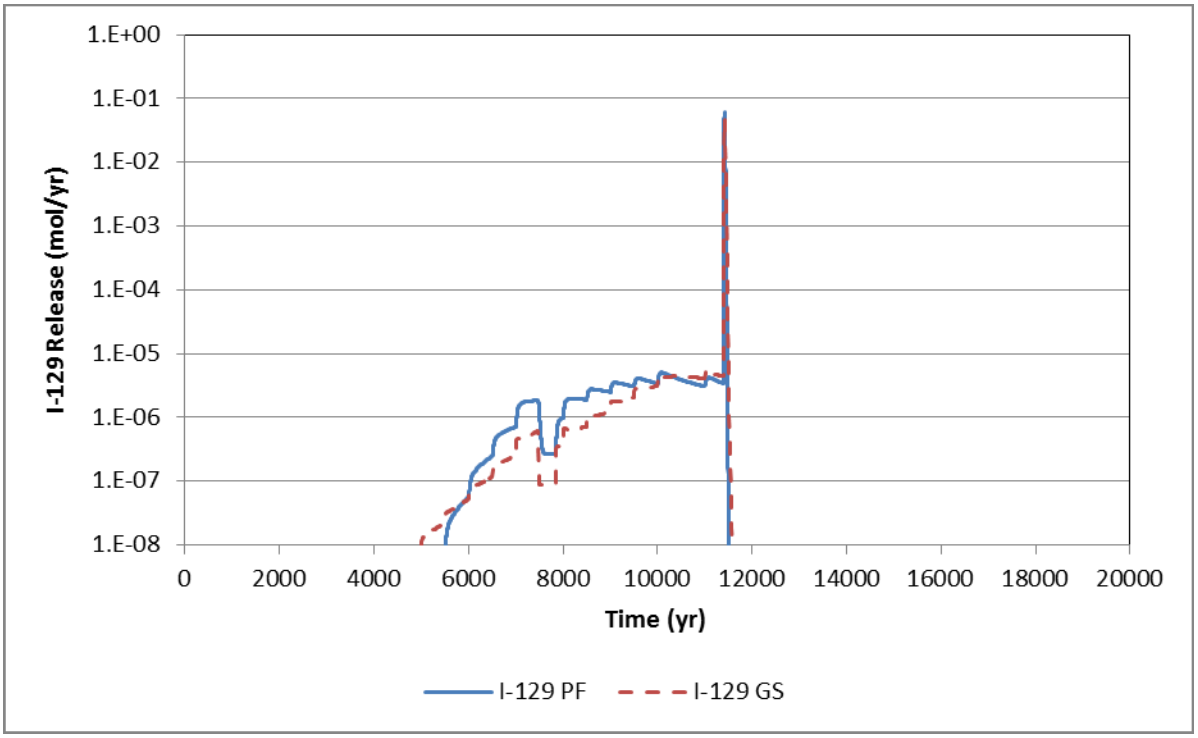

Figure 3-3: Tank 9 Tc-99 Release to the Saturated Zone

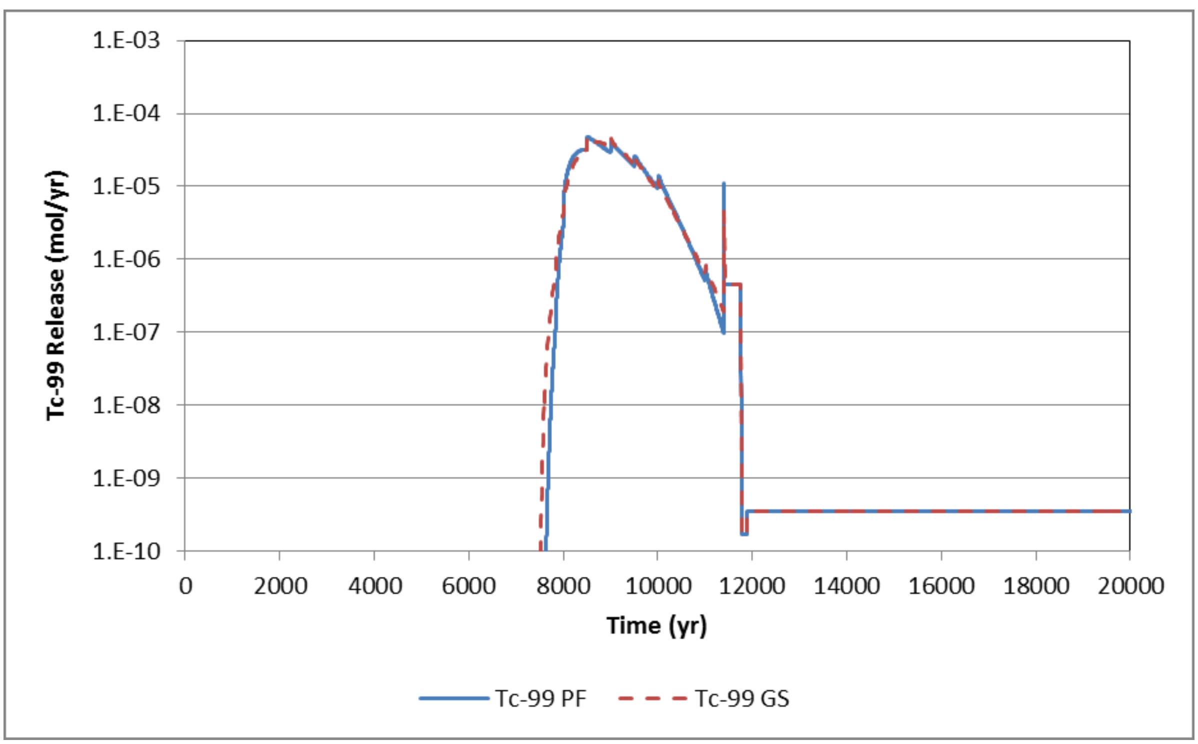

Figure 3-4: Tank 9 Am-243 Release to the Saturated Zone

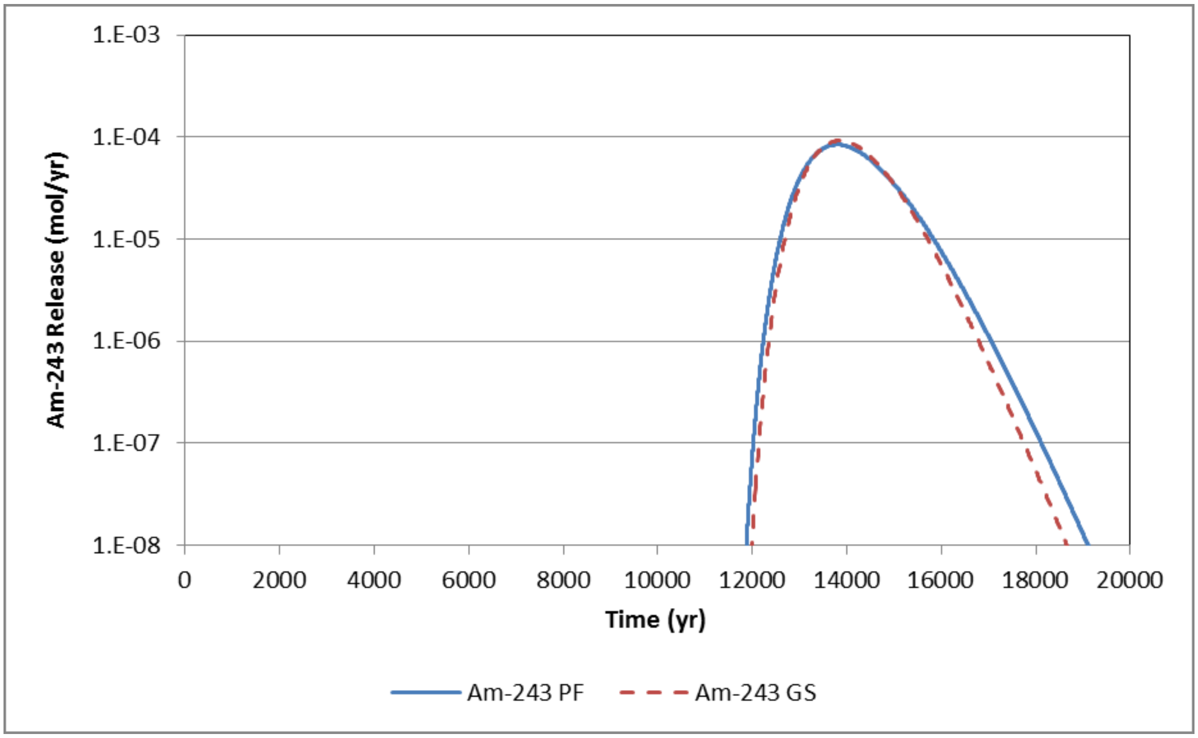

Figure 3-5: Tank 9 Pu-239 Release to the Saturated Zone

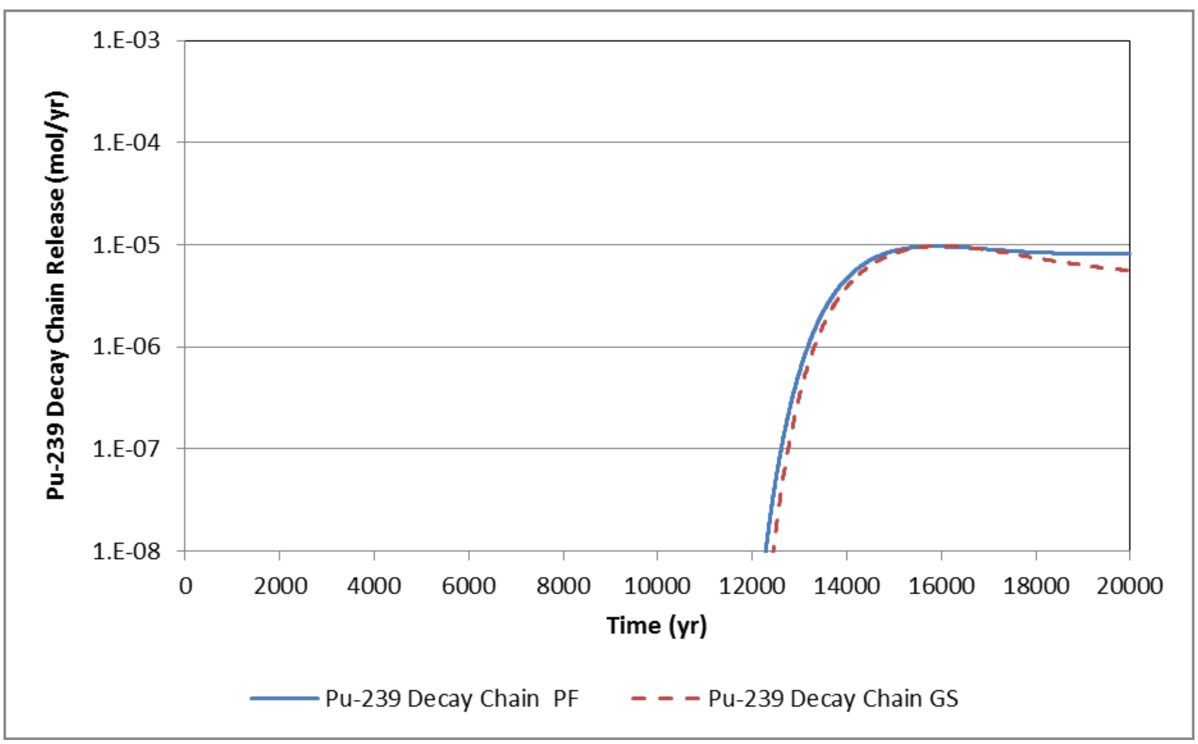

Figure 3-6: Tank 9 U-234 Release to the Saturated Zone

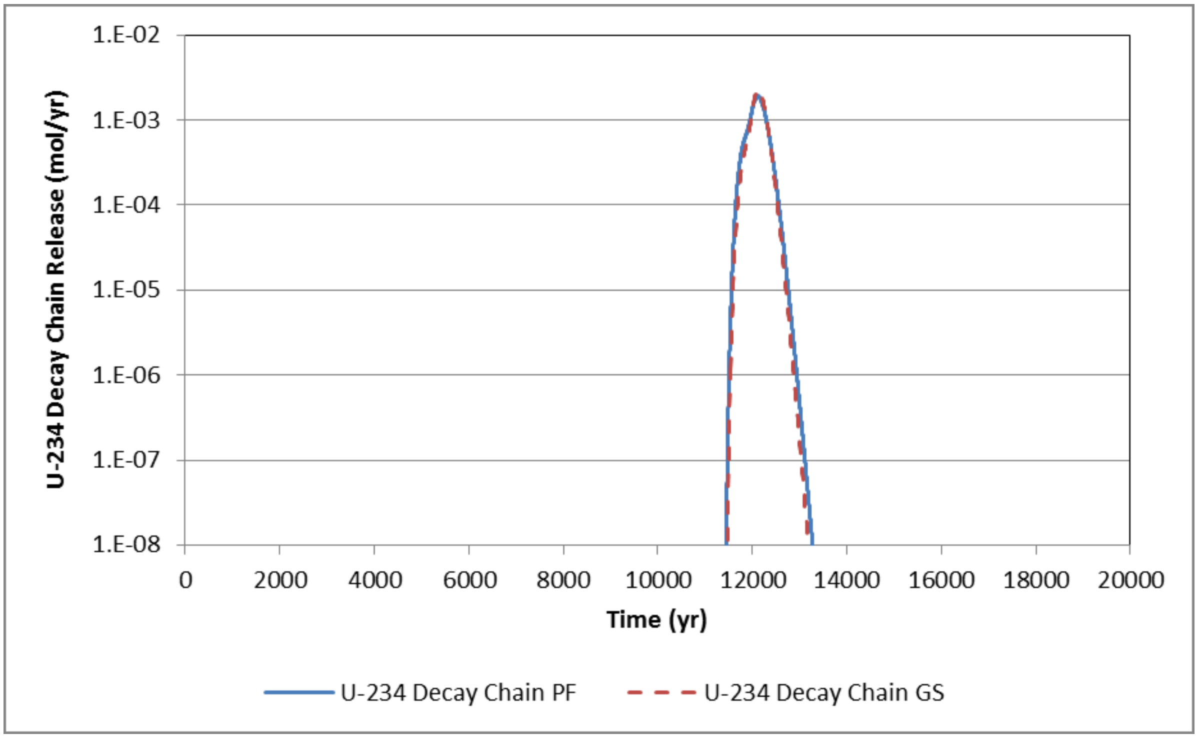

Figure 3-7: Tank 9 Ra-226 Release to the Saturated Zone

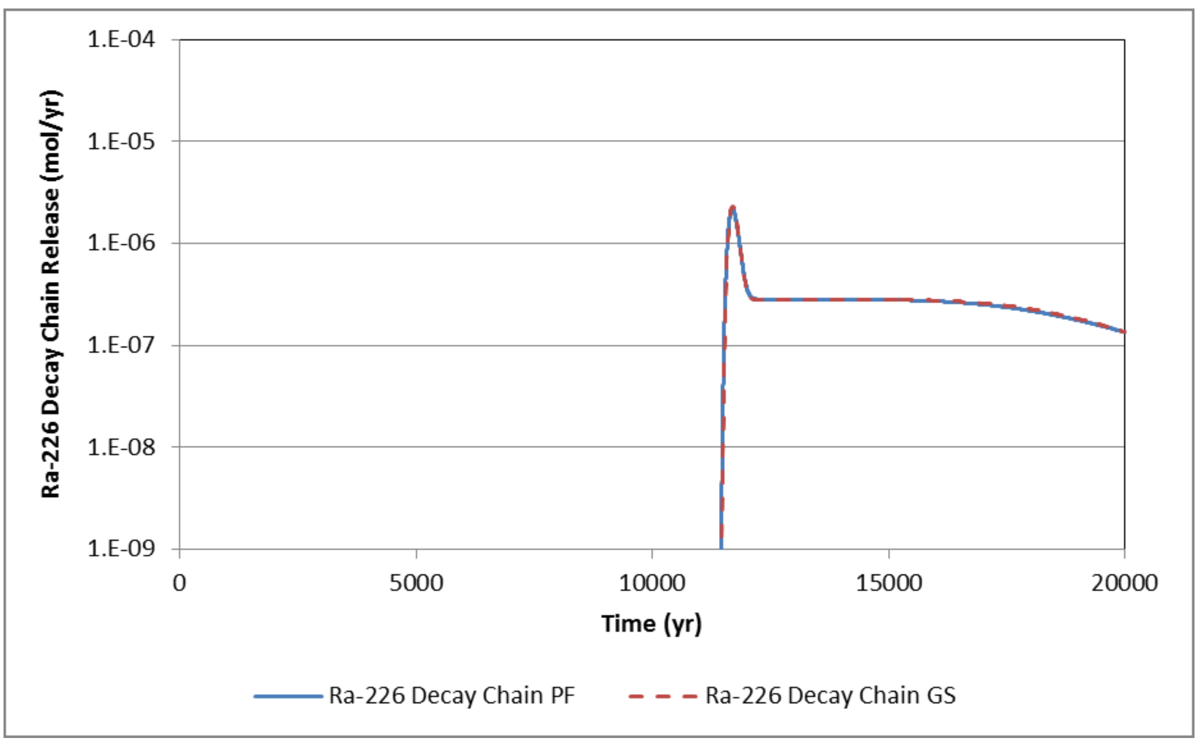

Figure 3-8: Tank 9 Am-241 Release to the Saturated Zone

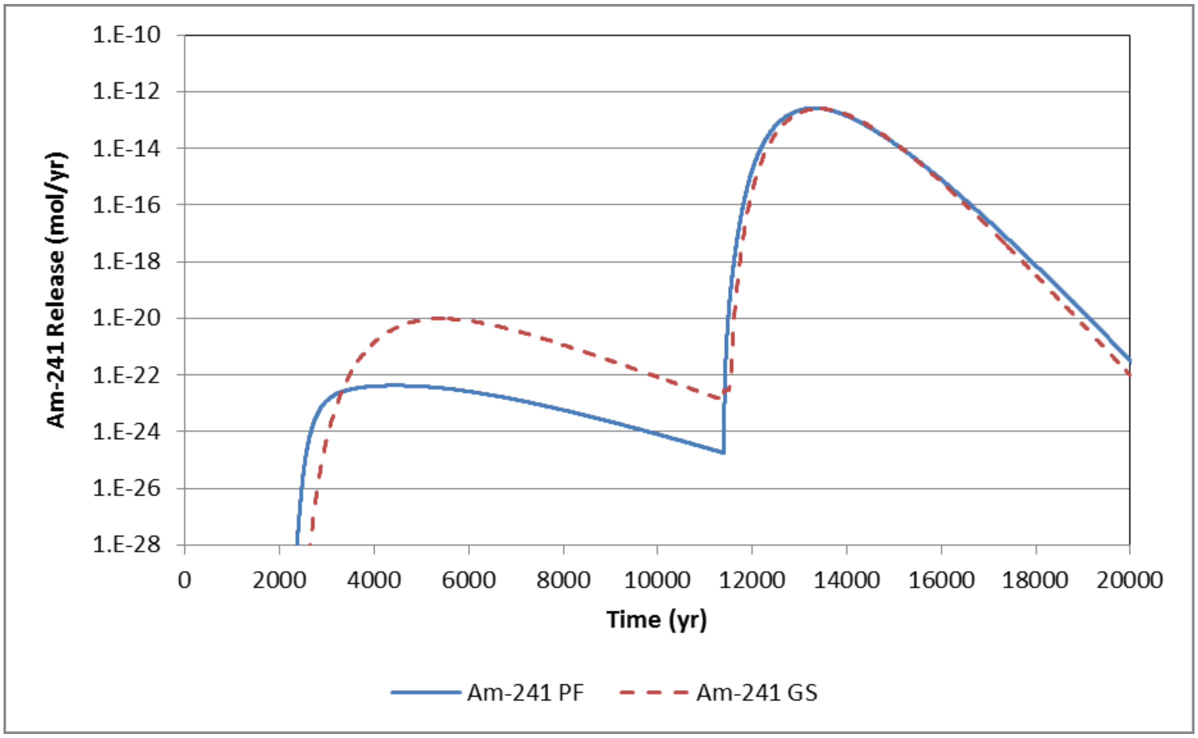

Figure 3-9: Tank 9 Np-237 Release to the Saturated Zone

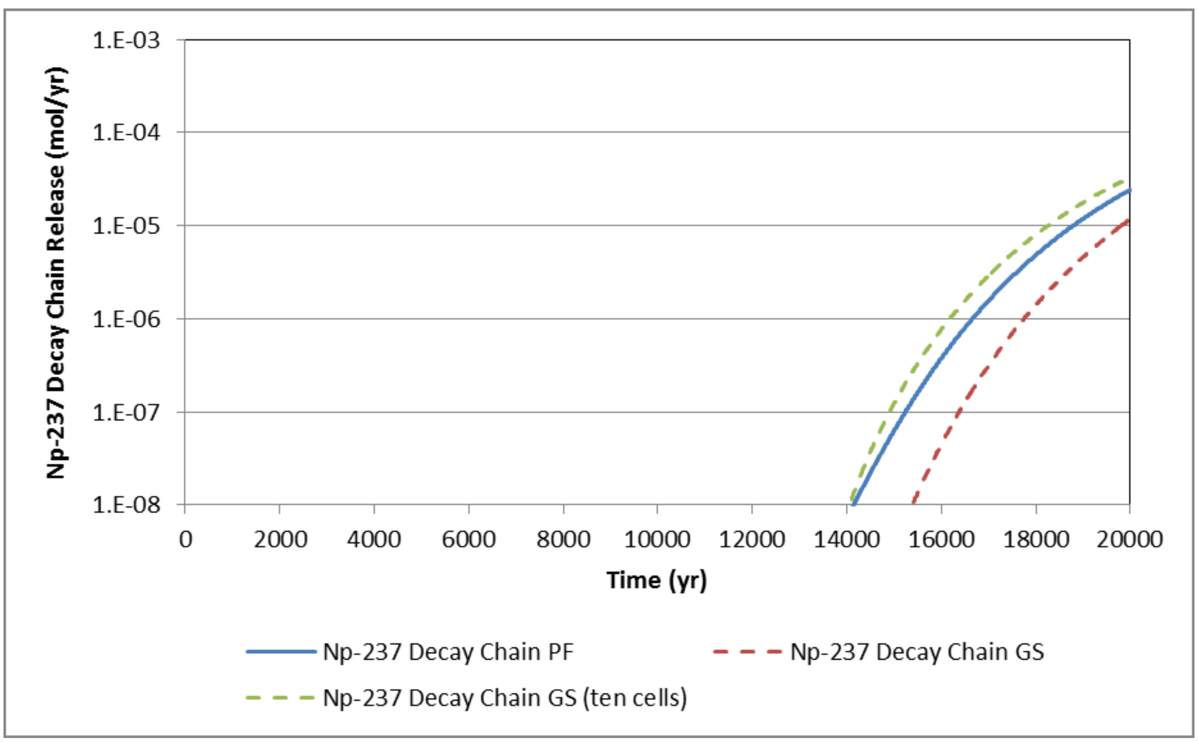

3.2.1.2 Type I Tank with Failed Liner (Tank 12)

A comparison of the PORFLOW HTF Model and the GoldSim HTF RAD Model mass releases of I-129, Tc-99, Am-243, Pu-239, U-234, Ra-226, Am-241, and Np-237, as presented in Figure 3-10 through Figure 3-17, indicate that the GoldSim model generally produces a good approximation of the releases from Tank 12 generated by the PORFLOW model. Table 3-2. summarizes the peak values for these releases showing that except for Tc-99 and Am-241, when comparing the two models the percent differences are below 50%.

Table 3-2: GoldSim and PORFLOW Model Peak Release from the UZ to the SZ Comparisons for Tank 12 within 20,000 years

Radionuclide	PORFLOW Peak Release (mol/yr)	PORFLOW Time of Peak Release (yr)	GoldSim Peak Release (mol/yr)	GoldSim Time of Peak Release (yr)	Peak Release Percent Difference GoldSim vs PORFLOW
I-129	1.0E-02	2,213	1.3E-02	2,250	30%
Tc-99	2.7E-04	6,806	5.5E-05	6,800	-80%
Am-243	3.7E-07	10,399	3.1E-07	10,330	-16%
Pu-239	3.9E-06	19,998	3.7E-06	20,000	-5%
U-234	1.6E-04	7,697	1.7E-04	7,830	6%
Ra-226	4.7E-08	8,281	4.8E-08	8,510	2%
Am-241	2.8E-10	5,152	7.6E-10	5,510	171%
Np-237	2.5E-05	20,000	2.3E-05	20,000	-8%

For the Tc-99 release from Tank 12 (see Table 3-2), the general trend is captured, but the spikes at 6,800 years differ by 80%. Over 6,800 years, the total Tc-99 release from the annulus in the GoldSim model is greater than for the PORFLOW model leaving less to be released from the annulus at the Eh transition time. Despite this minor difference the trends of the annulus releases from the two models are similar and the comparison is considered acceptable. For the Am-241 release from Tank 12, even though the releases of Am-241 are different, the trends are similar and differences at small release levels are not considered significant to overall dose.

Figure 3-10: Tank 12 I-129 Release to the Saturated Zone

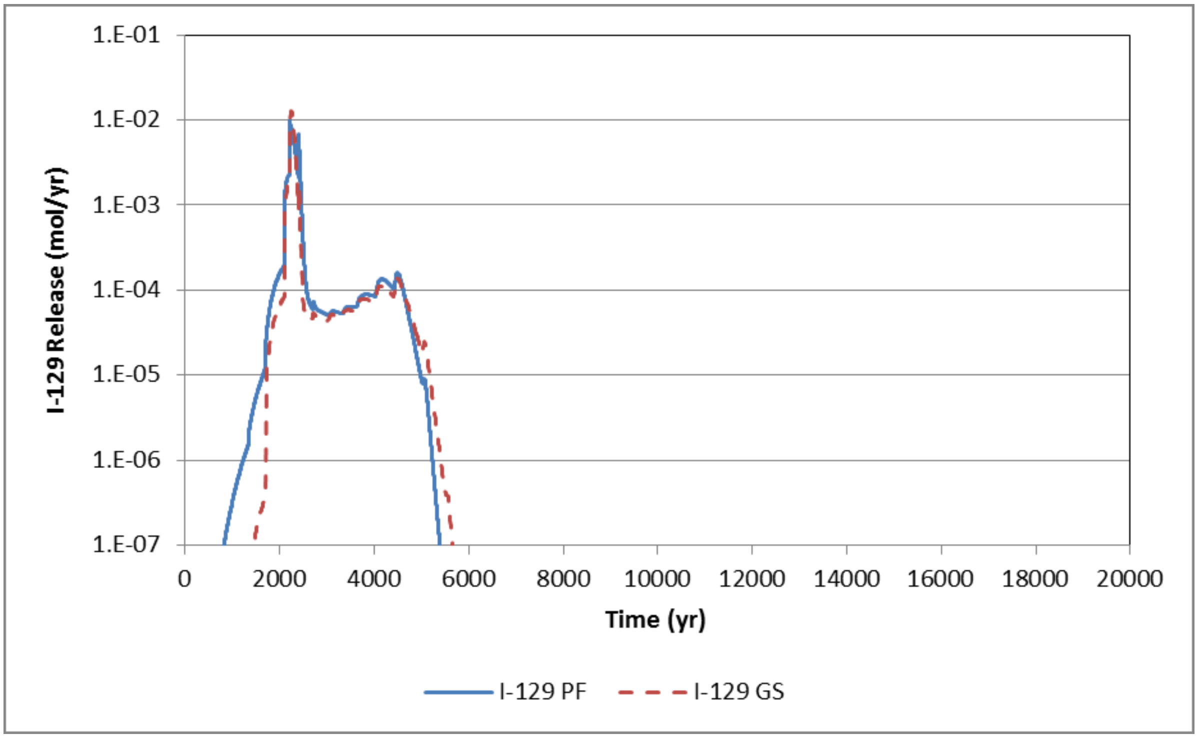

Figure 3-11: Tank 12 Tc-99 Release to the Saturated Zone

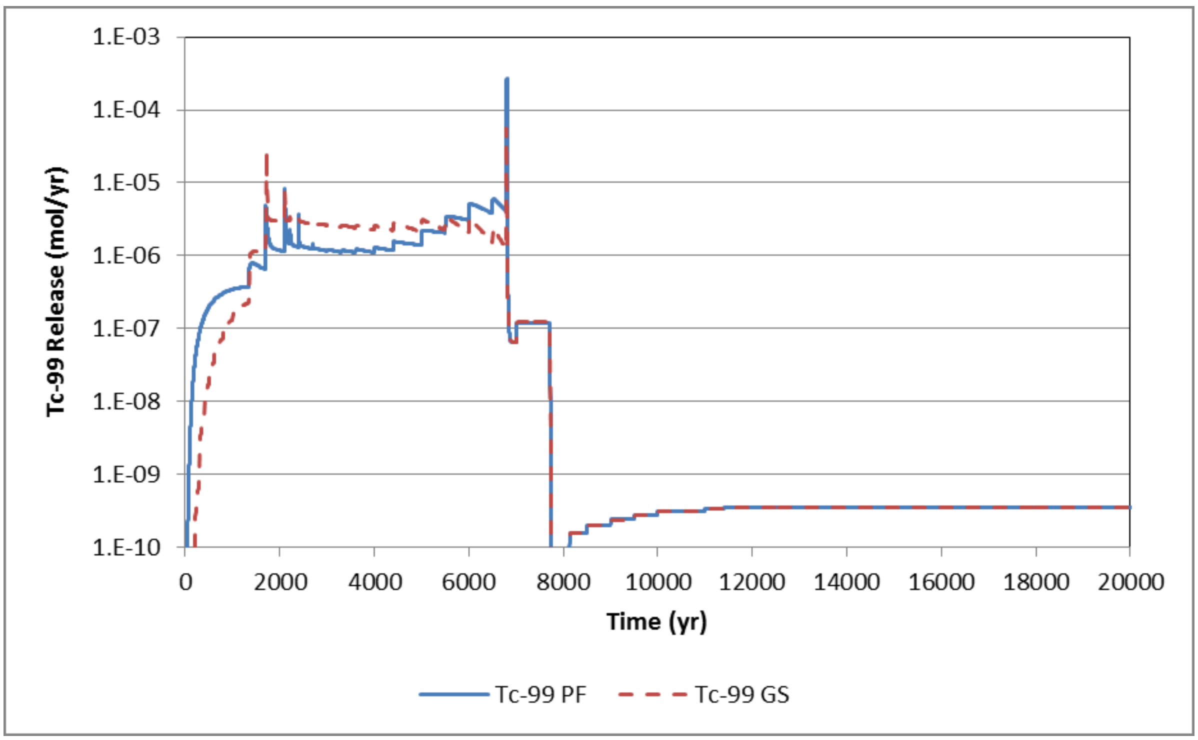

Figure 3-12: Tank 12 Am-243 Release to the Saturated Zone

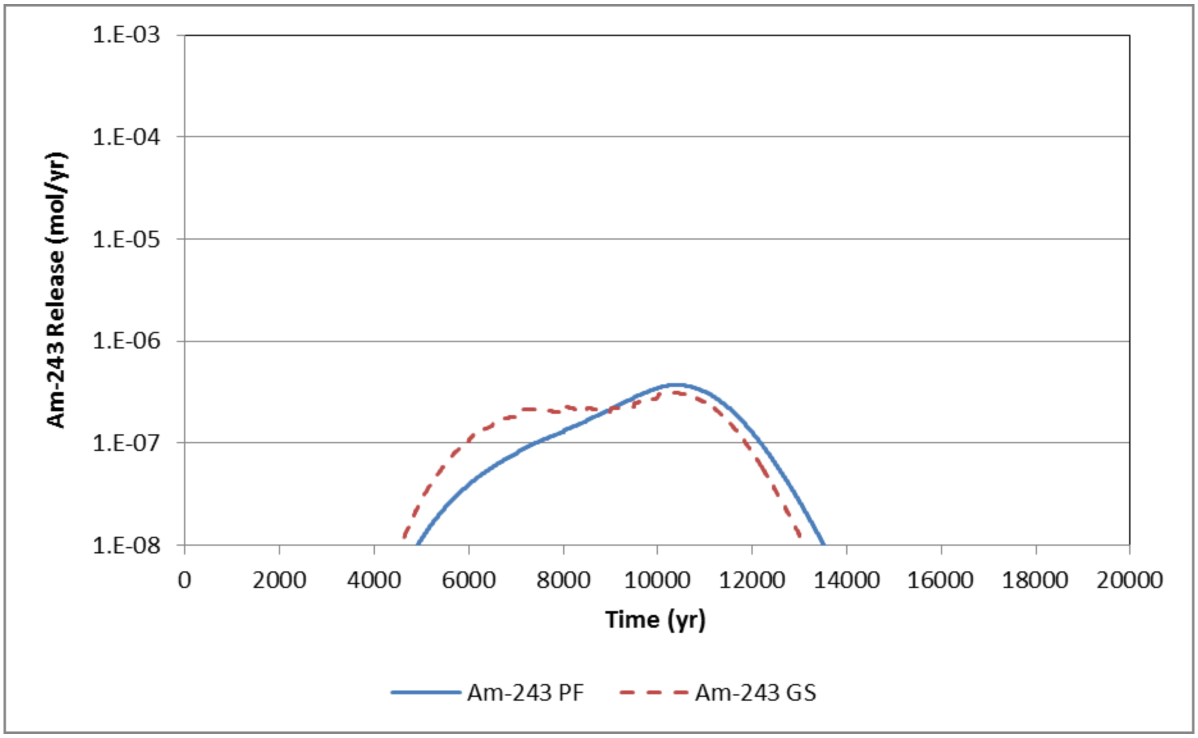

Figure 3-13: Tank 12 Pu-239 Release to the Saturated Zone

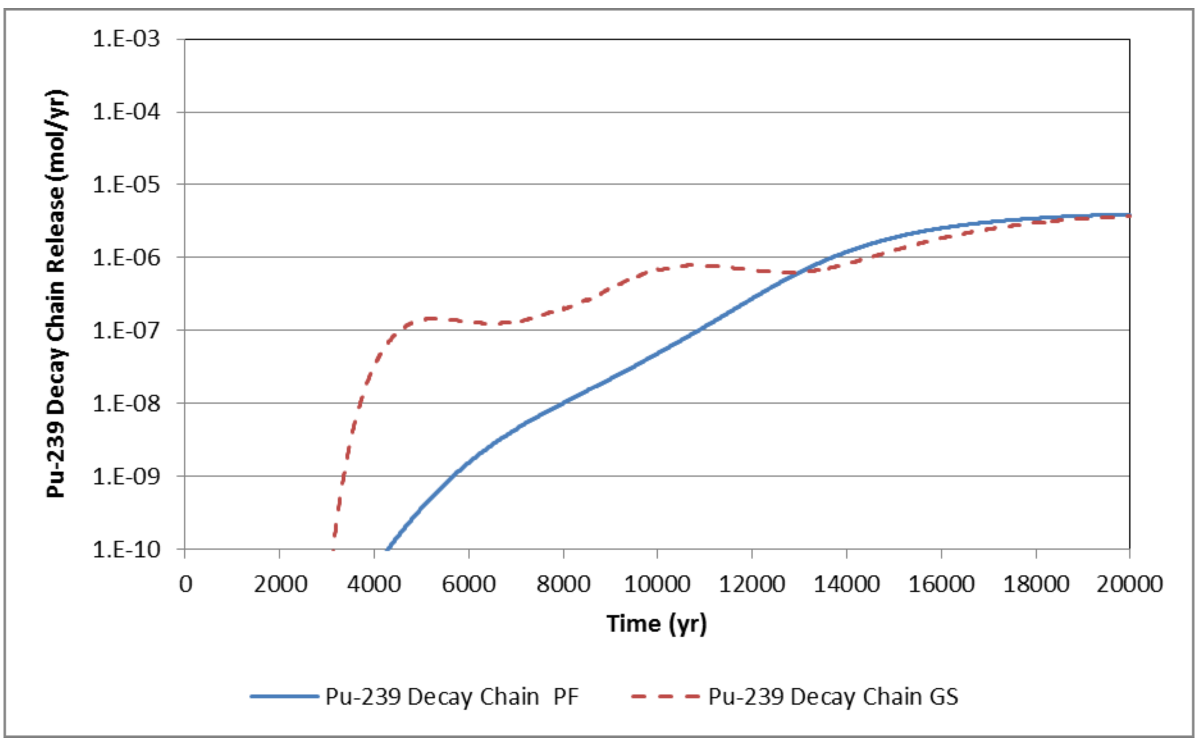

Figure 3-14: Tank 12 U-234 Release to the Saturated Zone

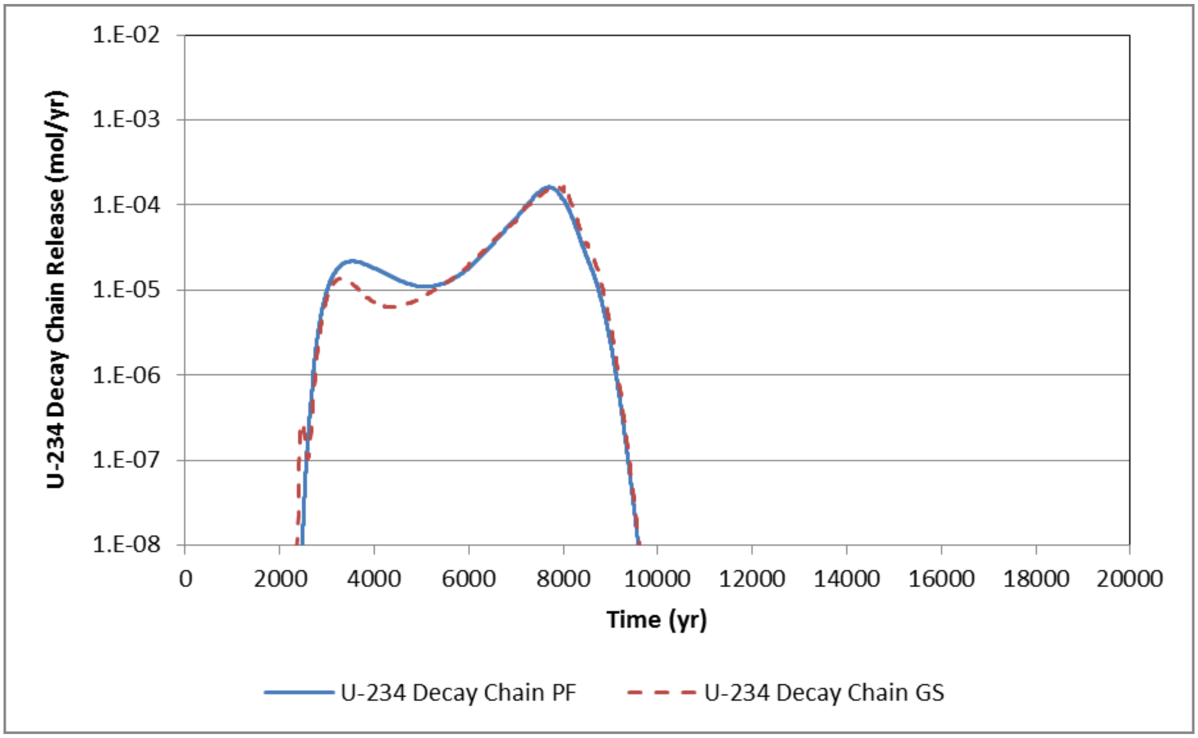

Figure 3-15: Tank 12 Ra-226 Release to the Saturated Zone

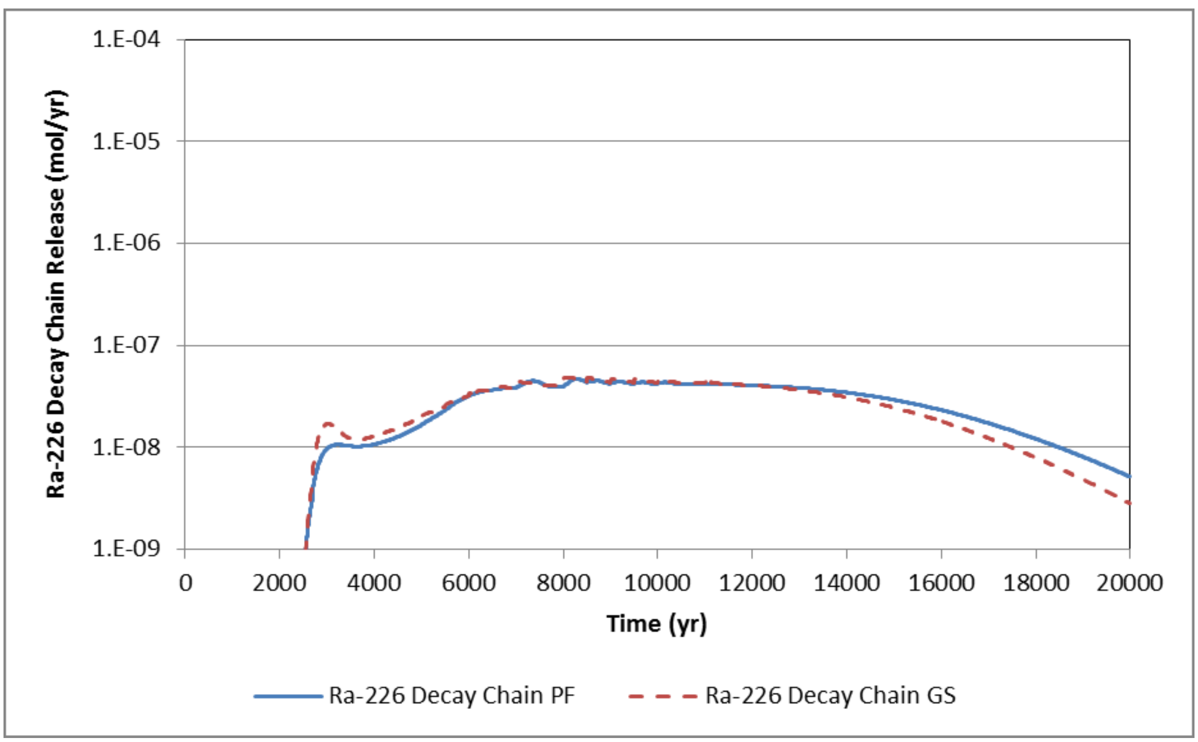

Figure 3-16: Tank 12 Am-241 Release to the Saturated Zone

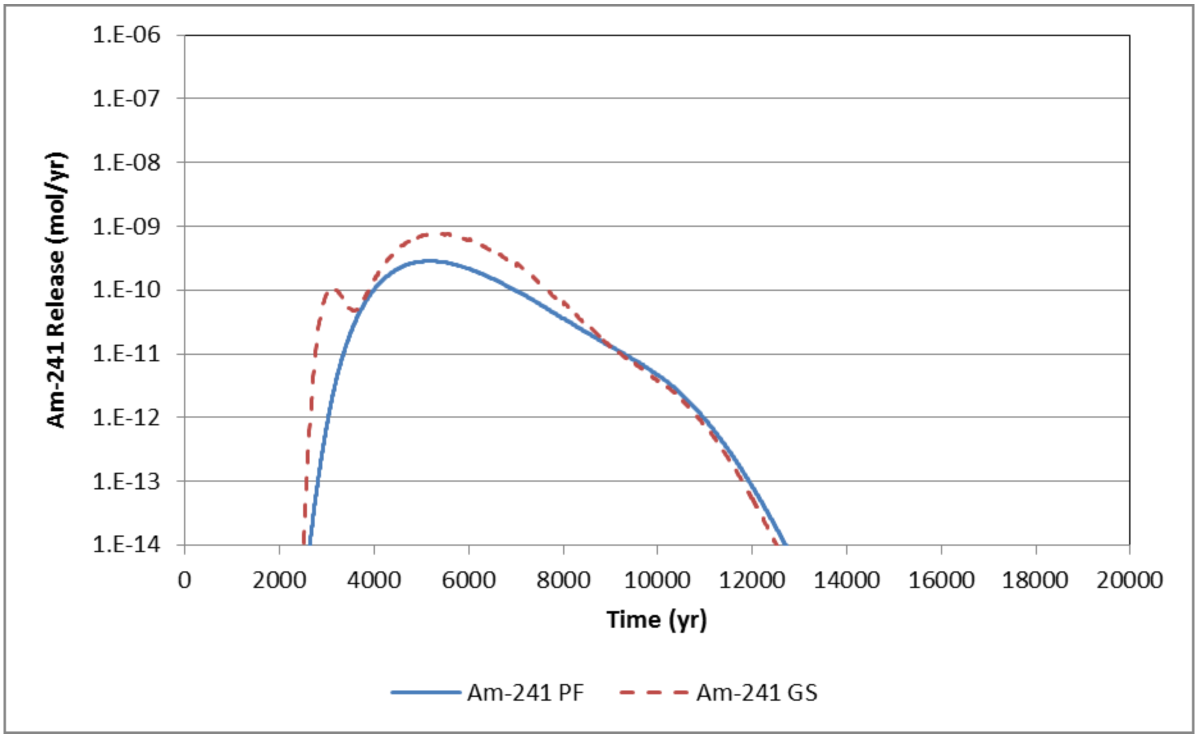

Figure 3-17: Tank 12 Np-237 Release to the Saturated Zone

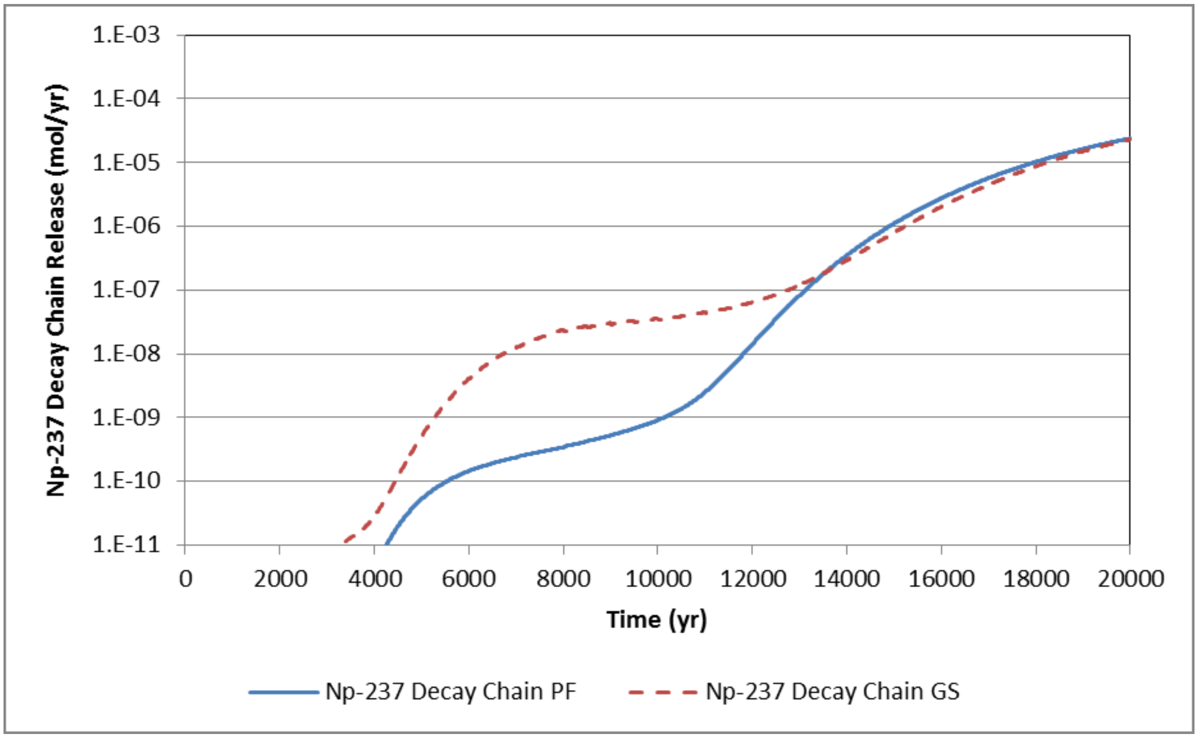

3.2.1.3 Type II Tank with Intact Liner (Tank 13)

A comparison of the PORFLOW HTF Model and the GoldSim HTF RAD Model mass releases of I-129, Tc-99, Am-243, Pu-239, U-234, Ra-226, Am-241, and Np-237, as presented in Figure 3-18 through Figure 3-25, indicate that the GoldSim model produces a good approximation of the releases from Tank 13 generated by the PORFLOW model. Table 3-3 summarizes the peak values for these releases showing that except for Am-241 and Np-237, when comparing the two models the percent differences are below 50%.

Table 3-3: GoldSim and PORFLOW Model Peak Release from the UZ to the SZ Comparisons for Tank 13 within 20,000 years

Radionuclide	PORFLOW Peak Release (mol/yr)	PORFLOW Time of Peak Release (yr)	GoldSim Peak Release (mol/yr)	GoldSim Time of Peak Release (yr)	Peak Release Percent Difference GoldSim vs PORFLOW
I-129	4.4E-02	12,725	3.7E-02	12,730	-16%
Tc-99	3.2E-03	12,692	2.4E-03	12,690	-25%
Am-243	3.6E-05	17,448	3.6E-05	17,200	0%
Pu-239	4.2E-06	20,000	4.5E-06	20,000	7%
U-234	7.1E-04	14,036	6.7E-04	14,180	-6%
Ra-226	1.5E-06	13,251	1.5E-06	13,230	0%
Am-241	3.0E-16	16,398	4.8E-16	16,070	60%
Np-237	4.1E-12	20,000	1.5E-10	20,000	3559%

For Am-241 (see Figure 3-24 and Table 3-3) percent differences are not much above 50% (60%) but the trends are similar. For Np-237 (see Figure 3-25 and Table 3-3) percent differences don't match well percentage-wise but this is very early in the breakthrough period when values are continuing to climb, and the trends are similar.

Figure 3-18: Tank 13 I-129 Release to the Saturated Zone

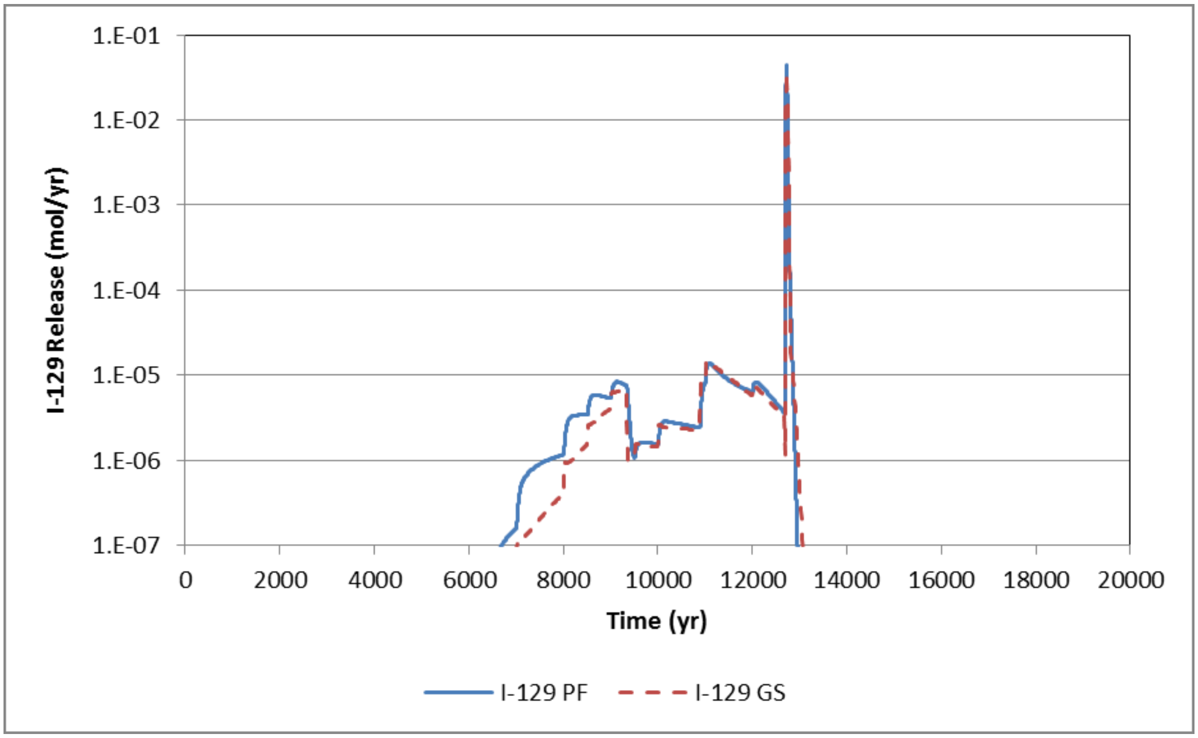

Figure 3-19: Tank 13 Tc-99 Release to the Saturated Zone

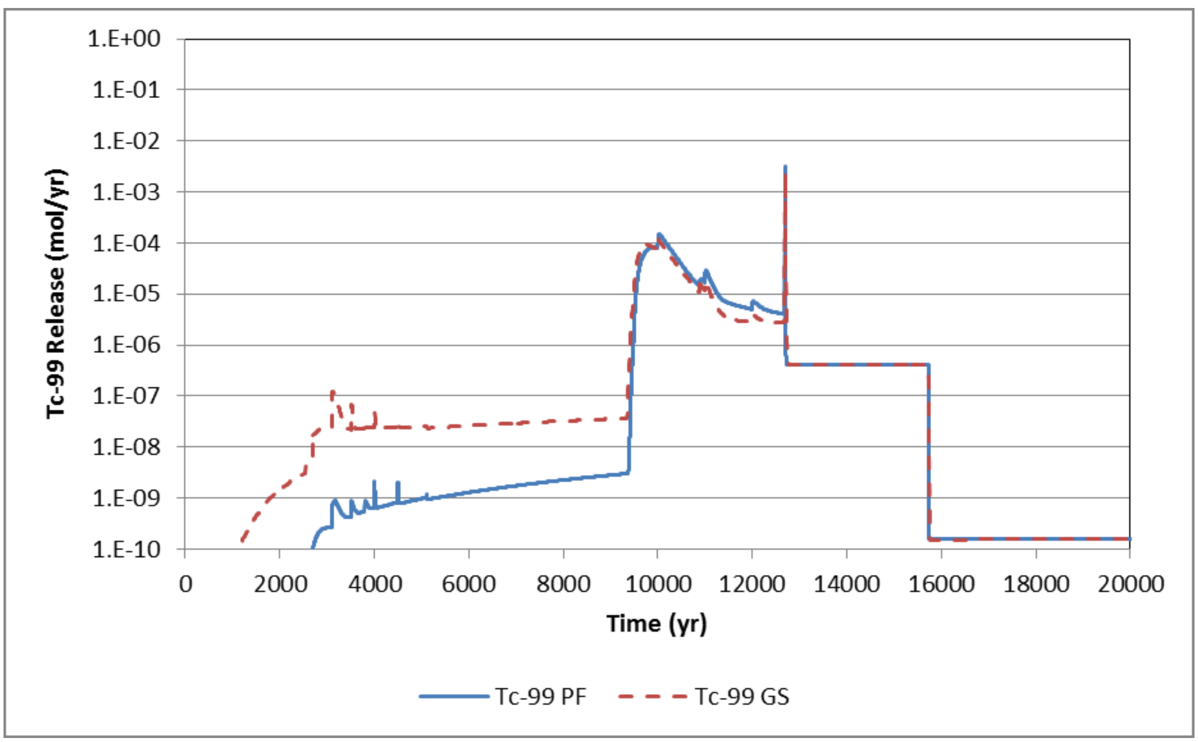

Figure 3-20: Tank 13 Am-243 Release to the Saturated Zone

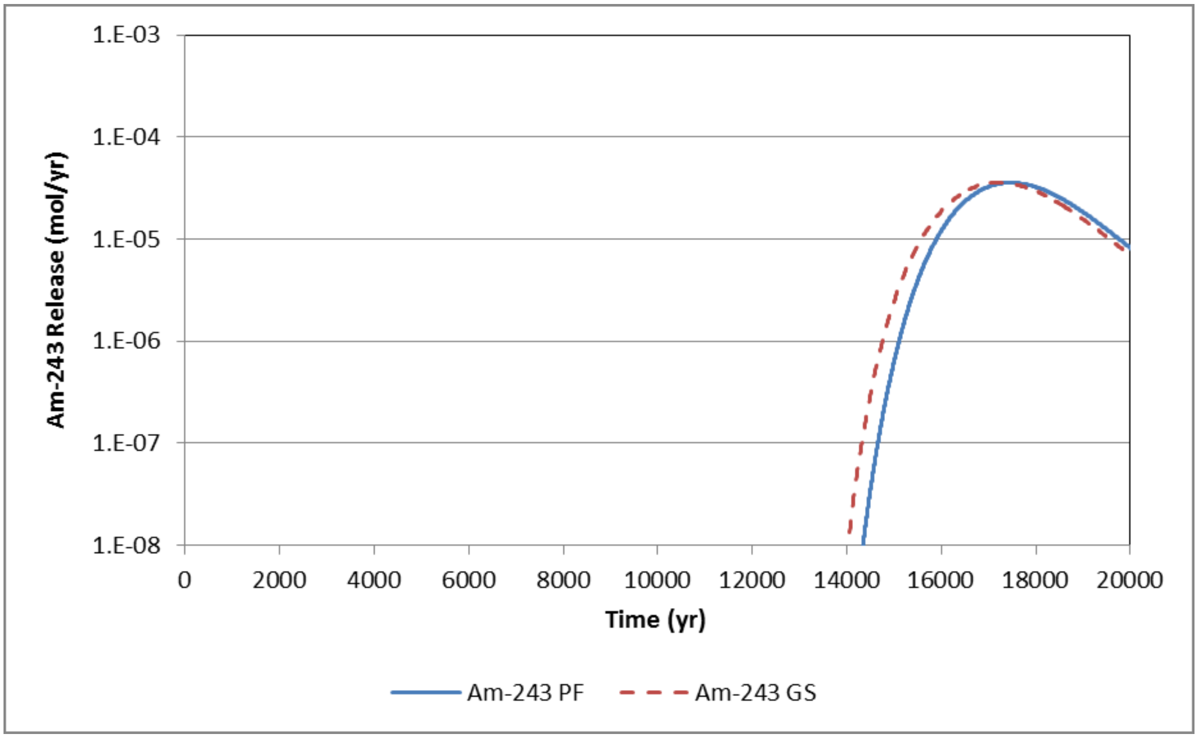

Figure 3-21: Tank 13 Pu-239 Release to the Saturated Zone

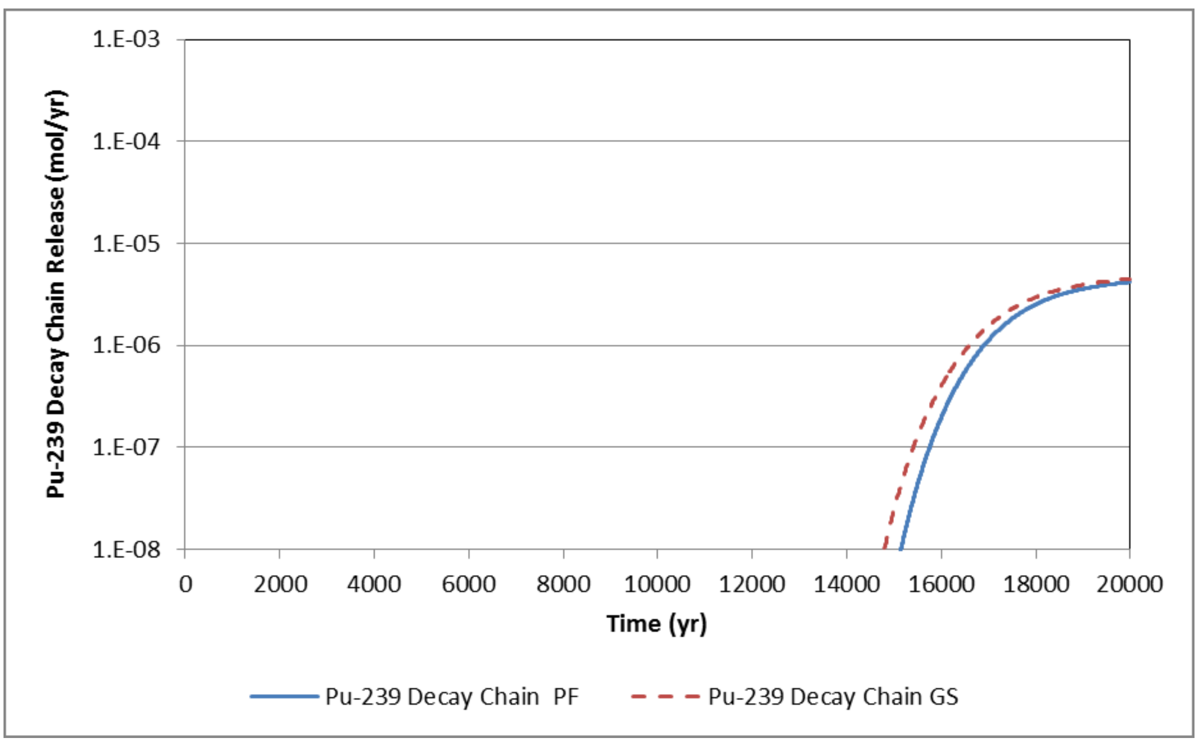

Figure 3-22: Tank 13 U-234 Release to the Saturated Zone

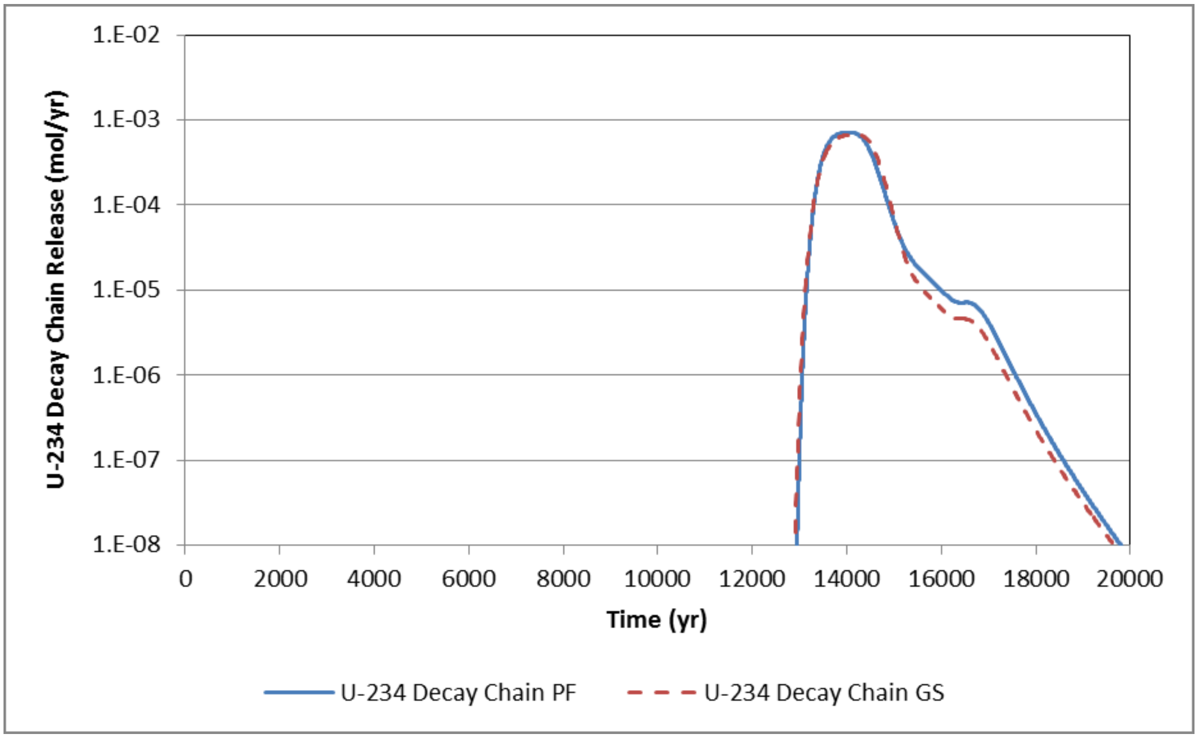

Figure 3-23: Tank 13 Ra-226 Release to the Saturated Zone

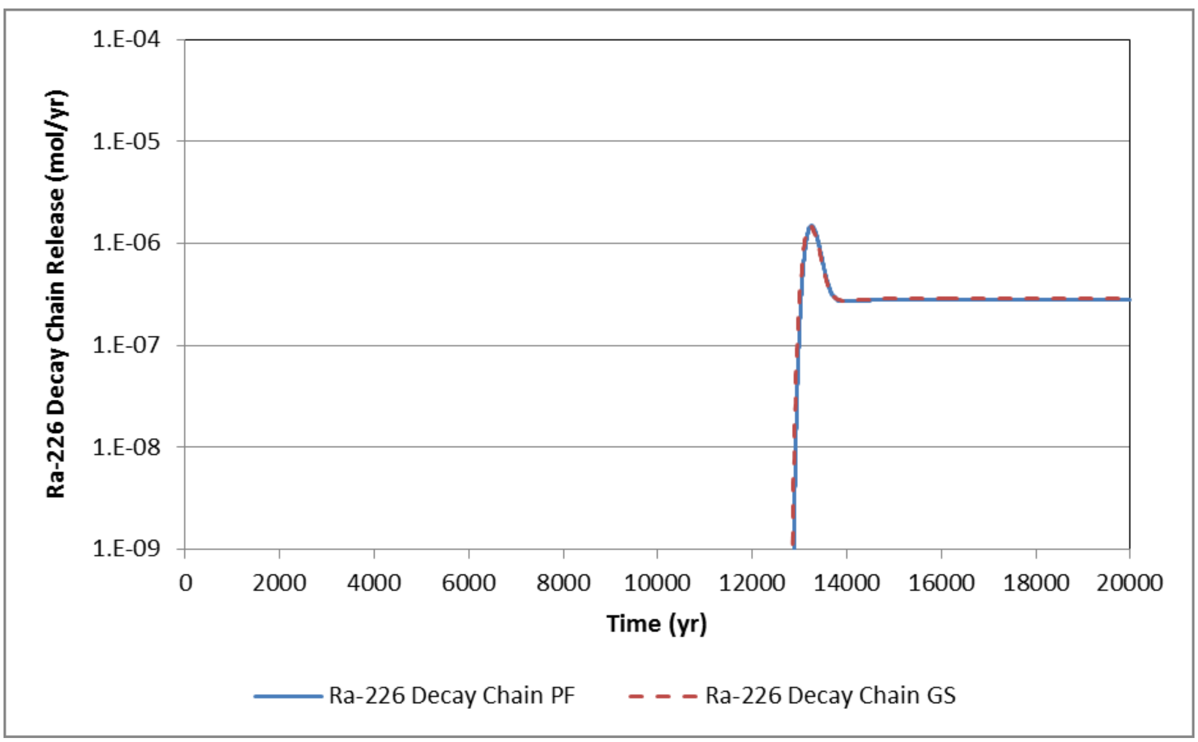

Figure 3-24: Tank 13 Am-241 Release to the Saturated Zone

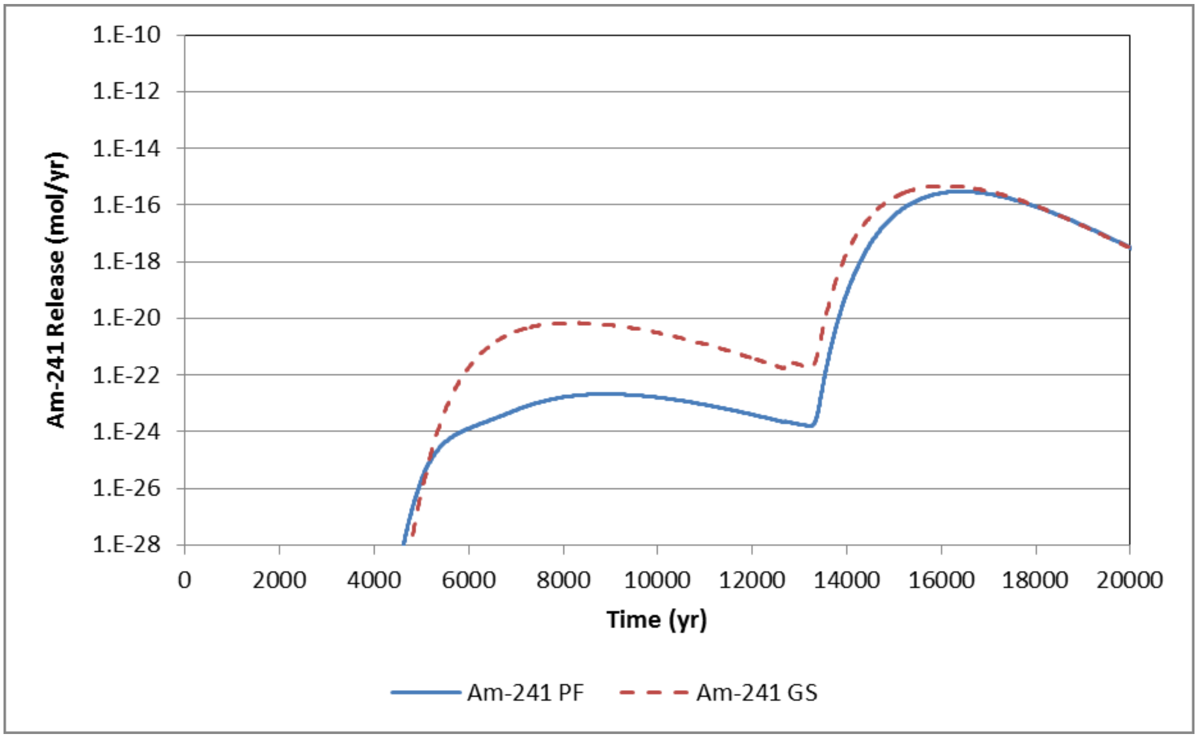

Figure 3-25: Tank 13 Np-237 Release to the Saturated Zone

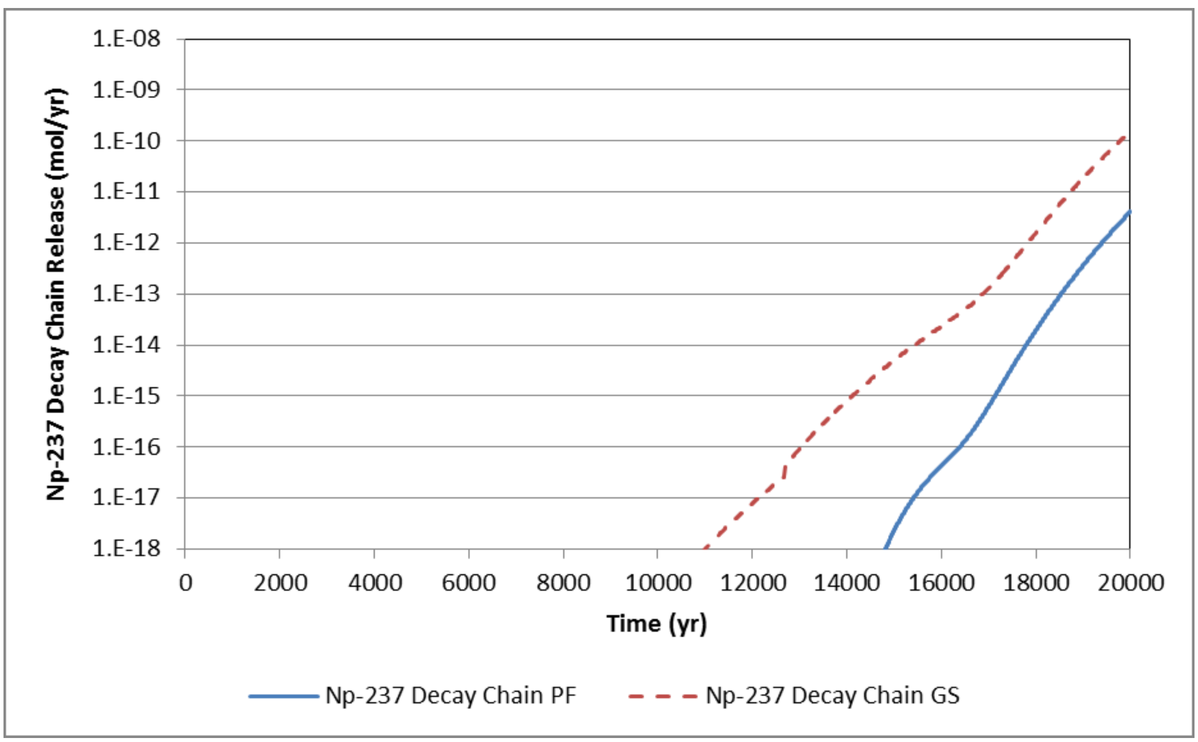

3.2.1.4 Type II Tank with Failed Liner (Tank 15)

A comparison of the PORFLOW HTF Model and the GoldSim HTF RAD Model mass releases of I-129, Tc-99, Am-243, Pu-239, U-234, Ra-226, Am-241, and Np-237, as presented in Figure 3-26 through Figure 3-33, indicate that the GoldSim model generally produces a good approximation of the releases from Tank 15 generated by the PORFLOW model. Table 3-4 summarizes the peak values for these releases showing that except for Tc-99, Am-241, and Np-237, when comparing the two models the percent differences are below 50%.

Table 3-4: GoldSim and PORFLOW Model Peak Release from the UZ to the SZ Comparisons for Tank 15 within 20,000 years

Radionuclide	PORFLOW Peak Release (mol/yr)	PORFLOW Time of Peak Release (yr)	GoldSim Peak Release (mol/yr)	GoldSim Time of Peak Release (yr)	Peak Release Percent Difference GoldSim vs PORFLOW
I-129	8.2E-03	3,598	8.6E-03	3,600	5%
Tc-99	5.0E-04	9,322	1.0E-04	9,320	-80%
Am-243	6.6E-05	11,949	6.4E-05	11,640	-3%
Pu-239	1.1E-05	20,000	1.0E-05	18,520	-9%
U-234	5.5E-04	8,638	5.8E-04	8,820	5%
Ra-226	2.6E-07	7,465	2.3E-07	7,090	-12%
Am-241	2.0E-11	9,721	6.2E-11	8,510	210%
Np-237	2.7E-08	20,000	2.8E-07	20,000	937%

For the Tc-99 release from Tank 15 (see Table 3-4), the general trend is well captured, but the spikes at 9,300 years differ by 80%. Despite this difference of 80%, the trends of the annulus releases from the two models are similar and the comparison is considered acceptable. In addition, differences in spikes developed over a very short time period will be dampened by dispersion in the SZ transport process.

For Am-241 (see Figure 3-32 and Table 3-4) percent differences are above 50% (210%) but the trends are very similar. For Np-237 (see Figure 3-33 and Table 3-4) percent differences are relatively high but the trends are very similar and the differences in magnitude reflect an early stage in the breakthrough.

Figure 3-26: Tank 15 I-129 Release to the Saturated Zone

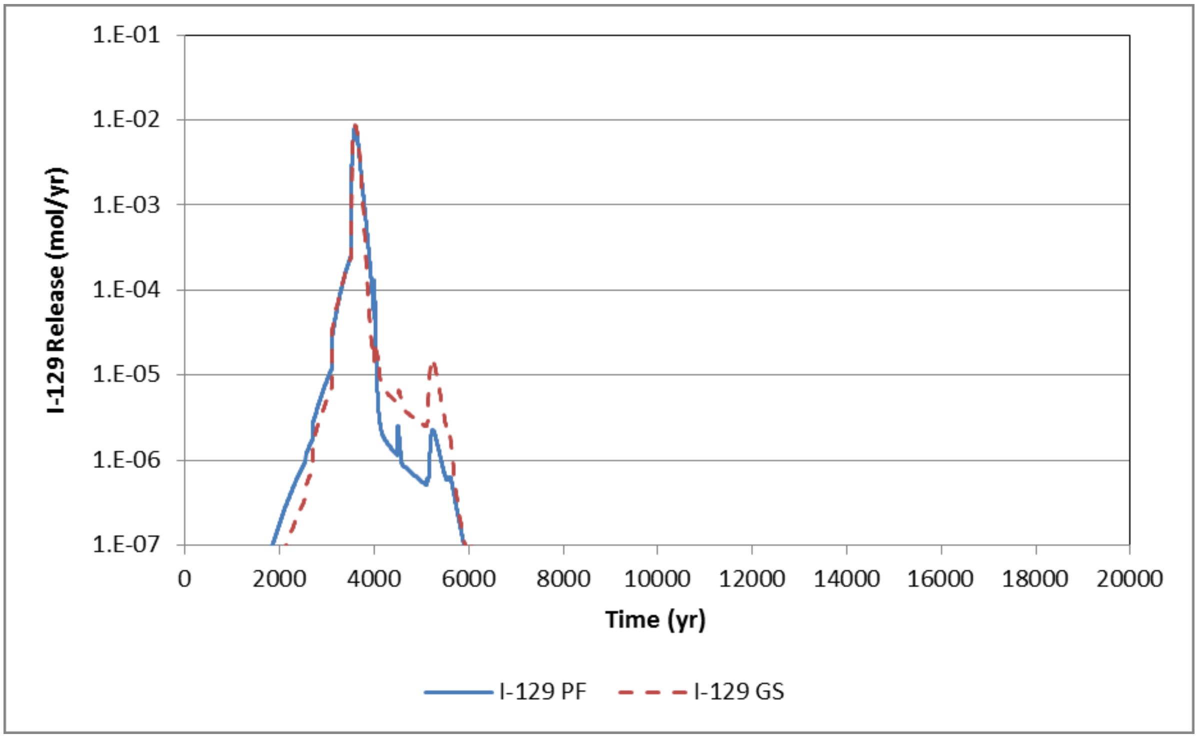

Figure 3-27: Tank 15 Tc-99 Release to the Saturated Zone

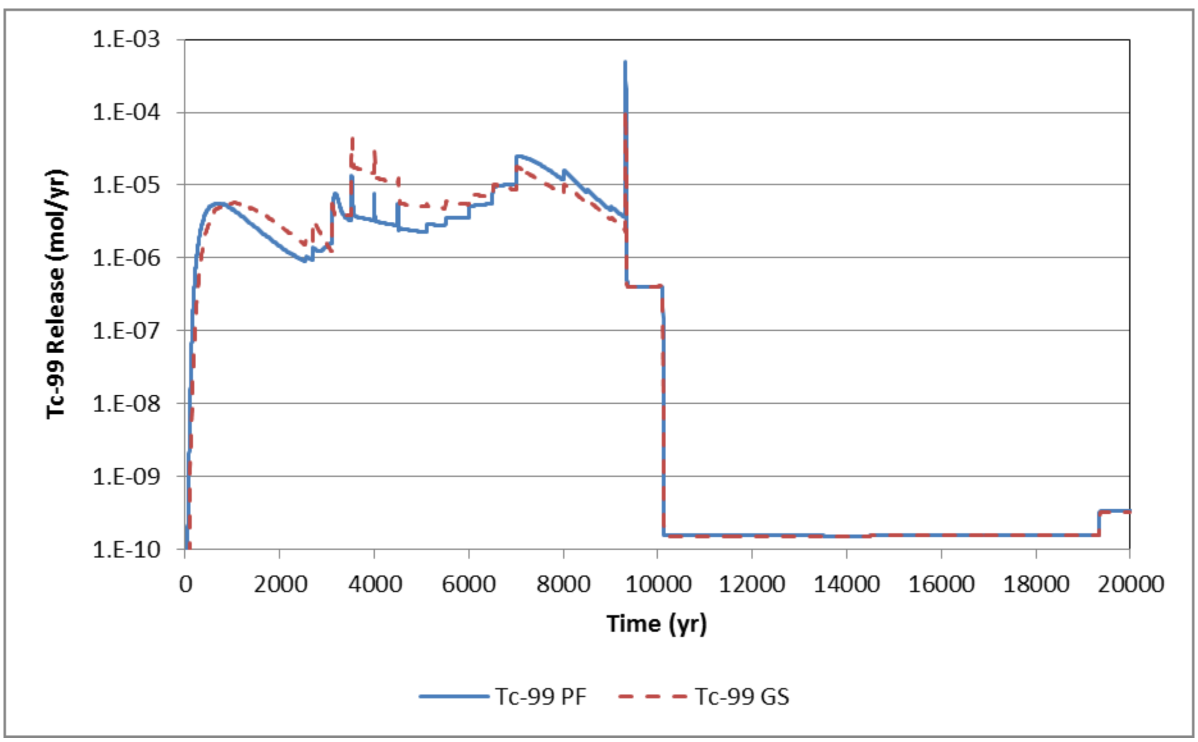

Figure 3-28: Tank 15 Am-243 Release to the Saturated Zone

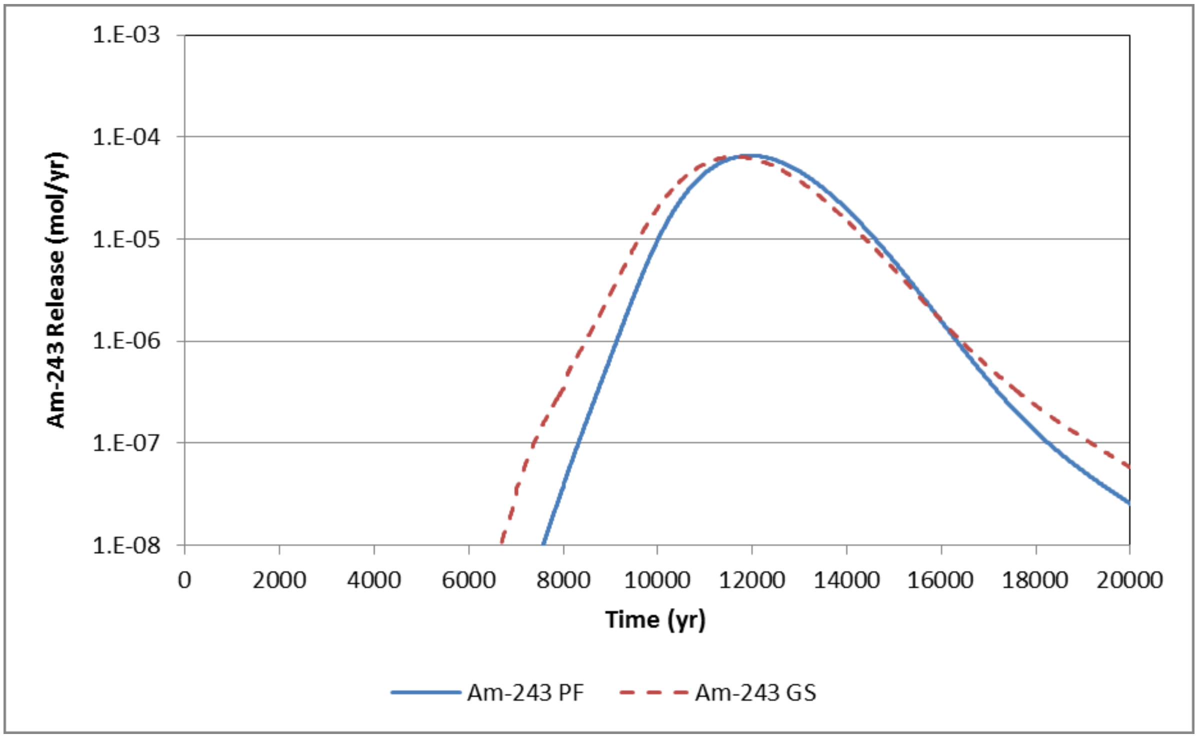

Figure 3-29: Tank 15 Pu-239 Release to the Saturated Zone

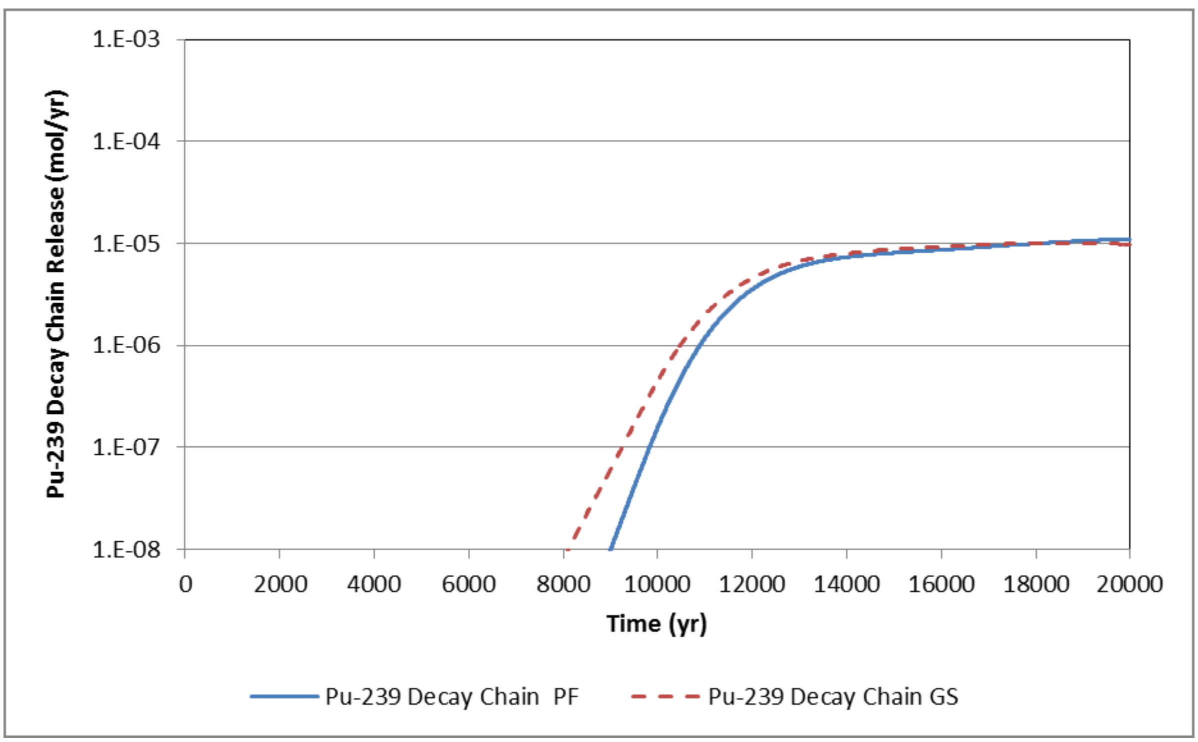

Figure 3-30: Tank 15 U-234 Release to the Saturated Zone

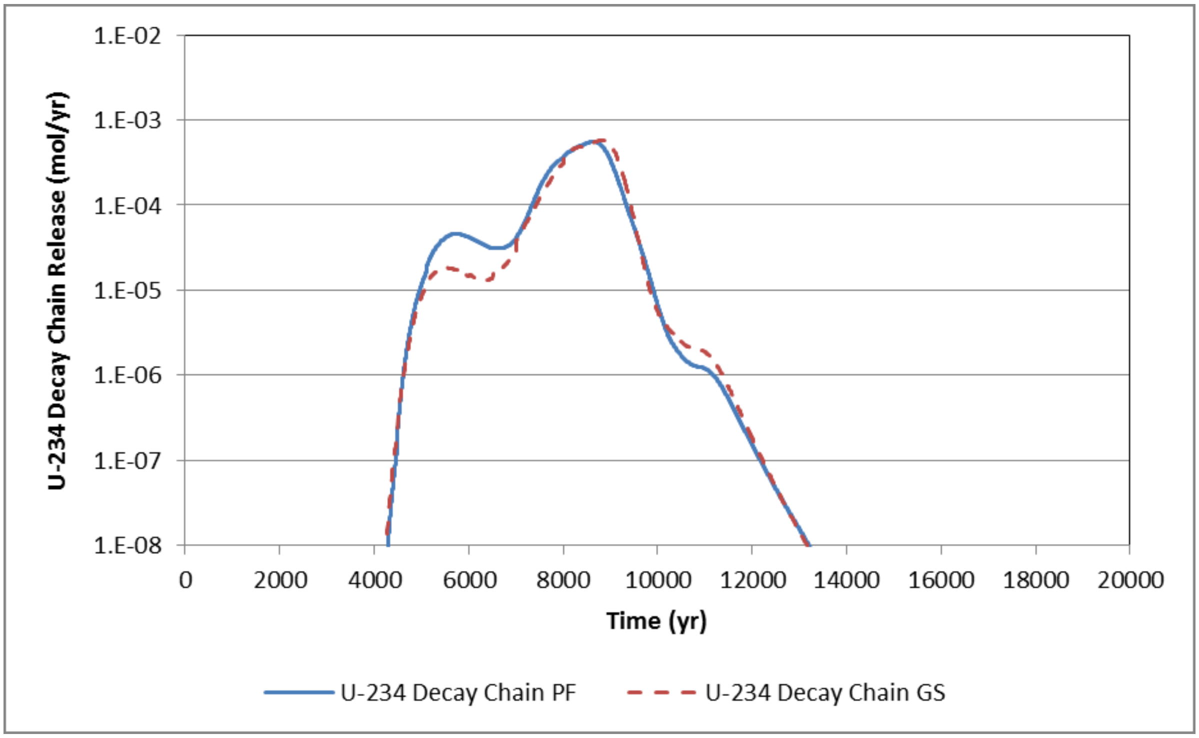

Figure 3-31: Tank 15 Ra-226 Release to the Saturated Zone

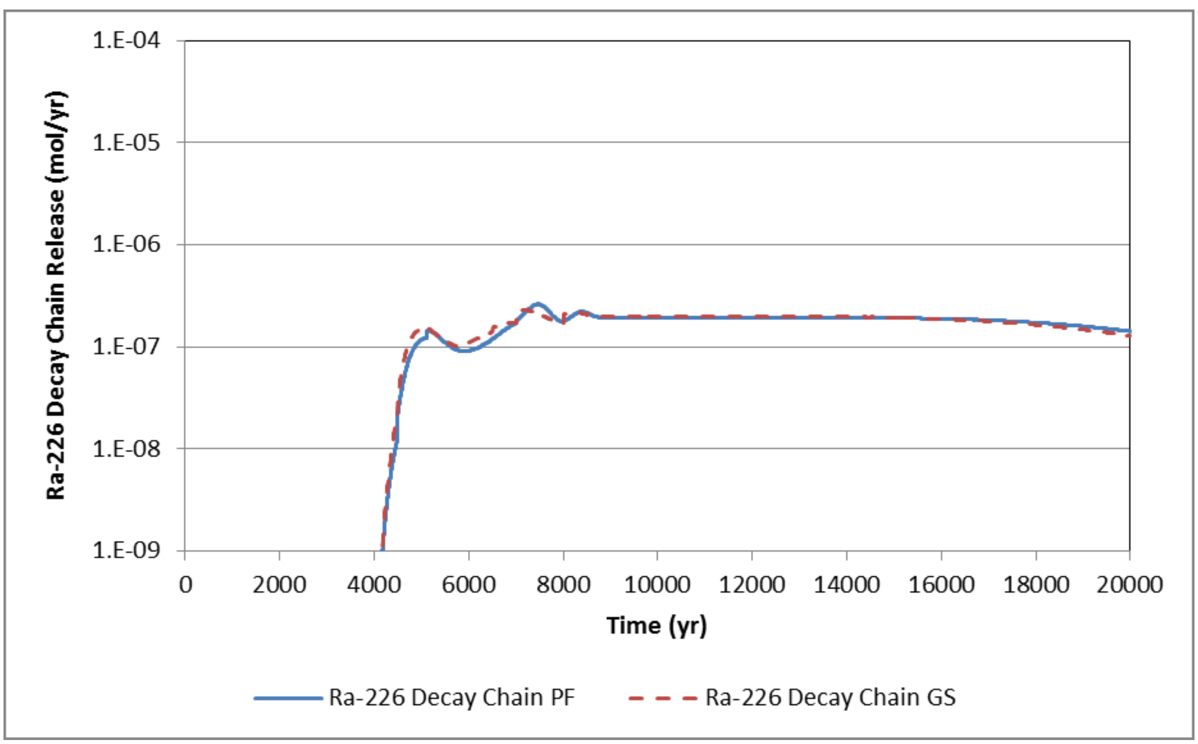

Figure 3-32: Tank 15 Am-241 Release to the Saturated Zone

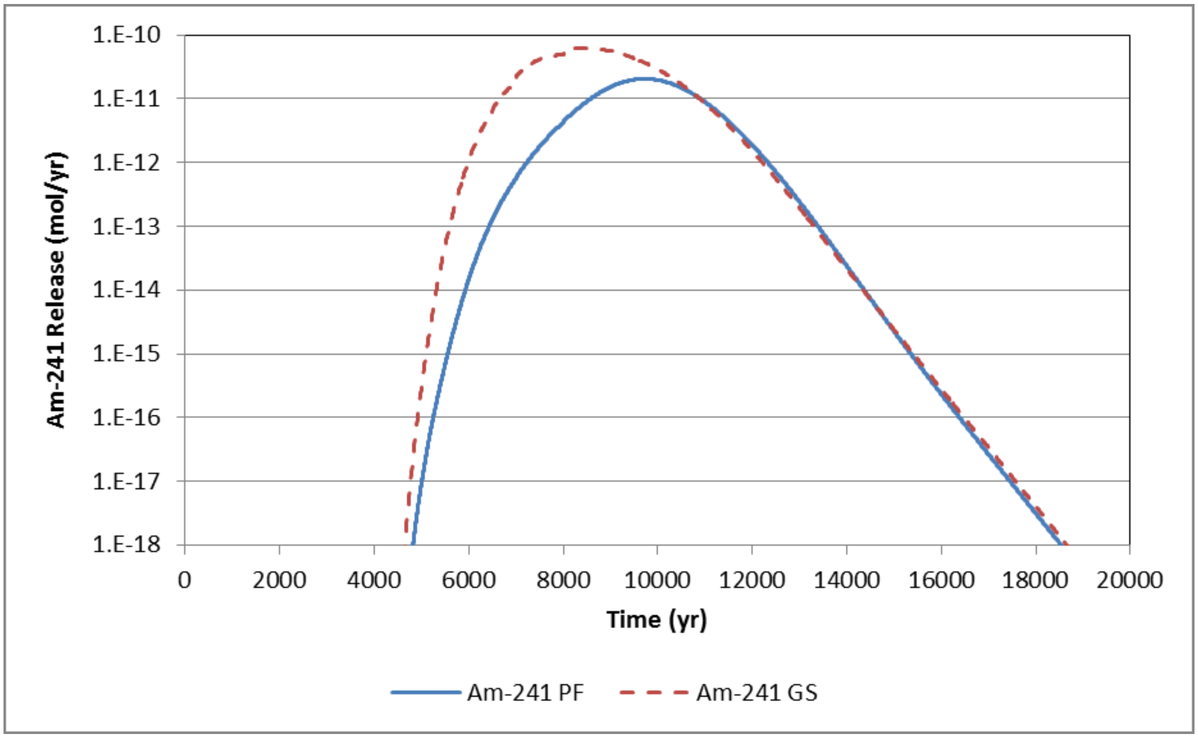

Figure 3-33: Tank 15 Np-237 Release to the Saturated Zone

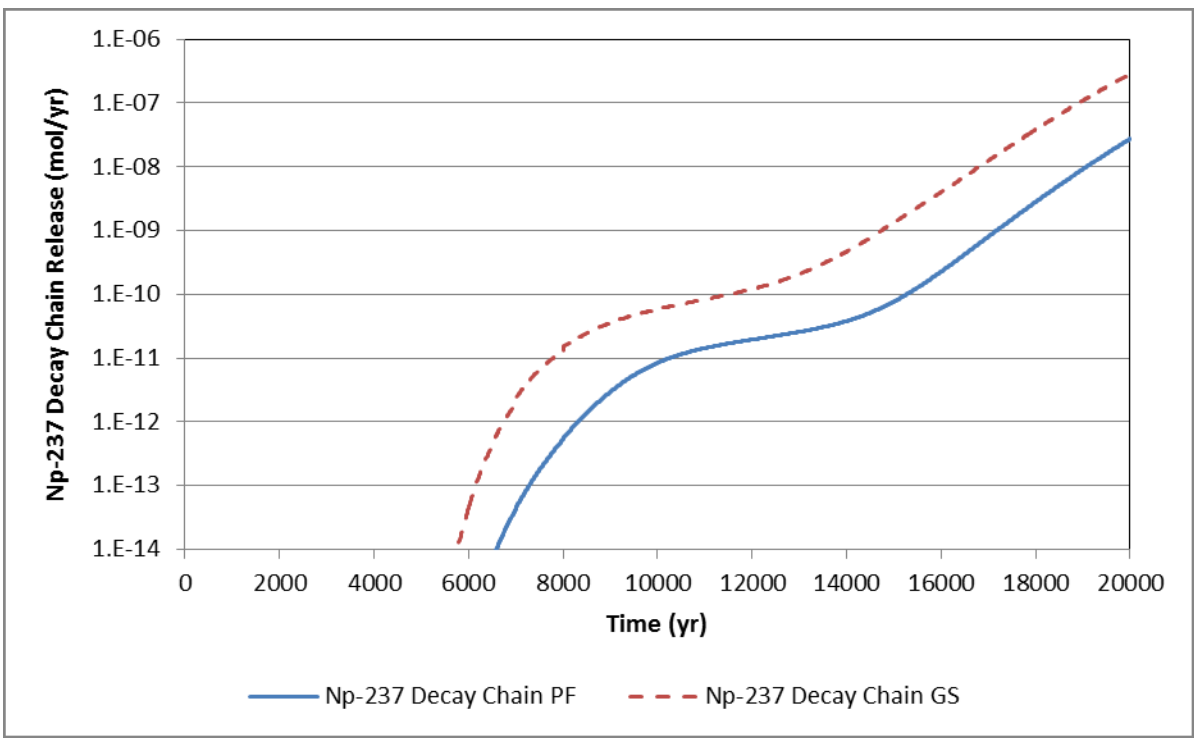

3.2.1.5 Type II Tank with Failed Liner (Tank 16)

A comparison of the PORFLOW HTF Model and the GoldSim HTF RAD Model mass releases of I-129, Tc-99, Am-243, Pu-239, U-234, Ra-226, Am-241, and Np-237, as presented in Figure 3-34 through Figure 3-41, indicate that the GoldSim model generally produces a good approximation of the releases from Tank 16 generated by the PORFLOW model. Table 3-5 summarizes the peak values for these releases showing that when comparing the two models except for Tc-99, Am-241, and Np-237, the percent differences are below or near 50%.

Table 3-5: GoldSim and PORFLOW Model Peak Release from the UZ to the SZ Comparisons for Tank 16 within 20,000 years

Radionuclide	PORFLOW Peak Release (mol/yr)	PORFLOW Time of Peak Release (yr)	GoldSim Peak Release (mol/yr)	GoldSim Time of Peak Release (yr)	Peak Release Percent Difference GoldSim vs PORFLOW
I-129	4.0E-03	3,614	4.2E-03	3,620	5%
Tc-99	9.3E-03	9,322	2.0E-03	9,320	-78%
Am-243	1.5E-08	11,337	1.5E-08	10,740	0%
Pu-239	1.3E-05	20,000	2.0E-05	20,000	54%
U-234	1.2E-05	5,647	1.3E-05	5,510	8%
Ra-226	9.4E-09	7,466	7.1E-09	7,050	-24%
Am-241	1.6E-13	9,501	2.5E-12	6,770	1463%
Np-237	1.1E-08	20,000	1.2E-07	20,000	991%

For the Tc-99 release from Tank 16 (see Figure 3-35 and Table 3-5), the general trend is well captured, but the spikes at 9,300 years differ by 78%. Despite this difference of 78%, the trends of the annulus releases from the two models are similar and the comparison is considered acceptable.

For Am-241 (see Figure 3-40 and Table 3-5) percent differences are well above 50% but the trends are similar. For Np-237 (see Figure 3-41 and Table 3-5) percent differences are again well above 50% but the trends are similar and the differences in magnitude reflect an early stage in the breakthrough.

Figure 3-34: Tank 16 I-129 Release to the Saturated Zone

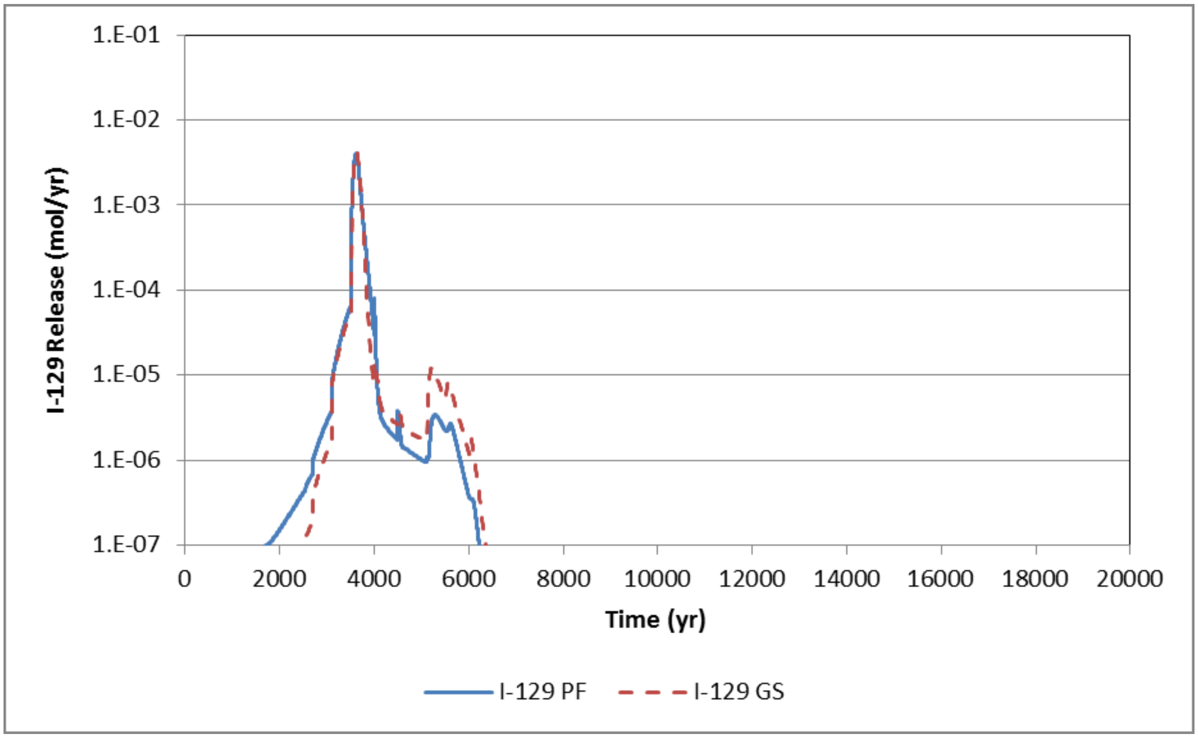

Figure 3-35: Tank 16 Tc-99 Release to the Saturated Zone

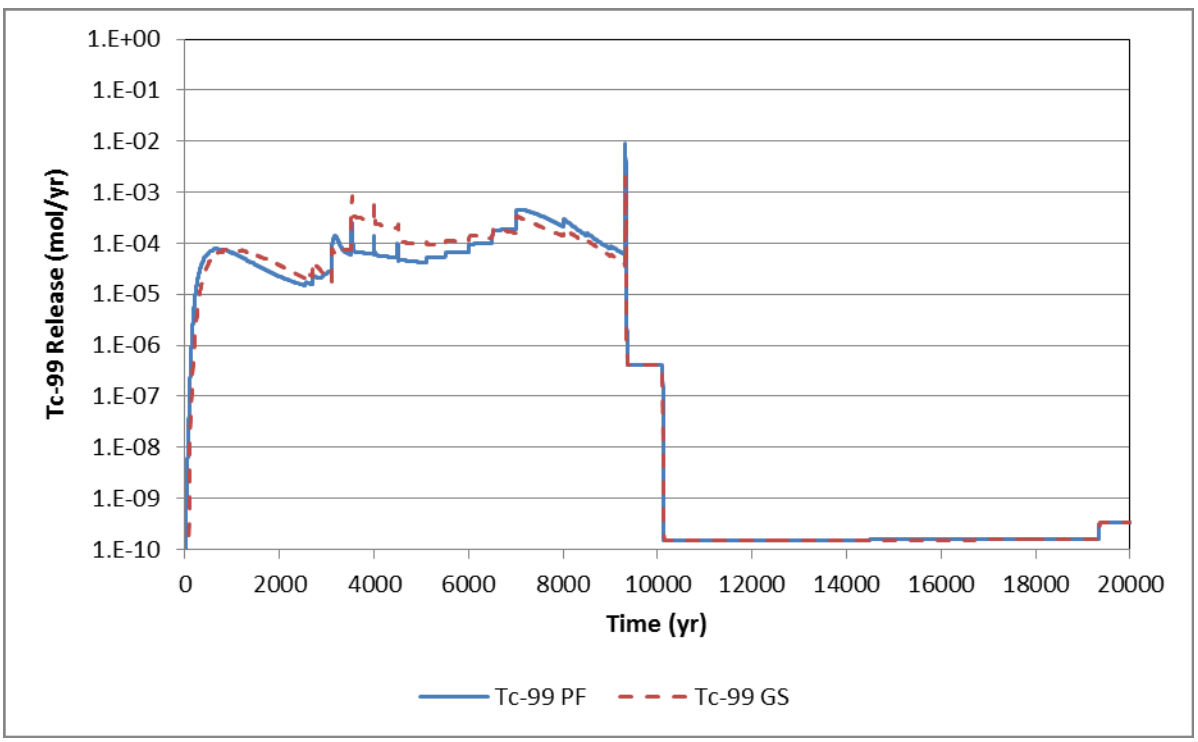

Figure 3-36: Tank 16 Am-243 Release to the Saturated Zone

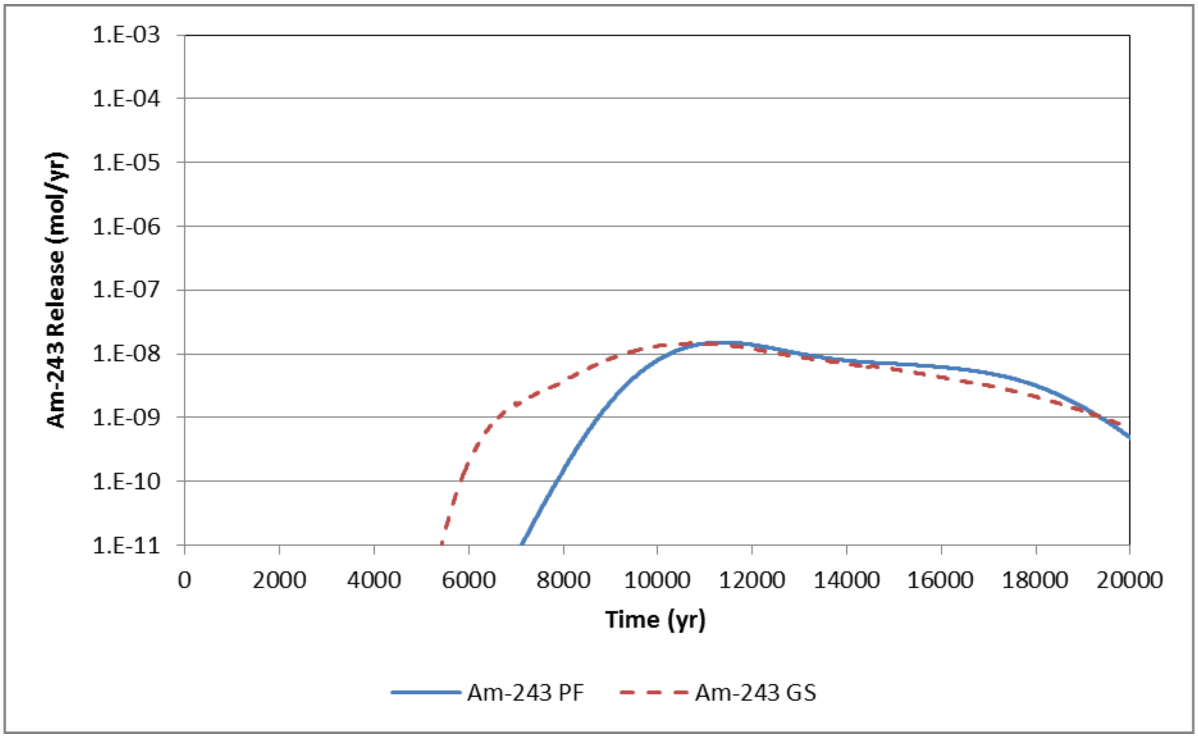

Figure 3-37: Tank 16 Pu-239 Release to the Saturated Zone

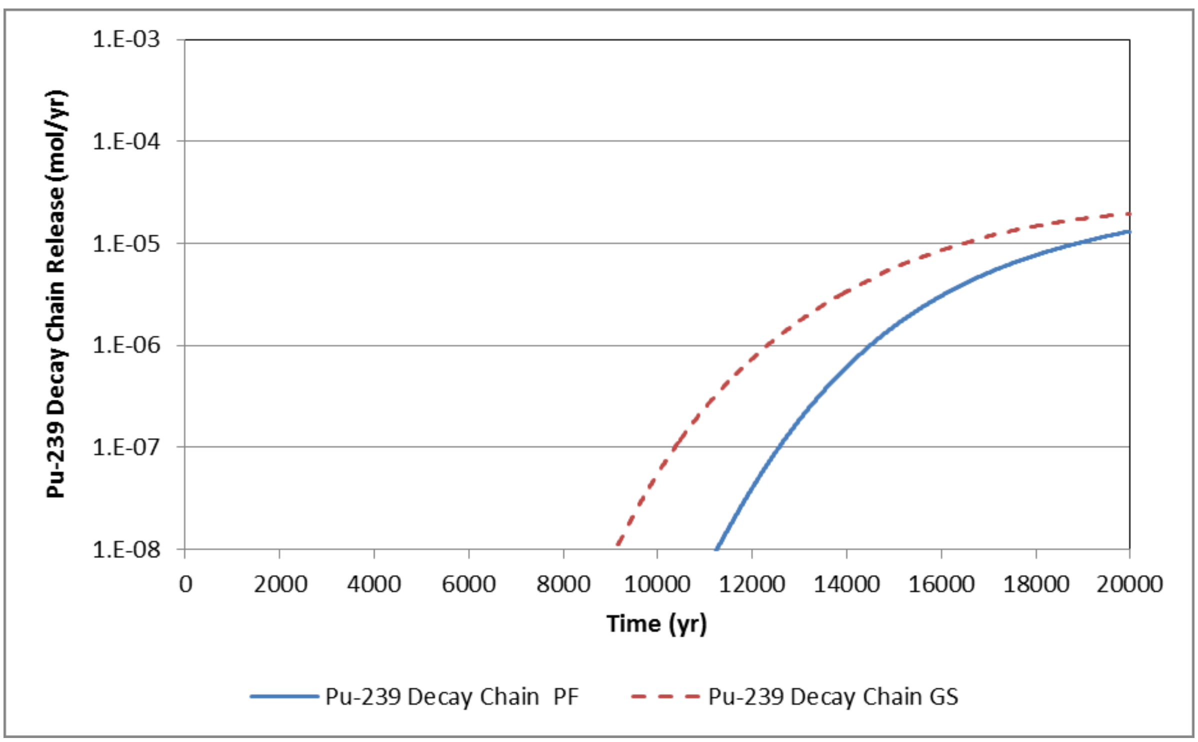

Figure 3-38: Tank 16 U-234 Release to the Saturated Zone

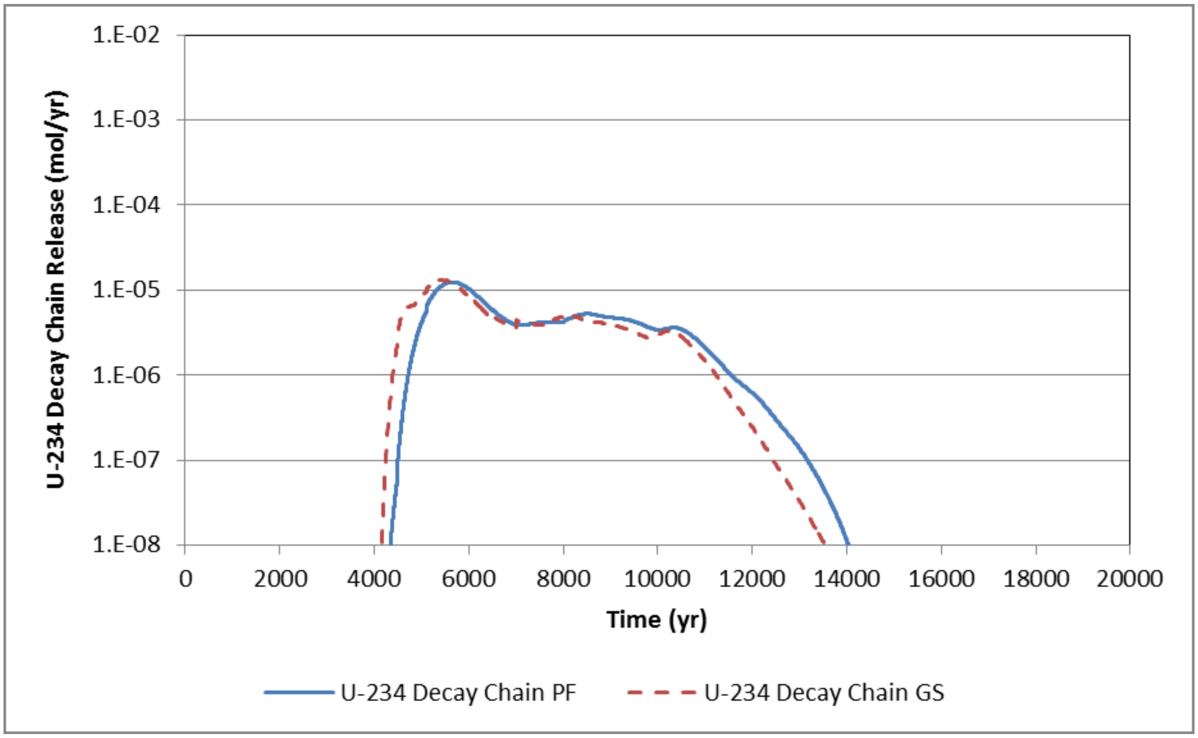

Figure 3-39: Tank 16 Ra-226 Release to the Saturated Zone

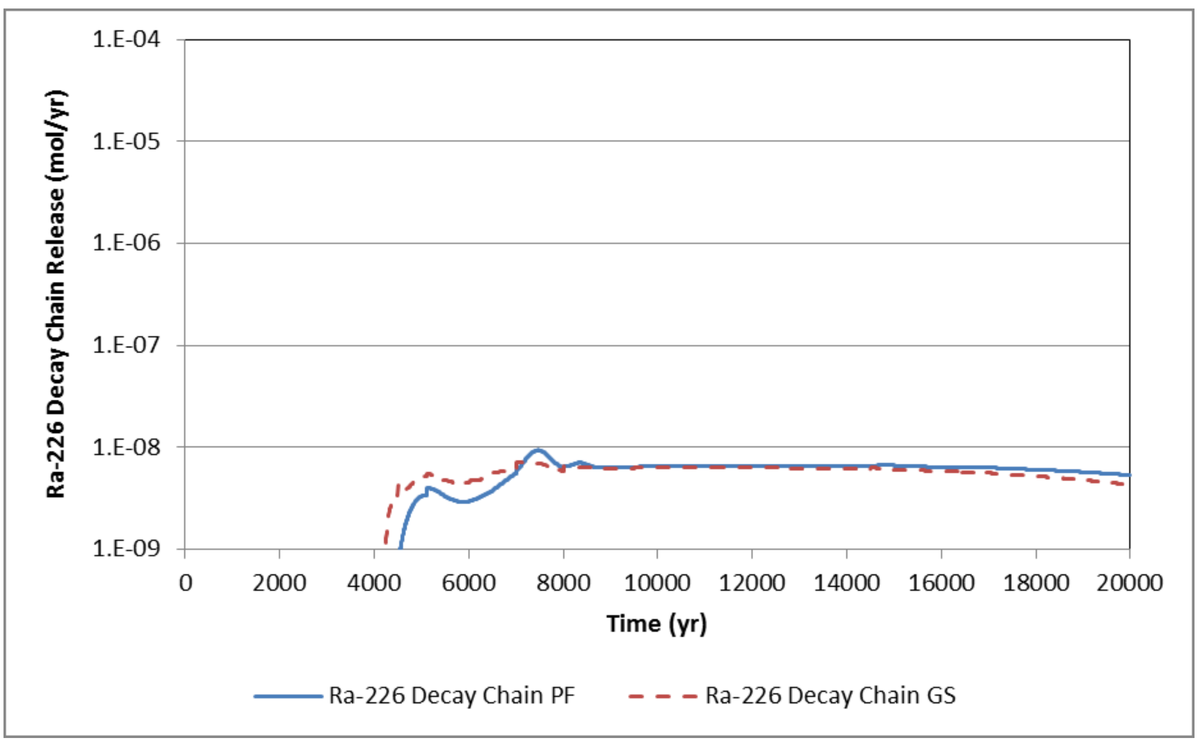

Figure 3-40: Tank 16 Am-241 Release to the Saturated Zone

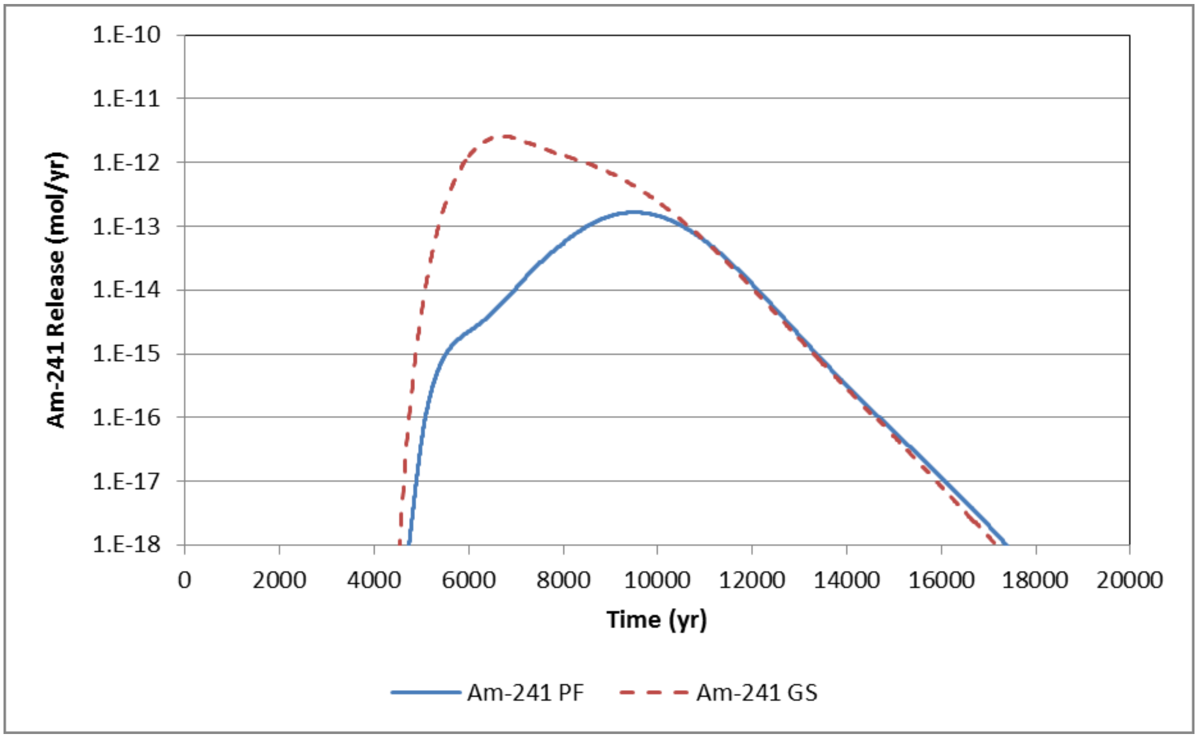

Figure 3-41: Tank 16 Np-237 Release to the Saturated Zone

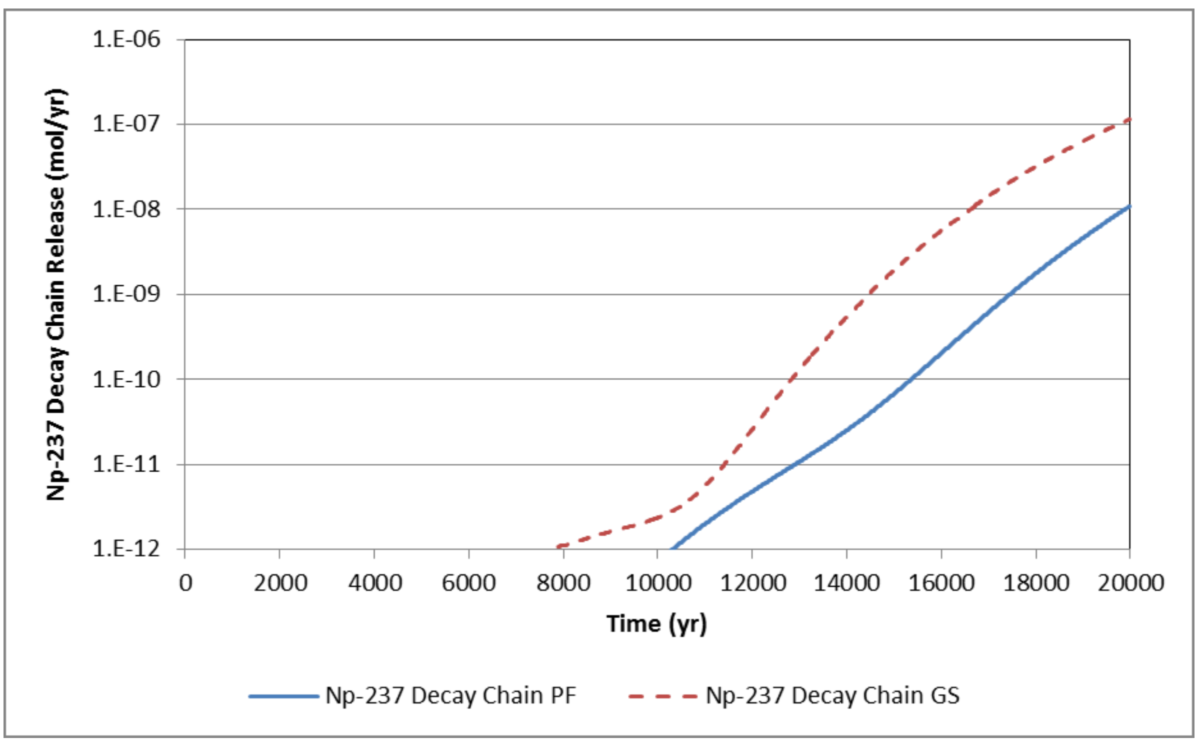

3.2.1.6 Type IV Tank (Tank 24)

A comparison of the PORFLOW HTF Model and the GoldSim HTF RAD Model mass releases of I-129, Tc-99, Am-243, Pu-239, U-234, Ra-226, Am-241, and Np-237, as presented in Figure 3-42 through Figure 3-49, indicate that the GoldSim model produces a very good approximation of the releases from Tank 24 generated by the PORFLOW model. Table 3-6 summarizes the peak values for these releases showing that when comparing the two models the percent differences, except for Am-241 are below 50%.

Table 3-6: GoldSim and PORFLOW Model Peak Release from the UZ to the SZ Comparisons for Tank 24 within 20,000 years

Radionuclide	PORFLOW Peak Release (mol/yr)	PORFLOW Time of Peak Release (yr)	GoldSim Peak Release (mol/yr)	GoldSim Time of Peak Release (yr)	Peak Release Percent Difference GoldSim vs PORFLOW
I-129	2.4E-04	3,670	2.3E-04	3,670	-4%
Tc-99	1.5E-08	11,001	1.5E-08	11,010	0%
Am-243	1.5E-07	15,765	1.5E-07	17,040	0%
Pu-239	1.8E-06	19,998	1.6E-06	20,000	-11%
U-234	2.3E-06	13,317	2.5E-06	13,540	13%
Ra-226	5.5E-08	4,725	5.7E-08	4,740	4%
Am-241	3.6E-14	6,686	1.1E-14	7,120	-69%
Np-237	1.2E-05	10,667	1.1E-05	9,750	-8%

The only species that when comparing the two models has a percent differences above 50% is Am-241 (see Figure 3-48 and Table 3-6) but the difference is still only 69% and the trends are similar.

Figure 3-42: Tank 24 I-129 Release to the Saturated Zone

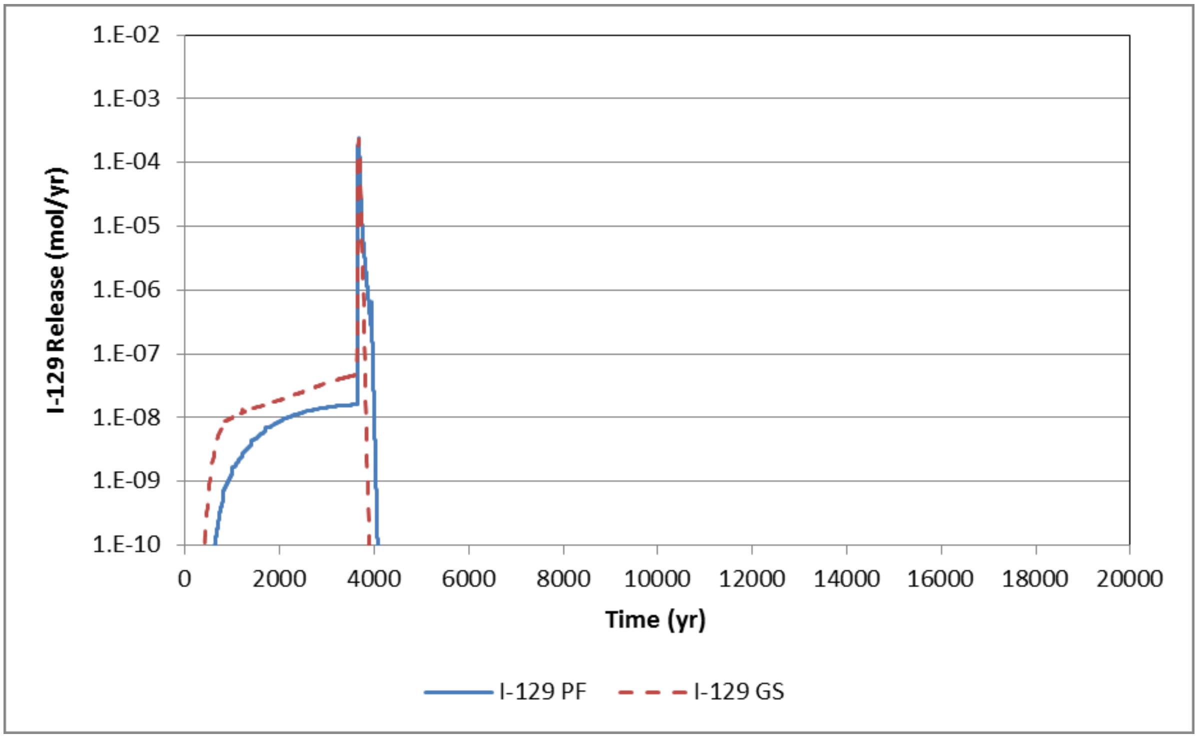

Figure 3-43: Tank 24 Tc-99 Release to the Saturated Zone

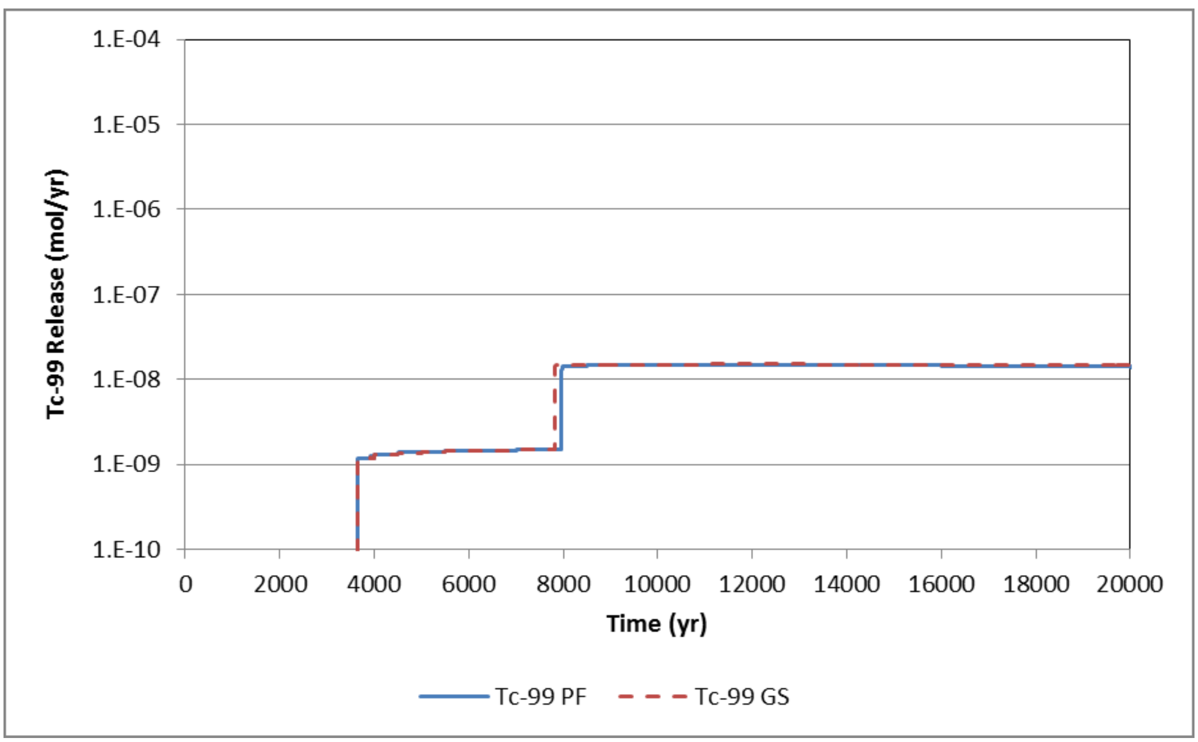

Figure 3-44: Tank 24 Am-243 Release to the Saturated Zone

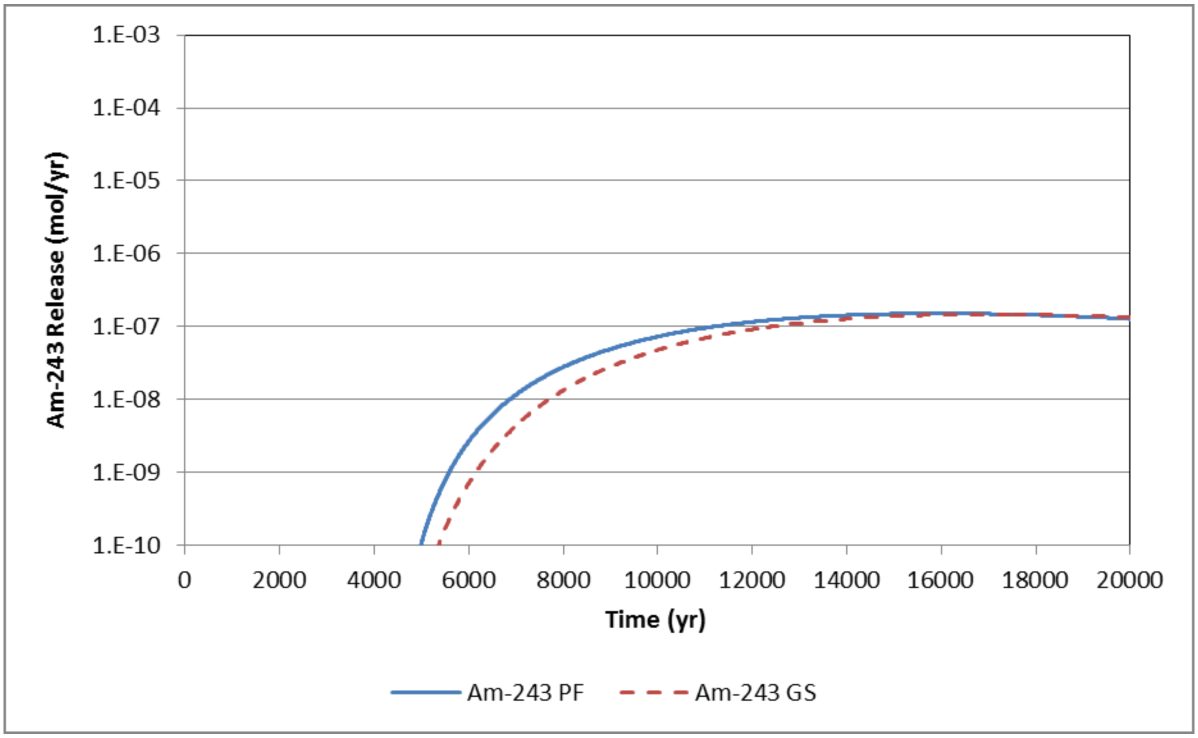

Figure 3-45: Tank 24 Pu-239 Release to the Saturated Zone

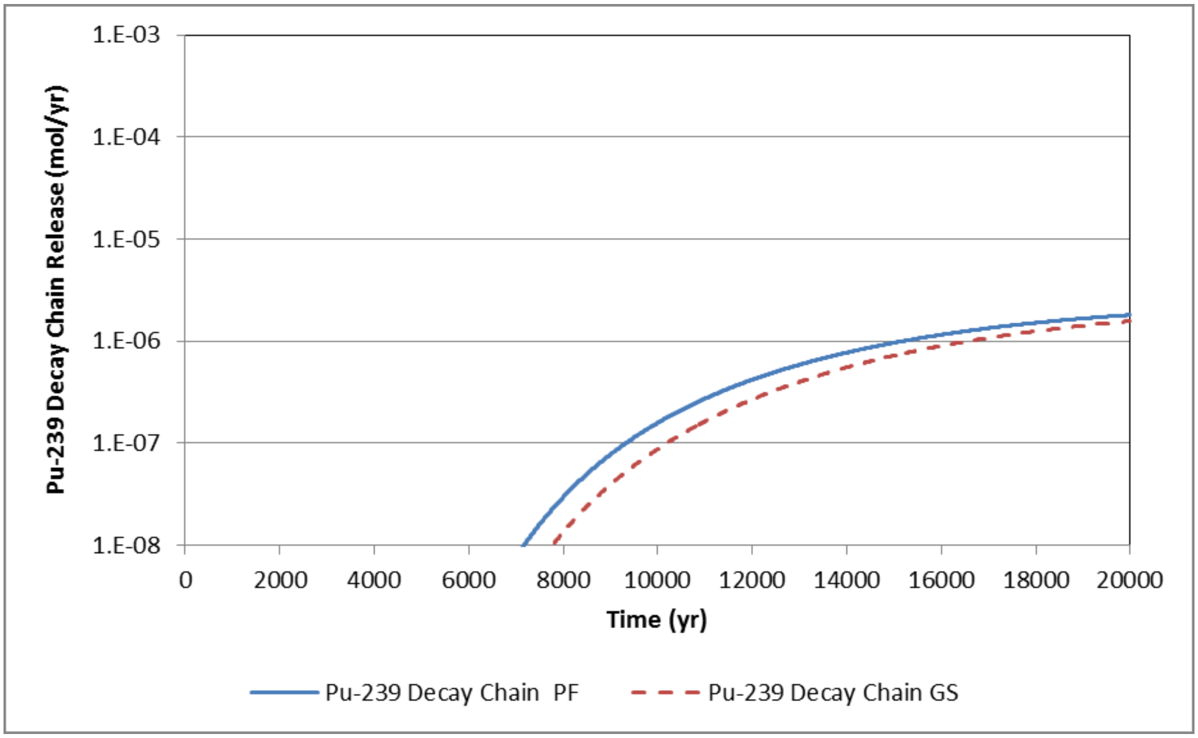

Figure 3-46: Tank 24 U-234 Release to the Saturated Zone

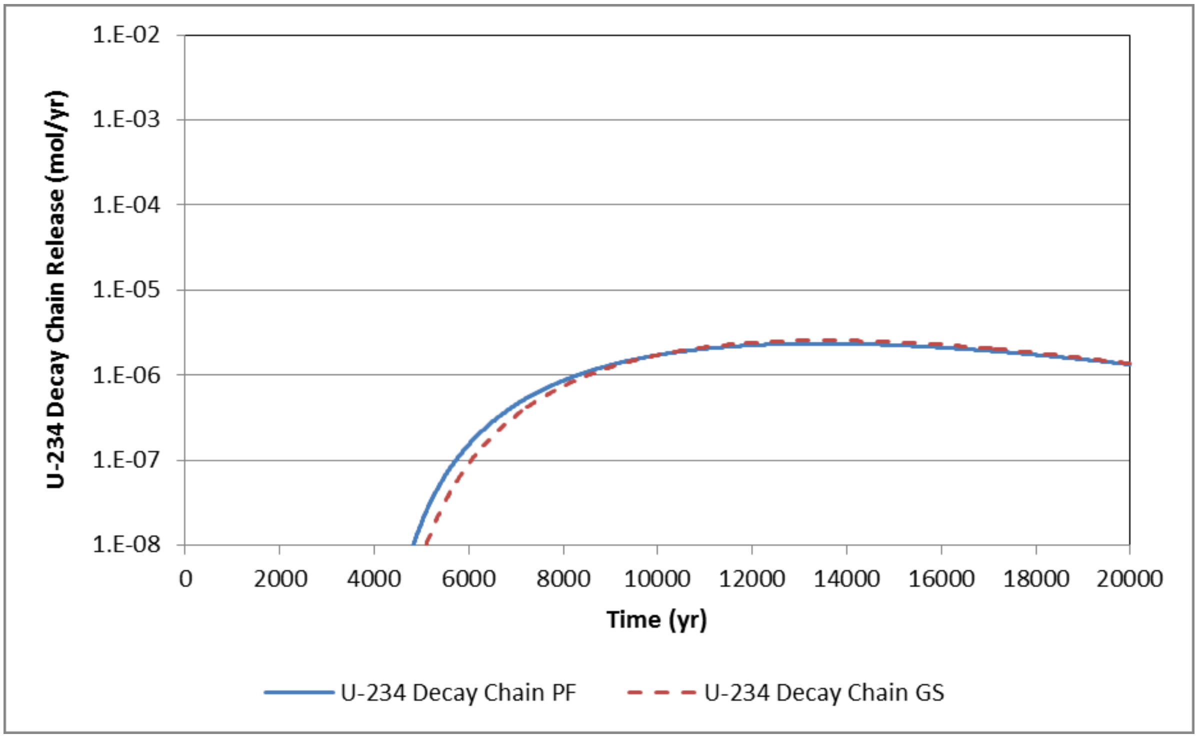

Figure 3-47: Tank 24 Ra-226 Release to the Saturated Zone

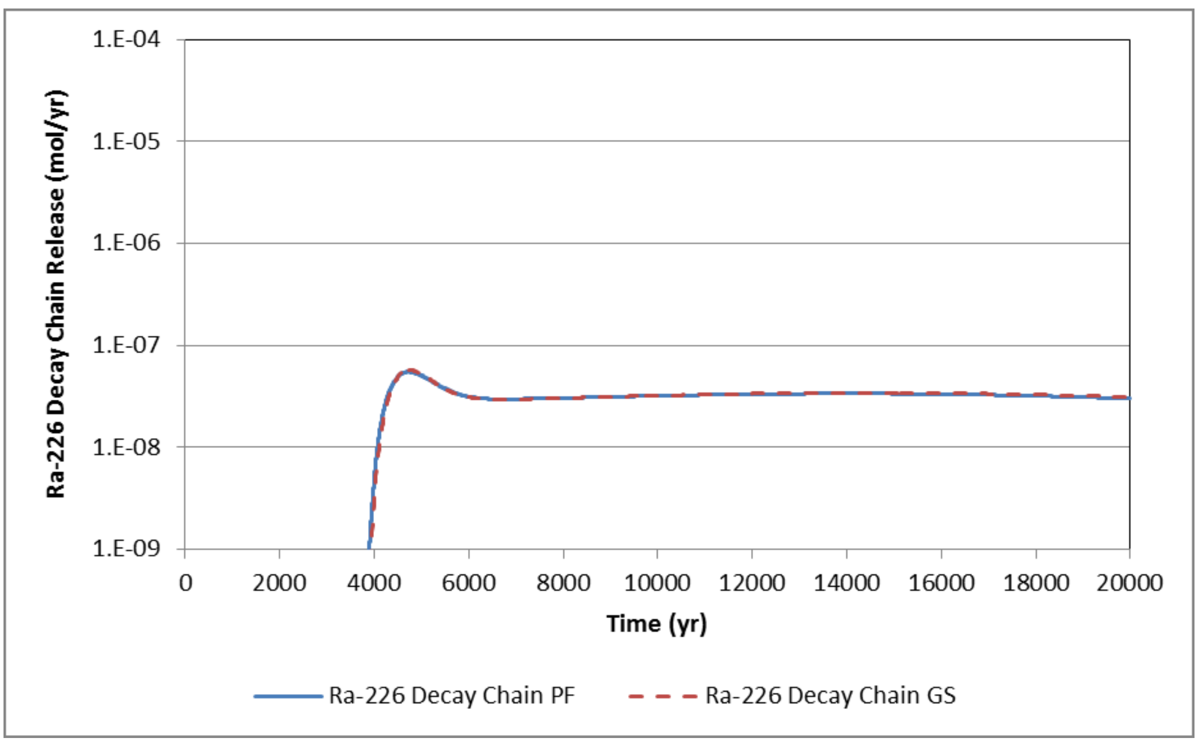

Figure 3-48: Tank 24 Am-241 Release to the Saturated Zone

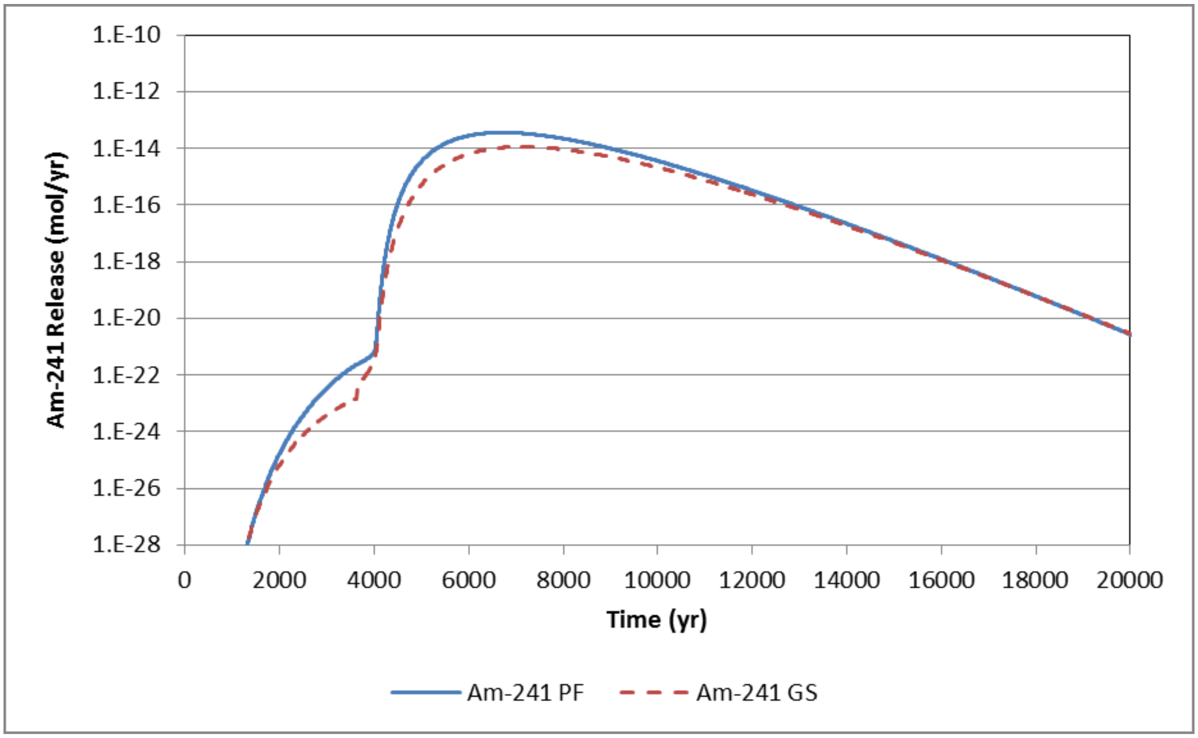

Figure 3-49: Tank 24 Np-237 Release to the Saturated Zone

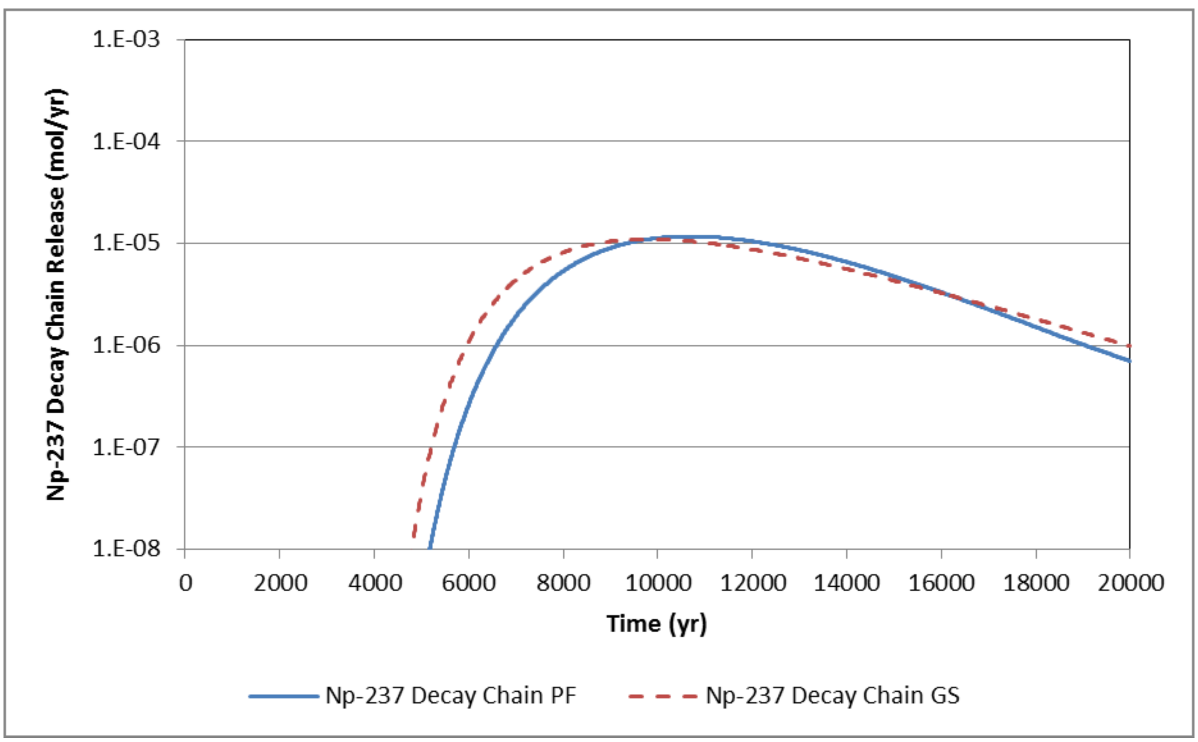

3.2.1.7 Type III Tank (Tank 31)

A comparison of the PORFLOW HTF Model and the GoldSim HTF RAD Model mass releases of I-129, Tc-99, Am-243, Pu-239, U-234, Ra-226, Am-241, and Np-237, as presented in Figure 3-50 through Figure 3-57, indicate that the GoldSim model generally produces a good approximation of the releases from Tank 31 generated by the PORFLOW model. Table 3-7. summarizes the peak values for these releases showing that except for Pu-239, U-234, and Np-237, when comparing the two models the percent differences are below 50%.

Table 3-7: GoldSim and PORFLOW Model Peak Release from the UZ to the SZ Comparisons for Tank 31 within 20,000 years

Radionuclide	PORFLOW Peak Release (mol/yr)	PORFLOW Time of Peak Release (yr)	GoldSim Peak Release (mol/yr)	GoldSim Time of Peak Release (yr)	Peak Release Percent Difference GoldSim vs PORFLOW
I-129	3.6E-03	12,874	3.7E-03	12,870	3%
Tc-99	1.6E-08	19,208	1.7E-08	19,230	6%
Am-243	2.5E-16	20,000	2.1E-16	20,000	-16%
Pu-239	5.5E-16	20,000	1.2E-15	19,990	118%
U-234	7.2E-07	20,000	2.3E-06	20,000	219%
Ra-226	4.1E-07	14,879	5.0E-07	14,600	22%
Am-241	1.2E-27	20,000	9.9E-28	20,000	-18%
Np-237	1.4E-13	20,000	6.1E-16	20,000	-100%
Np-237[1]	1.4E-13	20,000	1.8E-14	20,000	-87%

[1] Used coarser discretization on basemat.

Results for Pu-239 (Figure 3-53 and Table 3-7), U-234 (Figure 3-54 and Table 3-7), and Np-237 (Figure 3-57 and Table 3-7), reflect early differences in model results associated with early breakthrough times (for strongly sorbed species). Figure 3-57 also shows that by increasing the numerical dispersion (decreasing the number of mixing cells in the basemat) in the GoldSim model, a closer match is obtained.

Figure 3-50: Tank 31 I-129 Release to the Saturated Zone

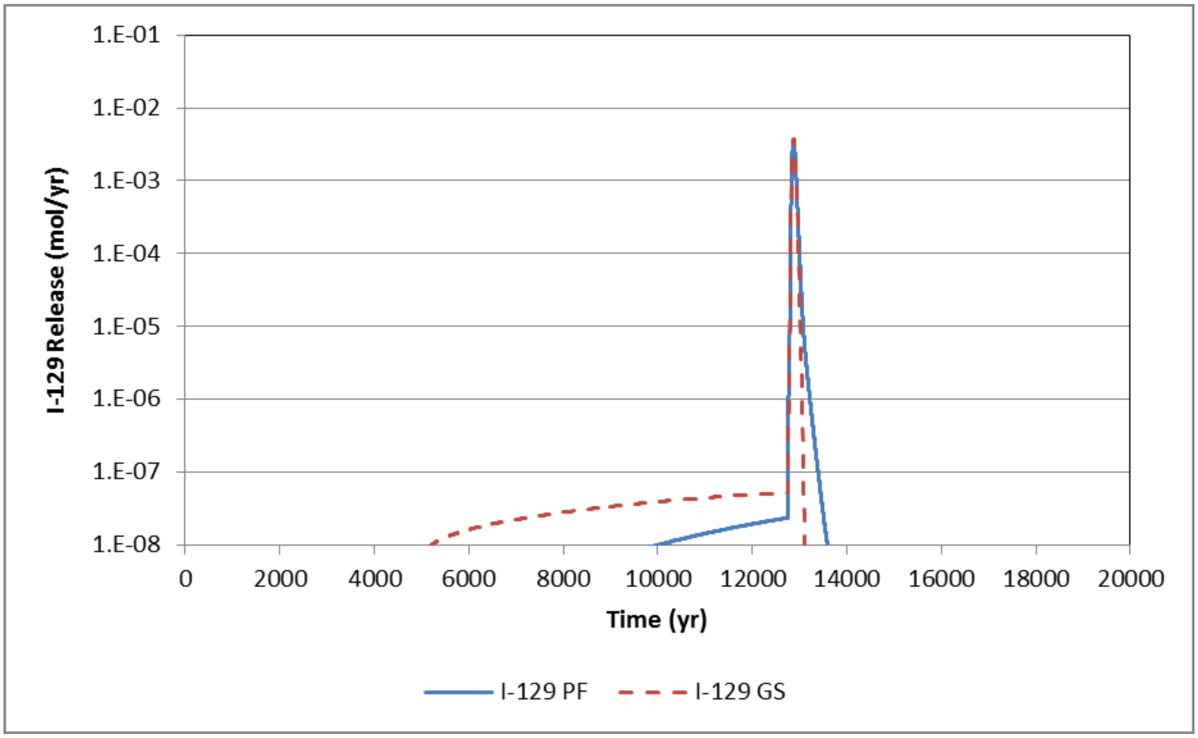

Figure 3-51: Tank 31 Tc-99 Release to the Saturated Zone

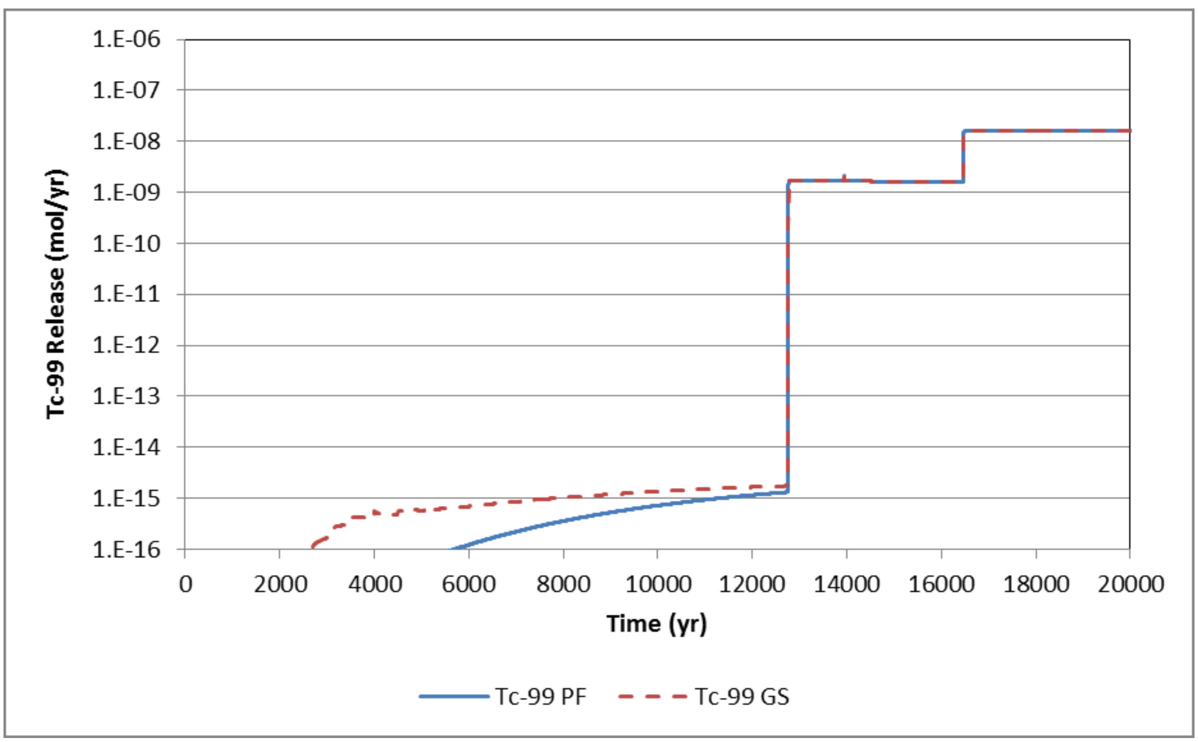

Figure 3-52: Tank 31 Am-243 Release to the Saturated Zone

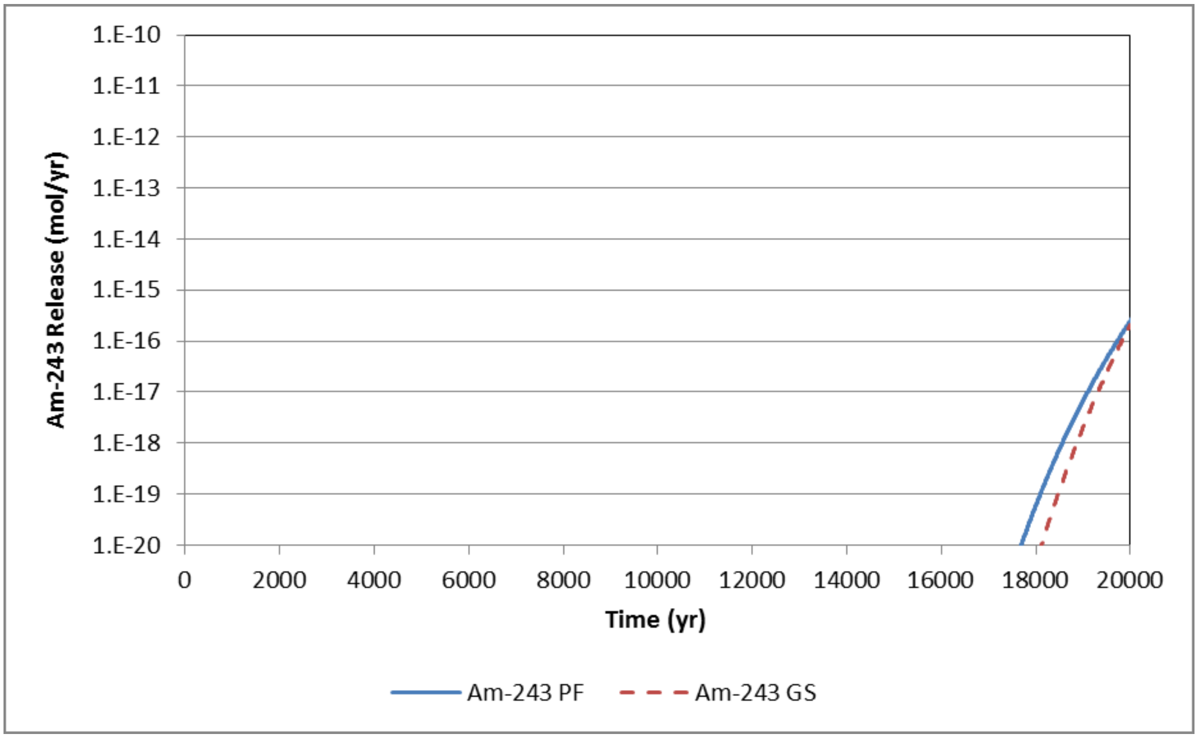

Figure 3-53: Tank 31 Pu-239 Release to the Saturated Zone

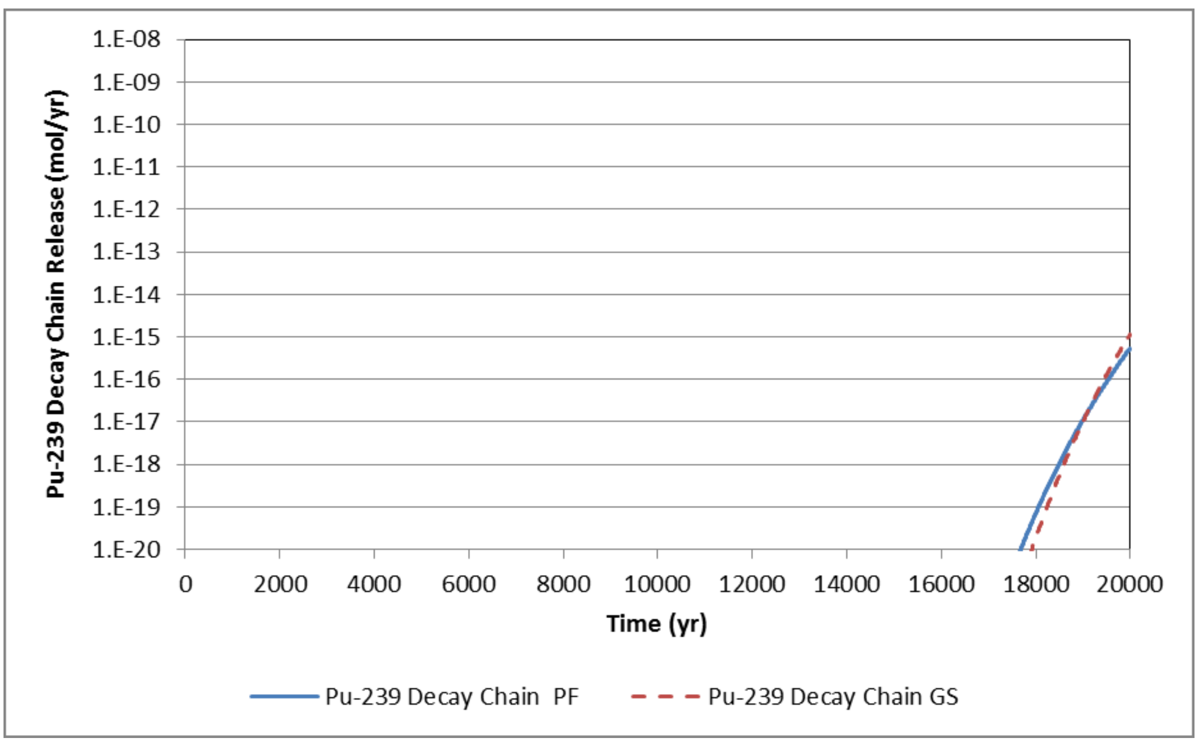

Figure 3-54: Tank 31 U-234 Release to the Saturated Zone

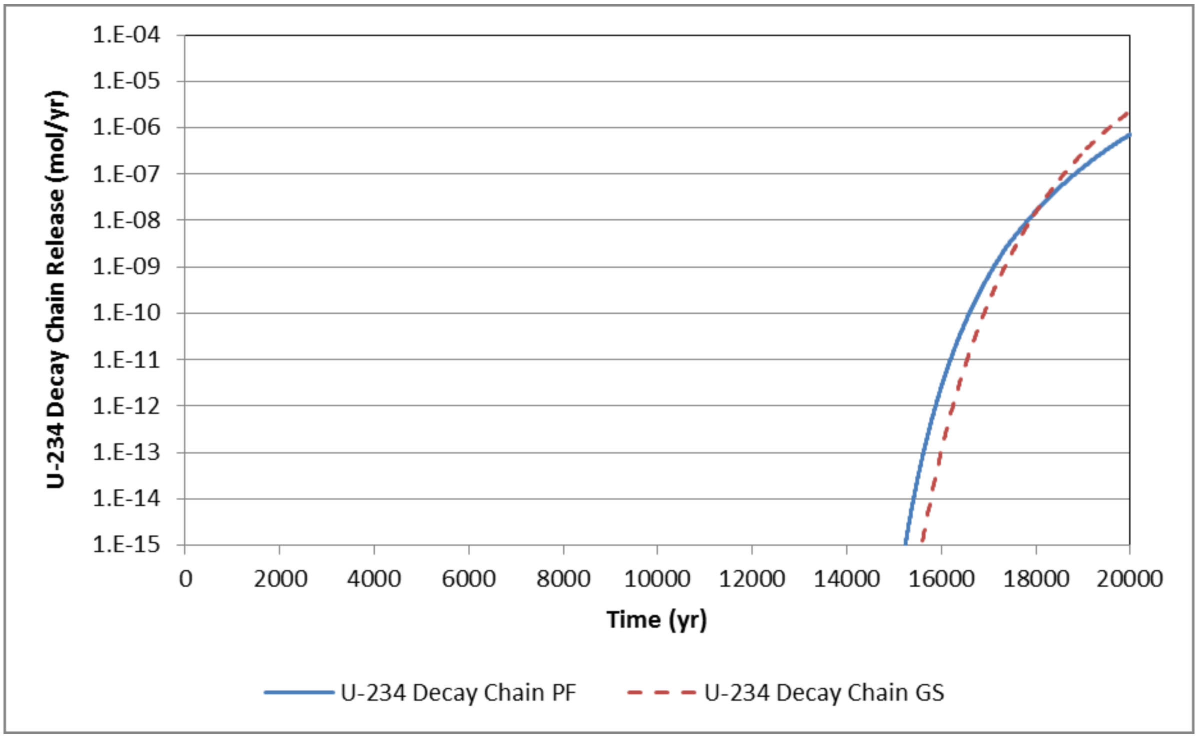

Figure 3-55: Tank 31 Ra-226 Release to the Saturated Zone

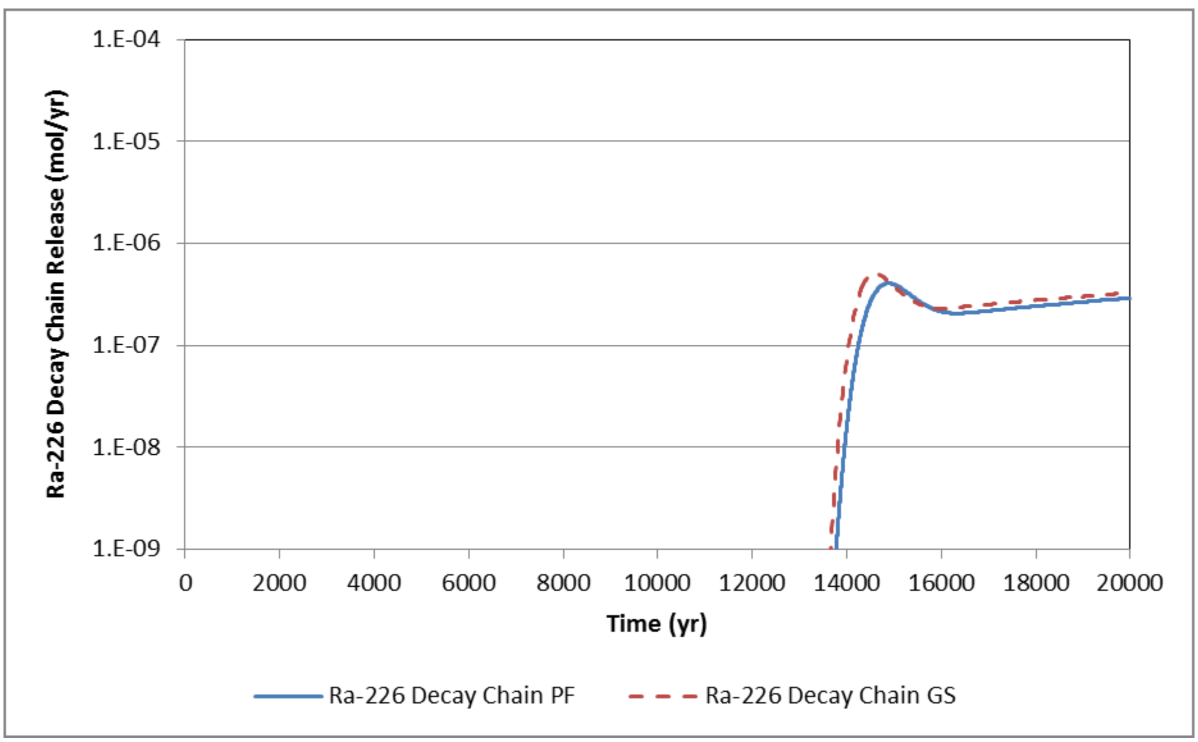

Figure 3-56: Tank 31 Am-241 Release to the Saturated Zone

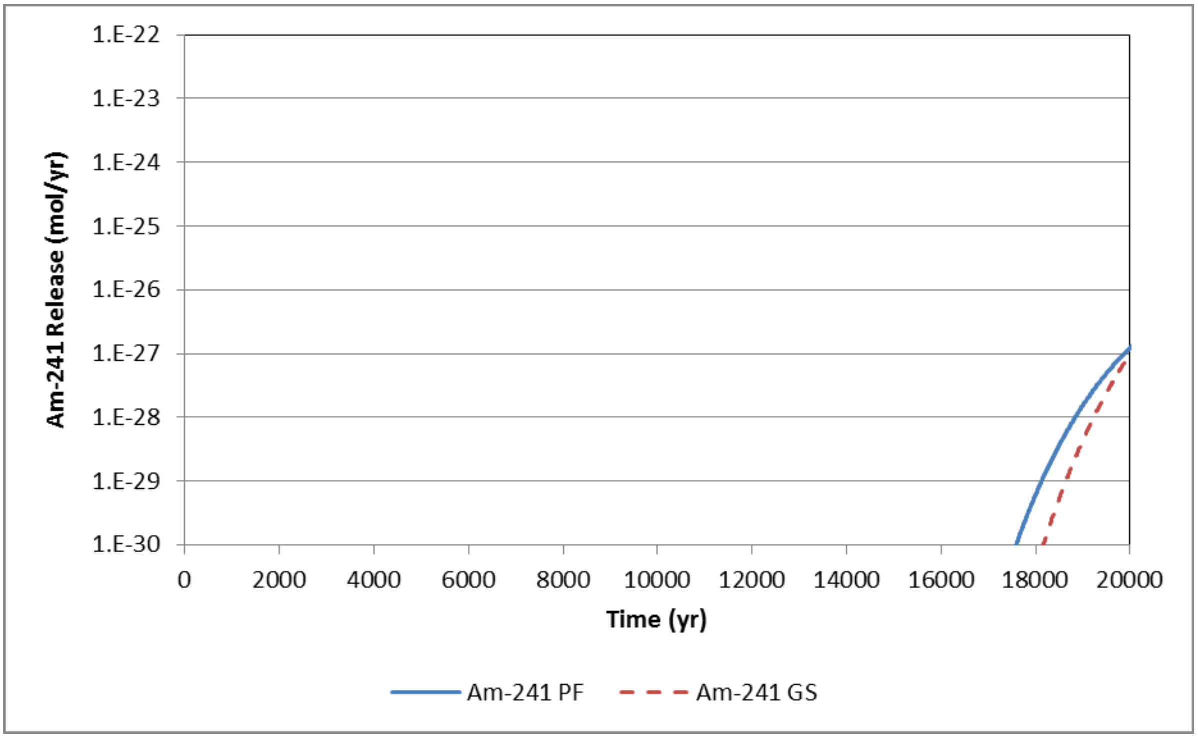

Figure 3-57: Tank 31 Np-237 Release to the Saturated Zone

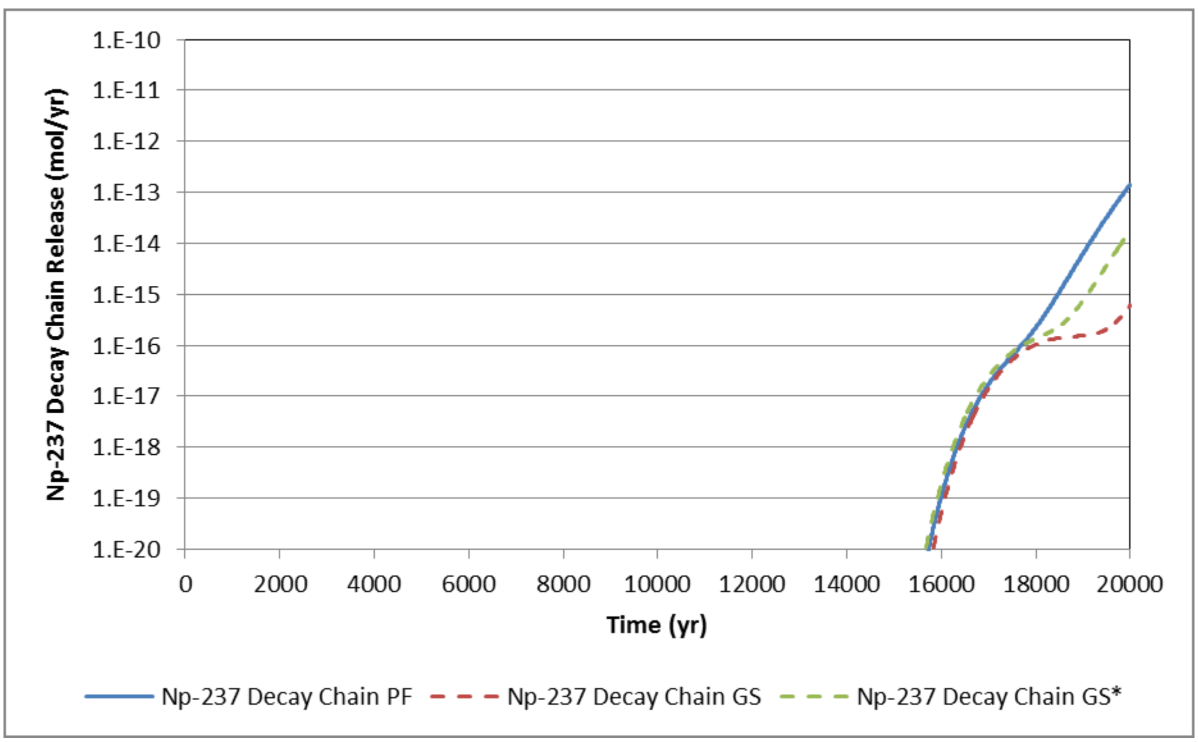

* Np-237 modeled using coarser discretization on basemat.

3.2.2 Phase 2: Radionuclide Doses at the 100-Meter Boundary

The second phase of the benchmarking process focuses on examining how well the abstracted model approximates the radionuclide transport behavior in the SZ to the 100-meter boundary. Radionuclide doses (in mrem/yr) in five sectors (A, B, C, E, and F), were examined for this task (Figure 3-58 through Figure 3-62). The 100-meter dose for each boundary sector is based upon the maximum concentration in each set of wells, based on the sectors shown in Figure 3-1. Sector D was omitted from this analysis because in the GoldSim model pathlines from the HTF tanks do not cross this sector (Figure 3-1). Dose comparisons between PORFLOW and GoldSim HTF Model results showed the most consistency in Sector A where pathlines generated from single-particles released from the tank-centers, migrated relatively straight to Sector A of the 100-meter boundary. For this exercise, PORFLOW and GoldSim model dose curves for four species (I-129, Np-237, Ra-226, and Tc-99), were examined.

3.2.2.1 Sector A

An examination of PORFLOW- and GoldSim-generated radionuclide dose contributions presented in Figure 3-58 indicates that the GoldSim model can provide a computationally efficient approximation of 100-meter boundary radionuclide dose contributions in Sector A. There is a good consistency in the trends observed in the two sets of model results throughout the 20,000-year simulation. The basic dilution/attenuation processes in the SZ are captured by the abstraction. Note that there are also differences but they will have little impact on the utility of the abstraction model to evaluate peak doses.

Figure 3-58 also shows that the GoldSim concentrations decrease at a faster rate than in the HTF PORFLOW model. One reason for the difference is the nature of the locations for a specific sector from which the maximum value can be chosen at each time step. In PORFLOW, a vertical plane through the surface trace defining each sector is evaluated for concentrations at each node within the plane, with the maximum nodal value representing the sector value. This vertical plane may be parallel or oblique to a particle released from the tank centroid. In the abstracted GoldSim model five to six locations along each sector line are evaluated (for each time step) and the maximum value from a sector's set of locations is chosen as the value for that specific sector.

Figure 3-58: Maximum Dose Contributions at the 100-Meter Boundary, Sector A

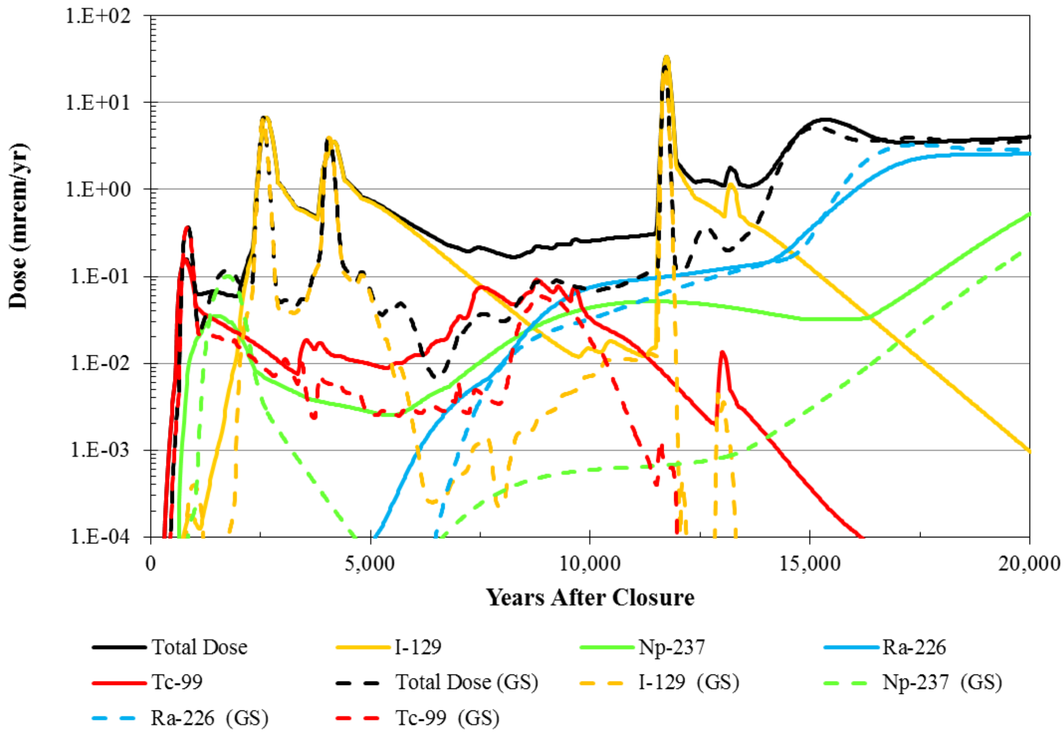

To simplify the analysis, each location along a sector line is assumed to be oriented perpendicular to the pathline of a particle released from the tank centroid. The degree of influence of a specific tank release on a specific location is then based on the one-dimensional transport calculation for concentration at the point of contact between the particle pathline and the sector line. The concentration is then adjusted for the influence of transverse dispersion based on its location relative to the pathline/sector-line contact. This simplification dictates that the more perpendicular a particle pathline is to a sector line, the more accurately the transverse dispersion effects can be approximated along the sector line.

When the pathline is perpendicular to the sector line peak values occur at the same time for all points along the sector line. This minimizes a pseudo-dispersive effect generated by changing evaluation locations over time as done in the PORFLOW model analysis. The difference in the breakthrough curves is also associated with the occurrence of storage zones such as the “green clay” layer (i.e., the Gordon Confining Unit), which are modeled explicitly in the PORFLOW model, but not in the GoldSim HTF Model. The “green clay” layer provides a storage zone for more sorptive elements which are subsequently slowly released over time. Since the dose-contribution curves differ at well below peak levels, the simplification in the GoldSim HTF Model is acceptable.

3.2.2.2 Sector B

An examination of PORFLOW- and GoldSim-generated radionuclide dose contributions presented in Figure 3-59 indicates that the GoldSim model can provide a computationally efficient approximation of 100-meter boundary radionuclide dose contributions in Sector B.

There is a good consistency in the trends observed in the two sets of model results throughout the 20,000-year simulation. The basic dilution/attenuation processes in the SZ are captured by the abstraction. Note that there are also differences but they will have little impact on the utility of the abstraction model to evaluate peak doses.

Figure 3-59: Maximum Dose Contributions at the 100-Meter Boundary, Sector B

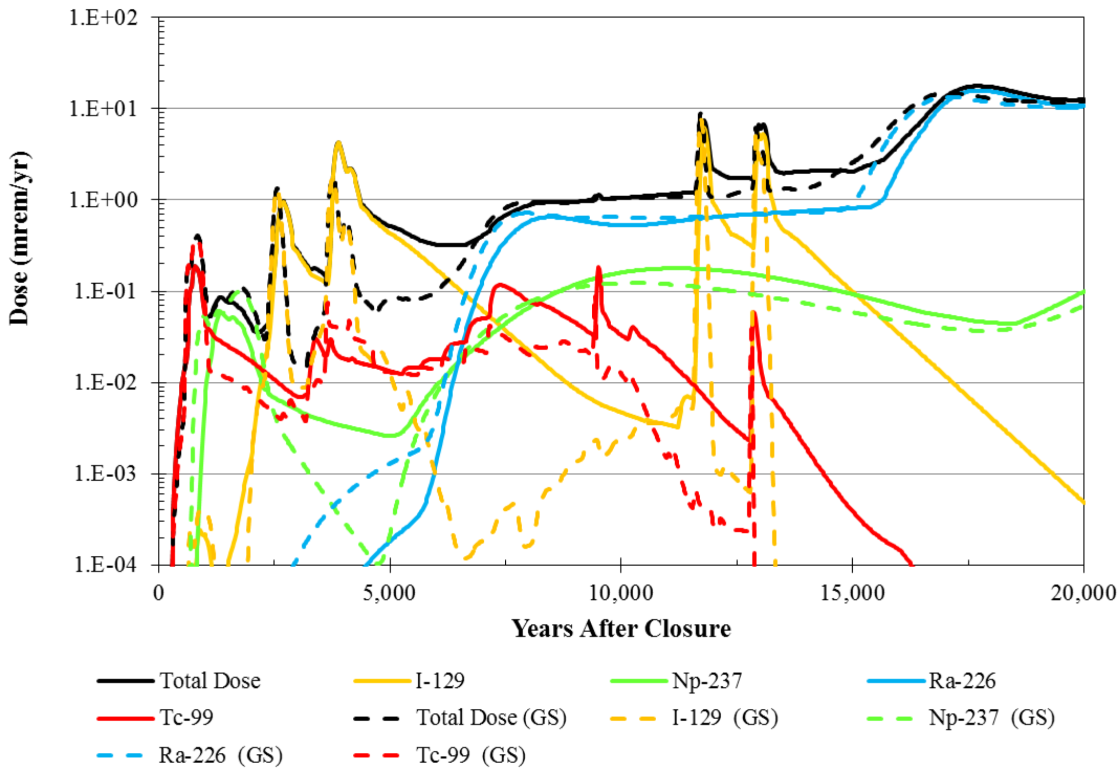

3.2.2.3 Sector C

An examination of PORFLOW- and GoldSim-generated radionuclide dose contributions presented in Figure 3-60 indicates that the model can provide a computationally efficient approximation of 100-meter boundary radionuclide dose contributions in Sector C. There is a good consistency in the trends observed in the two sets of model results throughout the 20,000-year simulation. The basic dilution/attenuation processes in the SZ are captured by the abstraction. Note that there are also differences but they will have little impact on the utility of the abstraction model to evaluate peak doses.

Figure 3-60: Maximum Dose Contributions at the 100-Meter Boundary, Sector C

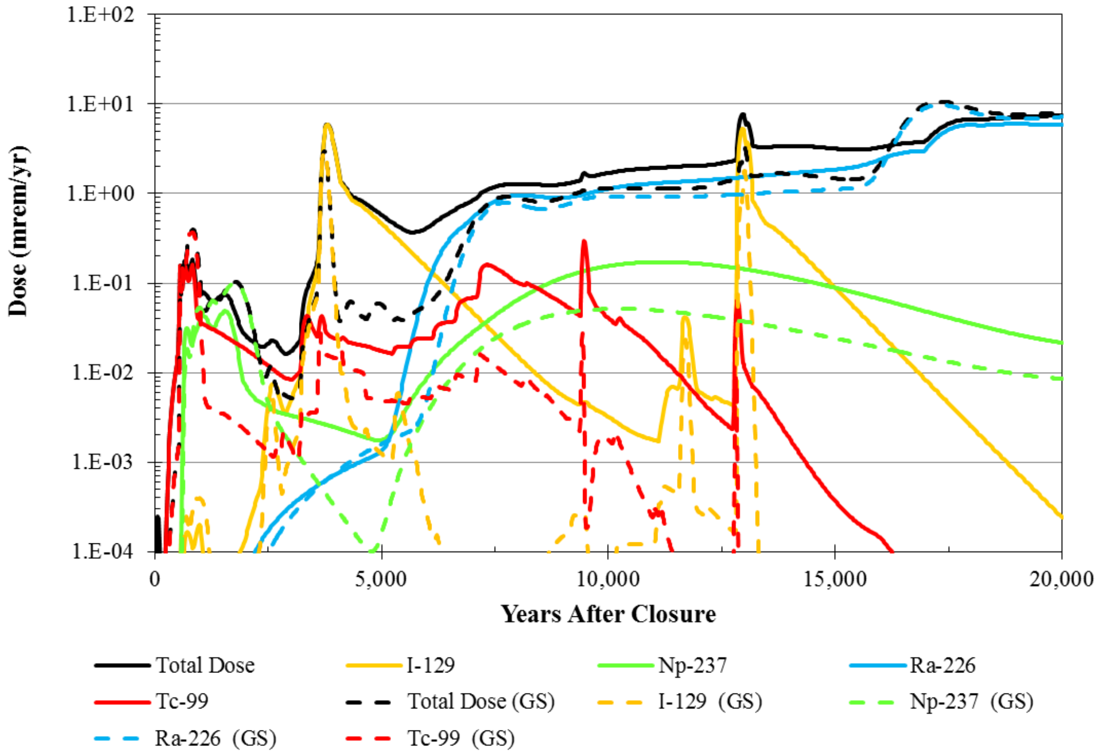

3.2.2.4 Sector E

An examination of PORFLOW- and GoldSim-generated radionuclide dose contributions presented in Figure 3-61 indicates that the GoldSim model can provide a computationally efficient approximation of 100-meter boundary radionuclide dose contributions in Sector E. There is a good consistency in the trends observed in the two sets of model results throughout the 20,000-year simulation. The basic dilution/attenuation processes in the SZ are captured by the abstraction. Note that there are also differences but they will have little impact on the utility of the abstraction model to evaluate peak doses.

Figure 3-61: Maximum Dose Contributions at the 100-Meter Boundary, Sector E

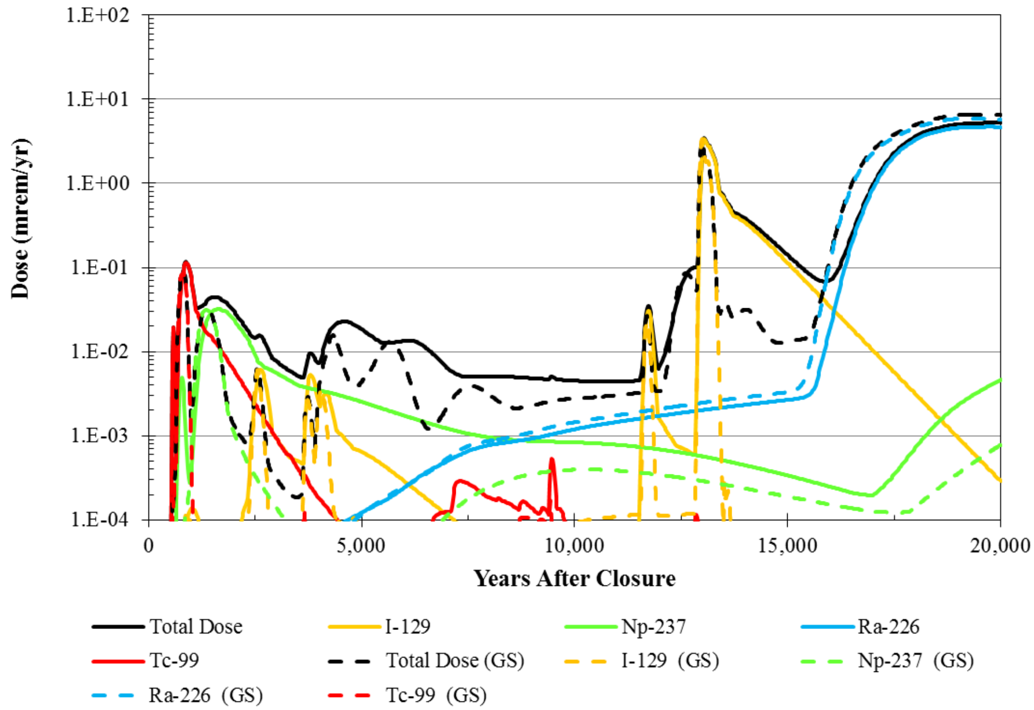

3.2.2.5 Sector F

An examination of PORFLOW- and GoldSim-generated radionuclide dose contributions presented in Figure 3-62 indicates that the GoldSim model can provide a computationally efficient approximation of 100-meter boundary radionuclide dose contributions in Sector F. There is a good consistency in the trends observed in the two sets of model results early and late during the 20,000-year simulation. The basic dilution/attenuation processes in the SZ are captured by the abstraction. Note that peak doses not well accounted for are low compared to peak doses well accounted for in Sectors A, B, and C.

Figure 3-62: Maximum Dose Contributions at the 100-Meter Boundary, Sector F

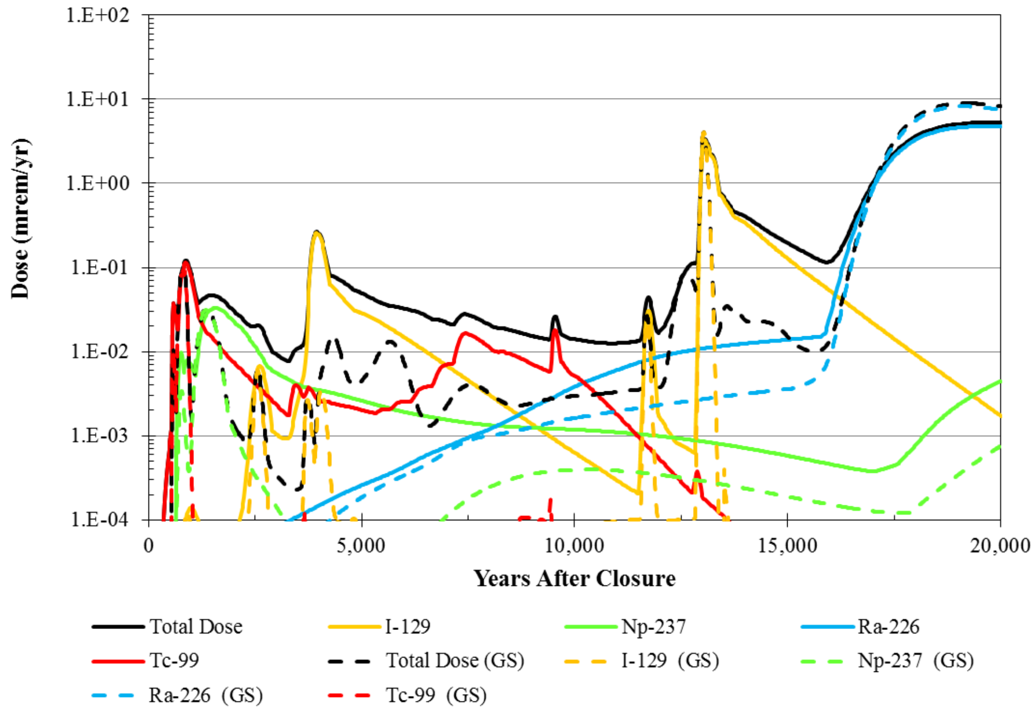

3.2.2.6 Maximum MOP Dose Time Histories

The next phase of the benchmarking process focuses on examining how well the abstracted model approximates the MOP dose results. Comparisons of the maximum total MOP doses (in millirem per year) generated by the two models form the basis of the benchmarking effort along with a comparison of dose contributions from the major contributing radionuclides.

Figure 3-63 provides a comparison of the maximum dose-contribution curves from the major species, regardless of sector, for both the PORFLOW and the GoldSim models. This figure shows that the GoldSim HTF Radionuclide Stochastic Fate and Transport Model closely approximates the maximum dose results calculated from the PORFLOW model. Figure 3-64 provides a comparison of the maximum dose curves, regardless of sector, for both the PORFLOW and the GoldSim models. This figure illustrates that the GoldSim HTF Radionuclide Stochastic Fate and Transport Model closely approximates the maximum dose results calculated from the PORFLOW model.

Despite the GoldSim model simplifications, the similarity between GoldSim model results and PORFLOW model results justifies the use of the GoldSim HTF Radionuclide Stochastic Fate and Transport Model for evaluating parameter sensitivity and the influence of parameter uncertainty on the system to support DOE decision-making related to reasonable expectation/assurance that performance objectives will be met for the HTF.

Figure 3-63: Maximum Dose Contributions at the 100-Meter Boundary

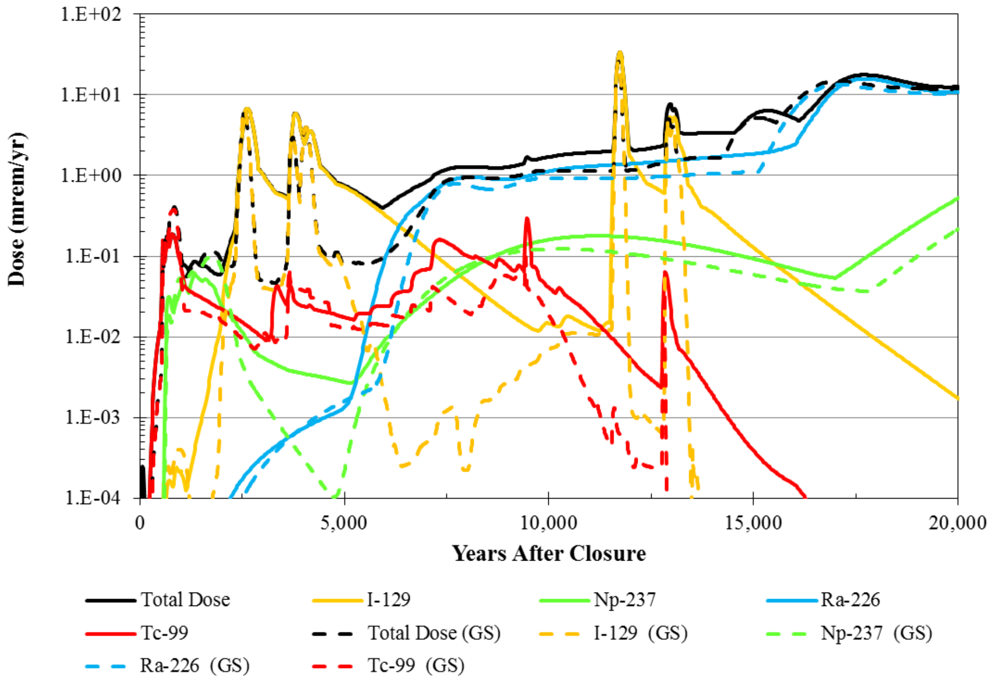

Figure 3-64: Maximum Dose from all Sources at the 100-Meter Boundary

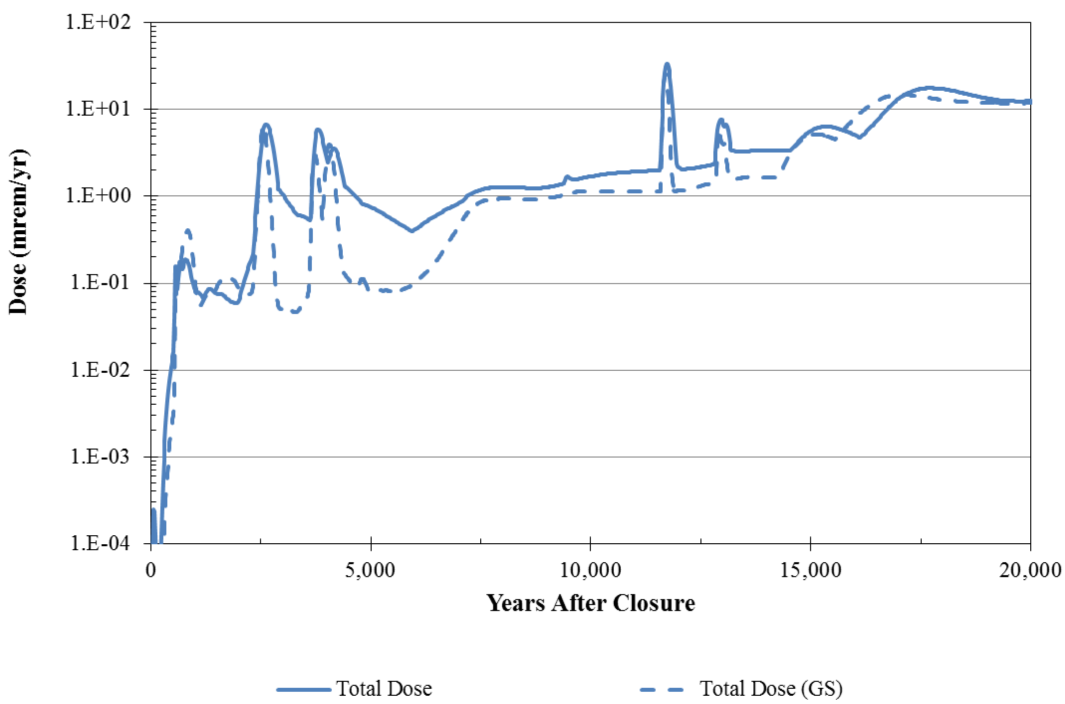

3.2.3 Phase 3: Radionuclide Doses at the 1-Meter Boundary

The third phase of the benchmarking process focuses on examining how well the abstracted model approximates the radionuclide transport behavior in the SZ, specifically to the 1-meter facility boundary (Figure 3-1). Radionuclide doses (in mrem/yr) in all six sectors (A through F), were examined for this task. Solubility controls for Am, Cm, Th, and U were turned off in the GoldSim model during this portion of the benchmarking process to better mimic conditions in the PORFLOW model. The reported dose for each sector along the 1-meter boundary is based upon the maximum concentration recorded at that sector's 1-meter wells (similar to the analysis performed in Section 3.2.2 for the 100-meter boundary).

Dose comparisons between PORFLOW and GoldSim HTF Model results showed excellent agreement in all HTF Sectors except Sector D. In Sector D, the HTF GoldSim model still provided a satisfactory approximation of the PORFLOW dose results at the 1-meter boundary, however the three dimensional flow behavior described by PORFLOW was more difficult to capture for this sector in the one-dimensional GoldSim model. For this exercise, PORFLOW and GoldSim model dose curves for four species (I-129, Np-237, Ra-226, and Tc-99), were examined.

3.2.3.1 Sector A

An examination of PORFLOW- and GoldSim-generated radionuclide dose contributions presented in Figure 3-65 indicates that the GoldSim model can provide a computationally efficient approximation of 1-meter boundary radionuclide dose contributions in Sector A. There is a good consistency in the trends observed in the two sets of model results throughout the 20,000-year simulation. The basic dilution/attenuation processes in the SZ are captured by the abstraction. Note that there are also differences but they will have little impact on the utility of the abstraction model to evaluate peak doses.

Figure 3-65 also shows that the GoldSim concentrations decrease at a faster rate than the HTF PORFLOW Model. One reason for the difference is the nature of the locations for a specific sector from which the maximum value can be chosen at each time step. In the HTF PORFLOW Model, a vertical plane through the surface trace defining each sector (see Figure 3-1) is evaluated for concentrations at each node within the plane, with the maximum nodal value representing the sector value. This vertical plane may be parallel or oblique to a particle released from the tank centroid. In the abstracted GoldSim model four locations along each sector line are evaluated (for each time step) and the maximum value from a sector's set of locations is chosen as the value for that specific sector.

To simplify the analysis, each location along a sector line is assumed to be oriented perpendicular to the pathline of a particle released from the tank centroid. The degree of influence of a specific tank release on a specific location is then based on the one-dimensional transport calculation for concentration at the point of contact between the particle pathline and the sector line. The concentration is then adjusted for the process of transverse dispersive process based on its location relative to the pathline/sector-line contact. This simplification dictates that the more perpendicular a particle pathline is to a sector line, the more accurately the transverse dispersion effects can be approximated along the sector line.

When the pathline is perpendicular to the sector line peak values occur at the same time for all points along the sector line. This minimizes a pseudo-dispersive effect generated by changing evaluation locations over time as done in the PORFLOW model analysis. The difference in the breakthrough curves is also associated with the occurrence of storage zones such as the "green clay" layer (i.e., the Gordon Confining Unit), which are modeled explicitly in the PORFLOW model, but not in the GoldSim HTF Model. The "green clay" layer provides a storage zone for more sorptive elements, from which, the radionuclides are released slowly over time. Since the dose-contribution curves differ at well below peak levels, the simplification in the GoldSim HTF Model is not important in dose calculations.

Figure 3-65: Maximum Dose Contributions at the 1-Meter Boundary, Sector A

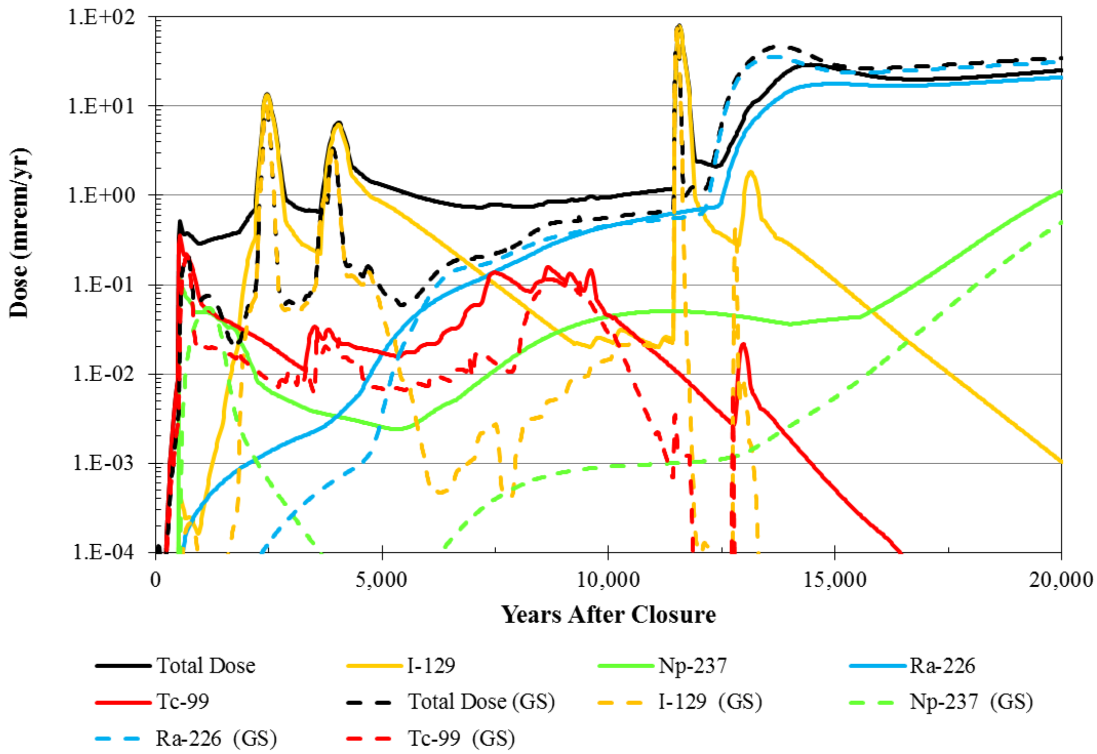

3.2.3.2 Sector B

An examination of PORFLOW- and GoldSim-generated radionuclide dose contributions presented in Figure 3-66 indicates that the GoldSim model can provide a computationally efficient approximation of 1-meter boundary radionuclide dose contributions in Sector B. There is a good consistency in the trends observed in the two sets of model results throughout the 20,000-year simulation. The basic dilution/attenuation processes in the SZ are captured by the abstraction. Note that there are also differences but they will have little impact on the utility of the abstraction model to evaluate peak doses.

Figure 3-66: Maximum Dose Contributions at the 1-Meter Boundary, Sector B

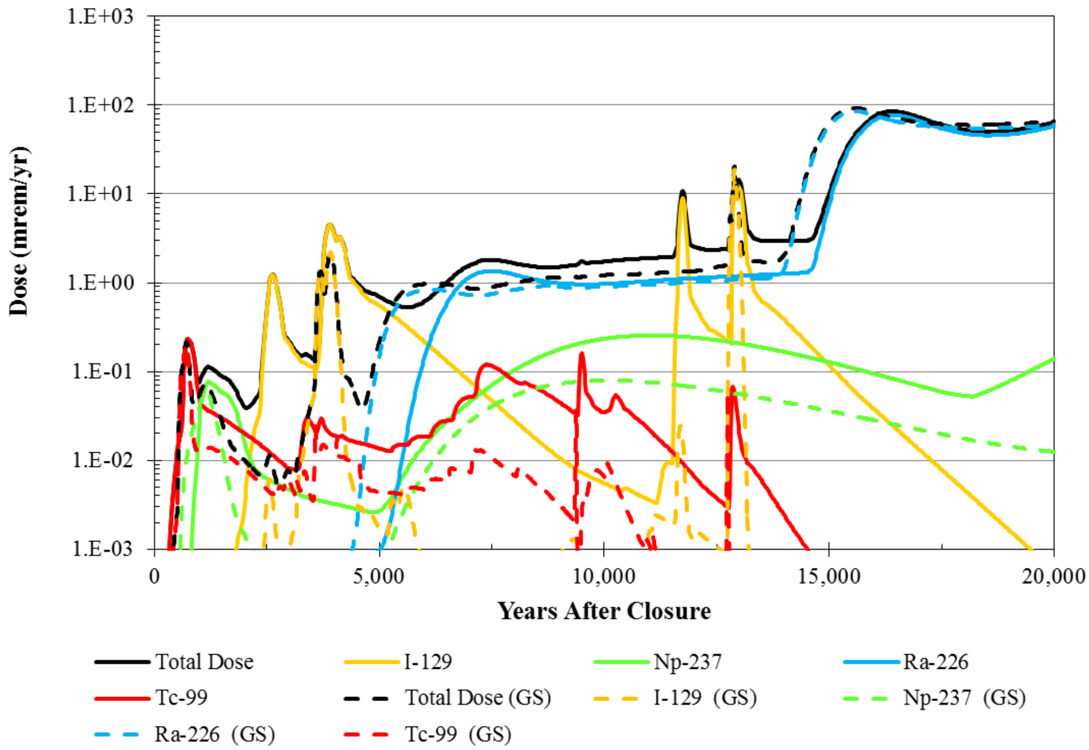

3.2.3.3 Sector C

An examination of PORFLOW- and GoldSim-generated radionuclide dose contributions presented in Figure 3-67 indicates that the GoldSim model can provide a computationally efficient approximation of 1-meter boundary radionuclide dose contributions in Sector C. There is a good consistency in the trends observed in the two sets of model results throughout the 20,000-year simulation. The basic dilution/attenuation processes in the SZ are captured by the abstraction. Note that there are also differences but they will have little impact on the utility of the abstraction model to evaluate peak doses.

Figure 3-67: Maximum Dose Contributions at the 1-Meter Boundary, Sector C

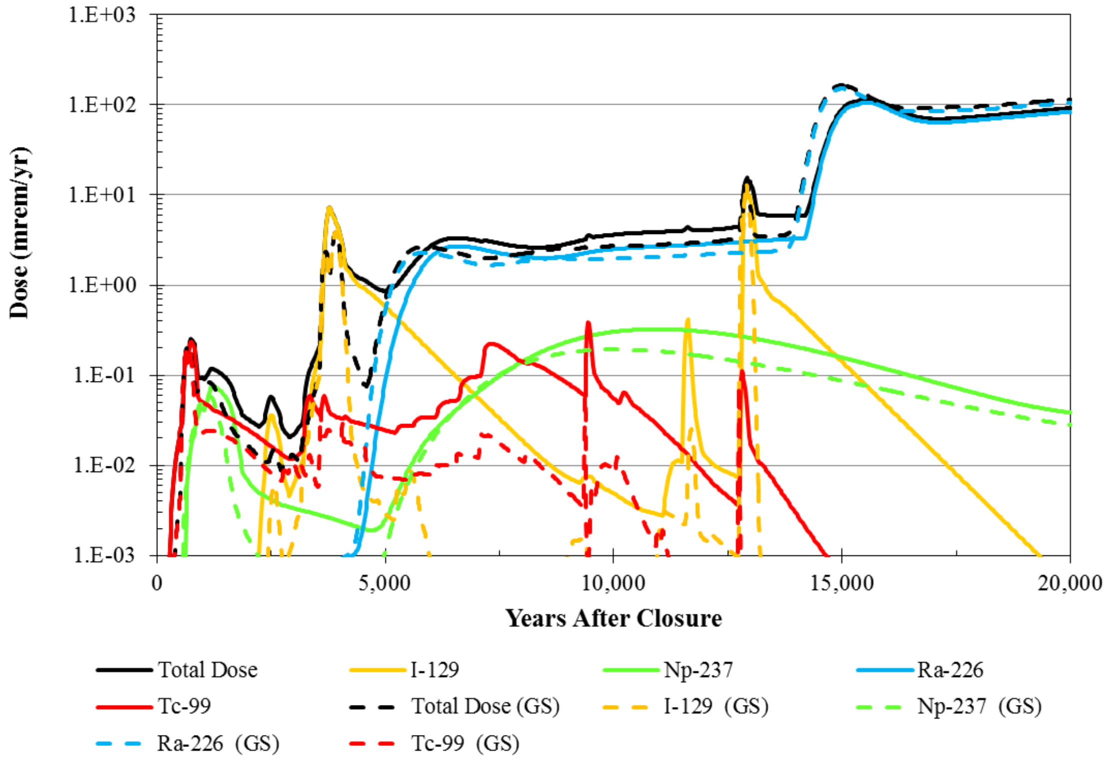

3.2.3.4 Sector D

An examination of PORFLOW- and GoldSim-generated radionuclide dose contributions presented in Figure 3-68 indicates that the GoldSim model can provide a computationally efficient approximation of 1-meter boundary radionuclide dose contributions in Sector D. Note that because of the proximity of the Type II tanks to Sector D of the 1-meter IHI boundary, Cm-248 and Am-243 can be important dose contributors along Sector D and are therefore included in Figure 3-68. There is a good consistency in the trends observed in the two sets of model results except near the end of the 20,000-year simulation. This difference is a function of the appearance of Am-243 and Cm-248 in the PORFLOW results while the GoldSim model allows solubility limit competition between americium isotopes and curium isotopes which can delay the release of Am-243 and Cm-248, respectively.

Figure 3-68: Maximum Dose Contributions at the 1-Meter Boundary, Sector D

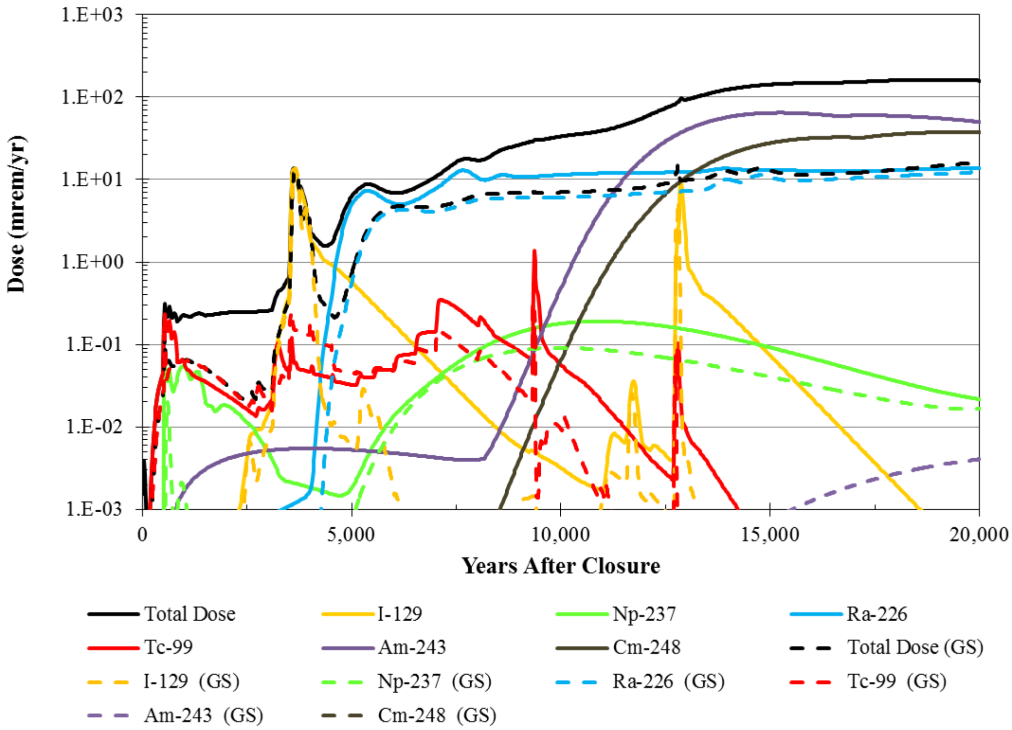

3.2.3.5 Sector E

An examination of PORFLOW- and GoldSim-generated radionuclide dose contributions presented in Figure 3-69 indicates that the GoldSim model can provide a computationally efficient approximation of 1-meter boundary radionuclide dose contributions in Sector E. There is good consistency in the trends observed in the two sets of model results throughout the 20,000-year simulation. The basic dilution/attenuation processes in the SZ are captured by the abstraction. Note that there are also differences but they will have little impact on the utility of the abstraction model to evaluate peak doses.

Figure 3-69: Maximum Dose Contributions at the 1-Meter Boundary, Sector E

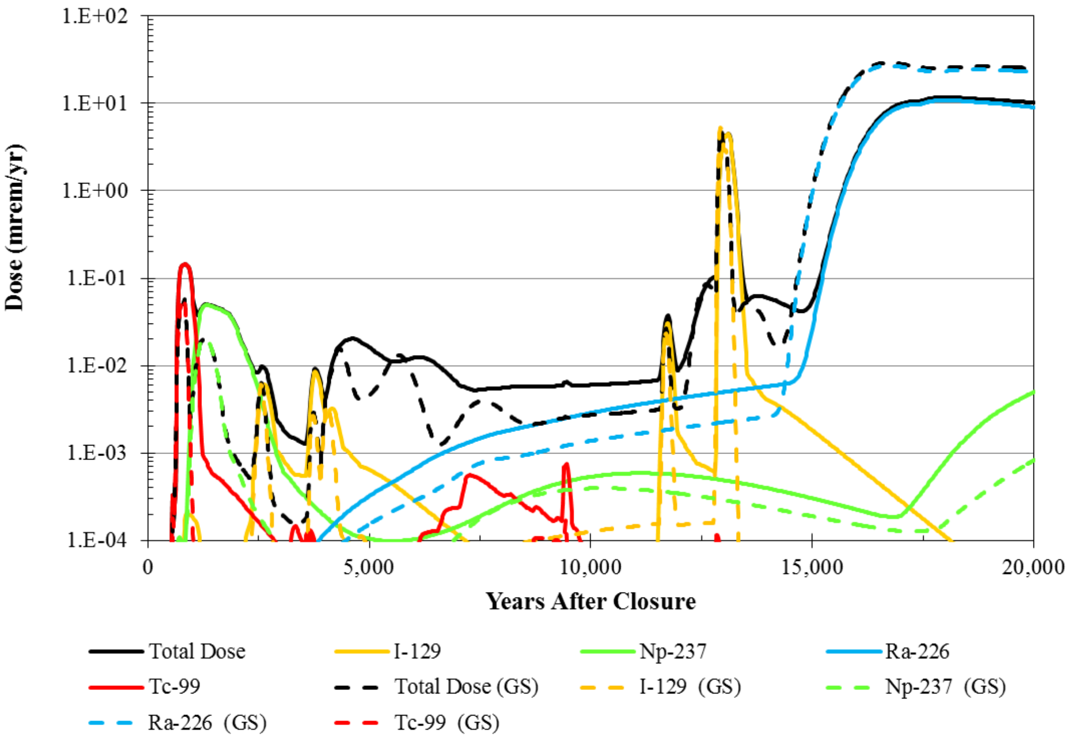

3.2.3.6 Sector F

An examination of PORFLOW- and GoldSim-generated radionuclide dose contributions presented in Figure 3-70 indicates that the model can provide a computationally efficient approximation of 1-meter boundary radionuclide dose contributions in Sector F. There is good consistency in the trends observed in the two sets of model results throughout the 20,000-year simulation. The basic dilution/attenuation processes in the SZ are captured by the abstraction. Note that there are also differences but they will have little impact on the utility of the abstraction model to evaluate peak doses.

Figure 3-70: Maximum Dose Contributions at the 1-Meter Boundary, Sector F

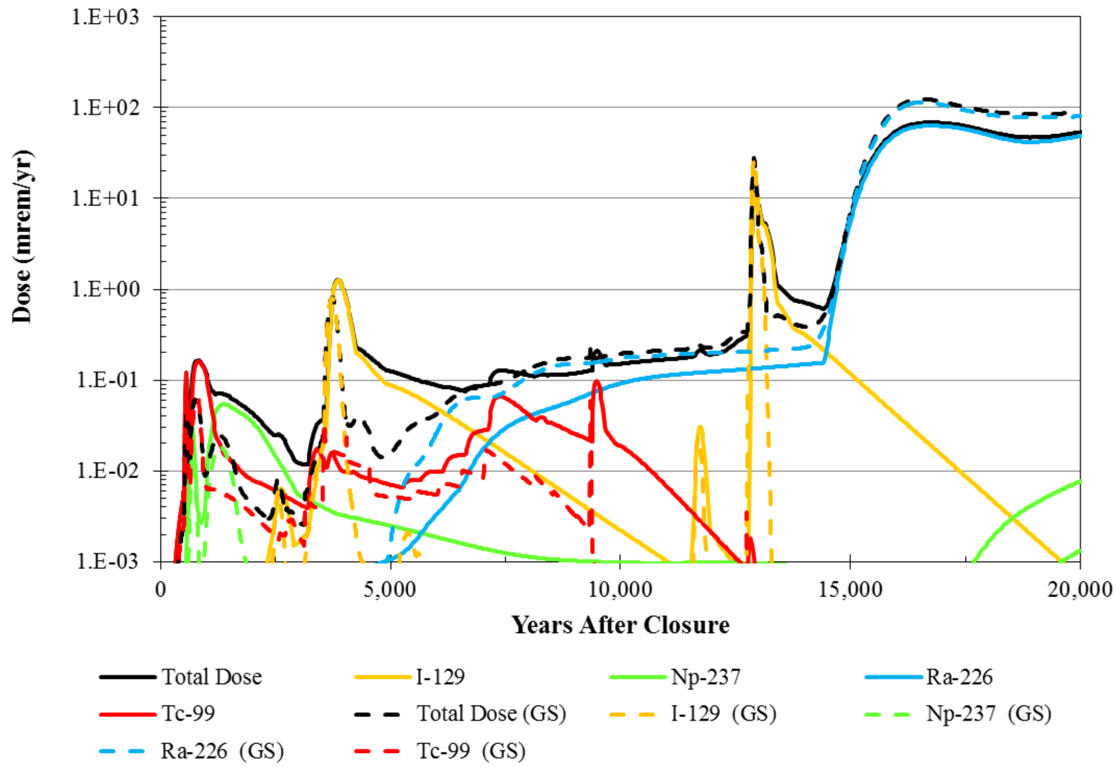

3.2.3.7 Maximum IHI Dose Time Histories

Next the benchmarking process focuses on examining how well the abstracted model approximates the IHI dose results. Comparisons of the maximum total MOP doses (in millirem per year) generated by the two models form the basis of the benchmarking effort along with a comparison of dose contributions from the major contributing radionuclides.

Figure 3-71 provides a comparison of the maximum dose-contribution curves from the major species, regardless of sector, for both the PORFLOW and the GoldSim models. This figure shows that the GoldSim model closely approximates the maximum dose results calculated from the PORFLOW model. Figure 3-72 provides a comparison of the maximum dose curves, regardless of sector, for both the PORFLOW and the GoldSim models. This figure shows that the GoldSim model closely approximates the maximum dose results calculated from the PORFLOW model.

Despite the GoldSim model simplifications, the similarity between GoldSim model results and PORFLOW model results justifies the use of the GoldSim model for evaluating parameter sensitivity and the influence of parameter uncertainty on the system to support DOE decision-making related to reasonable expectation/assurance that performance objectives will be met for the HTF.

Figure 3-71: Maximum Dose Contributions at the 1-Meter Boundary

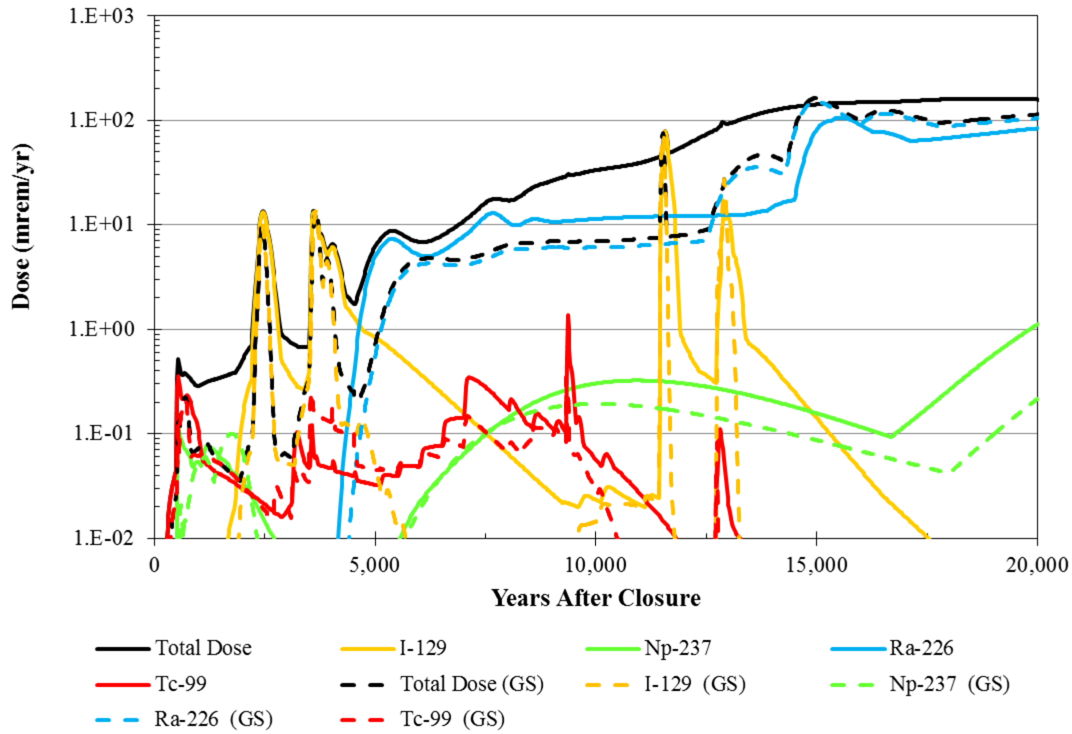

Figure 3-72: Maximum Dose from all Sources at the 1-Meter Boundary

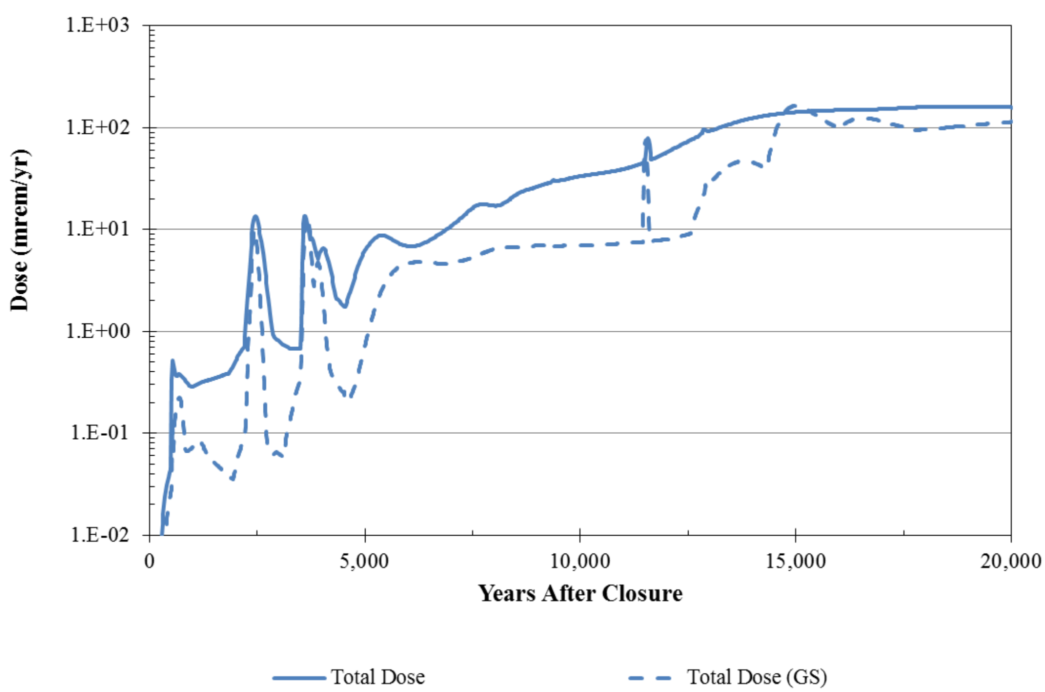

3.3 Benchmarking Conclusion

The GoldSim abstraction model is designed based on simplifying assumptions that allow it to reduce computation times and central processing unit (CPU) usage needed to evaluate tank releases and their impacts at POAs for the HTF. The reduction of computation times and CPU usage is especially critical for multi-realization stochastic studies using Monte Carlo/Latin Hypercube sampling techniques to evaluate uncertainty and parameter sensitivity. The benchmarking analysis described in Section 3 of this report was performed to validate the utility of the GoldSim abstraction model as an analogue for the HTF PORFLOW transport model when performing computationally intensive multi-realization stochastic studies.

A comparison of the tank release rates of I-129, Tc-99, Np-237, and Ra-226, as calculated by the GoldSim model, against the equivalent release rates from the PORFLOW HTF Model (see Section 3.2.1), shows that the GoldSim model (i.e., HTF_Transport_Model_v4.000_Rad) adequately reproduces the trends found in the PORFLOW model results.

Comparison of the 100-meter and 1-meter boundary dose calculations produced by the GoldSim model with those generated by the PORFLOW HTF Model (Sections 3.2.2 and 3.2.3, respectively), show that the GoldSim model reproduces the trends found in the PORFLOW model results. The comparisons between GoldSim and PORFLOW model generated total doses and the radionuclide dose contributions from species dominating the results (Figures 3-63 and 3-64 for the 100-meter boundary; Figures 3-71 and 3-72 for the 1-meter boundary) honor the peaks and show a good match in trends. Since the concentrations generated at these boundaries are used by the GoldSim dose-calculator to evaluate dose-based exposure to the MOP and IHI, the dose calculation comparison is also considered to be a validation of the boundary concentration calculations. Note that since the SZ transport modules are the same for the radionuclide and chemical transport models, the dose calculation comparisons can also be considered a validation of the SZ transport module used in the chemical transport simulations.

In conclusion, the GoldSim abstraction model is a satisfactory analogue for the PORFLOW HTF model. Because of the simplifying assumptions implicit to the GoldSim abstraction model, use of the abstraction model can effectively reduce limitations associated with excessive computation times and CPU usage when used in conjunction with a Latin Hypercube sampling technique to evaluate uncertainty and parameter sensitivity in HTF tank release modeling.

4 REFERENCES

Note: References identified as (Copyright) were used in the development of this document, but are protected by copyright laws. No part of the publication may be reproduced in any form or by any means, including photocopying or electronic transmittal, without permission in writing from the copyright owner.

GTG-2010c (Copyright), *GoldSim User's Guide, Volumes 1 & 2*, GoldSim Technology Group LLC, Issaquah, WA, January 2010.

GTG-2010d, (Copyright), *User's Guide, Probabilistic Simulation Environment, Version 10.5, Volumes 1 & 2*, GoldSim Technology Group LLC, Issaquah, WA, December 2010.

GTG-2010e, (Copyright), *GoldSim User's Guide, GoldSim Containment Transport Module,* Version 6.0, GoldSim Technology Group LLC, Issaquah, WA, December 2010.

SRNL-STI-2014-00612, Flach, G.P., and Taylor, G.A., *H-Area Tank Farm Tank 16 Special Analysis Model Support*, Savannah River Site, Aiken, SC, Rev. 0, December 2014.

SRNL-STI-2016-00224, Taylor, G.A., and Hang, T., *H-Area Tank Farm FY2016 Special Analysis Model Support*, Savannah River Site, Aiken, SC, Rev. 0, May 2016.

SRR-CWDA-2010-00023, Dean, W., *H-Tank Farm Waste Tank Closure Inventory for Use in Performance Assessment Modeling*, Savannah River Site, Aiken, SC, Rev. 3, May 2012.

SRR-CWDA-2010-00023, Dixon, K.D., *H-Tank Farm Waste Tank Closure Inventory for Use in Performance Assessment Modeling*, Savannah River Site, Aiken, SC, Rev. 4, November 2014.

SRR-CWDA-2010-00093, *H-Area Tank Farm Stochastic Fate and Transport Model,* Savannah River Site, Aiken, SC, Rev. 2, August 2012.

SRR-CWDA-2010-00128, *Performance Assessment for the H-Tank Farm at the Savannah River Site,* Savannah River Site, Aiken, SC, Rev. 1, November 2012.

SRR-CWDA-2011-00050, Pavletich, J. P., *Liquid Waste Tank Residuals Sampling and Analysis Program Plan,* Savannah River Site, Aiken, SC, Rev. 3, October 26, 2015.

SRR-CWDA-2011-00117, Pavletich, J. P., *Liquid Waste Tank Residuals Sampling-Quality Assurance Program Plan,* Savannah River Site, Aiken, SC, Rev. 2, October 26, 2015.

SRR-CWDA-2013-00058, Hommel, S., *Dose Calculation Methodology for Liquid Waste Performance Assessments at the Savannah River Site,* Savannah River Site, Aiken, SC, Rev. 1, July 2014.

SRR-CWDA-2014-00060, Lester, B., *Updates to the H-Area Tank Farm Stochastic Fate and Transport Model,* Savannah River Site, Aiken, SC, Rev. 0, January 2015.

SRR-CWDA-2014-00060, Mangold, J., *Updates to the H-Area Tank Farm Stochastic Fate and Transport Model,* Savannah River Site, Aiken, SC, Rev. 1, August 2015.

SRR-CWDA-2014-00106, *Tank 16 Special Analysis for the Performance Assessment for the H-Tank Farm at the Savannah River Site*, Savannah River Site, Aiken, SC, Rev. 1, February 2015.

SRR-CWDA-2014-00134, Hommel, S.P., *Tank 16 Special Analysis for the Performance Assessment for the H-Area Tank Farm at the Savannah River Site: Quality Assurance Report,* Savannah River Site, Aiken, SC, Rev. 0, February 2015.

SRR-CWDA-2015-00075, Dixon, K.D., *Tank 12 Inventory Determination,* Savannah River Site, Aiken, SC, Rev. 0, July 2015.

SRR-CWDA-2015-00166, Dixon, K.D., *Updated Radionuclide and Chemical Inventories in Tanks 9, 10, 11, 13, 14 and 15*, Savannah River Site, Aiken, SC, Rev. 1, January 2016.

SRR-CWDA-2016-00061, Mangold, J.E., *Evaluation of the Probabilistic Distribution used for Modeling Strontium Sorption to Sandy Soils*, Savannah River Site, Aiken, SC, Rev. 0, May 2016.

SRR-CWDA-2016-00062, Dixon, K.D., *Recommended Multipliers for H-Area Tank Farm Type II Tanks Sr-90 Inventories in Performance Assessment Modeling*, Savannah River Site, Aiken, SC, Rev. 0, June 2016.

APPENDIX A

A.1 MASS RELEASES TO THE SATURATED ZONE

The species evaluated during this benchmarking effort represent major dose contributors and parent species for major dose contributors that are part of decay chains. In addition, species chosen for the model comparison exhibit a wide range sorptive properties and solubility limits. Two independent species are used in the benchmarking including I-129 and Tc-99. The other species are members of the decay chains (or partial decay chains): 1) Am-241→ Np-237, 2) Am-243→Pu-239, and 3) Pu-238→U-234→Th-230→Ra-226. To limit the effort involved in assembling this document, breakthrough curves for the radionuclides Pu-238 and Th-230 are not presented with the results although their inventories are included in the ingrowth calculations.

During benchmarking, variances of ~50% or less for peak release-rates, were considered good. Because the PORFLOW flow-fields are more complex due the added fast zones peak releases differences between –75% and +100% are still considered acceptable, as long as the general trends matched well. Note that for some tanks, greater latitude in peak release comparisons was considered acceptable for releases. For example, where an event (such as Eh transition) associated with a many order of magnitude change in K_d or solubility (i.e. Tc-99), the one-day time steps used in the PORFLOW model may generate a breakthrough peak release of greater magnitude but narrower width.

In general, the GoldSim abstractions for all tanks accurately calculate Tc-99 releases from the CZ. They also accurately calculate the annulus releases over a long period prior to the Eh transition to Oxidized Region II. When most of the Tc-99 from the annulus has been released from the system, the remaining mass, which will be released in the Eh transition-induced surge, may be spatially distributed in a manner that may result in differences between GoldSim and PORFLOW breakthrough curve peaks. This distribution of mass associated with three-dimensional aspects of plume formation may not be fully captured by the GoldSim model. In addition, since the chemical region transition induced mass release peaks may occur over a short period of time relative to time step lengths, differences between GoldSim and PORFLOW model peaks may be enhanced.

For strongly sorbing radionuclides such as Np-237, early releases, which are dominated by diffusion may differ radically between the two models. The strongly sorptive nature of neptunium is reflected in a K_d of around 10,000 ml/g in concrete. The strongly sorptive nature of a dissolve species in conjuction with differences in disctretization between the two models may reflect large differences in numerical diffusion controlling the early shape of the breakthrough curve.

Note that all benchmark simulations used to compare tank releases were performed without using more than one isotope of any species. This circumvented differences between how the PORFLOW model and the GoldSim model are structured to handle the combined influence of isotopes on solubility calculations. The GoldSim model solves for elemental based concentrations and then apportions the dissolved mass among all species being modeled. The PORFLOW model does not simulate all species in the same tank release run, allowing greater concentrations of specific radionuclides to occur simultaneously.

Further discussion on the differences between how the GoldSim model and the PORFLOW model evaluate solubility, and examples showing comparisons of results of this report, can be found in Revision 1 of this report.

A.1.1 Type I Tank with Intact Liner (Tank 9) for Case B

For the Case B configuration, a comparison of the PORFLOW HTF Model and the GoldSim model mass releases of I-129, Tc-99, Am-243, Pu-239, U-234, Ra-226, Am-241, and Np-237, as presented in Figure A.1-1 through Figure A.1-8, indicate that the GoldSim model produces a good approximation of the releases from Tank 9 generated by the PORFLOW model.

Table A.1-1 summarizes the peak values for these releases. Variances of ~50% or less for peak releases, as seen in the I-129, Am-243, Pu-239, U-234, Ra-226, Am-241, and Np-237 results, were considered acceptable. The -55% variance for Tc-99 is only slightly more than the ~50% target and the shapes of the release curves indicate good agreement; therefore Tc-99 is also acceptable.

Note that in Figure A.1-7, the PORFLOW breakthrough curve indicates that there is an initial release of Am-241 ending at 501 years followed by a second release starting at 1,178 years. This pattern is based on calculations that measure the total release from the tank into the soil below and the backfill above and outside the tank walls. For this simulation, Tank 9 under Configuration B, the main release in the first 500 years is from diffusion out of the top of the tank into the backfill above. This mass reaches the top of the tank by diffusion upward through the fast zone. As time progresses and advection downwards starts to dominate the system, the mass advecting from the backfill above the tank, back into the tank, is greater than the mass leaving the tank on other boundaries creating a positive influx mass balance (or negative release). This negative release does not show up on a log-scale plot. After 1,178 years, the mass release is again greater than any mass influx from the overlying backfill and the results are as shown. Also note that the simplified abstraction used in the GoldSim model does not include the backfill therefore early-time low-level releases are not evaluated.

Table A.1-1: Case B GoldSim and PORFLOW Model Peak Releases from the UZ to the SZ Comparisons for Tank 9 within 20,000 years

Radionuclide	PORFLOW Peak Release (mol/yr)	PORFLOW Time of Peak Release (yr)	GoldSim Peak Release (mol/yr)	GoldSim Time of Peak Release (yr)	Peak Release Percent Difference GoldSim vs PORFLOW
I-129	4.1E-02	1,173	3.9E-02	1,180	-5%
Tc-99	1.1E-03	1,144	4.9E-04	1,150	-55%
Am-243	1.7E-04	4,156	2.2E-04	4,020	29%
Pu-239	1.8E-05	6,139	2.1E-05	5,810	17%
U-234	1.7E-03	2,022	2.0E-03	2,000	18%
Ra-226	2.1E-07	1,594	2.4E-07	1,570	14%
Am-241	2.3E-06	3,105	2.7E-06	3,280	17%
Np-237	2.1E-04	19,998	2.7E-04	20,000	29%

Figure A.1-1: Tank 9 I-129 Release to the Saturated Zone for Case B

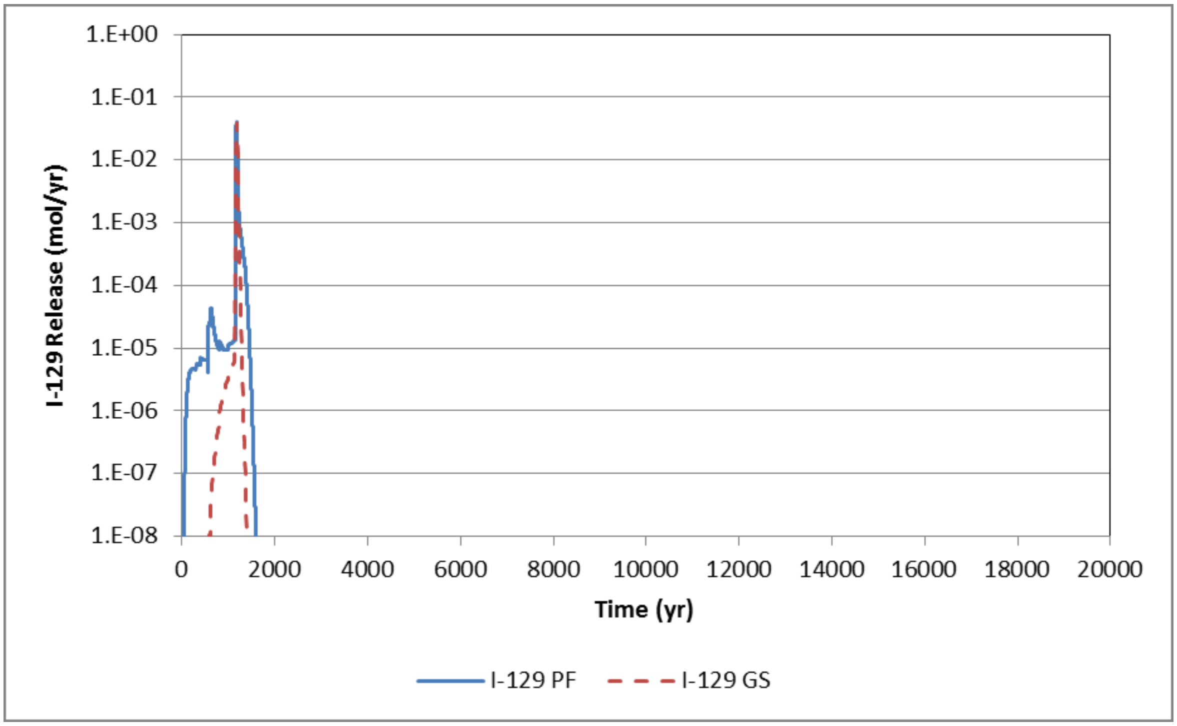

Figure A.1-2: Tank 9 Tc-99 Release to the Saturated Zone for Case B

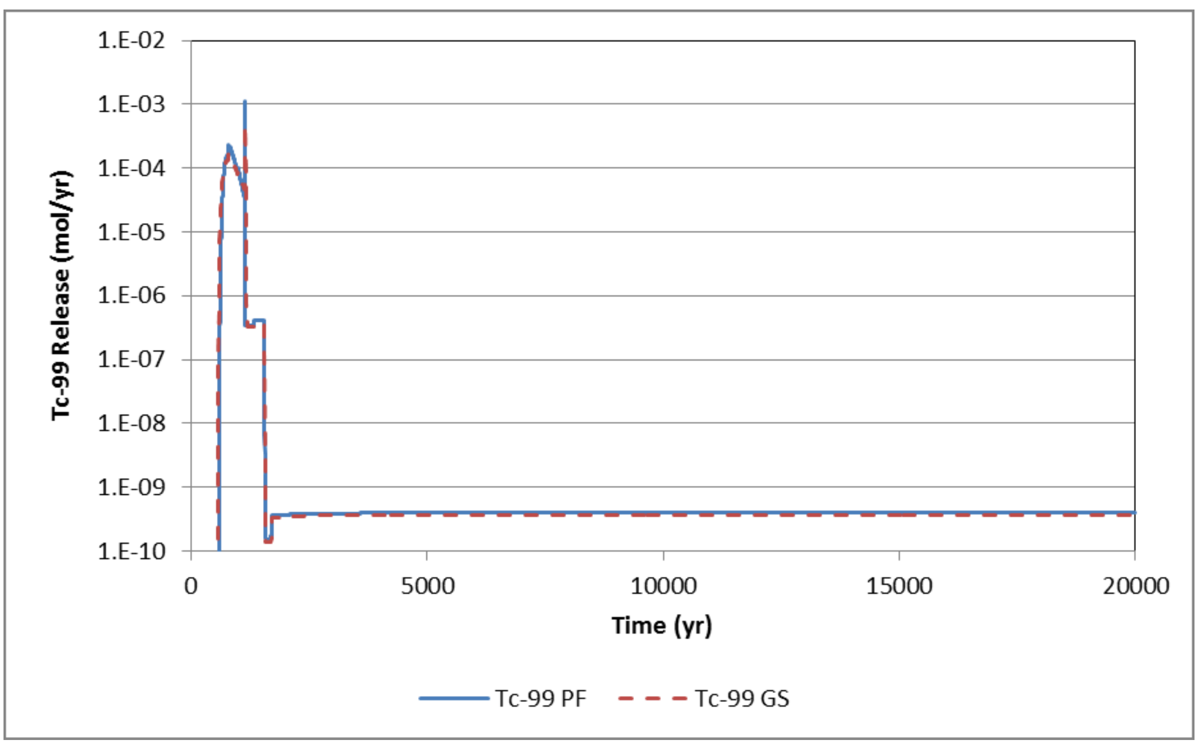

Figure A.1-3: Tank 9 Am-243 Release to the Saturated Zone for Case B

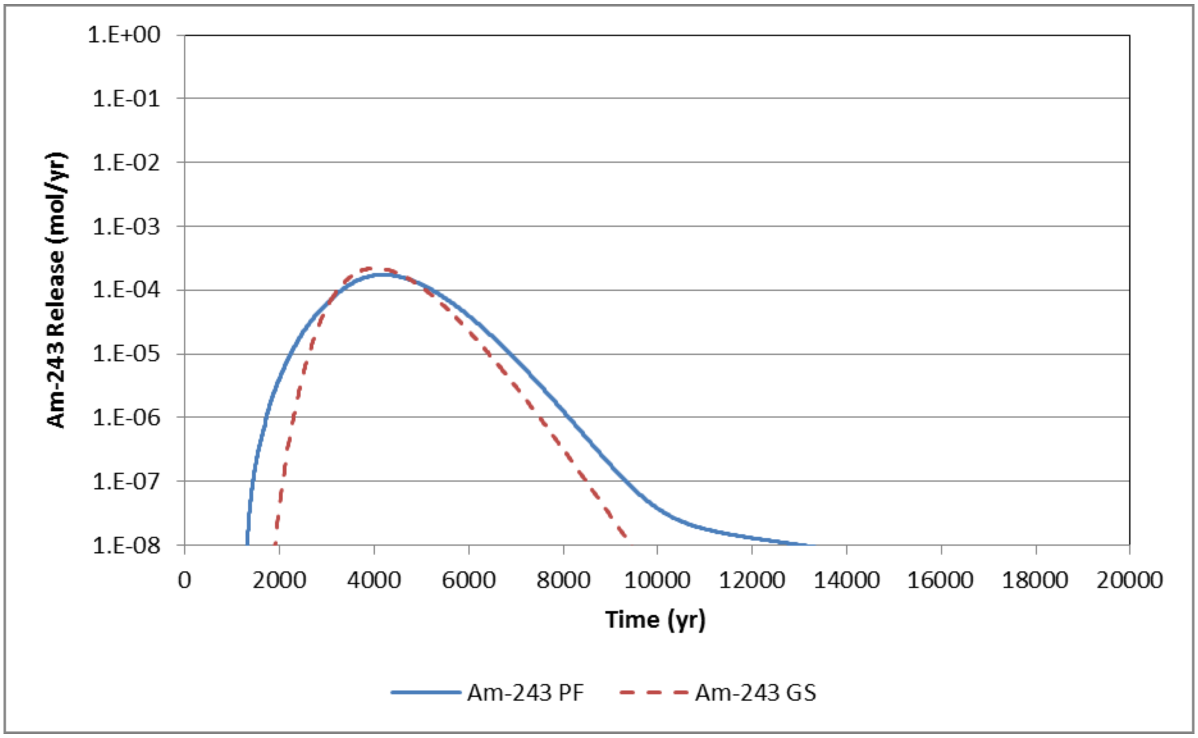

Figure A.1-4: Tank 9 Pu-239 Release to the Saturated Zone for Case B

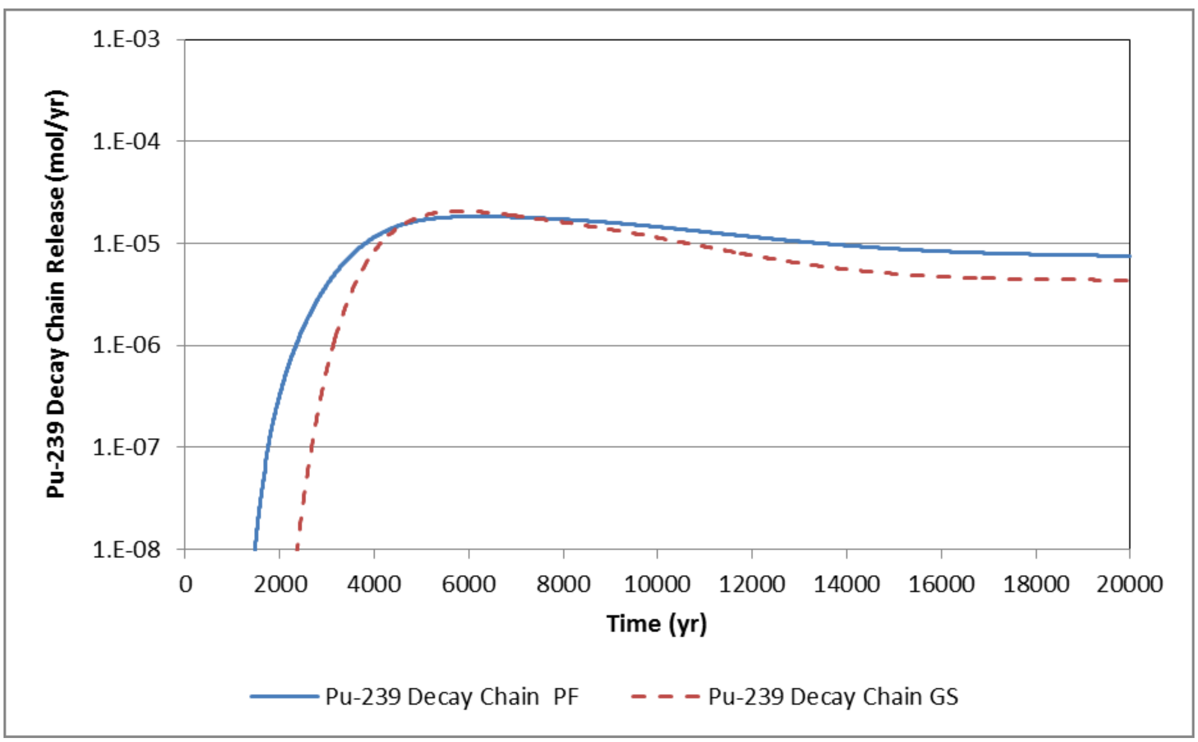

Figure A.1-5: Tank 9 U-234 Release to the Saturated Zone for Case B

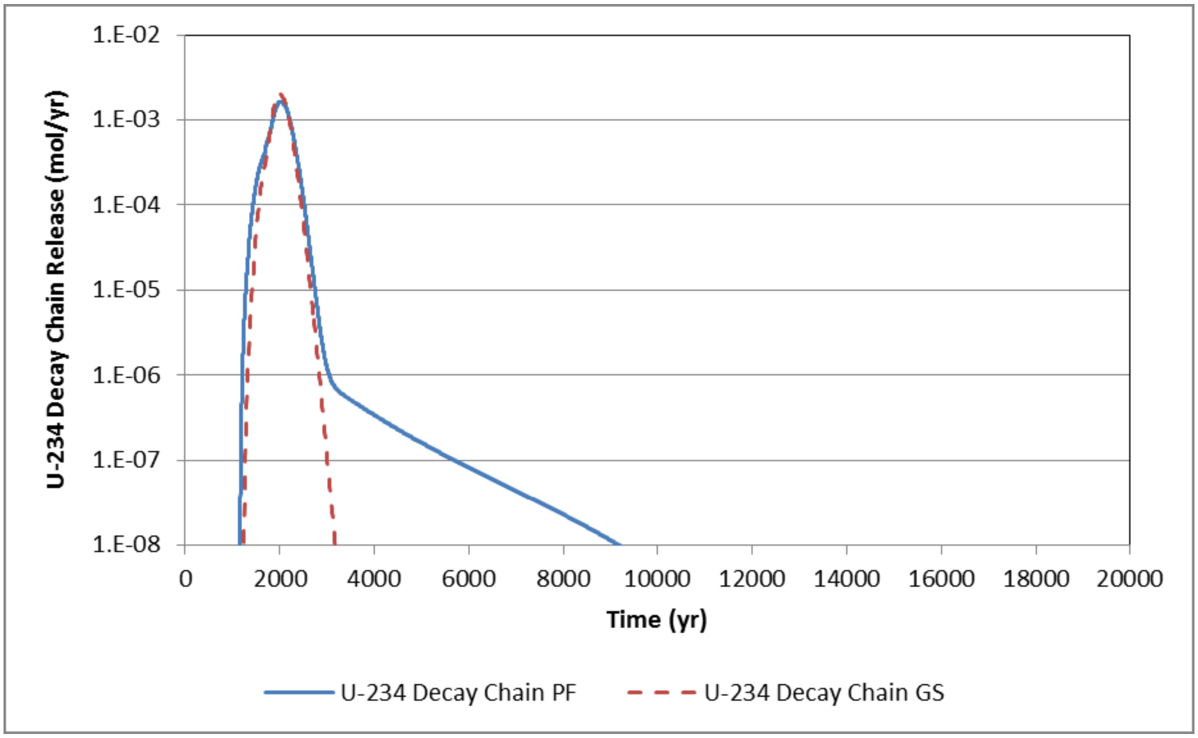

Figure A.1-6: Tank 9 Ra-226 Release to the Saturated Zone for Case B

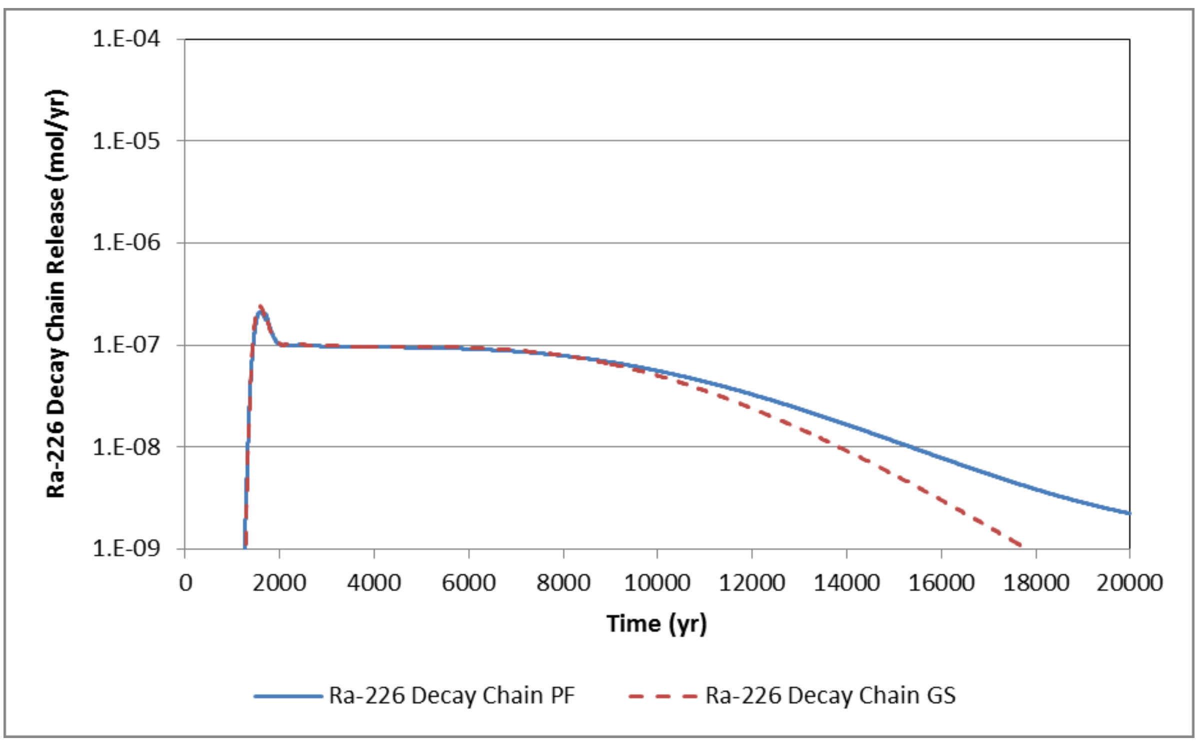

Figure A.1-7: Tank 9 Am-241 Release to the Saturated Zone for Case B

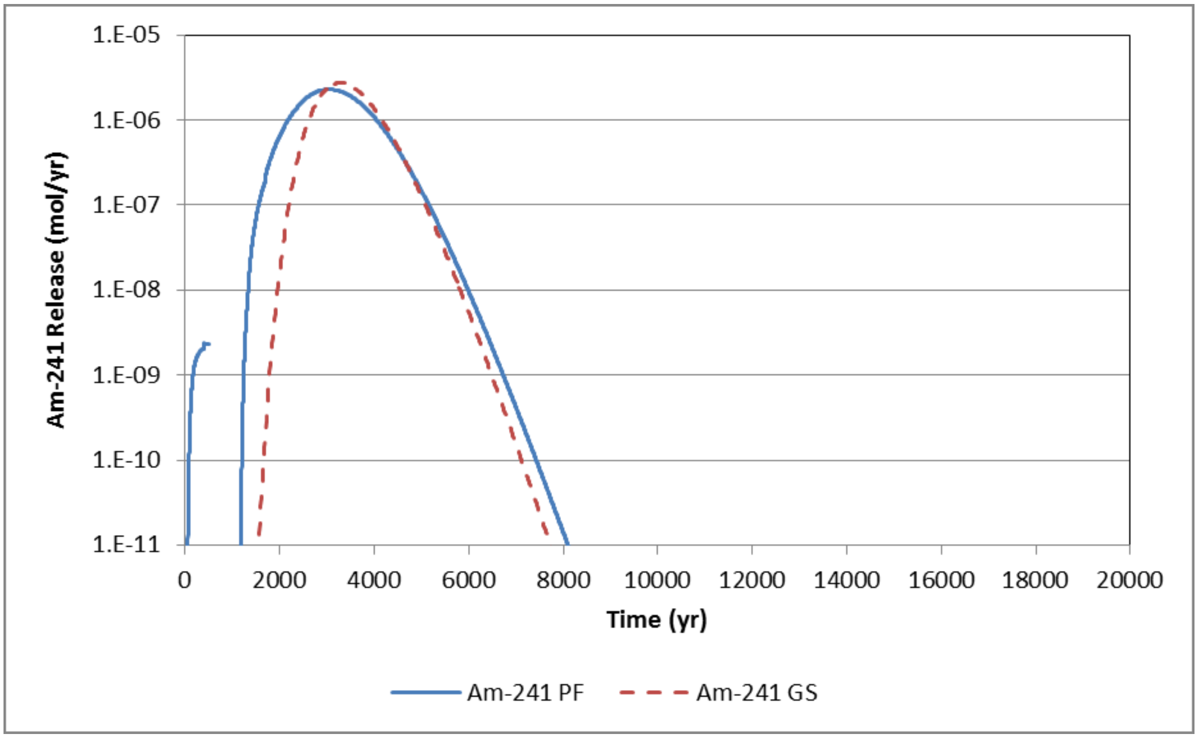

Figure A.1-8: Tank 9 Np-237 Release to the Saturated Zone for Case B

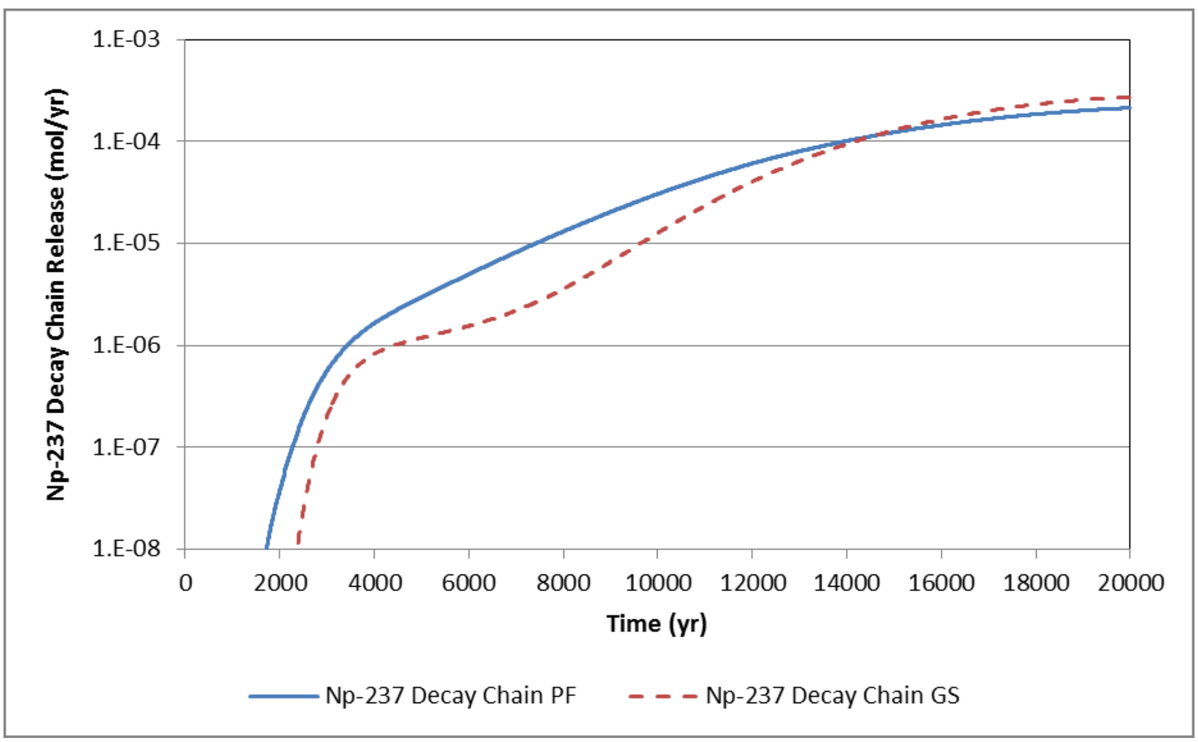

A.1.2 Type I Tank with Failed Liner (Tank 12) for Case B

For the Case B configuration, a comparison of the PORFLOW HTF Model and the GoldSim model mass releases of I-129, Tc-99, Am-243, Pu-239, U-234, Ra-226, Am-241, and Np-237, as presented in Figure A.1-9 through Figure A.1-16, indicate that the GoldSim model produces a good approximation of the releases from Tank 12 generated by the PORFLOW model. Table A.1-2 summarizes the peak values for these releases. Variances of ~50% or less for peak releases, as seen in the I-129, Tc-99, Am-243, Pu-239, U-234, Ra-226, Am-241, and Np-237 results, were considered acceptable.

Table A.1-2: Case B GoldSim and PORFLOW Model Peak Releases from the UZ to the SZ Comparisons for Tank 12 within 20,000 years

Radionuclide	PORFLOW Peak Release (mol/yr)	PORFLOW Time of Peak Release (yr)	GoldSim Peak Release (mol/yr)	GoldSim Time of Peak Release (yr)	Peak Release Percent Difference GoldSim vs PORFLOW
I-129	3.2E-02	601	2.6E-02	580	-19%
Tc-99	1.4E-03	546	9.4E-04	550	-33%
Am-243	9.9E-07	3,670	1.2E-06	3,520	21%
Pu-239	4.7E-06	19,887	4.3E-06	19,980	-9%
U-234	4.6E-04	1,506	5.5E-04	1,470	20%
Ra-226	1.4E-08	1,701	1.4E-08	1,710	0%
Am-241	4.3E-07	2,701	5.2E-07	2,870	21%
Np-237	5.5E-05	19,998	7.0E-05	20,000	27%

Figure A.1-9: Tank 12 I-129 Release to the Saturated Zone for Case B

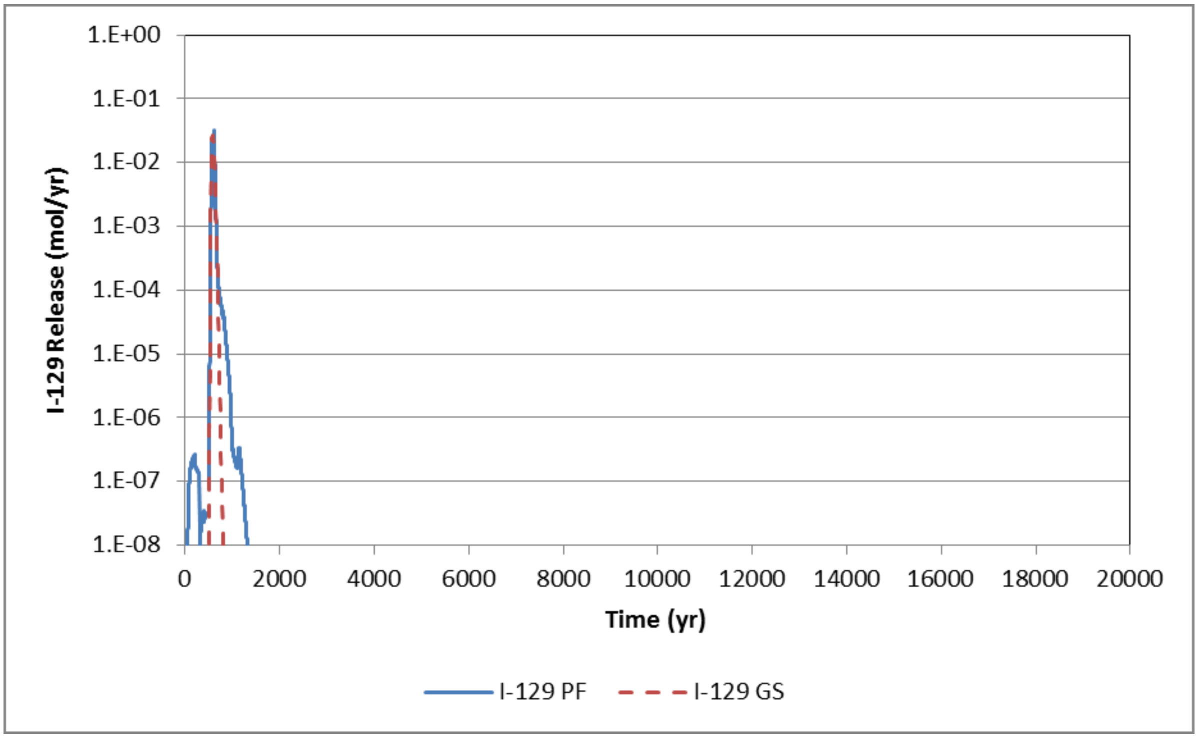

Figure A.1-10: Tank 12 Tc-99 Release to the Saturated Zone for Case B

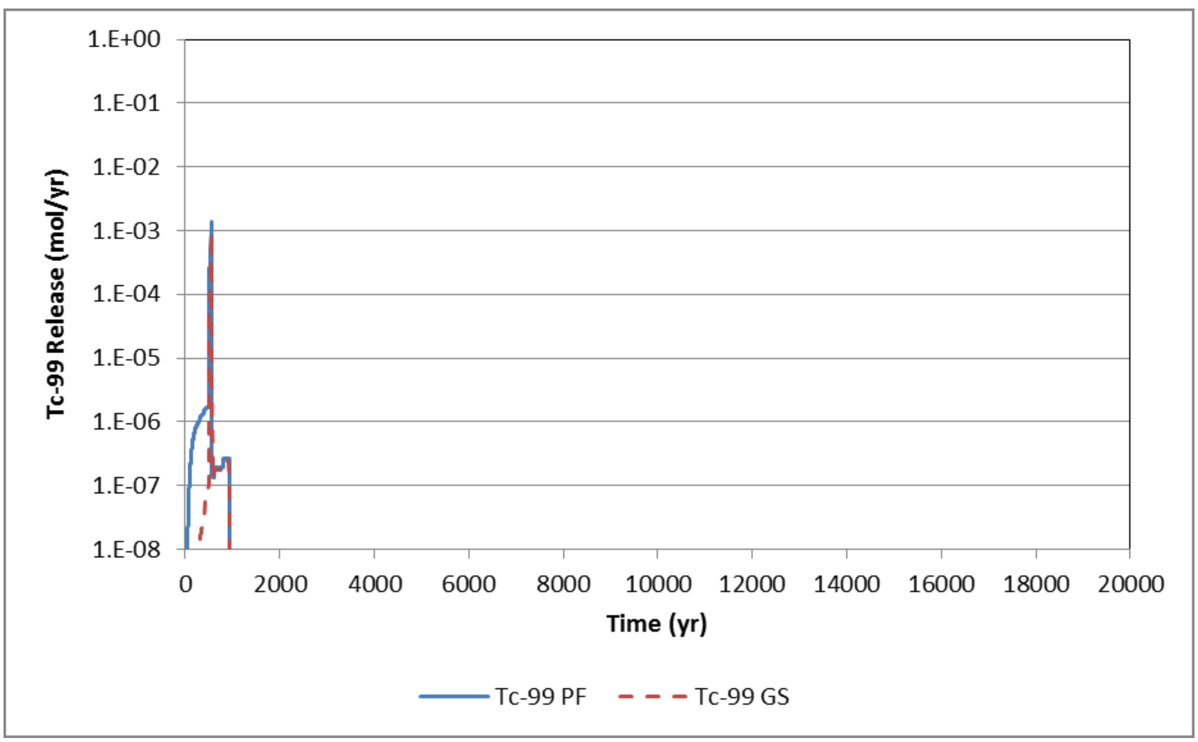

Figure A.1-11: Tank 12 Am-243 Release to the Saturated Zone for Case B

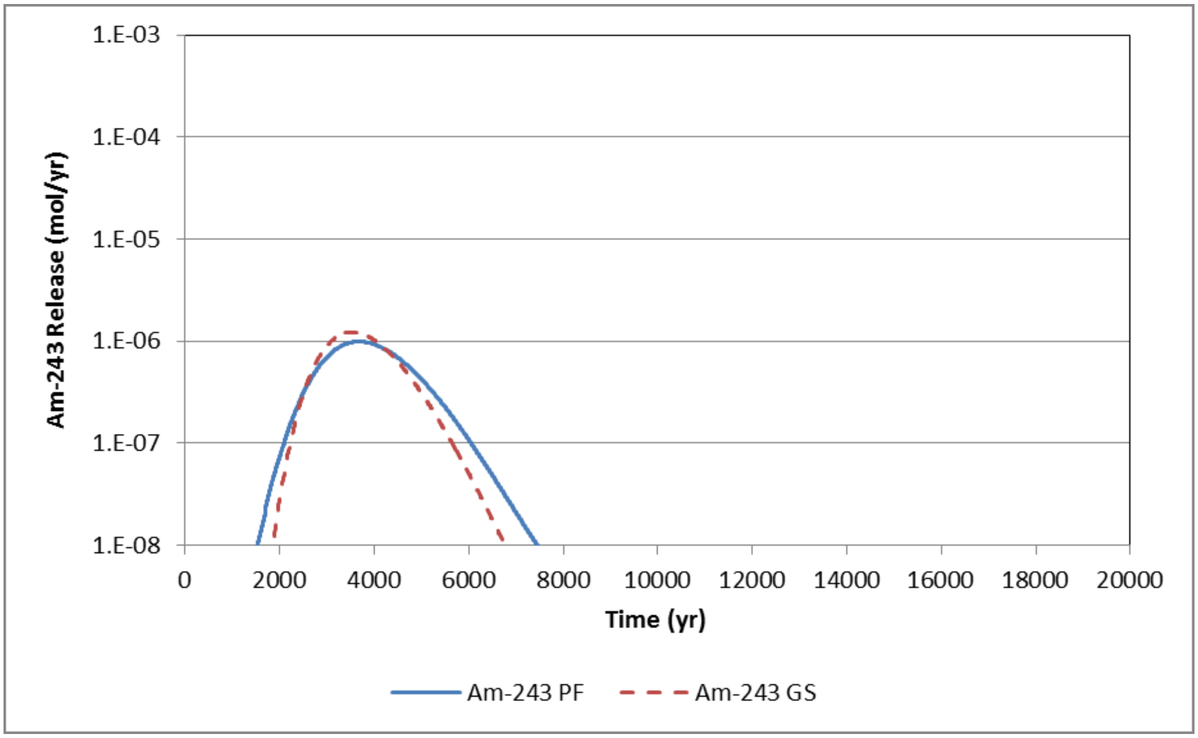

Figure A.1-12: Tank 12 Pu-239 Release to the Saturated Zone for Case B

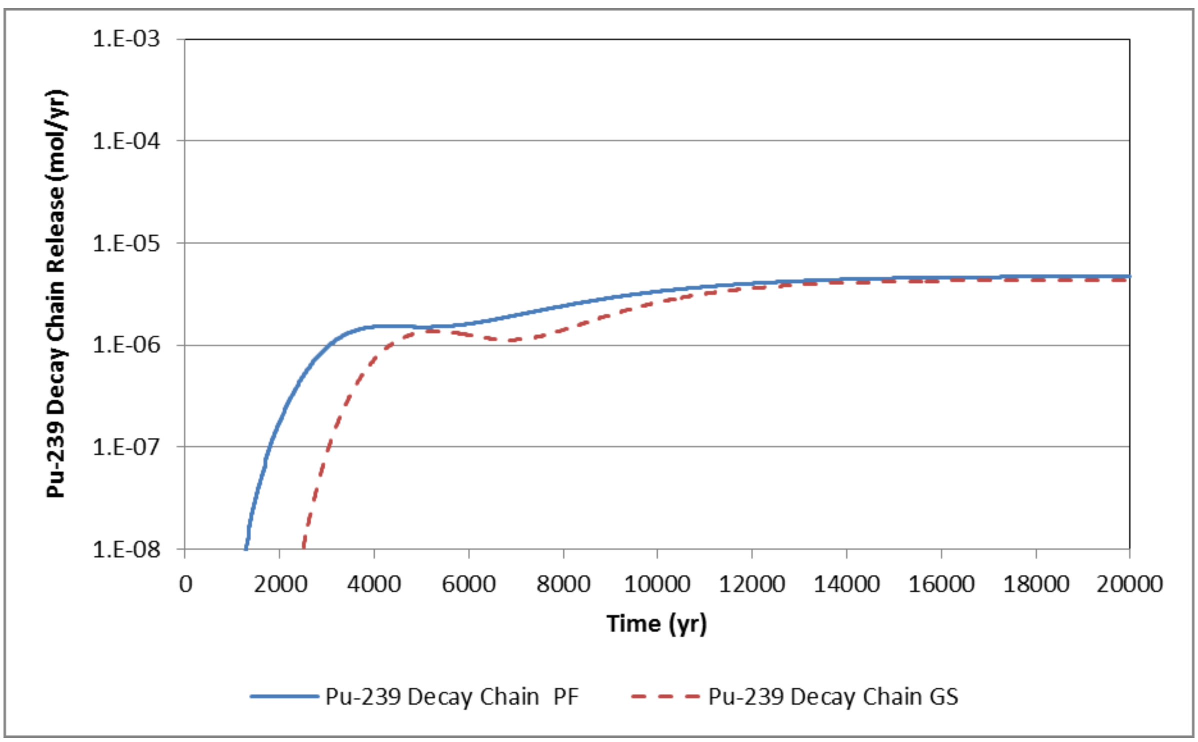

Figure A.1-13: Tank 12 U-234 Release to the Saturated Zone for Case B

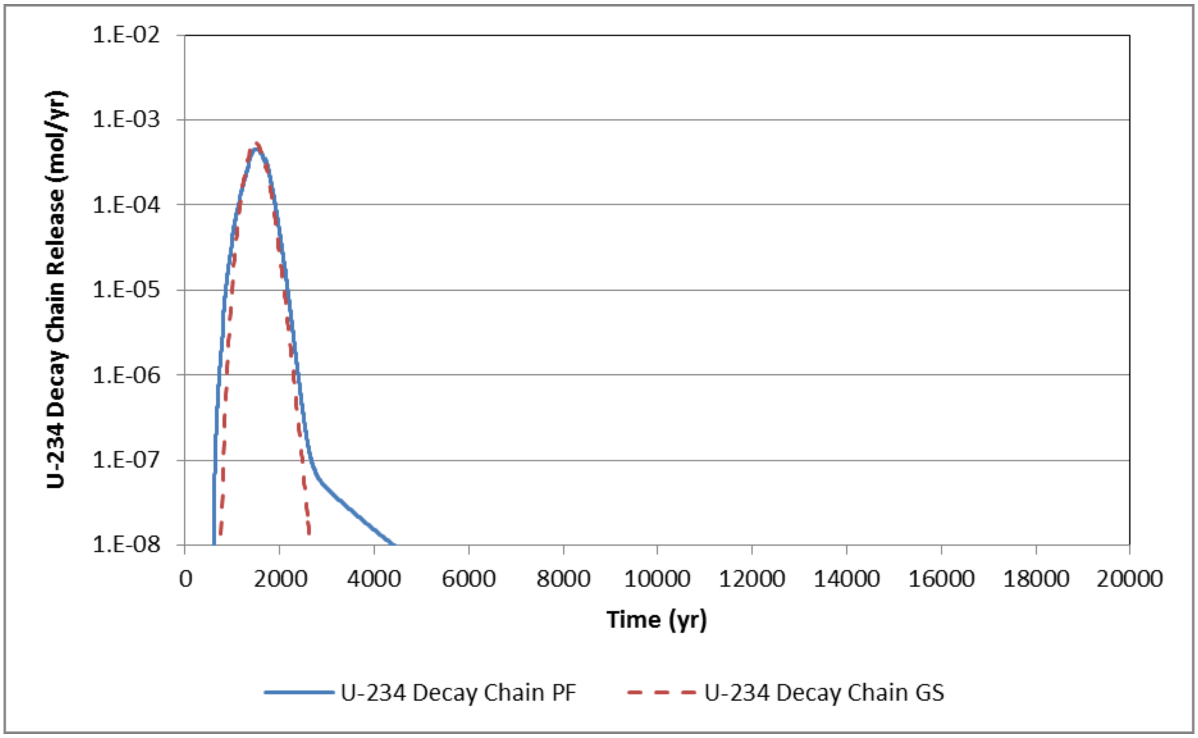

Figure A.1-14: Tank 12 Ra-226 Release to the Saturated Zone for Case B

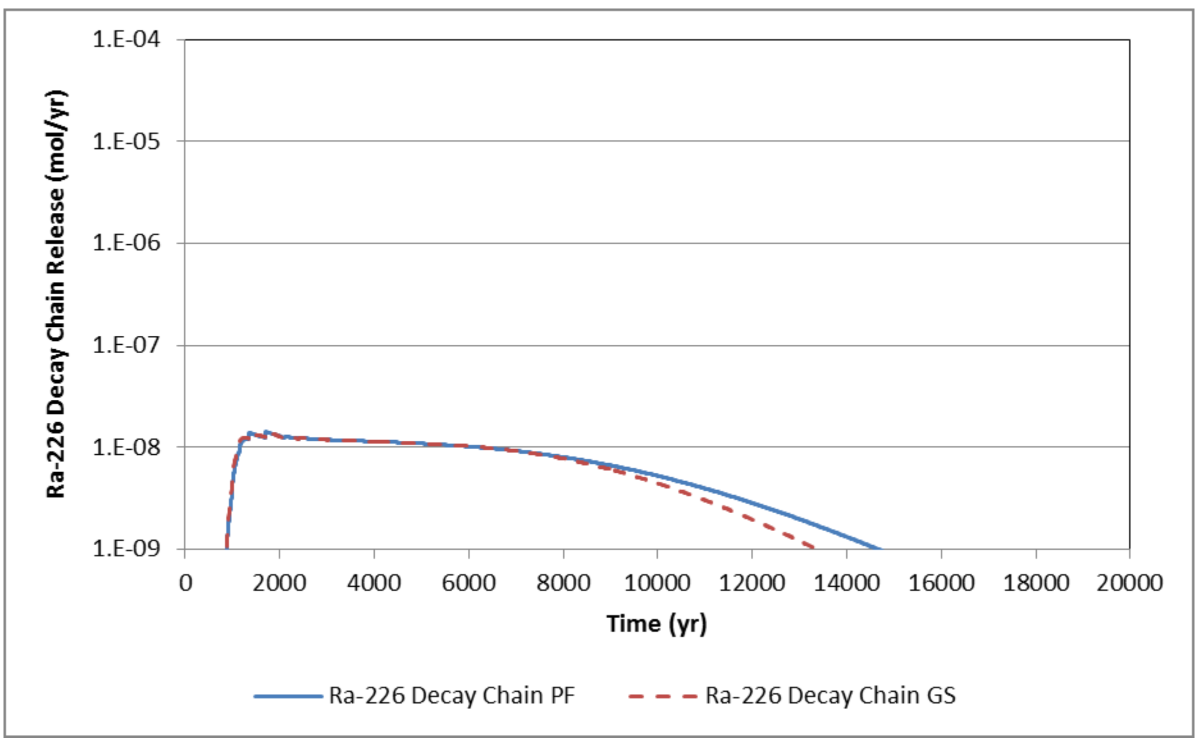

Figure A.1-15: Tank 12 Am-241 Release to the Saturated Zone for Case B

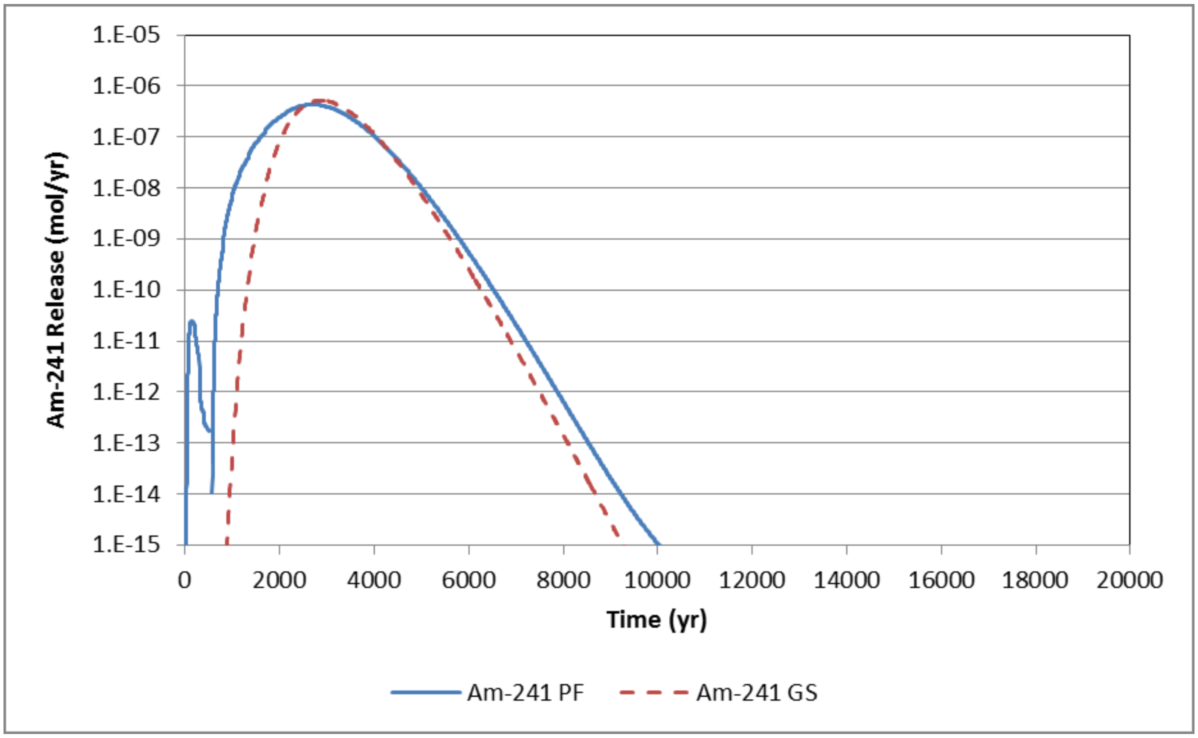

Figure A.1-16: Tank 12 Np-237 Release to the Saturated Zone for Case B

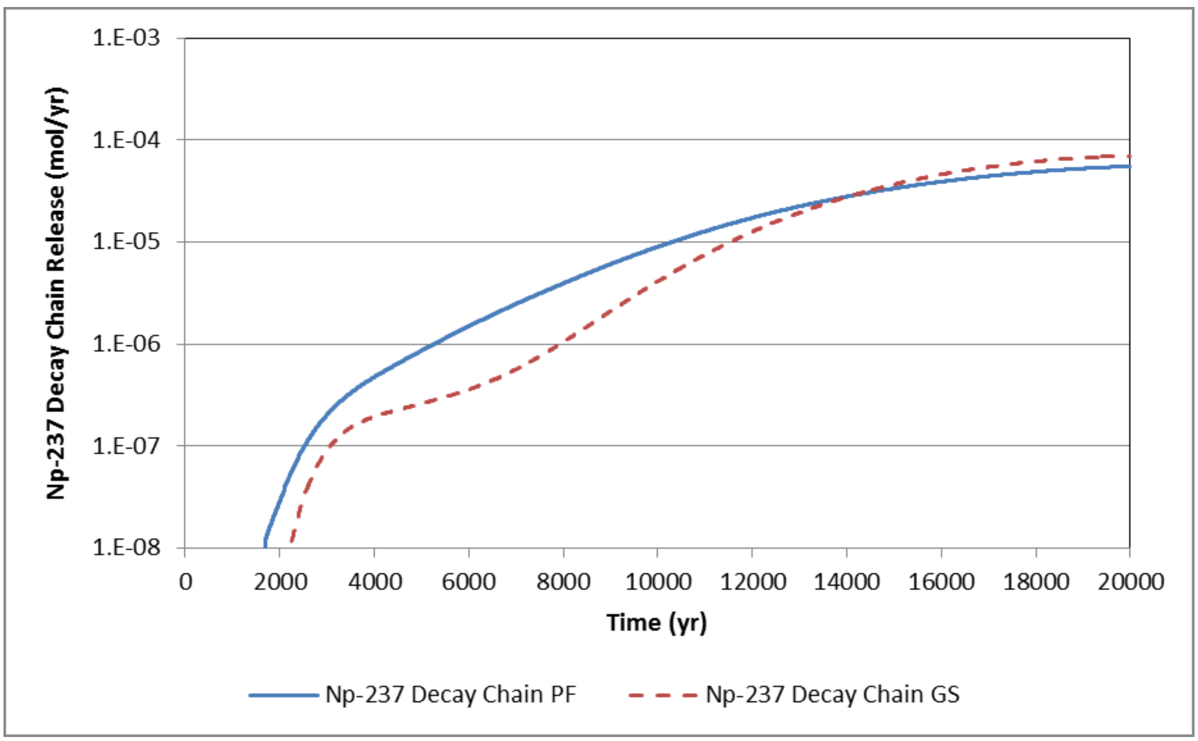

A.1.3 Type II Tank with Intact Liner (Tank 13) for Case B

For the Case B configuration, a comparison of the PORFLOW HTF Model and the GoldSim model mass releases of I-129, Tc-99, Am-243, Pu-239, U-234, Ra-226, Am-241, and Np-237, as presented in Figure A.1-17 through Figure A.1-24, indicate that the GoldSim model produces a good approximation of the releases from Tank 13 generated by the PORFLOW model.

Table A.1-3 summarizes the peak values for these releases showing that when comparing the two models except for Am-241 and Np-237 the percent differences are below 50%. Figure A.1-23 and Figure A.1-24, show that despite similar release patterns in the two models, the GoldSim model will conservatively overestimate the releases of Am-241 and Np-237, respectively.

Table A.1-3: Case B GoldSim and PORFLOW Model Peak Releases from the UZ to the SZ Comparisons for Tank 13 within 20,000 years

Radionuclide	PORFLOW Peak Release (mol/yr)	PORFLOW Time of Peak Release (yr)	GoldSim Peak Release (mol/yr)	GoldSim Time of Peak Release (yr)	Peak Release Percent Difference GoldSim vs PORFLOW
I-129	3.8E-02	2,543	3.9E-02	2,540	3%
Tc-99	4.0E-03	2,511	2.8E-03	2,510	-30%
Am-243	6.7E-05	7,458	9.8E-05	7,140	46%
Pu-239	1.4E-05	15,116	1.4E-05	13,200	0%
U-234	6.7E-04	3,721	7.2E-04	3,930	7%
Ra-226	3.4E-07	3,084	3.5E-07	3,060	3%
Am-241	4.8E-09	5,888	2.3E-08	5,240	379%
Np-237	2.8E-06	20,000	1.1E-05	20,000	293%

Figure A.1-17: Tank 13 I-129 Release to the Saturated Zone for Case B

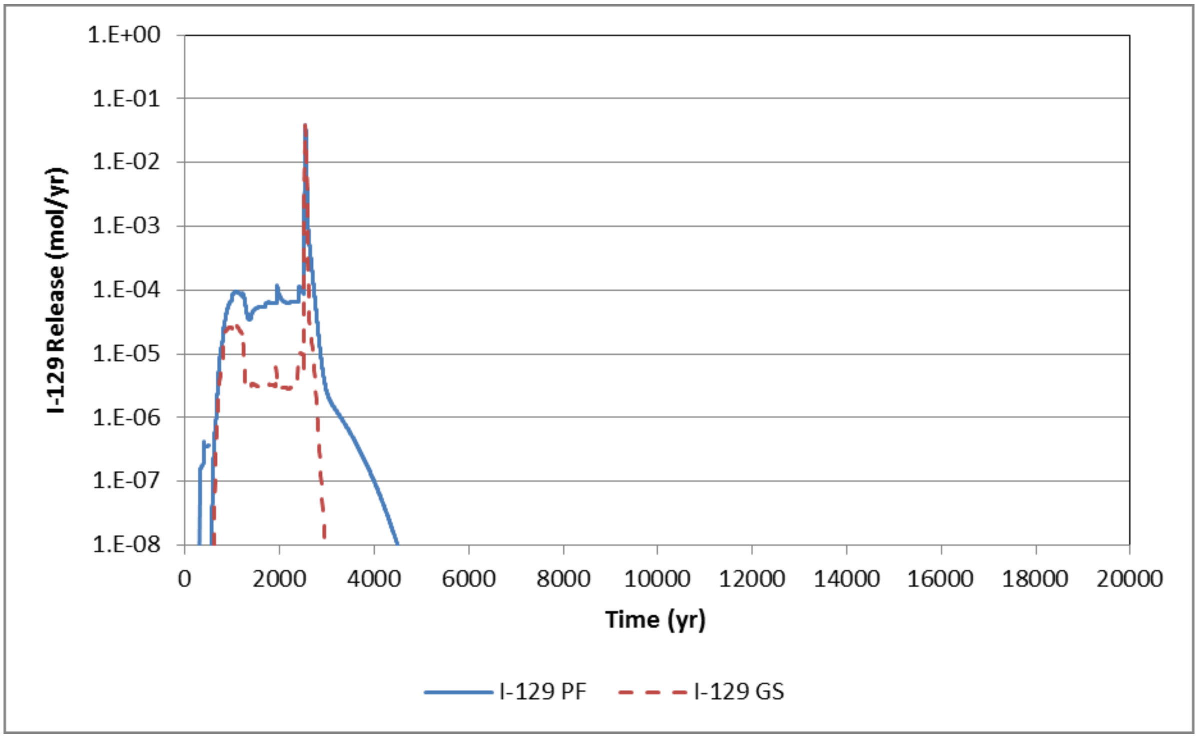

Figure A.1-18: Tank 13 Tc-99 Release to the Saturated Zone for Case B

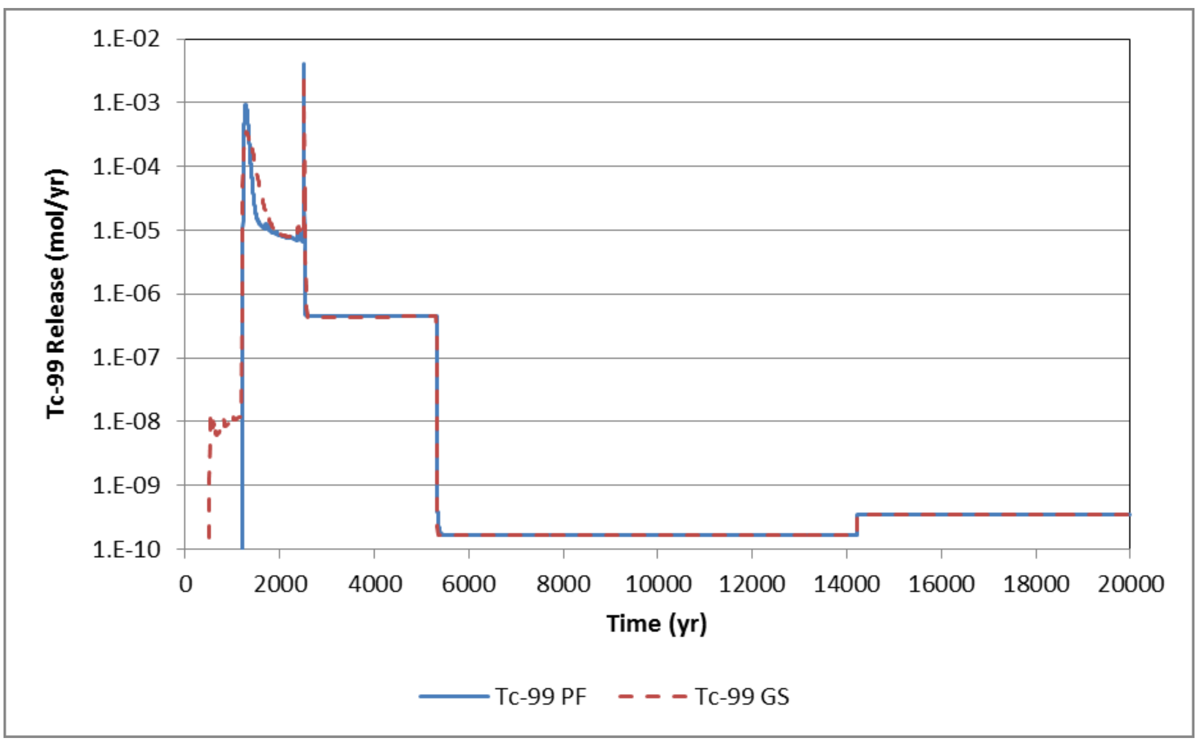

Figure A.1-19: Tank 13 Am-243 Release to the Saturated Zone for Case B

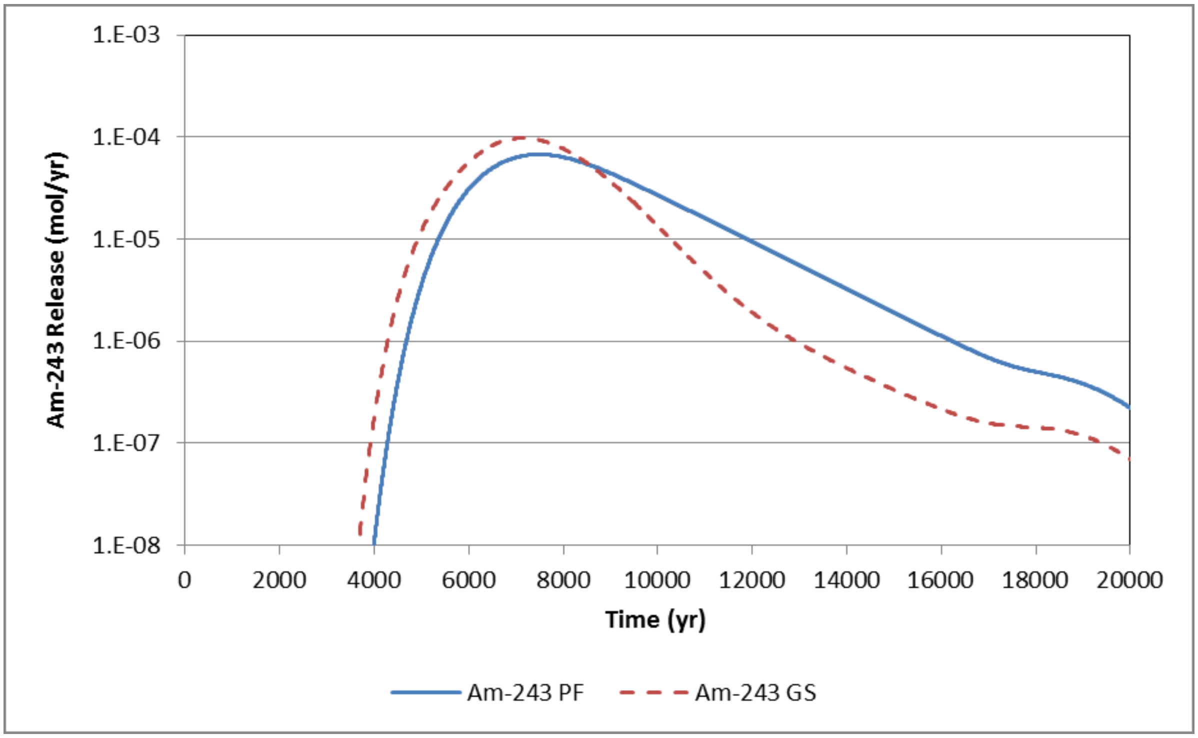

Figure A.1-20: Tank 13 Pu-239 Release to the Saturated Zone for Case B

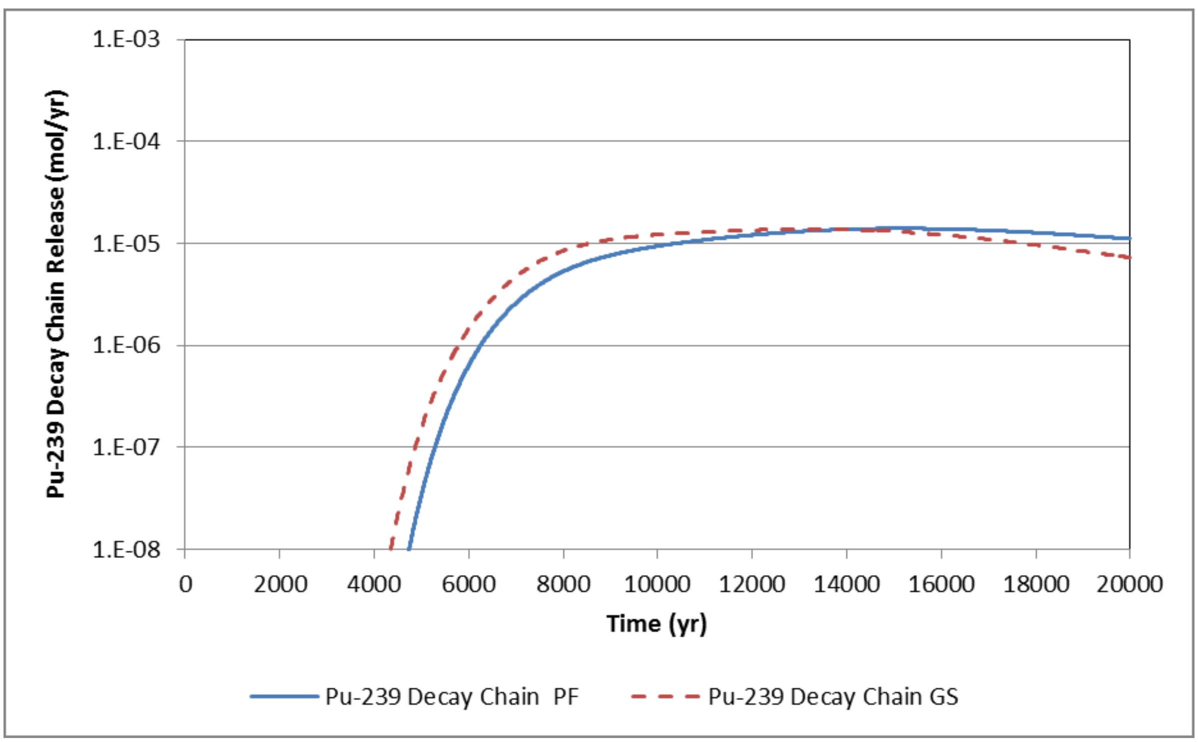

Figure A.1-21: Tank 13 U-234 Release to the Saturated Zone for Case B

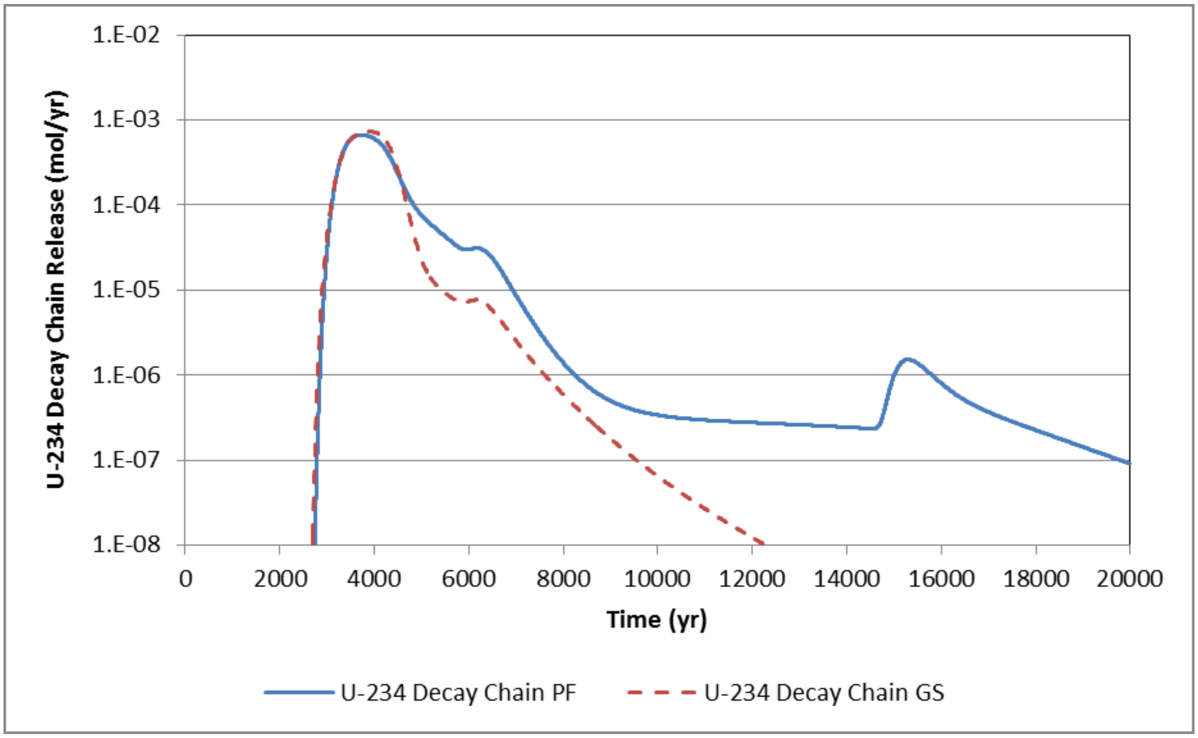

Figure A.1-22: Tank 13 Ra-226 Release to the Saturated Zone for Case B

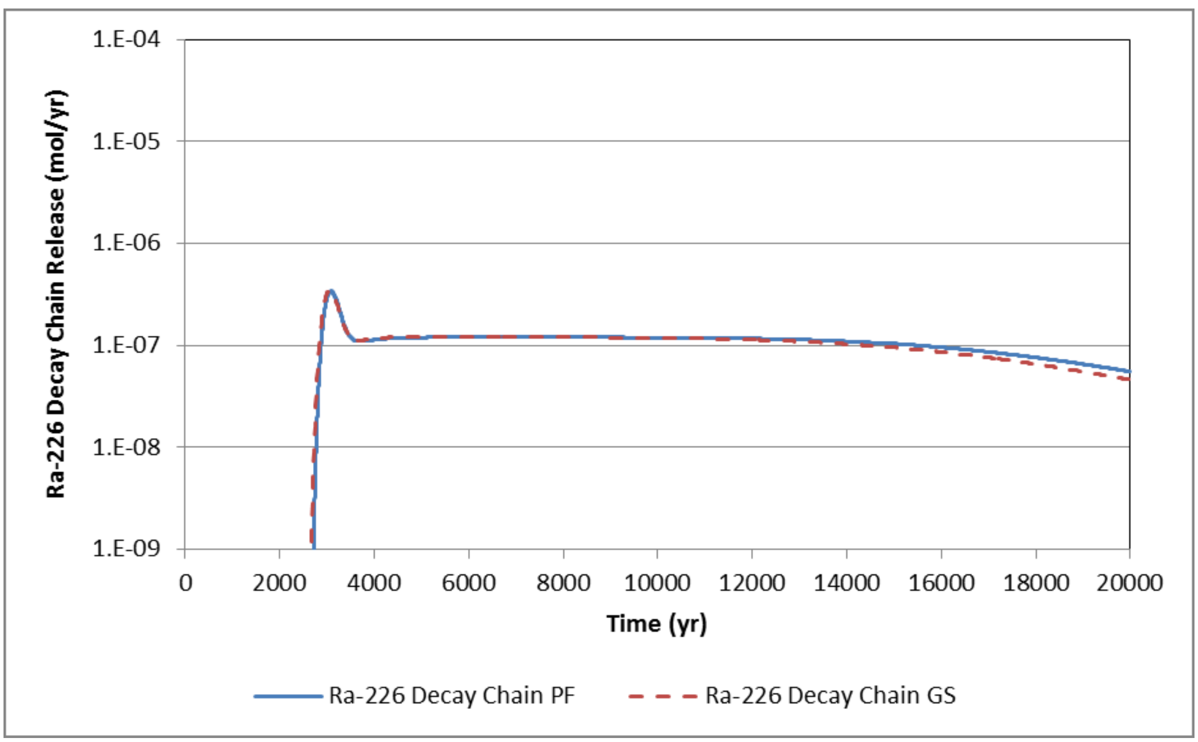

Figure A.1-23: Tank 13 Am-241 Release to the Saturated Zone for Case B

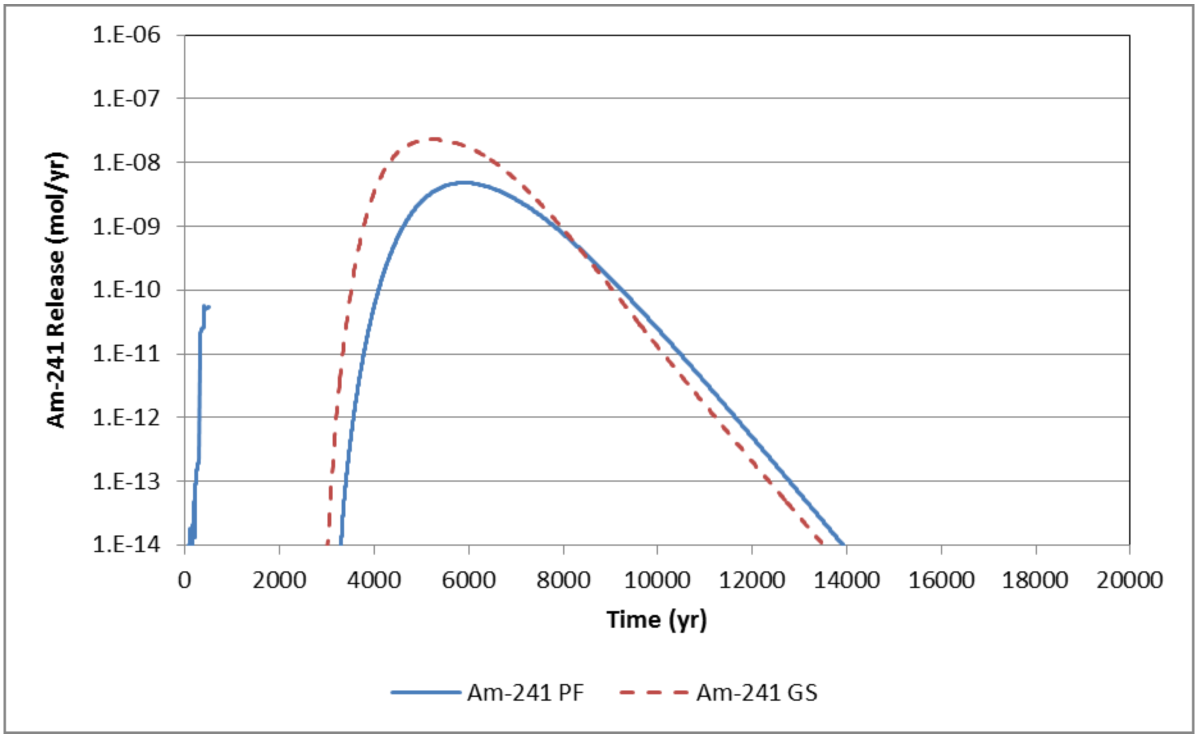

Figure A.1-24: Tank 13 Np-237 Release to the Saturated Zone for Case B

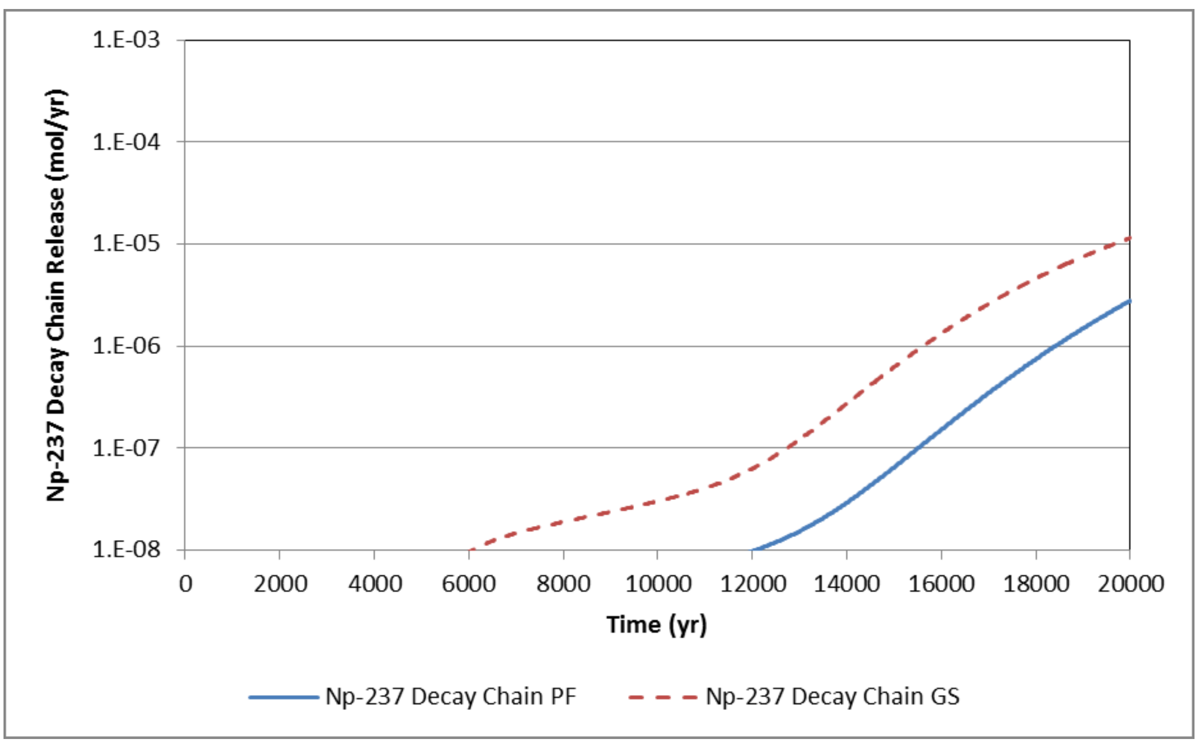

A.1.4 Type II Tank with Failed Liner (Tank 15) for Case B

For the Case B configuration, a comparison of the PORFLOW HTF Model and the GoldSim model mass releases of I-129, Tc-99, Am-243, Pu-239, U-234, Ra-226, Am-241, and Np-237, as presented in Figure A.1-25 through Figure A.1-32, indicate that the GoldSim model produces a good approximation of the releases from Tank 15 generated by the PORFLOW model.

Table A.1-4 summarizes the peak values for these releases showing that when comparing the two models except for Np-237 the percent differences are slightly above 50% or lower. Figure A.1-32, shows that despite similar release patterns in the two models, the GoldSim model will conservatively overestimate the releases of Np-237.

Table A.1-4: Case B GoldSim and PORFLOW Model Peak Releases from the UZ to the SZ Comparisons for Tank 15 within 20,000 years

Radionuclide	PORFLOW Peak Release (mol/yr)	PORFLOW Time of Peak Release (yr)	GoldSim Peak Release (mol/yr)	GoldSim Time of Peak Release (yr)	Peak Release Percent Difference GoldSim vs PORFLOW
I-129	1.5E-02	523	1.5E-02	520	0%
Tc-99	2.9E-04	318	1.3E-04	310	-55%
Am-243	1.1E-04	5,978	1.1E-04	5,680	0%
Pu-239	1.7E-05	12,946	1.6E-05	11,820	-6%
U-234	6.4E-04	2,201	7.0E-04	2,510	9%
Ra-226	1.2E-07	1,701	1.1E-07	1,710	-8%
Am-241	1.6E-07	4,355	2.5E-07	3,920	56%
Np-237	8.1E-06	20,000	2.1E-05	20,000	159%

Figure A.1-25: Tank 15 I-129 Release to the Saturated Zone for Case B

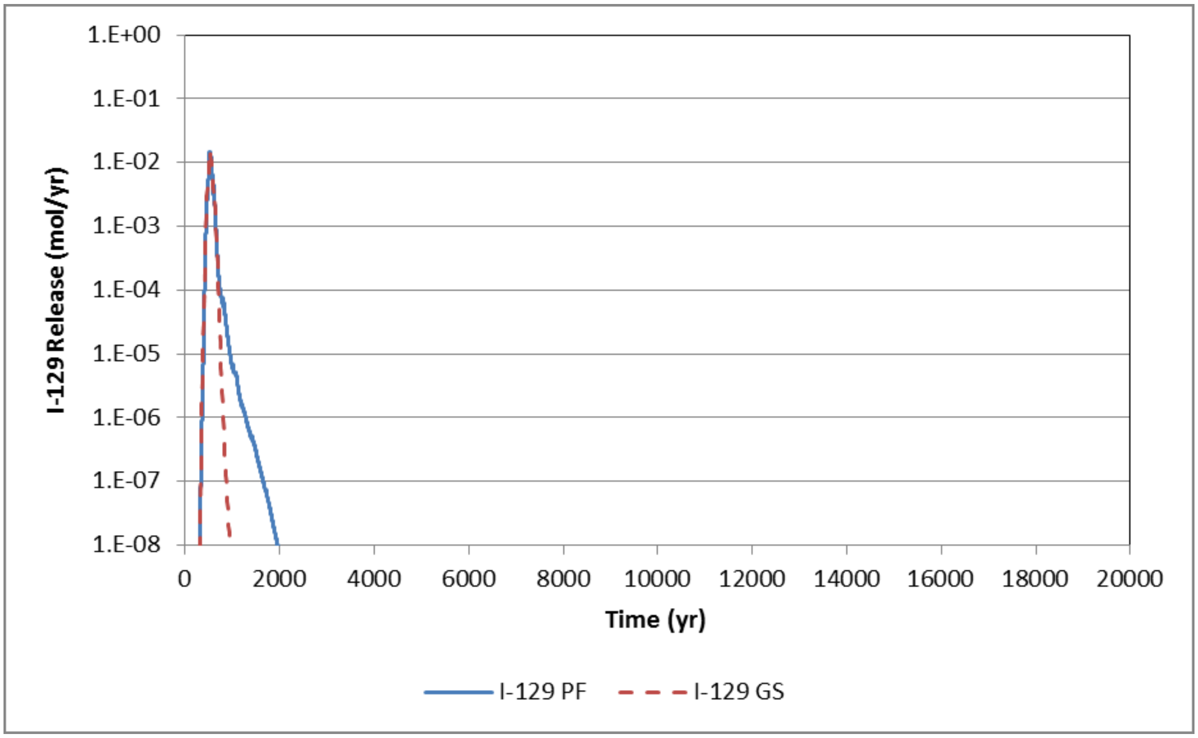

Figure A.1-26: Tank 15 Tc-99 Release to the Saturated Zone for Case B

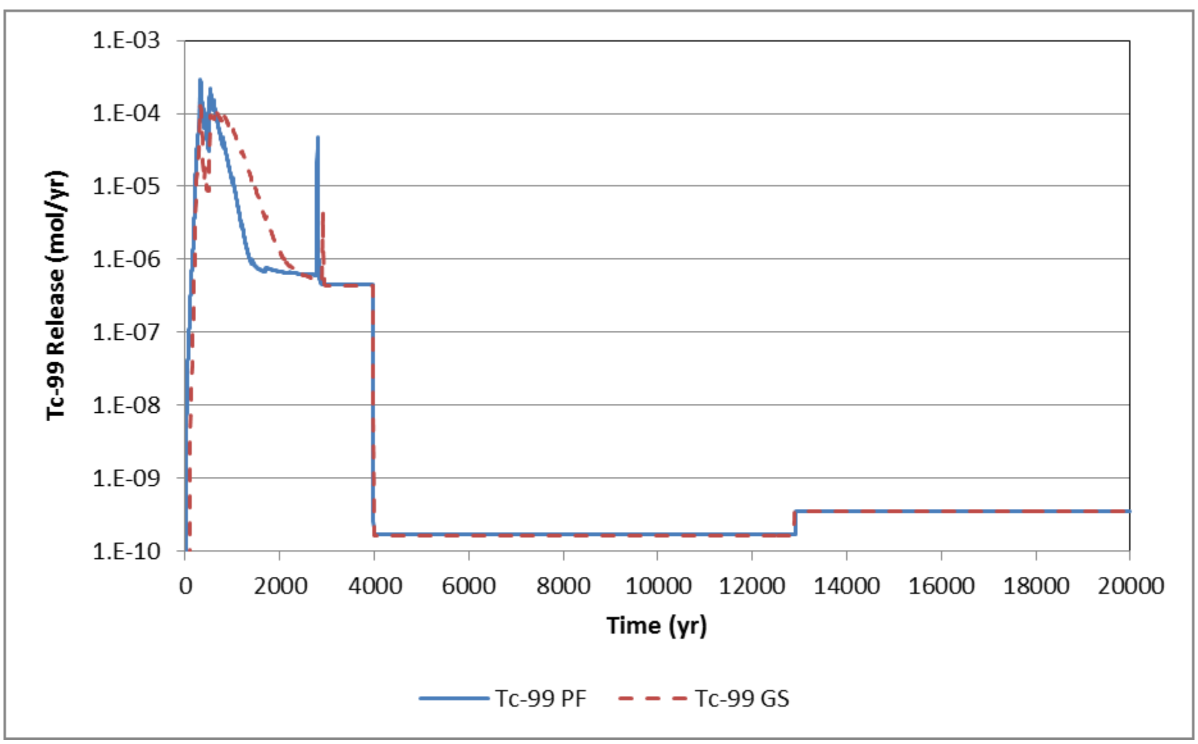

Figure A.1-27: Tank 15 Am-243 Release to the Saturated Zone for Case B

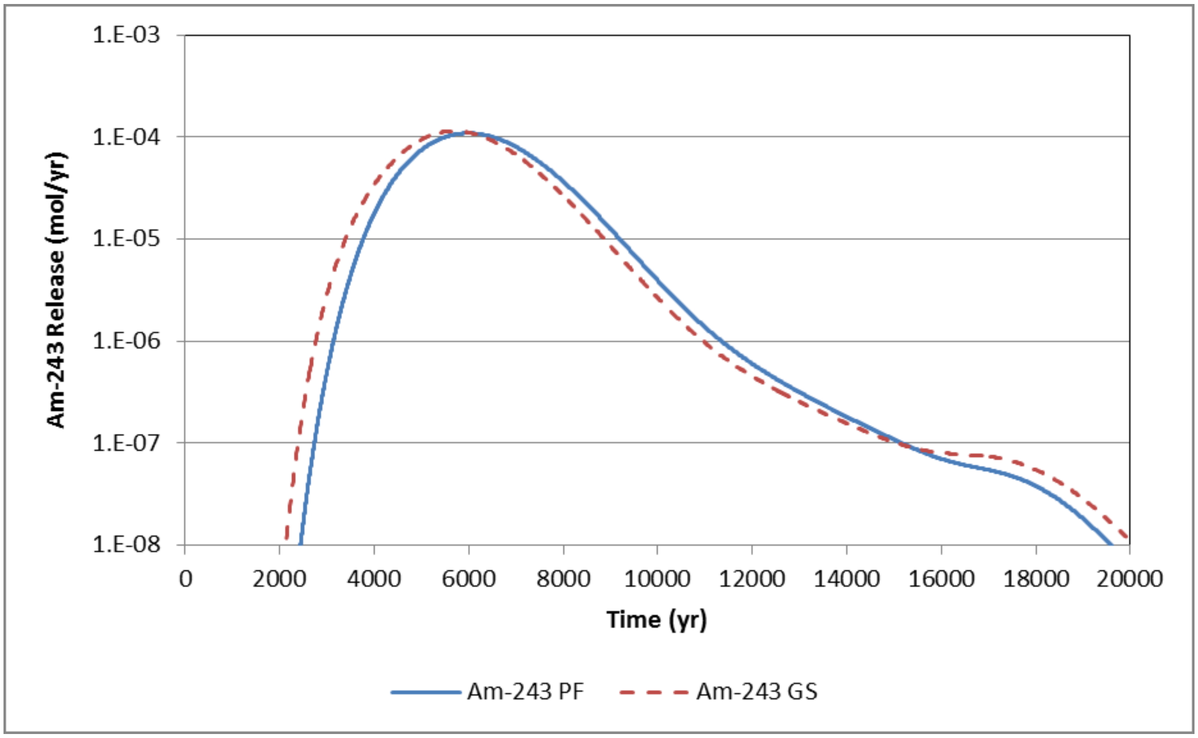

Figure A.1-28: Tank 15 Pu-239 Release to the Saturated Zone for Case B

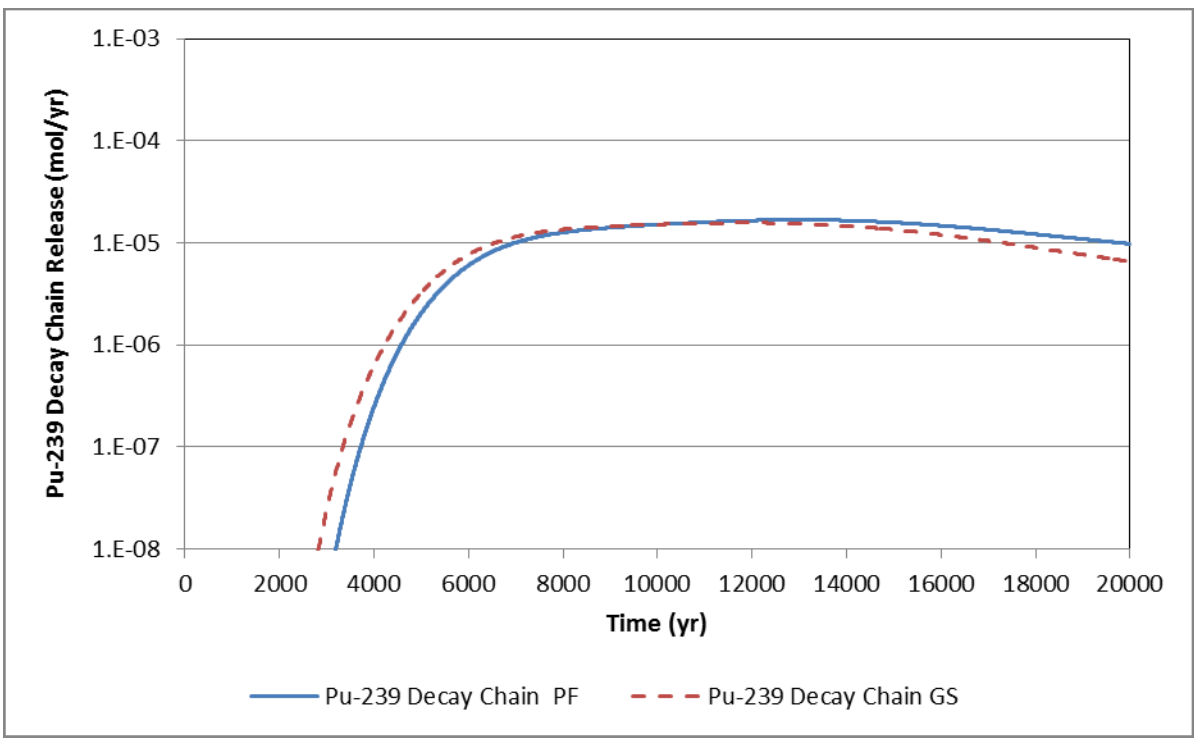

Figure A.1-29: Tank 15 U-234 Release to the Saturated Zone for Case B

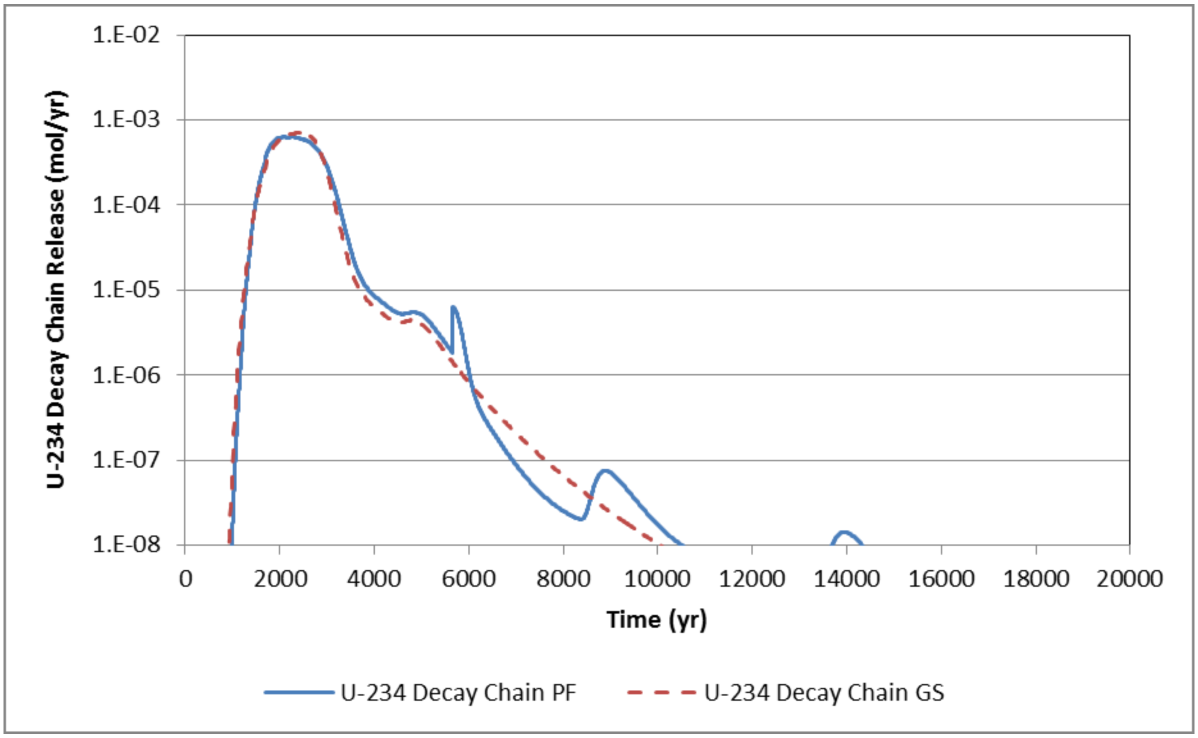

Figure A.1-30: Tank 15 Ra-226 Release to the Saturated Zone for Case B

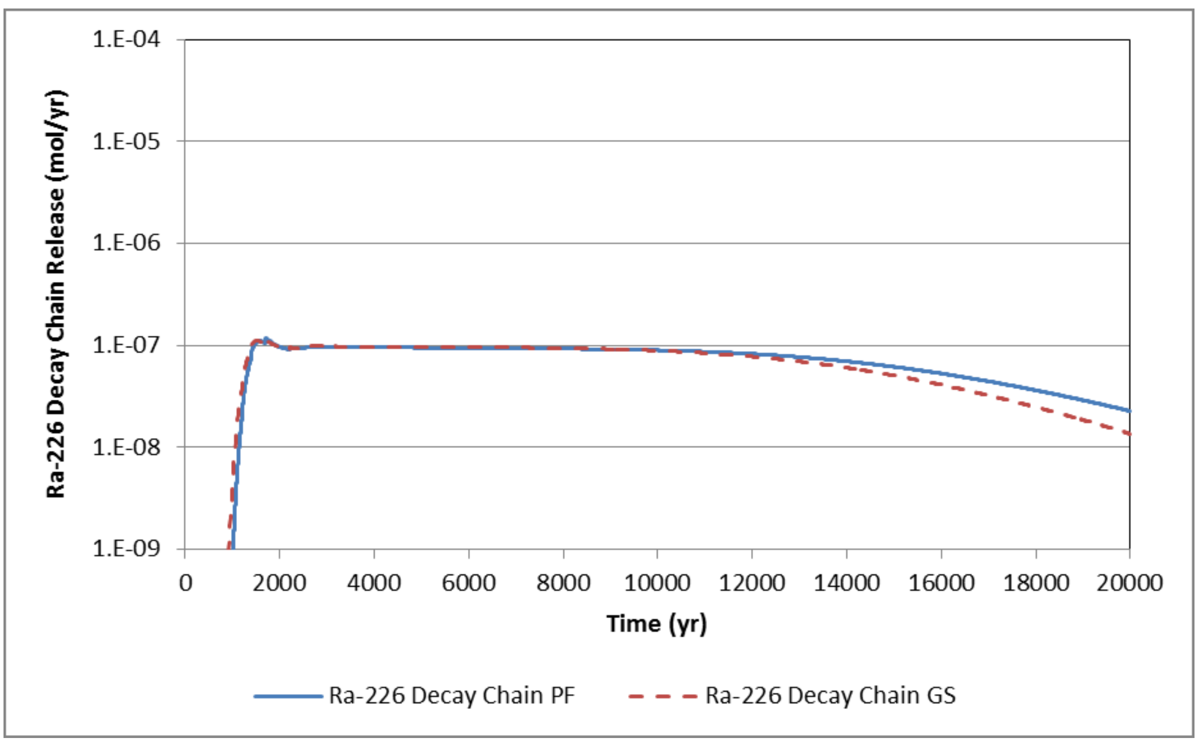

Figure A.1-31: Tank 15 Am-241 Release to the Saturated Zone for Case B

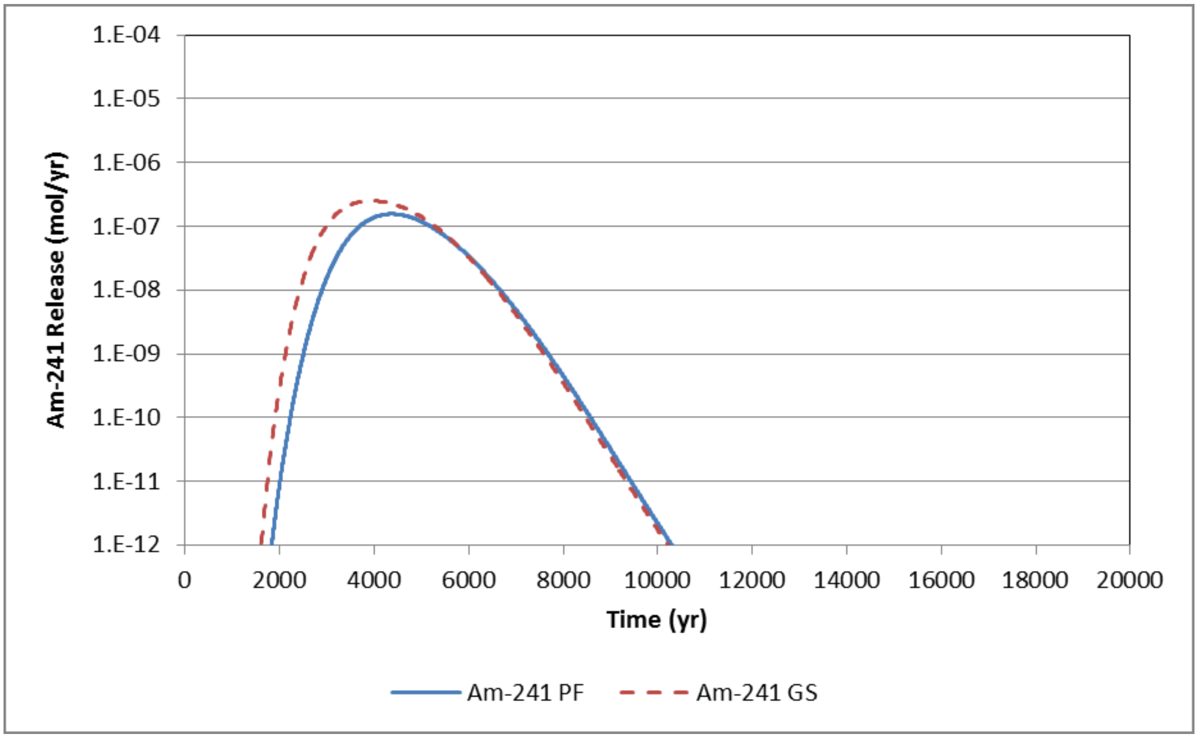

Figure A.1-32: Tank 15 Np-237 Release to the Saturated Zone for Case B

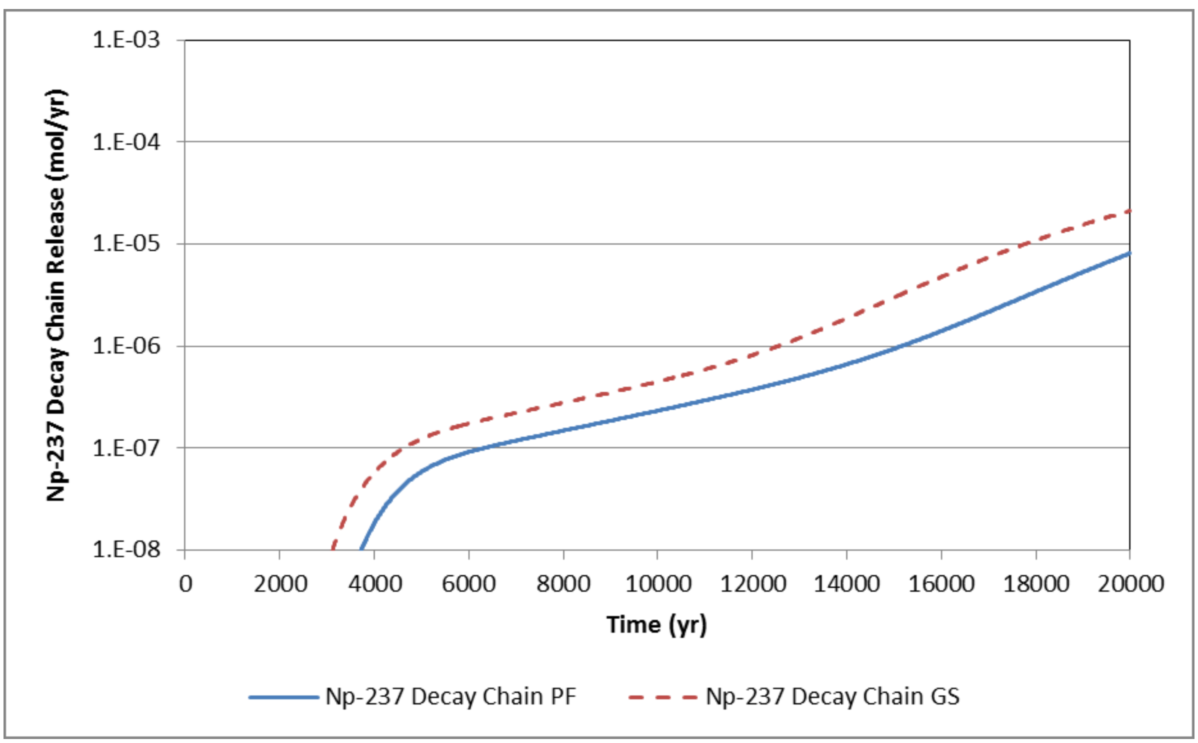

A.1.5 Type II Tank with Failed Liner (Tank 16) for Case B

For the Case B configuration, a comparison of the PORFLOW HTF Model and the GoldSim model mass releases of I-129, Tc-99, Am-243, Pu-239, U-234, Ra-226, Am-241, and Np-237, as presented in Figure A.1-33 through Figure A.1-40, indicate that the GoldSim model produces a good approximation of the releases from Tank 16 generated by the PORFLOW model.

Table A.1-5 summarizes the peak values for these releases showing that when comparing the two models the percent differences are slightly above 50% or lower.

Table A.1-5: Case B GoldSim and PORFLOW Model Peak Releases from the UZ to the SZ Comparisons for Tank 16 within 20,000 years

Radionuclide	PORFLOW Peak Release (mol/yr)	PORFLOW Time of Peak Release (yr)	GoldSim Peak Release (mol/yr)	GoldSim Time of Peak Release (yr)	Peak Release Percent Difference GoldSim vs PORFLOW
I-129	5.9E-03	518	8.0E-03	510	36%
Tc-99	4.7E-03	319	2.2E-03	610	-53%
Am-243	5.3E-08	4,920	5.6E-08	5,250	6%
Pu-239	4.2E-05	13,489	4.0E-05	13,930	-5%
U-234	4.6E-05	1,701	5.1E-05	1,730	11%
Ra-226	3.6E-09	1,701	3.5E-09	1,710	-3%
Am-241	4.4E-09	3,845	3.8E-09	3,910	-14%
Np-237	2.1E-06	20,000	2.3E-06	20,000	10%

Figure A.1-33: Tank 16 I-129 Release to the Saturated Zone for Case B

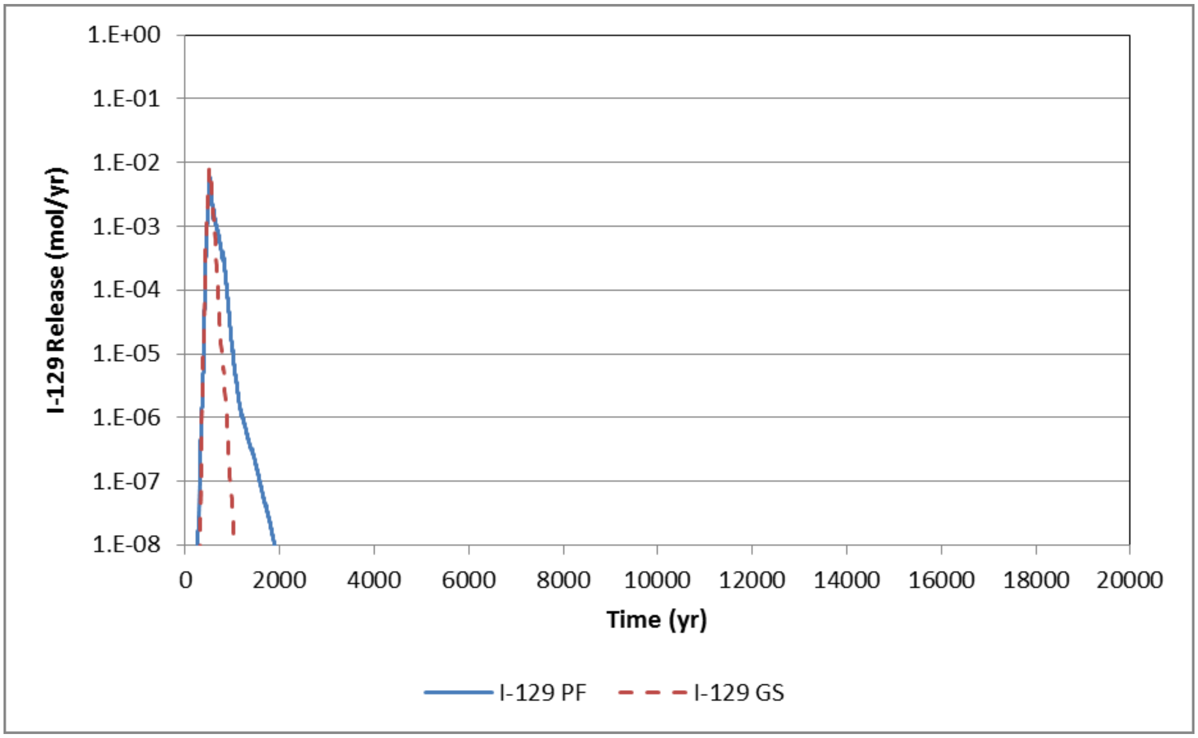

Figure A.1-34: Tank 16 Tc-99 Release to the Saturated Zone for Case B

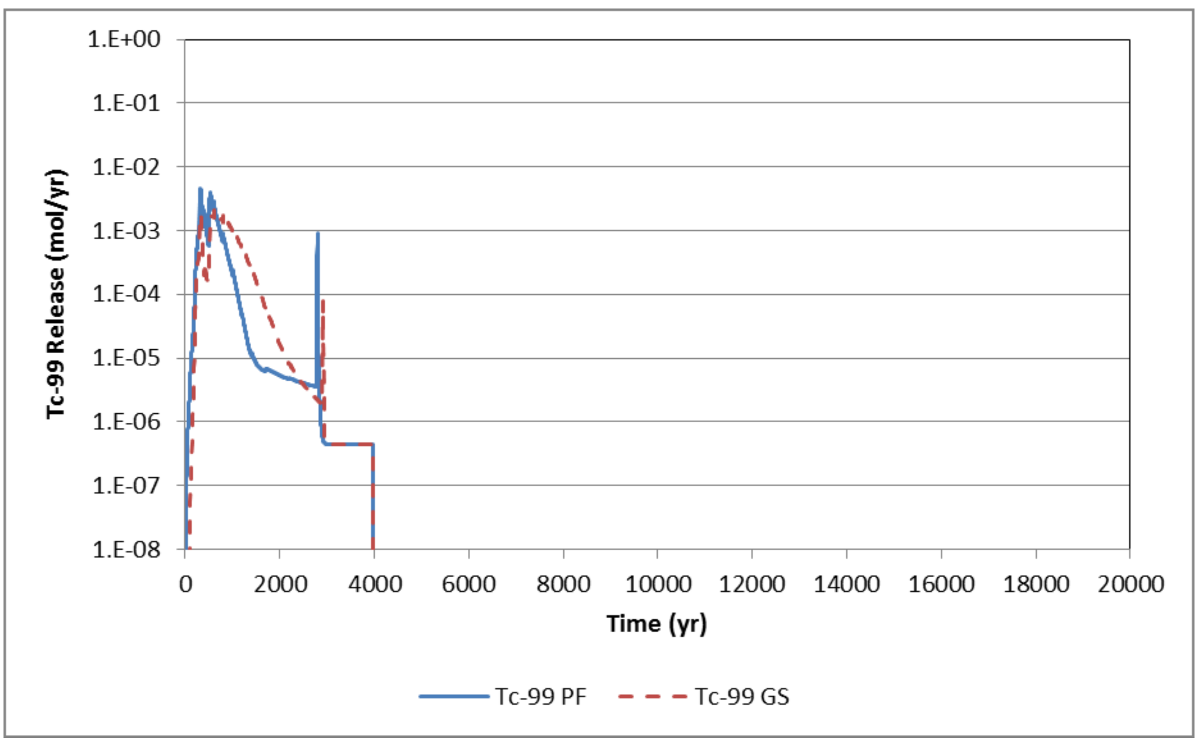

Figure A.1-35: Tank 16 Am-243 Release to the Saturated Zone for Case B

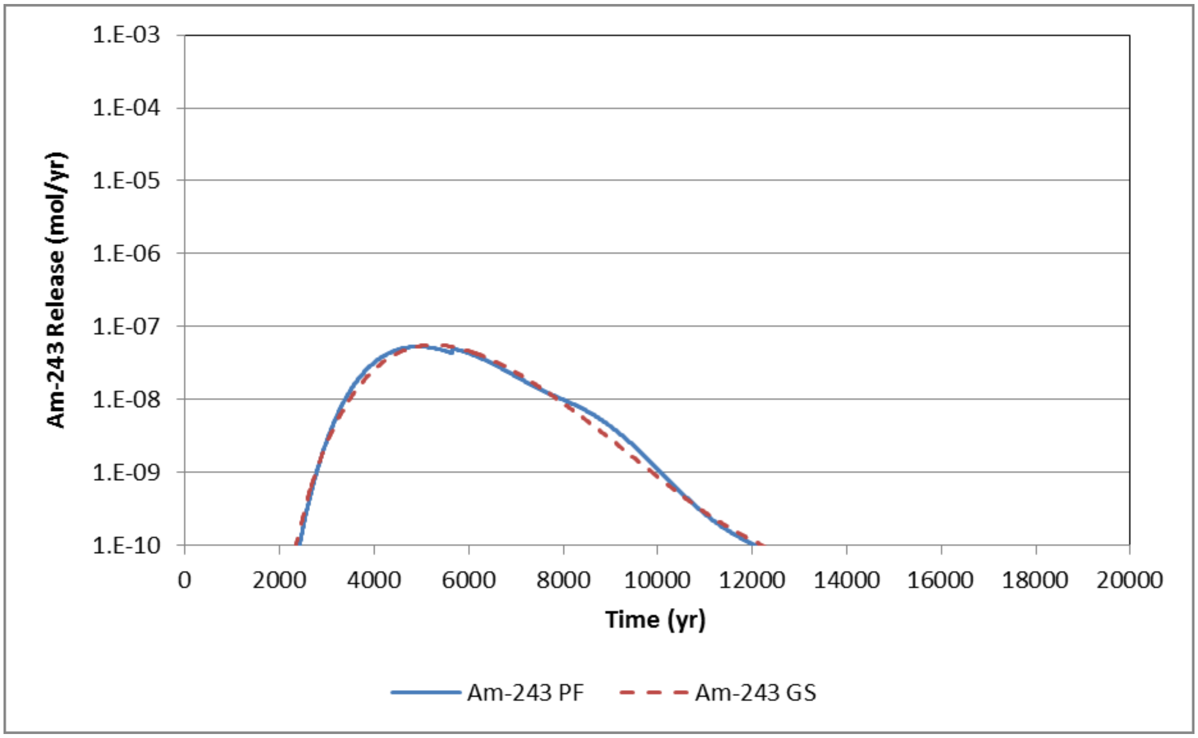

Figure A.1-36: Tank 16 Pu-239 Release to the Saturated Zone for Case B

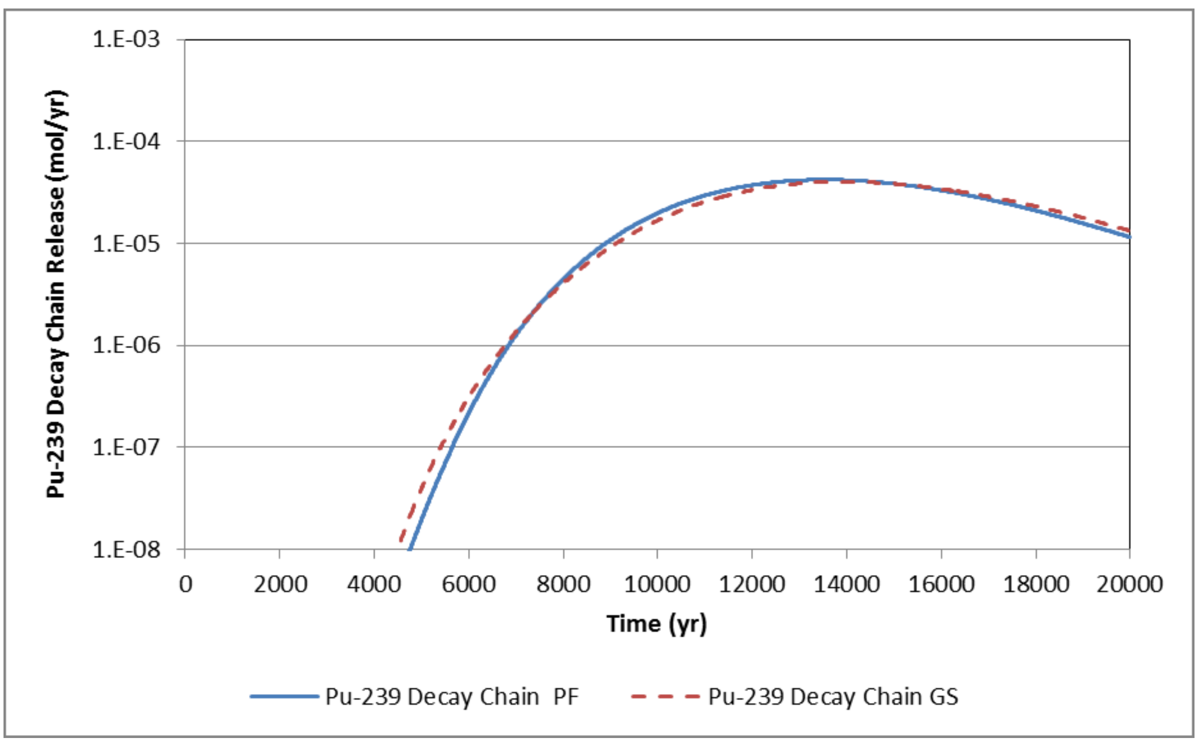

Figure A.1-37: Tank 16 U-234 Release to the Saturated Zone for Case B

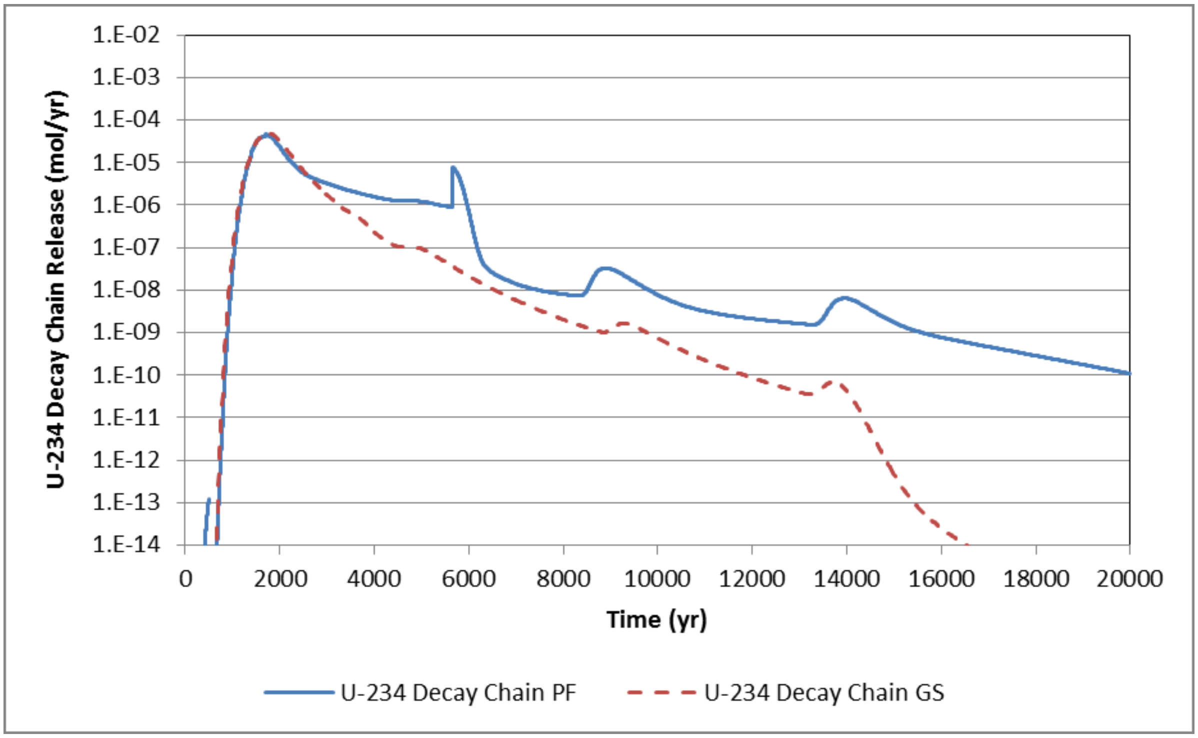

Figure A.1-38: Tank 16 Ra-226 Release to the Saturated Zone for Case B

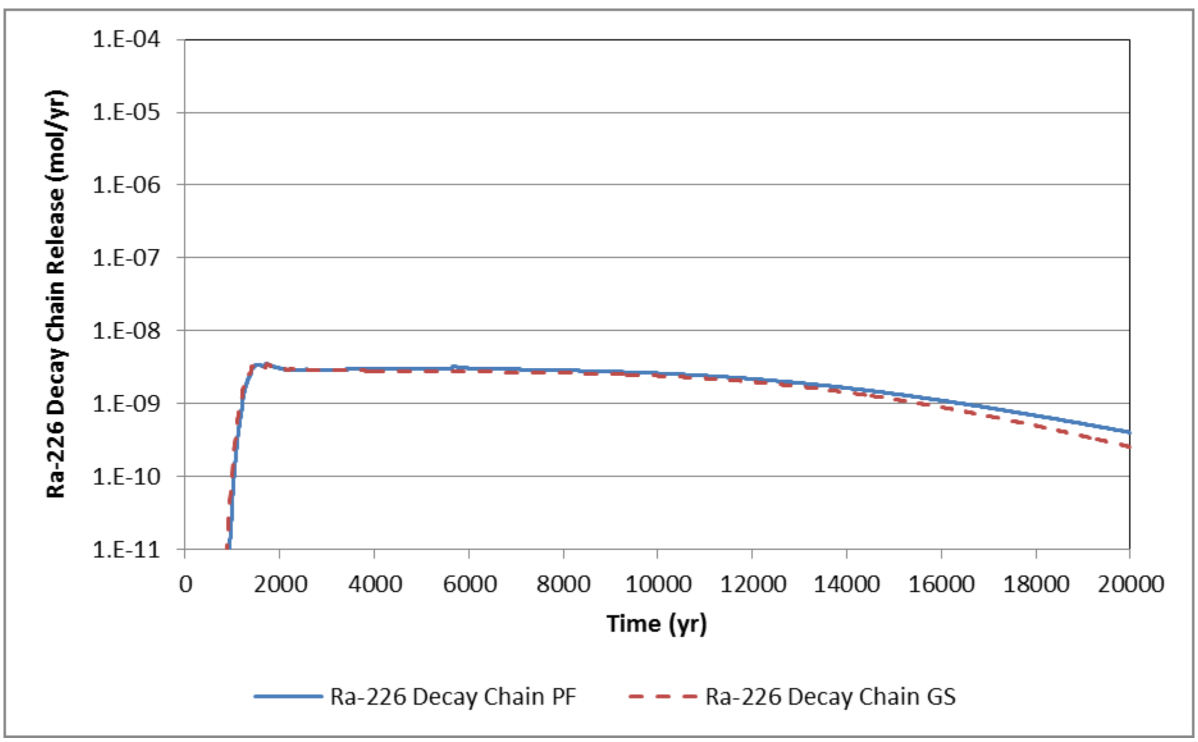

Figure A.1-39: Tank 16 Am-241 Release to the Saturated Zone for Case B

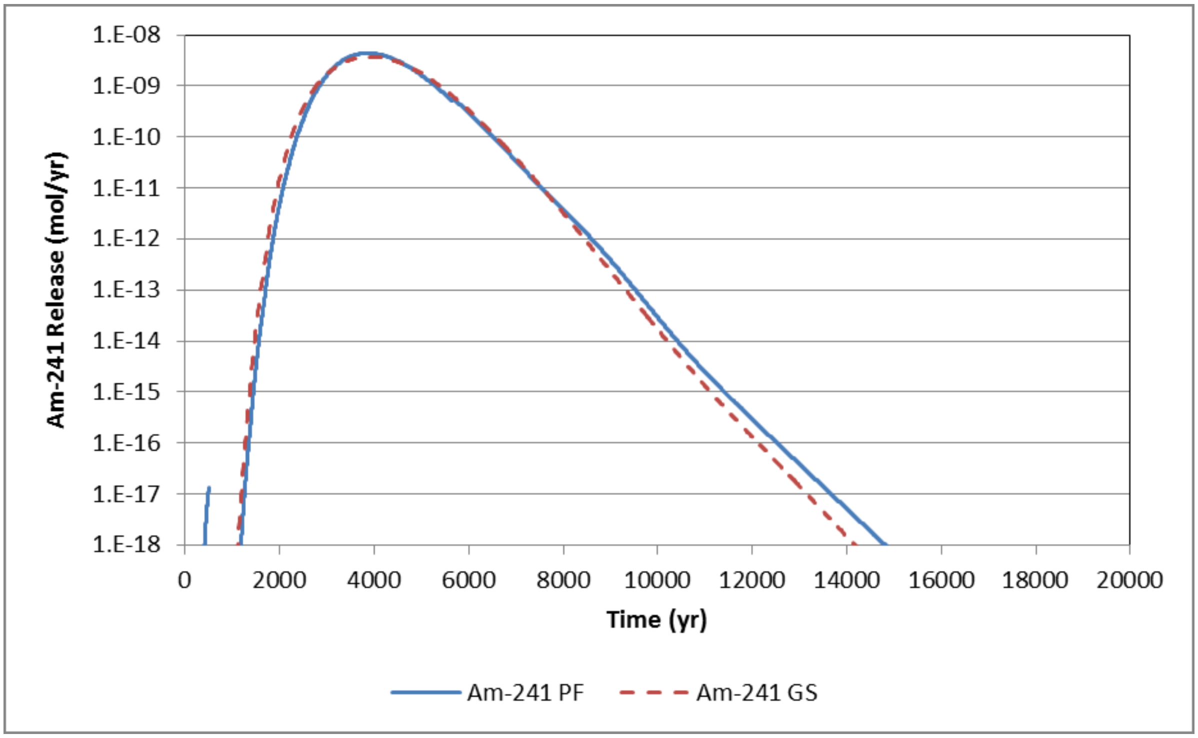

Figure A.1-40: Tank 16 Np-237 Release to the Saturated Zone for Case B

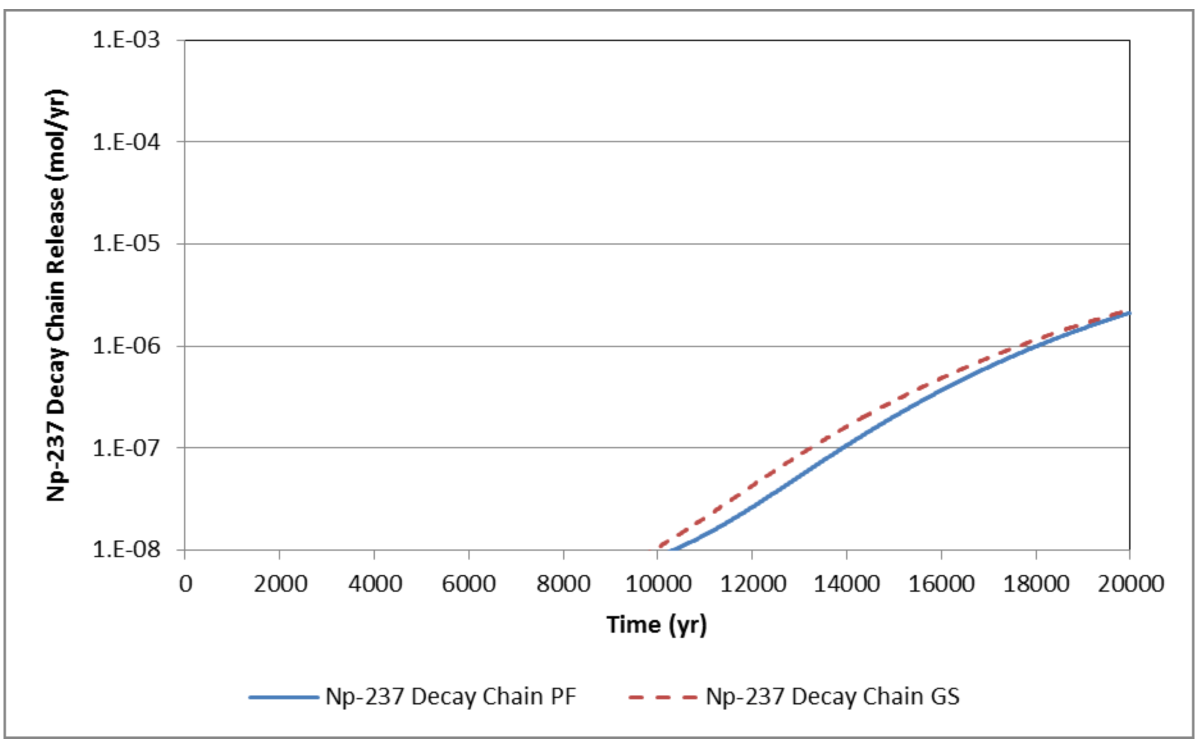

A.1.6 Type IV Tank (Tank 24) for Case B

For the Case B configuration, a comparison of the PORFLOW HTF Model and the GoldSim model mass releases of I-129, Tc-99, Am-243, Pu-239, U-234, Ra-226, Am-241, and Np-237, as presented in Figure A.1-41 through Figure A.1-48, indicate that the GoldSim model produces a good approximation of the releases from Tank 24 generated by the PORFLOW model.

Table A.1-6 summarizes the peak values for these releases showing that when comparing the two models except for Pu-239 and Ra-226 the percent differences are below 50%. The difference between the two model results is a function of the tank-grout pore-volume calculations used to evaluate Eh/pH transition times for the two models. The PORFLOW model calculations are based on a tank-grout volume defined by the tank-grout property zone assignments. For the GoldSim model pore-volume calculations, the calculations are based on a tank-grout volume defined by a cylindrical body which does not include the dome portion of the Type IV tanks. This difference in methodologies represent a conservative simplification for the GoldSim model, with the transition times occurring earlier.

Table A.1-6: Case B GoldSim and PORFLOW Model Peak Releases from the UZ to the SZ Comparisons for Tank 24 within 20,000 years

Radionuclide	PORFLOW Peak Release (mol/yr)	PORFLOW Time of Peak Release (yr)	GoldSim Peak Release (mol/yr)	GoldSim Time of Peak Release (yr)	Peak Release Percent Difference GoldSim vs PORFLOW
I-129	6.2E-05	501	6.4E-05	510	3%
Tc-99	1.9E-08	9.501	2.0E-08	10,010	5%
Am-243	2.2E-07	12,685	2.8E-07	18,100	27%
Pu-239	2.2E-06	19,980	5.4E-06	19,050	145%
U-234	2.5E-06	9,966	2.9E-06	9,630	16%
Ra-226	3.5E-08	2,301	7.7E-08	18,100	120%
Am-241	9.6E-12	3,501	5.5E-12	3,940	-43%
Np-237	1.2E-05	7,900	1.2E-05	6,440	0%

Figure A.1-41: Tank 24 I-129 Release to the Saturated Zone for Case B

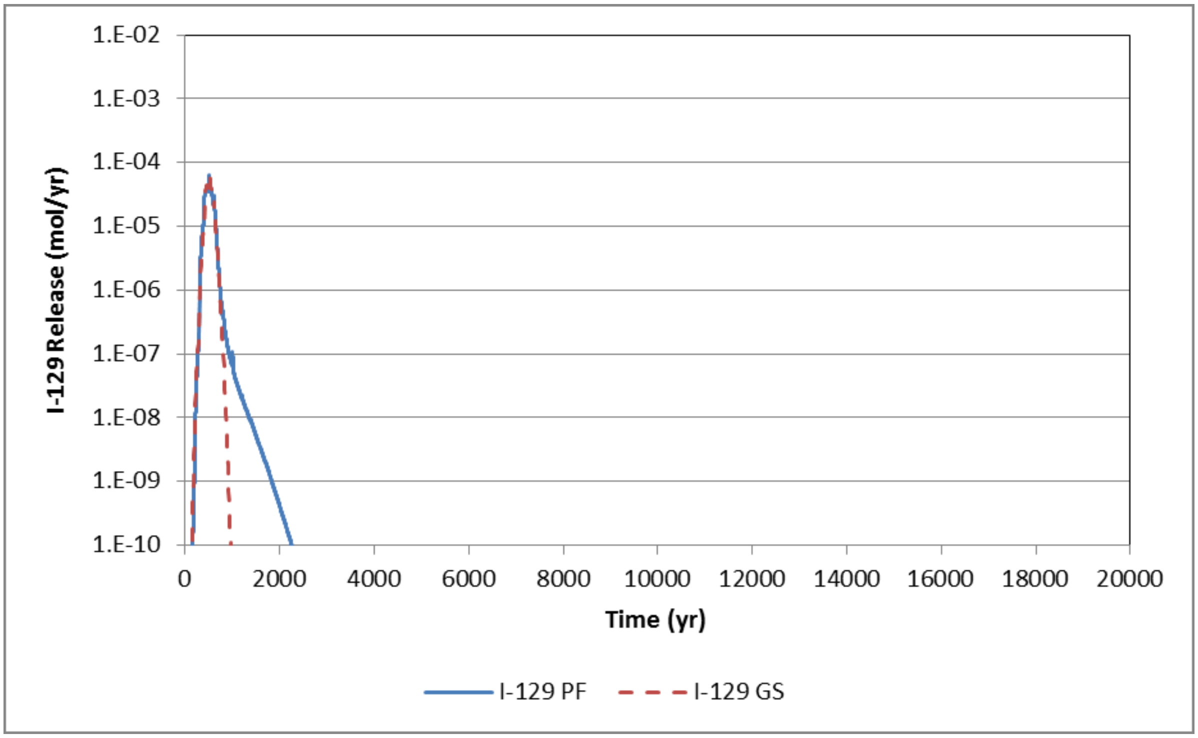

Figure A.1-42: Tank 24 Tc-99 Release to the Saturated Zone for Case B

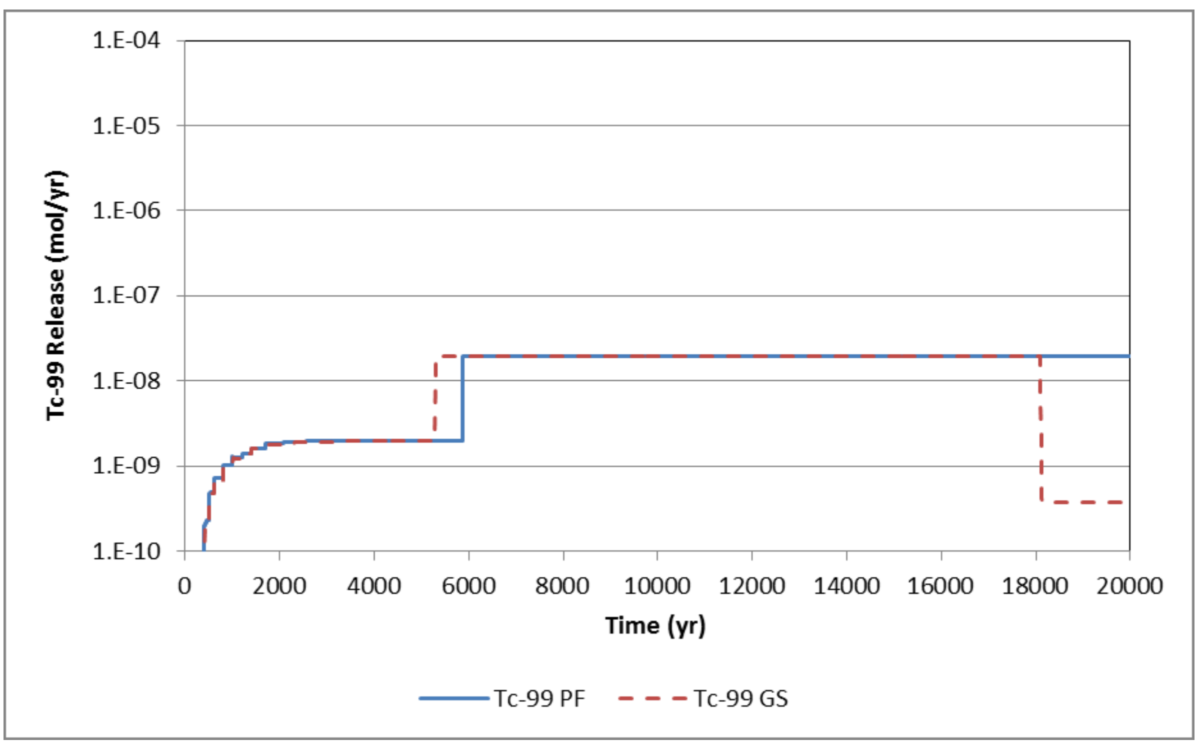

Figure A.1-43: Tank 24 Am-243 Release to the Saturated Zone for Case B

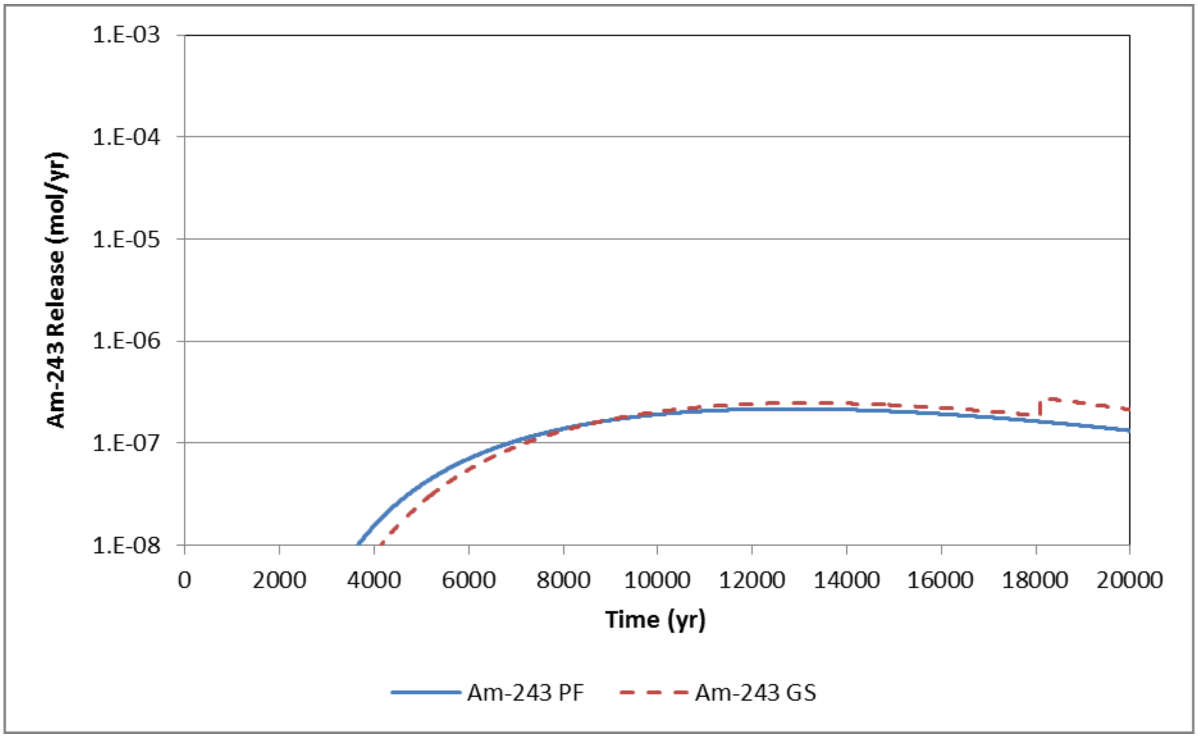

Figure A.1-44: Tank 24 Pu-239 Release to the Saturated Zone for Case B

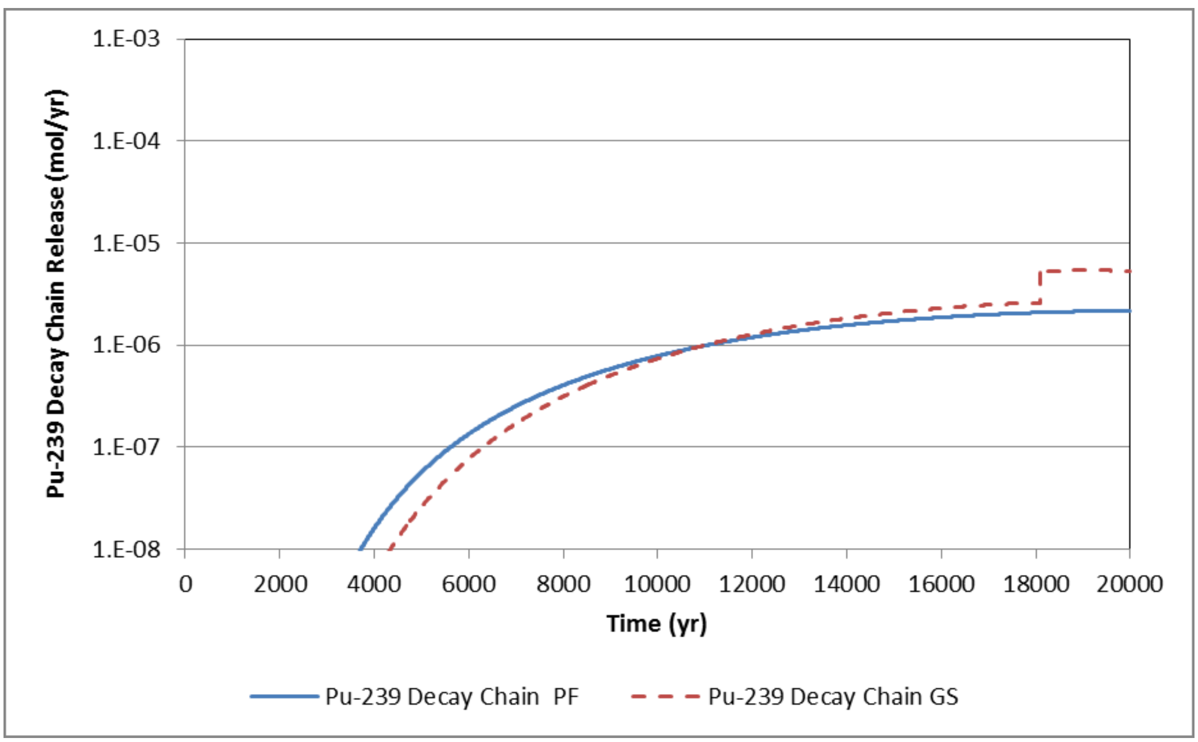

Figure A.1-45: Tank 24 U-234 Release to the Saturated Zone for Case B

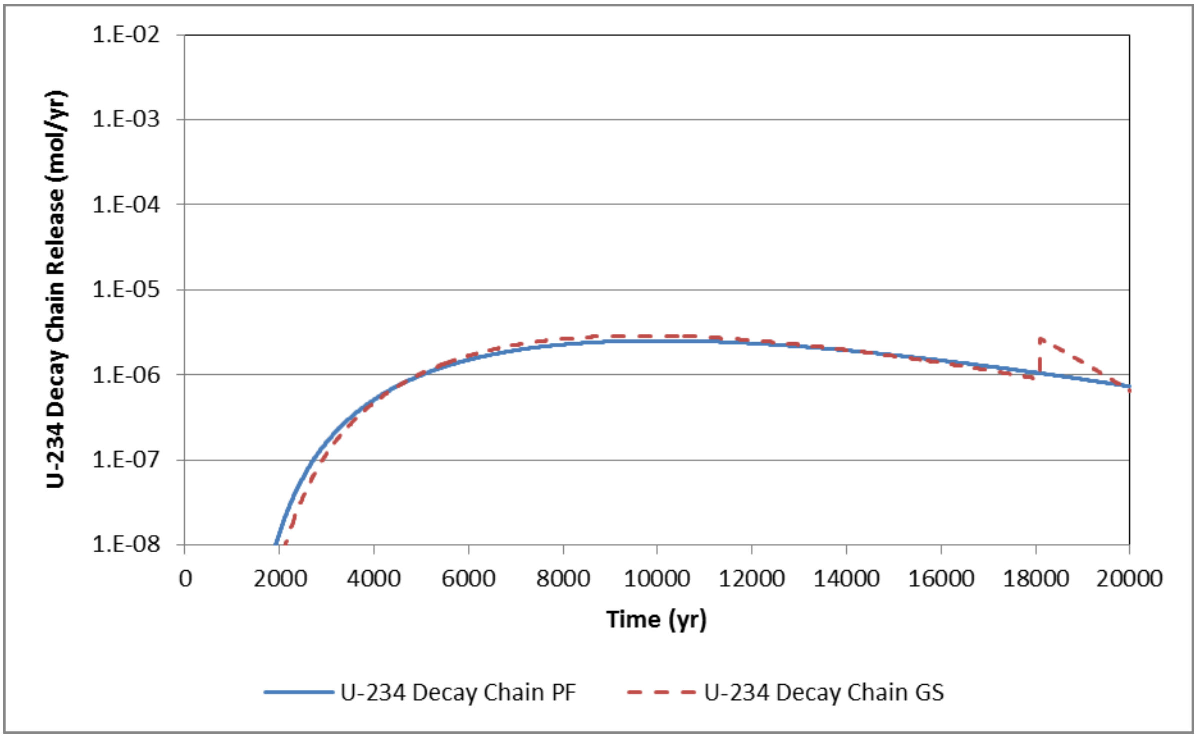

Figure A.1-46: Tank 24 Ra-226 Release to the Saturated Zone for Case B

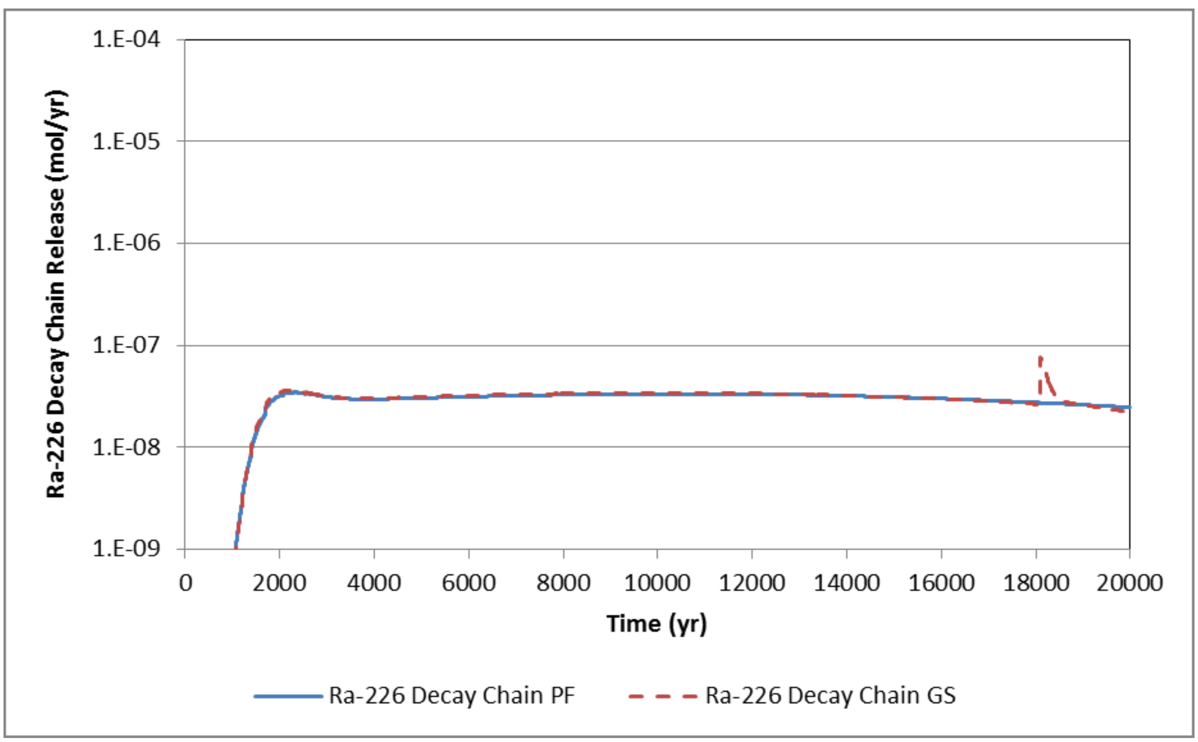

Figure A.1-47: Tank 24 Am-241 Release to the Saturated Zone for Case B

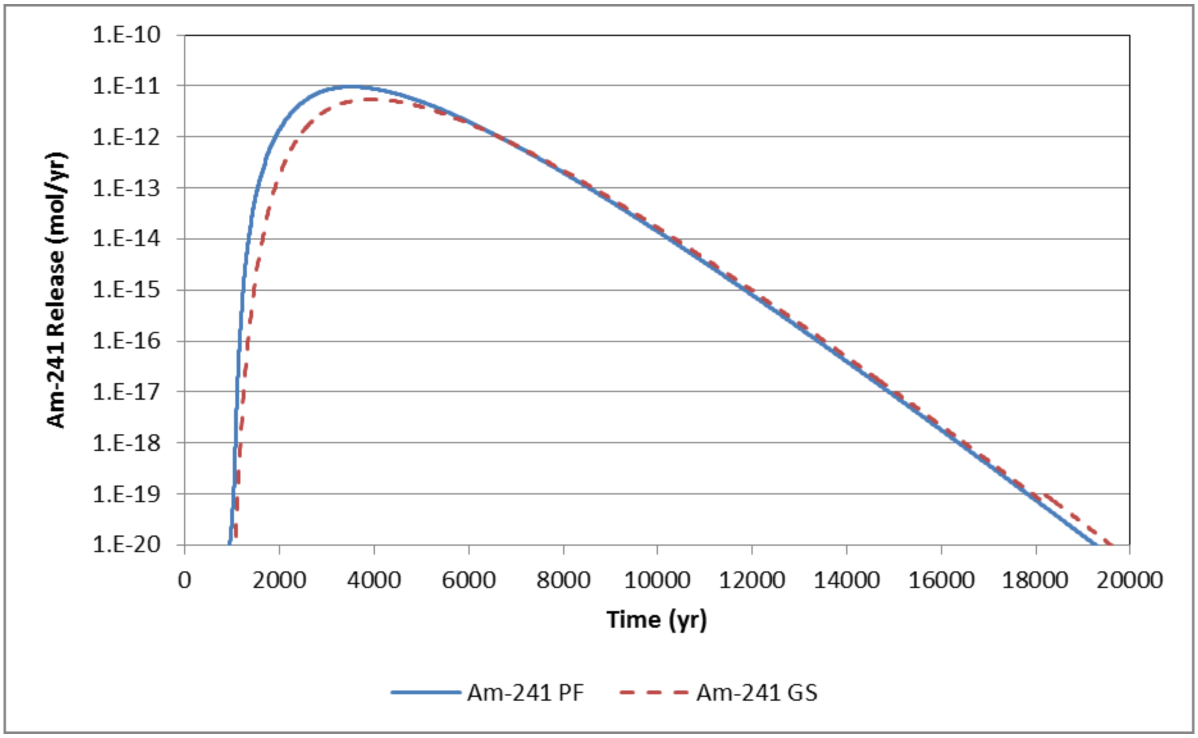

Figure A.1-48: Tank 24 Np-237 Release to the Saturated Zone for Case B

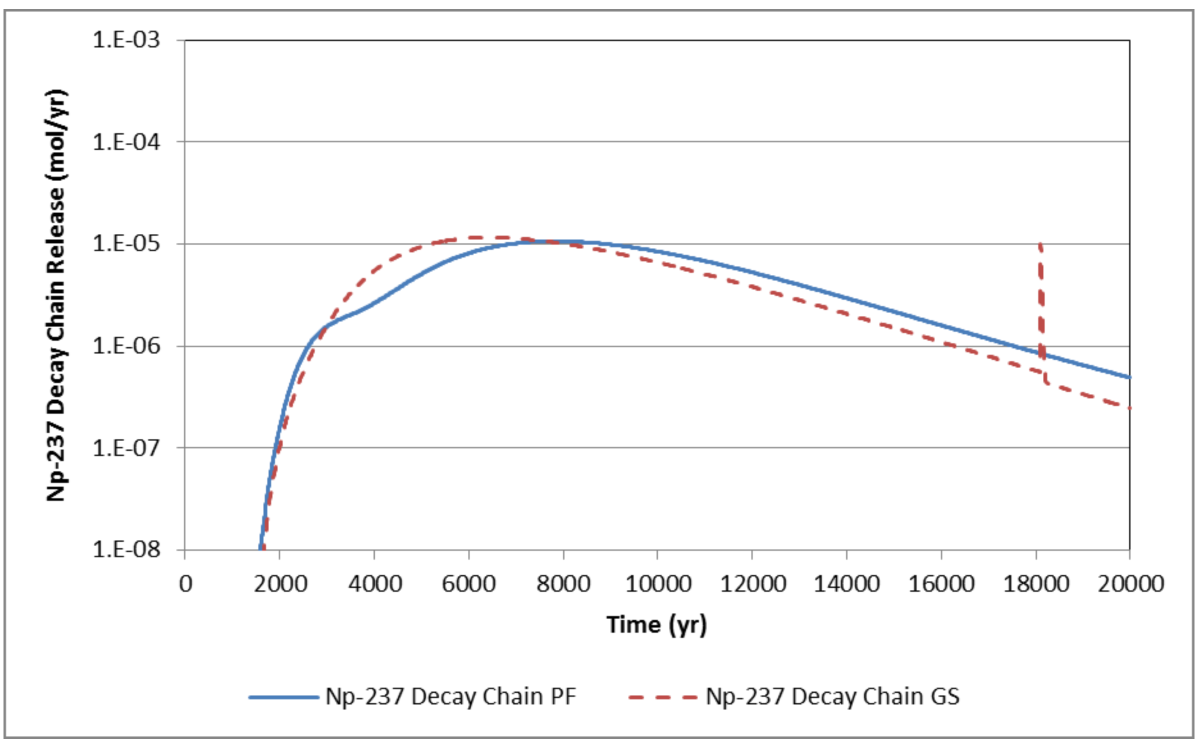

A.1.7 Type III Tank (Tank 31) for Case B

For the Case B configuration, a comparison of the PORFLOW HTF Model and the GoldSim model mass releases of I-129, Tc-99, Am-243, Pu-239, U-234, Ra-226, Am-241, and Np-237, as presented in Figure A.1-49 through Figure A.1-56, indicate that the GoldSim model produces a good approximation of the releases from Tank 31 generated by the PORFLOW model.

Table A.1-7 summarizes the peak values for these releases showing that when comparing the two models except for Am-243, Pu-239, Am-241 and Np-237 the percent differences are below 50%. Figure A.1-51 and Figure A.1-52, show that despite similar release patterns in the two models, the GoldSim model may conservatively overestimate the releases of Am-243, and Pu-239, respectively. Figure A.1-55 shows that despite similar release patterns in the two models, the GoldSim model may conservatively overestimate the releases of Am-241. Figure A.1-56, which contains GoldSim model release curves for a 15 cell basemat and a 10 cell basemat shows that if the numerical dispersion is increased the two models have closer results.

Table A.1-7: Case B GoldSim and PORFLOW Model Peak Releases from the UZ to the SZ Comparisons for Tank 31 within 20,000 years

Radionuclide	PORFLOW Peak Release (mol/yr)	PORFLOW Time of Peak Release (yr)	GoldSim Peak Release (mol/yr)	GoldSim Time of Peak Release (yr)	Peak Release Percent Difference GoldSim vs PORFLOW
I-129	2.5E-03	2,215	3.4E-03	2,210	36%
Tc-99	1.9E-08	9,501	1.9E-08	10,010	0%
Am-243	7.1E-09	20,000	5.6E-08	20,000	689%
Pu-239	2.0E-07	20,000	5.7E-07	20,000	185%
U-234	3.3E-04	18,488	3.1E-04	18,330	-6%
Ra-226	1.1E-06	18,325	9.5E-07	18,330	-14%
Am-241	3.3E-18	12,205	8.0E-18	13,810	142%
Np-237	3.1E-04	18,343	1.3E-06	18,350	-100%
Np-237[1]	3.1E-04	18,343	1.1E-04	18,340	-65%

[1] Used coarser discretization on basemat.

Figure A.1-49: Tank 31 I-129 Release to the Saturated Zone for Case B

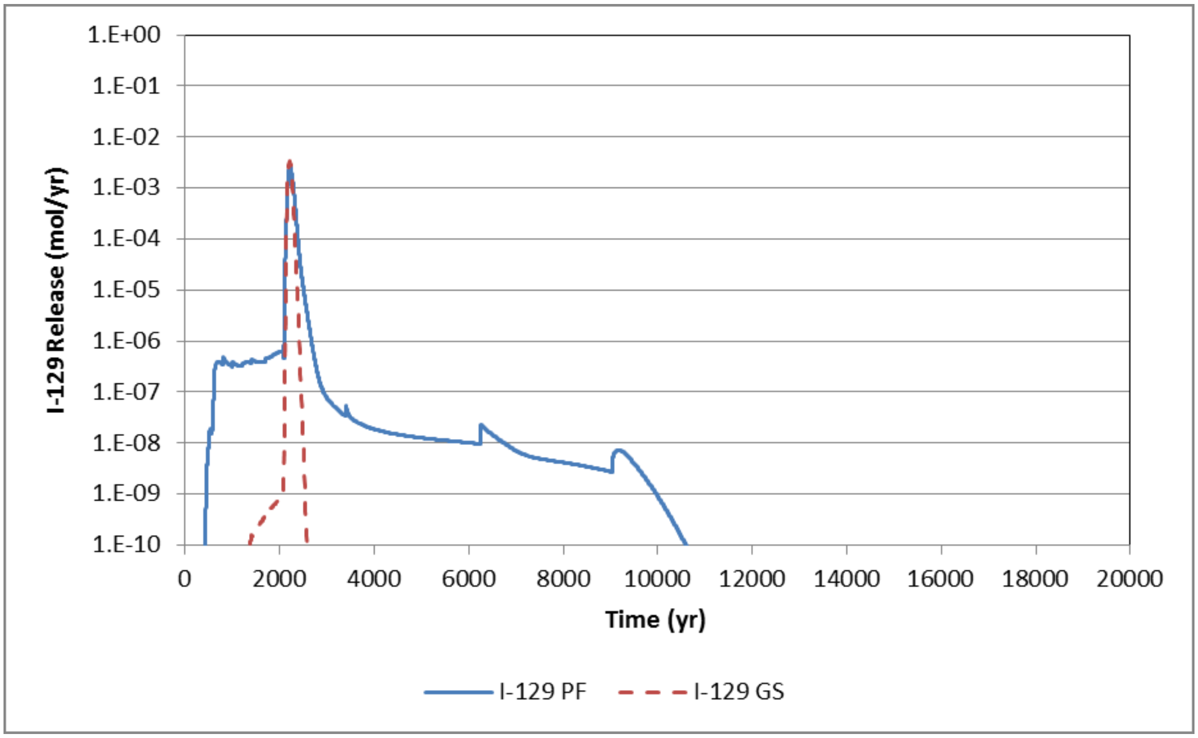

Figure A.1-50: Tank 31 Tc-99 Release to the Saturated Zone for Case B

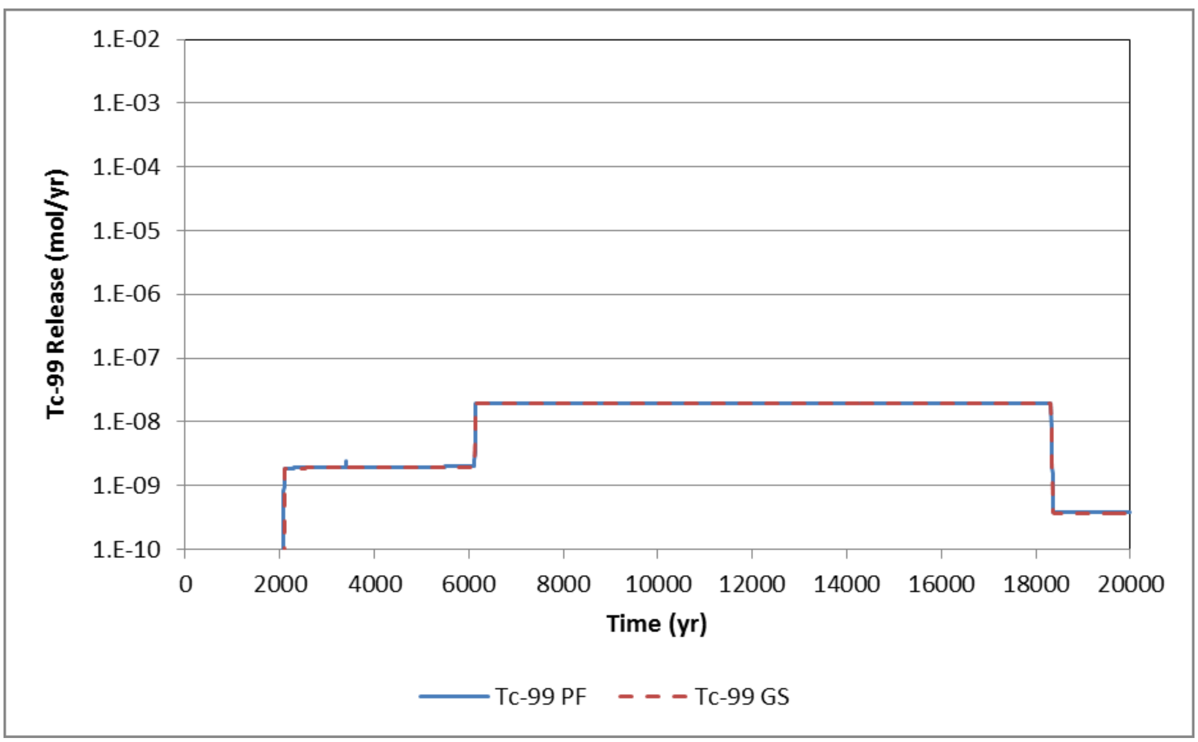

Figure A.1-51: Tank 31 Am-243 Release to the Saturated Zone for Case B

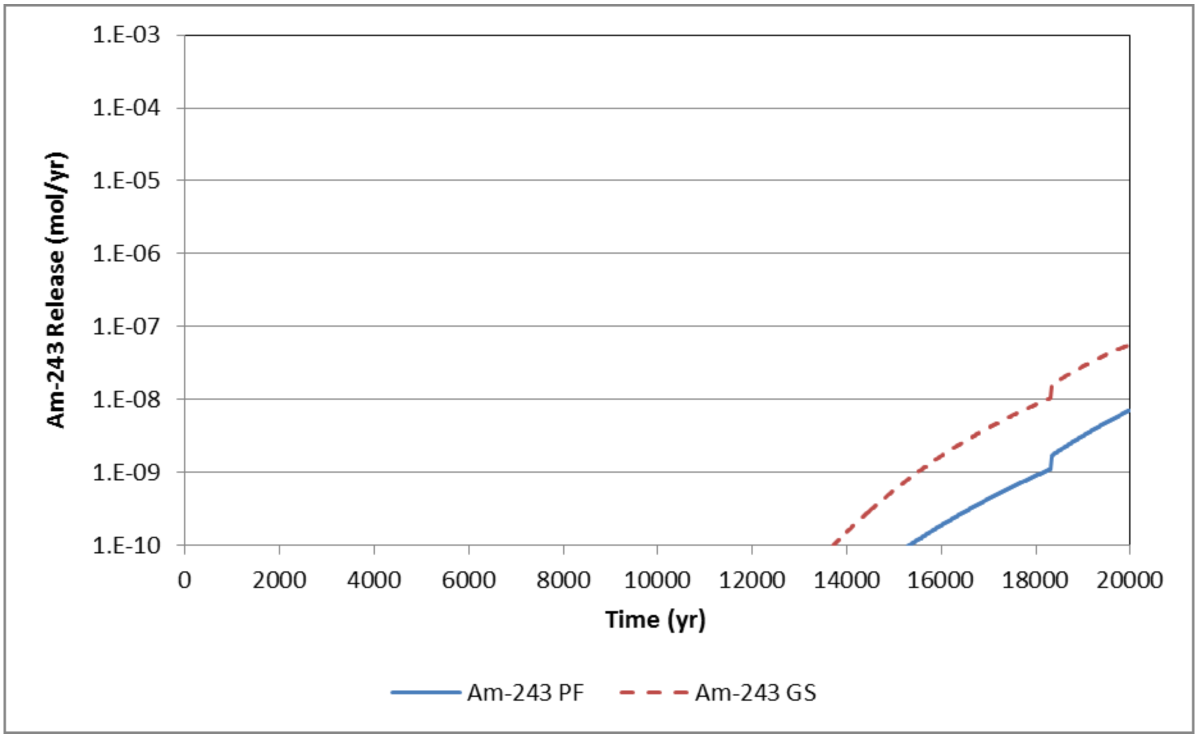

Figure A.1-52: Tank 31 Pu-239 Release to the Saturated Zone for Case B

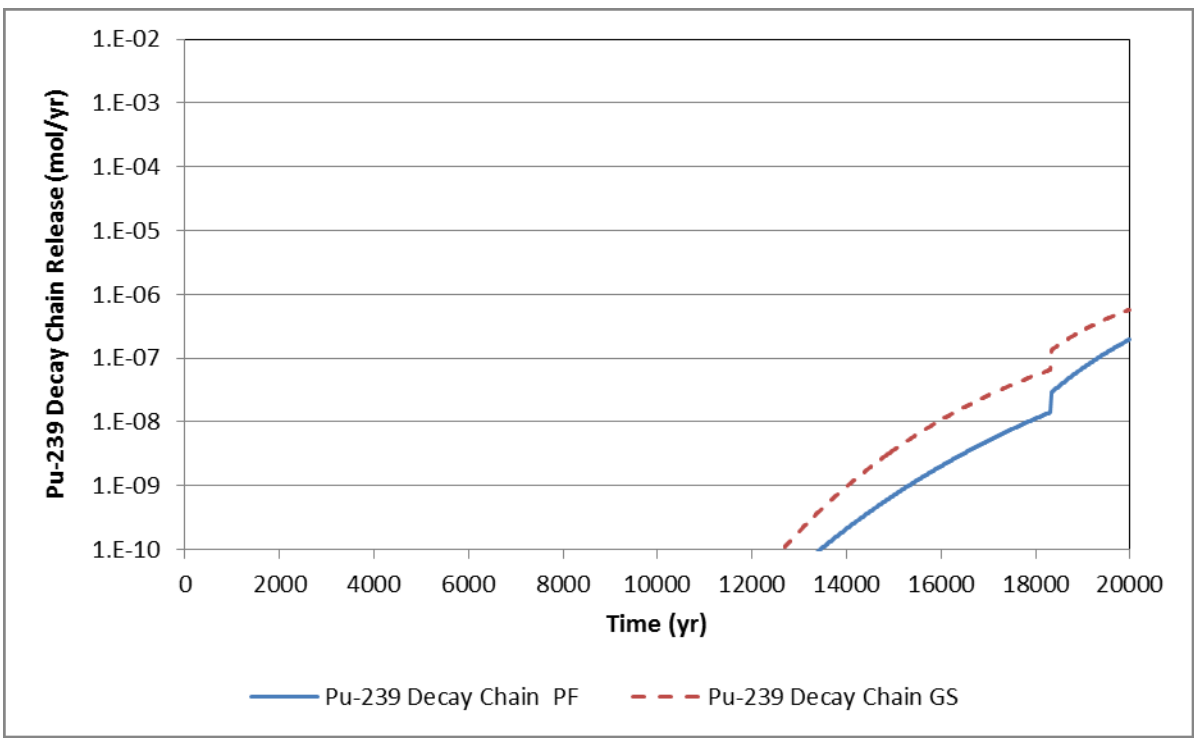

Figure A.1-53: Tank 31 U-234 Release to the Saturated Zone for Case B

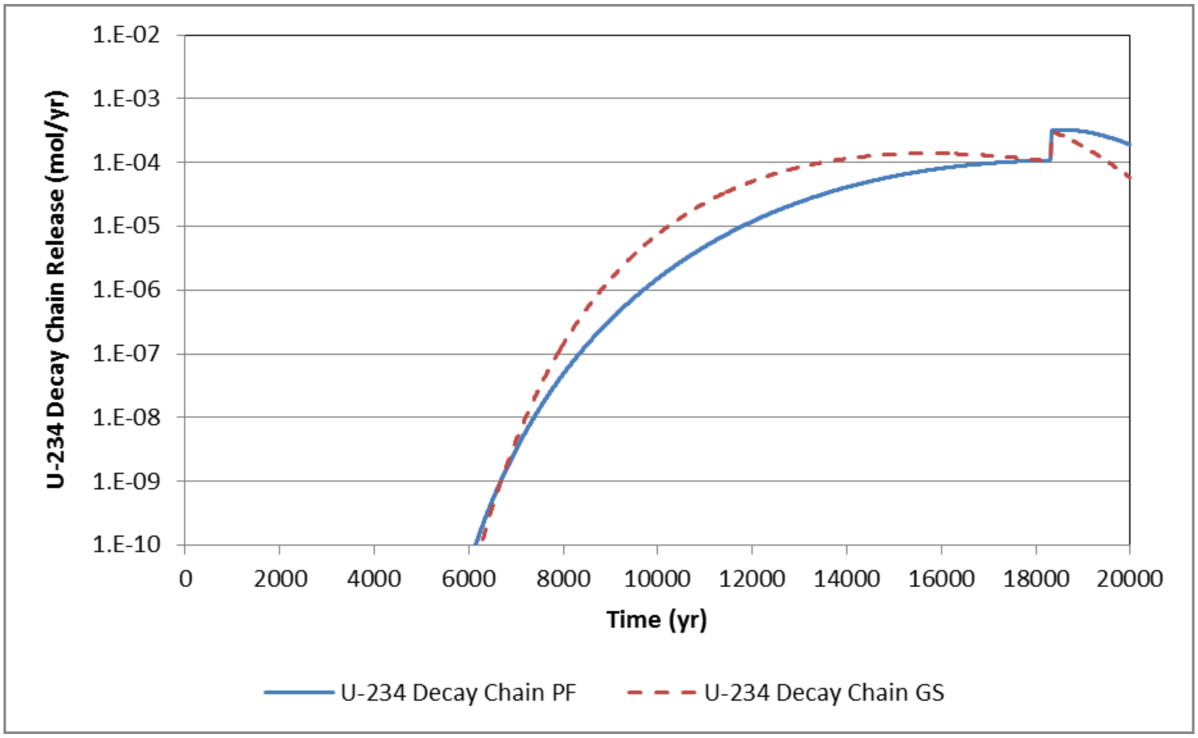

Figure A.1-54: Tank 31 Ra-226 Release to the Saturated Zone for Case B

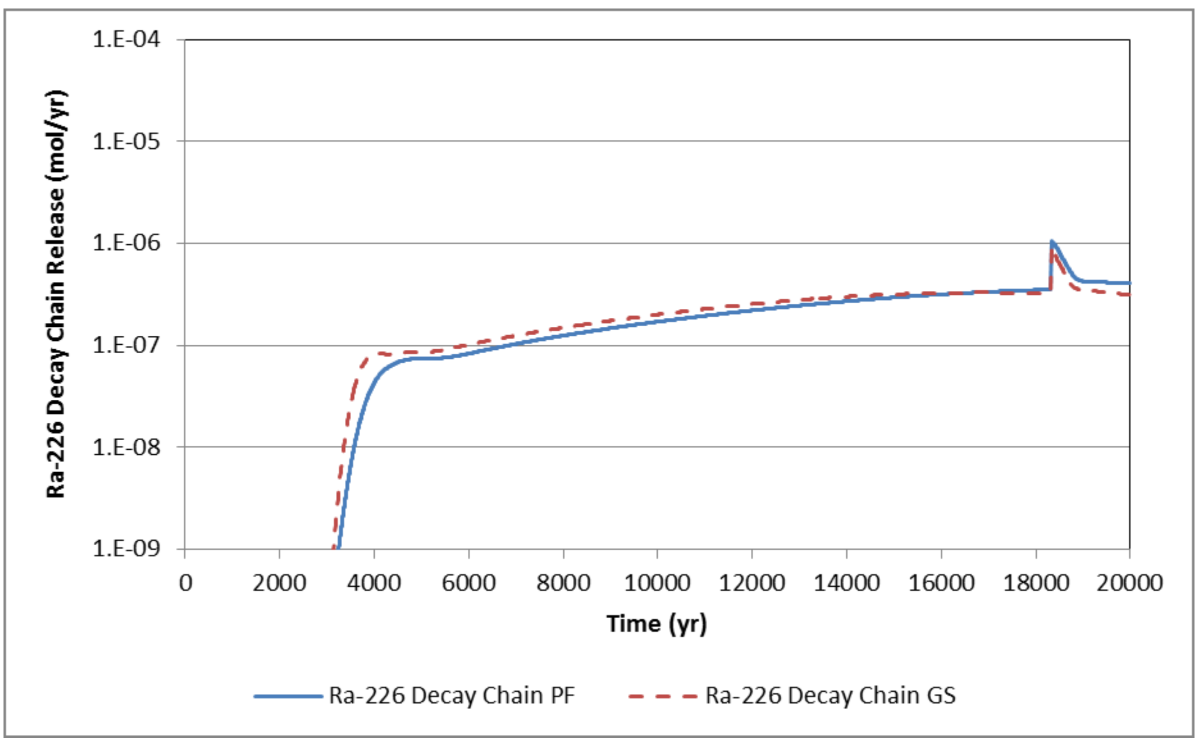

Figure A.1-55: Tank 31 Am-241 Release to the Saturated Zone for Case B

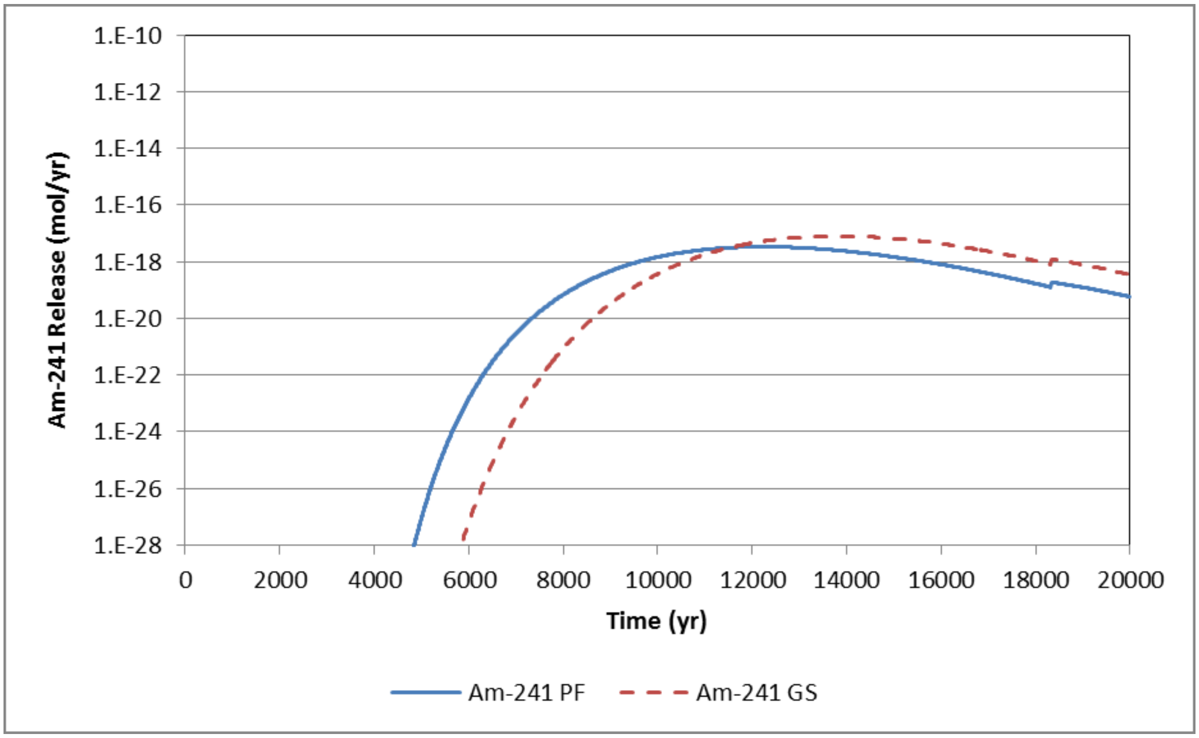

Figure A.1-56: Tank 31 Np-237 Release to the Saturated Zone for Case B

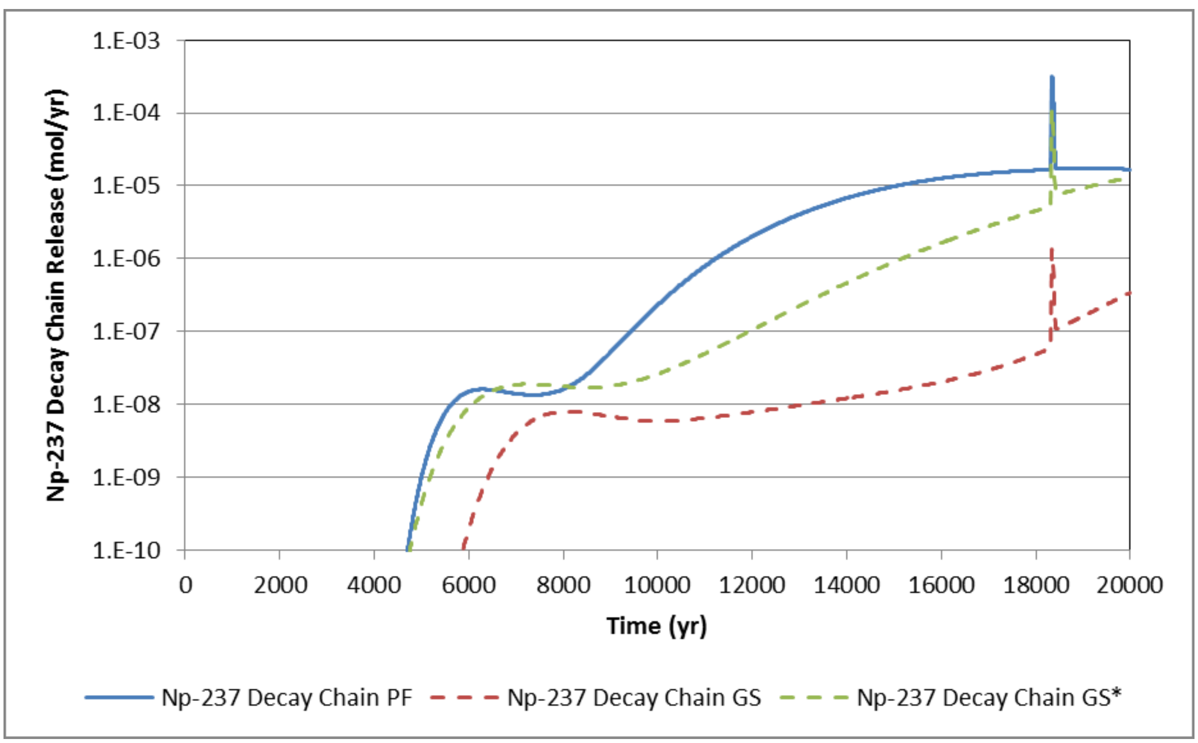

* Np-237 modeled using coarser discretization on basemat.

A.2.1 Type I Tank with Intact Liner (Tank 9) for Case C

For the Case C configuration, a comparison of the PORFLOW HTF Model and the GoldSim model mass releases of I-129, Tc-99, Am-243, Pu-239, U-234, Ra-226, Am-241, and Np-237, as presented in Figure A.2-1 through Figure A.2-8, indicate that the GoldSim model successfully captures the radionuclide release patterns seen in Tank 9 results generated by the PORFLOW model.

Table A.2-1 summarizes the peak values for these releases showing that when comparing the two models I-129, Pu-239, and Ra-226 have percent differences that are below 50%. The GoldSim results for Am-243, Pu-239, U-234, Am-241, and Np-237, tend to be slightly high, but not unreasonably when considering how similar the release patterns are as shown in Figures A.2-3, A.2-4, A.2-5, A.2-7, and A.2-8. Figure A.2-2 shows that the magnitude of the narrow Tc-99 release peaks are different, but the "spikey" peak readily disperses in the SZ, with a narrower spike dissipating quicker than a wider spike.

Table A.2-1: Case C GoldSim and PORFLOW Model Peak Releases from the UZ to the SZ Comparisons for Tank 9 within 20,000 years

Radionuclide	PORFLOW Peak Release (mol/yr)	PORFLOW Time of Peak Release (yr)	GoldSim Peak Release (mol/yr)	GoldSim Time of Peak Release (yr)	Peak Release Percent Difference GoldSim vs PORFLOW
I-129	2.2E-02	1,717	2.2E-02	1,710	0%
Tc-99	1.5E-03	6,813	5.4E-04	6,820	-64%
Am-243	9.3E-05	4,649	1.8E-04	4,150	94%
Pu-239	1.7E-05	9,551	1.4E-05	7,510	-18%
U-234	9.3E-04	2,232	1.6E-03	2,200	72%
Ra-226	2.3E-07	2,101	2.8E-07	2,110	22%
Am-241	5.1E-07	3,396	1.2E-06	3,610	135%
Np-237	1.1E-04	20,000	2.0E-04	20,000	82%

Figure A.2-1: Tank 9 I-129 Release to the Saturated Zone for Case C

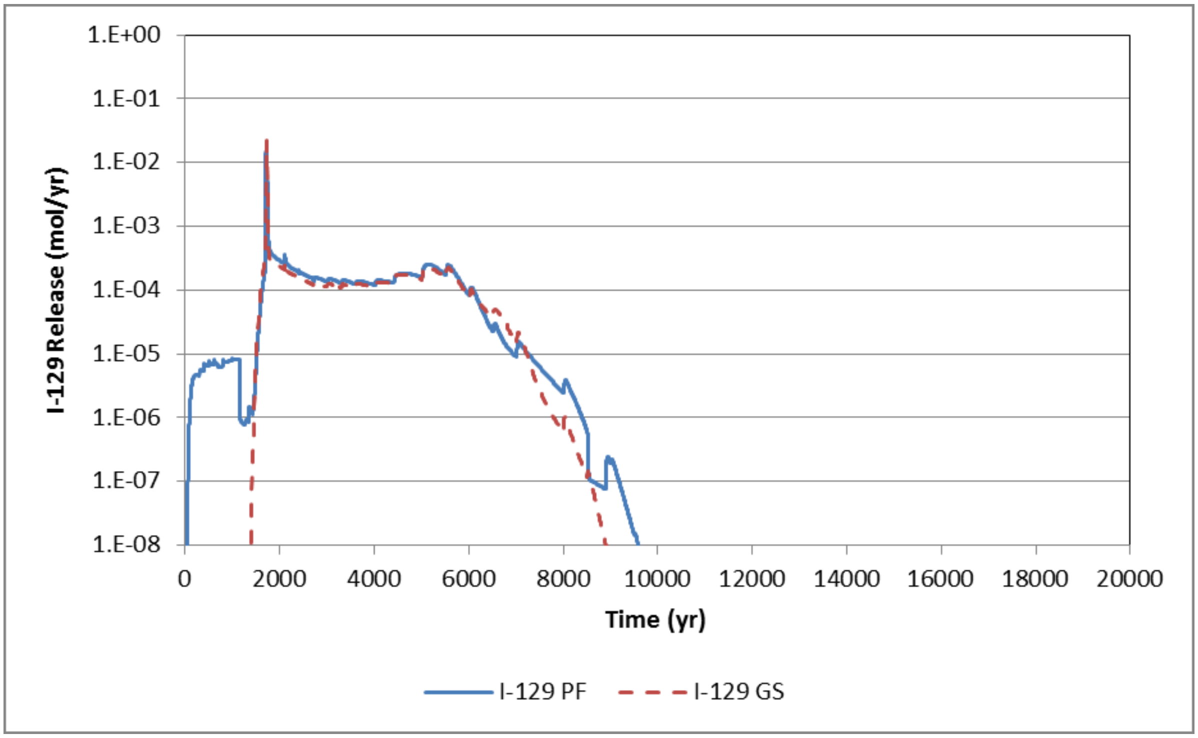

Figure A.2-2: Tank 9 Tc-99 Release to the Saturated Zone for Case C

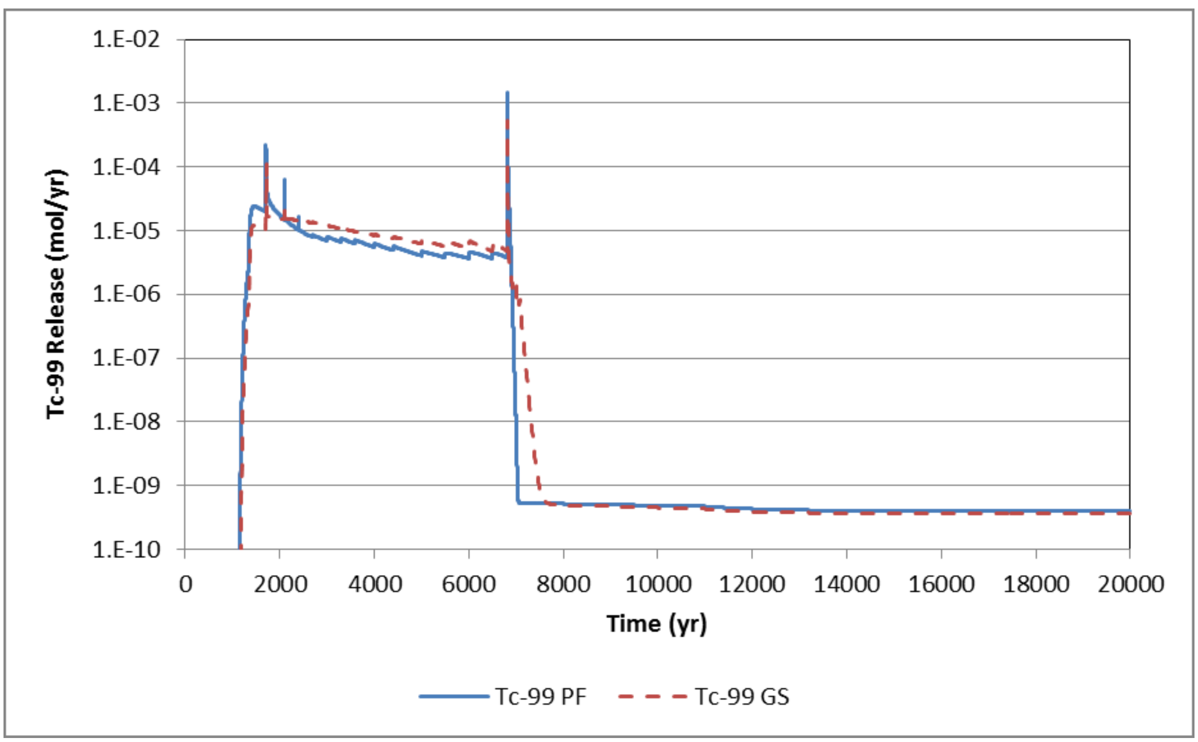

Figure A.2-3: Tank 9 Am-243 Release to the Saturated Zone for Case C

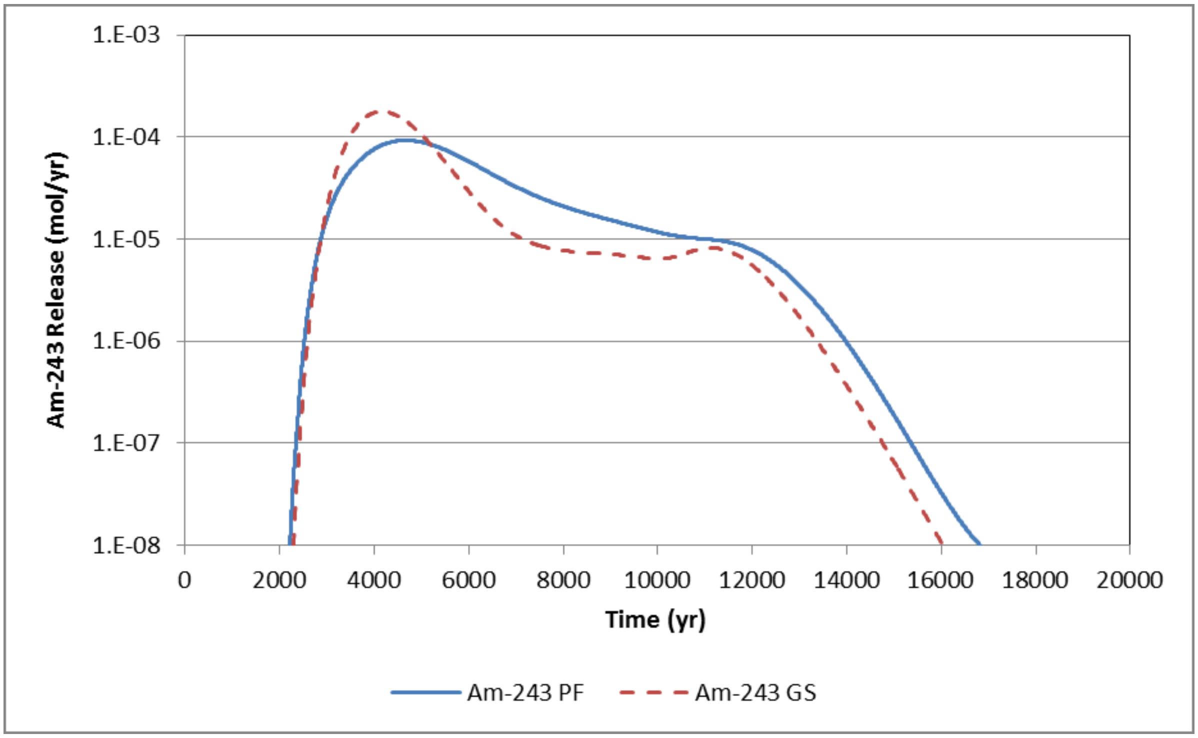

Figure A.2-4: Tank 9 Pu-239 Release to the Saturated Zone for Case C

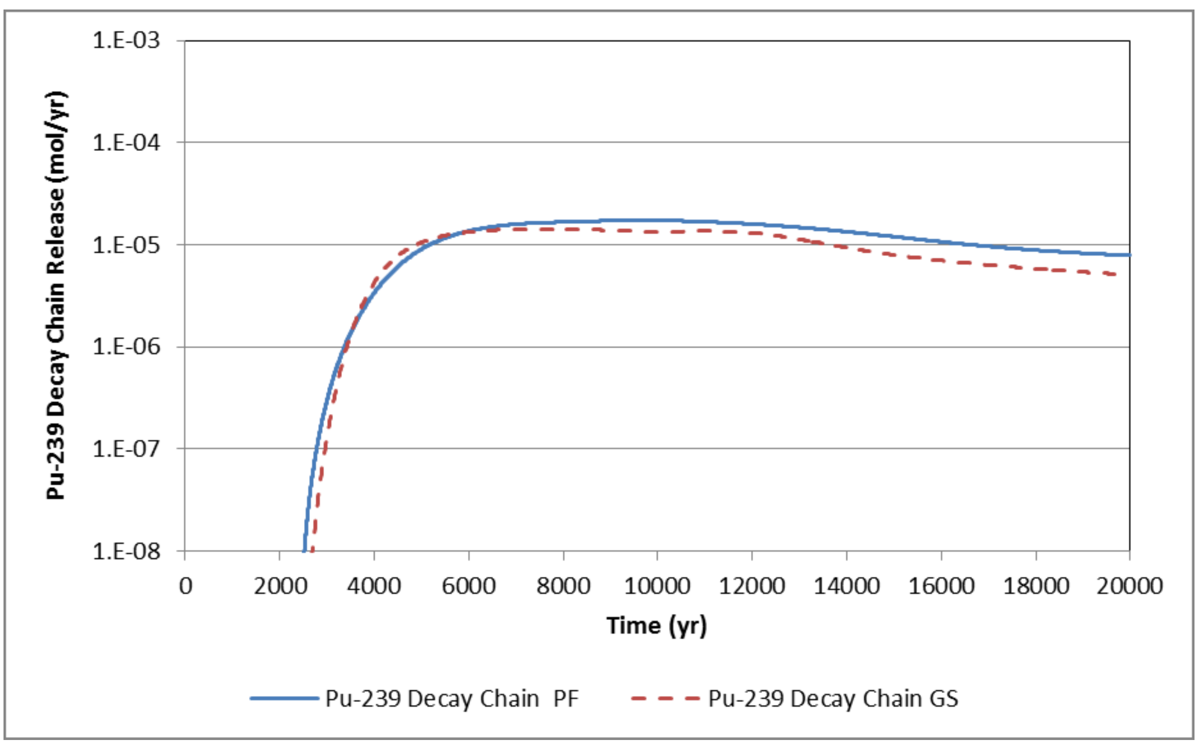

Figure A.2-5: Tank 9 U-234 Release to the Saturated Zone for Case C

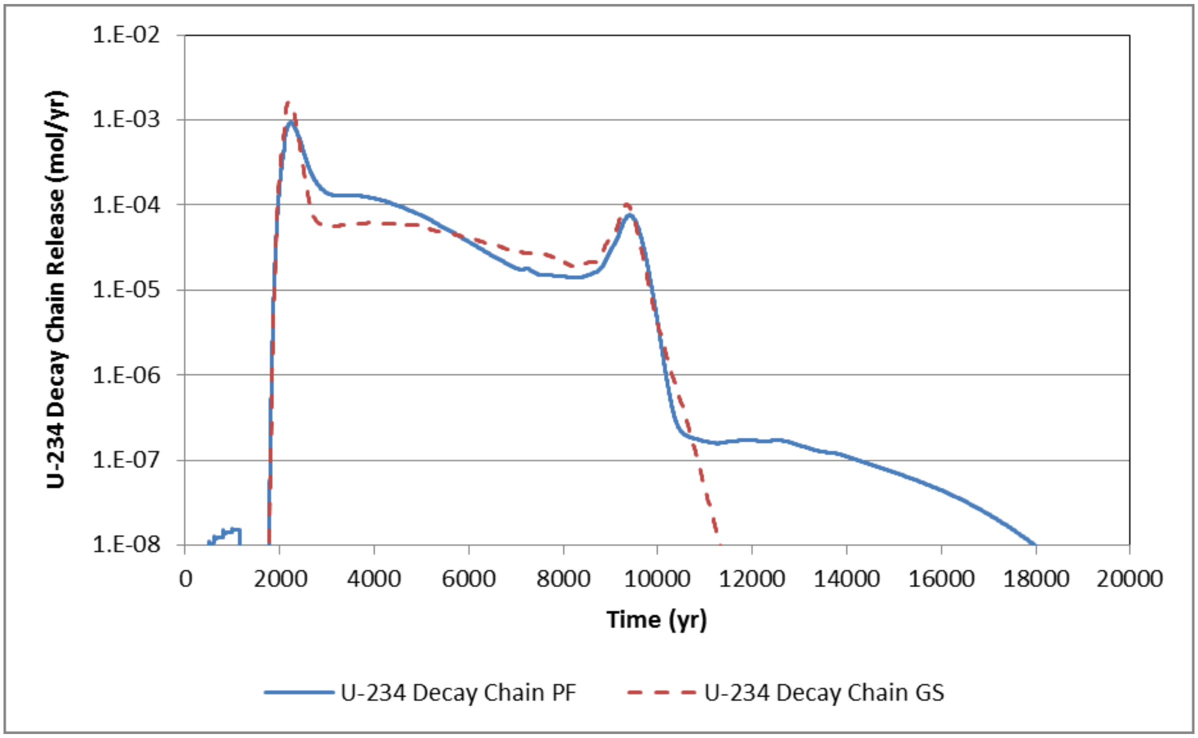

Figure A.2-6: Tank 9 Ra-226 Release to the Saturated Zone for Case C

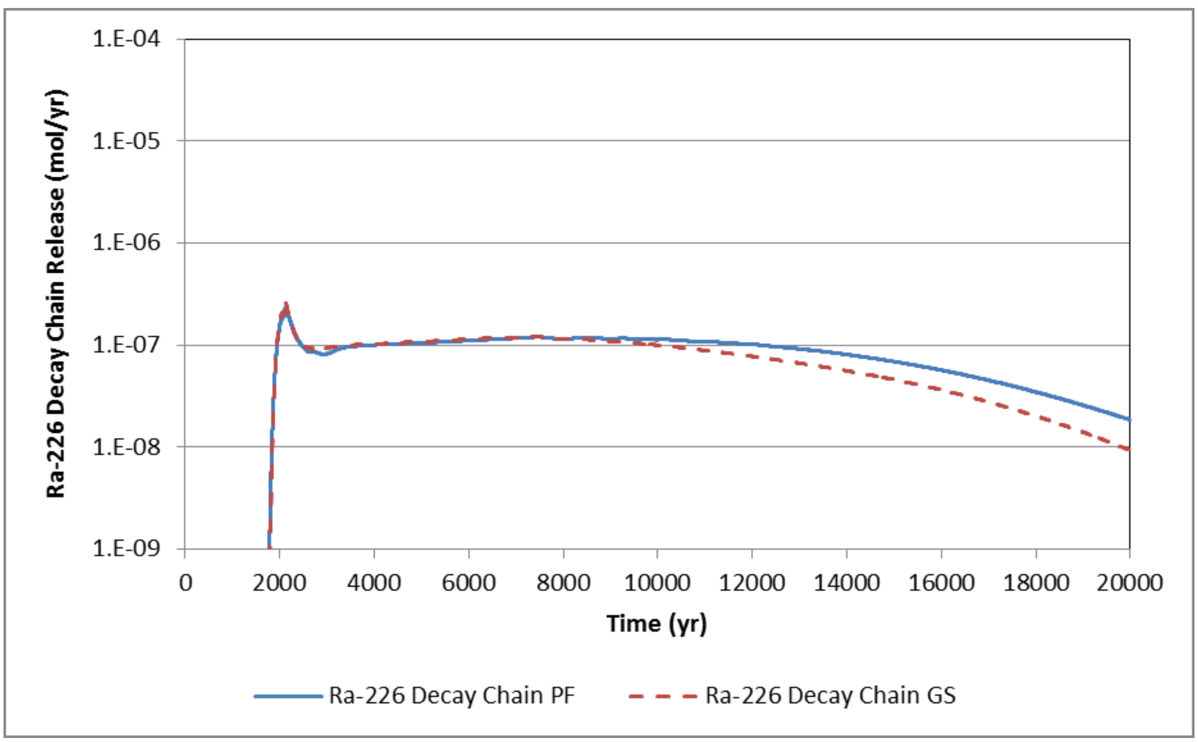

Figure A.2-7: Tank 9 Am-241 Release to the Saturated Zone for Case C

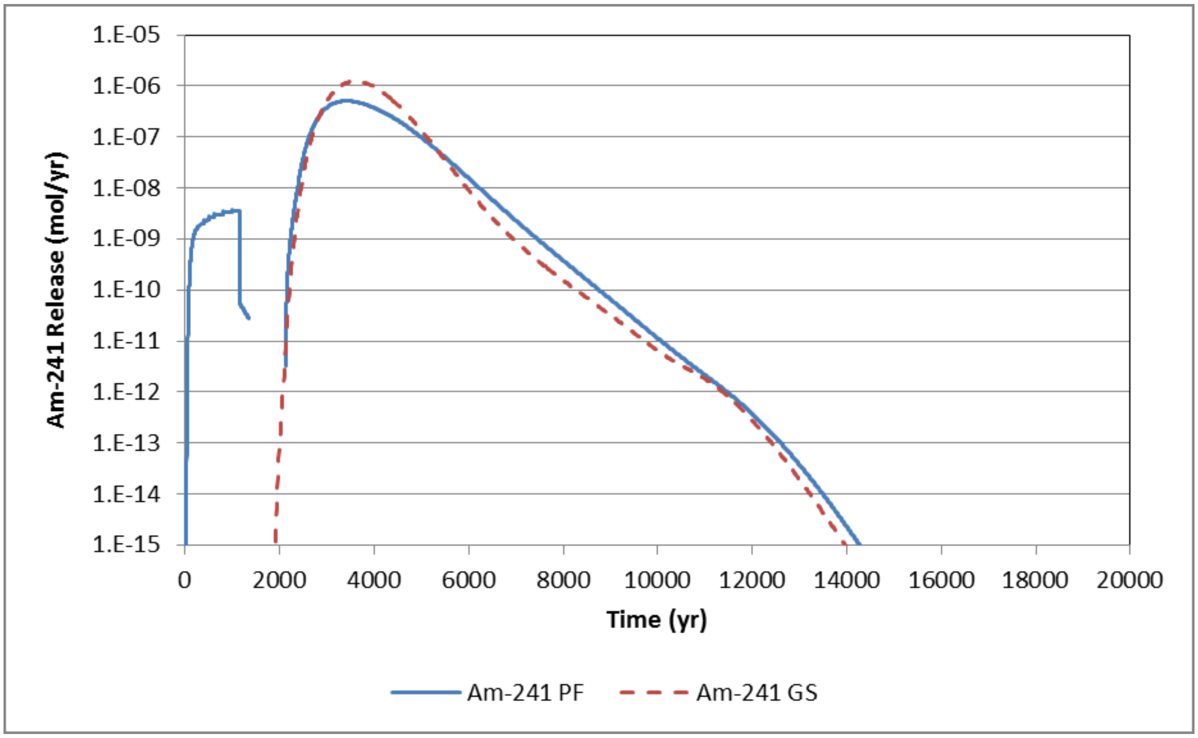

Figure A.2-8: Tank 9 Np-237 Release to the Saturated Zone for Case C

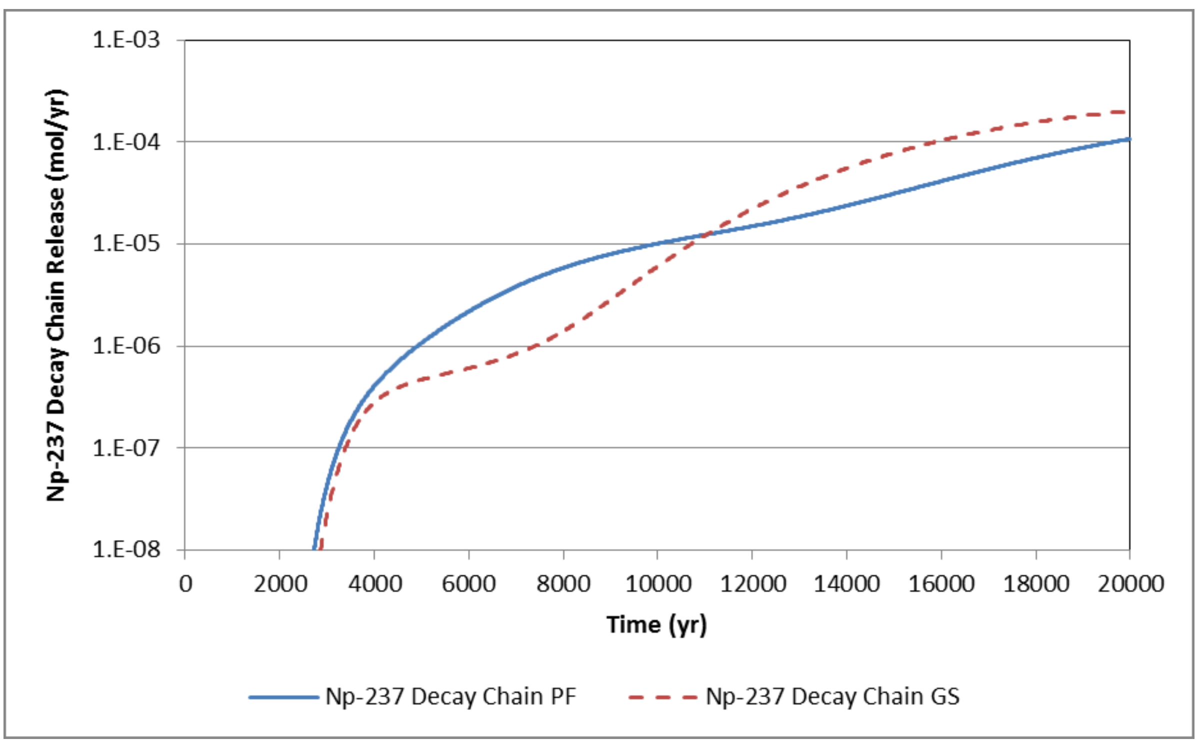

A.2.2 Type I Tank with Failed Liner (Tank 12) for Case C

For the Case C configuration, a comparison of the PORFLOW HTF Model and the GoldSim model mass releases of I-129, Tc-99, Am-243, Pu-239, U-234, Ra-226, Am-241, and Np-237, as presented in Figure A.2-9 through Figure A.2-16, indicate that the GoldSim model produces a good approximation of the releases from Tank 12 generated by the PORFLOW model.

Table A.2-2 summarizes the peak values for these releases showing that when comparing the two models although not all of the percent differences are below 50% the values are reasonably close when considered in conjunction with the release patterns shown in Figure A.2-9 through Figure A.2-16. Note in Figure A.2-15, the PORFLOW results show a small early release of Am-241 escaping into the backfill at the top of the vault, that is not accounted for in the GoldSim model.

Table A.2-2: Case C GoldSim and PORFLOW Model Peak Releases from the UZ to the SZ Comparisons for Tank 12 within 20,000 years

Radionuclide	PORFLOW Peak Release (mol/yr)	PORFLOW Time of Peak Release (yr)	GoldSim Peak Release (mol/yr)	GoldSim Time of Peak Release (yr)	Peak Release Percent Difference GoldSim vs PORFLOW
I-129	1.5E-02	1,701	9.4E-03	1,710	-37%
Tc-99	3.7E-04	6,506	1.3E-04	6,800	-65%
Am-243	2.4E-07	4,839	4.7E-07	4,170	96%
Pu-239	5.2E-06	11,397	5.7E-06	14,260	10%
U-234	2.5E-04	2,200	3.7E-04	2,180	48%
Ra-226	3.3E-08	2,101	3.7E-08	2,110	12%
Am-241	4.6E-08	3,219	7.2E-08	3,580	57%
Np-237	2.5E-05	20,000	4.3E-05	20,000	72%

Figure A.2-9: Tank 12 I-129 Release to the Saturated Zone for Case C

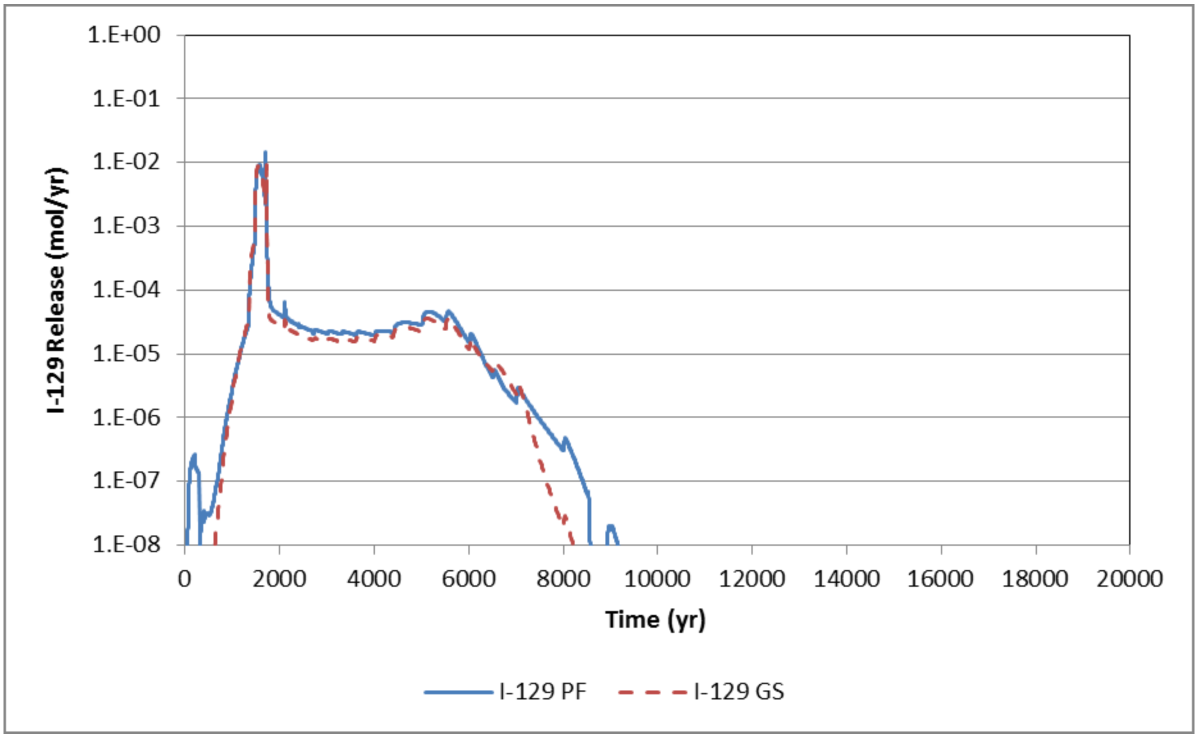

Figure A.2-10: Tank 12 Tc-99 Release to the Saturated Zone for Case C

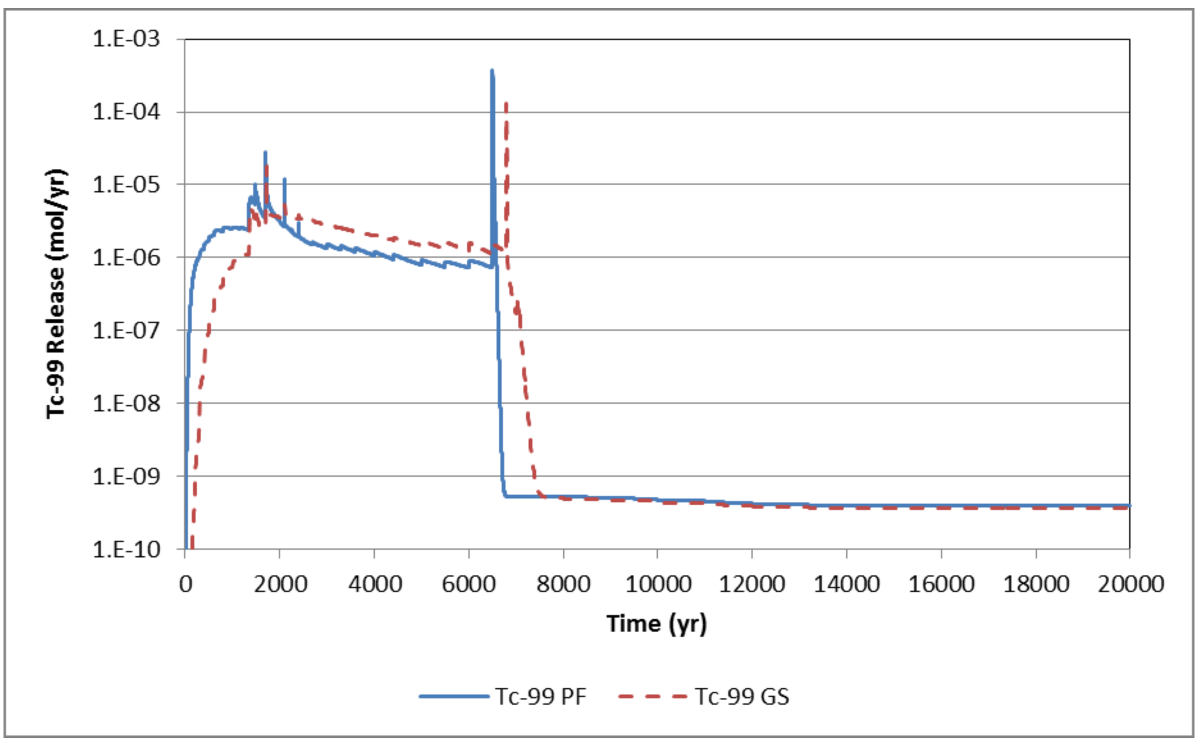

Figure A.2-11: Tank 12 Am-243 Release to the Saturated Zone for Case C

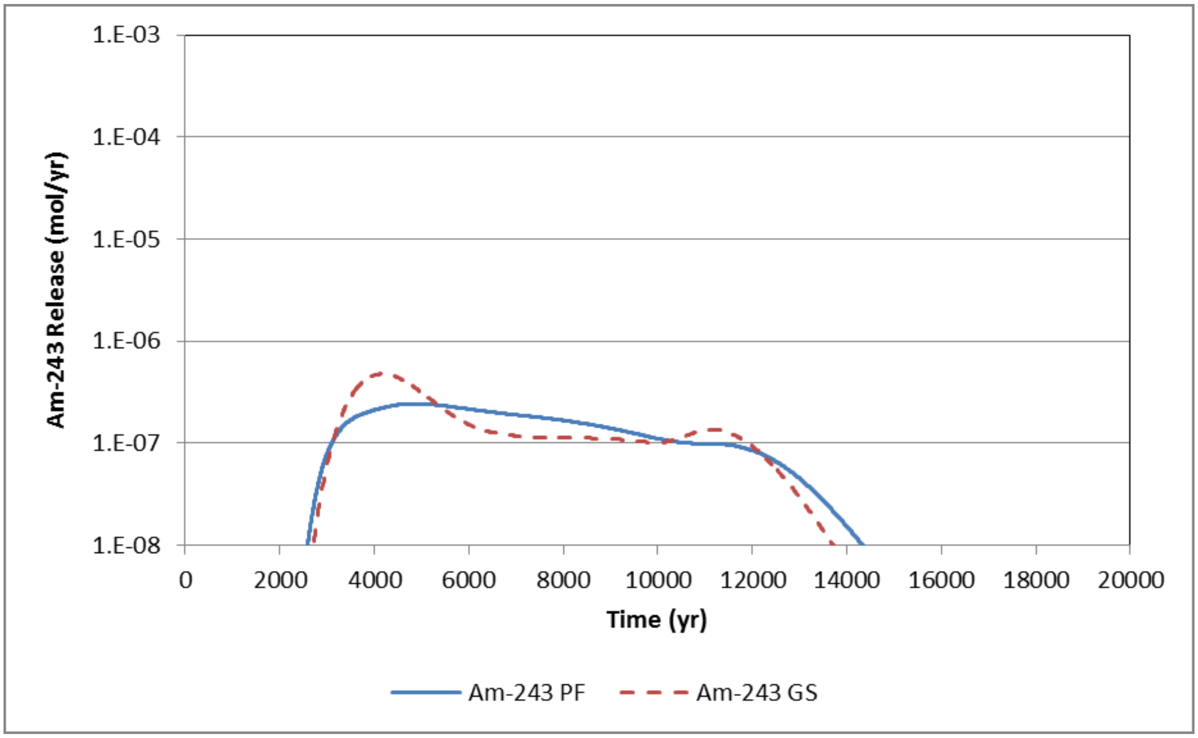

Figure A.2-12: Tank 12 Pu-239 Release to the Saturated Zone for Case C

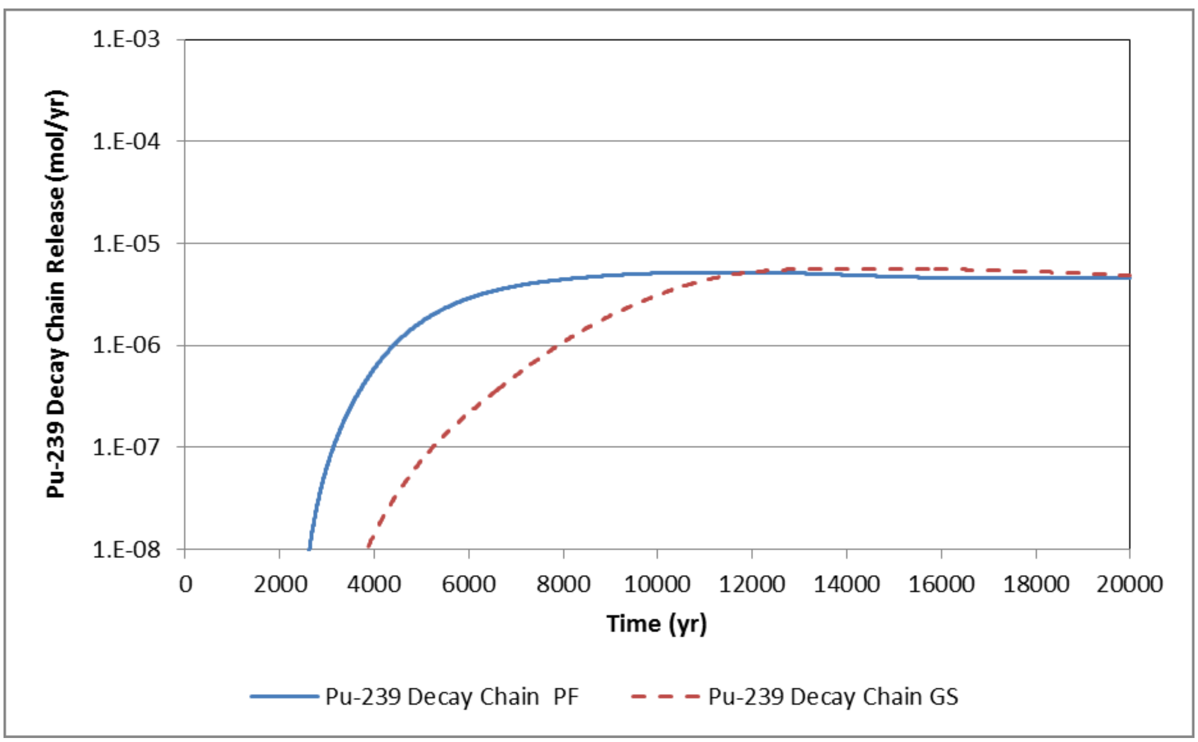

Figure A.2-13: Tank 12 U-234 Release to the Saturated Zone for Case C

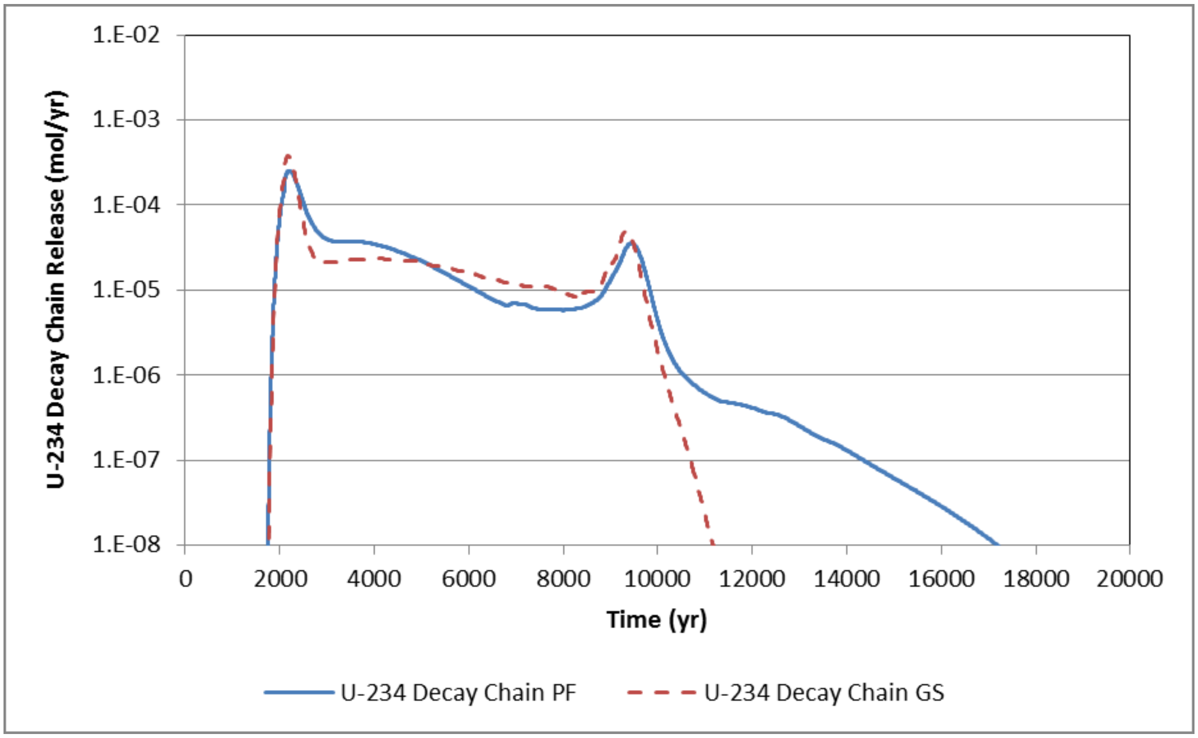

Figure A.2-14: Tank 12 Ra-226 Release to the Saturated Zone for Case C

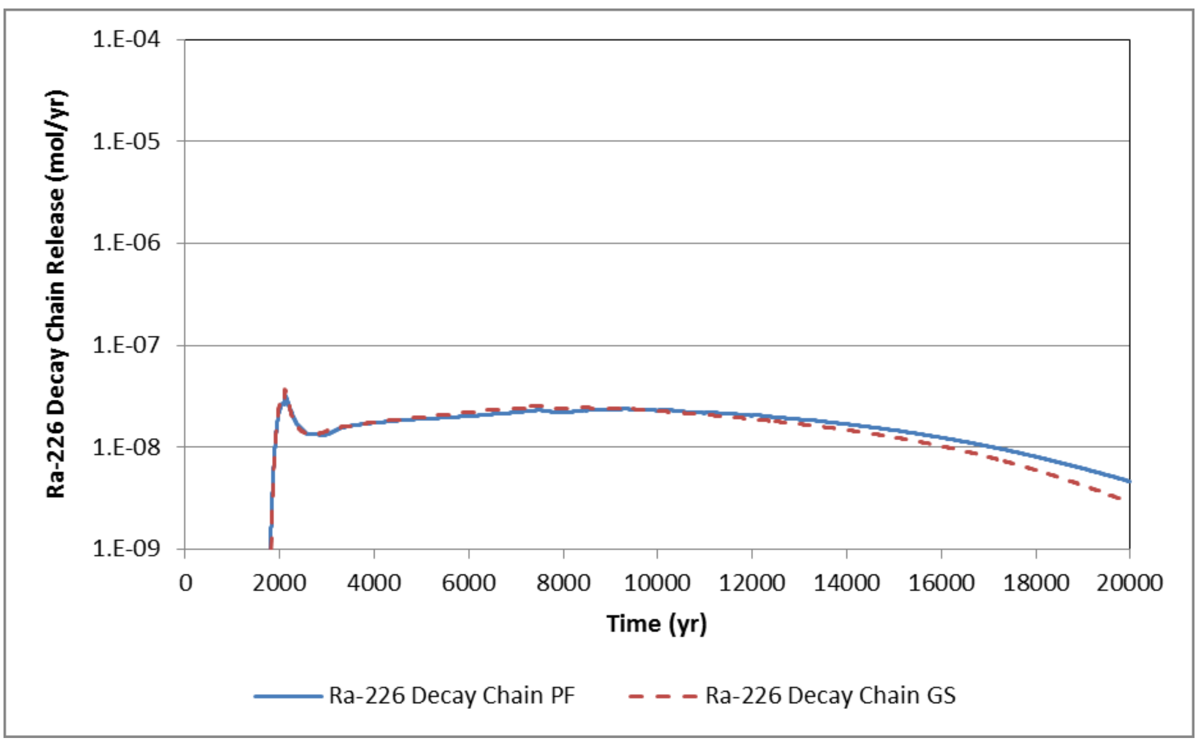

Figure A.2-15: Tank 12 Am-241 Release to the Saturated Zone for Case C

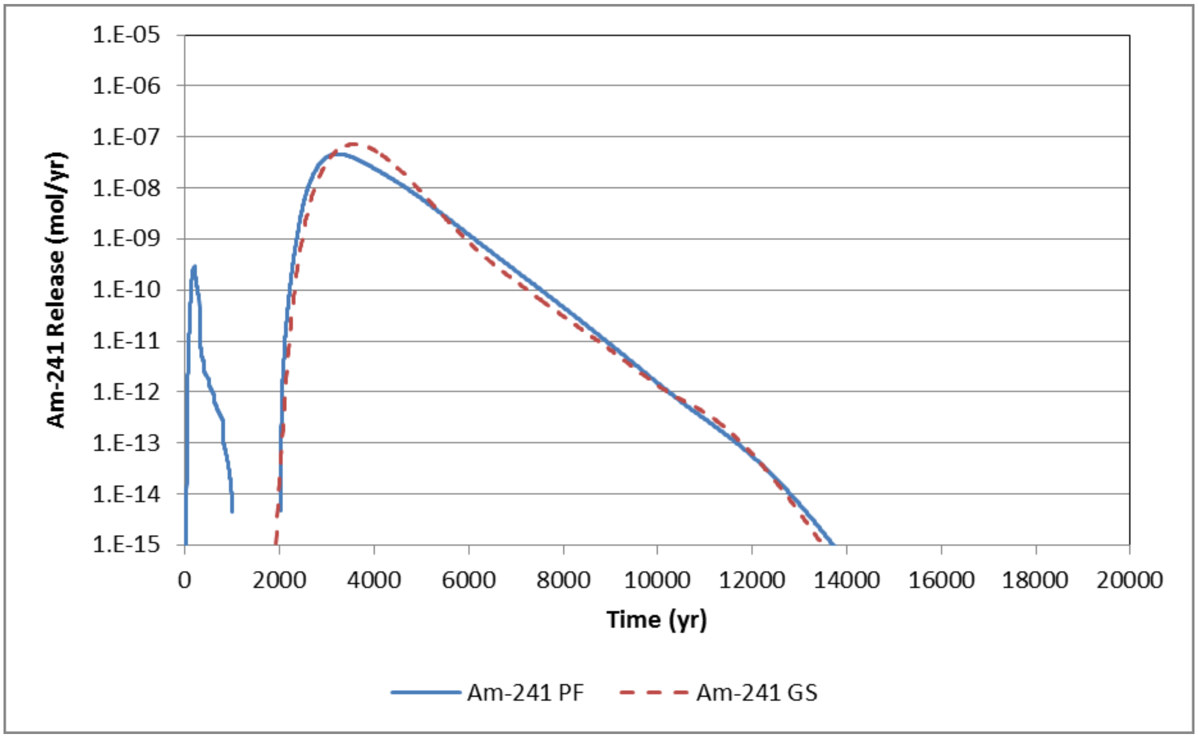

Figure A.2-16: Tank 12 Np-237 Release to the Saturated Zone for Case C

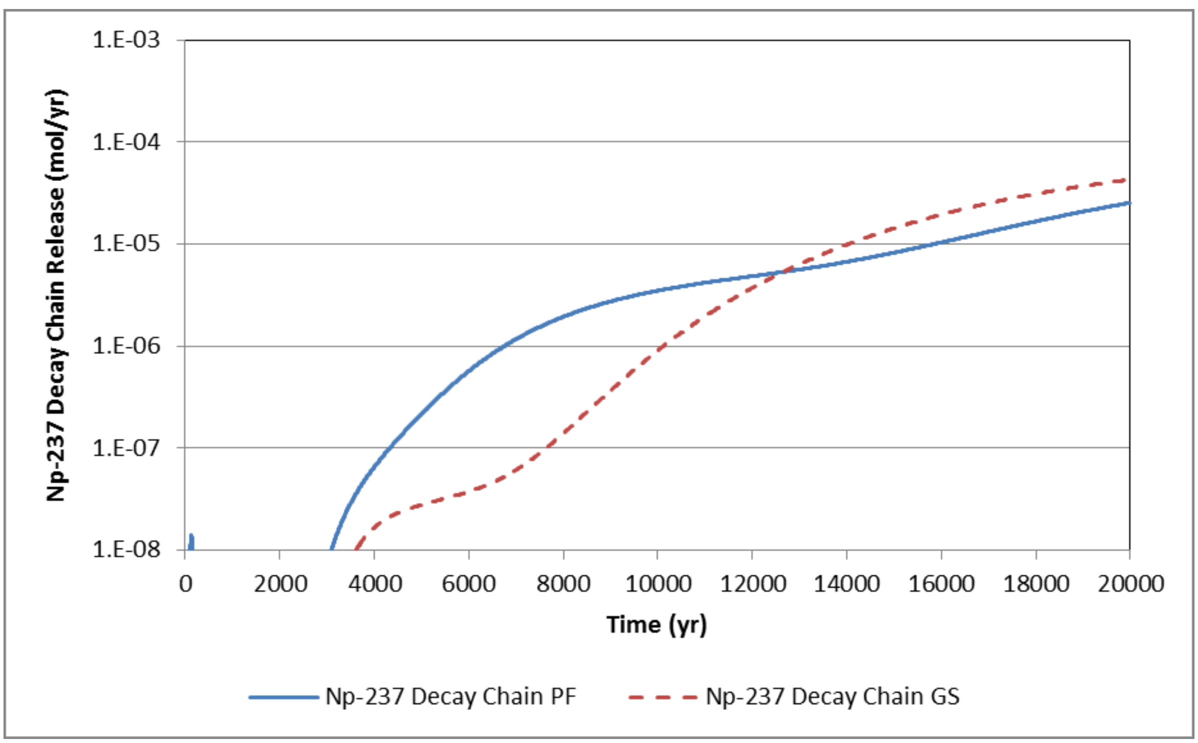

A.2.3 Type II Tank with Intact Liner (Tank 13) for Case C

For the Case C configuration, a comparison of the PORFLOW HTF Model and the GoldSim model mass releases of I-129, Tc-99, Am-243, Pu-239, U-234, Ra-226, Am-241, and Np-237, as presented in Figure A.2-17 through Figure A.2-24, indicate that the GoldSim model produces a good approximation of the releases from Tank 13 generated by the PORFLOW model.

Table A.2-3 summarizes the peak values for these releases showing that when comparing the two models although not all of the percent differences are below 50% the values, except for Am-241 and Np-237 are reasonably close when considered in conjunction with the release patterns shown in Figure A.2-17 through Figure A.2-22. As can be seen in Figure A.2-23 and Figure A.2-24, releases of Am-241 and Np-237, show similar trends but will be conservatively overestimated by the GoldSim model.

Table A.2-3: Case C GoldSim and PORFLOW Model Peak Releases from the UZ to the SZ Comparisons for Tank 13 within 20,000 years

Radionuclide	PORFLOW Peak Release (mol/yr)	PORFLOW Time of Peak Release (yr)	GoldSim Peak Release (mol/yr)	GoldSim Time of Peak Release (yr)	Peak Release Percent Difference GoldSim vs PORFLOW
I-129	7.2E-03	2,701	6.4E-03	2,690	-11%
Tc-99	1.3E-03	2,528	7.5E-04	2,530	-42%
Am-243	6.4E-05	8,001	1.1E-04	7,190	72%
Pu-239	1.4E-05	16,709	1.4E-05	12,990	0%
U-234	8.3E-04	3,585	1.7E-03	3,550	105%
Ra-226	1.6E-07	7,517	1.4E-07	6,570	-13%
Am-241	1.8E-09	6,046	1.4E-08	6,010	678%
Np-237	4.1E-06	20,000	1.3E-05	20,000	217%

Figure A.2-17: Tank 13 I-129 Release to the Saturated Zone for Case C

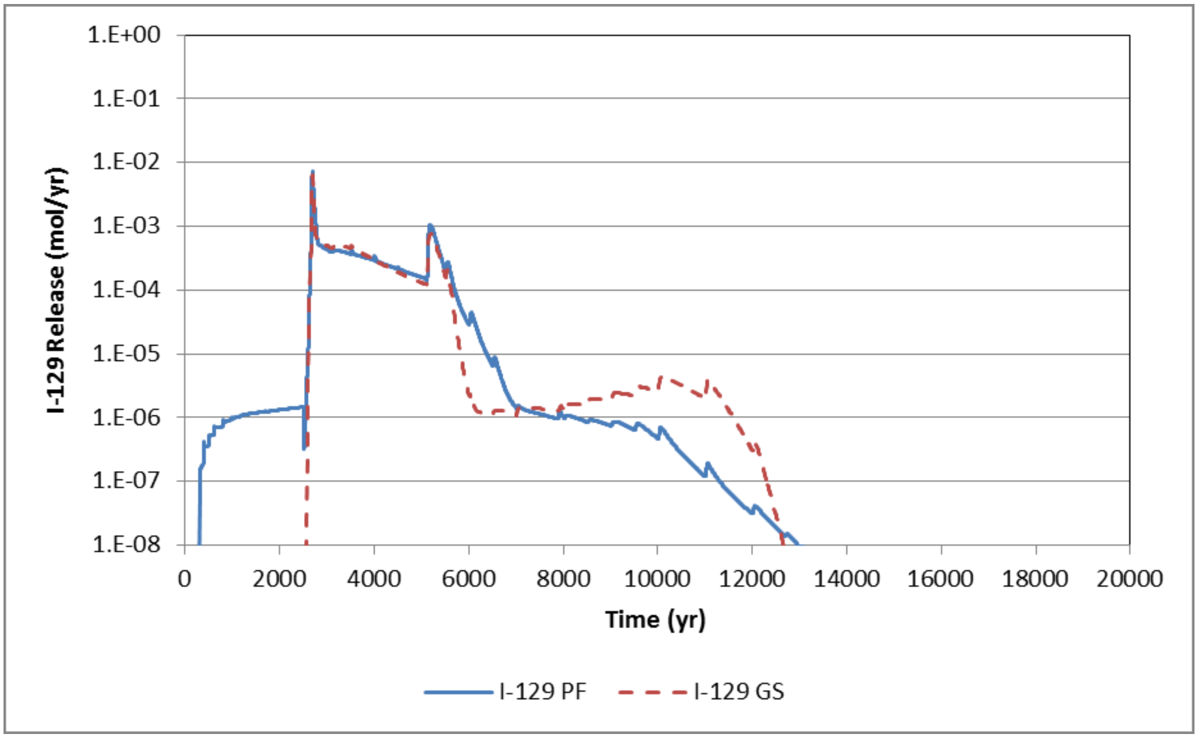

Figure A.2-18: Tank 13 Tc-99 Release to the Saturated Zone for Case C

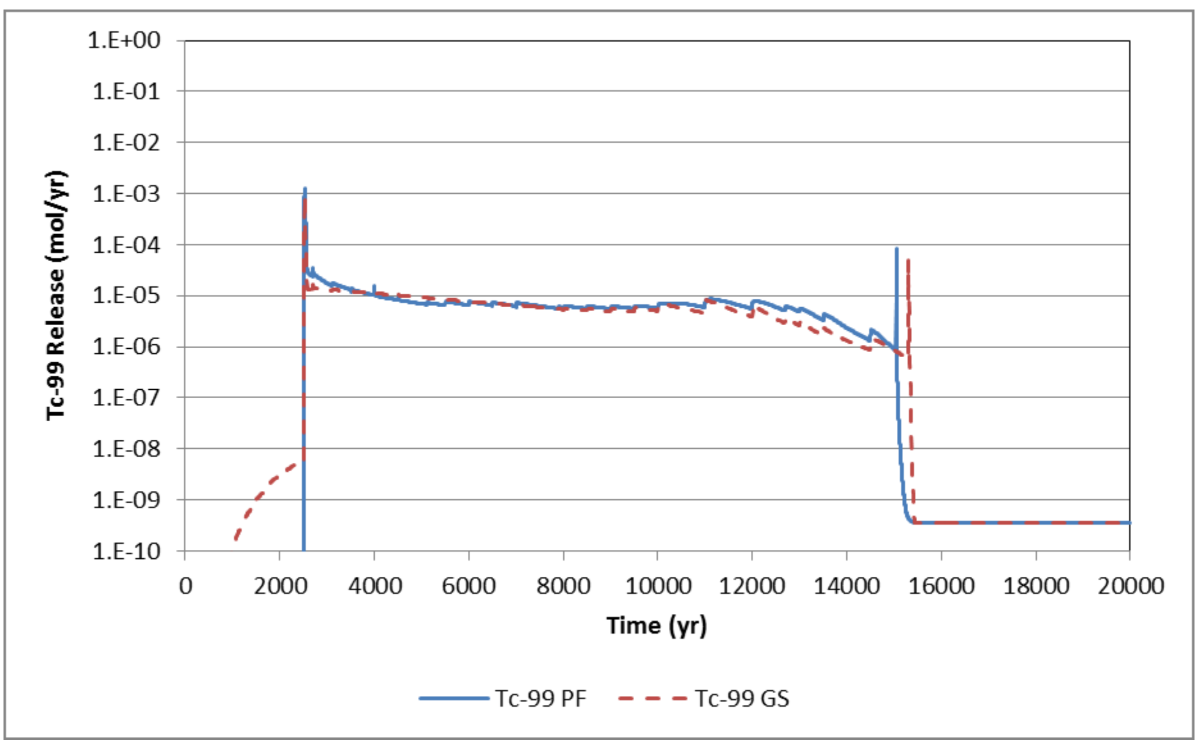

Figure A.2-19: Tank 13 Am-243 Release to the Saturated Zone for Case C

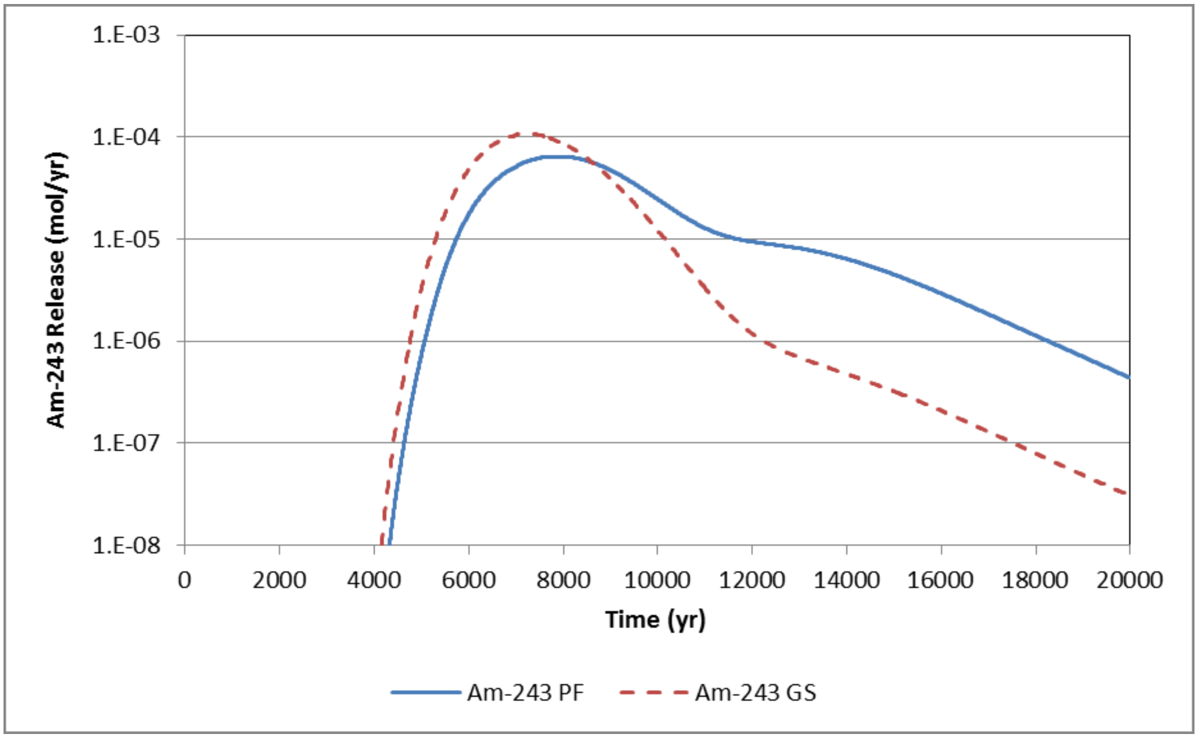

Figure A.2-20: Tank 13 Pu-239 Release to the Saturated Zone for Case C

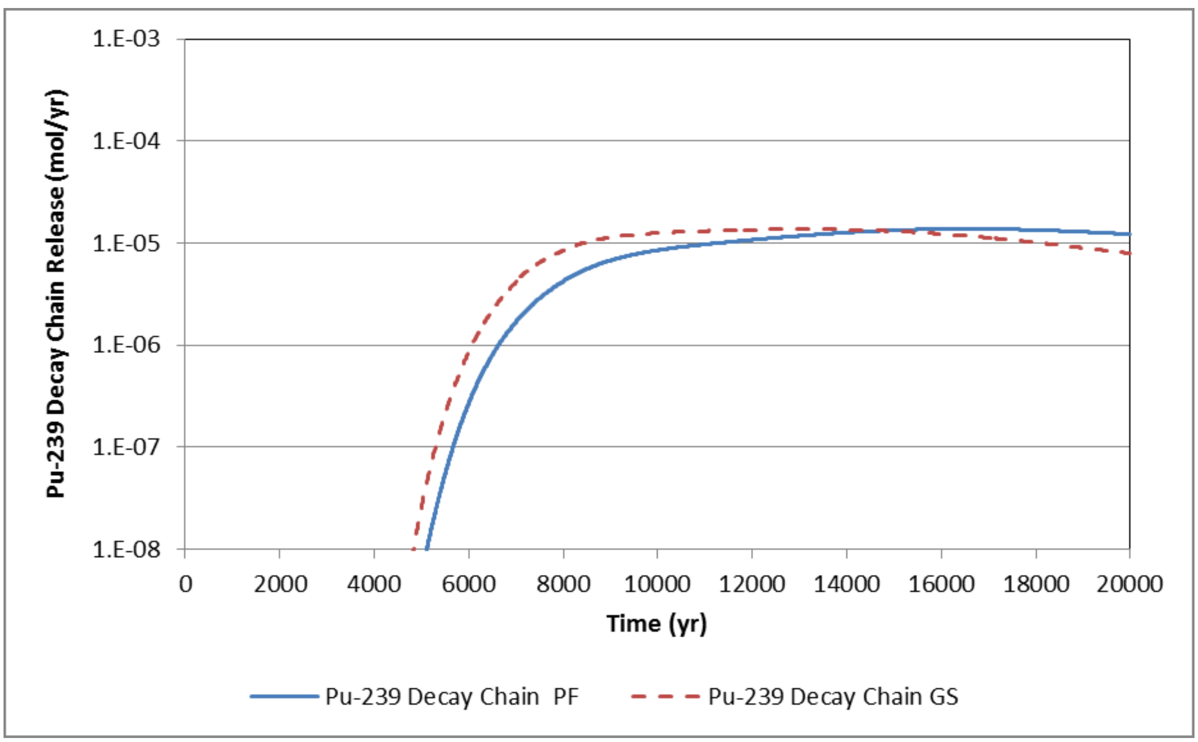

Figure A.2-21: Tank 13 U-234 Release to the Saturated Zone for Case C

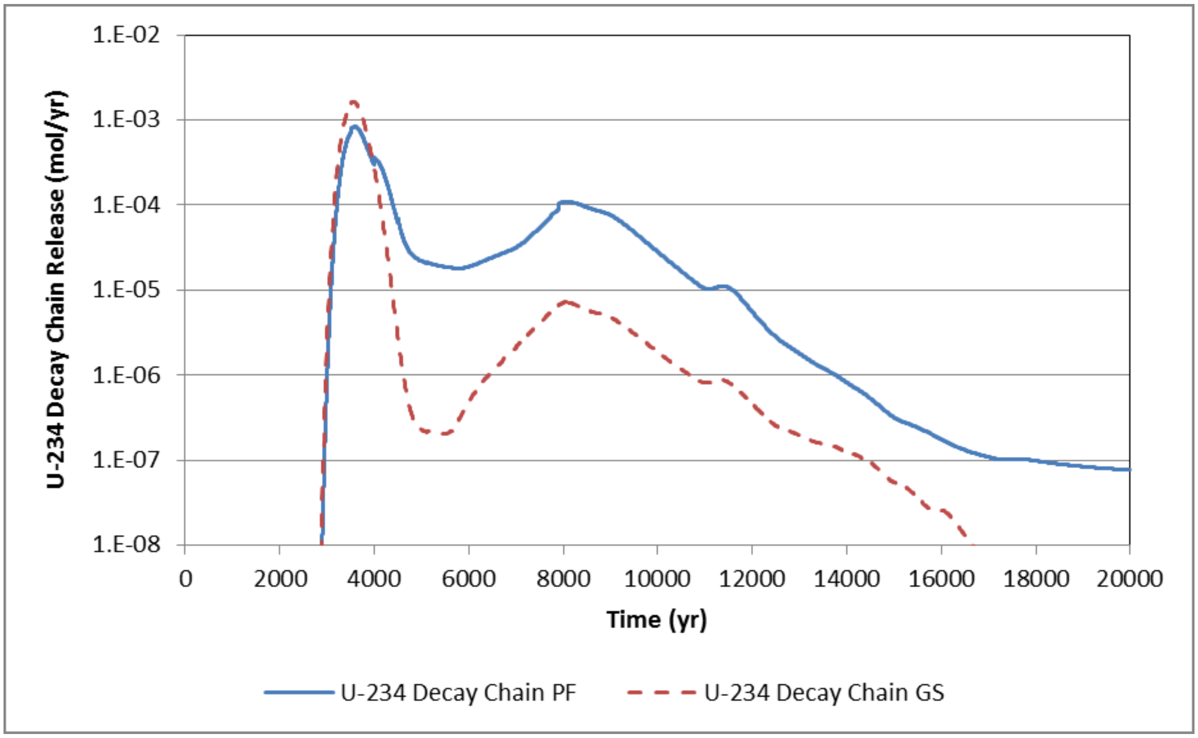

Figure A.2-22: Tank 13 Ra-226 Release to the Saturated Zone for Case C

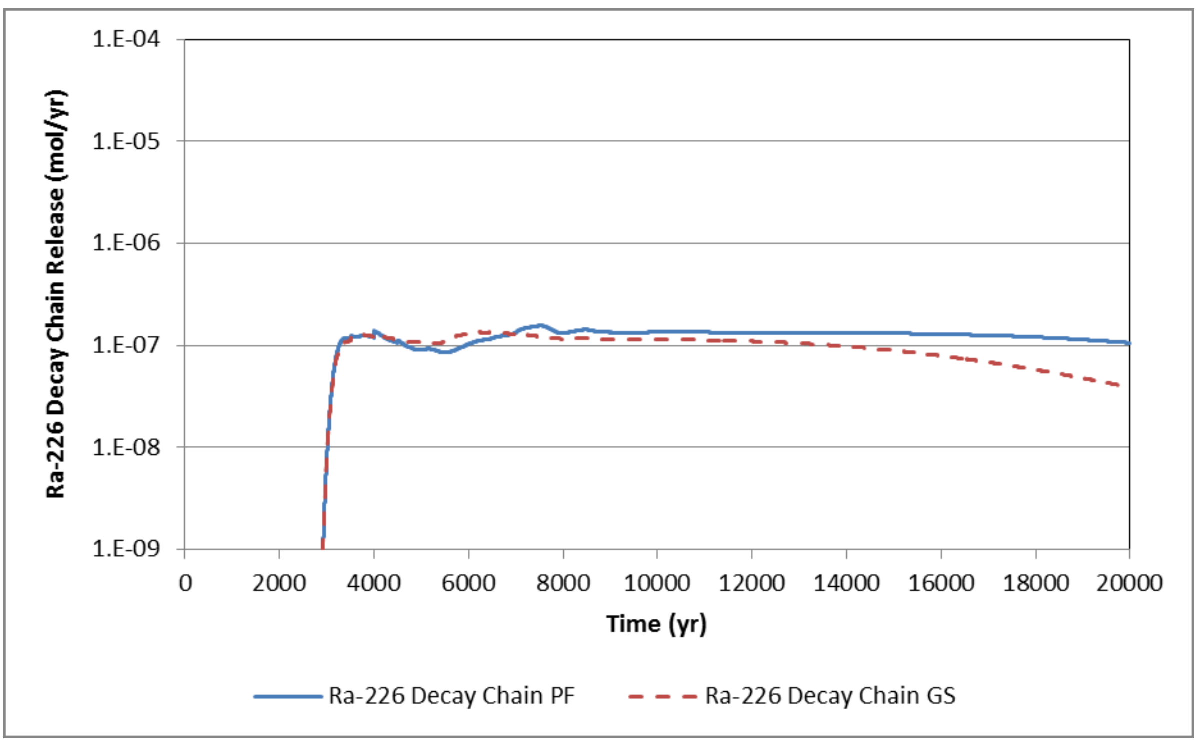

Figure A.2-23: Tank 13 Am-241 Release to the Saturated Zone for Case C

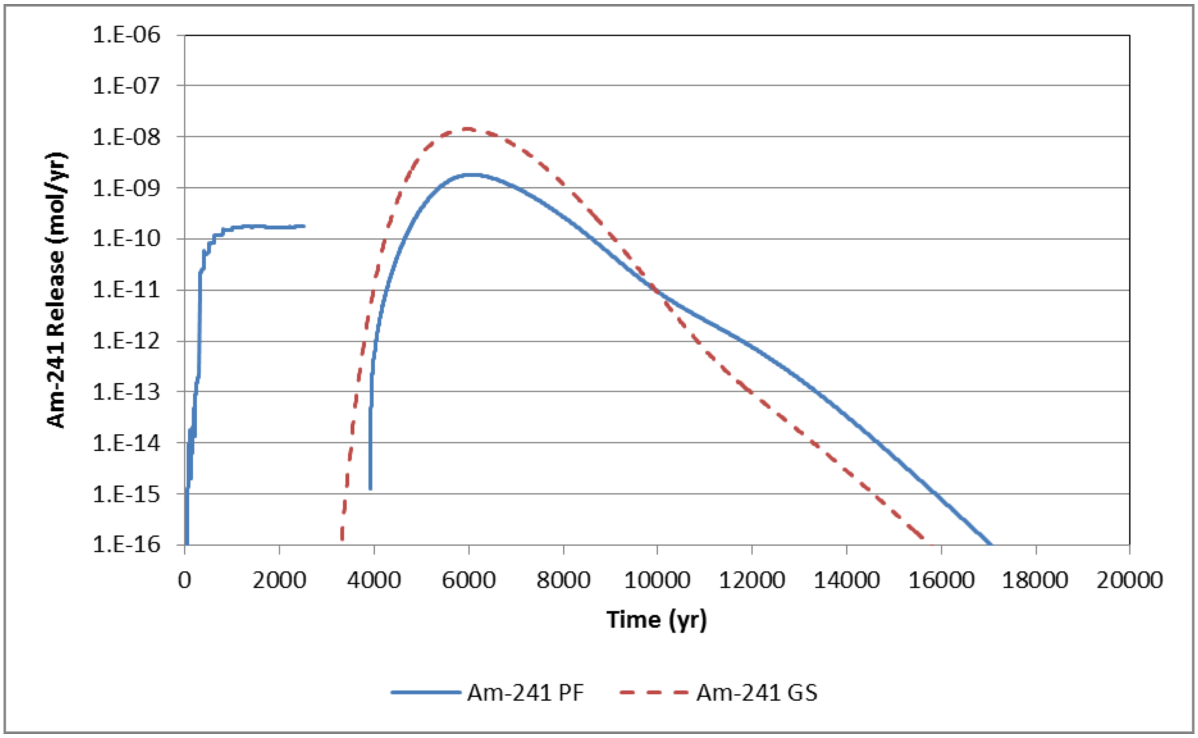

Figure A.2-24: Tank 13 Np-237 Release to the Saturated Zone for Case C

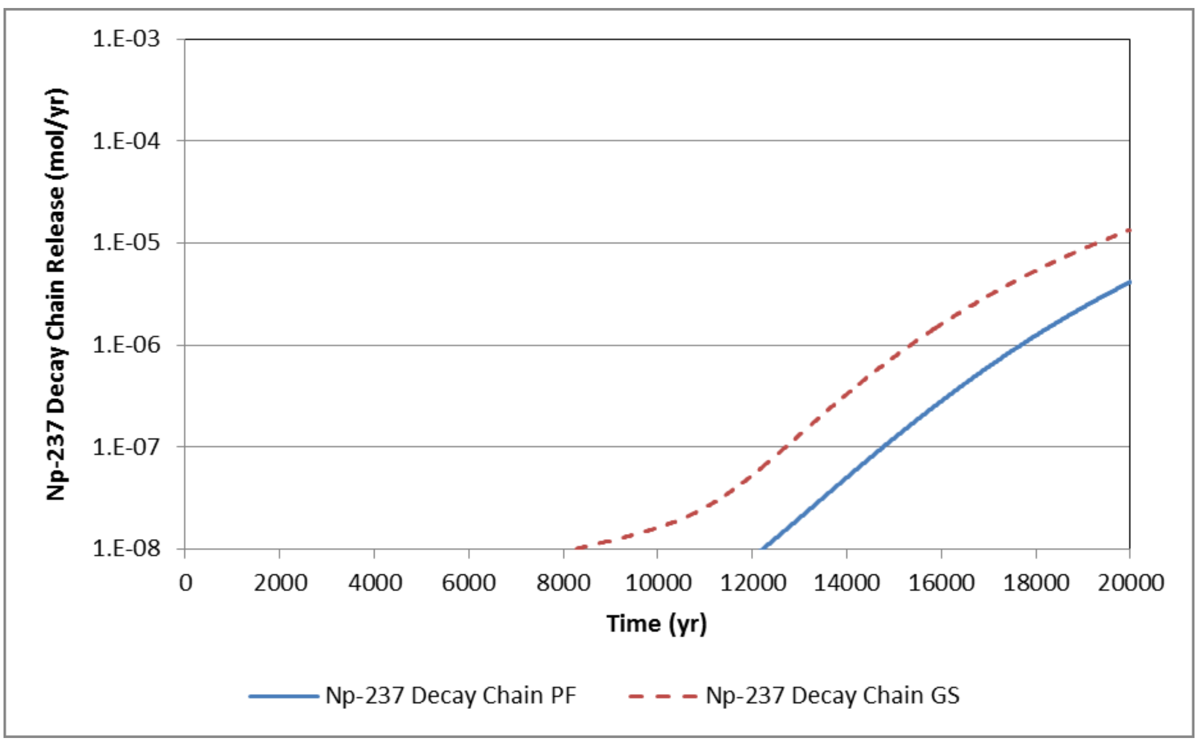

A.2.4 Type II Tank with Failed Liner (Tank 15) for Case C

For the Case C configuration, a comparison of the PORFLOW HTF Model and the GoldSim model mass releases of I-129, Tc-99, Am-243, Pu-239, U-234, Ra-226, Am-241, and Np-237, as presented in Figure A.2-25 through Figure A.2-32, indicate that the GoldSim model produces a good approximation of the releases from Tank 15 generated by the PORFLOW model.

Table A.2-4 summarizes the peak values for these releases showing that when comparing the two models although not all of the percent differences are below 50% the values, except for Am-241 and Np-237 are reasonably close when considered in conjunction with the release patterns shown in Figure A.2-25 through Figure A.2-30. As can be seen in Figure A.2-31 and Figure A.2-32, releases of Am-241 and Np-237, show similar trends but will be conservatively overestimated by the GoldSim model.

Table A.2-4: Case C GoldSim and PORFLOW Model Peak Releases from the UZ to the SZ Comparisons for Tank 15 within 20,000 years

Radionuclide	PORFLOW Peak Release (mol/yr)	PORFLOW Time of Peak Release (yr)	GoldSim Peak Release (mol/yr)	GoldSim Time of Peak Release (yr)	Peak Release Percent Difference GoldSim vs PORFLOW
I-129	1.1E-02	524	1.2E-02	520	9%
Tc-99	2.9E-04	318	1.3E-04	310	-55%
Am-243	7.2E-05	7,119	1.1E-04	6,560	53%
Pu-239	1.7E-05	15,962	1.8E-05	13,940	6%
U-234	7.0E-04	2,812	1.3E-03	2,790	86%
Ra-226	1.4E-07	7,470	1.8E-07	2,990	29%
Am-241	1.6E-08	5,586	3.8E-08	5,390	138%
Np-237	4.3E-06	20,000	1.7E-05	20,000	295%

Figure A.2-25: Tank 15 I-129 Release to the Saturated Zone for Case C

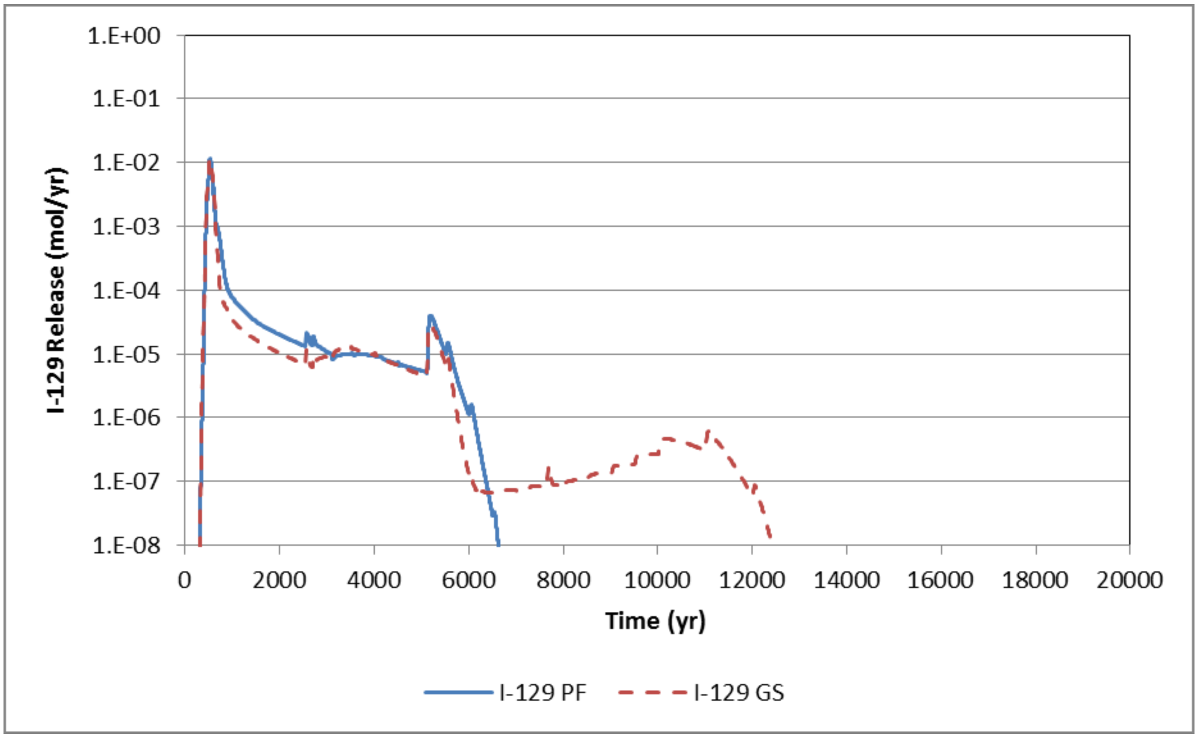

Figure A.2-26: Tank 15 Tc-99 Release to the Saturated Zone for Case C

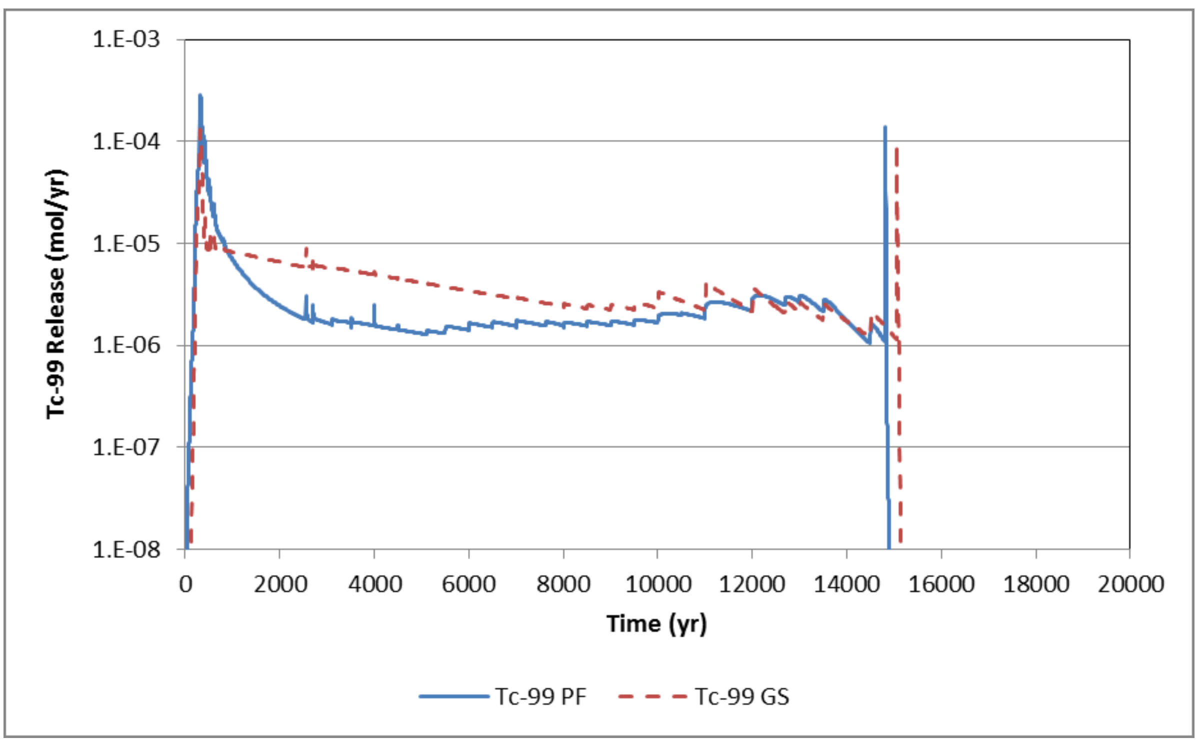

Figure A.2-27: Tank 15 Am-243 Release to the Saturated Zone for Case C

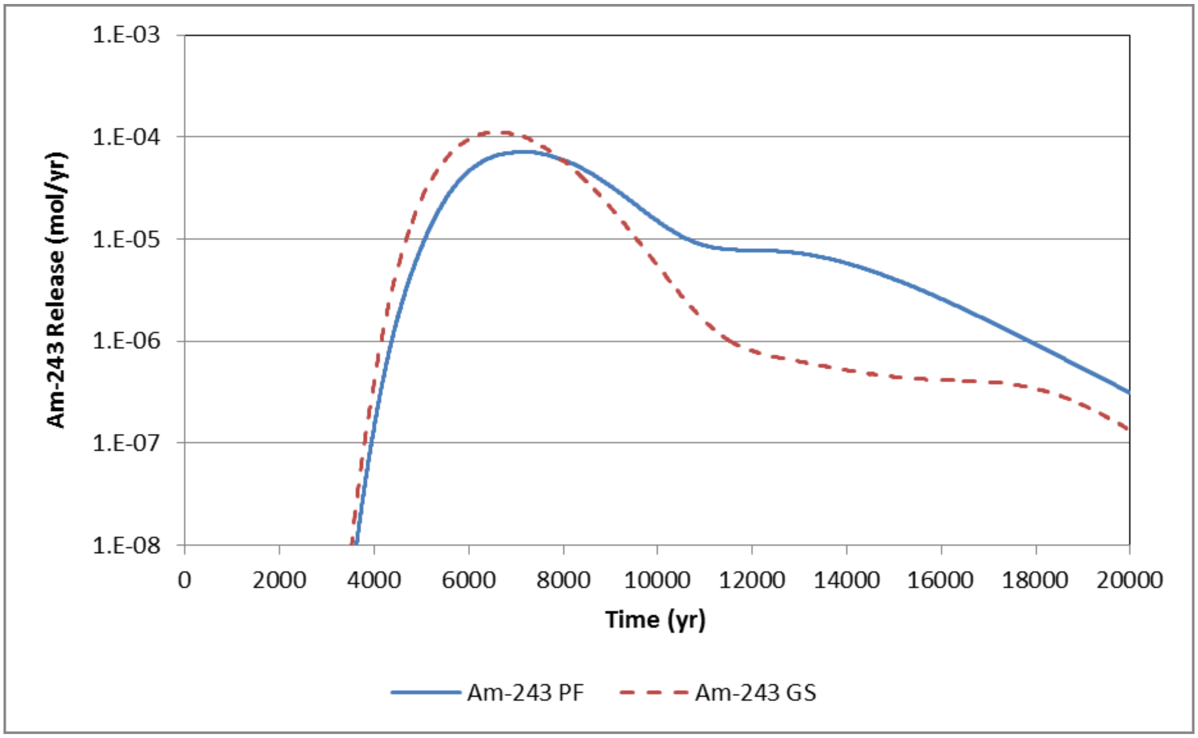

Figure A.2-28: Tank 15 Pu-239 Release to the Saturated Zone for Case C

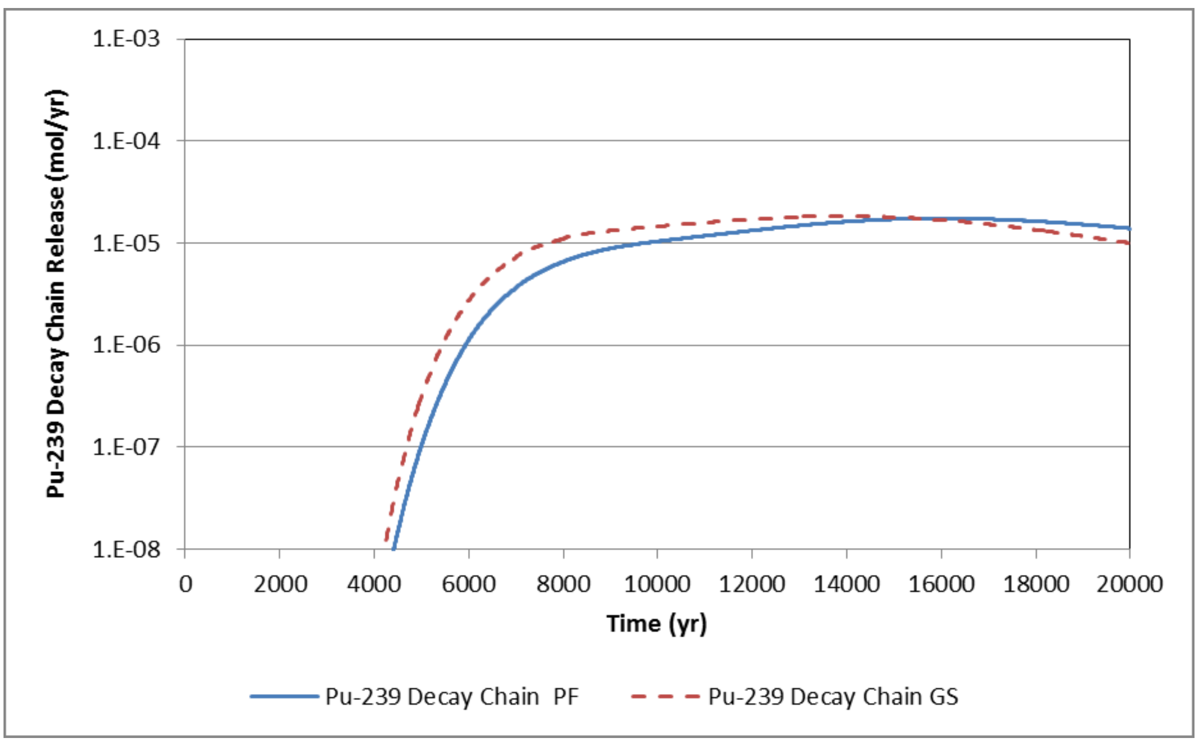

Figure A.2-29: Tank 15 U-234 Release to the Saturated Zone for Case C

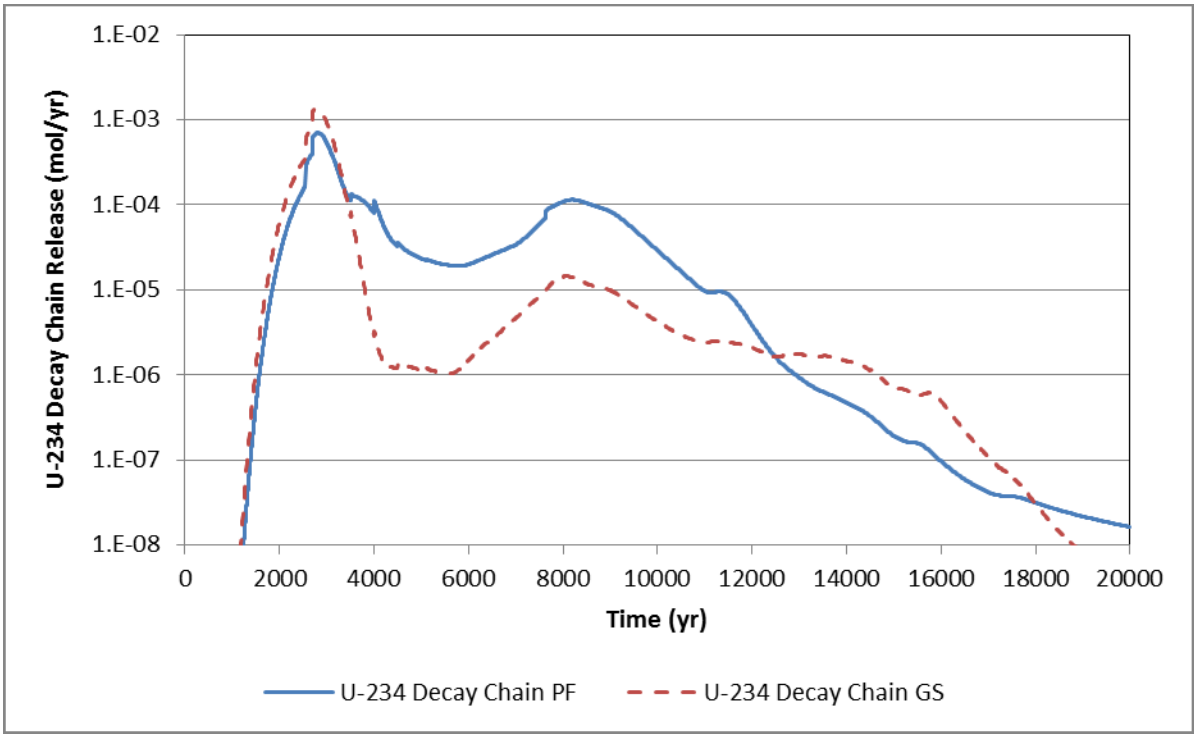

Figure A.2-30: Tank 15 Ra-226 Release to the Saturated Zone for Case C

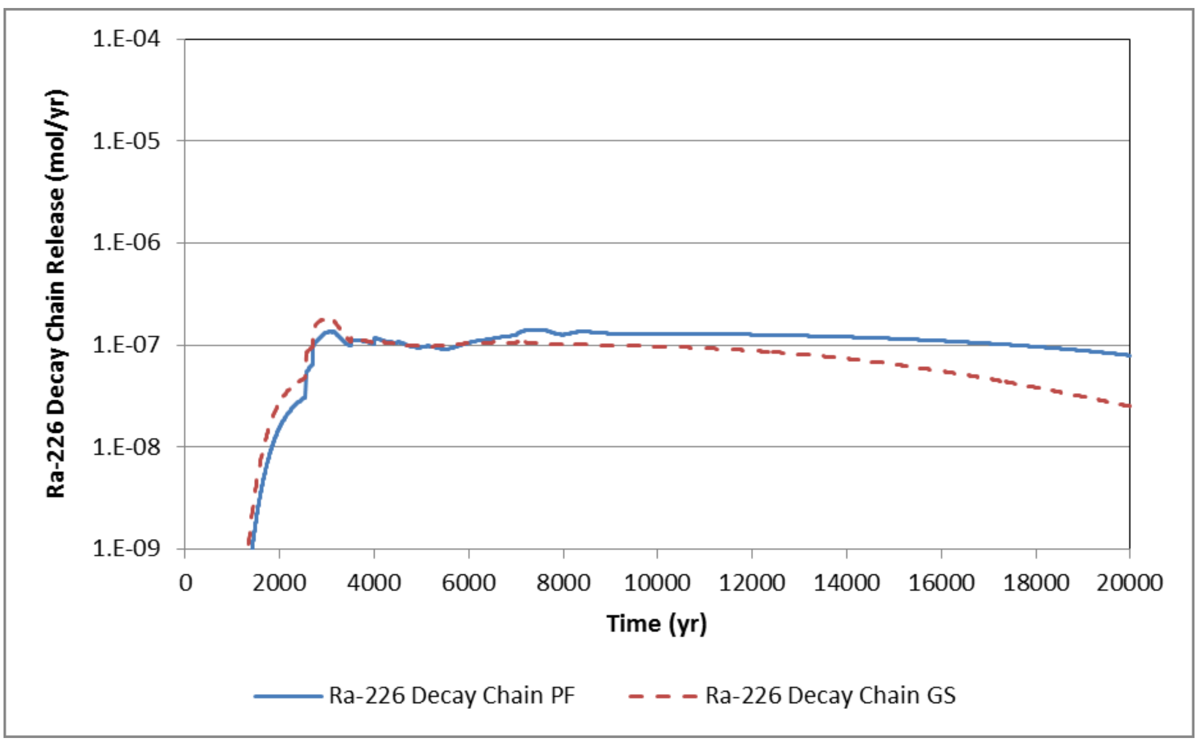

Figure A.2-31: Tank 15 Am-241 Release to the Saturated Zone for Case C

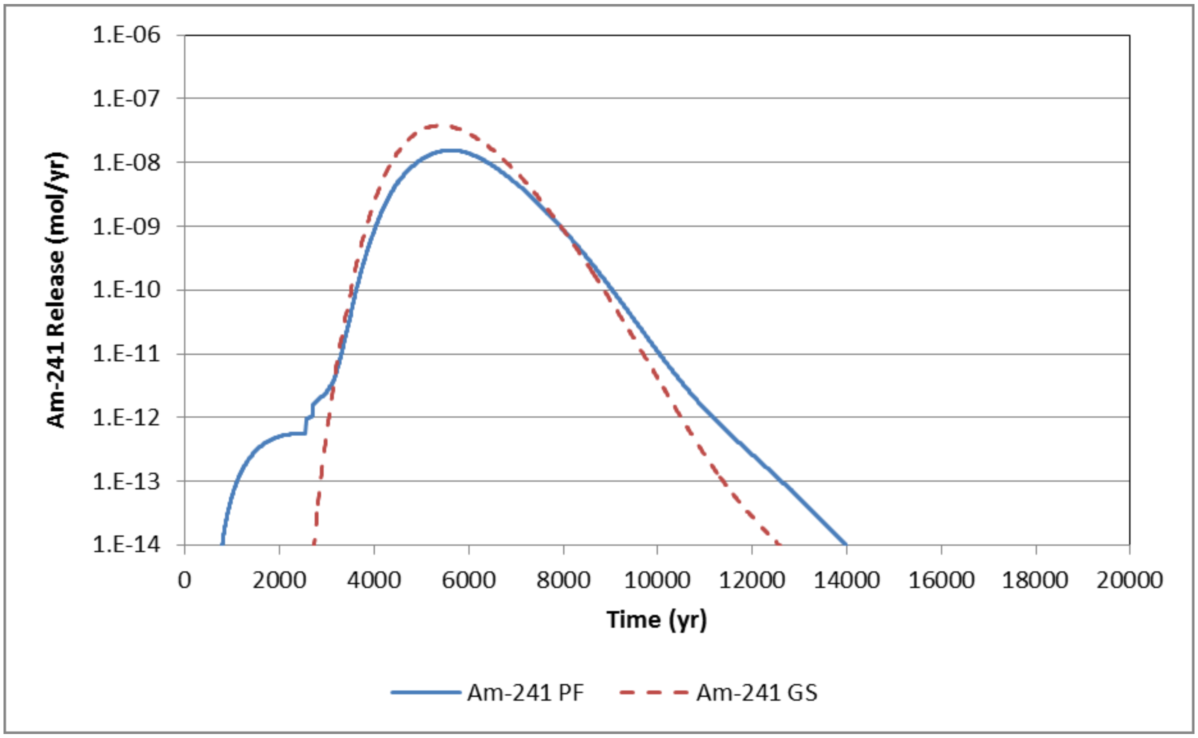

Figure A.2-32: Tank 15 Np-237 Release to the Saturated Zone for Case C

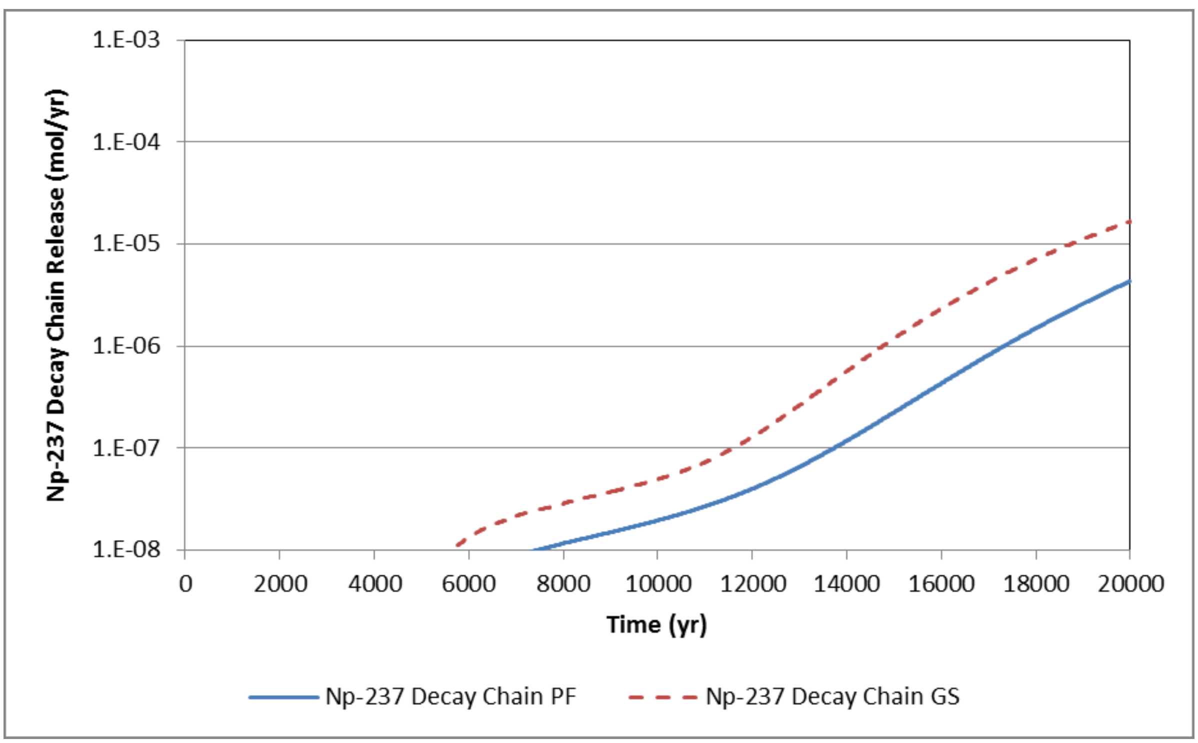

A.2.5 Type II Tank with Failed Liner (Tank 16) for Case C

For the Case C configuration, a comparison of the PORFLOW HTF Model and the GoldSim model mass releases of I-129, Tc-99, Am-243, Pu-239, U-234, Ra-226, Am-241, and Np-237, as presented in Figure A.2-33 through Figure A.2-40, indicate that the GoldSim model produces a good approximation of the releases from Tank 16 generated by the PORFLOW model.

Table A.2-5 summarizes the peak values for these releases showing that when comparing the two models although not all of the percent differences are below 50% the values are reasonably close when considered in conjunction with the release patterns shown in Figure A.2-33 through Figure A.2-40.

Table A.2-5: Case C GoldSim and PORFLOW Model Peak Releases from the UZ to the SZ Comparisons for Tank 16 within 20,000 years

Radionuclide	PORFLOW Peak Release (mol/yr)	PORFLOW Time of Peak Release (yr)	GoldSim Peak Release (mol/yr)	GoldSim Time of Peak Release (yr)	Peak Release Percent Difference GoldSim vs PORFLOW
I-129	4.4E-03	523	5.8E-03	520	32%
Tc-99	4.7E-03	319	1.8E-03	15,060	-62%
Am-243	3.2E-08	6,285	2.6E-08	6,510	-19%
Pu-239	2.8E-05	16,193	1.8E-05	16,070	-36%
U-234	2.8E-05	2,772	3.4E-05	2,780	21%
Ra-226	5.0E-09	7,635	5.0E-09	11,580	0%
Am-241	3.1E-10	5,338	2.4E-10	5,380	-23%
Np-237	5.6E-07	20,000	4.9E-07	20,000	-13%

Figure A.2-33: Tank 16 I-129 Release to the Saturated Zone for Case C

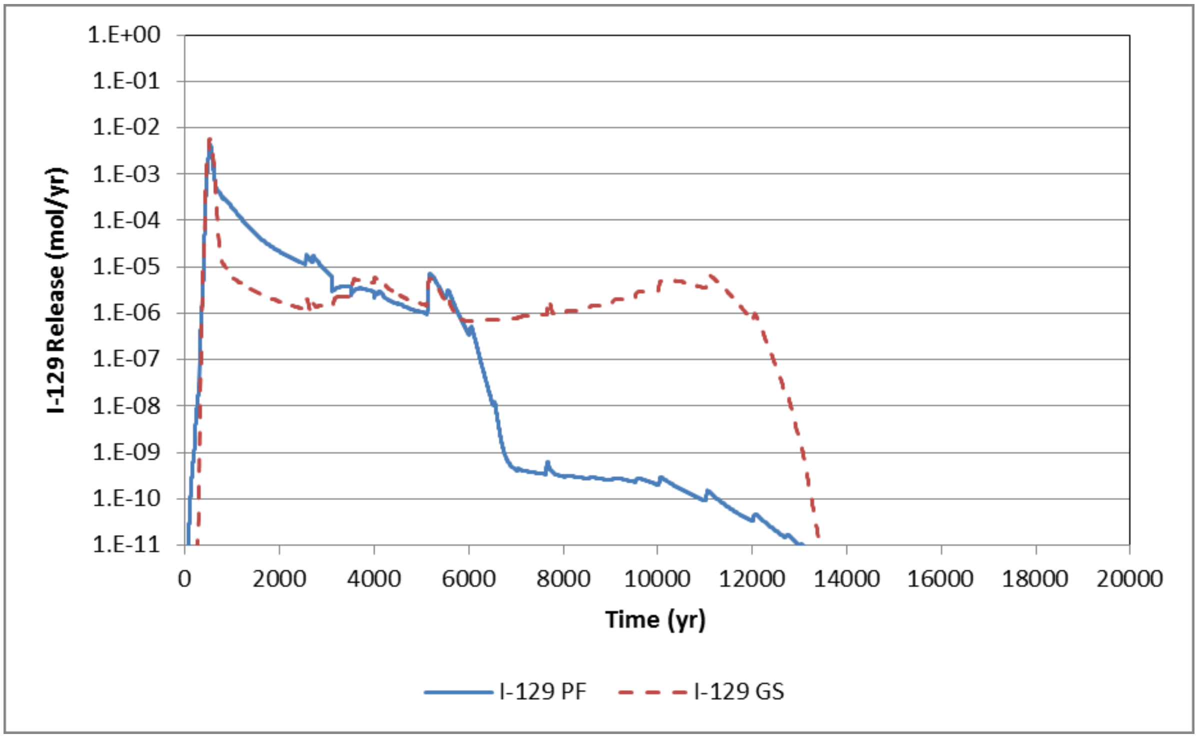

Figure A.2-34: Tank 16 Tc-99 Release to the Saturated Zone for Case C

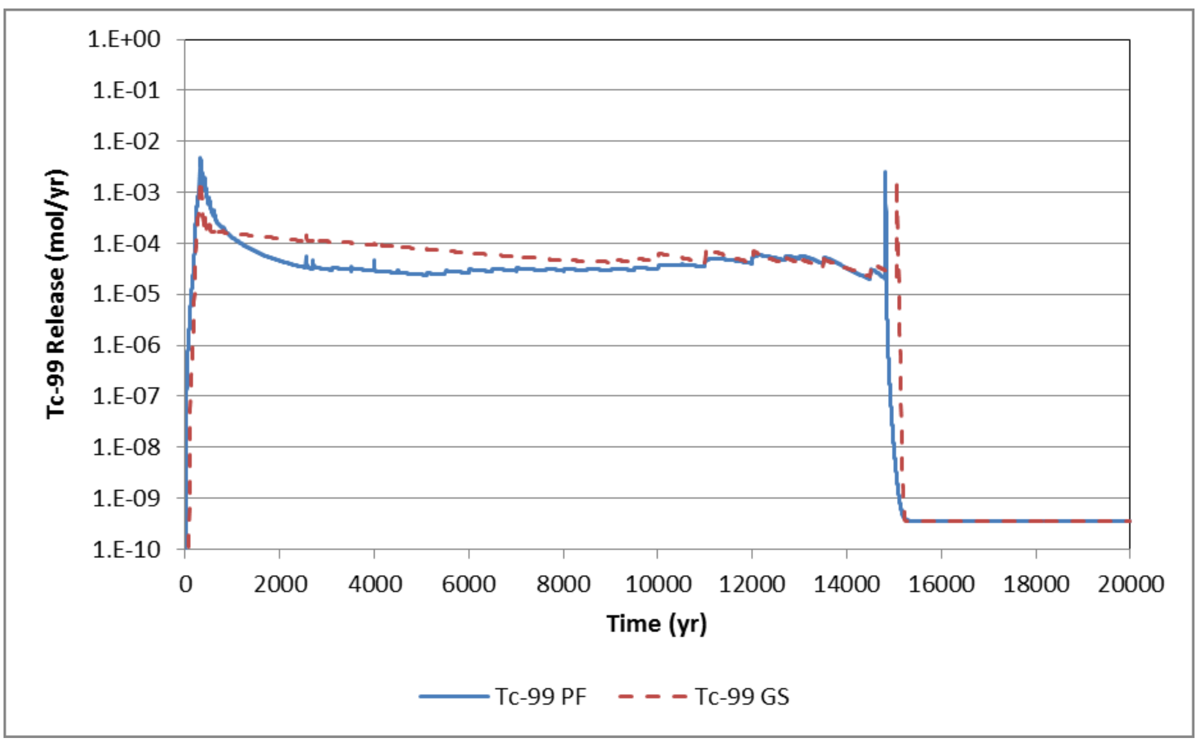

Figure A.2-35: Tank 16 Am-243 Release to the Saturated Zone for Case C

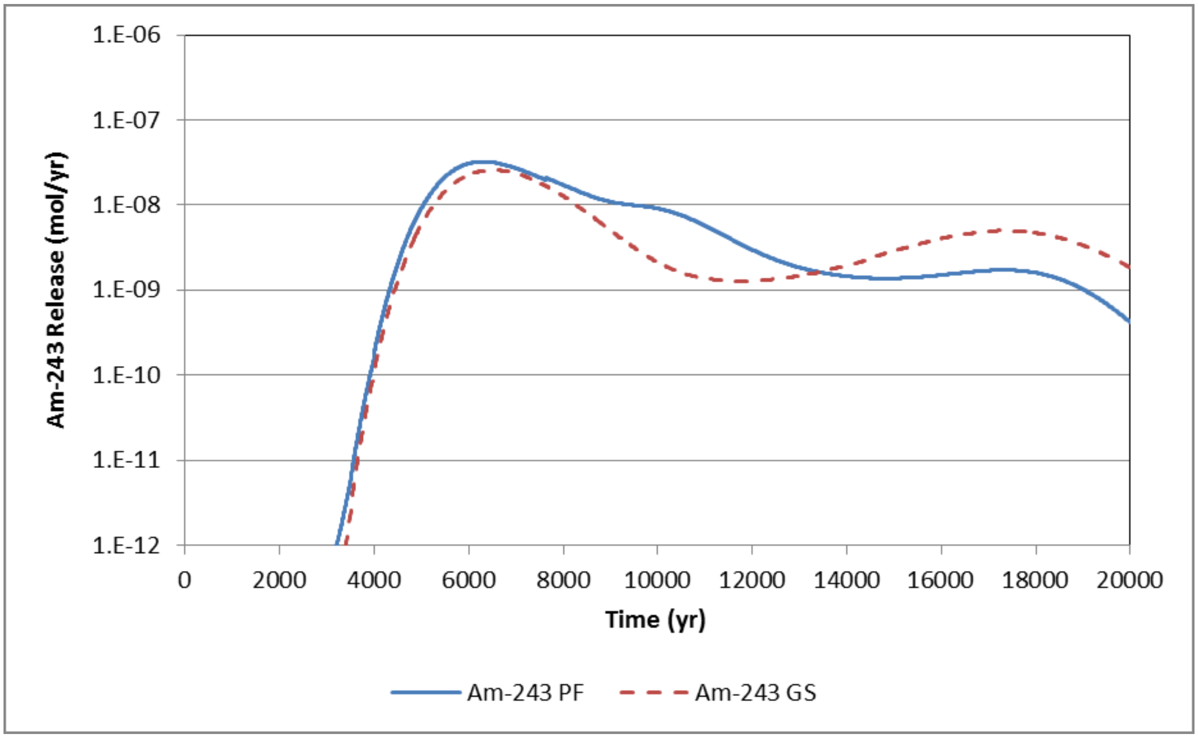

Figure A.2-36: Tank 16 Pu-239 Release to the Saturated Zone for Case C

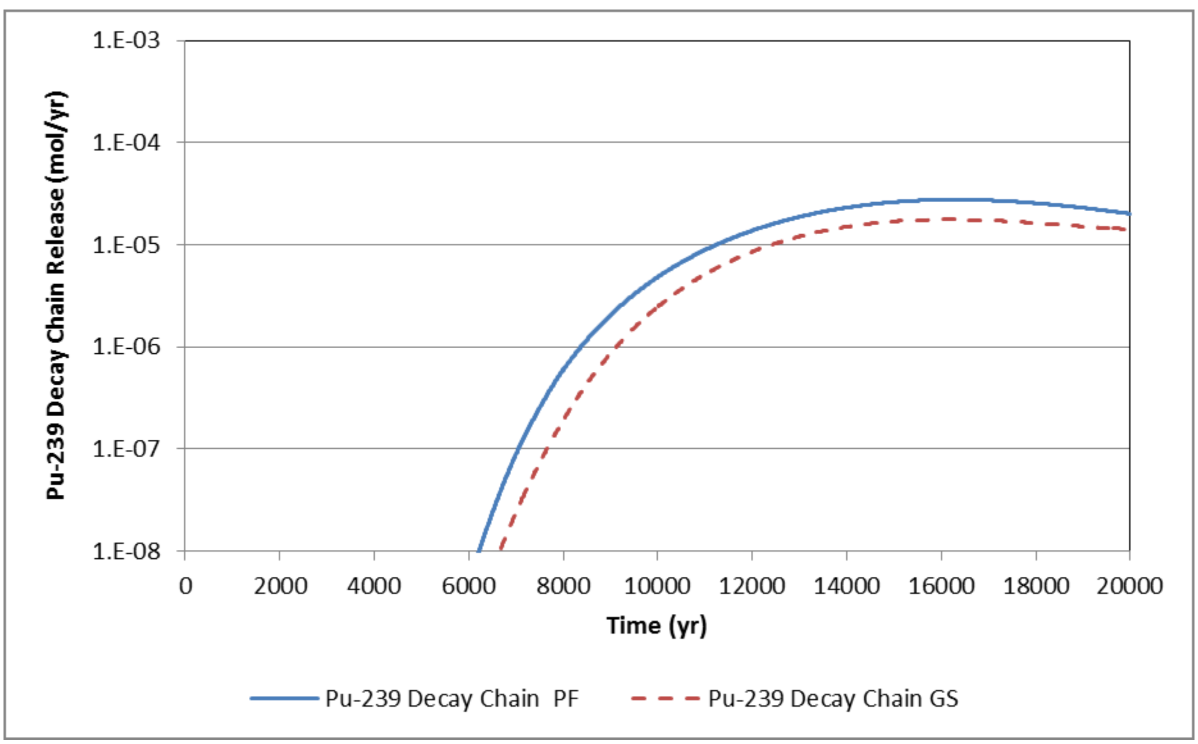

Figure A.2-37: Tank 16 U-234 Release to the Saturated Zone for Case C

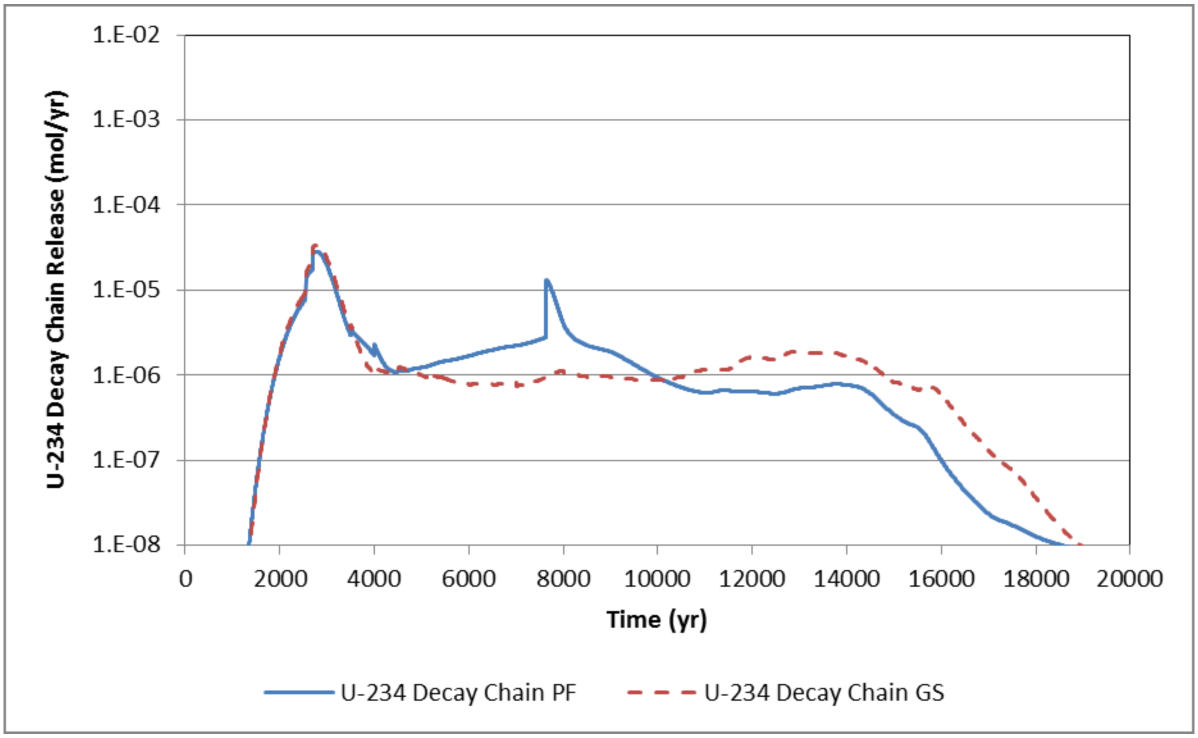

Figure A.2-38: Tank 16 Ra-226 Release to the Saturated Zone for Case C

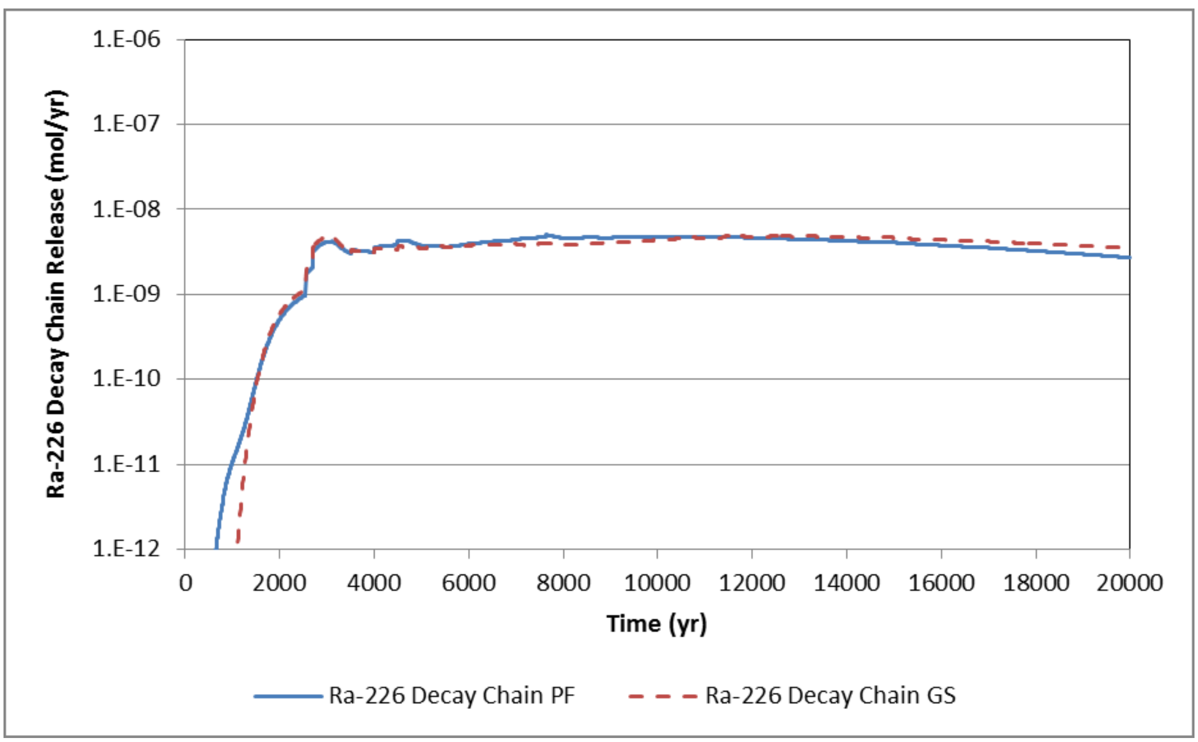

Figure A.2-39: Tank 16 Am-241 Release to the Saturated Zone for Case C

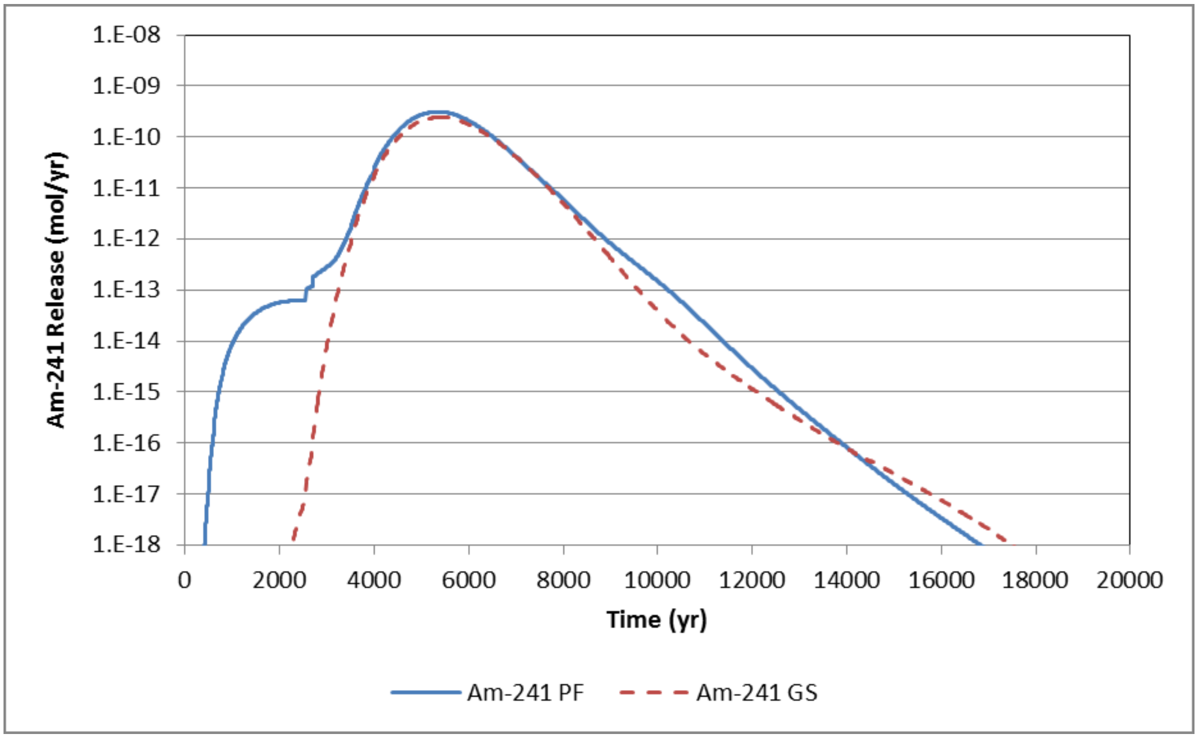

Figure A.2-40: Tank 16 Np-237 Release to the Saturated Zone for Case C

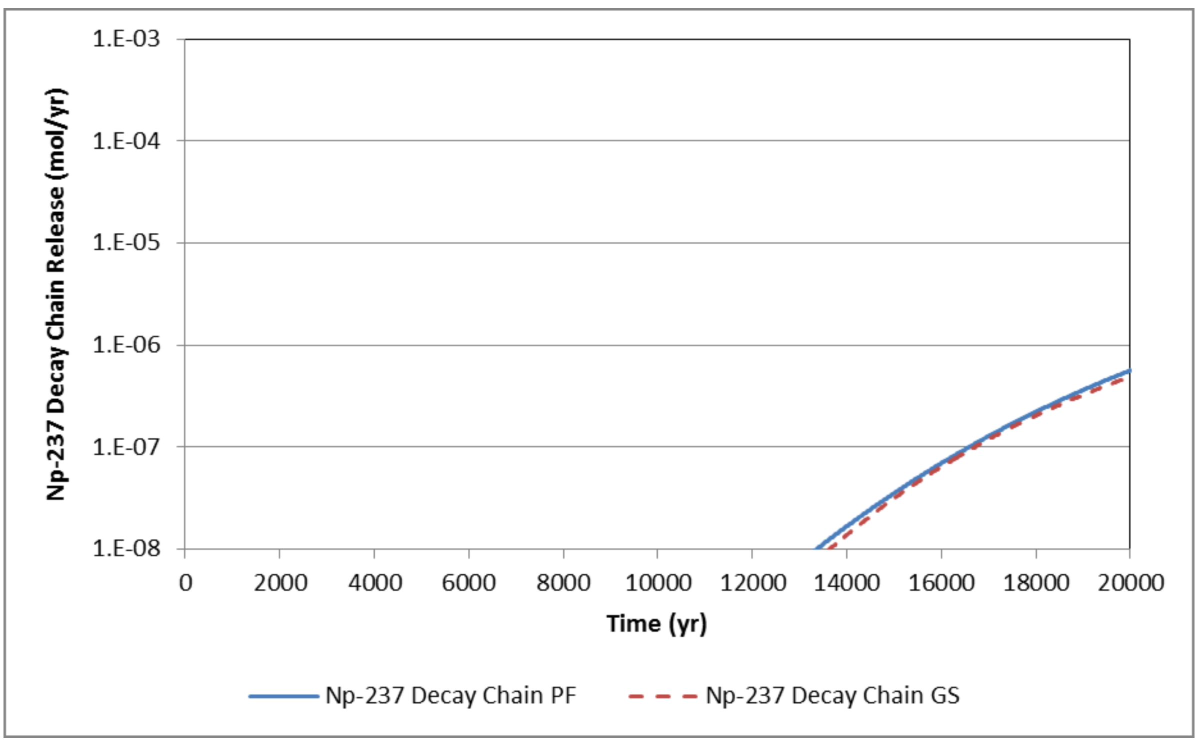

A.2.6 Type IV Tank (Tank 24) for Case C

For the Case C configuration, a comparison of the PORFLOW HTF Model and the GoldSim model mass releases of I-129, Tc-99, Am-243, Pu-239, U-234, Ra-226, Am-241, and Np-237, as presented in Figure A.2-41 through Figure A.2-48, indicate that the GoldSim model produces a good approximation of the releases from Tank 24 generated by the PORFLOW model.

Table A.2-6 summarizes the peak values for these releases showing that when comparing the two models although not all of the percent differences are below 50% the values are reasonably close when considered in conjunction with the release patterns shown in Figure A.2-41 through Figure A.2-48.

Table A.2-6: Case C GoldSim and PORFLOW Model Peak Releases from the UZ to the SZ Comparisons for Tank 24 within 20,000 years

Radionuclide	PORFLOW Peak Release (mol/yr)	PORFLOW Time of Peak Release (yr)	GoldSim Peak Release (mol/yr)	GoldSim Time of Peak Release (yr)	Peak Release Percent Difference GoldSim vs PORFLOW
I-129	3.7E-05	501	4.1E-05	530	11%
Tc-99	3.6E-09	531	3.0E-09	550	-17%
Am-243	3.8E-07	11,737	5.0E-07	11,030	32%
Pu-239	3.5E-06	16,649	4.5E-06	14,690	29%
U-234	6.3E-06	6,096	8.3E-06	5,010	32%
Ra-226	5.6E-08	2,846	5.1E-08	1,810	-9%
Am-241	2.8E-11	2,958	8.0E-12	4,580	-71%
Np-237	1.0E-05	8,779	1.2E-05	6,580	20%

Figure A.2-41: Tank 24 I-129 Release to the Saturated Zone for Case C

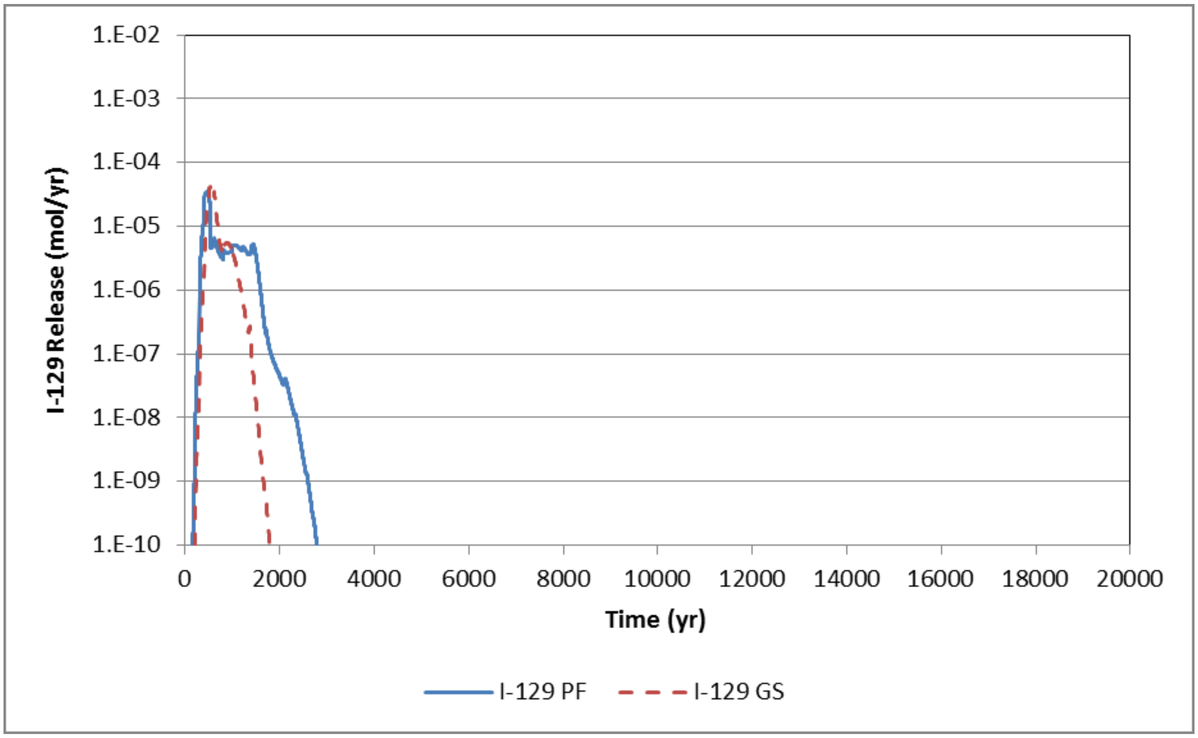

Figure A.2-42: Tank 24 Tc-99 Release to the Saturated Zone for Case C

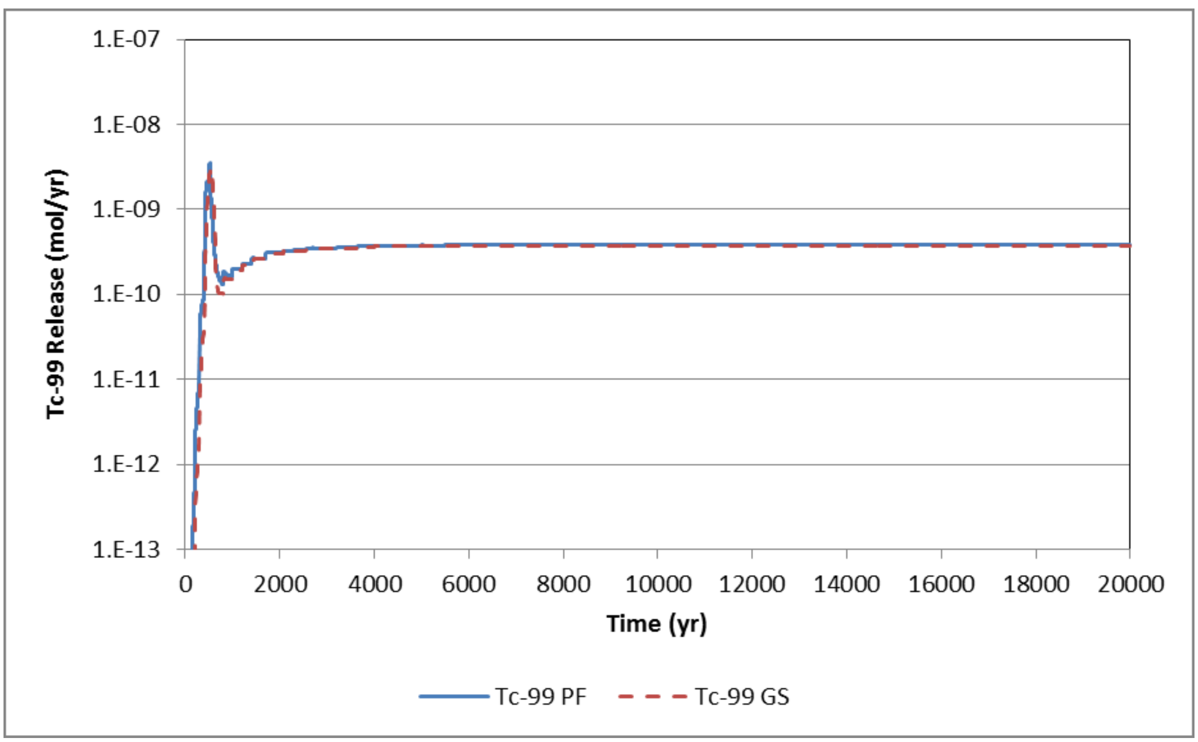

Figure A.2-43: Tank 24 Am-243 Release to the Saturated Zone for Case C

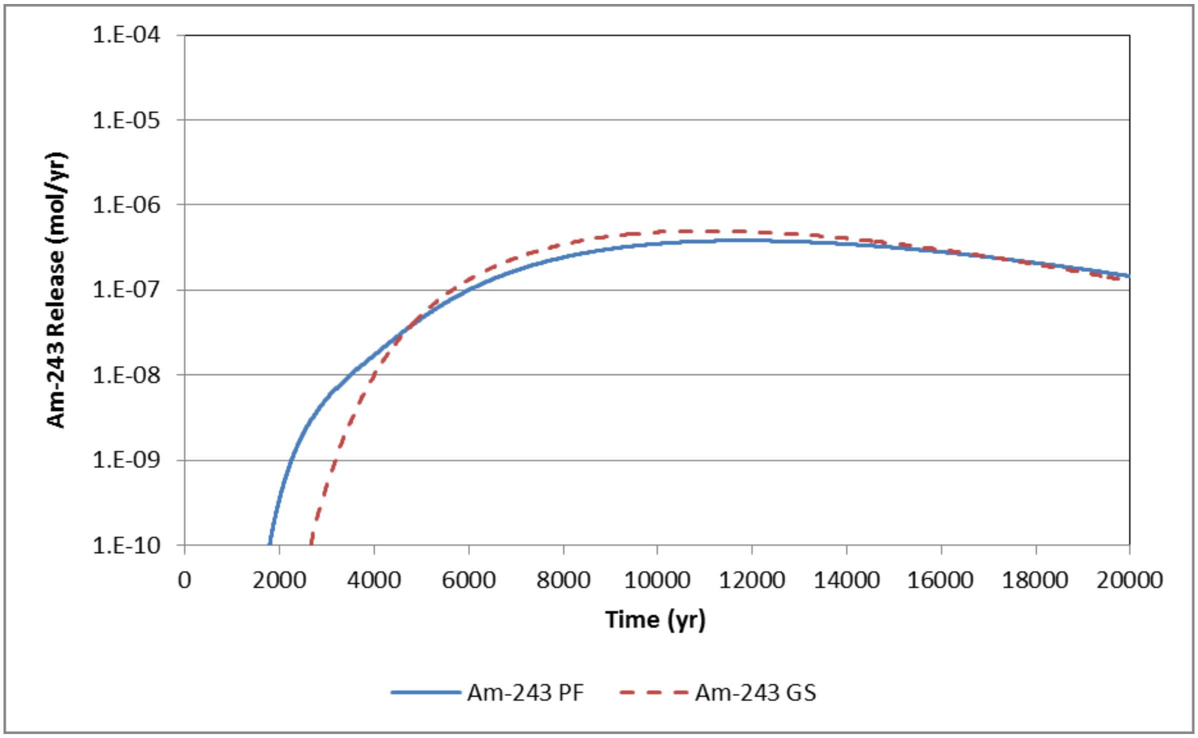

Figure A.2-44: Tank 24 Pu-239 Release to the Saturated Zone for Case C

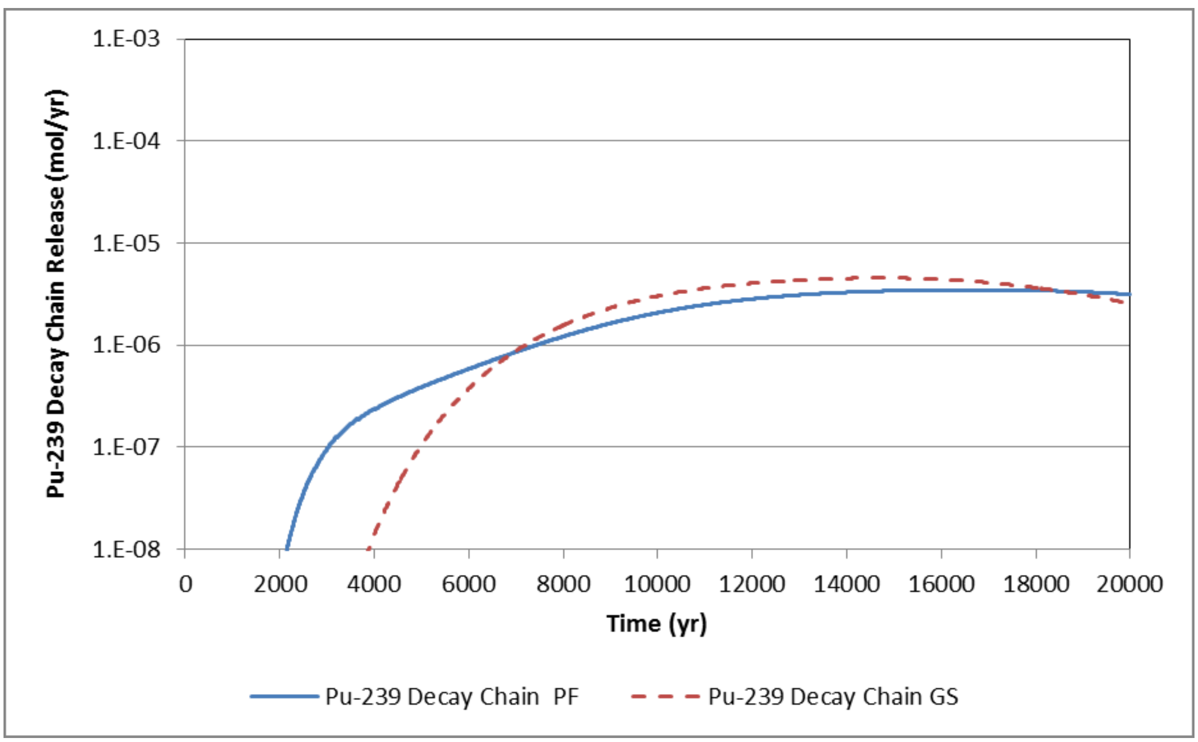

Figure A.2-45: Tank 24 U-234 Release to the Saturated Zone for Case C

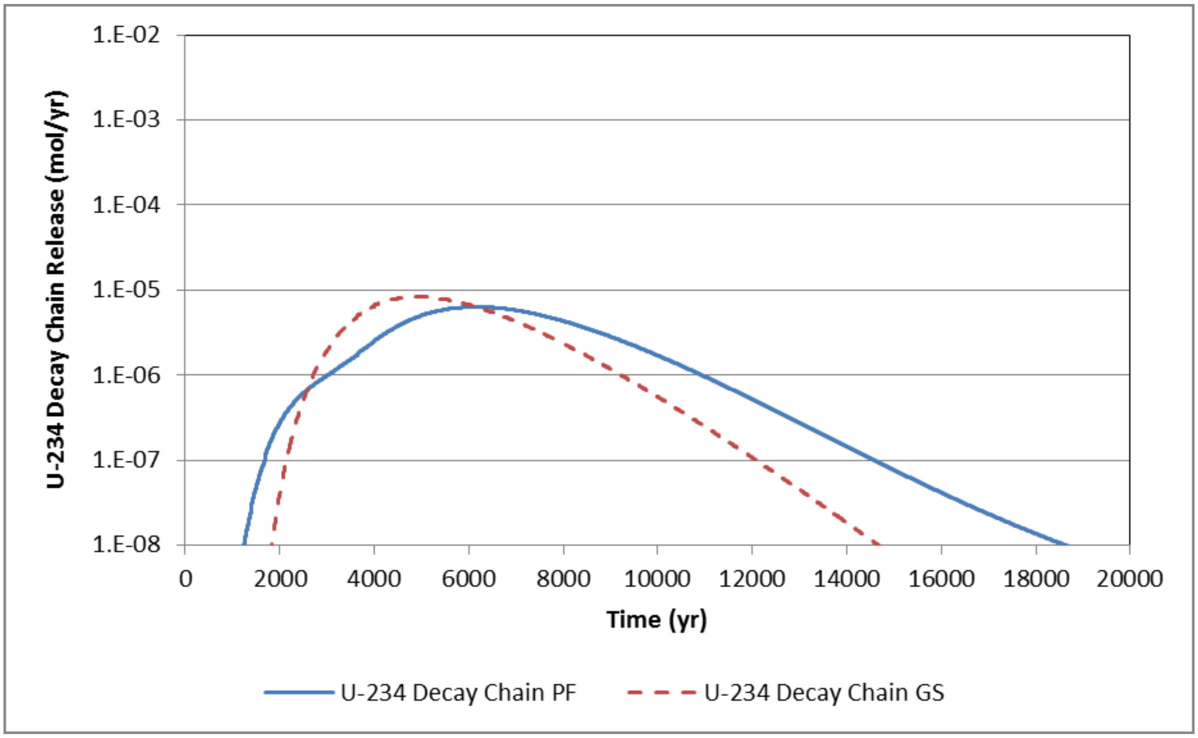

Figure A.2-46: Tank 24 Ra-226 Release to the Saturated Zone for Case C

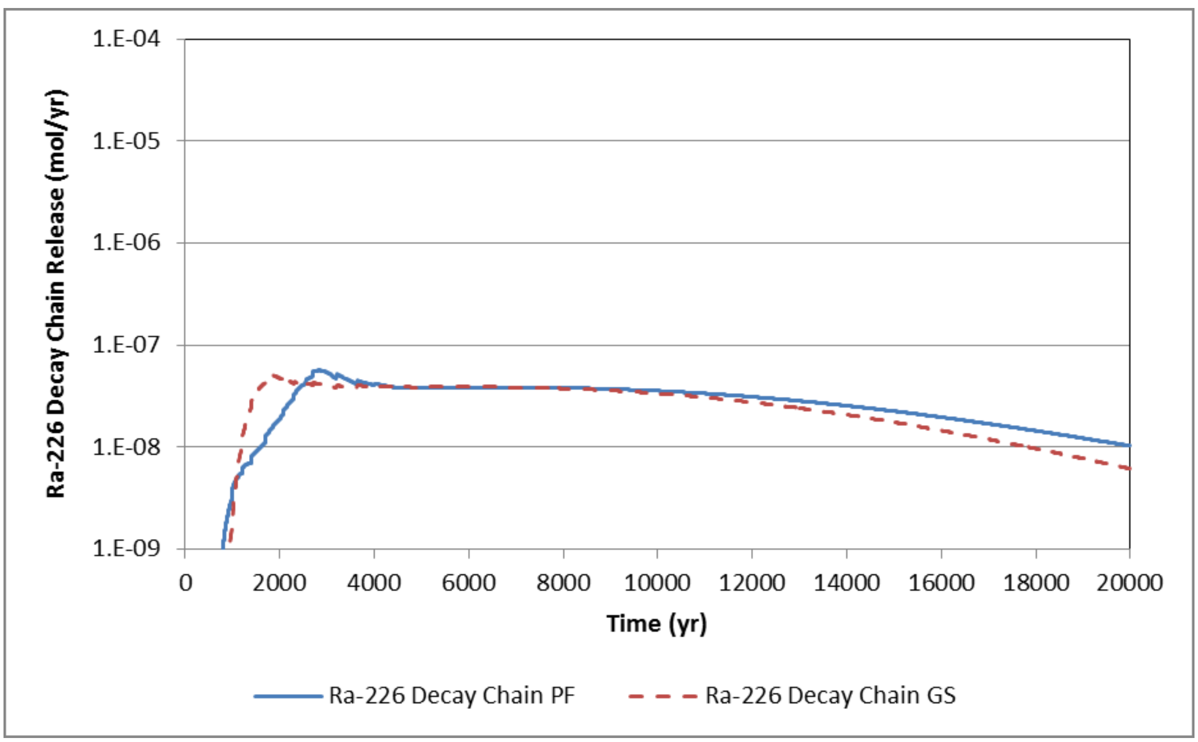

Figure A.2-47: Tank 24 Am-241 Release to the Saturated Zone for Case C

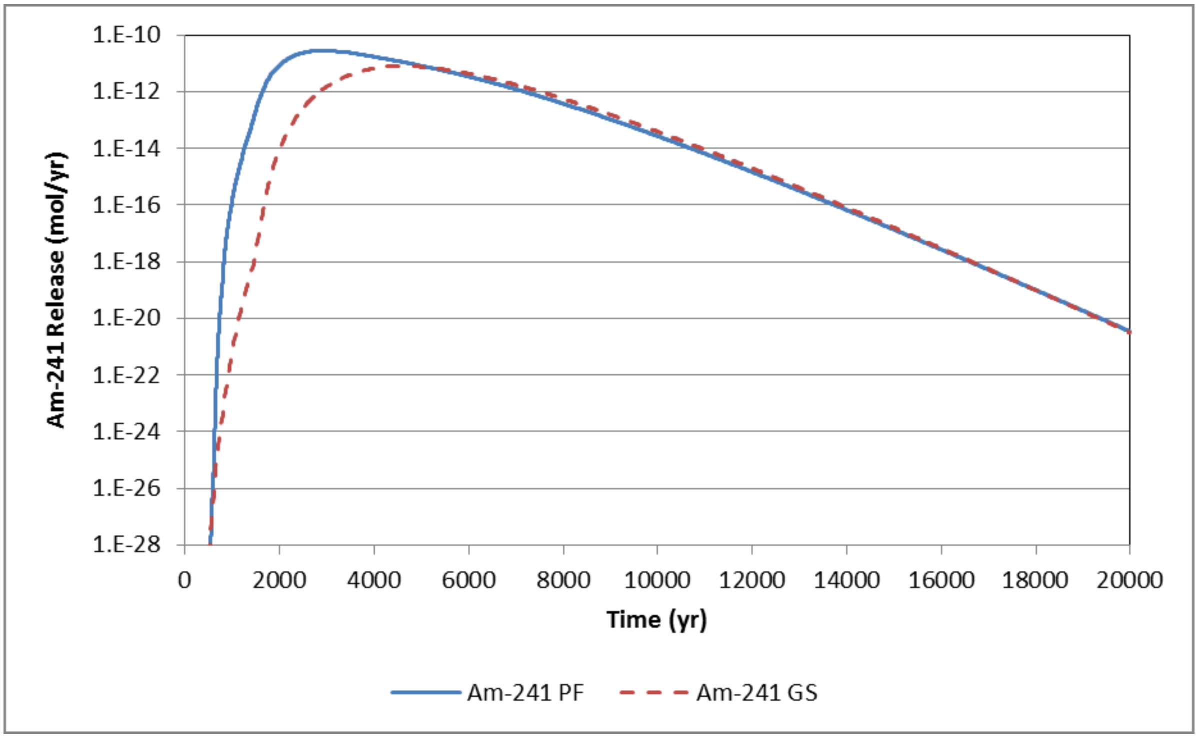

Figure A.2-48: Tank 24 Np-237 Release to the Saturated Zone for Case C

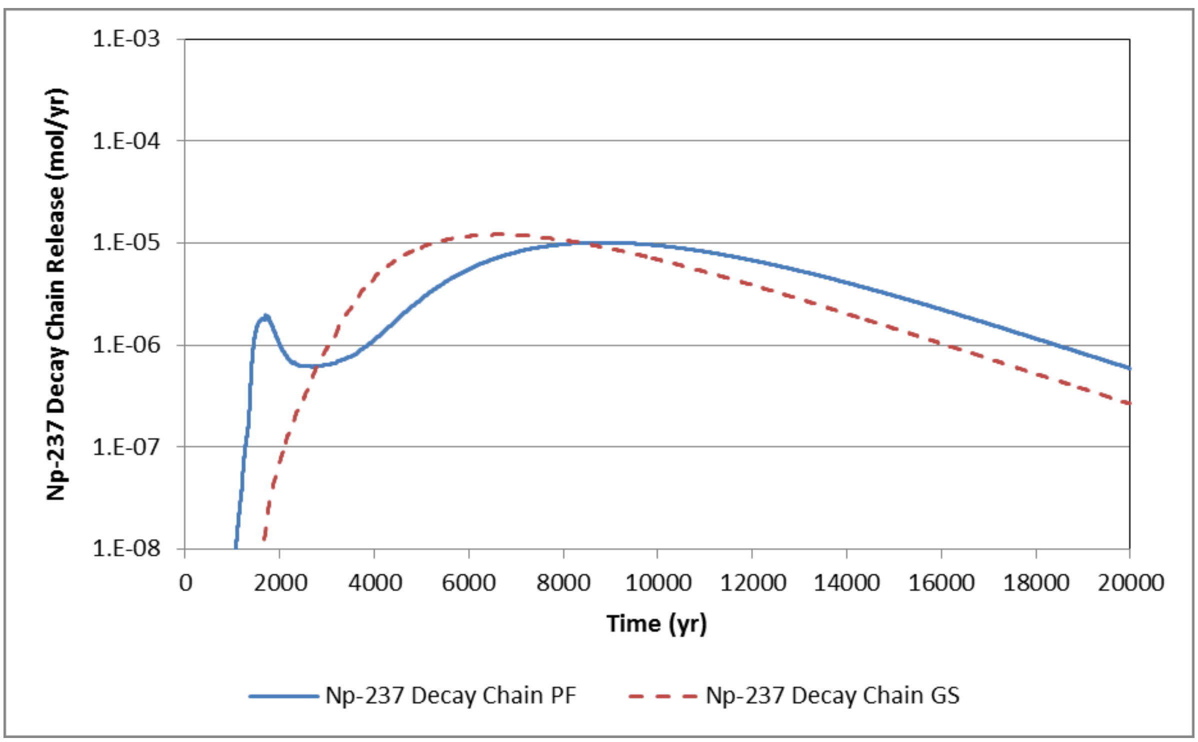

A.2.7 Type III Tank (Tank 31) for Case C

For the Case C configuration, a comparison of the PORFLOW HTF Model and the GoldSim model mass releases of I-129, Tc-99, Am-243, Pu-239, U-234, Ra-226, Am-241, and Np-237, as presented in Figure A.2-49 through Figure A.2-56, indicate that the GoldSim model produces a good approximation of the releases from Tank 15 generated by the PORFLOW model.

Table A.2-7 summarizes the peak values for these releases showing that when comparing the two models although not all of the percent differences are below 50% the values, except for Am-243, Am-241 and Np-237 are reasonably close when considered in conjunction with the release patterns shown in Figure A.2-49, Figure A.2-50, and Figure A.2-52 through Figure A.2-54. As can be seen in Figure A.2-51, A.2-55 and Figure A.2-56, the release of Am-243 is conservatively overestimated and the releases of Am-241 and Np-237 are underestimated over the 20,000 year time period.

Table A.2-7: Case C GoldSim and PORFLOW Model Peak Releases from the UZ to the SZ Comparisons for Tank 31 within 20,000 years

Radionuclide	PORFLOW Peak Release (mol/yr)	PORFLOW Time of Peak Release (yr)	GoldSim Peak Release (mol/yr)	GoldSim Time of Peak Release (yr)	Peak Release Percent Difference GoldSim vs PORFLOW
I-129	3.8E-04	2,369	3.9E-04	2,360	3%
Tc-99	7.7E-09	2,132	7.9E-09	2,130	3%
Am-243	6.7E-09	20,000	1.2E-07	20,000	1691%
Pu-239	9.5E-07	16,328	7.4E-07	20,000	-22%
U-234	3.0E-04	12,711	3.6E-04	9,420	20%
Ra-226	3.9E-07	8,387	2.6E-07	8,550	-33%
Am-241	5.7E-15	8,892	1.6E-17	15,070	-100%
Np-237	2.0E-05	5,842	3.2E-07	20,000	-98%

Figure A.2-49: Tank 31 I-129 Release to the Saturated Zone for Case C

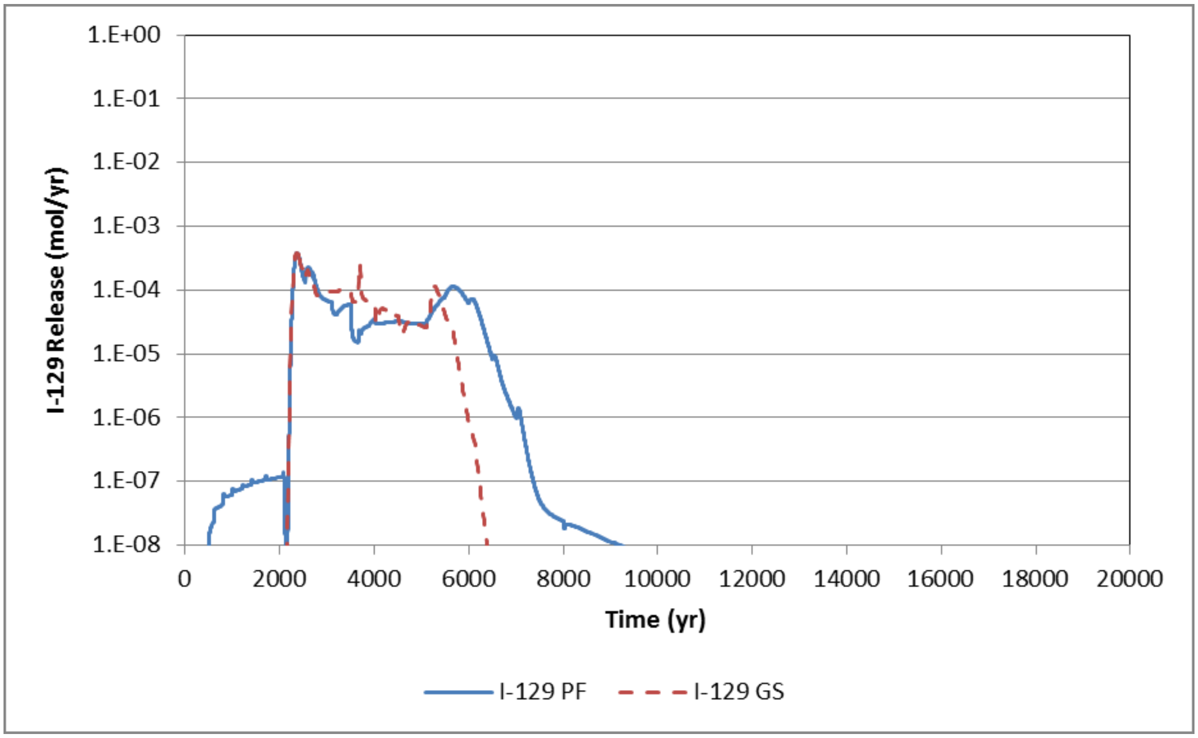

Figure A.2-50: Tank 31 Tc-99 Release to the Saturated Zone for Case C

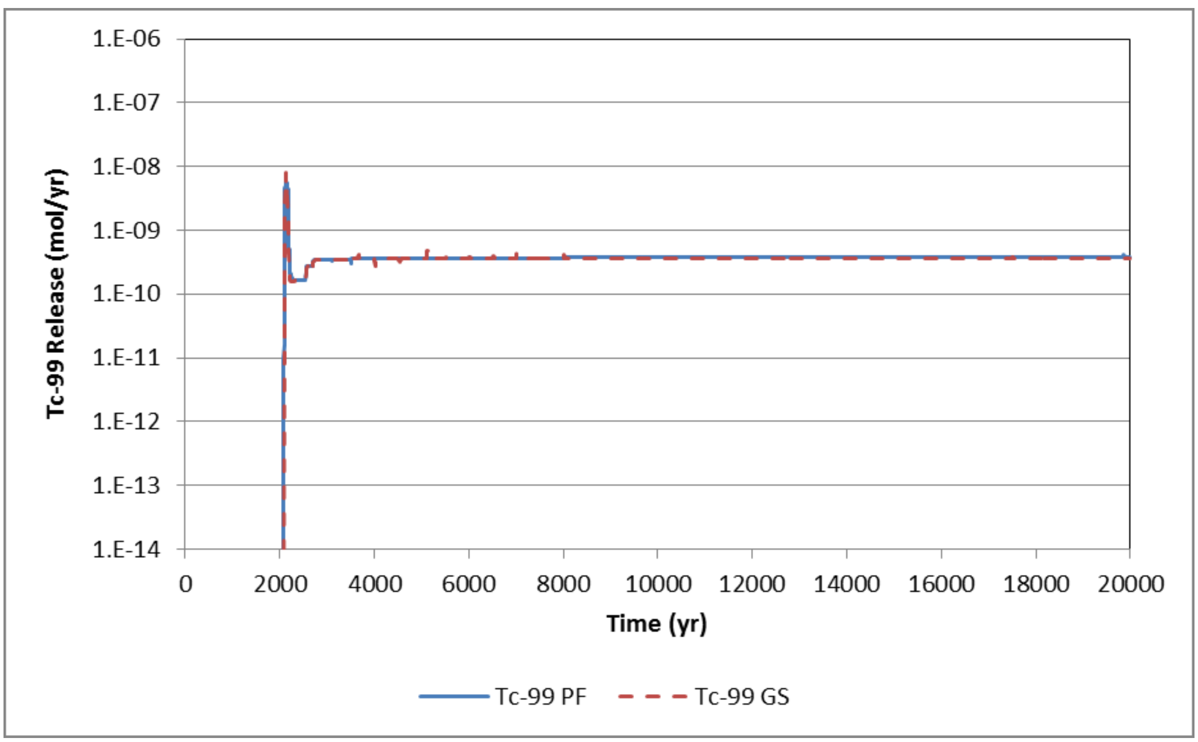

Figure A.2-51: Tank 31 Am-243 Release to the Saturated Zone for Case C

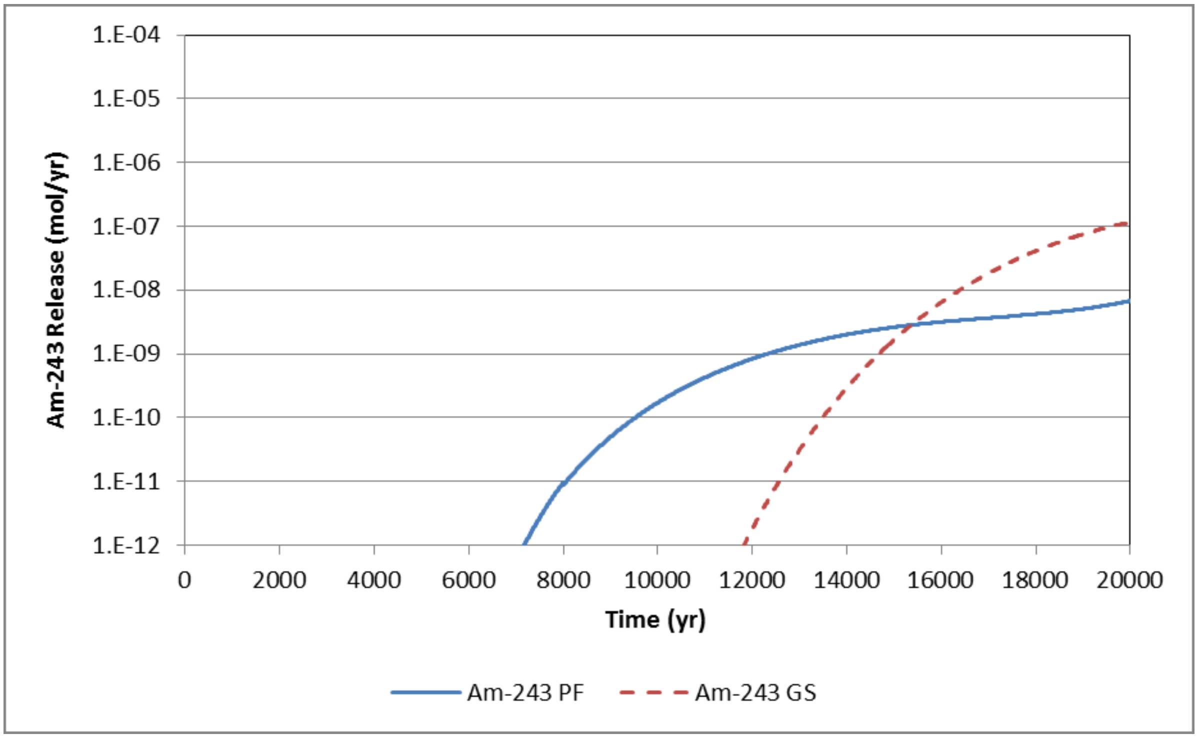

Figure A.2-52: Tank 31 Pu-239 Release to the Saturated Zone for Case C

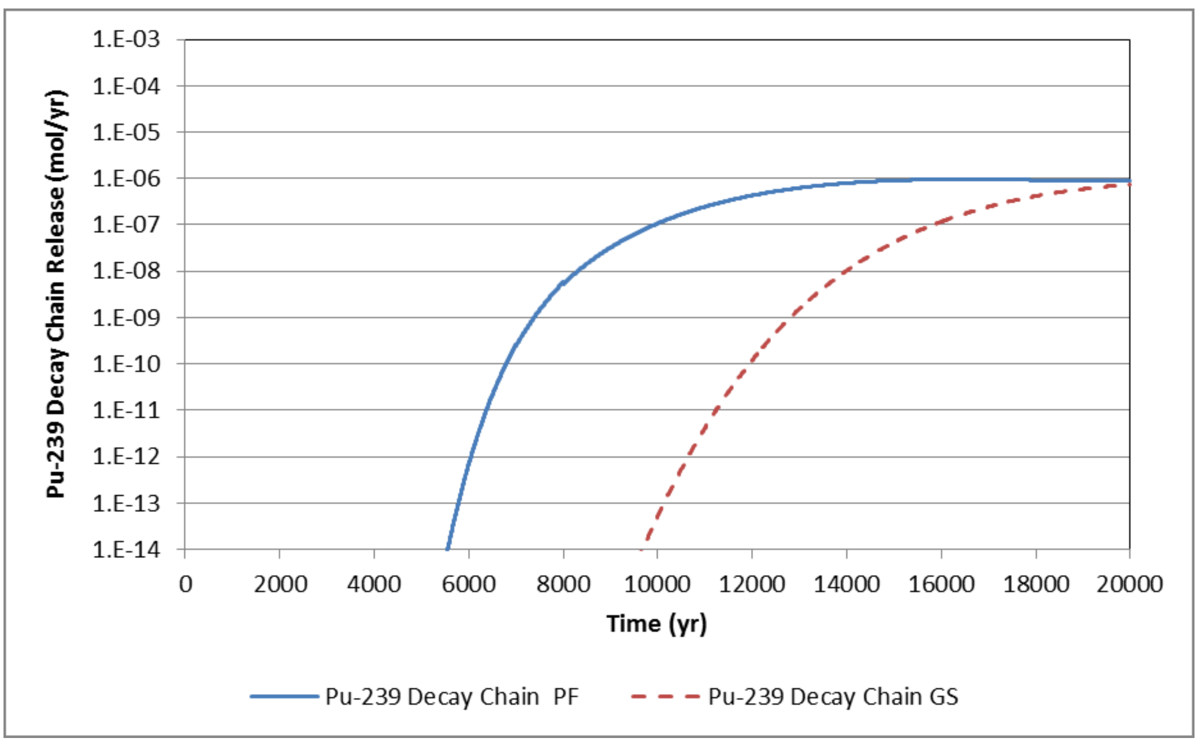

Figure A.2-53: Tank 31 U-234 Release to the Saturated Zone for Case C

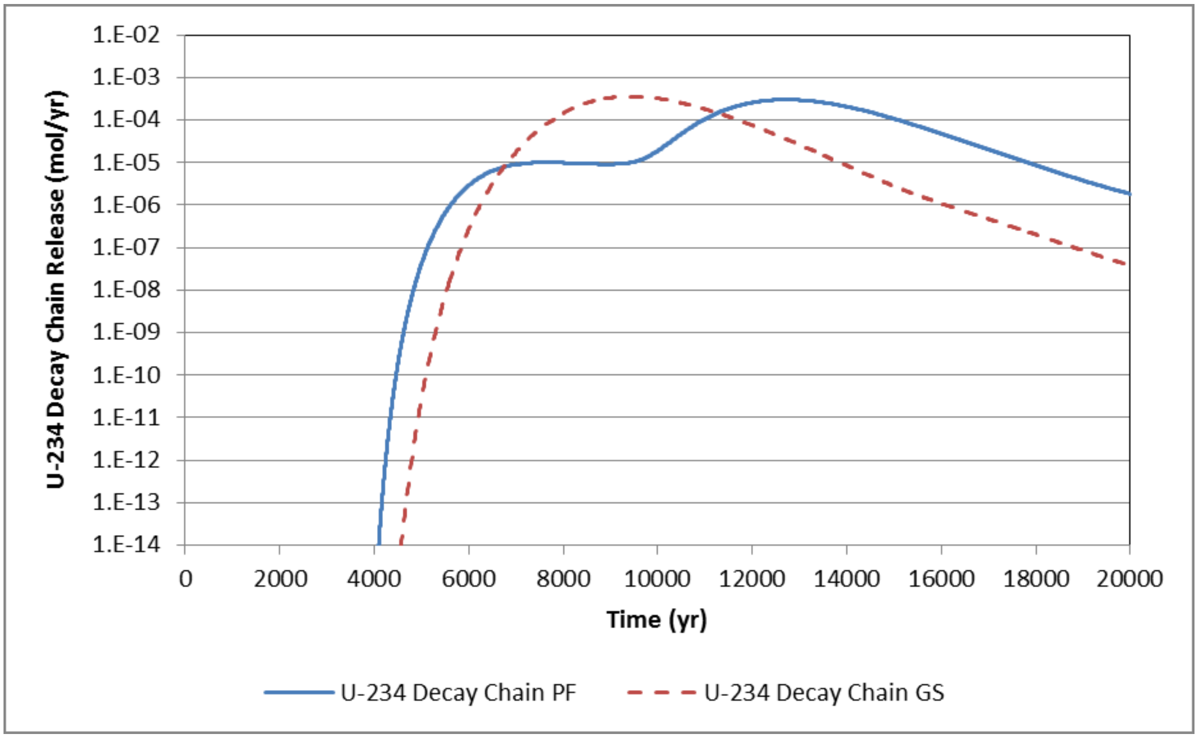

Figure A.2-54: Tank 31 Ra-226 Release to the Saturated Zone for Case C

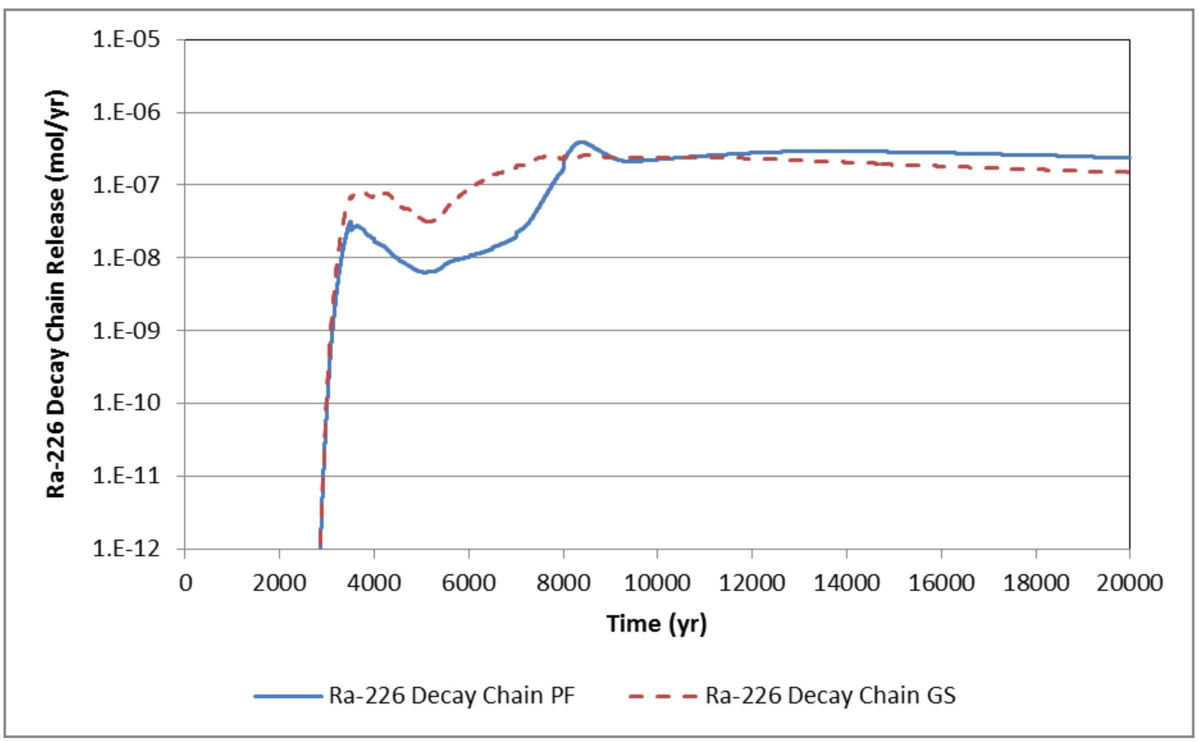

Figure A.2-55: Tank 31 Am-241 Release to the Saturated Zone for Case C

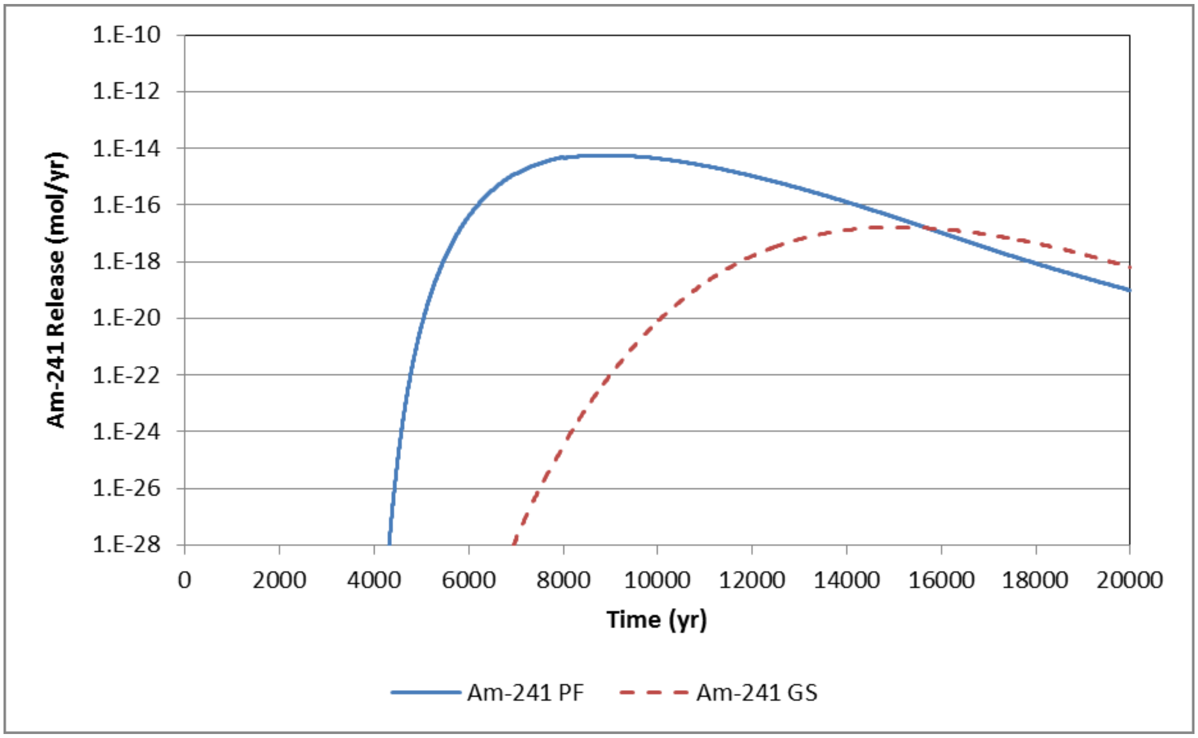

Figure A.2-56: Tank 31 Np-237 Release to the Saturated Zone for Case C

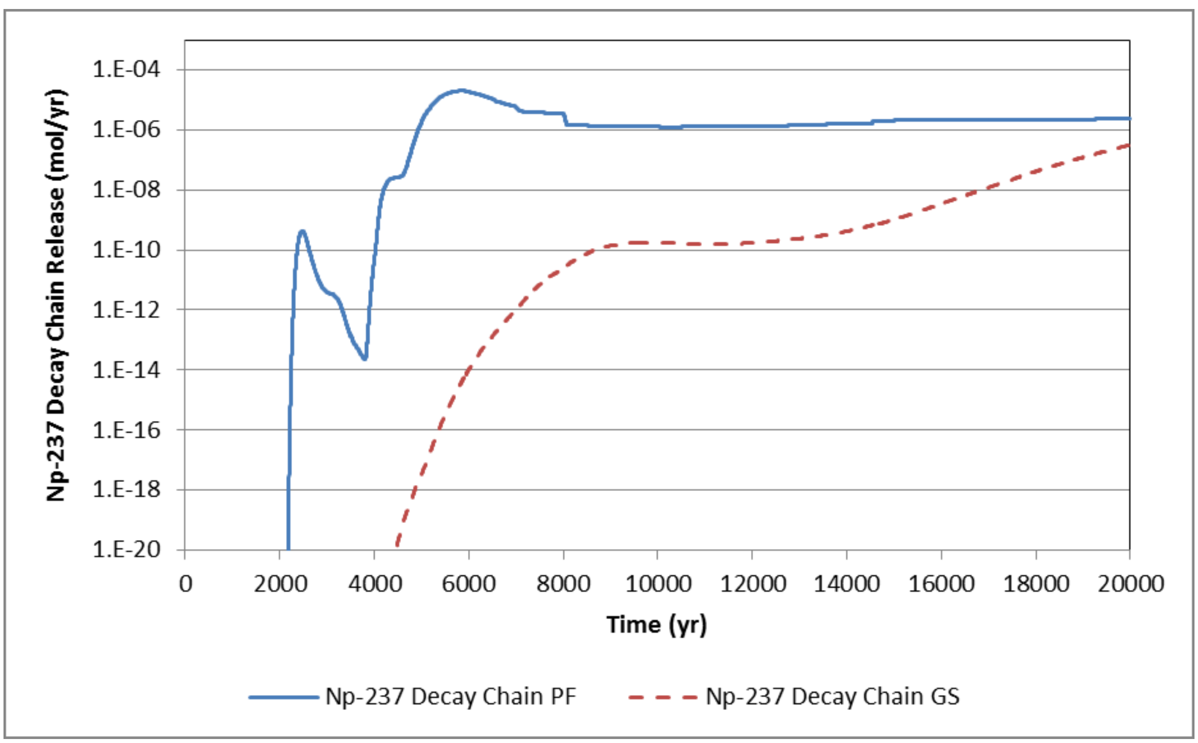

A.3.1 Type I Tank with Intact Liner (Tank 9) for Case D

For the Case D configuration, a comparison of the PORFLOW HTF Model and the GoldSim model mass releases of I-129, Tc-99, Am-243, Pu-239, U-234, Ra-226, Am-241, and Np-237, as presented in Figure A.3-1 through Figure A.3-8, indicate that the GoldSim model successfully captures the radionuclide release patterns seen in Tank 9 results generated by the PORFLOW model.

Table A.3-1 summarizes the peak values for these releases showing that when comparing the two models although not all of the percent differences are below 50% the values are reasonably close when considered in conjunction with the release patterns shown in Figure A.3-1 through Figure A.3-8.

Table A.3-1: Case D GoldSim and PORFLOW Model Peak Releases from the UZ to the SZ Comparisons for Tank 9 within 20,000 years

Radionuclide	PORFLOW Peak Release (mol/yr)	PORFLOW Time of Peak Release (yr)	GoldSim Peak Release (mol/yr)	GoldSim Time of Peak Release (yr)	Peak Release Percent Difference GoldSim vs PORFLOW
I-129	3.7E-02	1,174	3.7E-02	1,180	0%
Tc-99	1.1E-03	1,144	4.9E-04	1,150	-55%
Am-243	4.1E-04	1,719	5.6E-04	1,730	37%
Pu-239	1.8E-05	6,113	2.0E-05	5,820	11%
U-234	6.5E-03	1,563	3.0E-03	1,560	-54%
Ra-226	1.9E-07	1,596	2.3E-07	1,580	21%
Am-241	2.5E-05	1,453	3.1E-05	1,370	24%
Np-237	6.5E-02	1,562	2.1E-02	1,560	-68%

Figure A.3-1: Tank 9 I-129 Release to the Saturated Zone for Case D

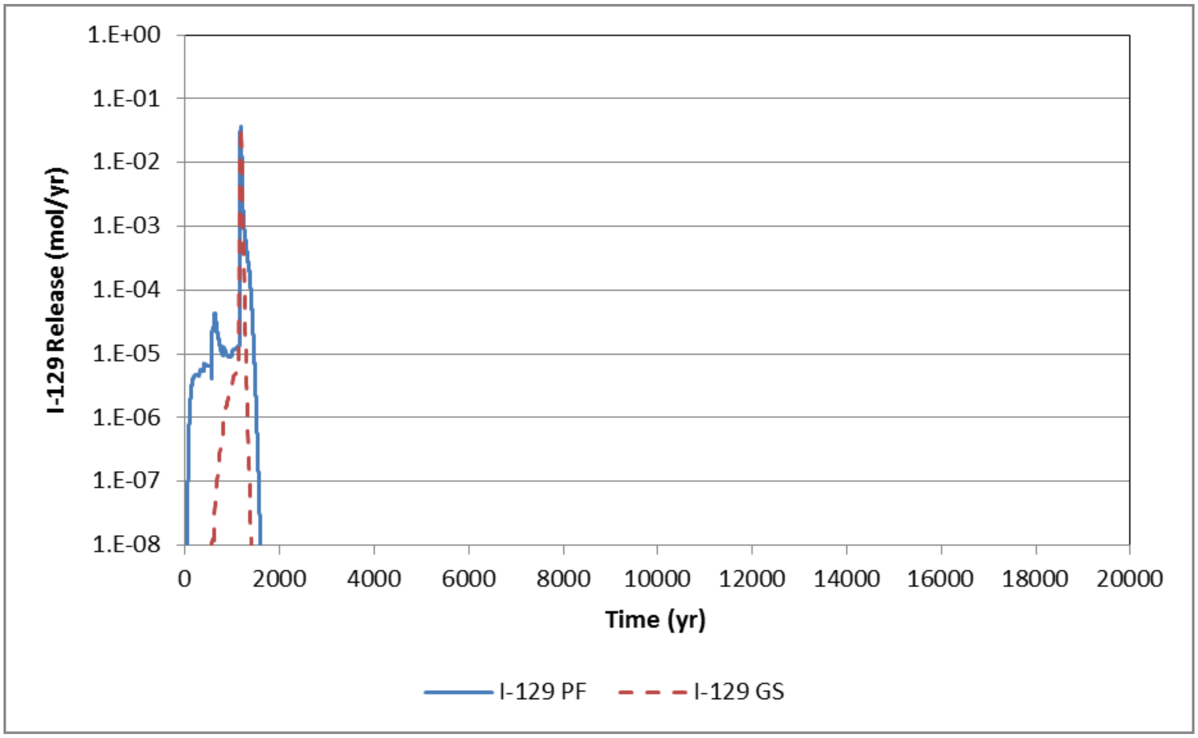

Figure A.3-2: Tank 9 Tc-99 Release to the Saturated Zone for Case D

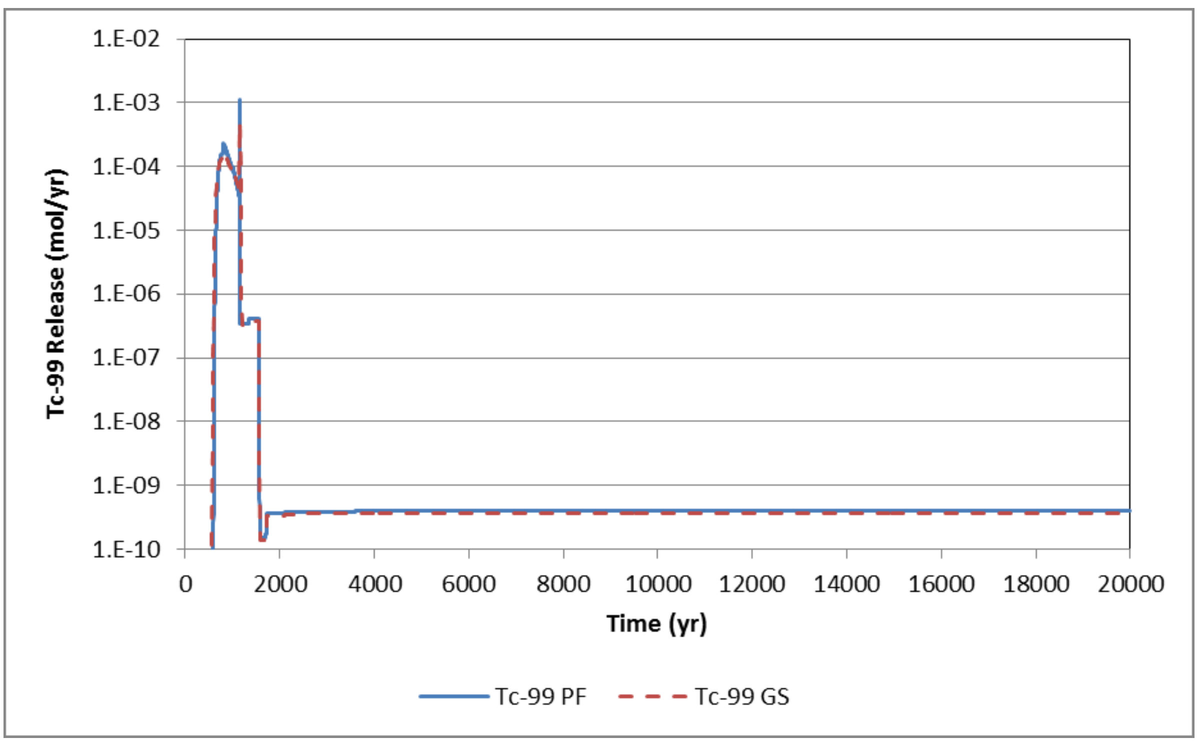

Figure A.3-3: Tank 9 Am-243 Release to the Saturated Zone for Case D

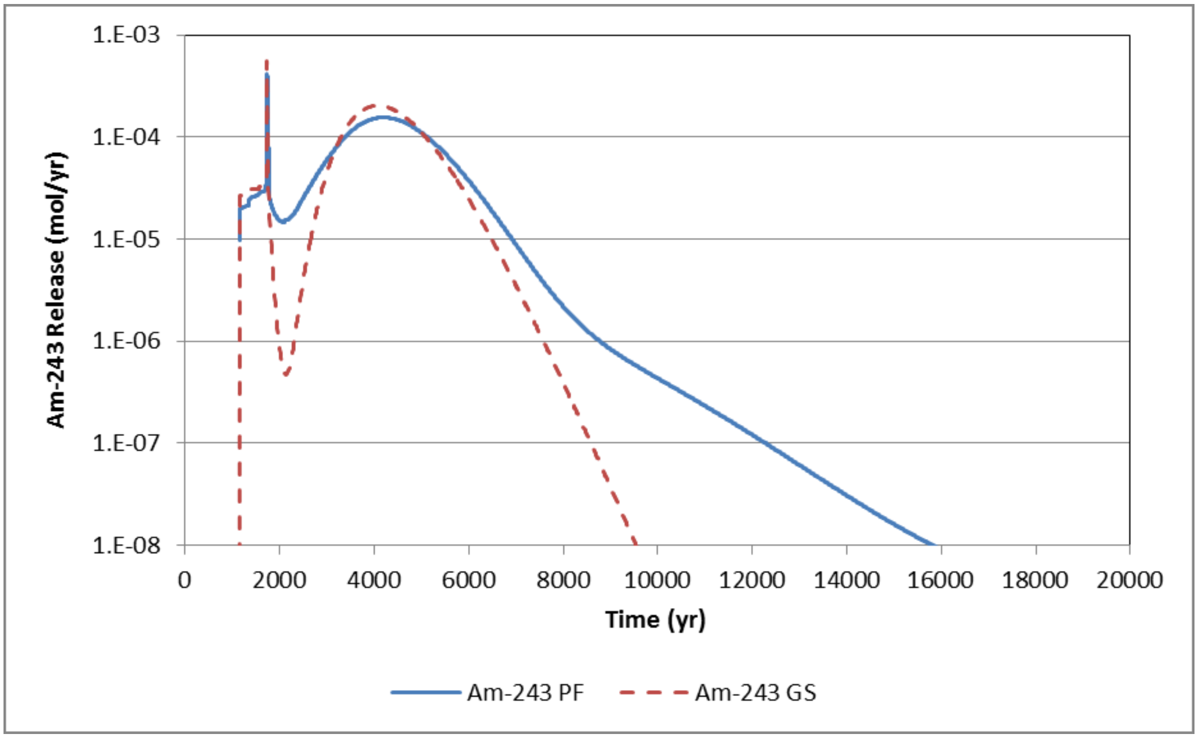

Figure A.3-4: Tank 9 Pu-239 Release to the Saturated Zone for Case D

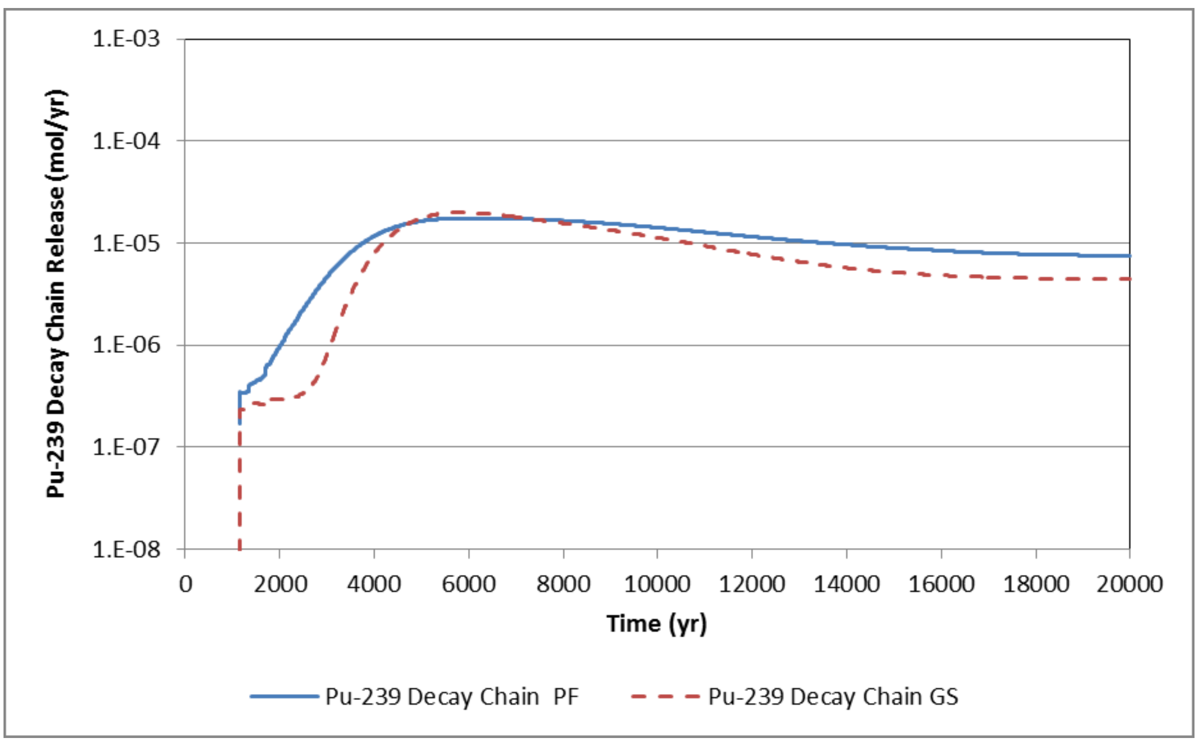

Figure A.3-5: Tank 9 U-234 Release to the Saturated Zone for Case D

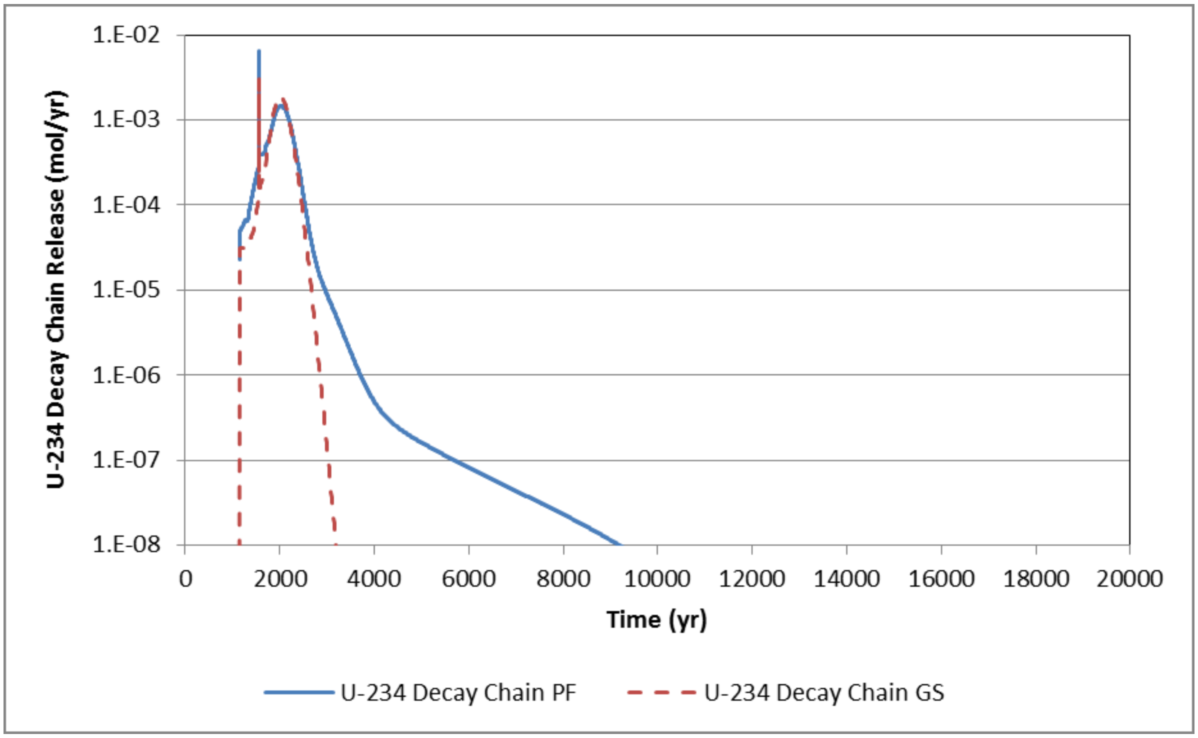

Figure A.3-6: Tank 9 Ra-226 Release to the Saturated Zone for Case D

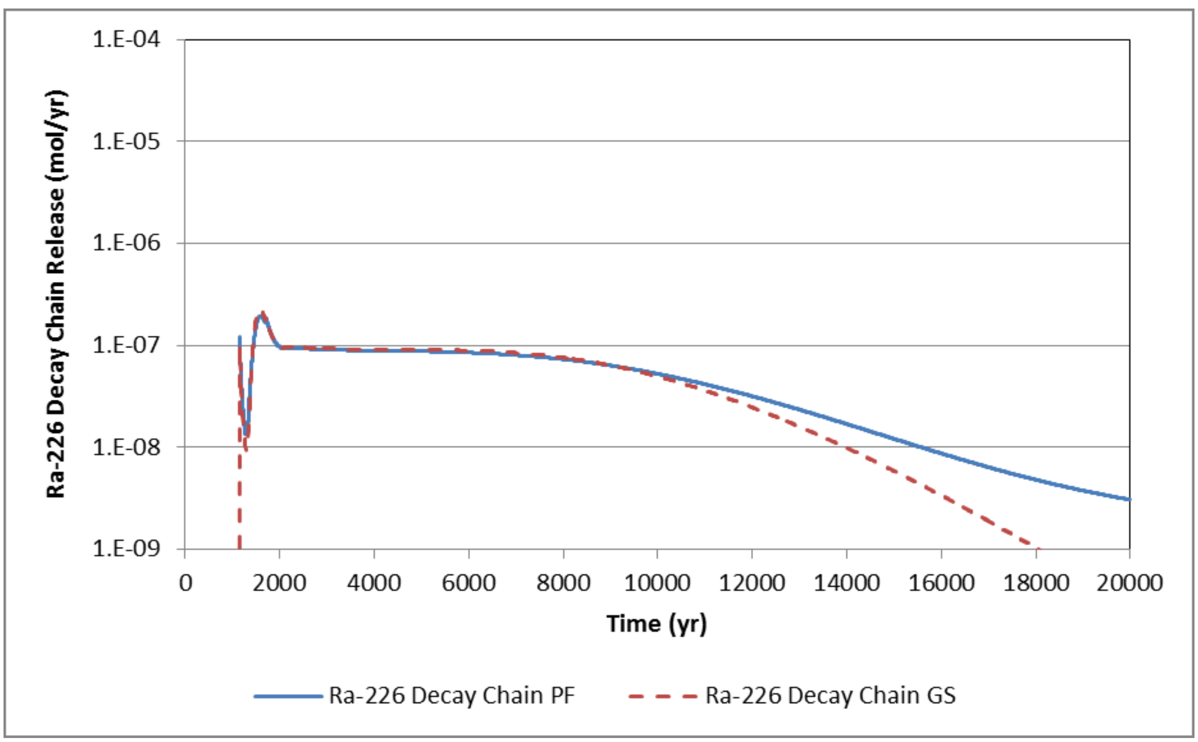

Figure A.3-7: Tank 9 Am-241 Release to the Saturated Zone for Case D

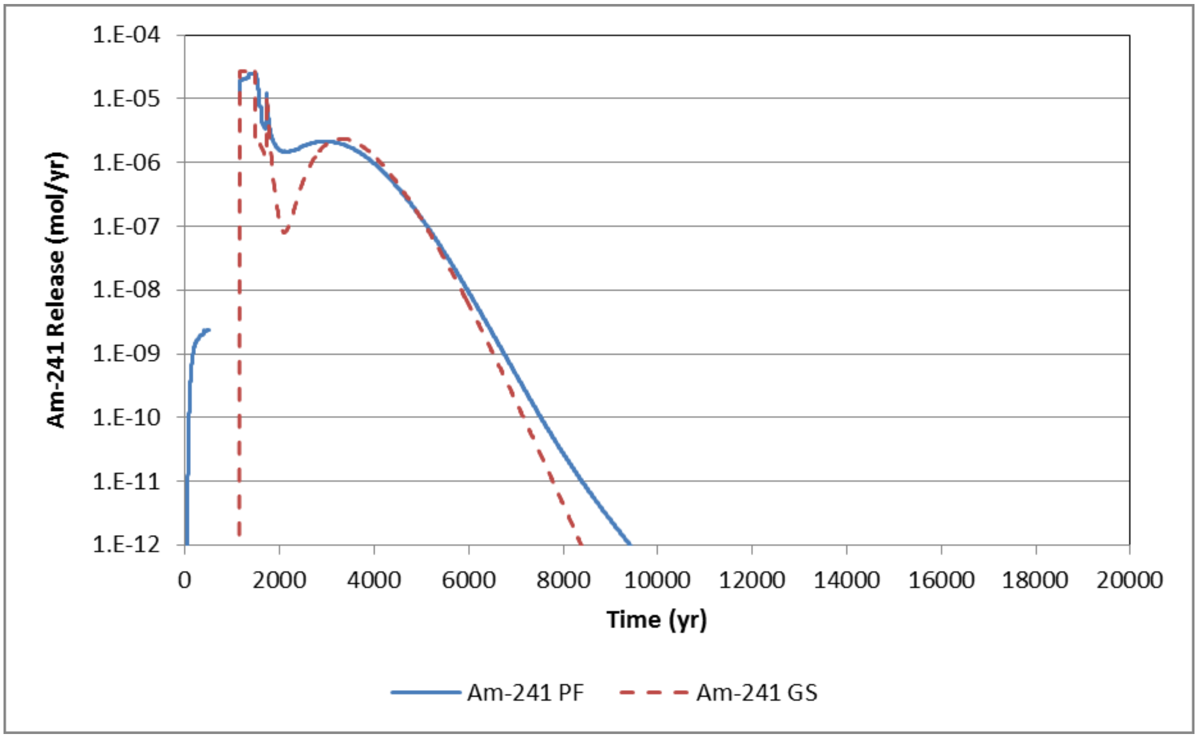

Figure A.3-8: Tank 9 Np-237 Release to the Saturated Zone for Case D

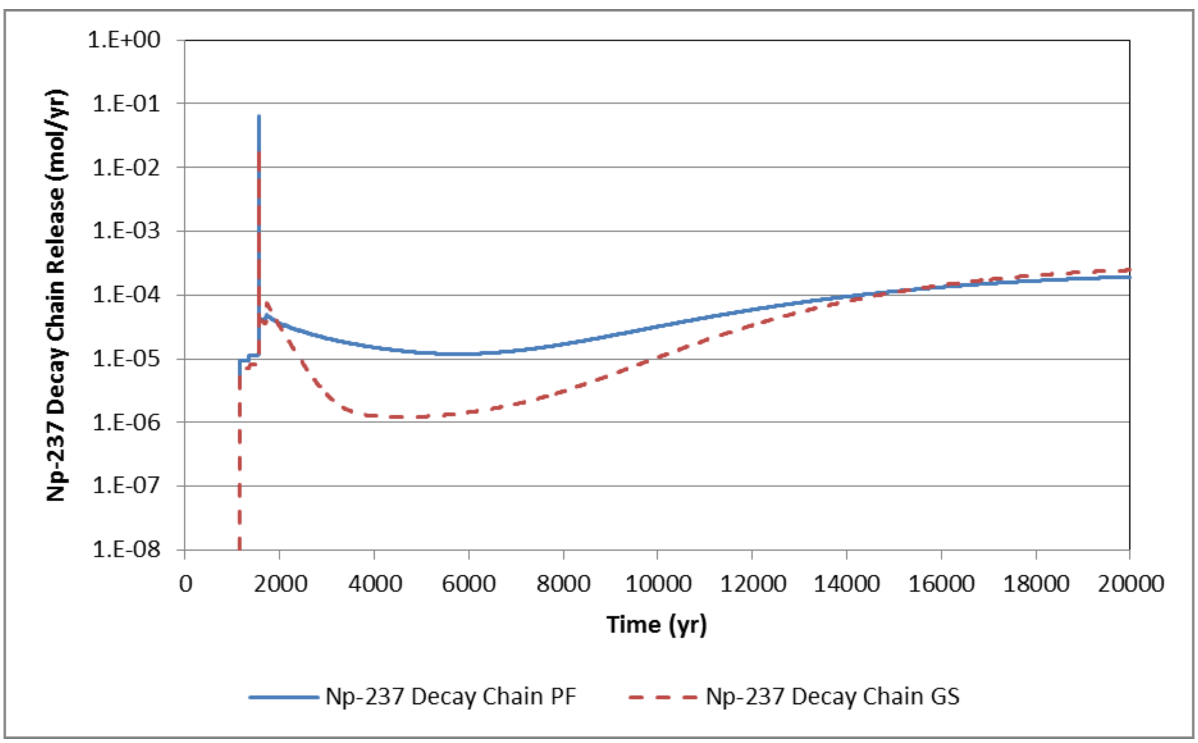

A.3.2 Type I Tank with Failed Liner (Tank 12) for Case D

For the Case D configuration, a comparison of the PORFLOW HTF Model and the GoldSim model mass releases of I-129, Tc-99, Am-243, Pu-239, U-234, Ra-226, Am-241, and Np-237, as presented in Figure A.3-9 through Figure A.3-16, indicate that the GoldSim model sucessfully captures the radionuclide release patterns seen in Tank 12 results generated by the PORFLOW model.

Table A.3-2 summarizes the peak values for these releases showing that when comparing the two models although not all of the percent differences are below 50% the values are reasonably close when considered in conjunction with the release patterns shown in Figure A.3-9 through Figure A.3-16.

Table A.3-2: Case D GoldSim and PORFLOW Model Peak Releases from the UZ to the SZ Comparisons for Tank 12 within 20,000 years

Radionuclide	PORFLOW Peak Release (mol/yr)	PORFLOW Time of Peak Release (yr)	GoldSim Peak Release (mol/yr)	GoldSim Time of Peak Release (yr)	Peak Release Percent Difference GoldSim vs PORFLOW
I-129	2.0E-02	601	2.0E-02	580	0%
Tc-99	1.4E-03	546	9.4E-04	550	-33%
Am-243	1.2E-06	1,092	1.8E-06	150	50%
Pu-239	4.7E-06	19,941	4.4E-06	19,990	-6%
U-234	1.6E-03	933	4.9E-04	1,480	-69%
Ra-226	1.2E-08	1,701	1.2E-08	1,710	0%
Am-241	3.3E-05	403	3.5E-05	420	6%
Np-237	1.6E-02	933	4.7E-03	930	-71%

Figure A.3-9: Tank 12 I-129 Release to the Saturated Zone for Case D

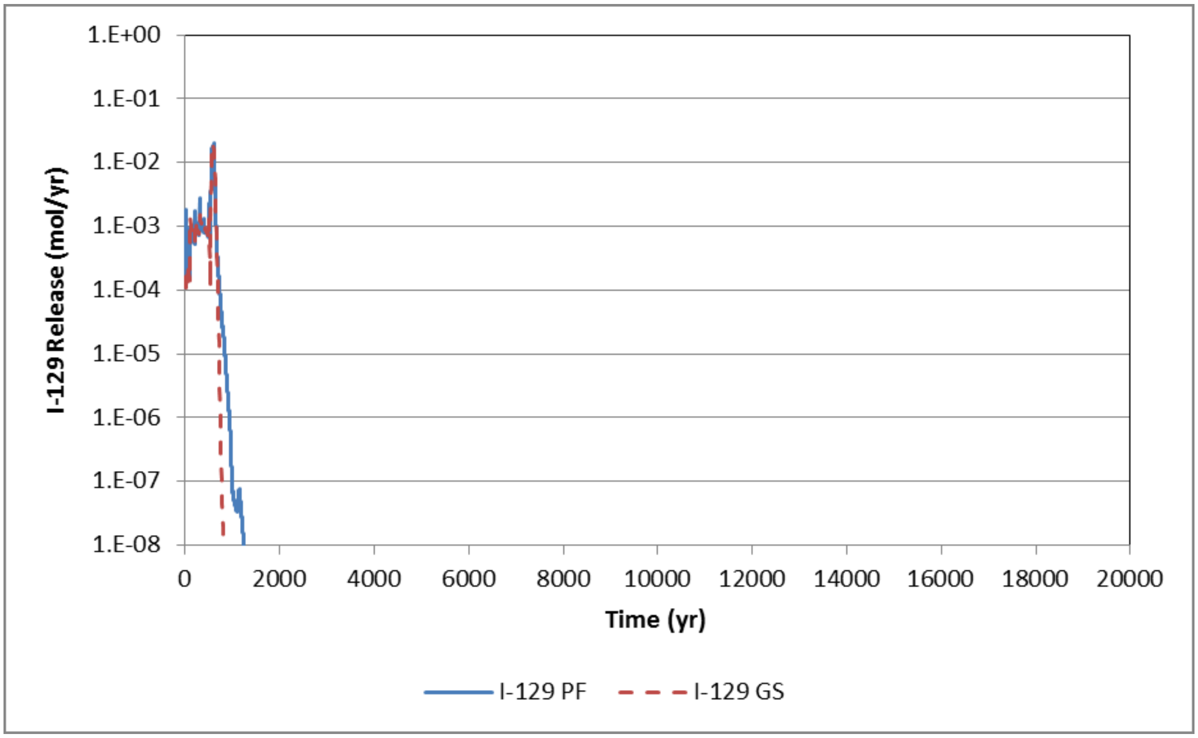

Figure A.3-10: Tank 12 Tc-99 Release to the Saturated Zone for Case D

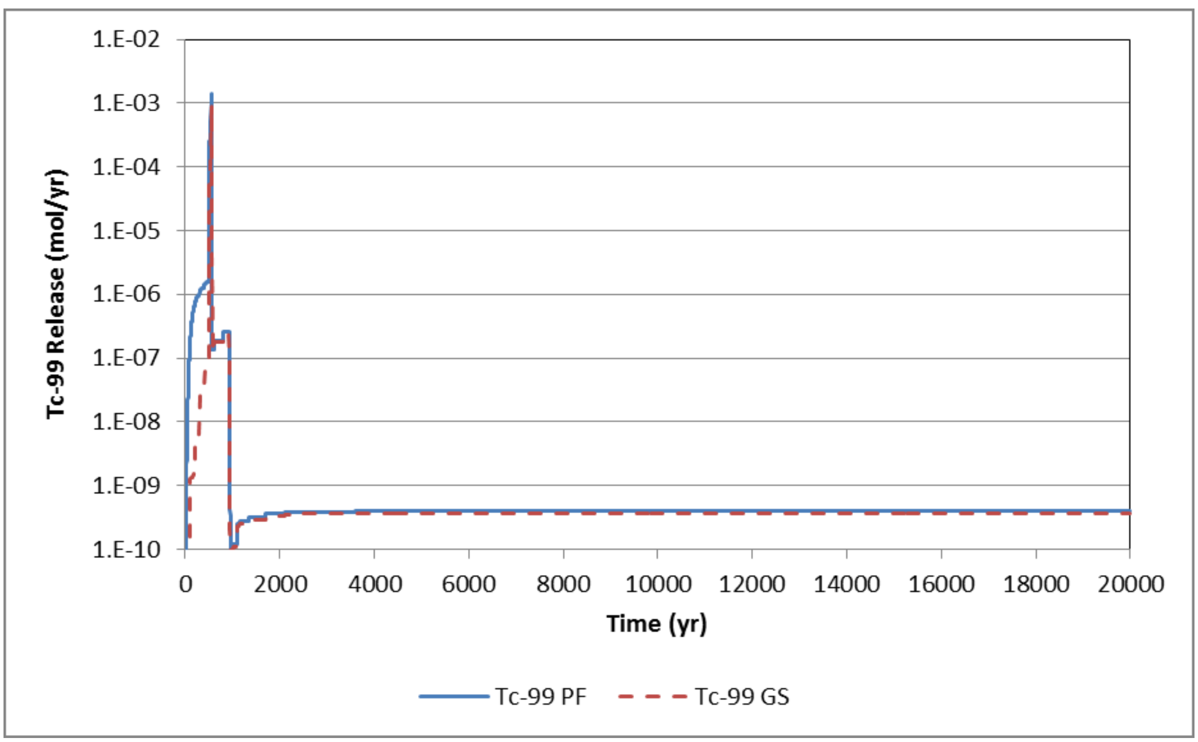

Figure A.3-11: Tank 12 Am-243 Release to the Saturated Zone for Case D

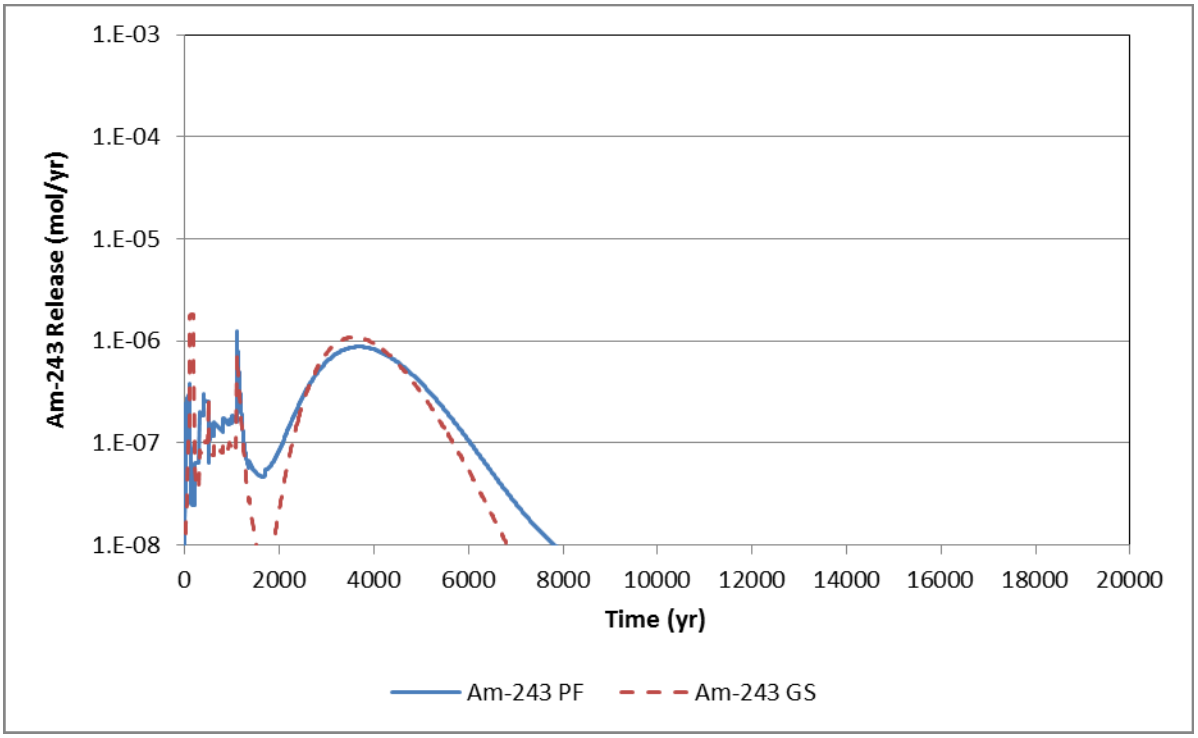

Figure A.3-12: Tank 12 Pu-239 Release to the Saturated Zone for Case D

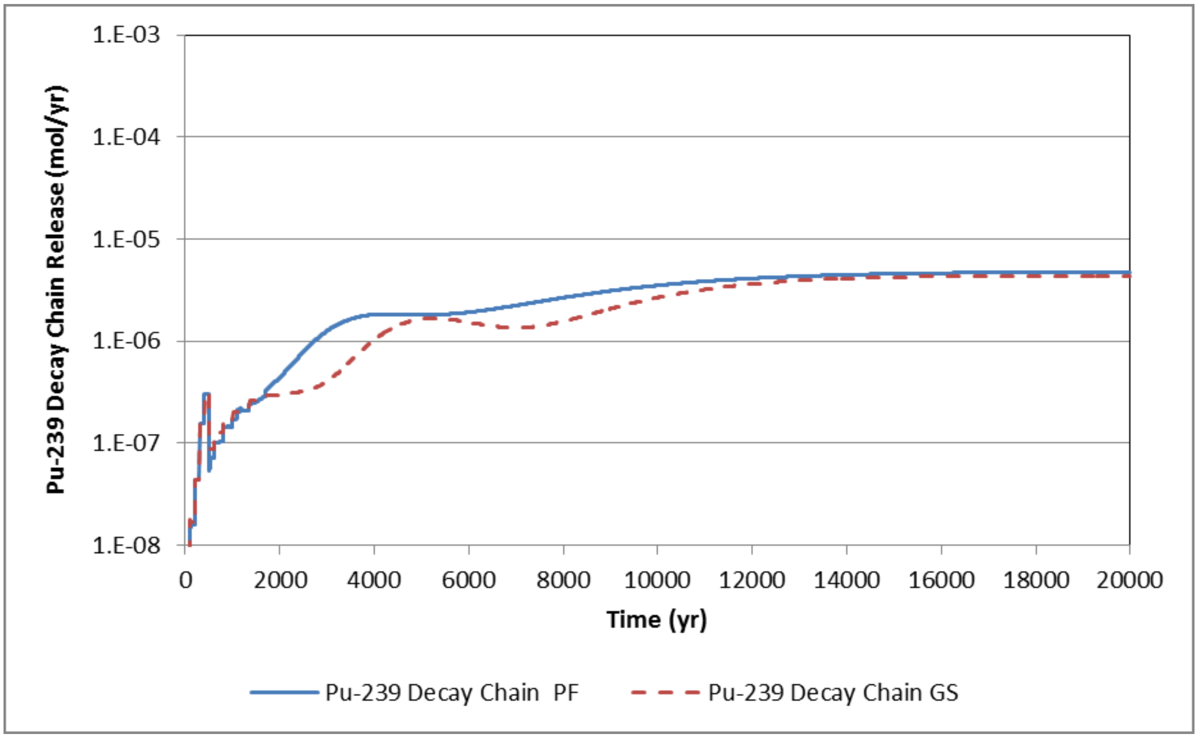

Figure A.3-13: Tank 12 U-234 Release to the Saturated Zone for Case D

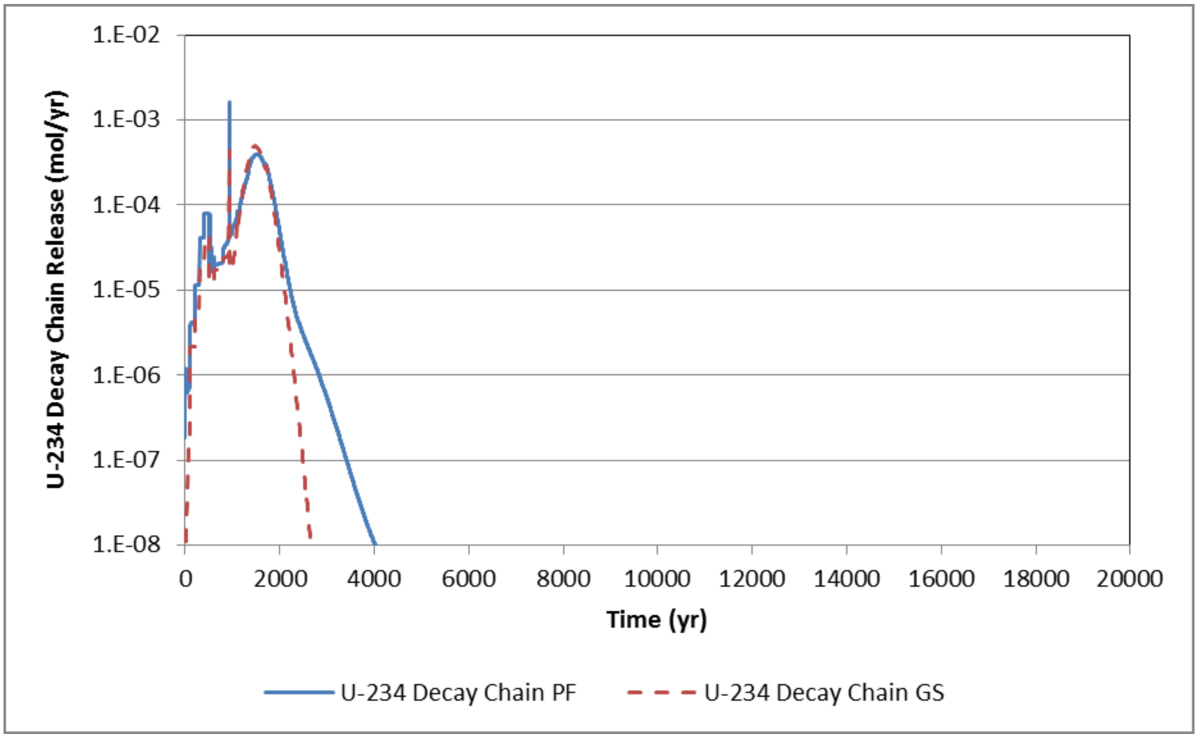

Figure A.3-14: Tank 12 Ra-226 Release to the Saturated Zone for Case D

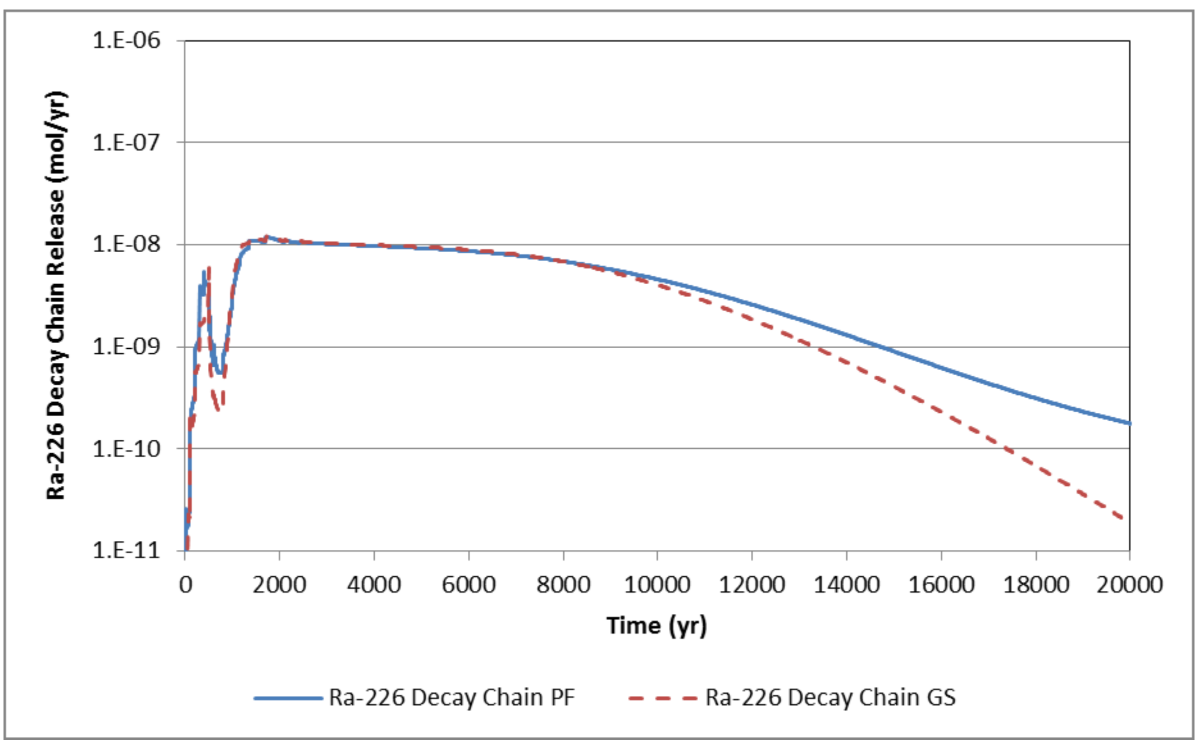

Figure A.3-15: Tank 12 Am-241 Release to the Saturated Zone for Case D

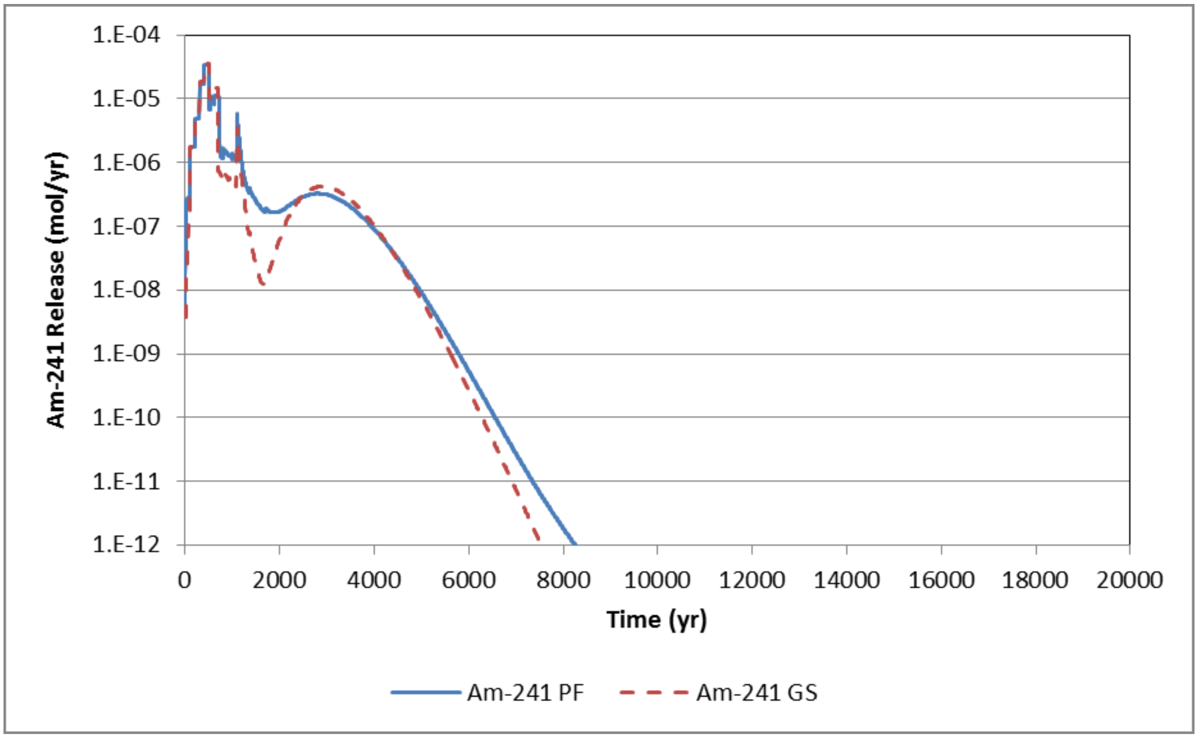

Figure A.3-16: Tank 12 Np-237 Release to the Saturated Zone for Case D

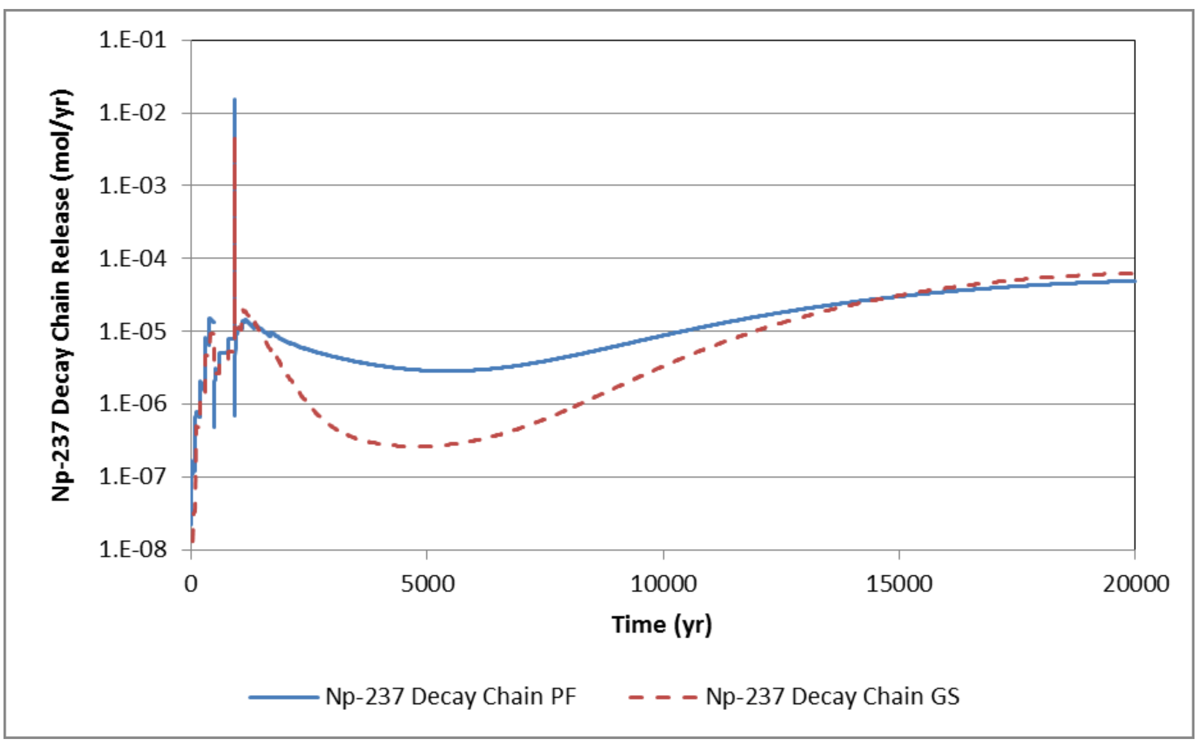

A.3.3 Type II Tank with Intact Liner (Tank 13) for Case D

For the Case D configuration, a comparison of the PORFLOW HTF Model and the GoldSim model mass releases of I-129, Tc-99, Am-243, Pu-239, U-234, Ra-226, Am-241, and Np-237, as presented in Figure A.3-17 through Figure A.3-24, indicate that the GoldSim model successfully captures the radionuclide release patterns seen in Tank 13 results generated by the PORFLOW model.

Table A.3-3 summarizes the peak values for these releases showing that when comparing the two models except for Am-241, the percent differences are at or below 50%. For Am-241, as seen in Figure A.3-23, the release trend is captured, but the magnitude of the peak will be conservatively overestimated.

Table A.3-3: Case D GoldSim and PORFLOW Model Peak Releases from the UZ to the SZ Comparisons for Tank 13 within 20,000 years

Radionuclide	PORFLOW Peak Release (mol/yr)	PORFLOW Time of Peak Release (yr)	GoldSim Peak Release (mol/yr)	GoldSim Time of Peak Release (yr)	Peak Release Percent Difference GoldSim vs PORFLOW
I-129	3.3E-02	2,545	3.5E-02	2,550	6%
Tc-99	3.4E-03	2,511	2.6E-03	2510	-24%
Am-243	5.8E-05	7,581	8.7E-05	7,390	50%
Pu-239	1.4E-05	15,265	1.3E-05	13,780	-7%
U-234	5.8E-04	3,748	6.6E-04	4,010	14%
Ra-226	3.0E-07	3,102	3.2E-07	3,090	7%
Am-241	5.9E-07	2,790	6.6E-06	2,590	1019%
Np-237	4.4E-02	5,319	3.5E-02	5,320	-20%

Figure A.3-17: Tank 13 I-129 Release to the Saturated Zone for Case D

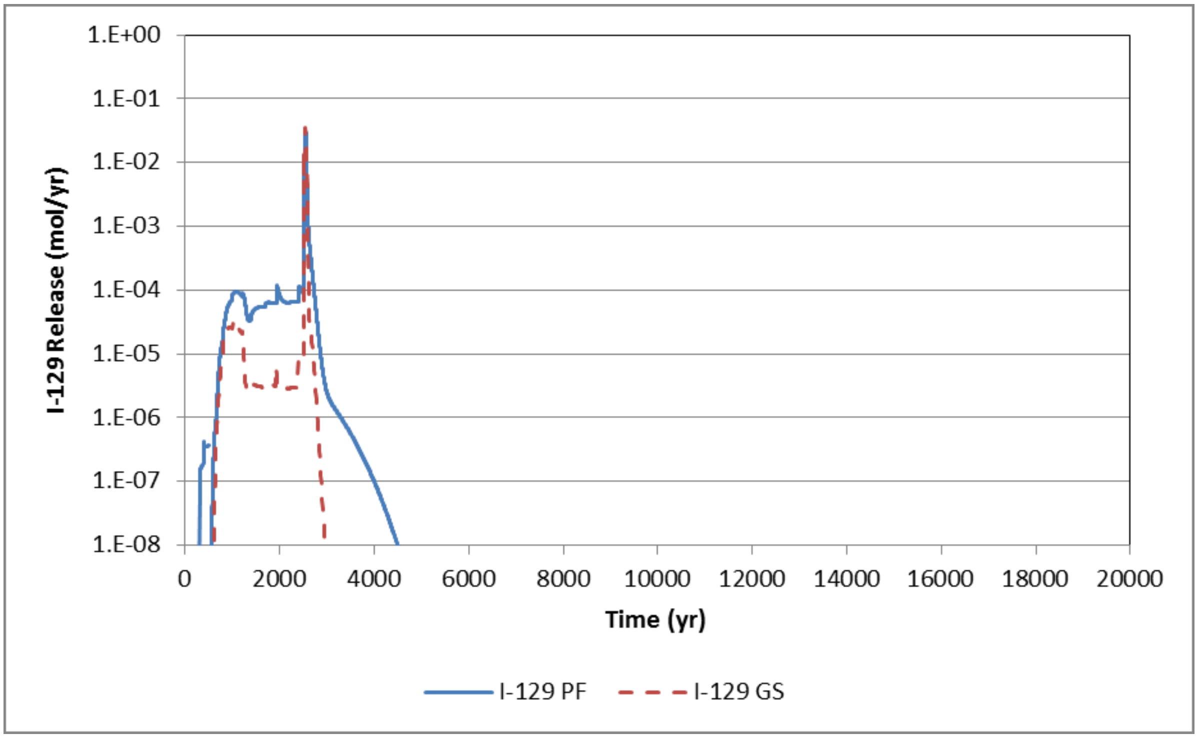

Figure A.3-18: Tank 13 Tc-99 Release to the Saturated Zone for Case D

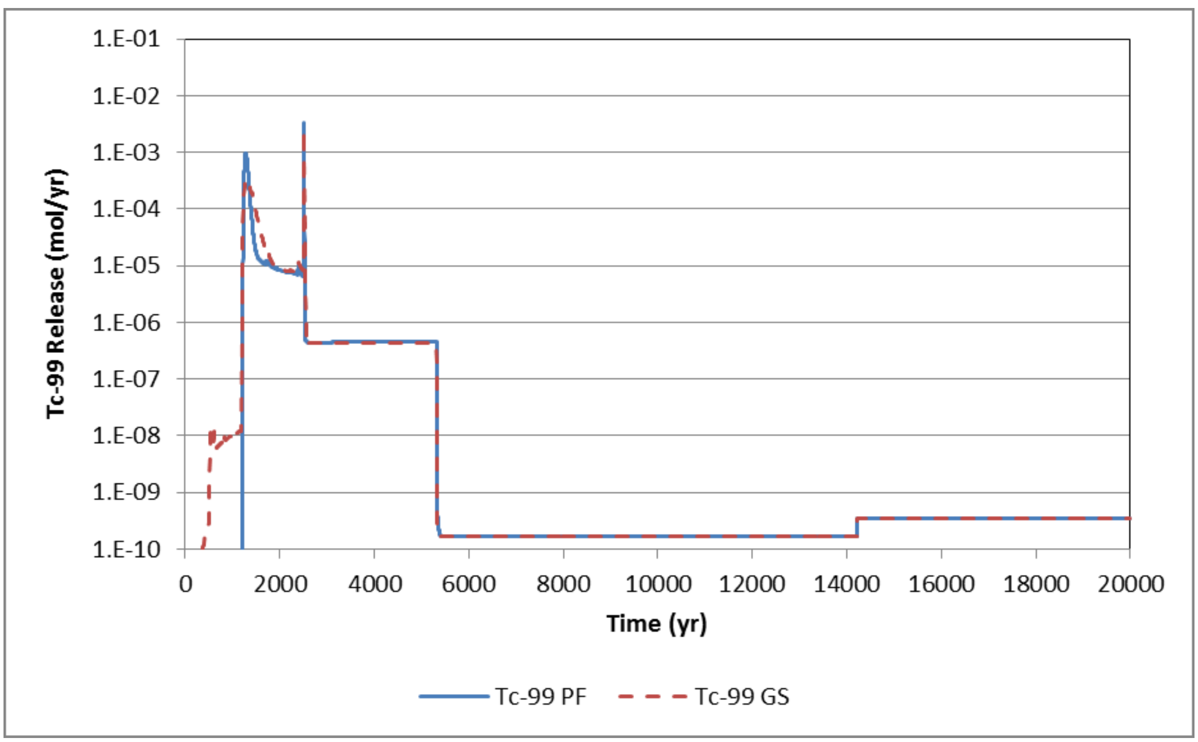

Figure A.3-19: Tank 13 Am-243 Release to the Saturated Zone for Case D

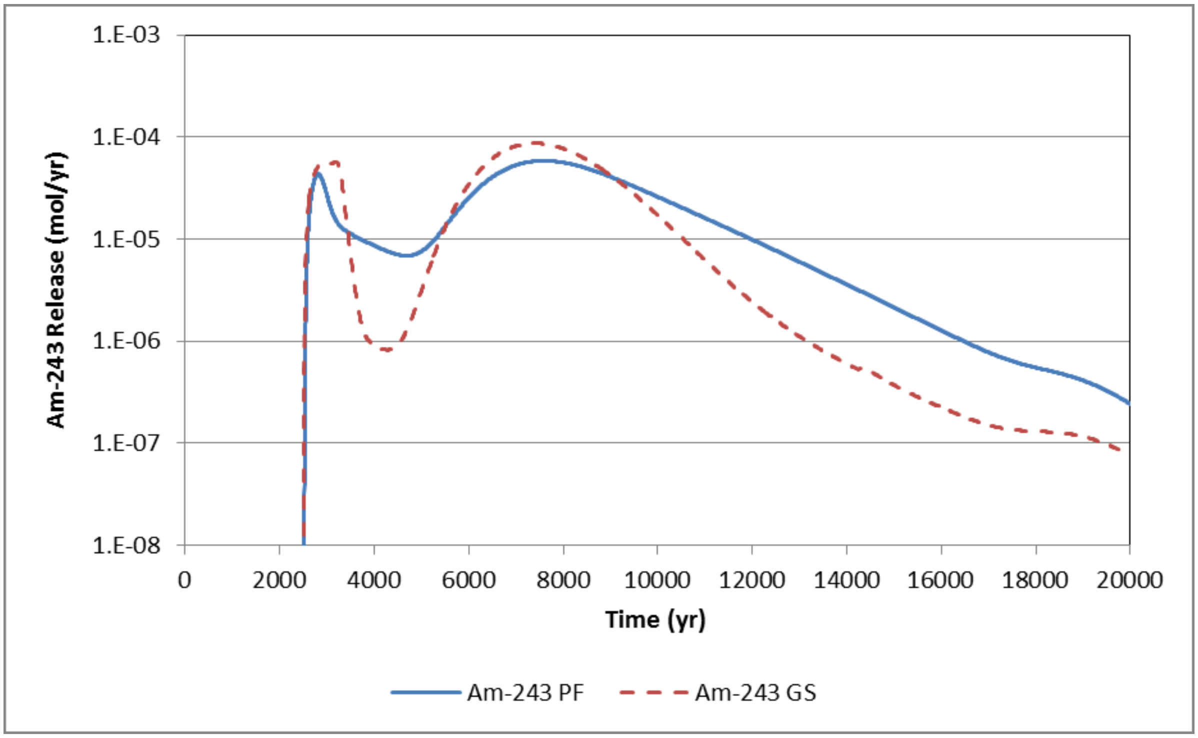

Figure A.3-20: Tank 13 Pu-239 Release to the Saturated Zone for Case D

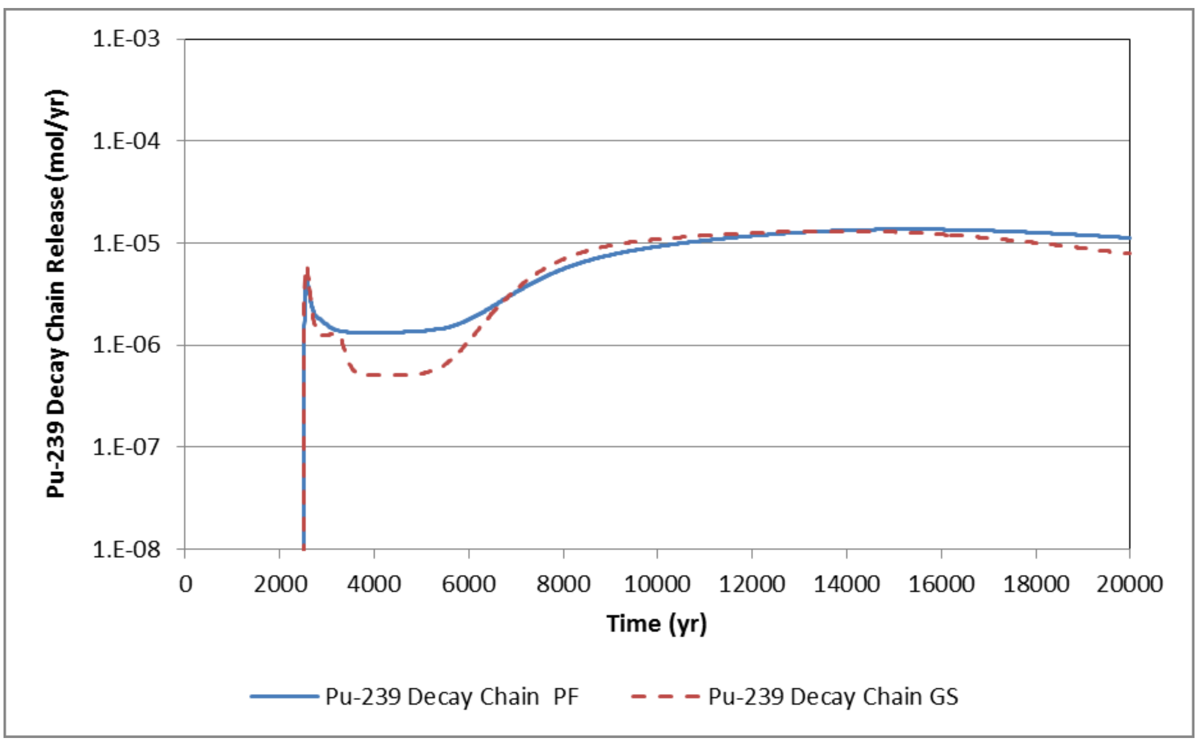

Figure A.3-21: Tank 13 U-234 Release to the Saturated Zone for Case D

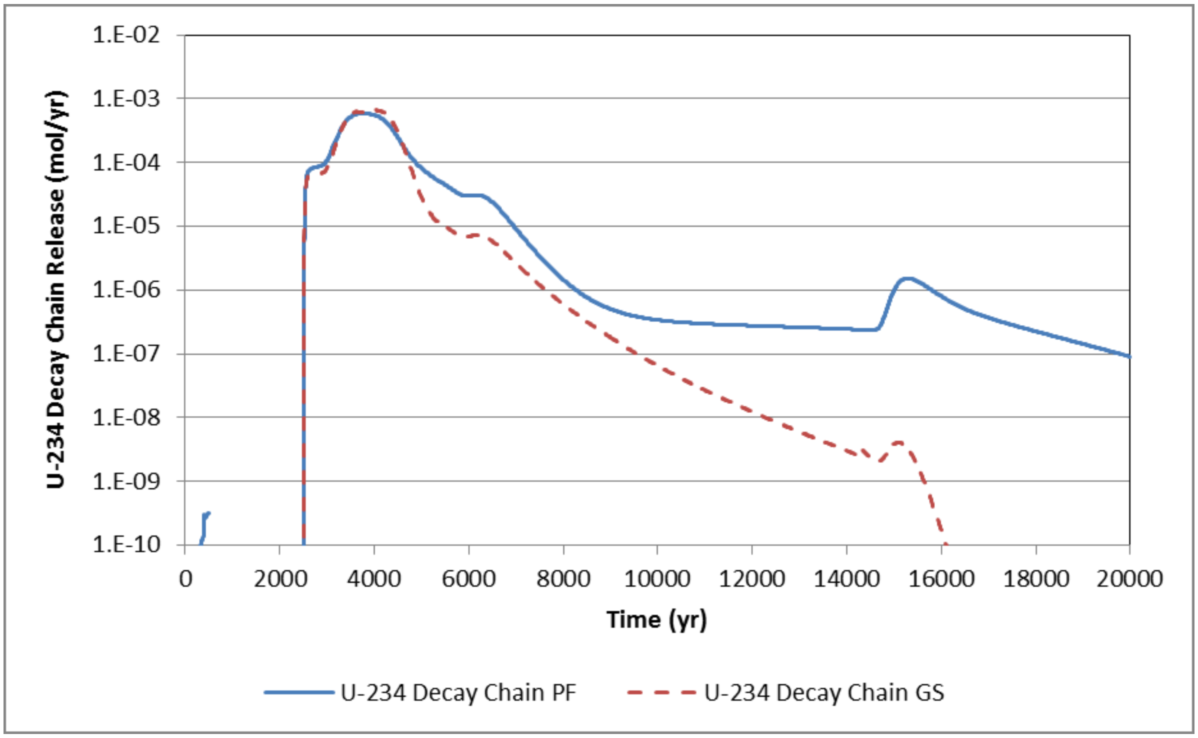

Figure A.3-22: Tank 13 Ra-226 Release to the Saturated Zone for Case D

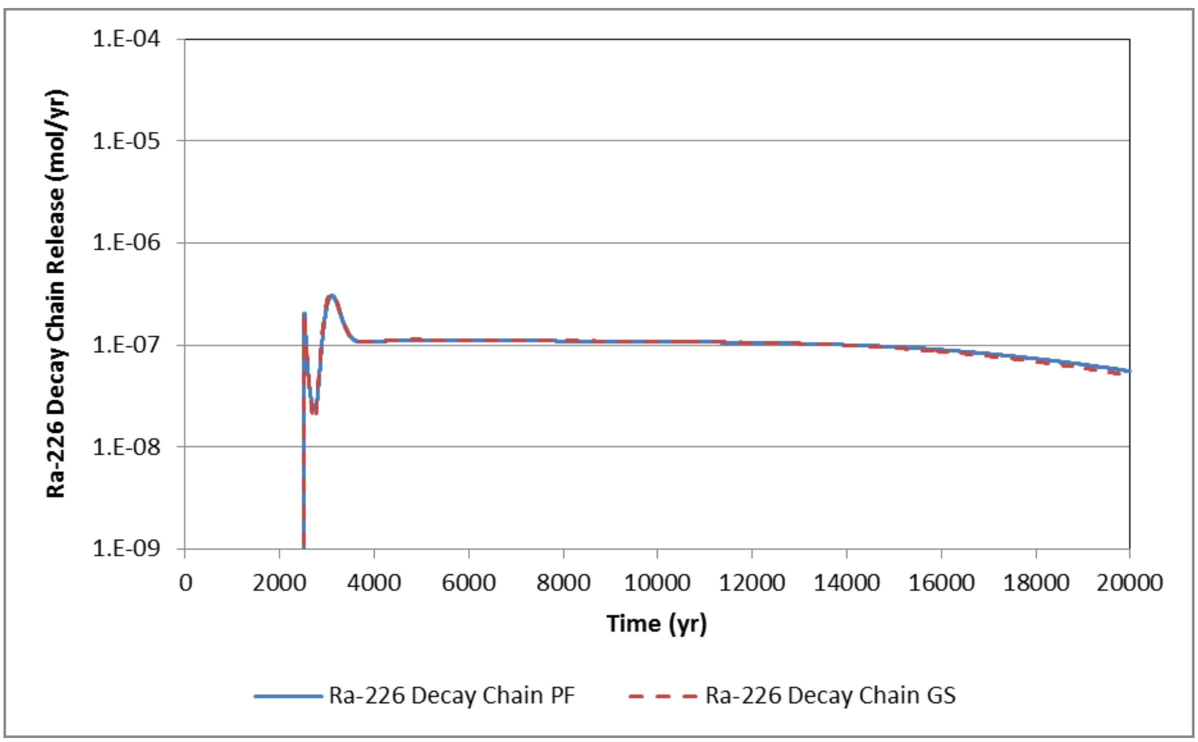

Figure A.3-23: Tank 13 Am-241 Release to the Saturated Zone for Case D

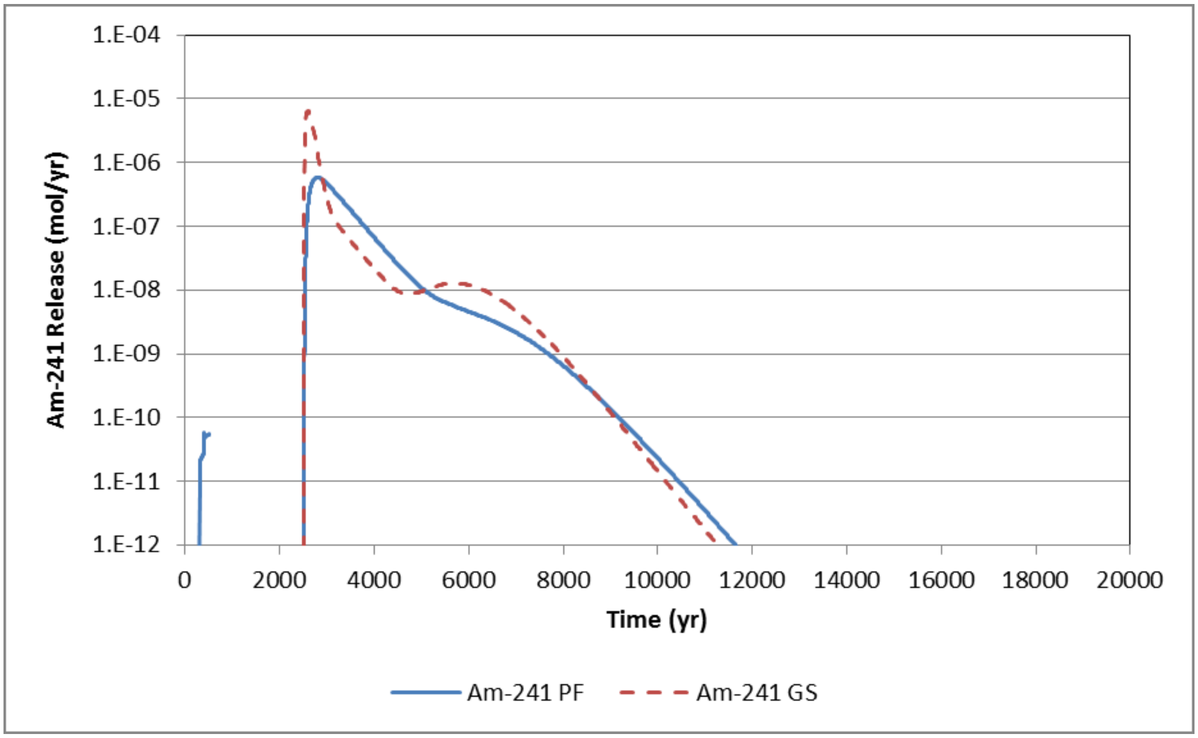

Figure A.3-24: Tank 13 Np-237 Release to the Saturated Zone for Case D

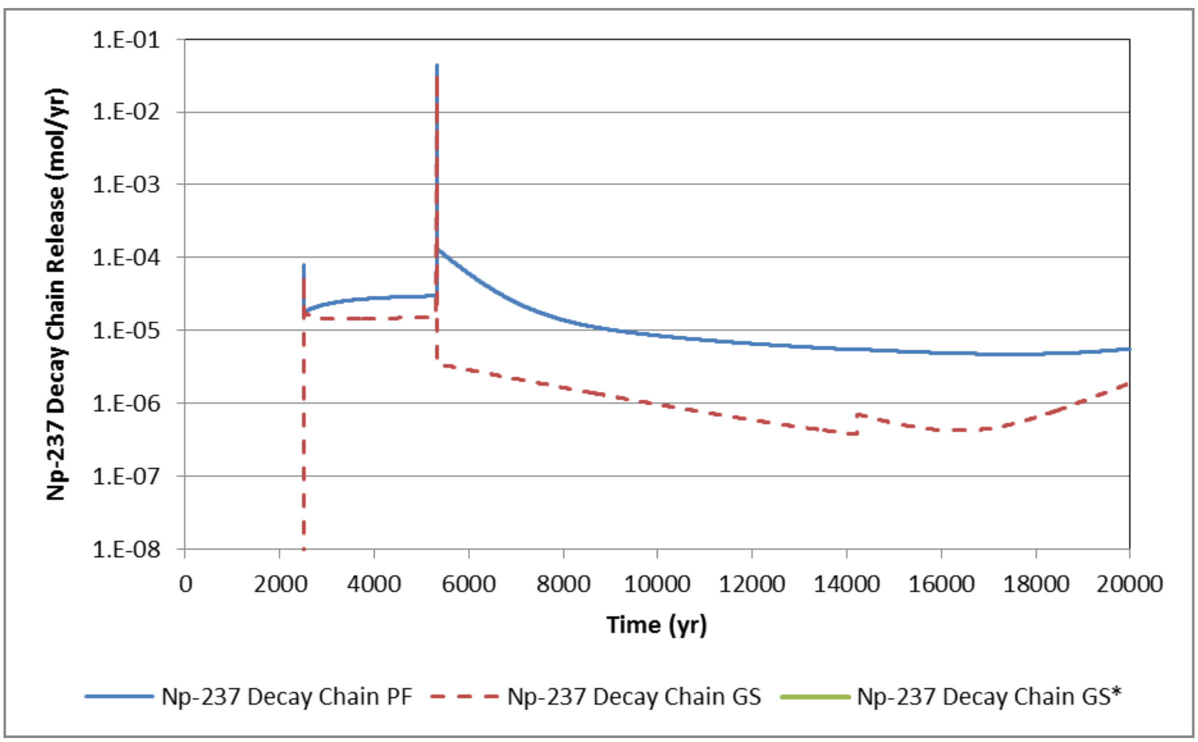

A.3.4 Type II Tank with Failed Liner (Tank 15) for Case D

For the Case D configuration, a comparison of the PORFLOW HTF Model and the GoldSim model mass releases of I-129, Tc-99, Am-243, Pu-239, U-234, Ra-226, Am-241, and Np-237, as presented in Figure A.3-25 through Figure A.3-32, indicate that the GoldSim model successfully captures the radionuclide release patterns seen in Tank 15 results generated by the PORFLOW model.

Table A.3-4 summarizes the peak values for these releases showing that when comparing the two models although not all of the percent differences are below 50%, the values are reasonably close when considered in conjunction with the release patterns shown in Figure A.3-25 through Figure A.3-32.

Table A.3-4: Case D GoldSim and PORFLOW Model Peak Releases from the UZ to the SZ Comparisons for Tank 15 within 20,000 years

Radionuclide	PORFLOW Peak Release (mol/yr)	PORFLOW Time of Peak Release (yr)	GoldSim Peak Release (mol/yr)	GoldSim Time of Peak Release (yr)	Peak Release Percent Difference GoldSim vs PORFLOW
I-129	1.3E-02	640	1.4E-02	640	8%
Tc-99	7.0E-04	512	2.1E-04	510	-70%
Am-243	9.1E-05	6132	9.8E-05	5,950	8%
Pu-239	1.5E-05	13,114	1.5E-05	12,610	0%
U-234	5.5E-04	2,201	6.5E-04	2,560	18%
Ra-226	8.5E-08	1,701	9.8E-08	310	15%
Am-241	8.2E-05	500	8.2E-05	500	0%
Np-237	4.1E-02	3,971	3.2E-02	3,960	-22%

Figure A.3-25: Tank 15 I-129 Release to the Saturated Zone for Case D

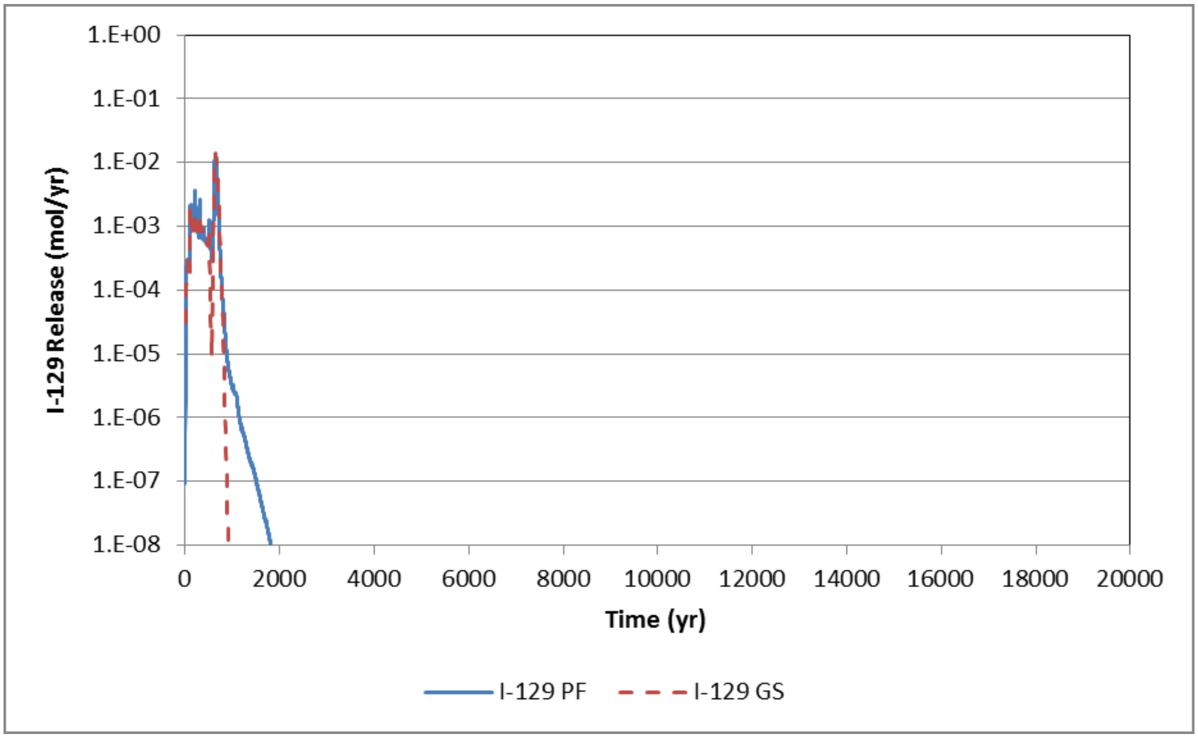

Figure A.3-26: Tank 15 Tc-99 Release to the Saturated Zone for Case D

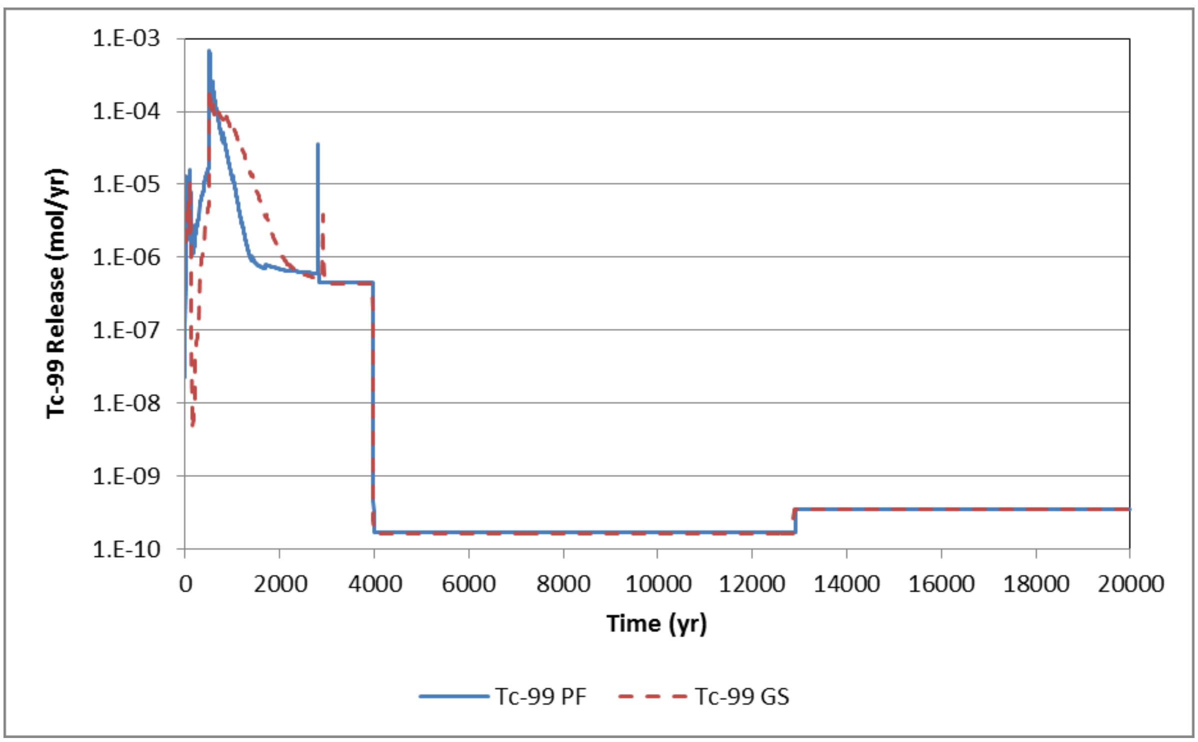

Figure A.3-27: Tank 15 Am-243 Release to the Saturated Zone for Case D

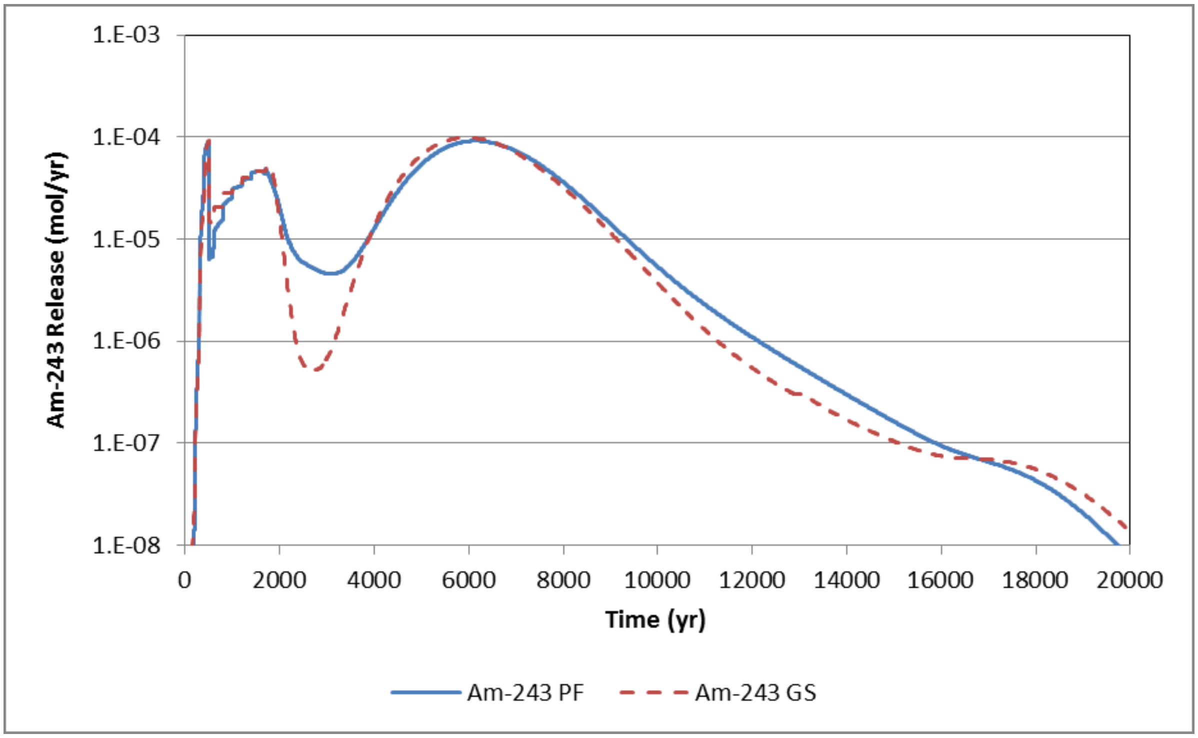

Figure A.3-28: Tank 15 Pu-239 Release to the Saturated Zone for Case D

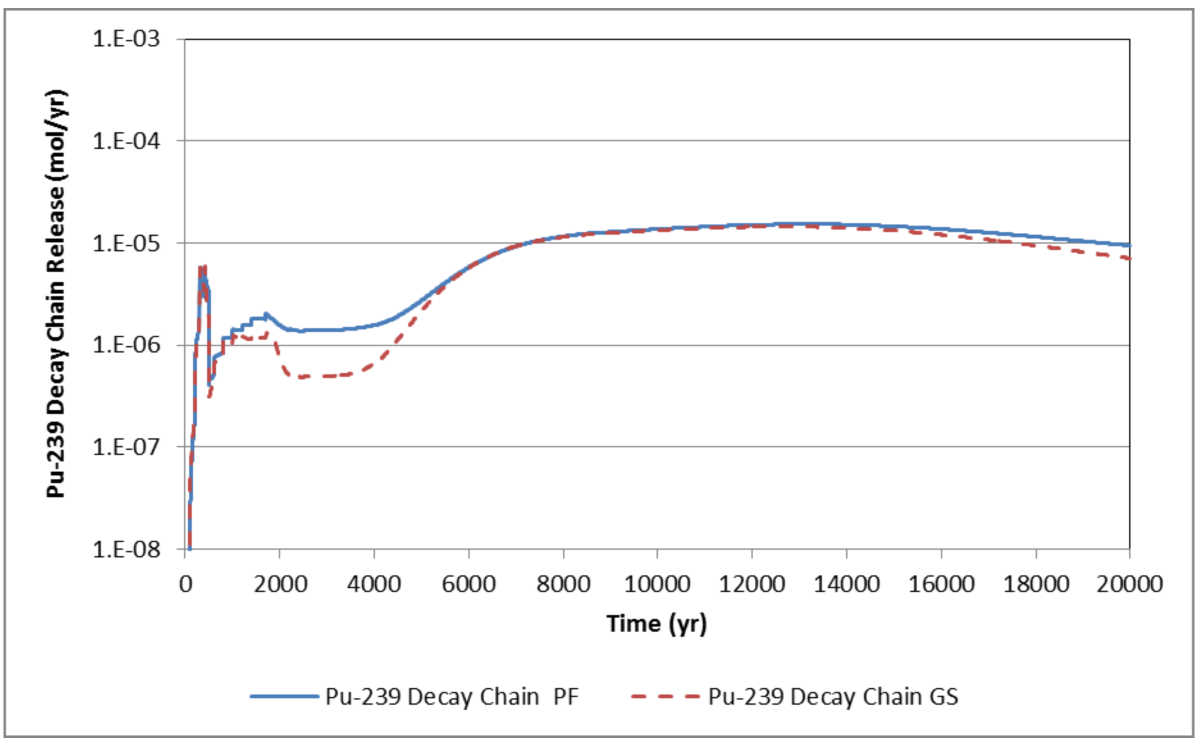

Figure A.3-29: Tank 15 U-234 Release to the Saturated Zone for Case D

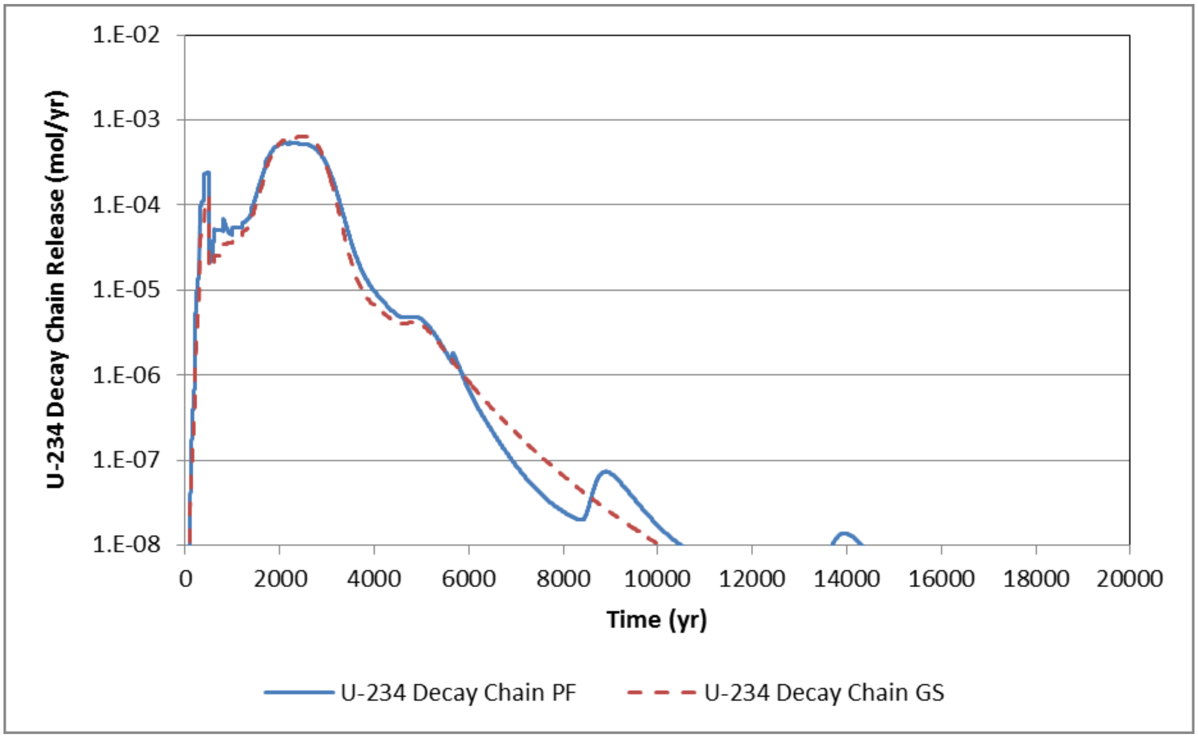

Figure A.3-30: Tank 15 Ra-226 Release to the Saturated Zone for Case D

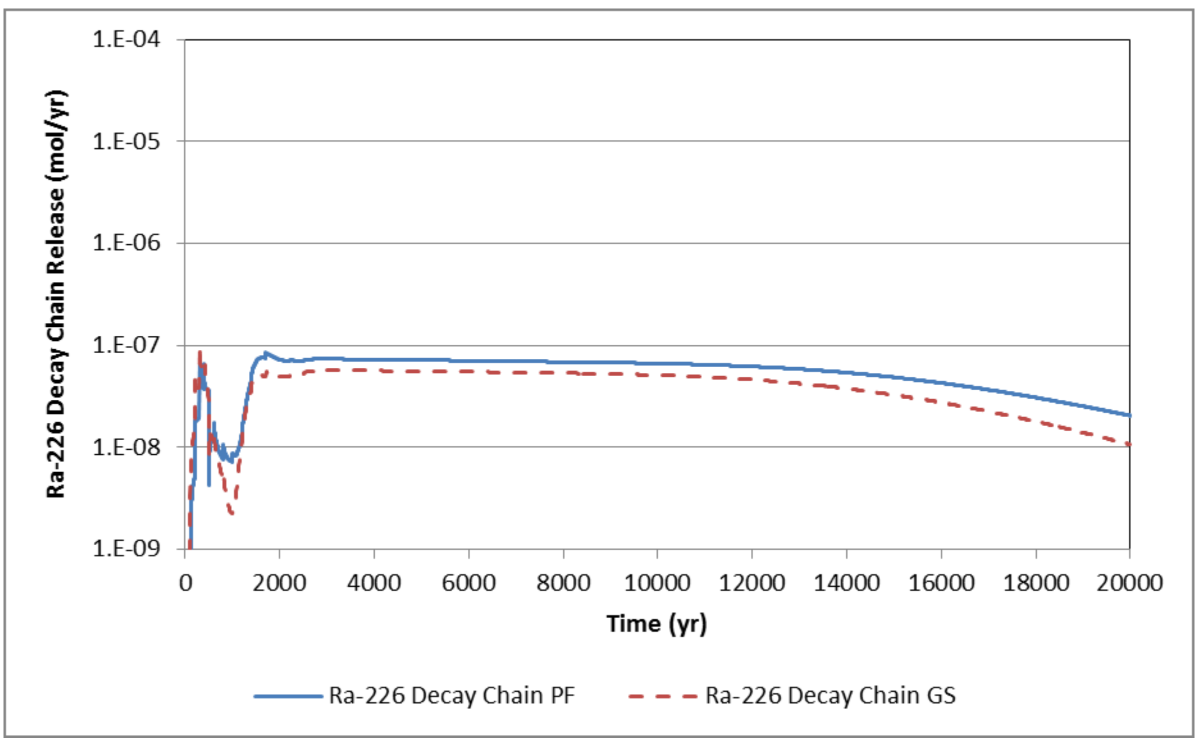

Figure A.3-31: Tank 15 Am-241 Release to the Saturated Zone for Case D

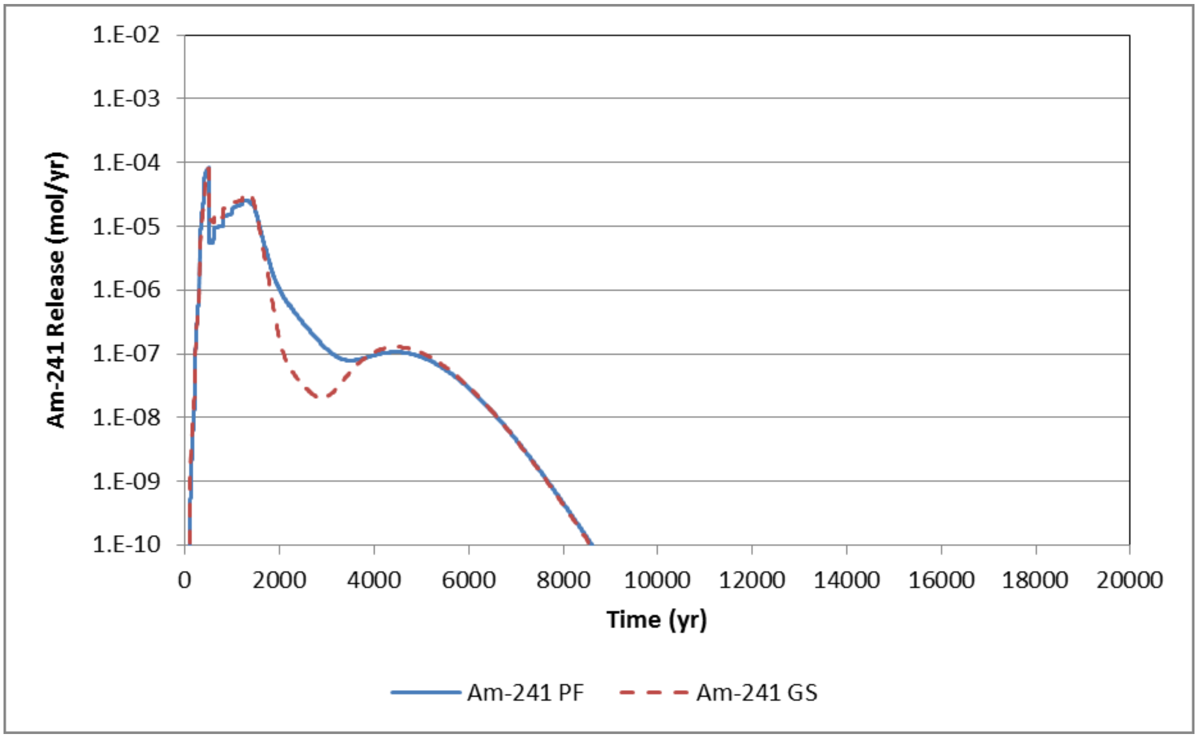

Figure A.3-32: Tank 15 Np-237 Release to the Saturated Zone for Case D

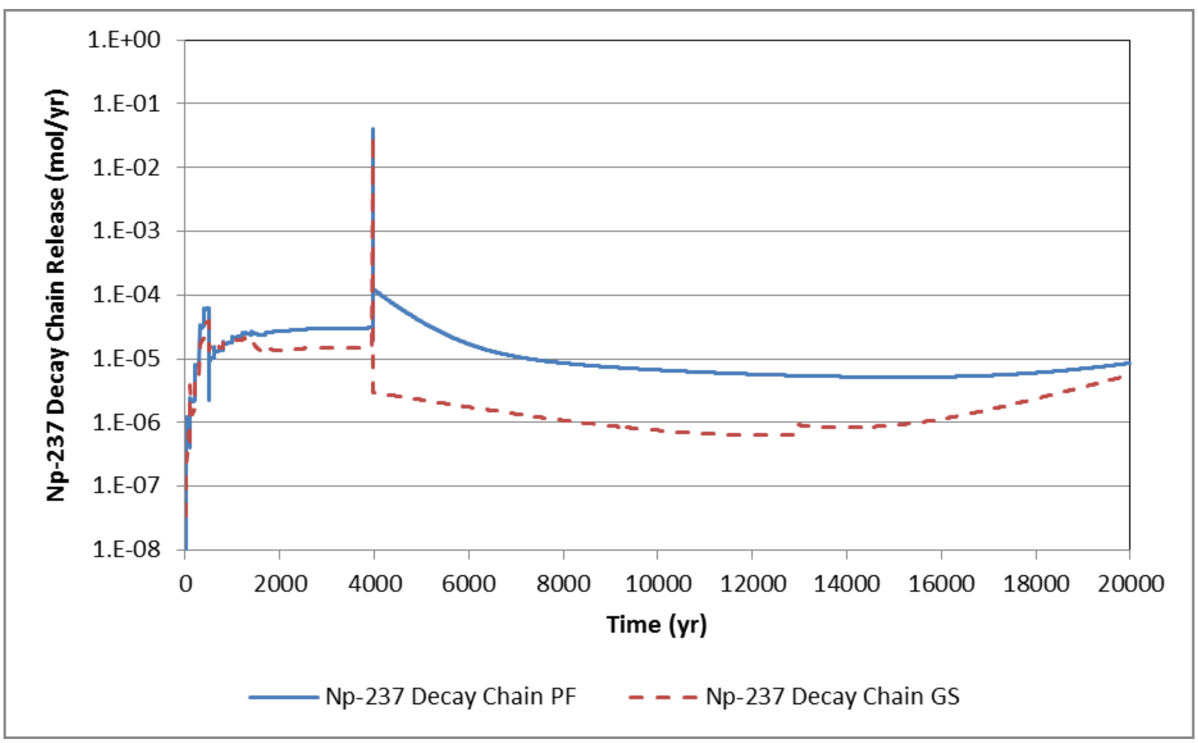

A.3.5 Type II Tank with Failed Liner (Tank 16) for Case D

For the Case D configuration, a comparison of the PORFLOW HTF Model and the GoldSim model mass releases of I-129, Tc-99, Am-243, Pu-239, U-234, Ra-226, Am-241, and Np-237, as presented in Figure A.3-33 through Figure A.3-40, indicate that the GoldSim model successfully captures the radionuclide release patterns seen in Tank 16 results generated by the PORFLOW model.

Table A.3-5 summarizes the peak values for these releases showing that when comparing the two models although not all of the percent differences are below 50% the values are reasonably close when considered in conjunction with the release patterns shown in Figure A.3-33 through Figure A.3-40. Note that for Am-243, U-234, and Np-237, two model comparisons are presented in Table A.3-5. These comparisons were made because the GoldSim and PORFLOW model maximum values occurred at different peaks (see Figure A.3-35, Figure A.3-37, and Figure A.3-40). The first comparison represents a comparison of the PORFLOW and GoldSim model peak values over 20,000 years. The second comparison is for the PORFLOW model peak value and the GoldSim model peak nearest the same simulation time. The number associated with the second comparison is the position of the GoldSim value in the sorted (from high to low) data.

Table A.3-5: Case D GoldSim and PORFLOW Model Peak Releases from the UZ to the SZ Comparisons for Tank 16 within 20,000 years

Radionuclide	PORFLOW Peak Release (mol/yr)	PORFLOW Time of Peak Release (yr)	GoldSim Peak Release (mol/yr)	GoldSim Time of Peak Release (yr)	Peak Release Percent Difference GoldSim vs PORFLOW
I-129	8.0E-03	633	8.9E-03	630	11%
Tc-99	1.2E-02	512	3.1E-03	520	-74%
Am-243	5.1E-08	4,913	5.6E-08	410	10%
Am-243 (#2)	5.1E-08	4,913	5.3E-08	5,360	4%
Pu-239	7.1E-05	303	7.2E-05	320	1%
U-234	4.3E-05	1,701	4.9E-05	330	14%
U-234 (#4)	4.3E-05	1,701	4.2E-05	1,780	-2%
Ra-226	3.3E-09	1,701	3.2E-09	1,710	-3%
Am-241	1.4E-06	401	2.1E-06	410	50%
Np-237	2.9E-05	401	3.7E-05	110	28%
Np-237 (#2)	2.9E-05	401	2.7E-05	410	-7%

Figure A.3-33: Tank 16 I-129 Release to the Saturated Zone for Case D

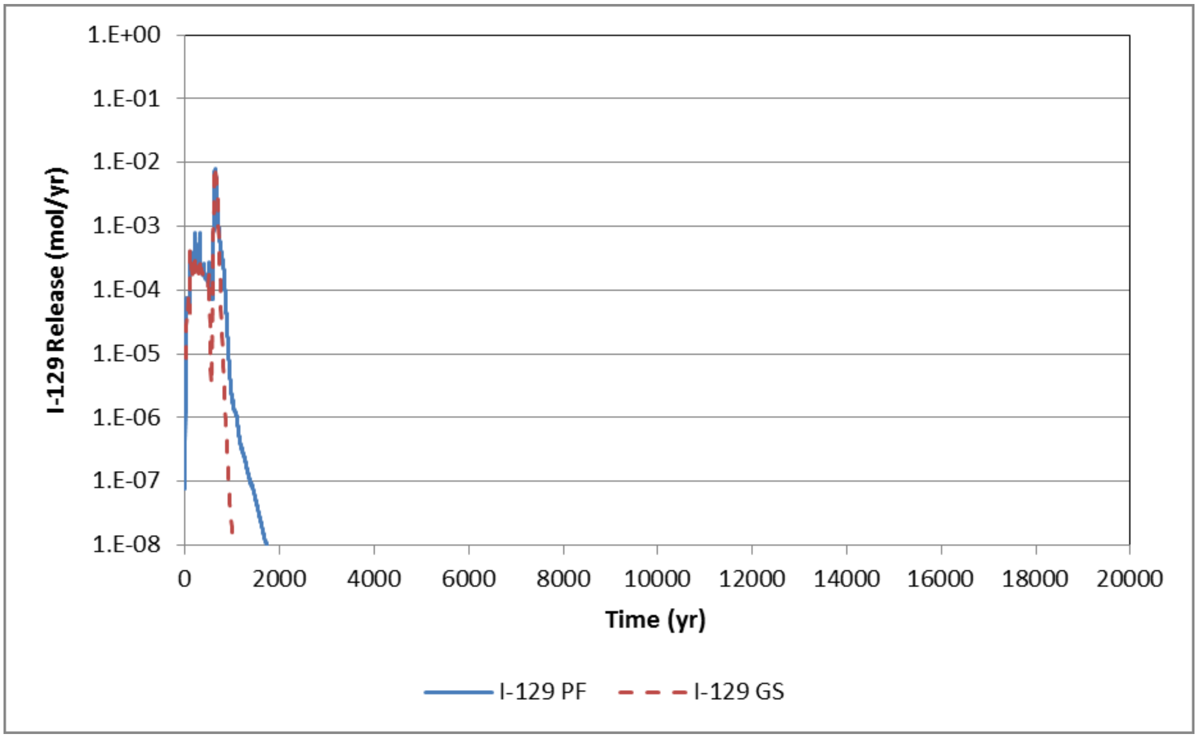

Figure A.3-34: Tank 16 Tc-99 Release to the Saturated Zone for Case D

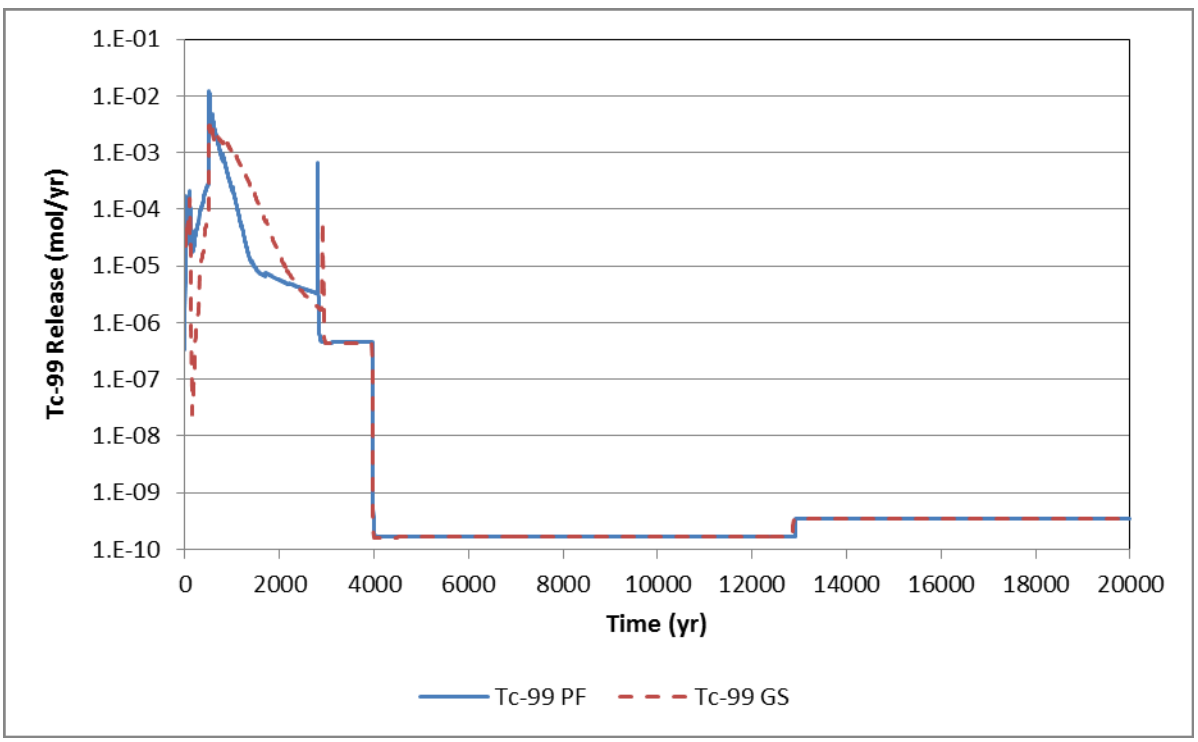

Figure A.3-35: Tank 16 Am-243 Release to the Saturated Zone for Case D

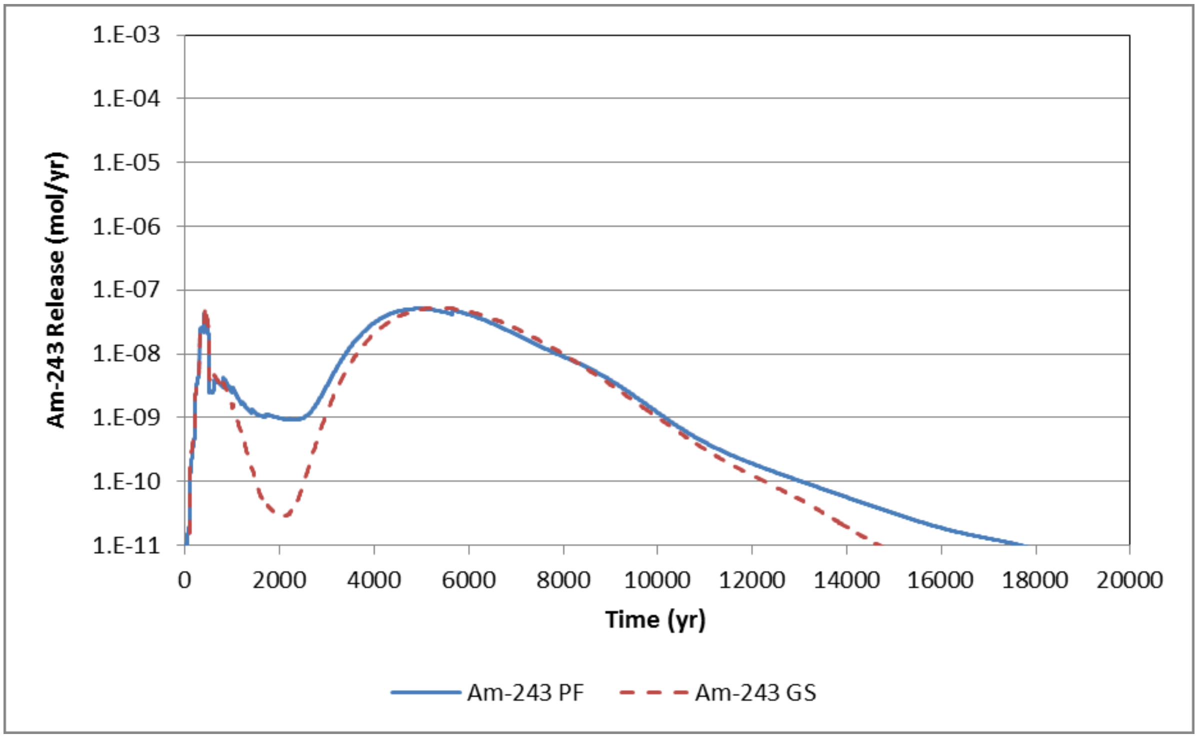

Figure A.3-36: Tank 16 Pu-239 Release to the Saturated Zone for Case D

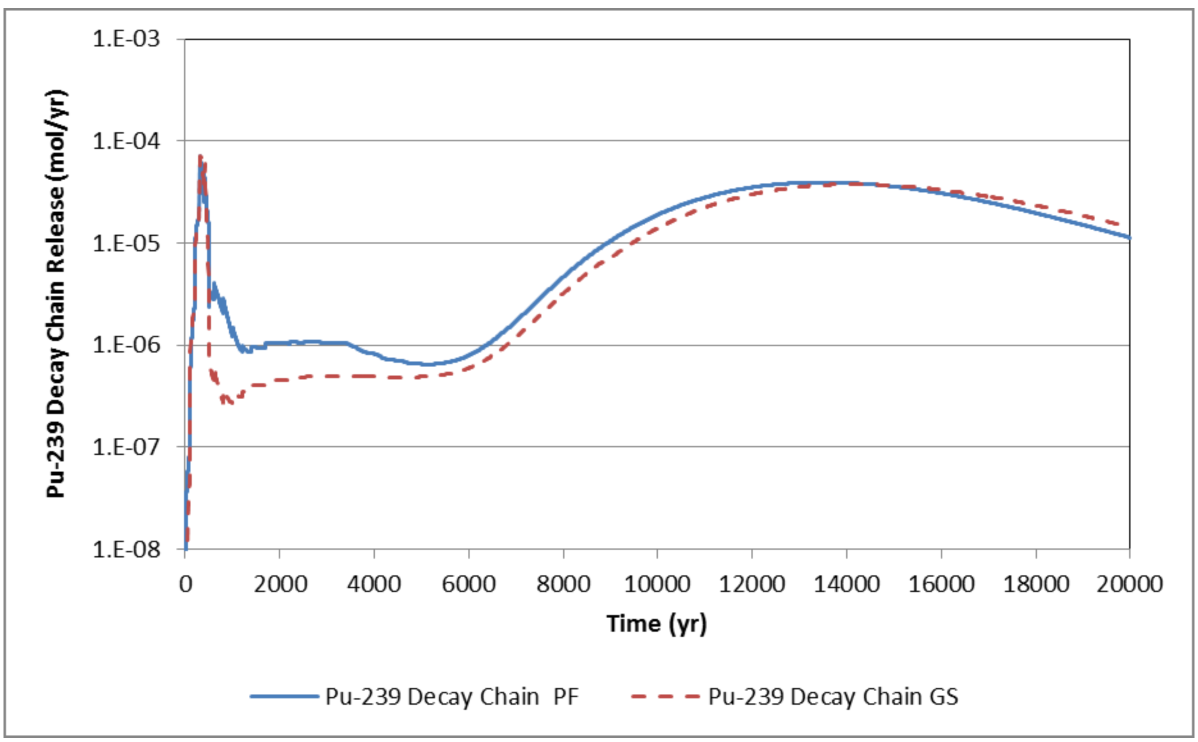

Figure A.3-37: Tank 16 U-234 Release to the Saturated Zone for Case D

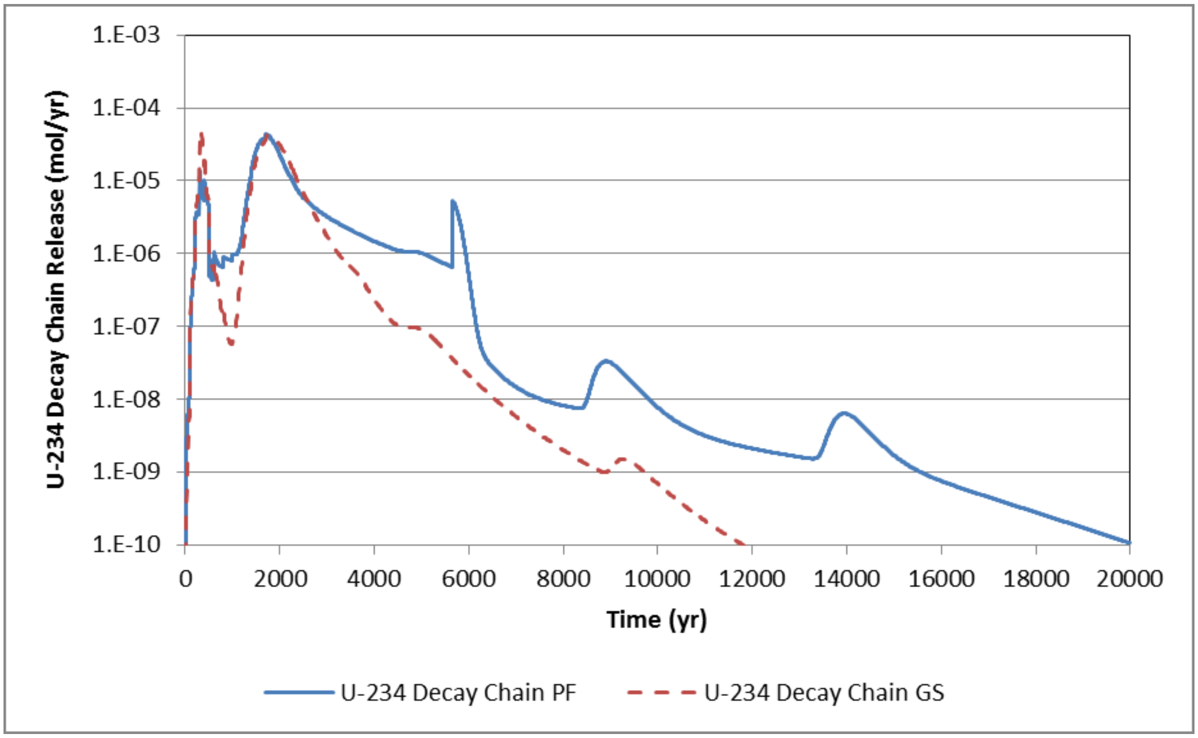

Figure A.3-38: Tank 16 Ra-226 Release to the Saturated Zone for Case D

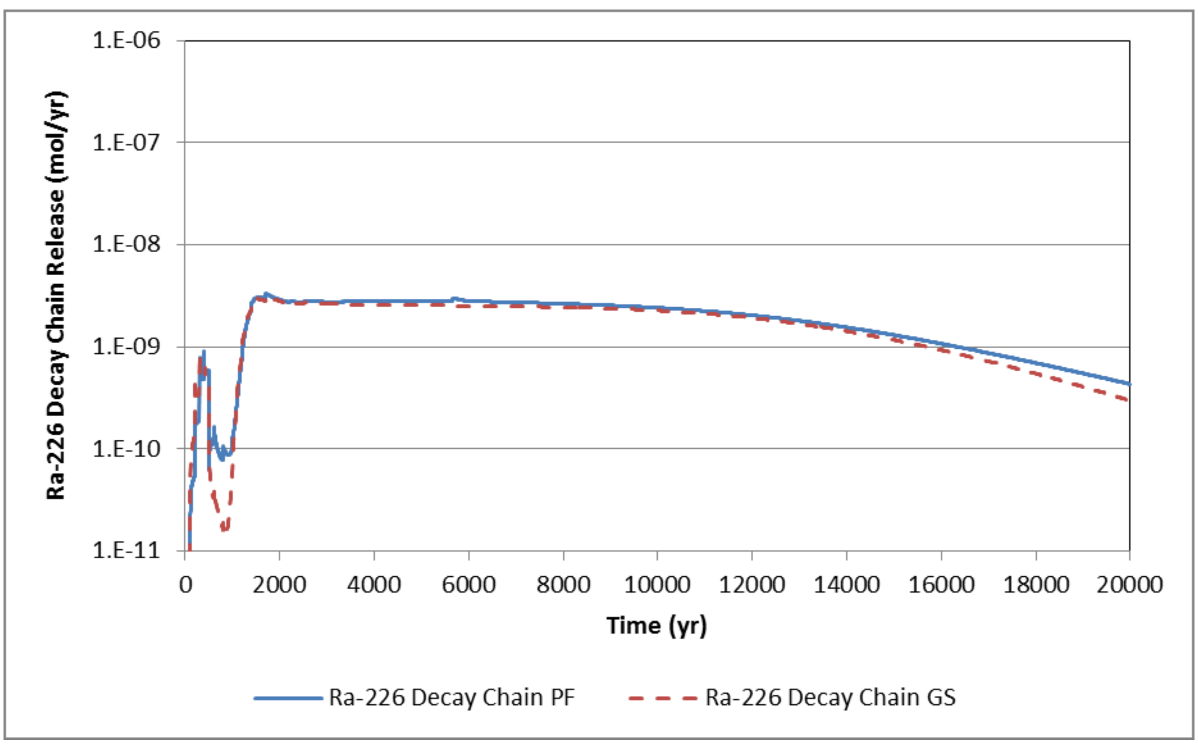

Figure A.3-39: Tank 16 Am-241 Release to the Saturated Zone for Case D

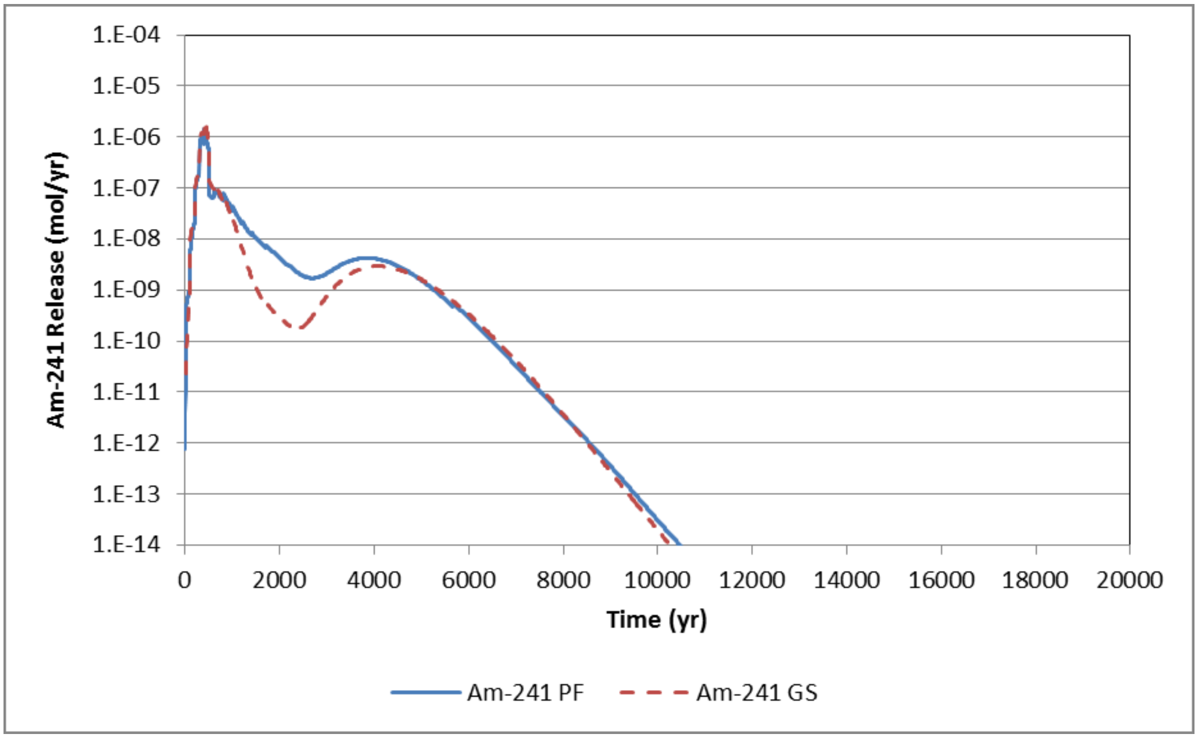

Figure A.3-40: Tank 16 Np-237 Release to the Saturated Zone for Case D

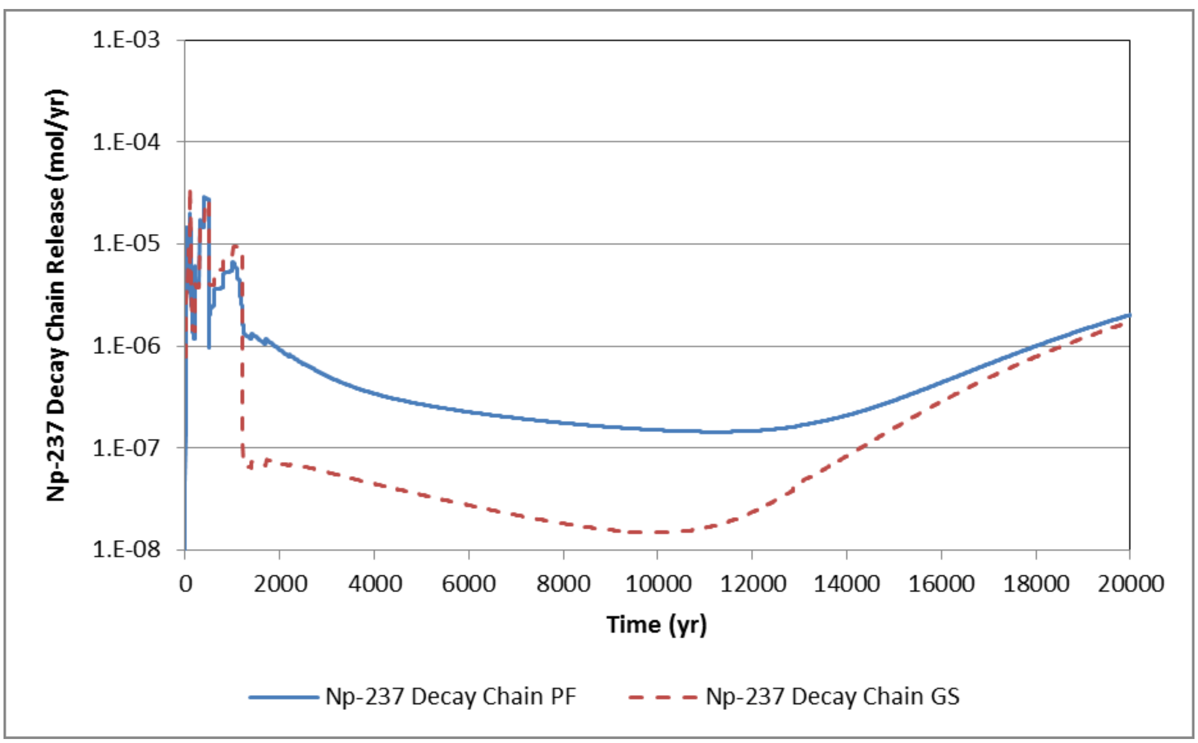

A.3.6 Type IV Tank (Tank 24) for Case D

For the Case D configuration, a comparison of the PORFLOW HTF Model and the GoldSim model mass releases of I-129, Tc-99, Am-243, Pu-239, U-234, Ra-226, Am-241, and Np-237, as presented in Figure A.3-41 through Figure A.3-48, indicate that the GoldSim model successfully captures the radionuclide release patterns seen in Tank 24 results generated by the PORFLOW model.

Table A.3-6 summarizes the peak values for these releases showing that when comparing the two models although not all of the percent differences are below 50% the values are reasonably close when considered in conjunction with the release patterns shown in Figure A.3-41 through Figure A.3-48. Note that the larger percent differences presented in Table A-3-6 reflect anomalous PORFLOW results caused by the slight difference in GoldSim and PORFLOW model chemical transition times (see Figure A.3-42 through Figure A.3-48) as discussed in Section A.1.6.

Table A.3-6: Case D GoldSim and PORFLOW Model Peak Releases from the UZ to the SZ Comparisons for Tank 24 within 20,000 years

Radionuclide	PORFLOW Peak Release (mol/yr)	PORFLOW Time of Peak Release (yr)	GoldSim Peak Release (mol/yr)	GoldSim Time of Peak Release (yr)	Peak Release Percent Difference GoldSim vs PORFLOW
I-129	6.3E-05	501	6.0E-05	510	-5%
Tc-99	1.9E-08	9,501	2.0E-08	10,010	5%
Am-243[1]	2.2E-07	12,727	2.8E-07	18,100	27%
Pu-239[1]	2.2E-06	19,979	5.4E-06	19,050	145%
U-234[1]	2.5E-06	9,899	2.9E-06	9,630	16%
Ra-226[1]	3.5E-08	2,302	7.7E-08	18,100	120%
Am-241	9.8E-12	3,481	5.8E-12	3,920	-41%
Np-237	1.0E-05	7,874	1.1E-05	6,510	10%

[1] Peak comparison influenced by mismatch in PORFLOW transition timing (see following figures).

Figure A.3-41: Tank 24 I-129 Release to the Saturated Zone for Case D

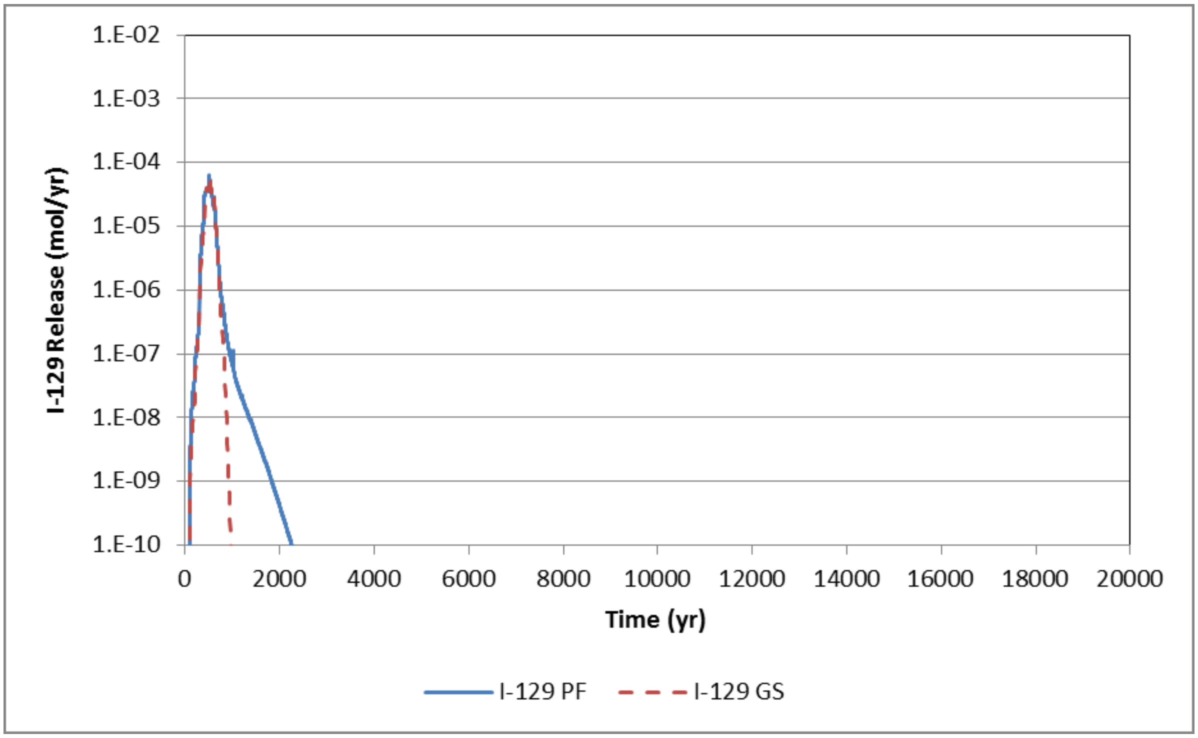

Figure A.3-42: Tank 24 Tc-99 Release to the Saturated Zone for Case D

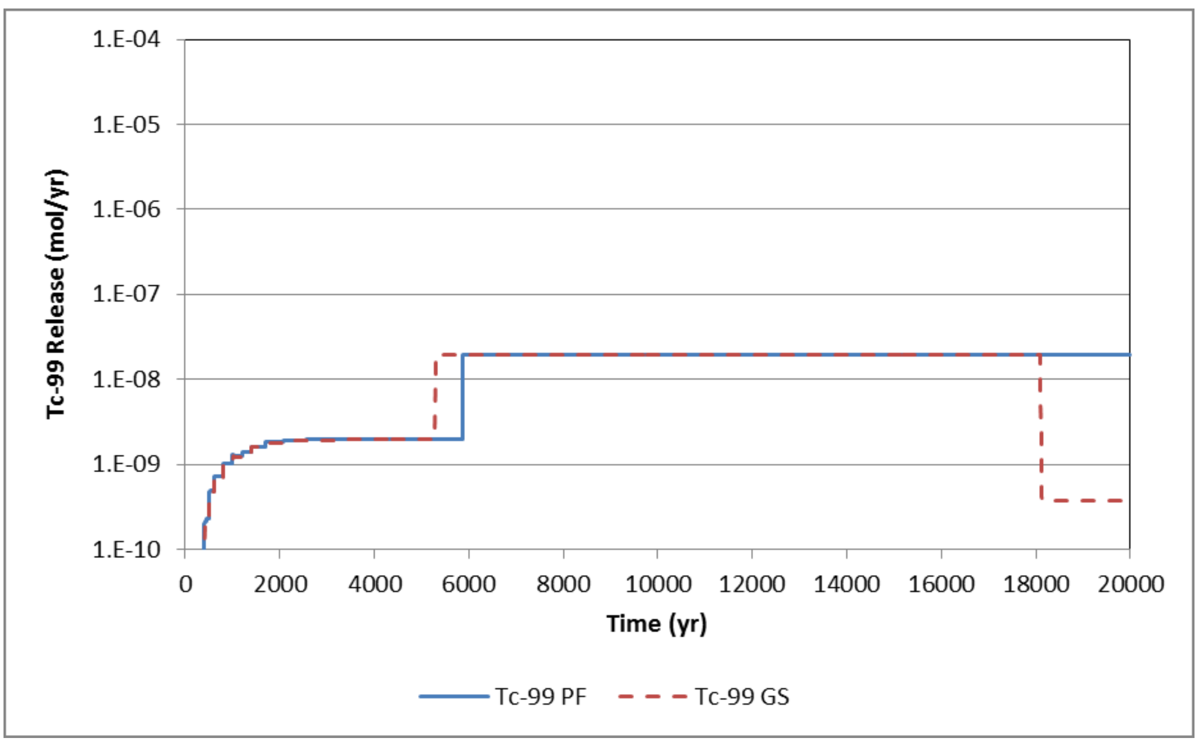

Figure A.3-43: Tank 24 Am-243 Release to the Saturated Zone for Case D

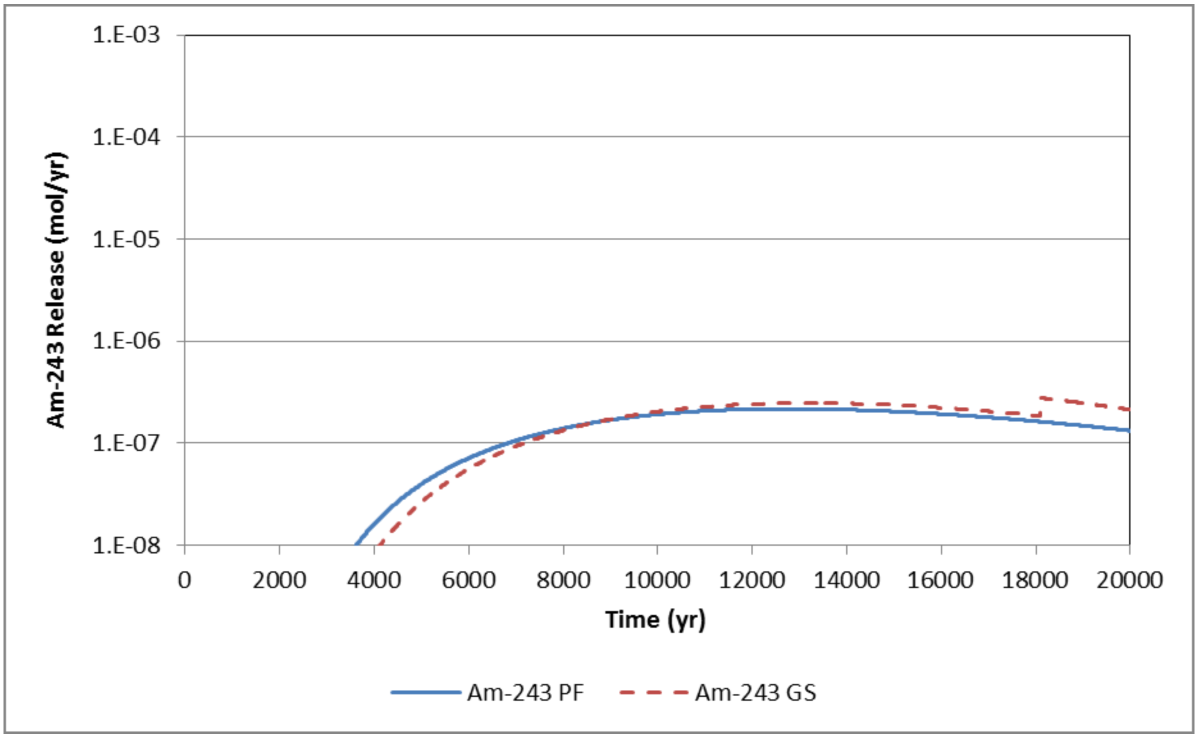

Figure A.3-44: Tank 24 Pu-239 Release to the Saturated Zone for Case D

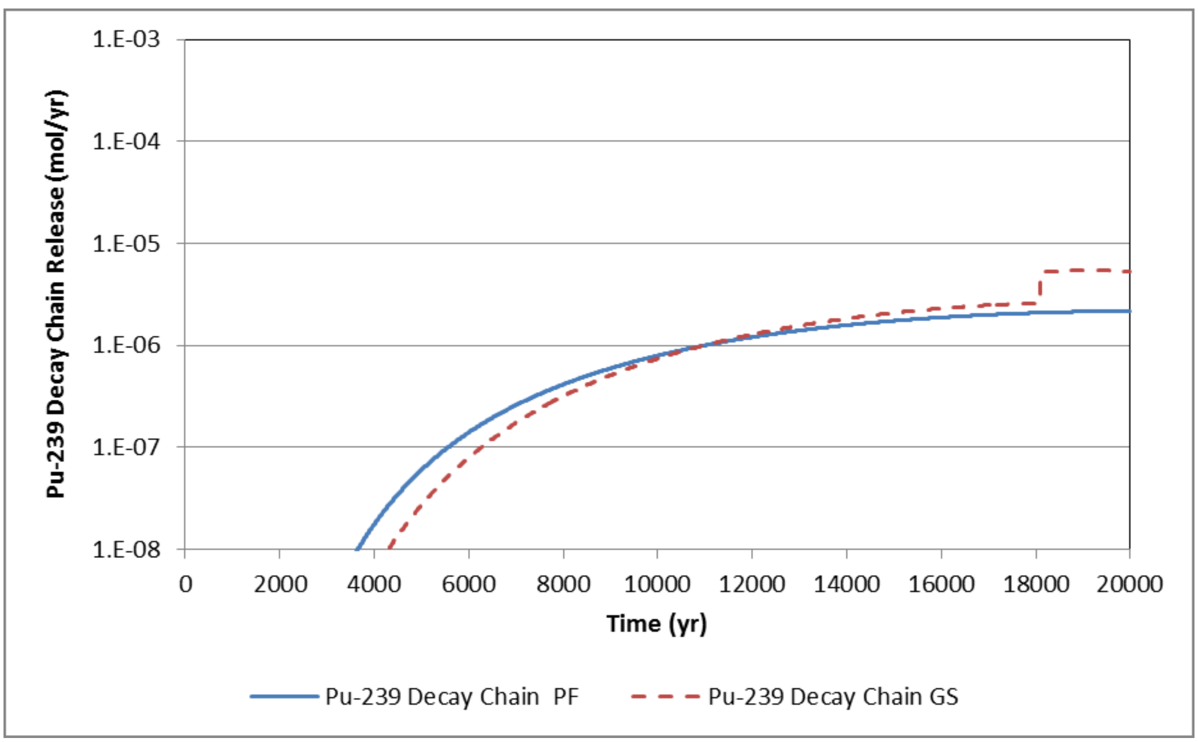

Figure A.3-45: Tank 24 U-234 Release to the Saturated Zone for Case D

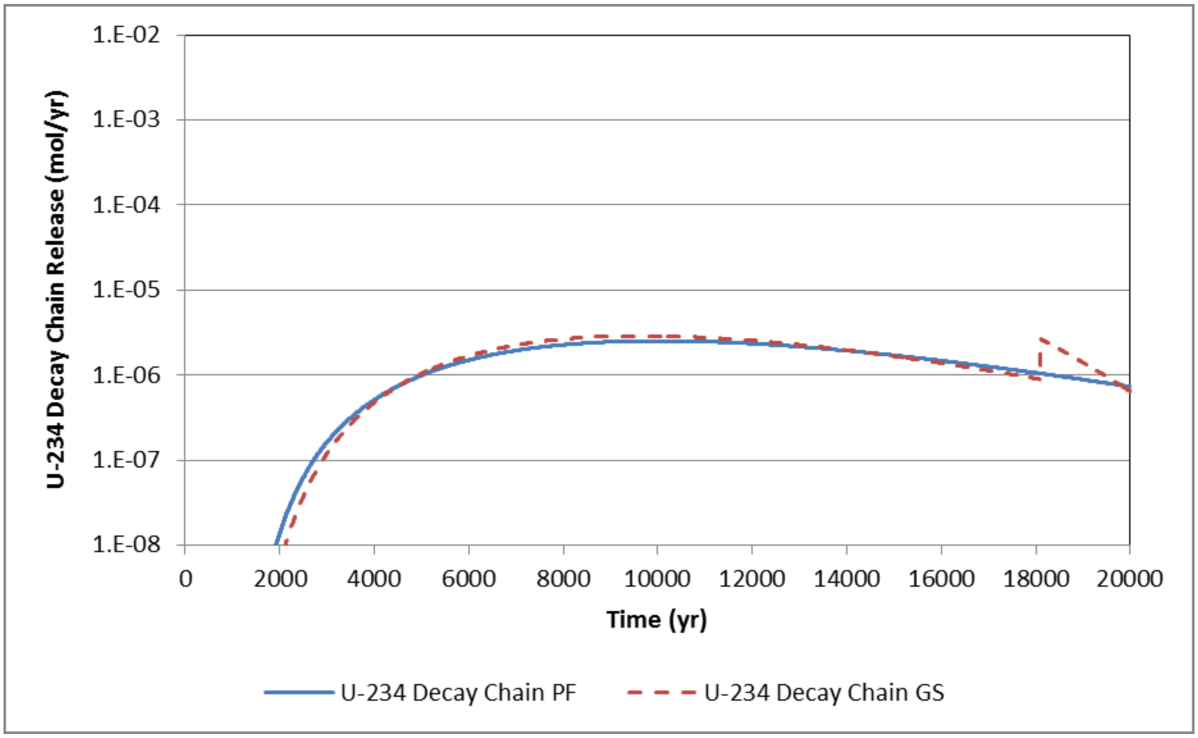

Figure A.3-46: Tank 24 Ra-226 Release to the Saturated Zone for Case D

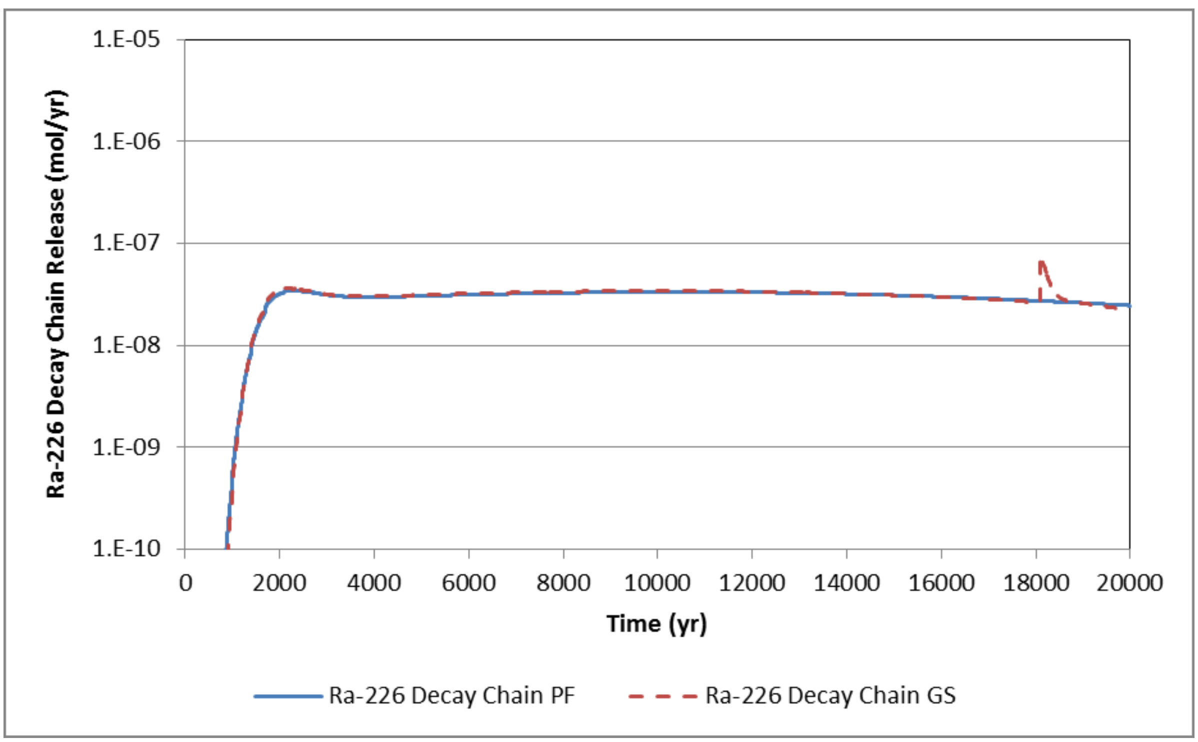

Figure A.3-47: Tank 24 Am-241 Release to the Saturated Zone for Case D

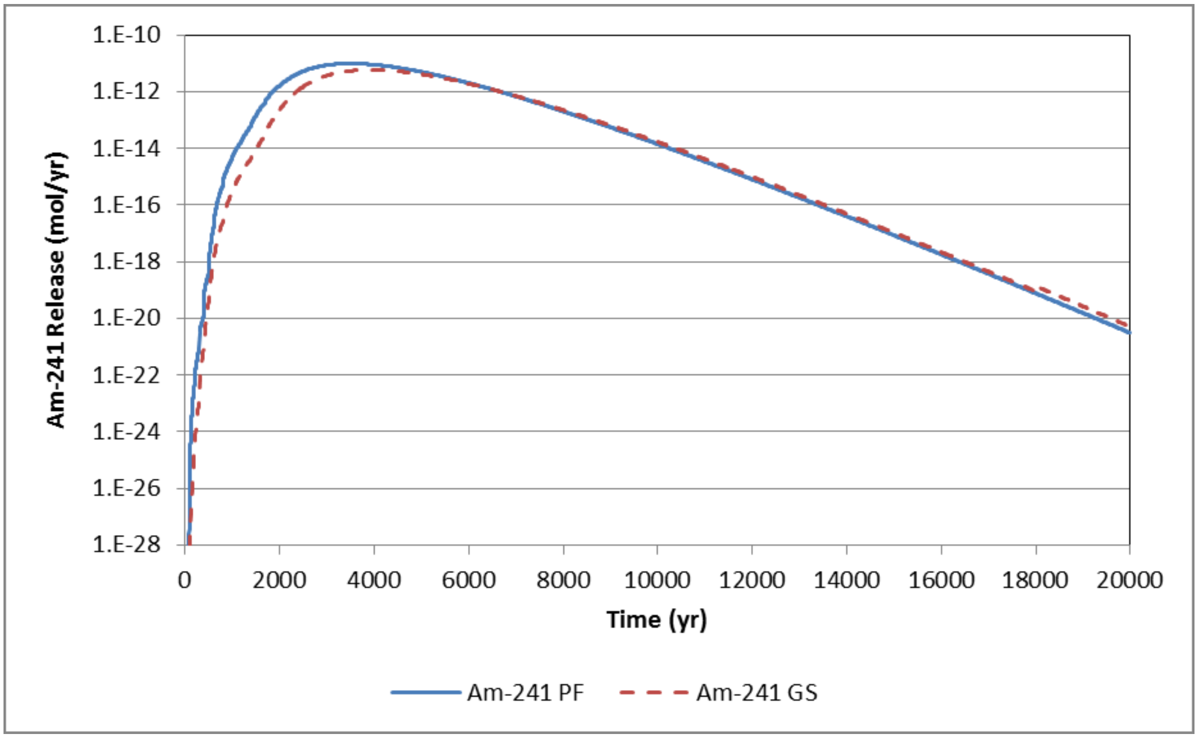

Figure A.3-48: Tank 24 Np-237 Release to the Saturated Zone for Case D

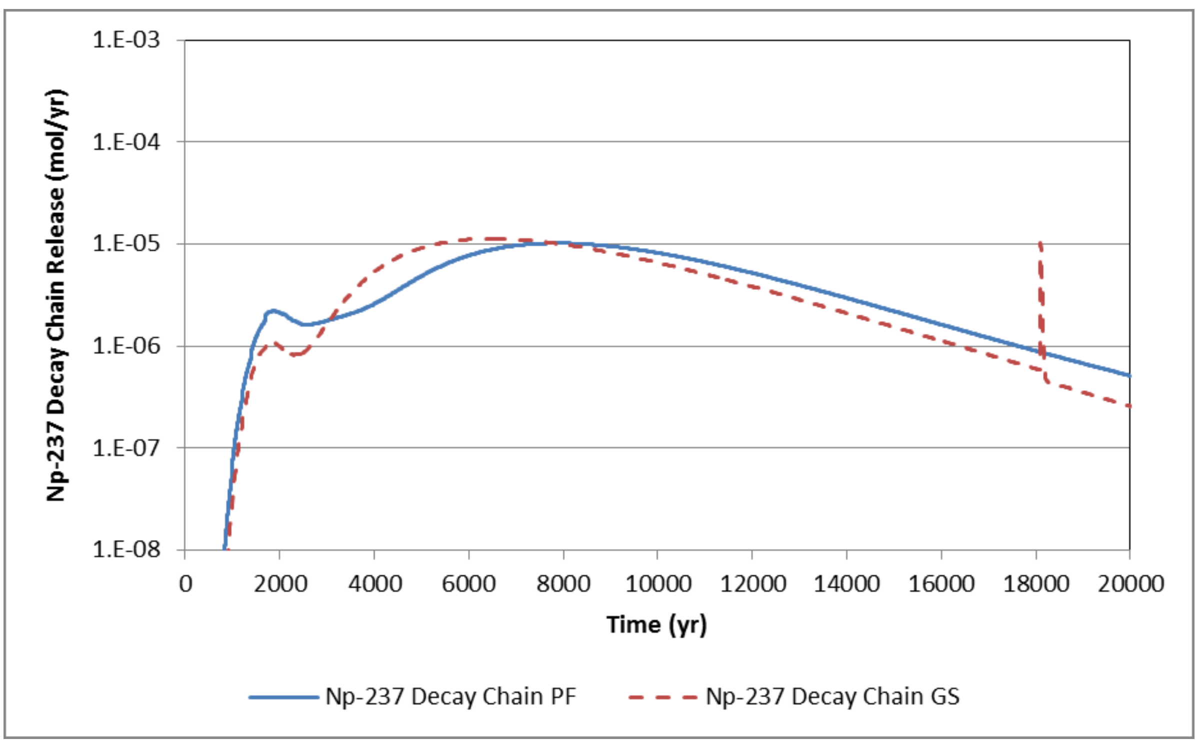

A.3.7 Type III Tank (Tank 31) for Case D

For the Case D configuration, a comparison of the PORFLOW HTF Model and the GoldSim model mass releases of I-129, Tc-99, Am-243, Pu-239, U-234, Ra-226, Am-241, and Np-237, as presented in Figure A.3-49 through Figure A.3-56, indicate that the GoldSim model successfully captures the radionuclide release patterns seen in Tank 31 results generated by the PORFLOW model.

Table A.3-7 summarizes the peak values for these releases showing that when comparing the two models that except for Am-243 and Am-241, all of the percent differences are below 50%. For Am-243, the trends of the model releases are similar (Figure A.3-51) , but the peak of the release is overestimated. With respect to Am-241, the trends of the model releases are similar (Figure A.3-55) , but the peak of the release is underestimated. Because the release of Am-241 is so low, the underestimation can be disregarded. The second comparison for Np-237 releases presented in Table A.3-7 shows what happens when the numerical dispersion in the basemat is increased by decreasing the number of mixing cells (from 15 to 10), representing it. Figure A.3-56 shows how the GoldSim model release pattern for Np-237 more closely matches the PORFLOW release when the numerical dispersion is increased in the GoldSim model.

Table A.3-7: Case D GoldSim and PORFLOW Model Peak Releases from the UZ to the SZ Comparisons for Tank 31 within 20,000 years

Radionuclide	PORFLOW Peak Release (mol/yr)	PORFLOW Time of Peak Release (yr)	GoldSim Peak Release (mol/yr)	GoldSim Time of Peak Release (yr)	Peak Release Percent Difference GoldSim vs PORFLOW
I-129	2.4E-03	2,214	3.1E-03	2,210	29%
Tc-99	1.9E-08	9,501	1.9E-08	10,010	0%
Am-243	2.4E-08	19,998	6.4E-08	20,000	167%
Pu-239	7.0E-07	20,000	9.1E-07	20,000	30%
U-234	3.1E-04	18,564	3.1E-04	18,330	0%
Ra-226	1.0E-06	18,325	9.5E-07	18,330	-5%
Am-241	6.2E-14	7,222	1.5E-15	9,350	-98%
Np-237	3.2E-04	6,822	3.2E-04	6,930	0%
Np-237[1]	3.2E-04	6,822	3.3E-04	6,930	3%

[1] Used coarser discretization on basemat.

Figure A.3-49: Tank 31 I-129 Release to the Saturated Zone for Case D

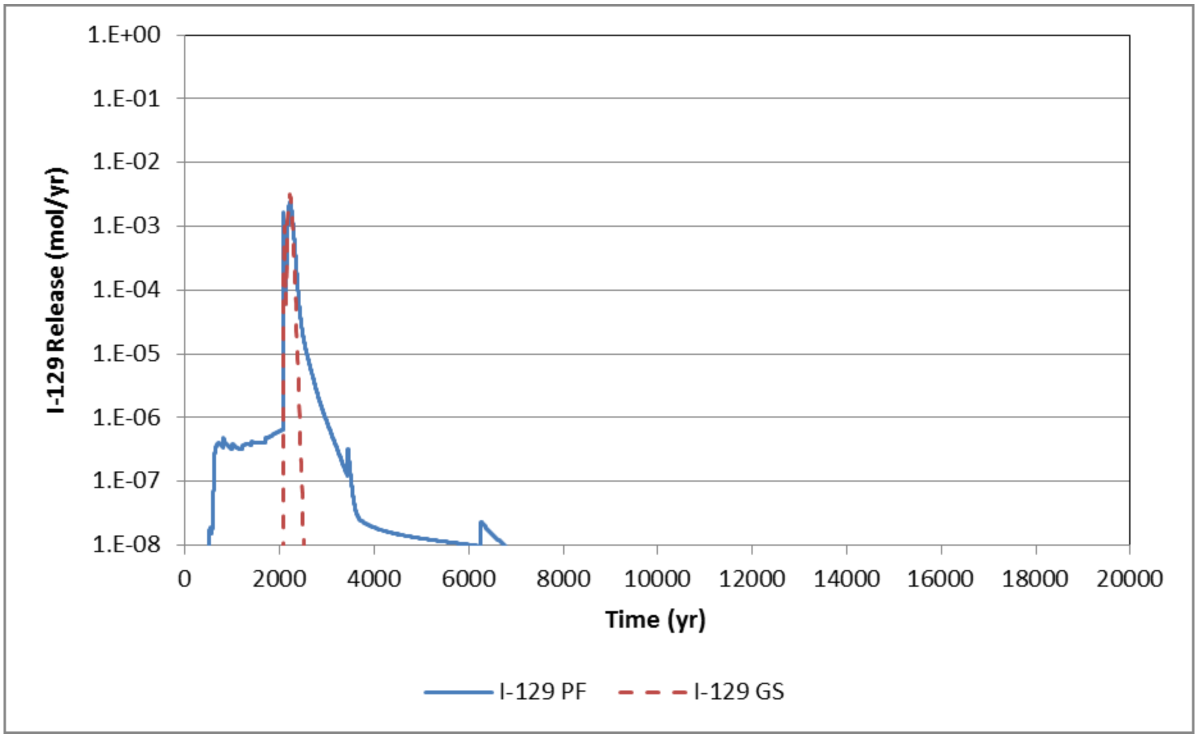

Figure A.3-50: Tank 31 Tc-99 Release to the Saturated Zone for Case D

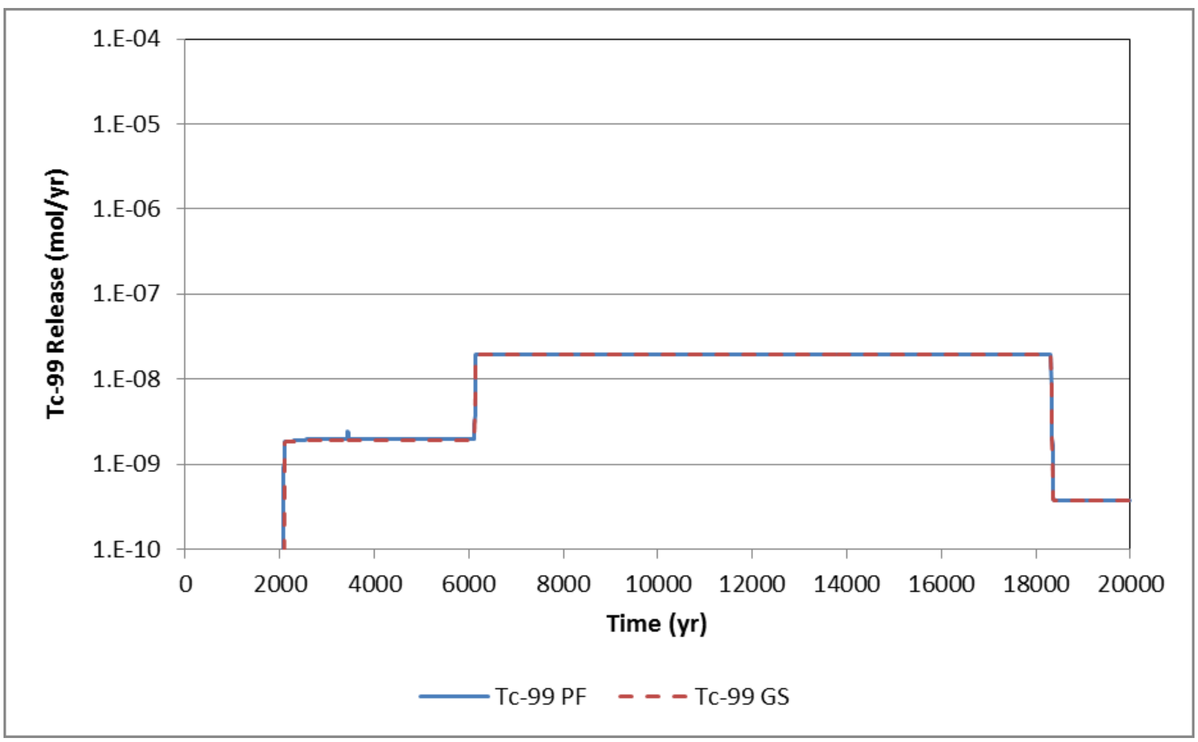

Figure A.3-51: Tank 31 Am-243 Release to the Saturated Zone for Case D

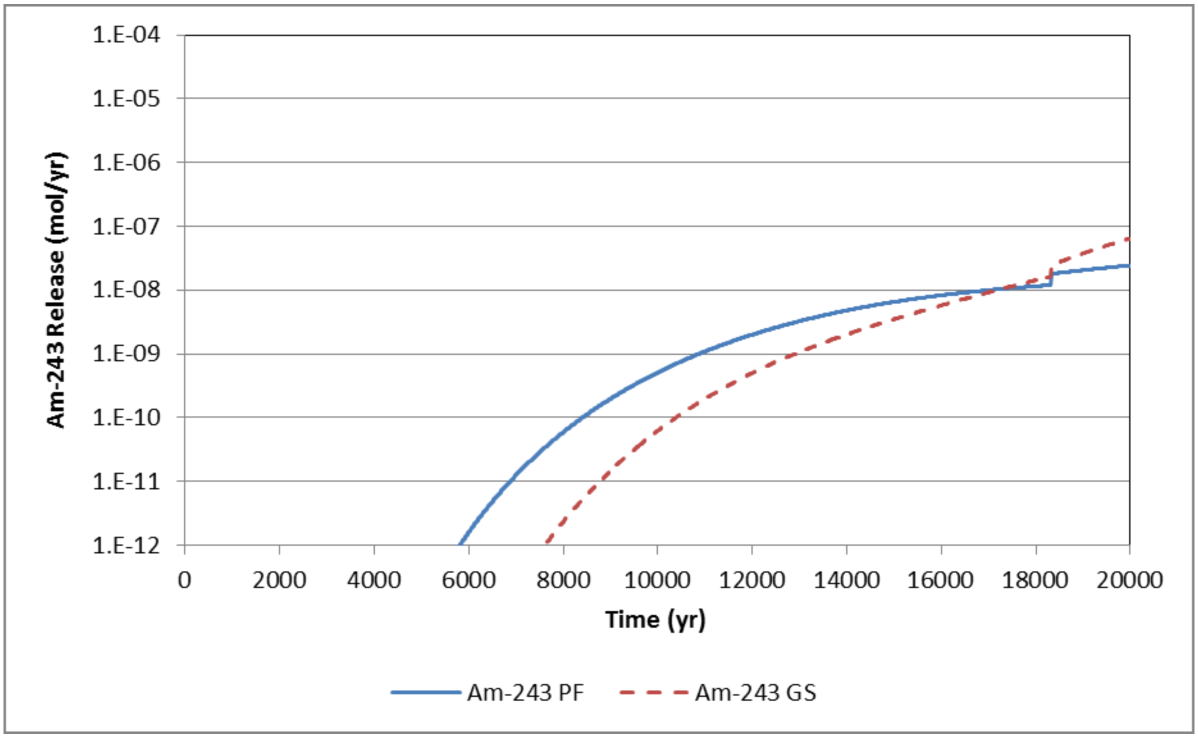

Figure A.3-52: Tank 31 Pu-239 Release to the Saturated Zone for Case D

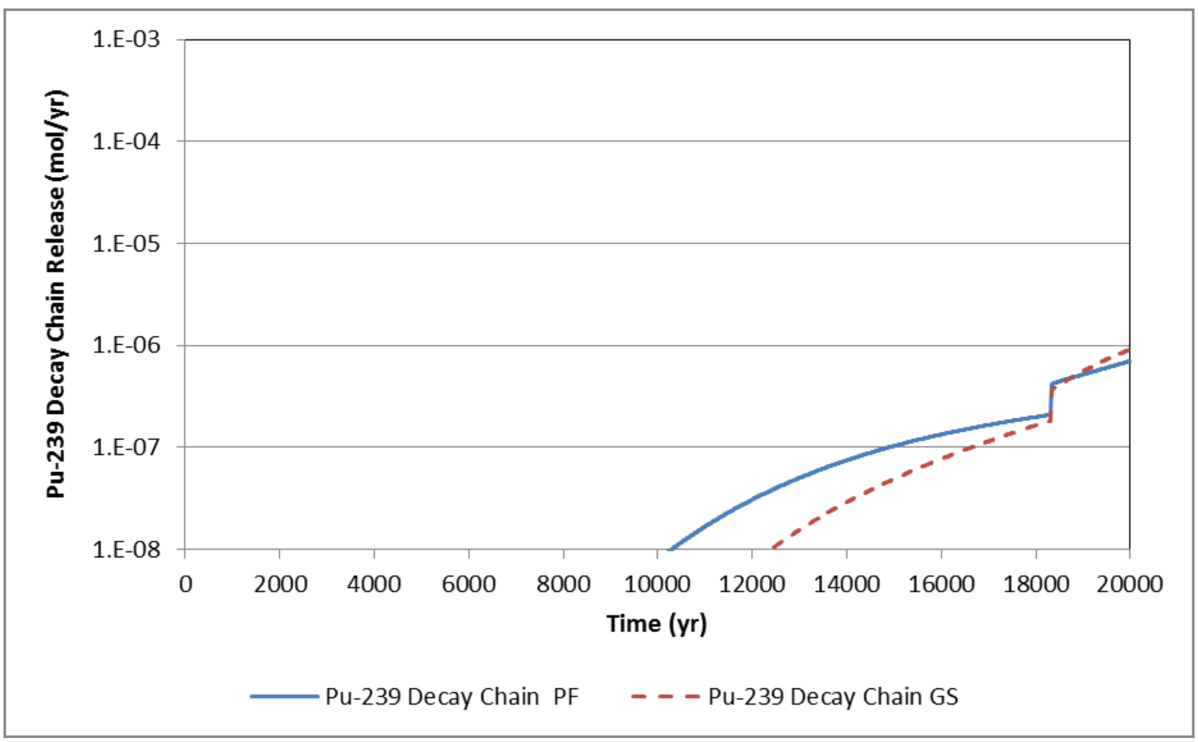

Figure A.3-53: Tank 31 U-234 Release to the Saturated Zone for Case D

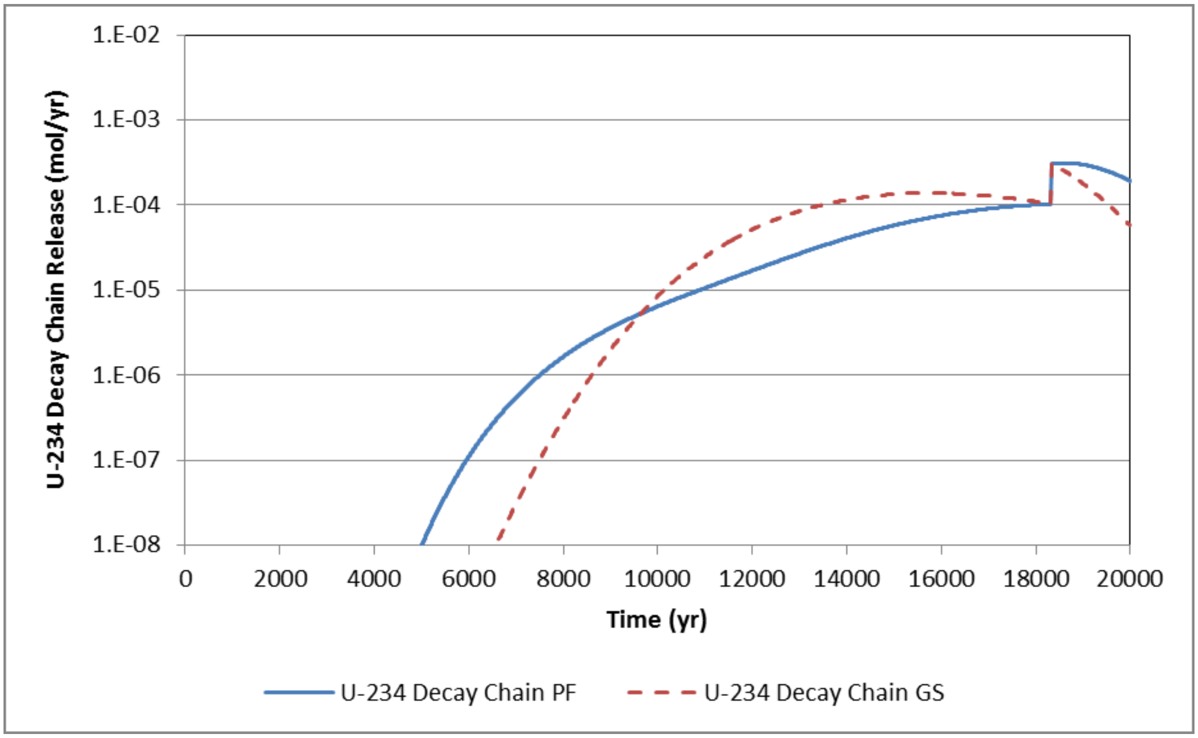

Figure A.3-54: Tank 31 Ra-226 Release to the Saturated Zone for Case D

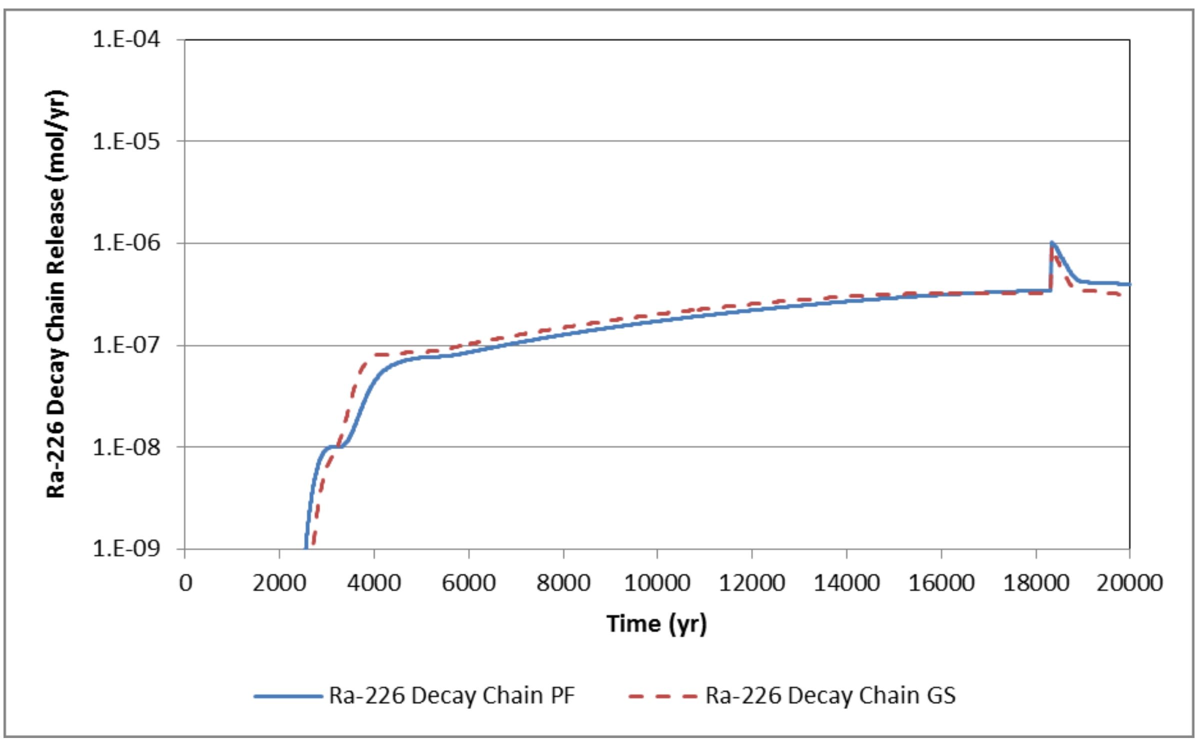

Figure A.3-55: Tank 31 Am-241 Release to the Saturated Zone for Case D

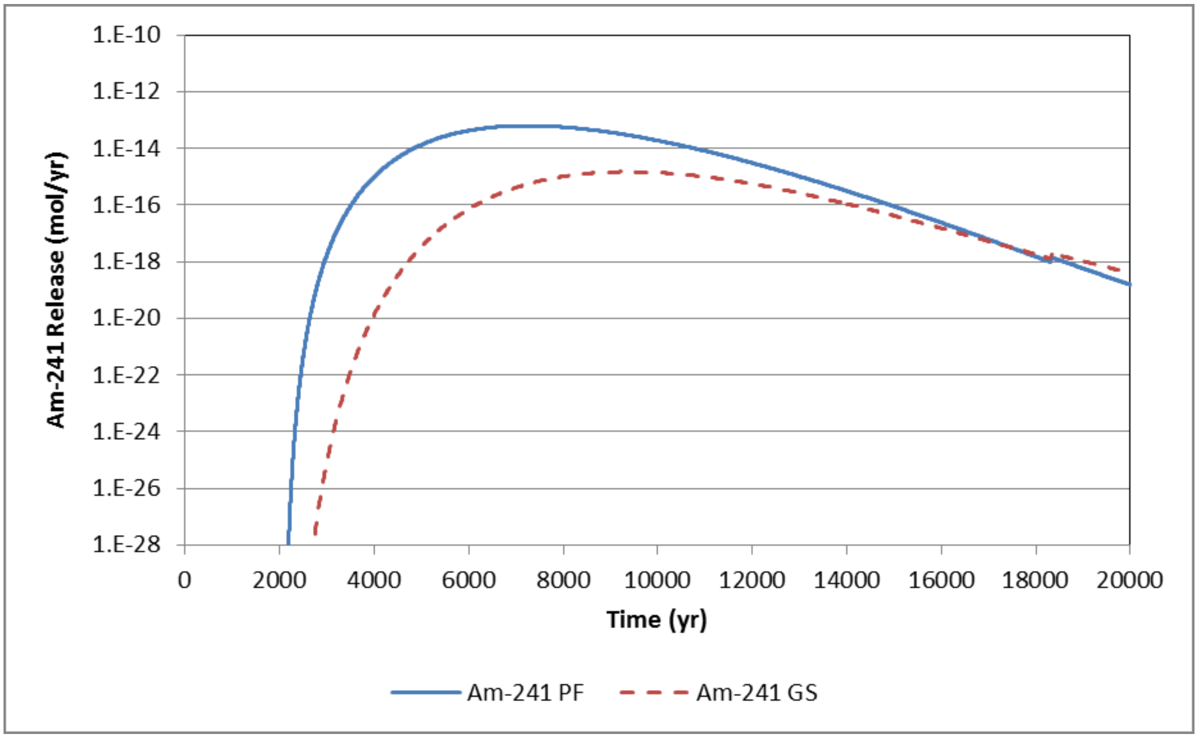

Figure A.3-56: Tank 31 Np-237 Release to the Saturated Zone for Case D

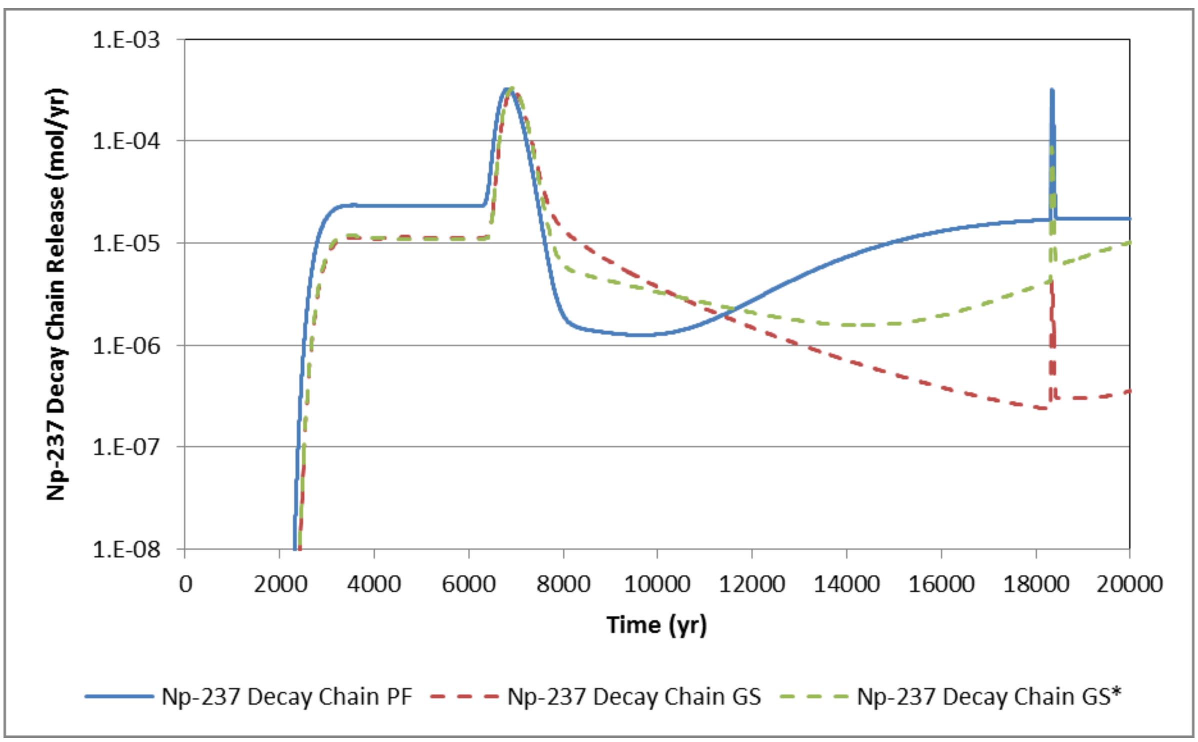

A.4.1 Type I Tank with Intact Liner (Tank 9) for Case E

For the Case E configuration, a comparison of the PORFLOW HTF Model and the GoldSim model mass releases of I-129, Tc-99, Am-243, Pu-239, U-234, Ra-226, Am-241, and Np-237, as presented in Figure A.4-1 through Figure A.4-8, indicate that the GoldSim model successfully captures the radionuclide release patterns seen in Tank 9 results generated by the PORFLOW model.

Table A.4-1 summarizes the peak values for these releases showing that when comparing the two models although not all of the percent differences are below 50% the values are reasonably close except for Np-237, when considered in conjunction with the release patterns shown in Figure A.4-1 through Figure A.4-7. With respect to Np-237, the spike defining the PORFLOW model peak is higher and the spike defining the GoldSim model peak is broader.

Table A.4-1: Case E GoldSim and PORFLOW Model Peak Releases from the UZ to the SZ Comparisons for Tank 9 within 20,000 years

Radionuclide	PORFLOW Peak Release (mol/yr)	PORFLOW Time of Peak Release (yr)	GoldSim Peak Release (mol/yr)	GoldSim Time of Peak Release (yr)	Peak Release Percent Difference GoldSim vs PORFLOW
I-129	2.6E-02	1,143	2.5E-02	1,150	-4%
Tc-99	1.5E-03	6,817	5.5E-04	6,820	-63%
Am-243	2.1E-03	1,304	2.2E-03	1,160	5%
Pu-239	8.3E-06	10,686	8.6E-06	12,150	4%
U-234	1.4E-01	1,147	8.8E-02	1,150	-37%
Ra-226	5.6E-07	1,143	4.1E-07	1,150	-27%
Am-241	2.1E-03	1,190	2.2E-03	1,160	5%
Np-237[1]	8.8E-01	1,146	6.0E-02	1,160	-93%

[1] In the Np-237 breakthrough curves, the PORFLOW spike contains 3.1 mols and the GoldSim spike contains 3.6 mols.

Figure A.4-1: Tank 9 I-129 Release to the Saturated Zone for Case E

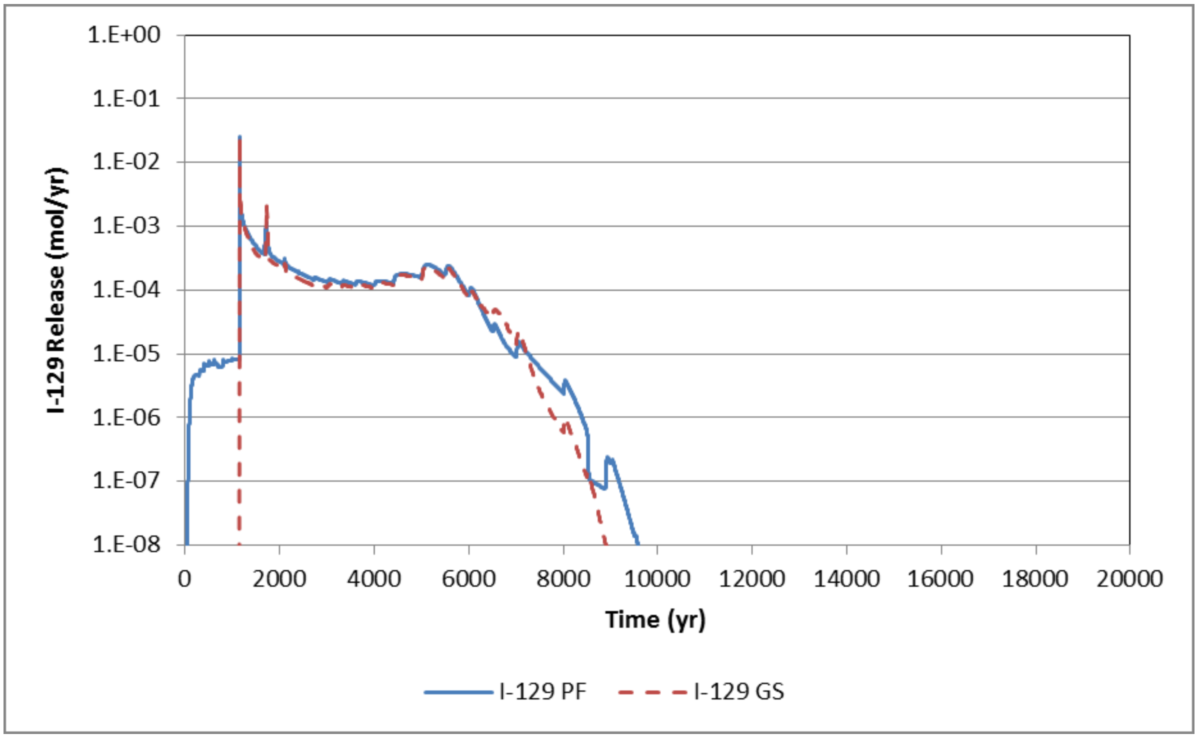

Figure A.4-2: Tank 9 Tc-99 Release to the Saturated Zone for Case E

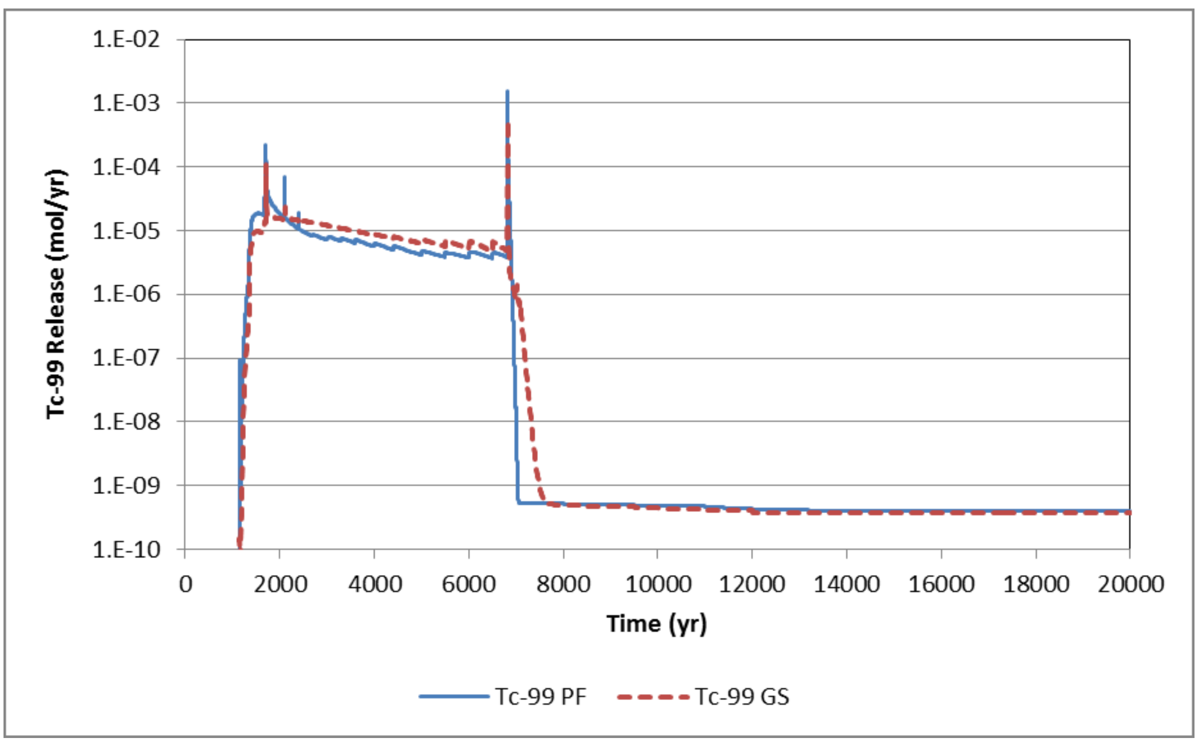

Figure A.4-3: Tank 9 Am-243 Release to the Saturated Zone for Case E

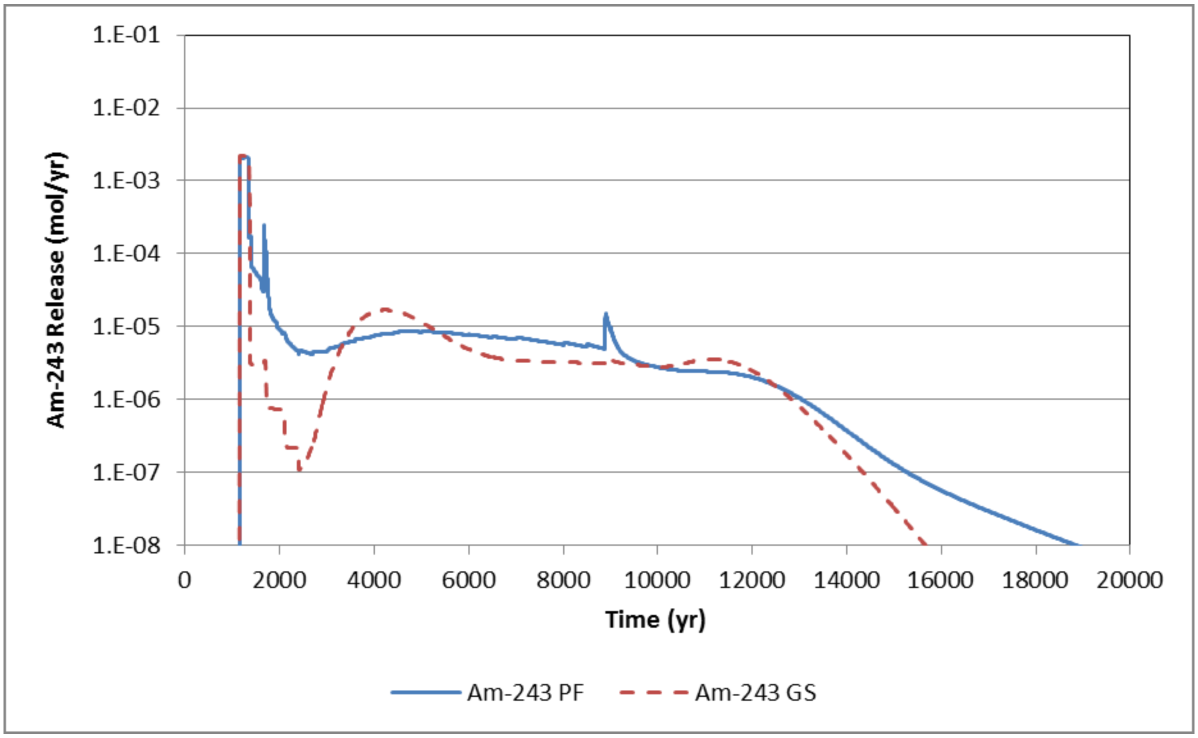

Figure A.4-4: Tank 9 Pu-239 Release to the Saturated Zone for Case E

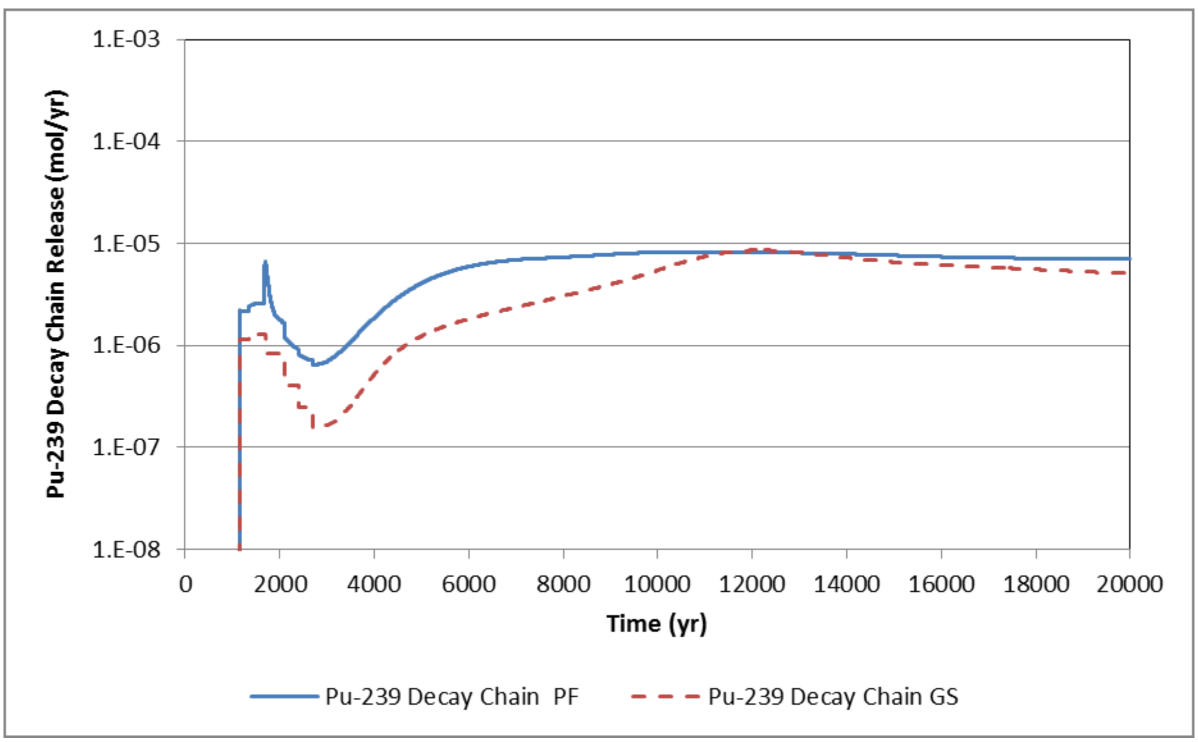

Figure A.4-5: Tank 9 U-234 Release to the Saturated Zone for Case E

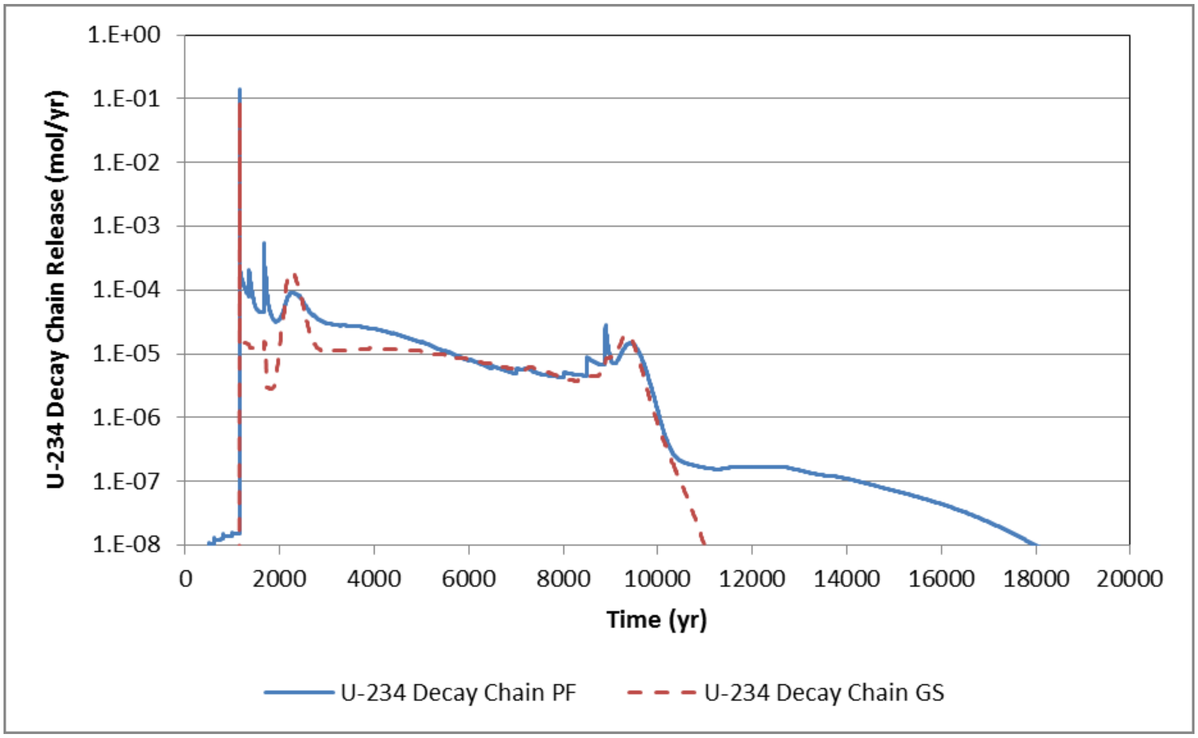

Figure A.4-6: Tank 9 Ra-226 Release to the Saturated Zone for Case E

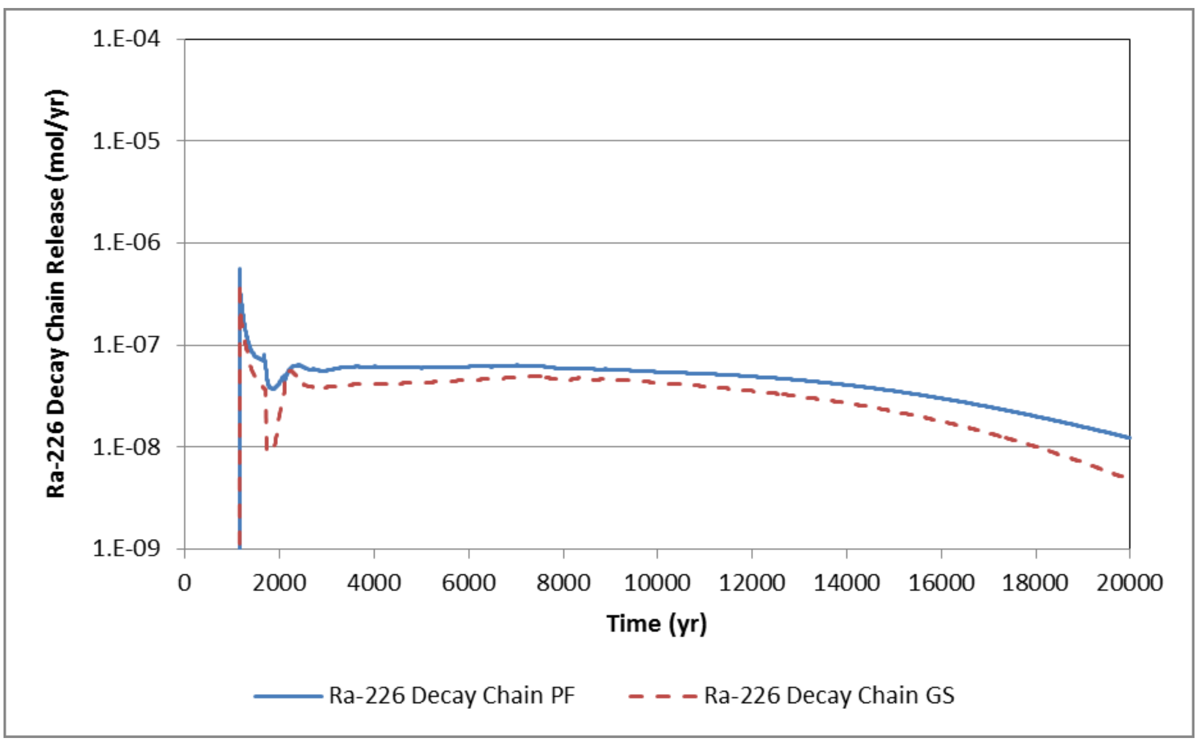

Figure A.4-7: Tank 9 Am-241 Release to the Saturated Zone for Case E

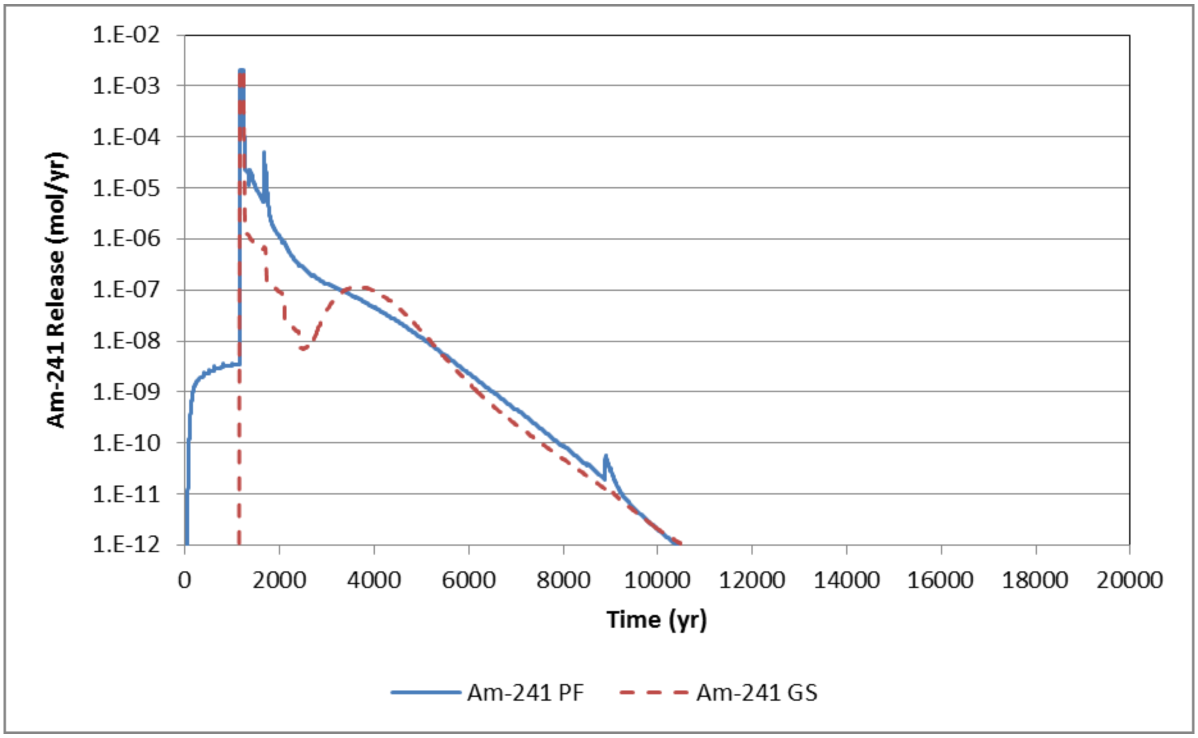

Figure A.4-8: Tank 9 Np-237 Release to the Saturated Zone for Case E

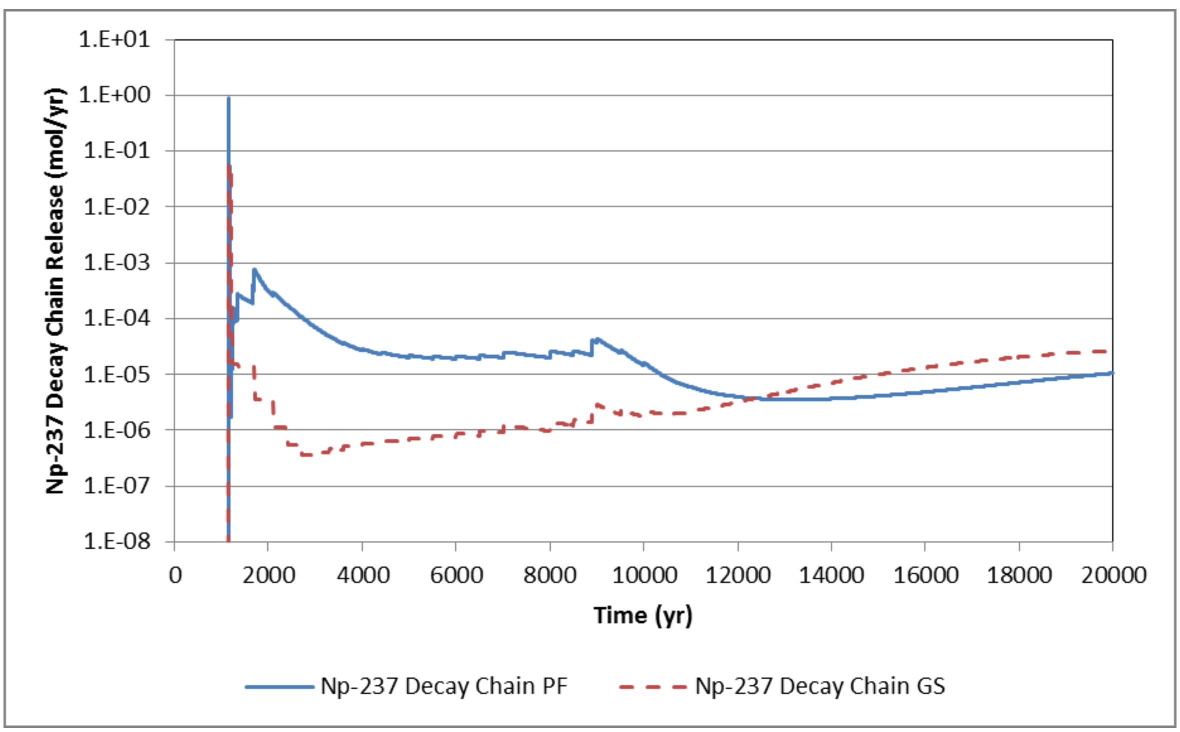

A.4.2 Type I Tank with Failed Liner (Tank 12) for Case E

For the Case E configuration, a comparison of the PORFLOW HTF Model and the GoldSim model mass releases of I-129, Tc-99, Am-243, Pu-239, U-234, Ra-226, Am-241, and Np-237, as presented in Figure A.4-9 through Figure A.4-16, indicate that the GoldSim model successfully captures the radionuclide release patterns seen in Tank 12 results generated by the PORFLOW model.

Table A.4-2 summarizes the peak values for these releases showing that when comparing the two models although not all of the percent differences are below 50%, except for Am-241 and Np-237, the compared values are reasonably close when considered in conjunction with the release patterns shown in Figure A.4-9 through Figure A.4-14. With respect to Am-241 and Np-237, the early peak generated by the GoldSim Model, will conservatively overestimate the release.

Table A.4-2: Case E GoldSim and PORFLOW Model Peak Releases from the UZ to the SZ Comparisons for Tank 12 within 20,000 years

Radionuclide	PORFLOW Peak Release (mol/yr)	PORFLOW Time of Peak Release (yr)	GoldSim Peak Release (mol/yr)	GoldSim Time of Peak Release (yr)	Peak Release Percent Difference GoldSim vs PORFLOW
I-129	9.3E-03	1,701	9.0E-03	1,710	-3%
Tc-99	3.8E-04	6,516	1.3E-04	6,810	-66%
Am-243	1.7E-06	13	4.3E-07	4,220	-75%
Pu-239	5.4E-06	11,297	5.7E-06	14,310	6%
U-234	1.7E-04	1,352	2.5E-04	2,230	47%
Ra-226	1.4E-08	8,924	2.2E-08	7,390	57%
Am-241	7.6E-05	213	3.0E-04	320	295%
Np-237	1.0E-04	11	8.0E-04	120	700%

Figure A.4-9: Tank 12 I-129 Release to the Saturated Zone for Case E

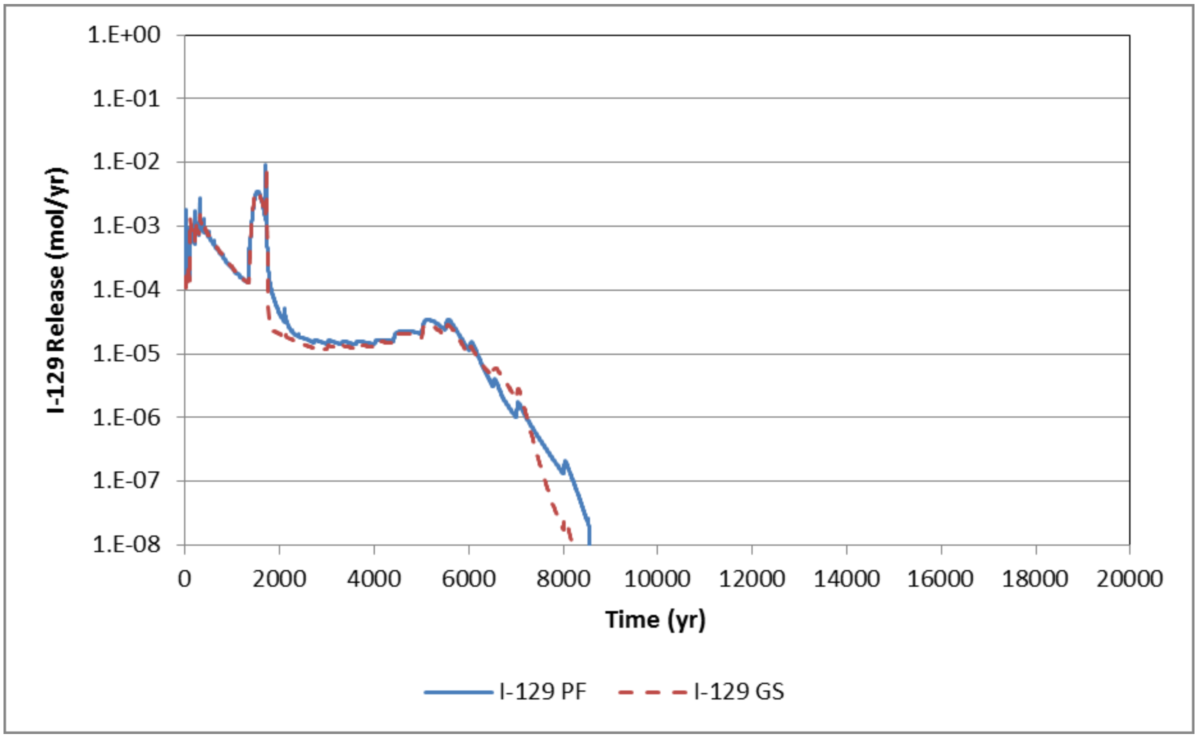

Figure A.4-10: Tank 12 Tc-99 Release to the Saturated Zone for Case E

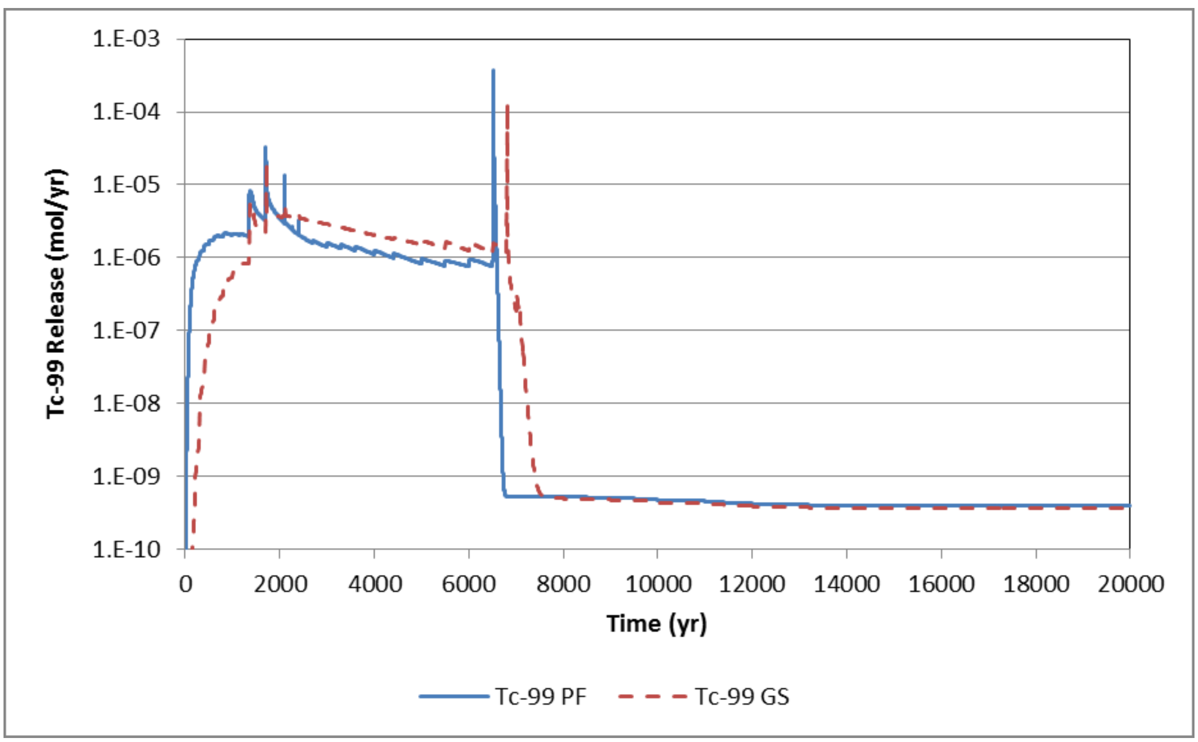

Figure A.4-11: Tank 12 Am-243 Release to the Saturated Zone for Case E

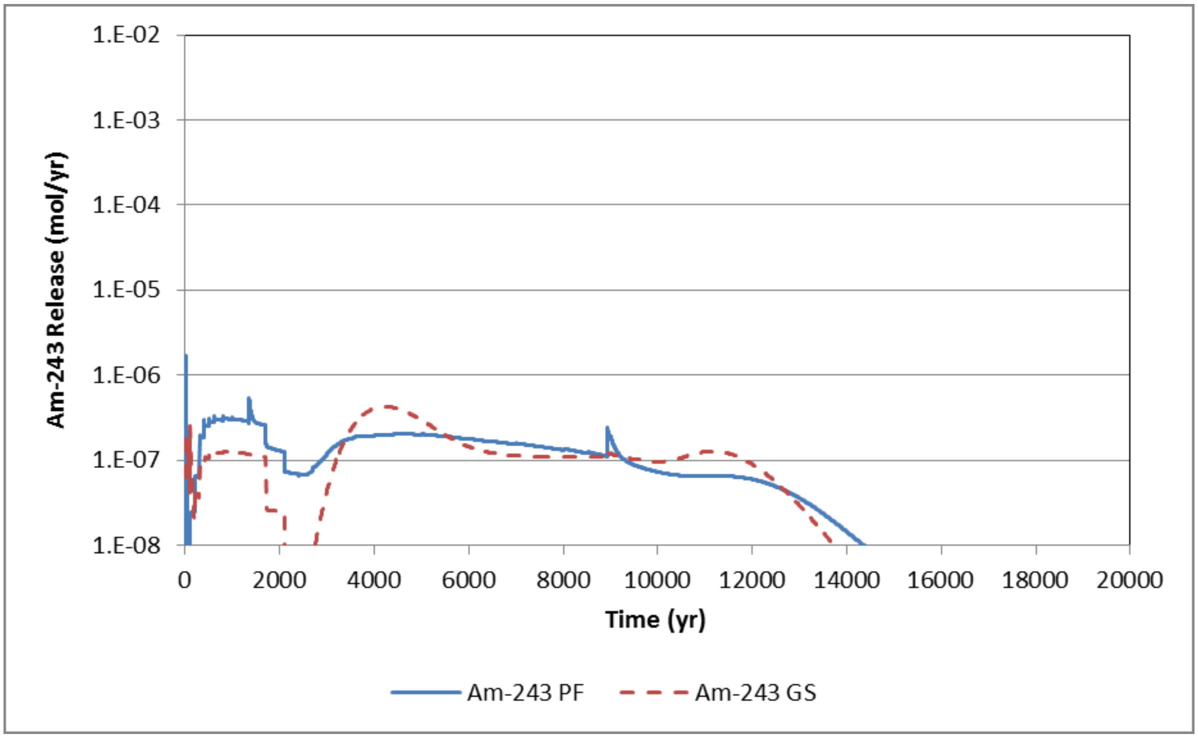

Figure A.4-12: Tank 12 Pu-239 Release to the Saturated Zone for Case E

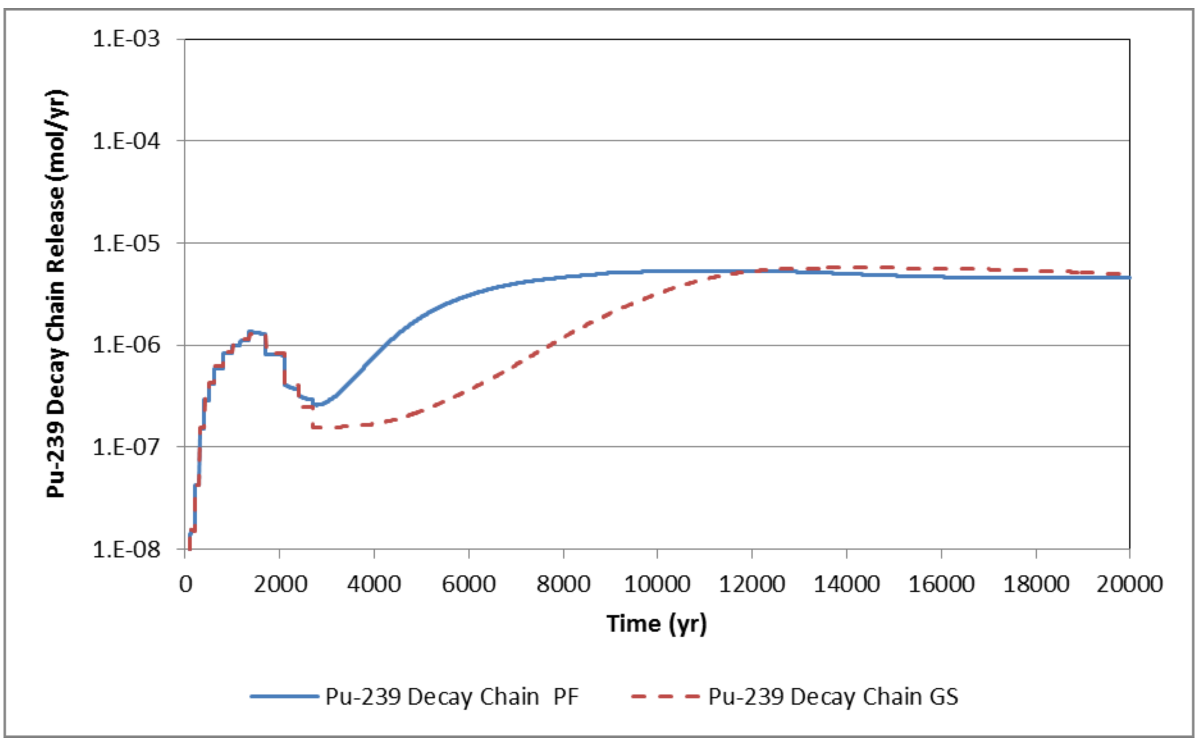

Figure A.4-13: Tank 12 U-234 Release to the Saturated Zone for Case E

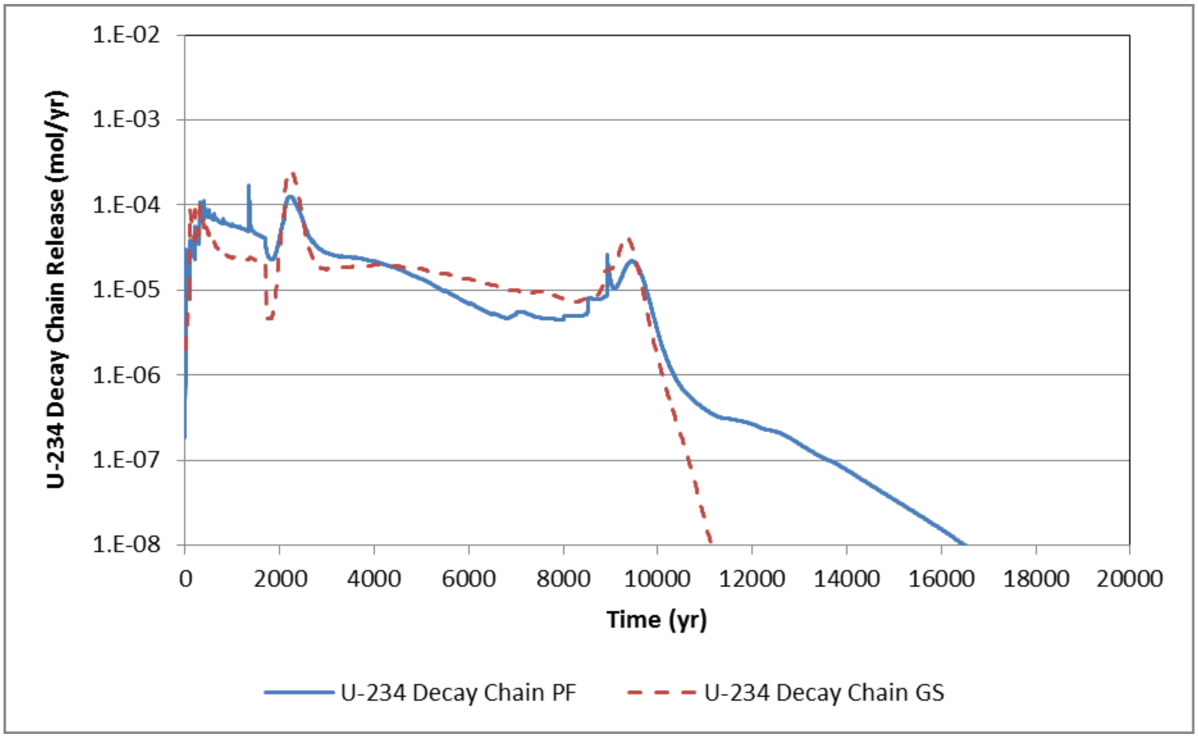

Figure A.4-14: Tank 12 Ra-226 Release to the Saturated Zone for Case E

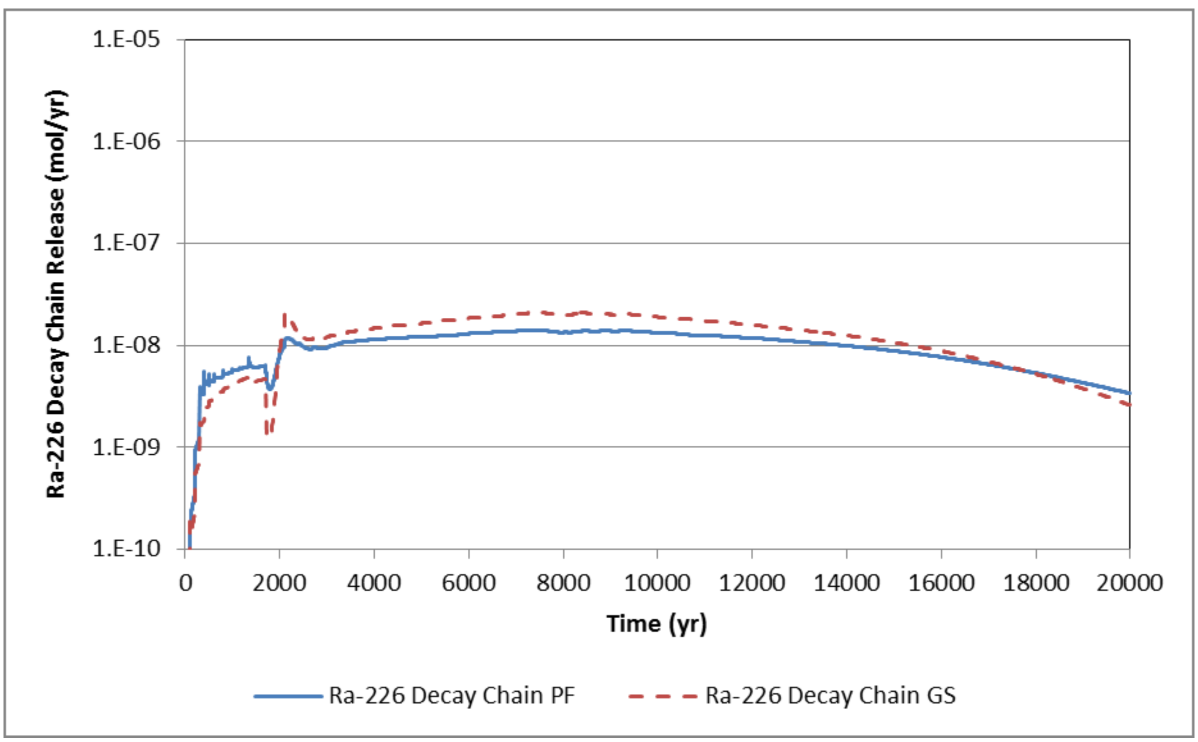

Figure A.4-15: Tank 12 Am-241 Release to the Saturated Zone for Case E

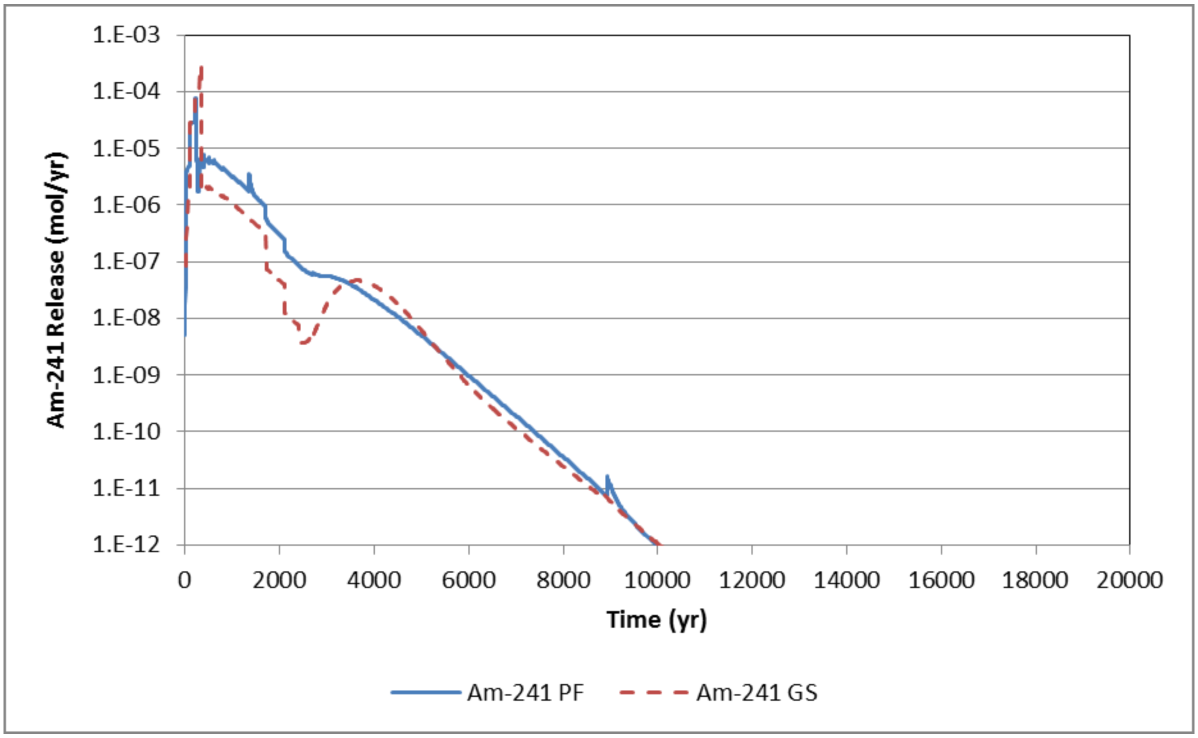

Figure A.4-16: Tank 12 Np-237 Release to the Saturated Zone for Case E

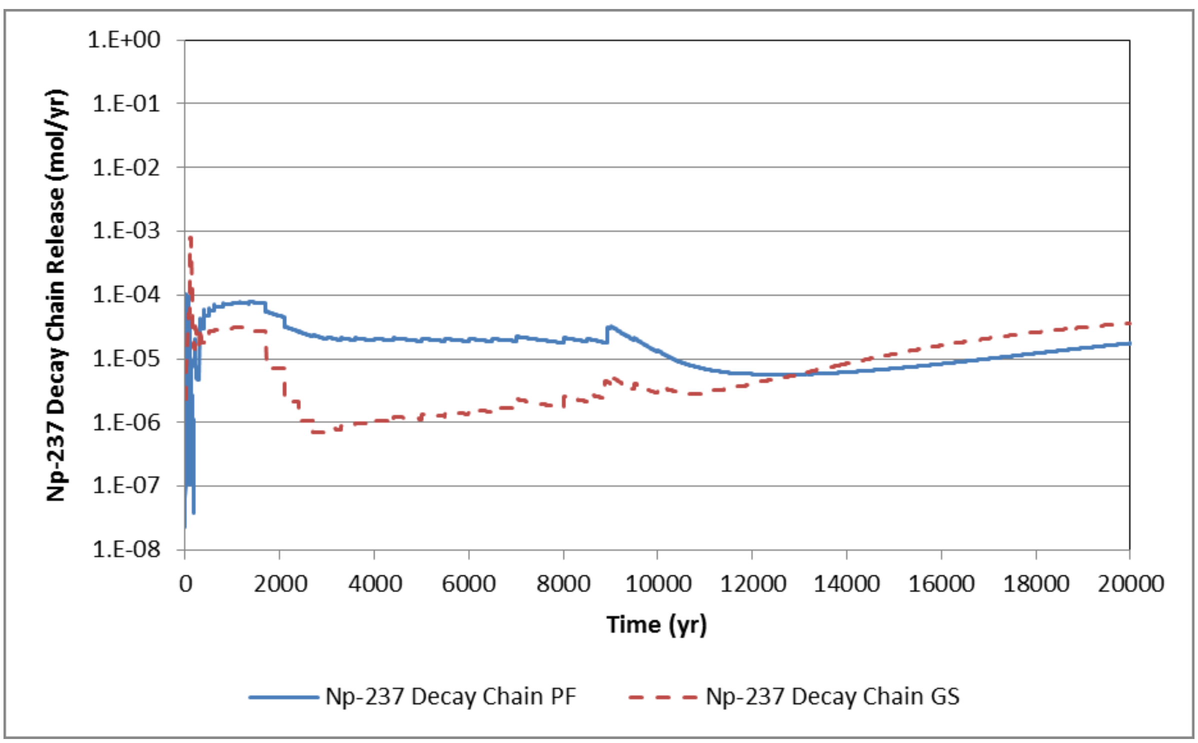

A.4.3 Type II Tank with Intact Liner (Tank 13) for Case E

For the Case E configuration, a comparison of the PORFLOW HTF Model and the GoldSim model mass releases of I-129, Tc-99, Am-243, Pu-239, U-234, Ra-226, Am-241, and Np-237, as presented in Figure A.4-17 through Figure A.4-24, indicate that the GoldSim model successfully captures the radionuclide release patterns seen in Tank 13 results generated by the PORFLOW model.

Table A.4-3 summarizes the peak values for these releases showing that when comparing the two models Am-243, Pu-239, U-234, produce similar peak releases in the two models. For the other radionuclides, the transition time releases do not match as well, but since they are reflected in very short term spikes, the differences in magnitude will not become less relavent as the mass disperses while it migrates downgradiant.

Table A.4-3: Case E GoldSim and PORFLOW Model Peak Releases from the UZ to the SZ Comparisons for Tank 13 within 20,000 years

Radionuclide	PORFLOW Peak Release (mol/yr)	PORFLOW Time of Peak Release (yr)	GoldSim Peak Release (mol/yr)	GoldSim Time of Peak Release (yr)	Peak Release Percent Difference GoldSim vs PORFLOW
I-129	3.2E-02	2,507	3.0E-02	2,510	-6%
Tc-99	3.7E-03	2,507	3.0E-04	2,510	-92%
Am-243	8.2E-03	2,570	8.5E-03	2,580	4%
Pu-239	5.7E-05	2,511	4.3E-05	2,520	-25%
U-234	9.0E-02	2,516	6.4E-02	2,520	-18%
Ra-226	3.0E-07	2,507	1.2E-06	2,510	300%
Am-241	3.0E-04	2,520	7.2E-04	2,540	140%
Np-237	2.4E-00	2,513	4.0E-01	2,520	-83%

Figure A.4-17: Tank 13 I-129 Release to the Saturated Zone for Case E

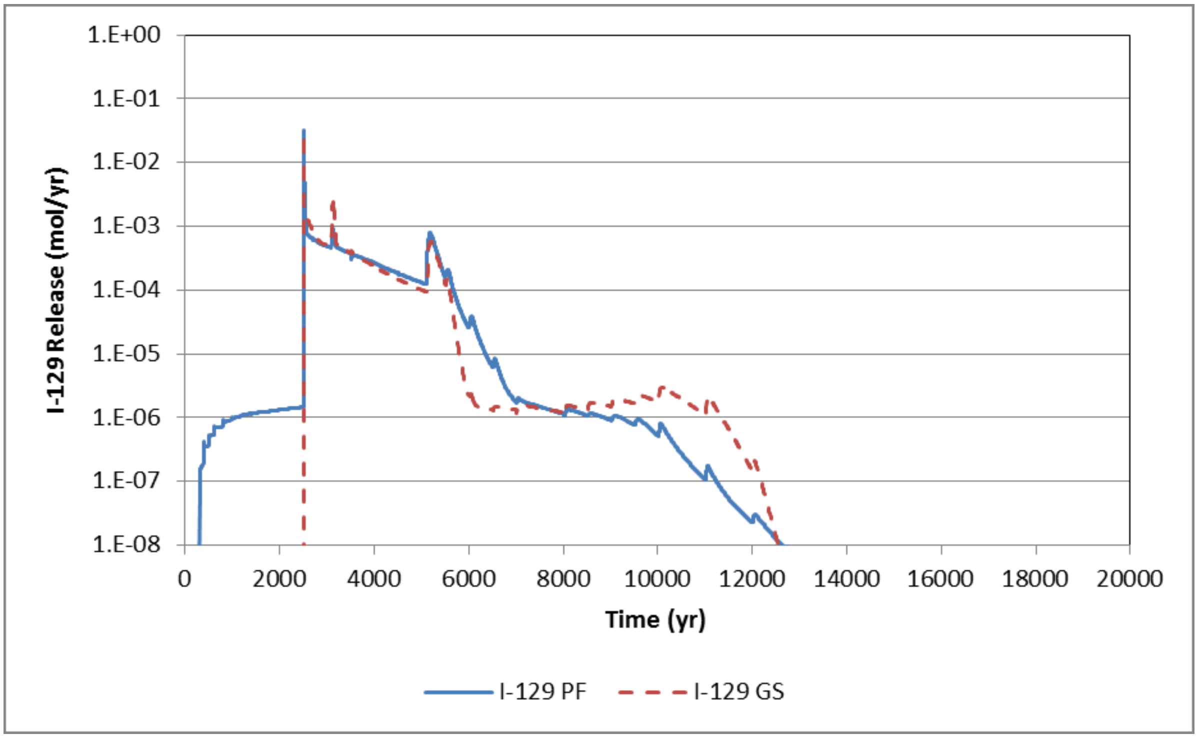

Figure A.4-18: Tank 13 Tc-99 Release to the Saturated Zone for Case E

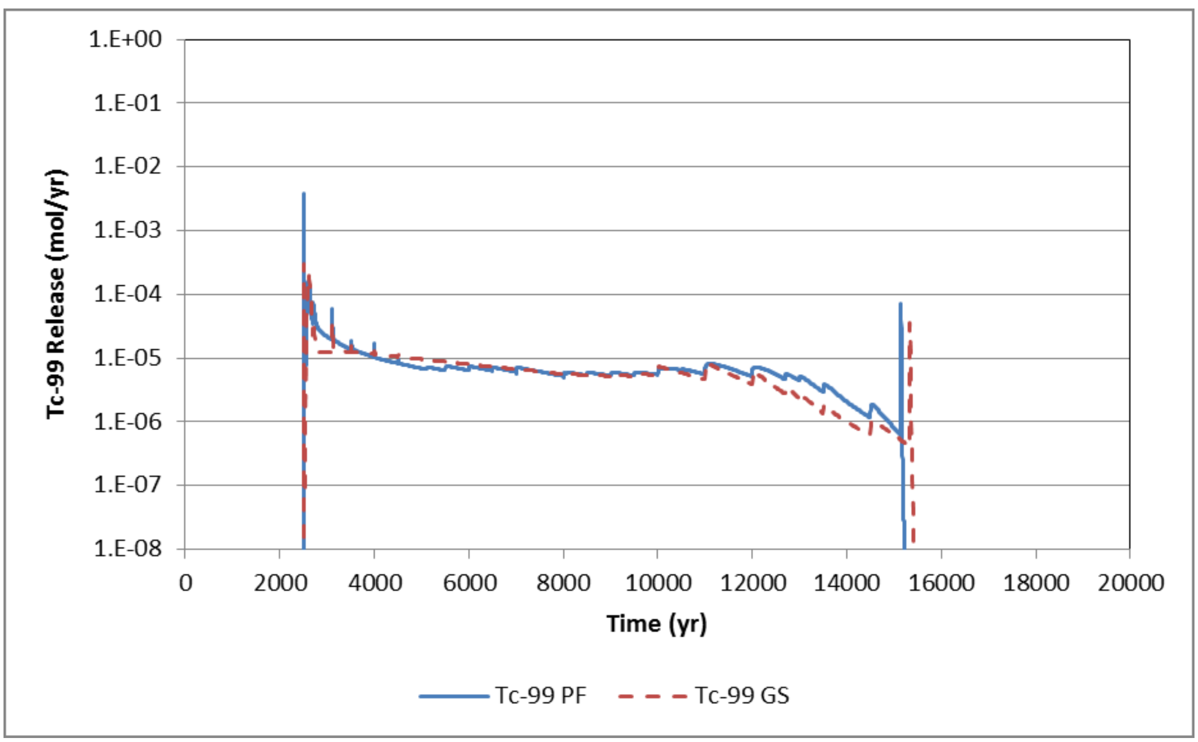

Figure A.4-19: Tank 13 Am-243 Release to the Saturated Zone for Case E

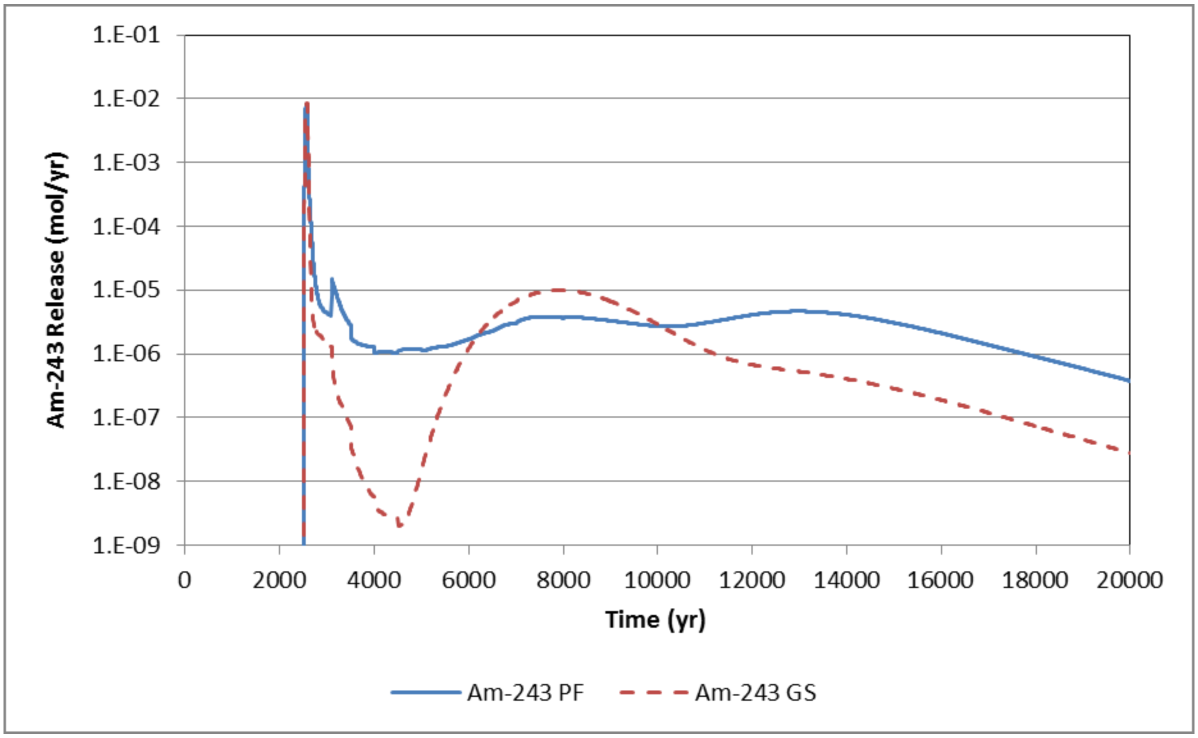

Figure A.4-20: Tank 13 Pu-239 Release to the Saturated Zone for Case E

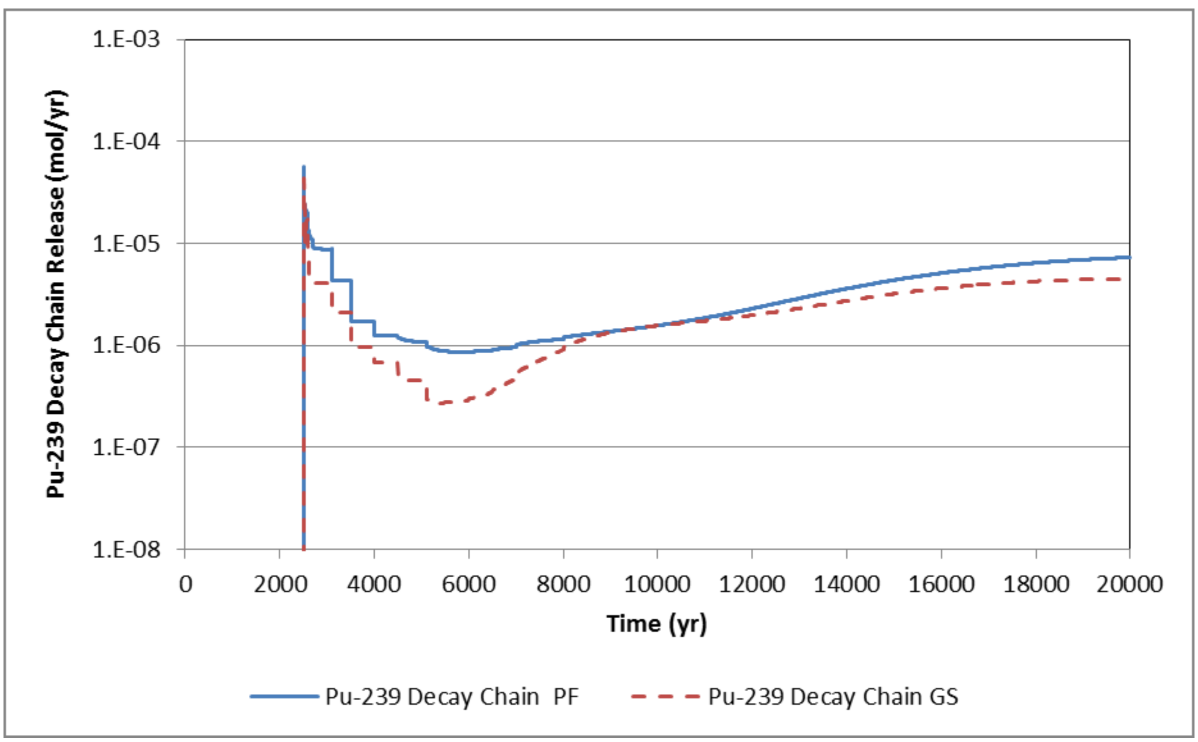

Figure A.4-21: Tank 13 U-234 Release to the Saturated Zone for Case E

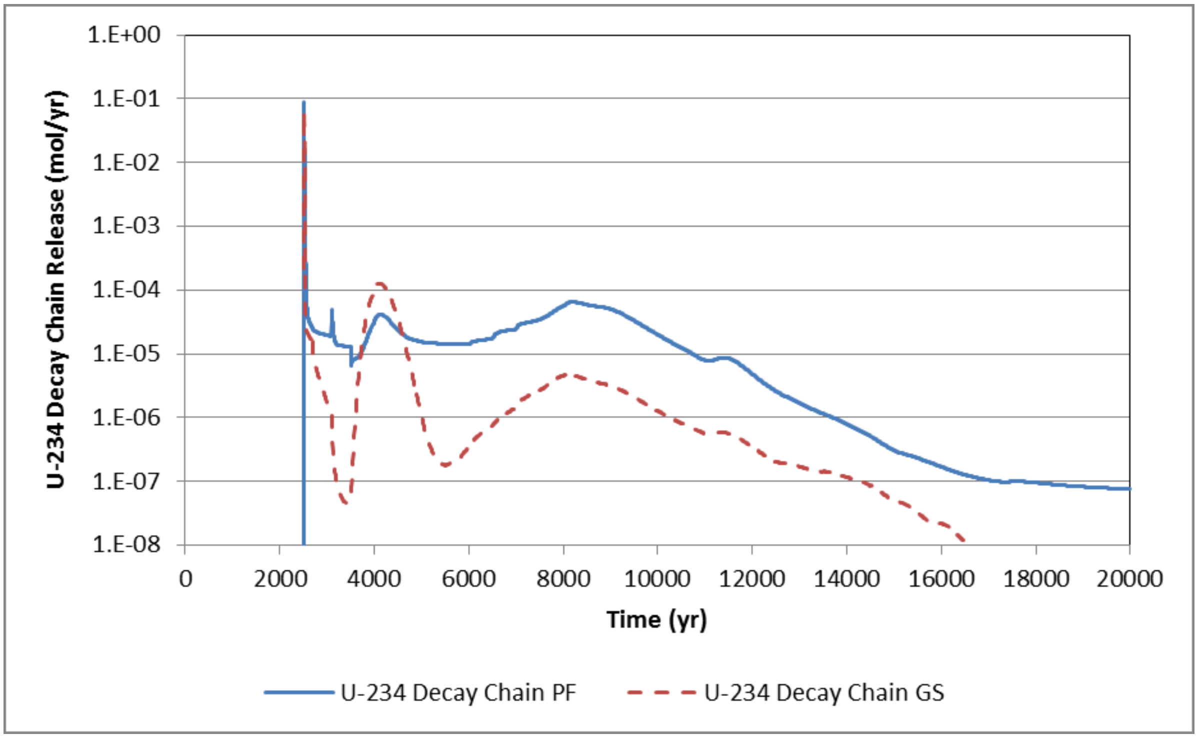

Figure A.4-22: Tank 13 Ra-226 Release to the Saturated Zone for Case E

Figure A.4-23: Tank 13 Am-241 Release to the Saturated Zone for Case E

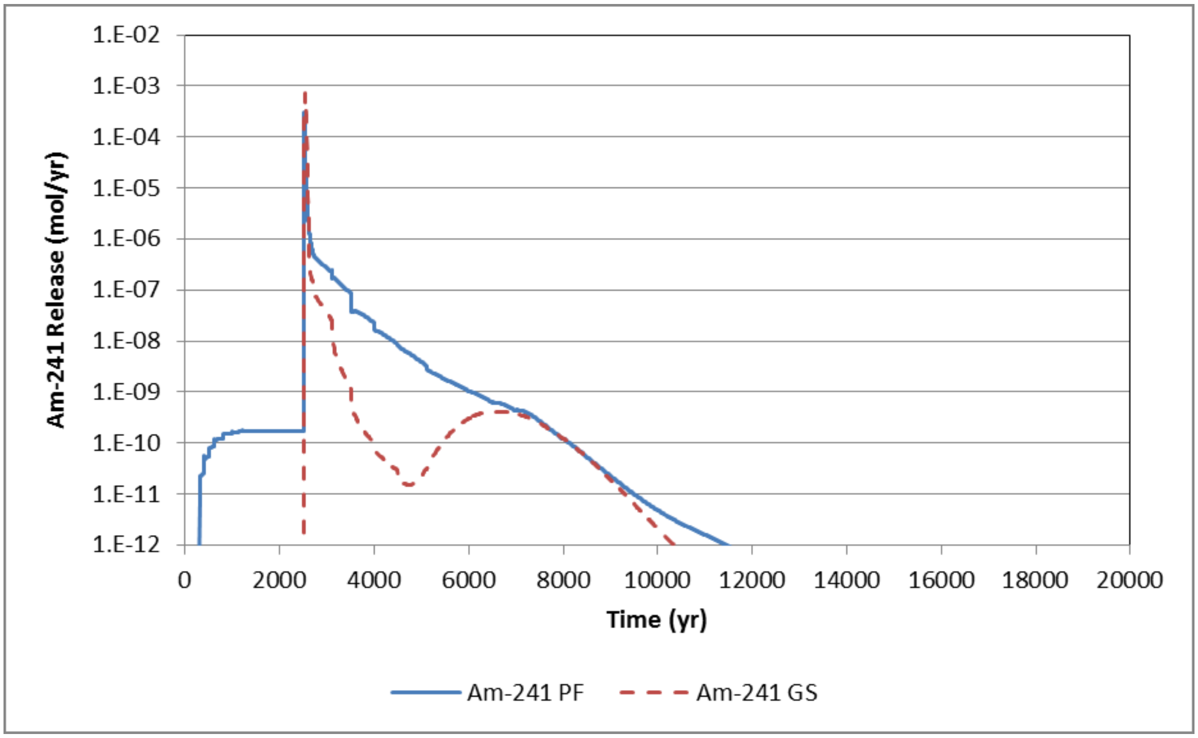

Figure A.4-24: Tank 13 Np-237 Release to the Saturated Zone for Case E

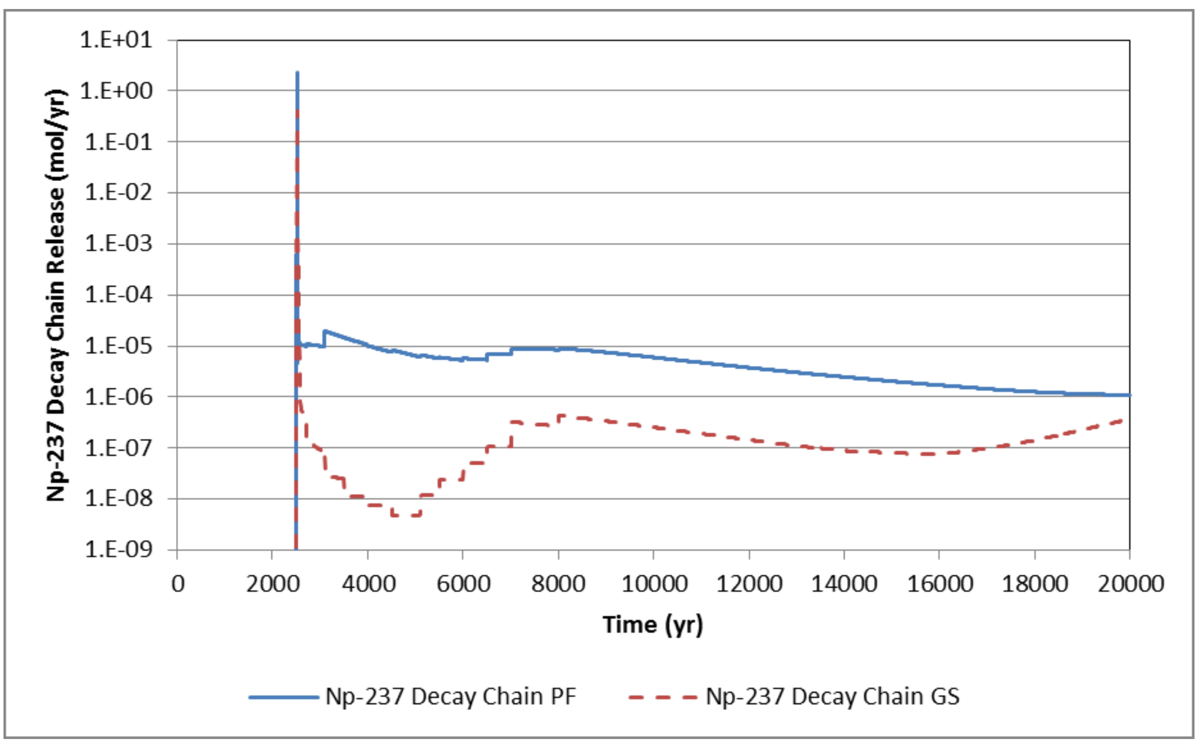

A.4.4 Type II Tank with Failed Liner (Tank 15) for Case E

For the Case E configuration, a comparison of the PORFLOW HTF Model and the GoldSim model mass releases of I-129, Tc-99, Am-243, Pu-239, U-234, Ra-226, Am-241, and Np-237, as presented in Figure A.4-25 through Figure A.4-32, indicate that the GoldSim model successfully captures the radionuclide release patterns seen in Tank 15 results generated by the PORFLOW model.

Table A.4-4 summarizes the peak values for these releases showing that when comparing the two models although not all of the percent differences are below 50%, the compared values are reasonably close when considered in conjunction with the release patterns shown in Figure A.4-25 through Figure A.4-32.

Table A.4-4: Case E GoldSim and PORFLOW Model Peak Releases from the UZ to the SZ Comparisons for Tank 15 within 20,000 years

Radionuclide	PORFLOW Peak Release (mol/yr)	PORFLOW Time of Peak Release (yr)	GoldSim Peak Release (mol/yr)	GoldSim Time of Peak Release (yr)	Peak Release Percent Difference GoldSim vs PORFLOW
I-129	3.7E-03	201	2.0E-03	110	-46%
Tc-99	1.1E-04	15,082	2.4E-05	15,330	-78%
Am-243	3.3E-03	646	3.5E-03	650	6%
Pu-239	1.8E-05	601	1.7E-05	610	-6%
U-234	1.0E-02	369	8.2E-03	370	-18%
Ra-226	7.8E-08	301	9.8E-08	310	26%
Am-241	3.2E-03	657	3.3E-03	660	3%
Np-237	2.9E-01	343	2.2E-01	340	-24%

Figure A.4-25: Tank 15 I-129 Release to the Saturated Zone for Case E

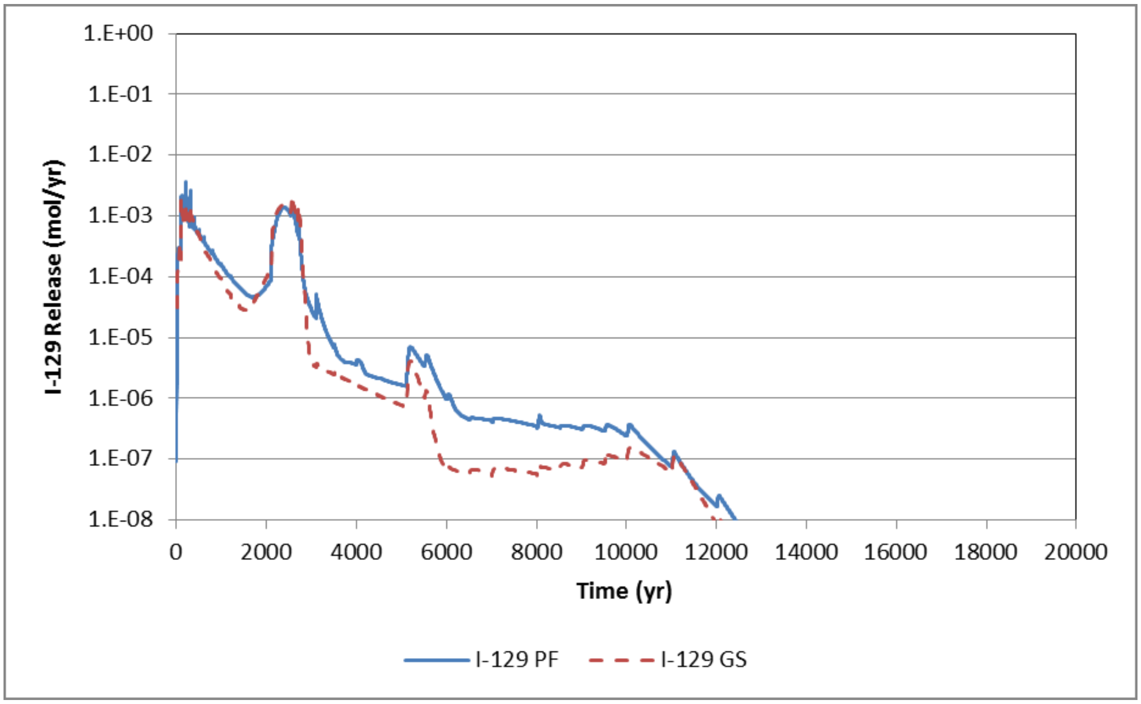

Figure A.4-26: Tank 15 Tc-99 Release to the Saturated Zone for Case E

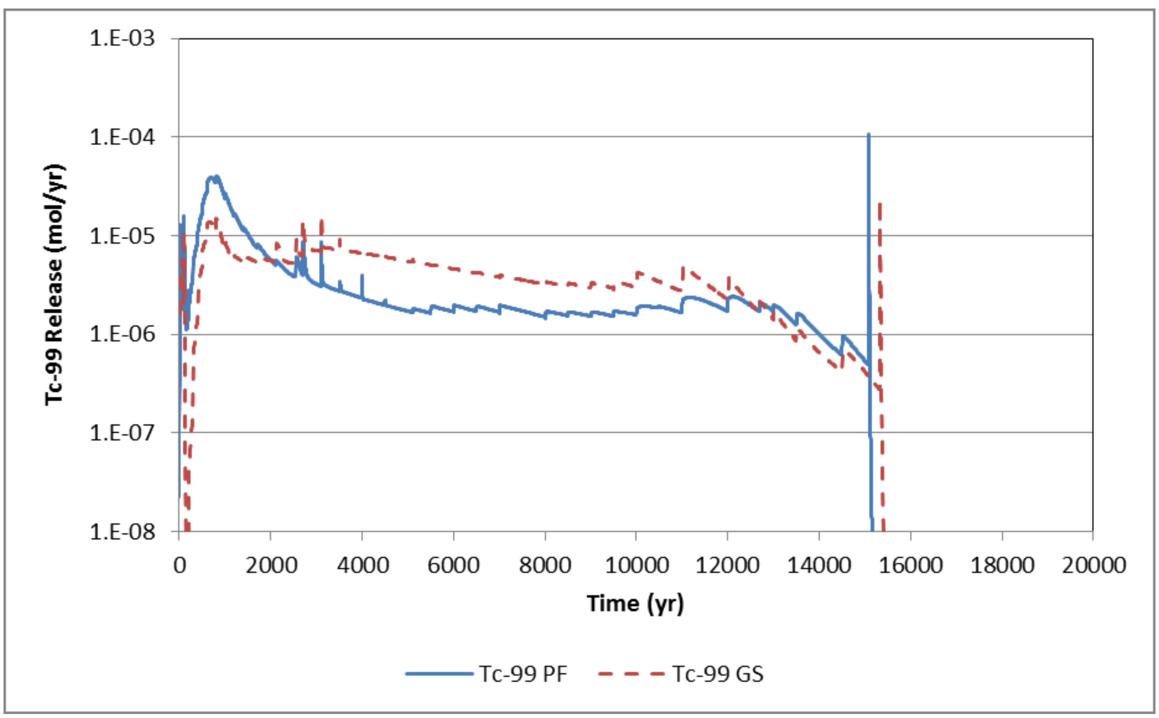

Figure A.4-27: Tank 15 Am-243 Release to the Saturated Zone for Case E

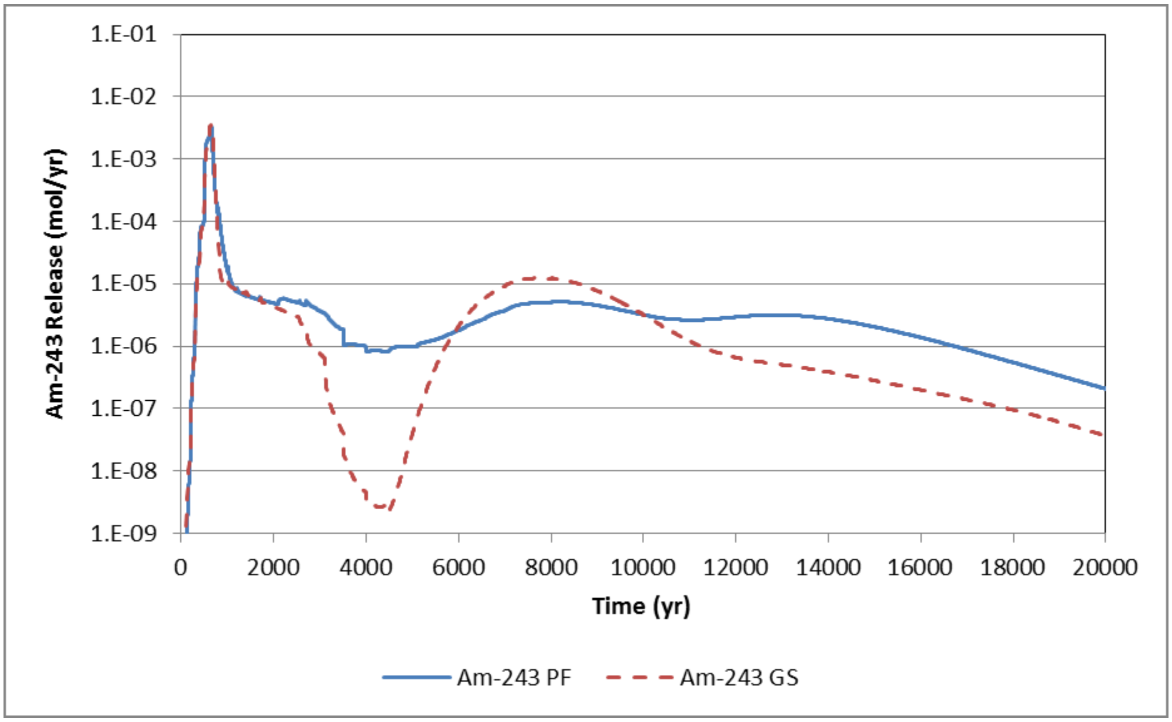

Figure A.4-28: Tank 15 Pu-239 Release to the Saturated Zone for Case E

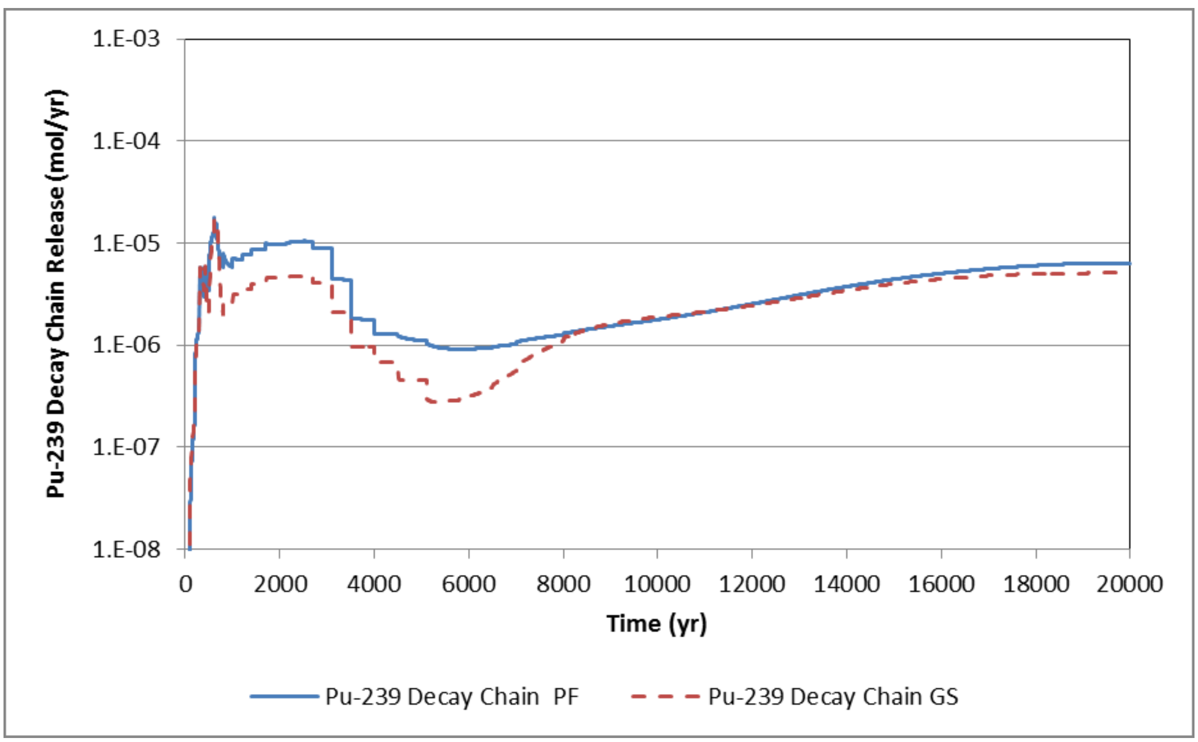

Figure A.4-29: Tank 15 U-234 Release to the Saturated Zone for Case E

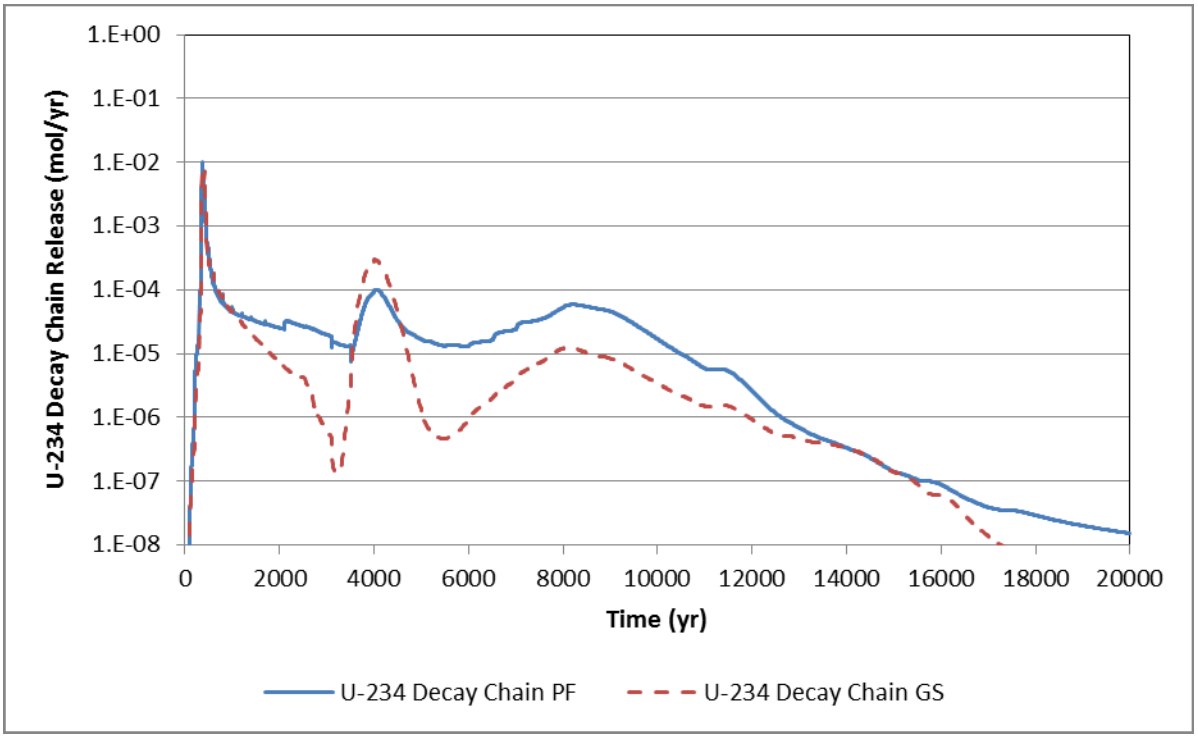

Figure A.4-30: Tank 15 Ra-226 Release to the Saturated Zone for Case E

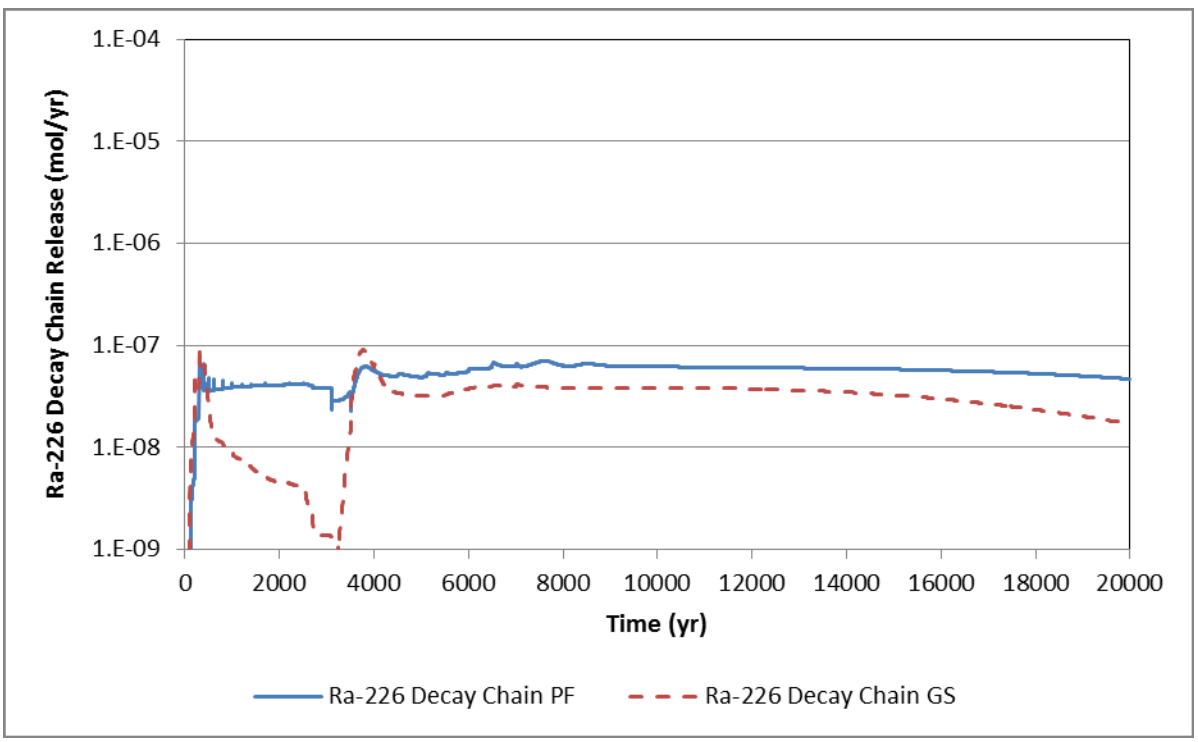

Figure A.4-31: Tank 15 Am-241 Release to the Saturated Zone for Case E

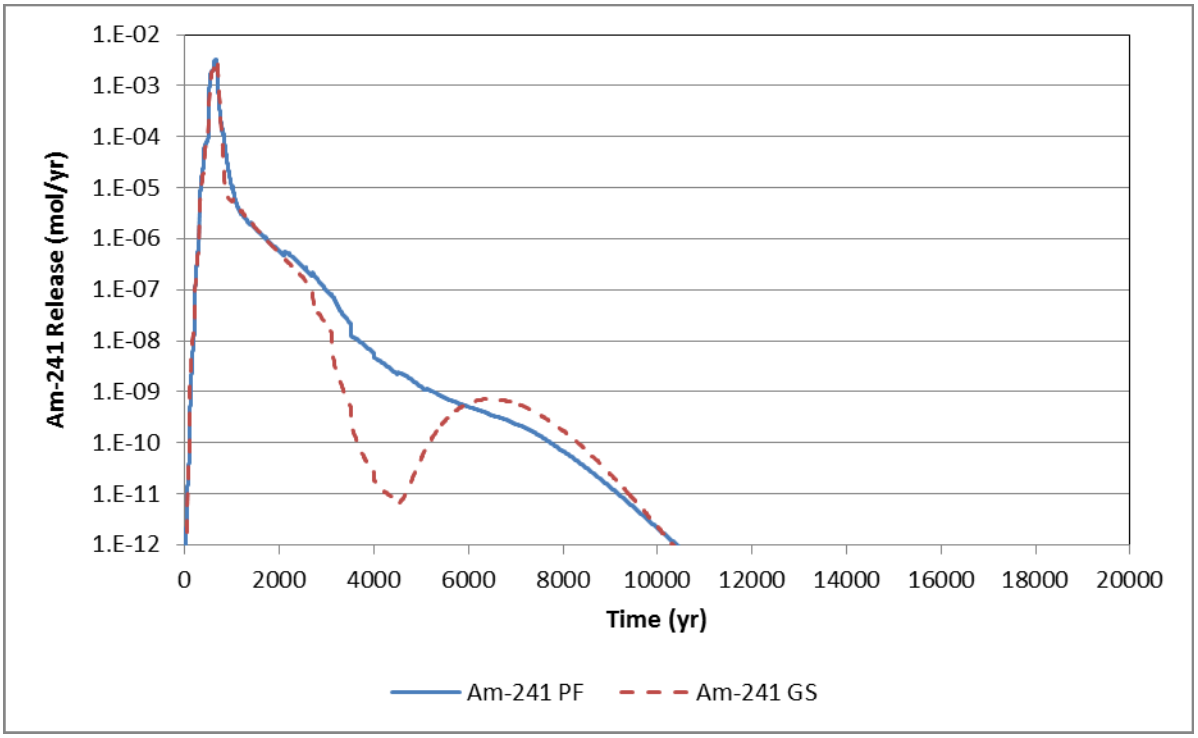

Figure A.4-32: Tank 15 Np-237 Release to the Saturated Zone for Case E

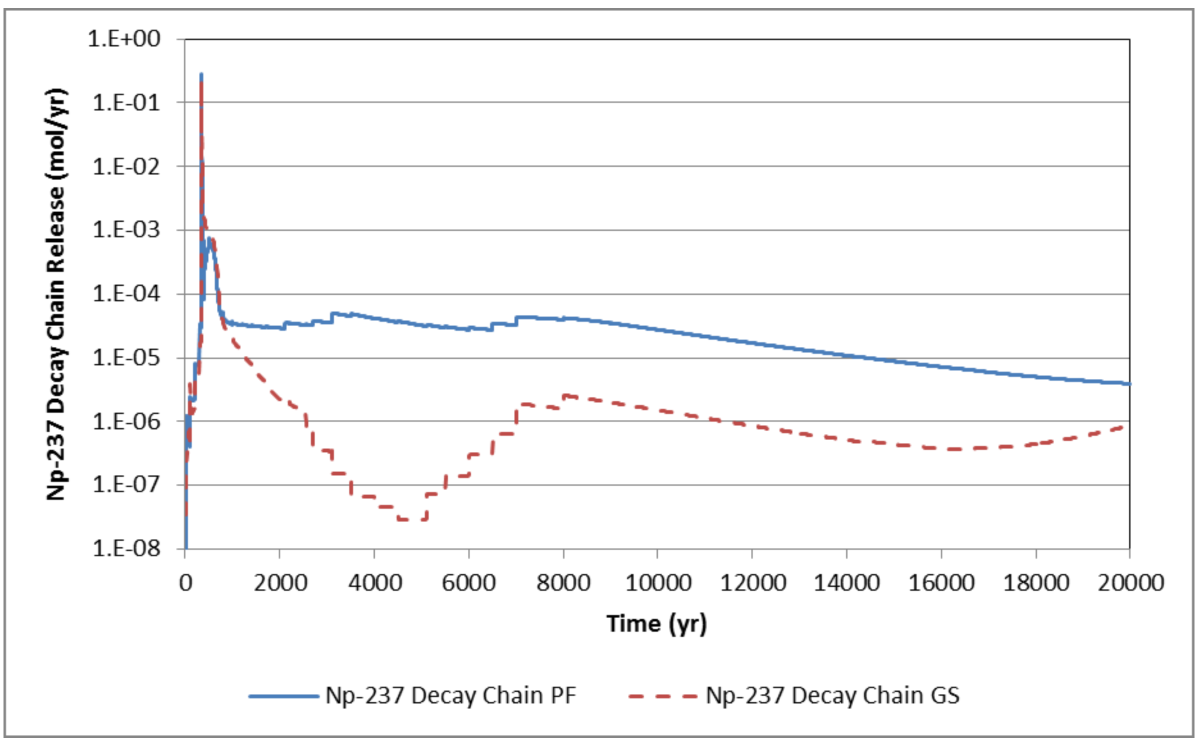

A.4.5 Type II Tank with Failed Liner (Tank 16) for Case E

For the Case E configuration, a comparison of the PORFLOW HTF Model and the GoldSim model mass releases of I-129, Tc-99, Am-243, Pu-239, U-234, Ra-226, Am-241, and Np-237, as presented in Figure A.4-33 through Figure A.4-40, indicate that the GoldSim model successfully captures the radionuclide release patterns seen in Tank 16 results generated by the PORFLOW model.

Table A.4-5 summarizes the peak values for these releases showing that when comparing the two models although not all of the percent differences are below 50%, the compared values are reasonably close when considered in conjunction with the release patterns shown in Figure A.4-33 through Figure A.4-40. The first row for U-234 in Table A.4-5 presents the peak values for each model and the second row for U-234 presents the peak PORFLOW model value along with the GoldSim model value at the same time. The position of the GoldSim model result in the sorted (from high to low) data is noted in parentheses.

Table A.4-5: Case E GoldSim and PORFLOW Model Peak Releases from the UZ to the SZ Comparisons for Tank 16 within 20,000 years

Radionuclide	PORFLOW Peak Release (mol/yr)	PORFLOW Time of Peak Release (yr)	GoldSim Peak Release (mol/yr)	GoldSim Time of Peak Release (yr)	Peak Release Percent Difference GoldSim vs PORFLOW
I-129	8.0E-04	2,551	1.2E-03	2,560	50%
Tc-99	2.0E-03	15,082	4.6E-04	15,330	-77%
Am-243	4.2E-08	401	5.6E-08	410	33%
Pu-239	7.1E-05	303	7.2E-05	320	1%
U-234	2.7E-05	4,001	4.9E-05	330	81%
U-234 (#7)	2.7E-05	4,001	2.5E-05	4010	-7%
Ra-226	5.2E-09	3,788	7.0E-09	3,780	35%
Am-241	1.4E-06	401	2.1E-06	410	50%
Np-237	1.0E-02	342	4.6E-03	340	-54%

Figure A.4-33: Tank 16 I-129 Release to the Saturated Zone for Case E

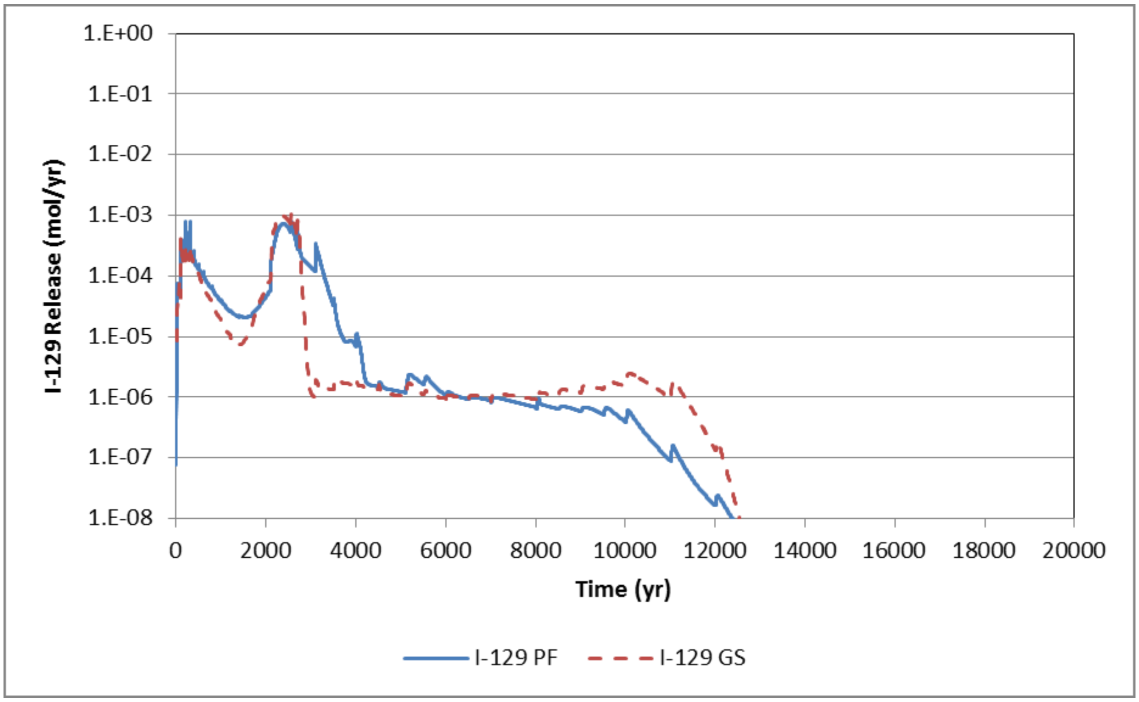

Figure A.4-34: Tank 16 Tc-99 Release to the Saturated Zone for Case E

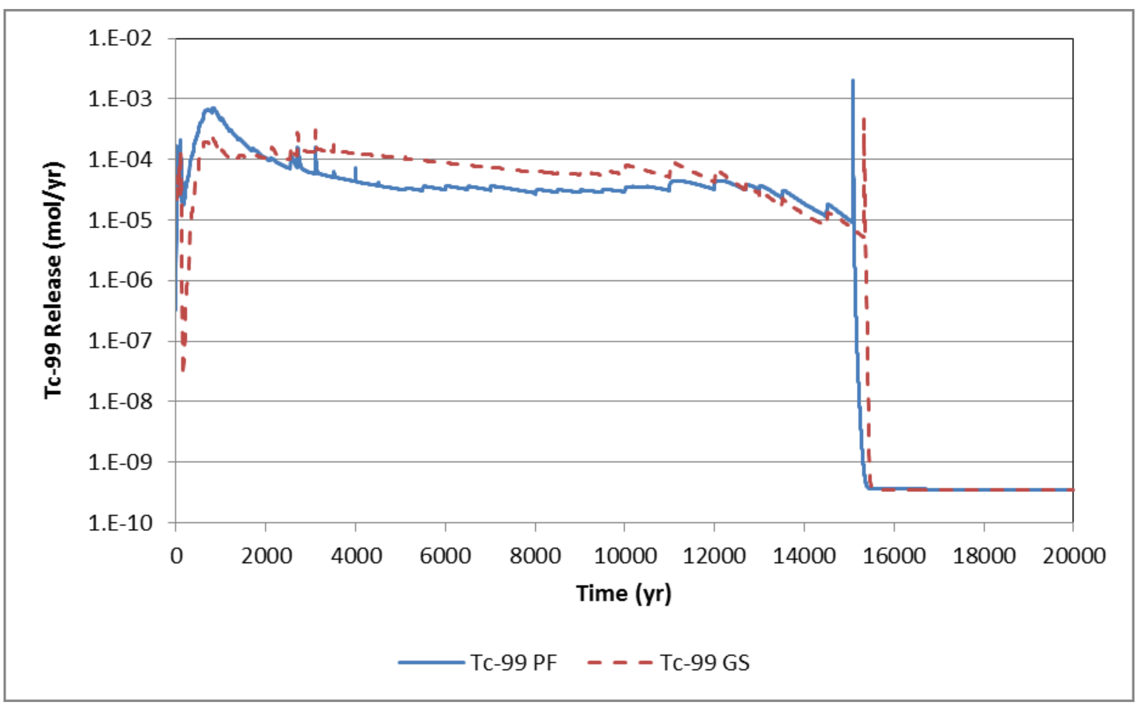

Figure A.4-35: Tank 16 Am-243 Release to the Saturated Zone for Case E

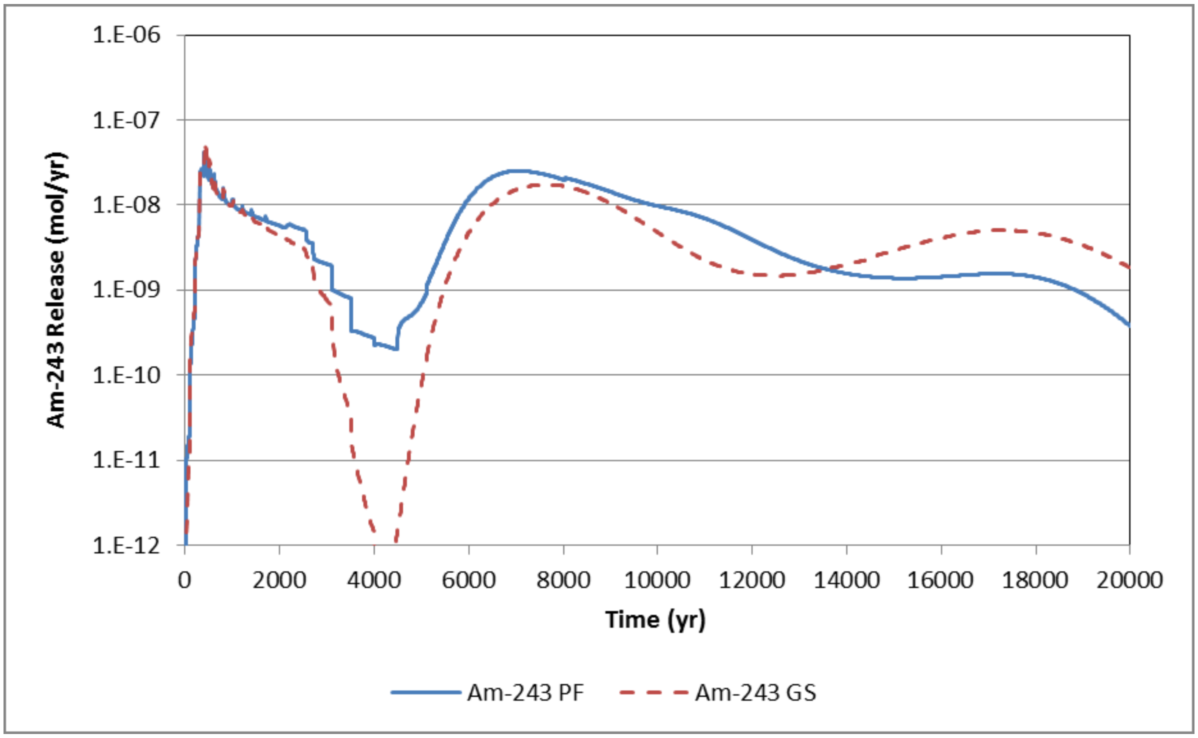

Figure A.4-36: Tank 16 Pu-239 Release to the Saturated Zone for Case E

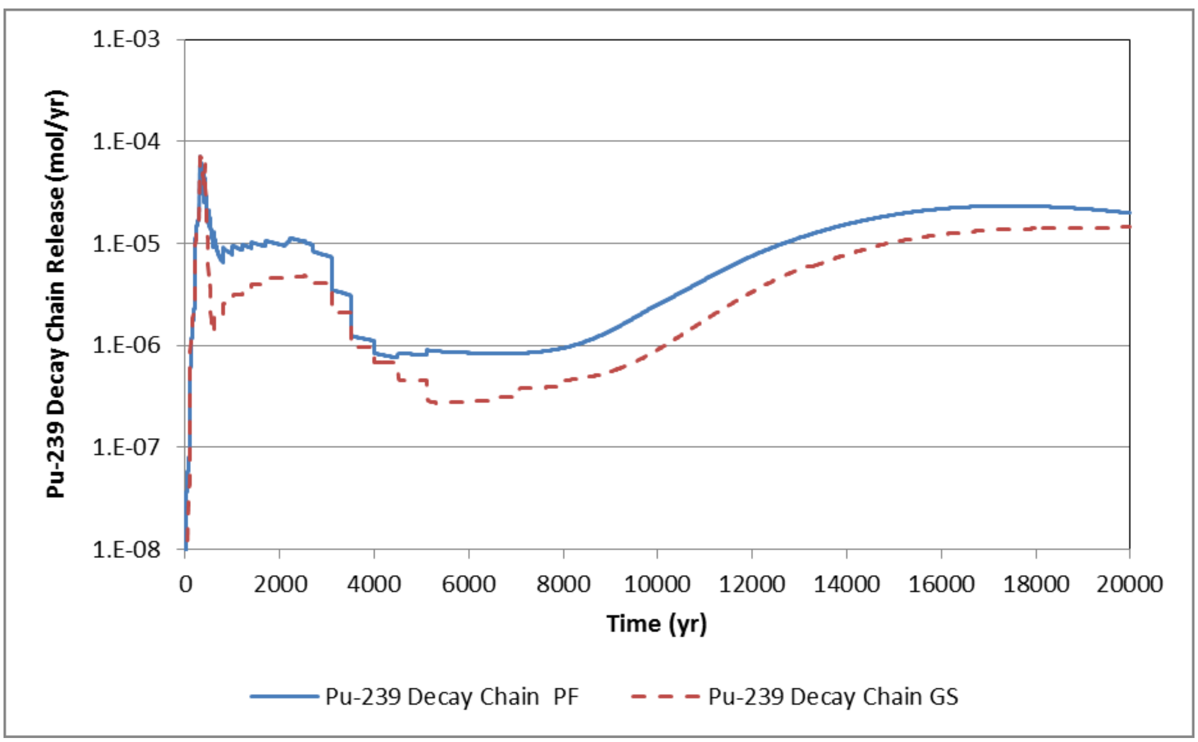

Figure A.4-37: Tank 16 U-234 Release to the Saturated Zone for Case E

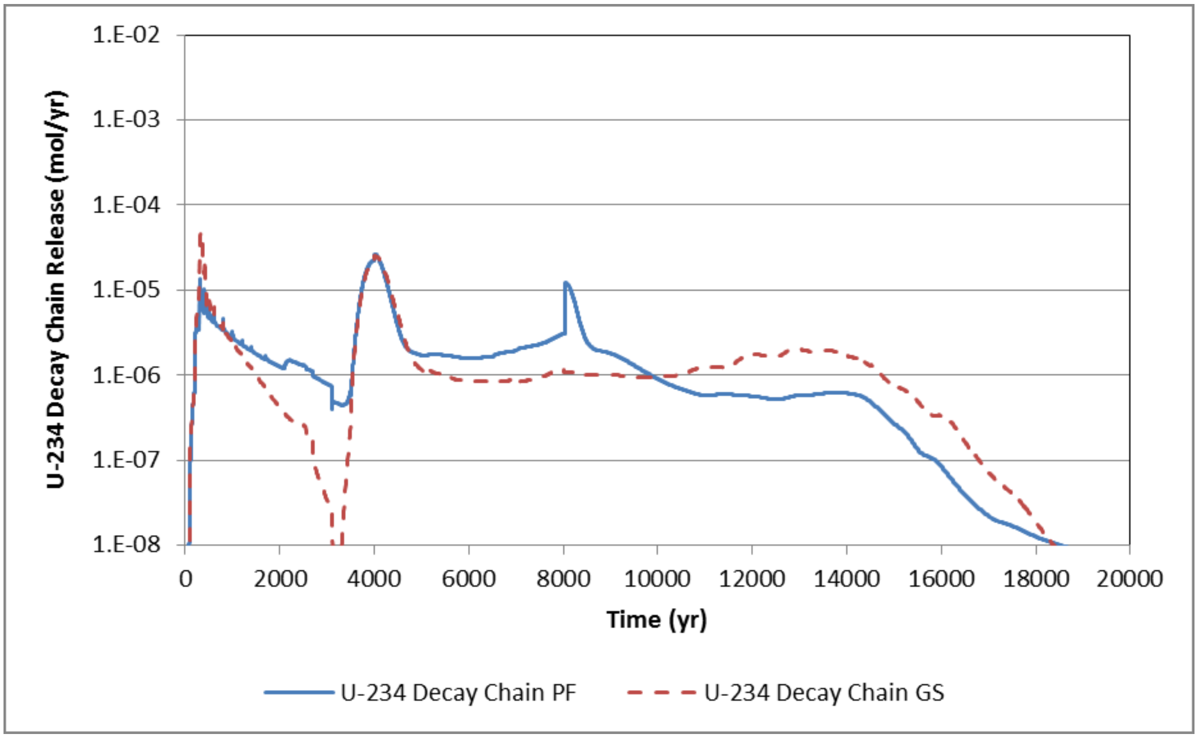

Figure A.4-38: Tank 16 Ra-226 Release to the Saturated Zone for Case E

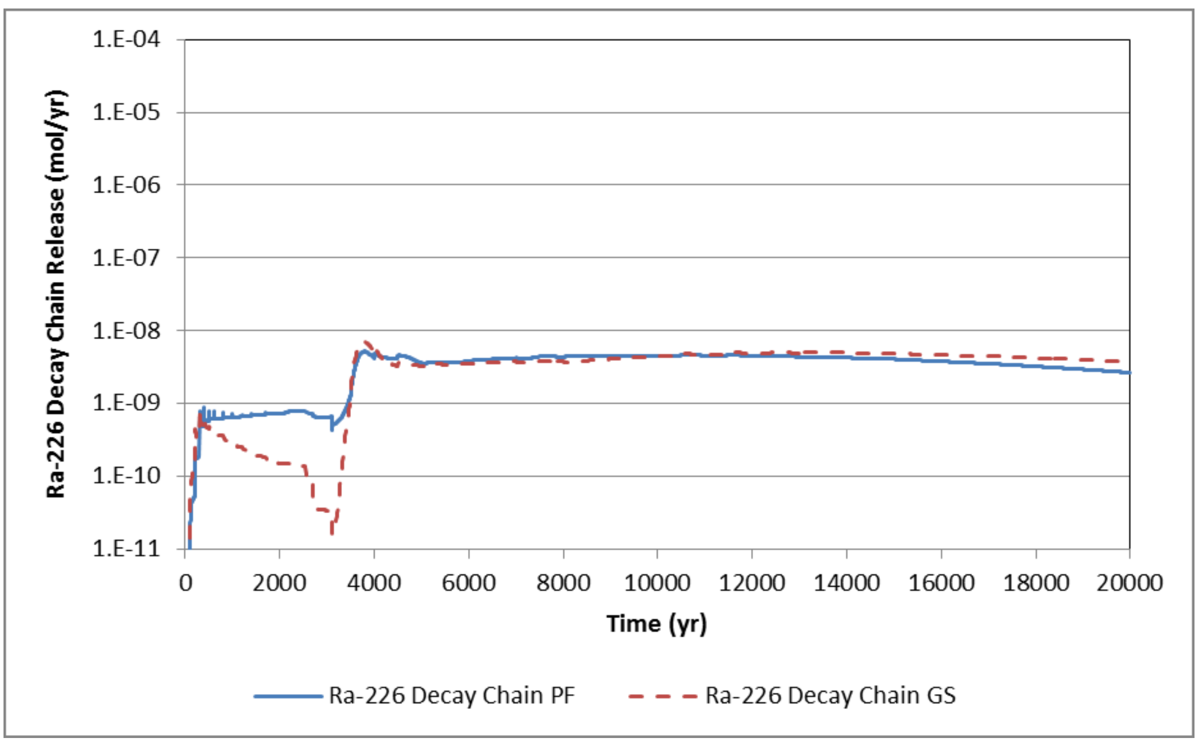

Figure A.4-39: Tank 16 Am-241 Release to the Saturated Zone for Case E

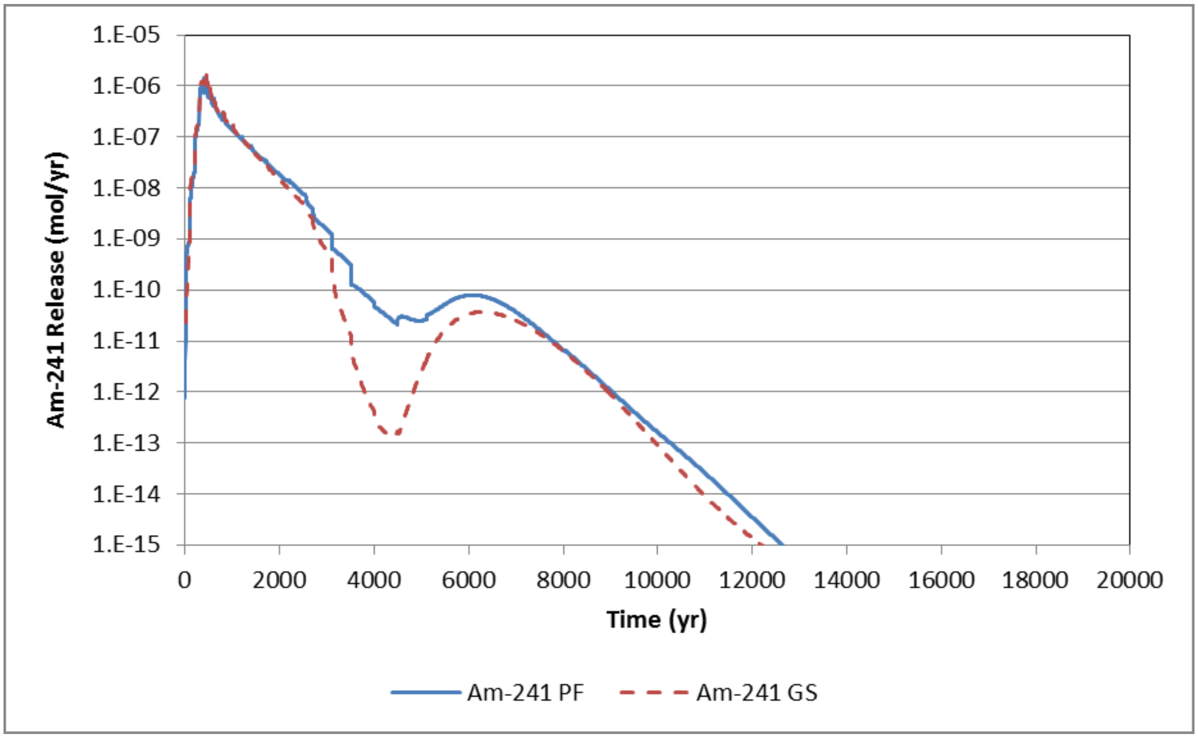

Figure A.4-40: Tank 16 Np-237 Release to the Saturated Zone for Case E

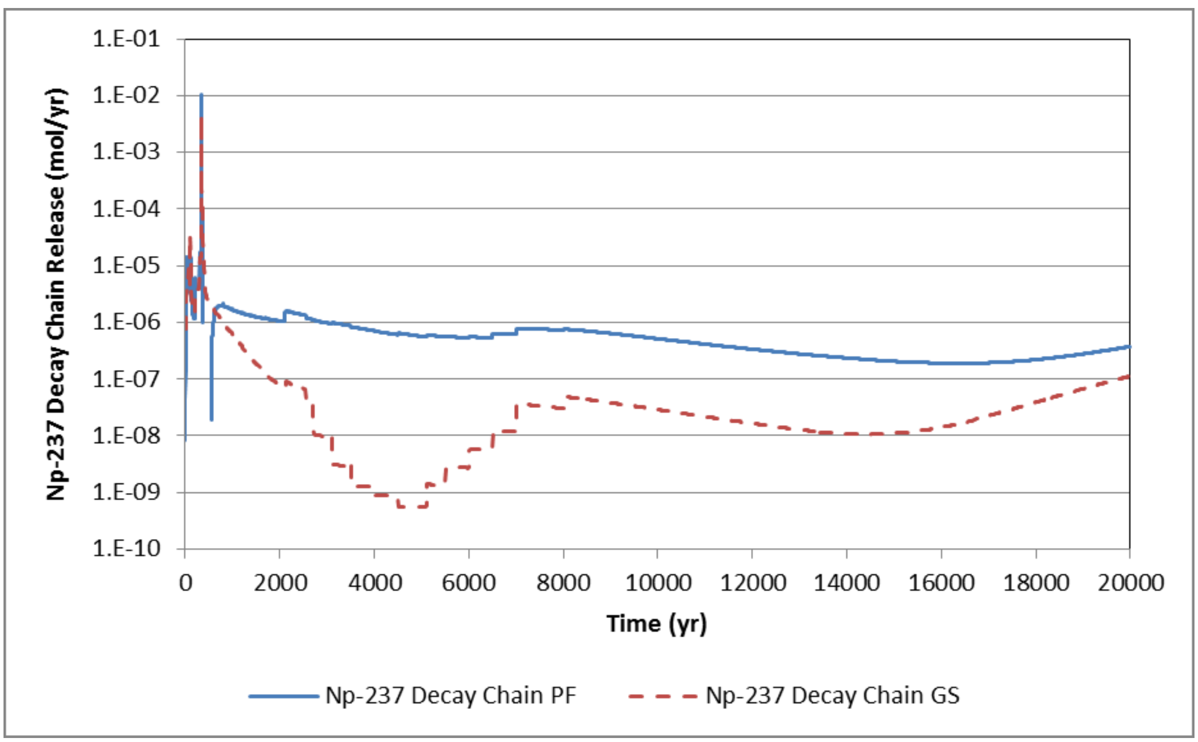

A.4.6 Type IV Tank (Tank 24) fo Case E

For the Case E configuration, a comparison of the PORFLOW HTF Model and the GoldSim model mass releases of I-129, Tc-99, Am-243, Pu-239, U-234, Ra-226, Am-241, and Np-237, as presented in Figure A.4-41 through Figure A.4-48, indicate that the GoldSim model successfully captures the radionuclide release patterns seen in Tank 24 results generated by the PORFLOW model.

Table A.4-6 summarizes the peak values for these releases showing that when comparing the two models although not all of the percent differences are below 50%, the compared values are reasonably close when considered in conjunction with the release patterns shown in Figure A.4-41 through Figure A.4-48.

Table A.4-6: Case E GoldSim and PORFLOW Model Peak Releases from the UZ to the SZ Comparisons for Tank 24 within 20,000 years

Radionuclide	PORFLOW Peak Release (mol/yr)	PORFLOW Time of Peak Release (yr)	GoldSim Peak Release (mol/yr)	GoldSim Time of Peak Release (yr)	Peak Release Percent Difference GoldSim vs PORFLOW
I-129	3.7E-05	501	4.5E-05	530	22%
Tc-99	3.6E-09	531	3.0E-09	550	-17%
Am-243	3.8E-07	11,712	5.0E-07	11,030	32%
Pu-239	3.5E-06	16,527	4.5E-06	14,700	29%
U-234	6.3E-06	6,135	8.4E-06	5,010	33%
Ra-226	5.6E-08	2,838	5.1E-08	1,790	-9%
Am-241	2.8E-11	2,959	8.1E-12	4,570	-71%
Np-237	9.8E-06	8,753	1.2E-05	6,590	22%

Figure A.4-41: Tank 24 I-129 Release to the Saturated Zone for Case E

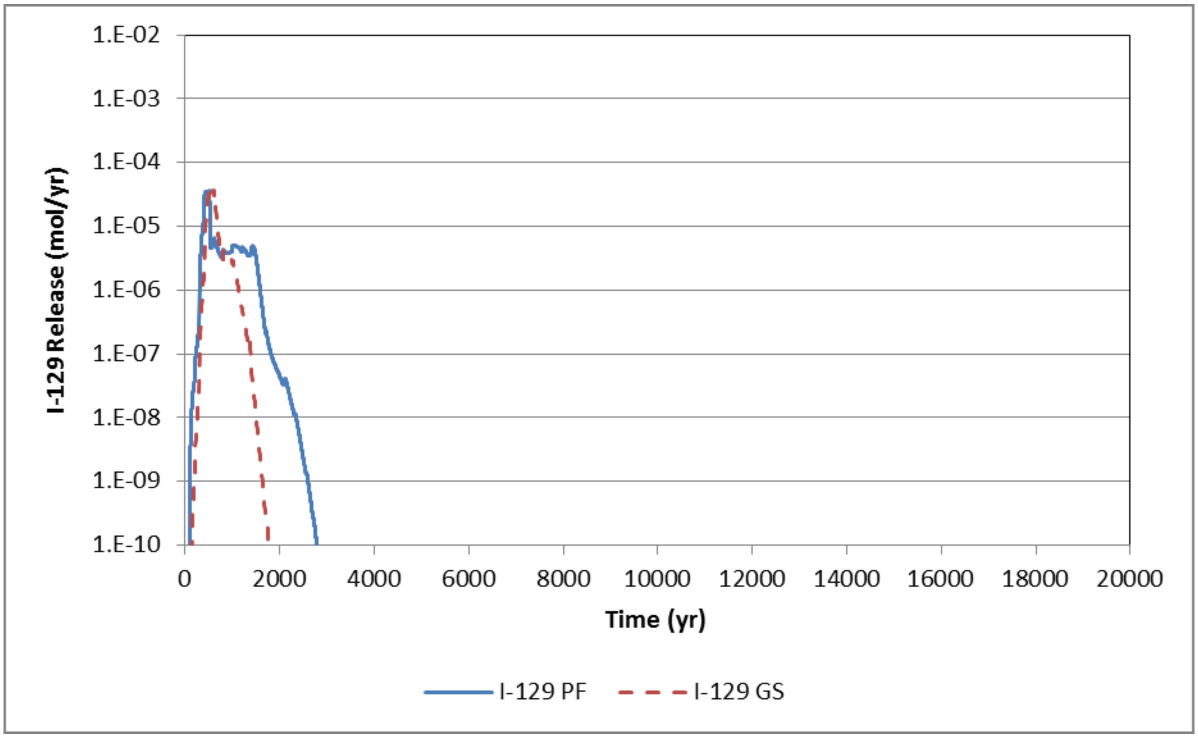

Figure A.4-42: Tank 24 Tc-99 Release to the Saturated Zone for Case E

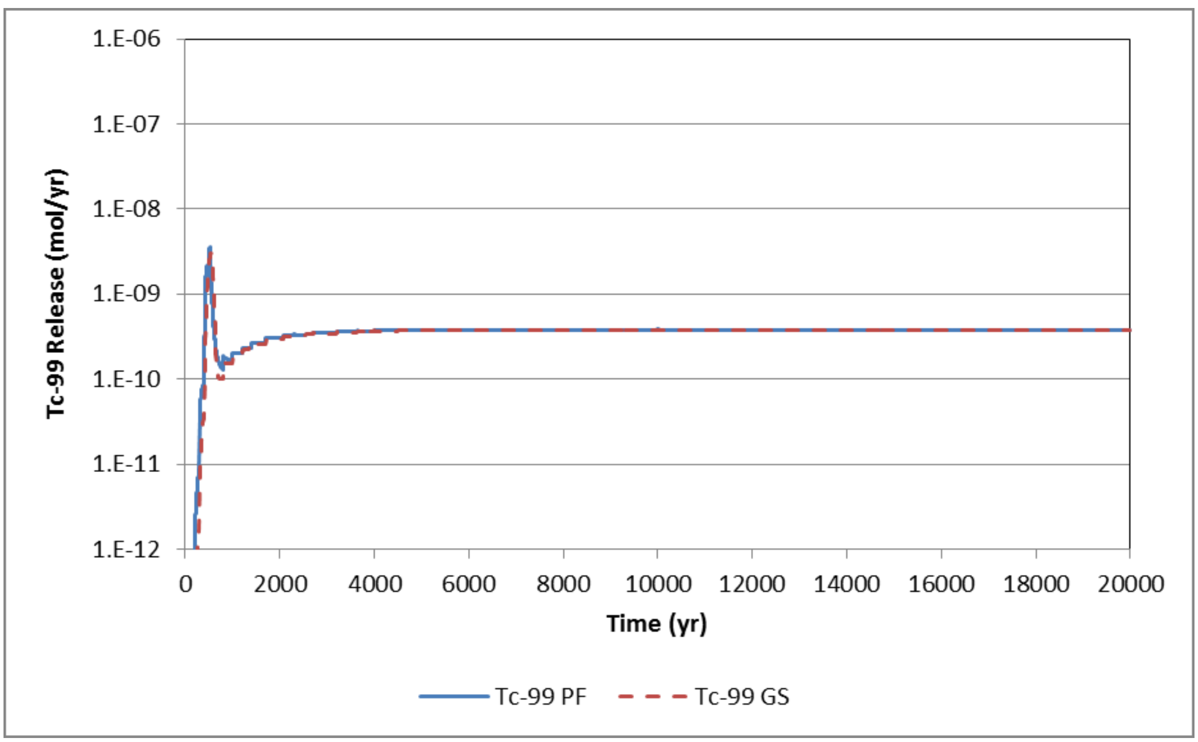

Figure A.4-43: Tank 24 Am-243 Release to the Saturated Zone for Case E

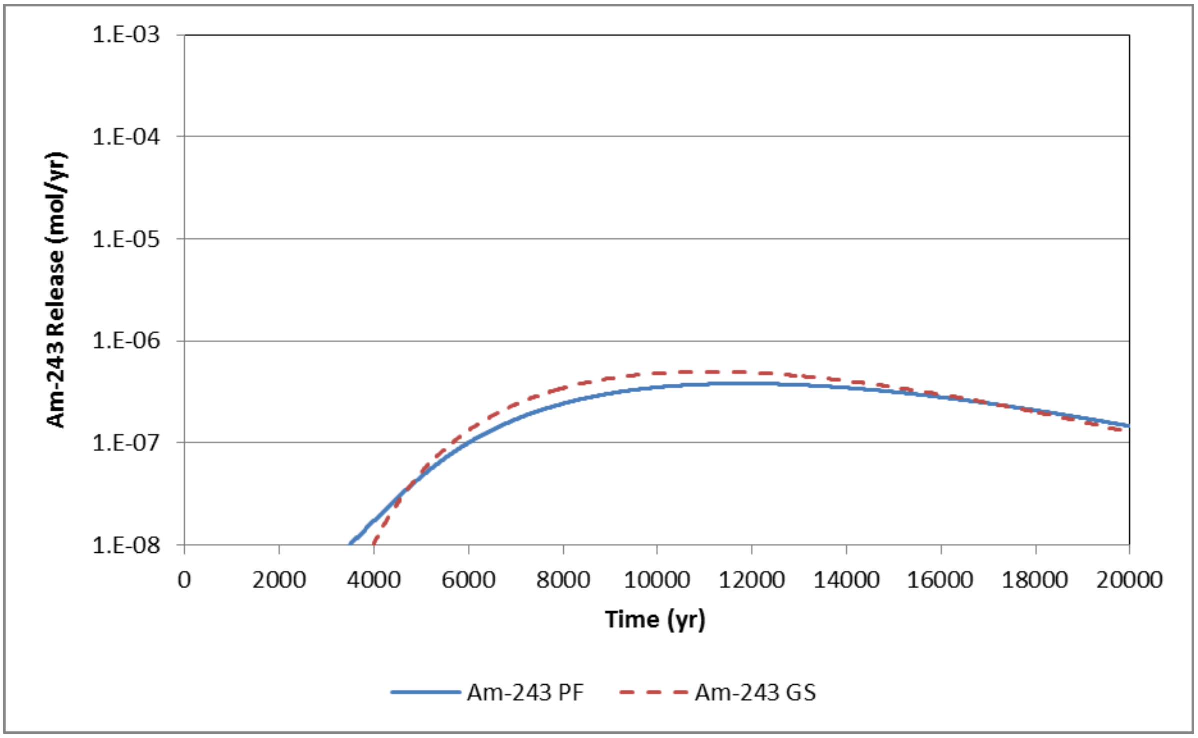

Figure A.4-44: Tank 24 Pu-239 Release to the Saturated Zone for Case E

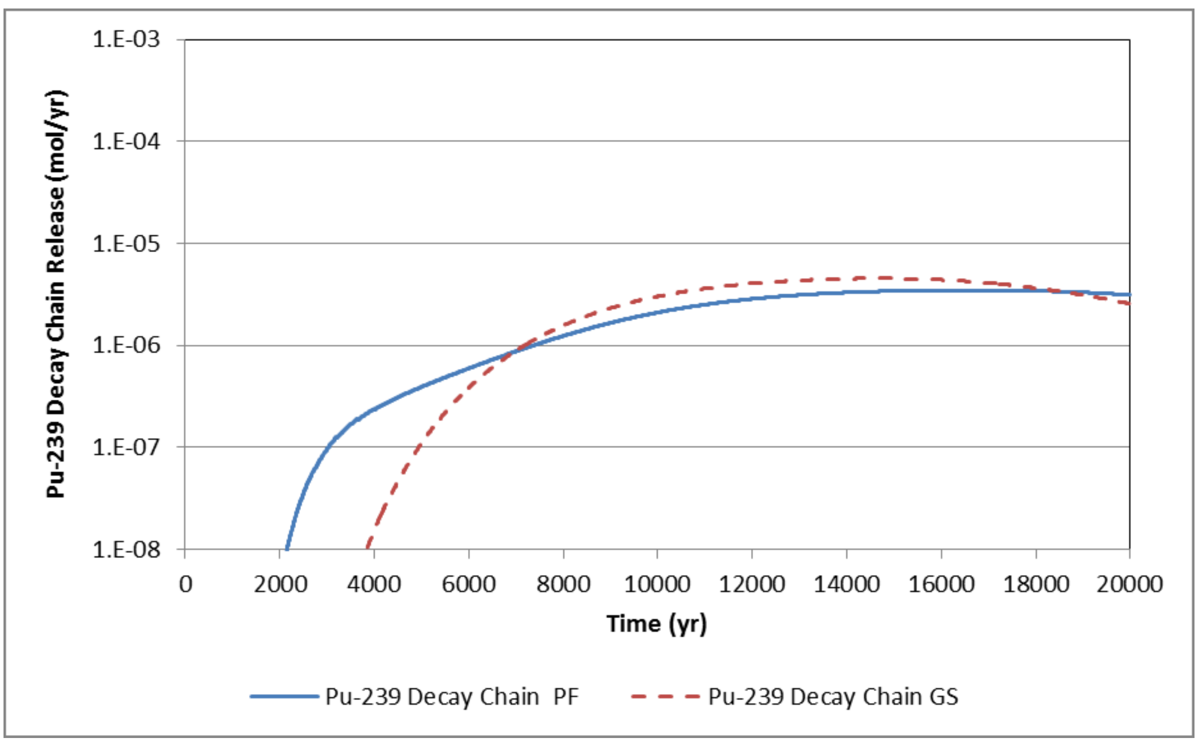

Figure A.4-45: Tank 24 U-234 Release to the Saturated Zone for Case E

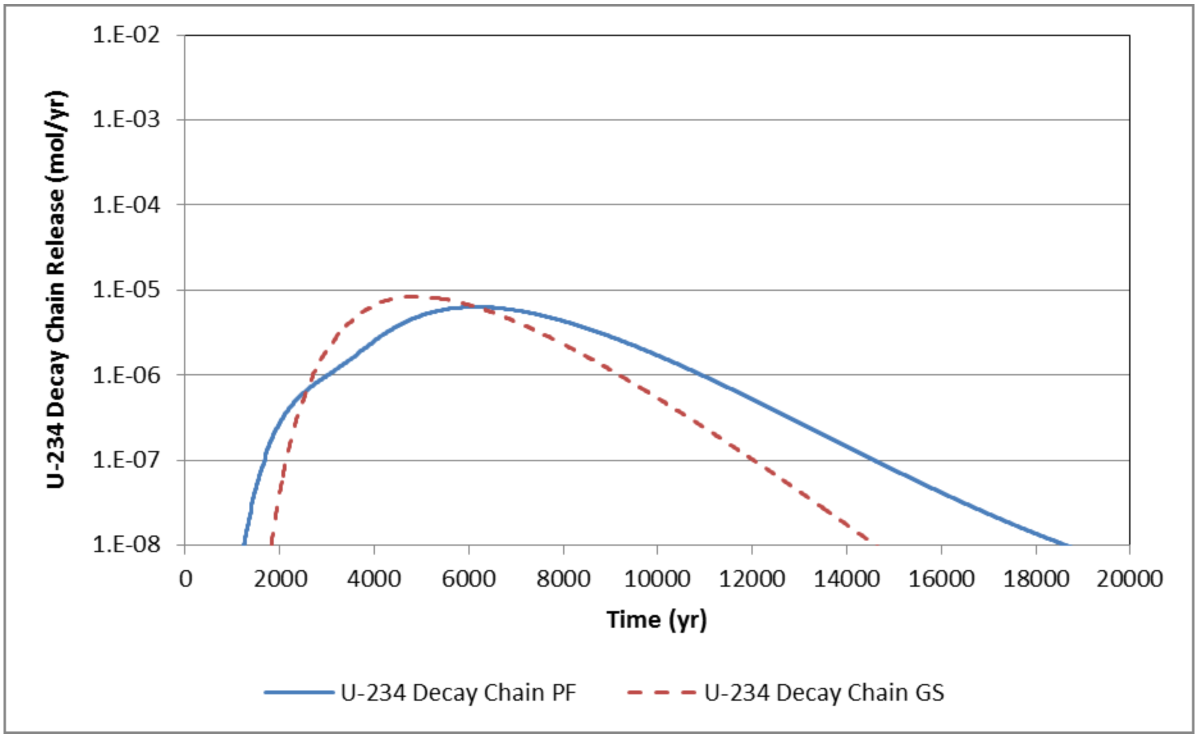

Figure A.4-46: Tank 24 Ra-226 Release to the Saturated Zone for Case E

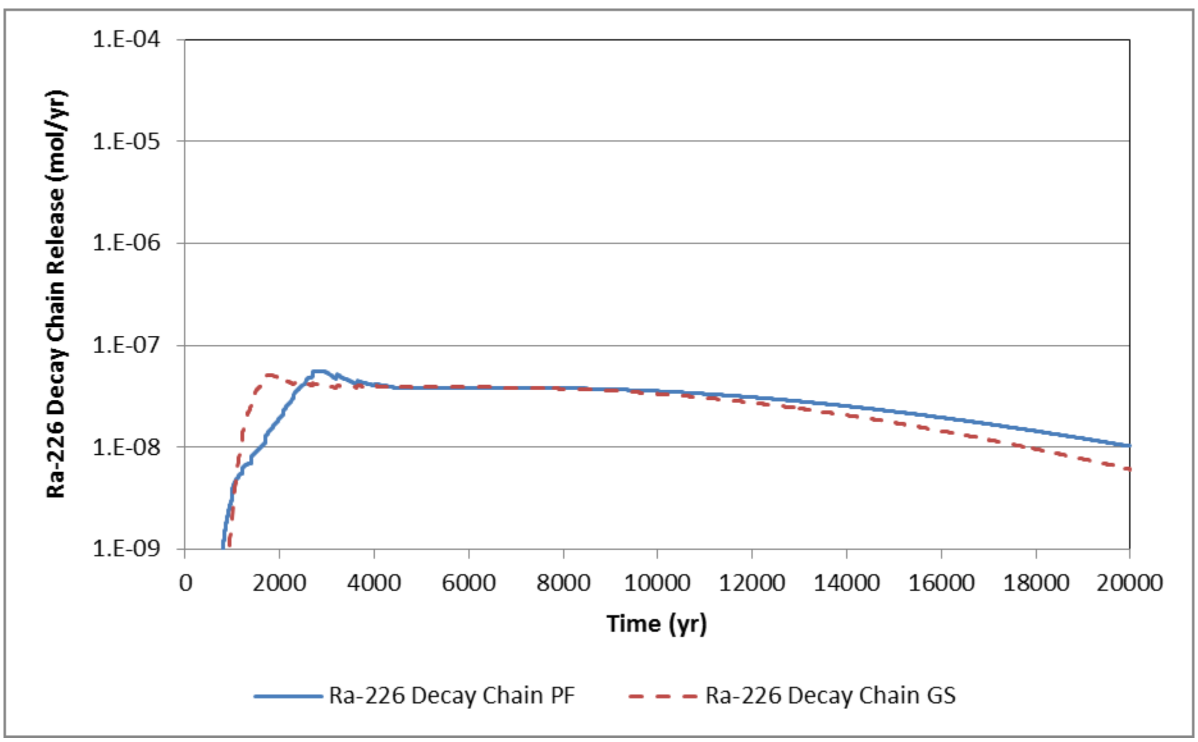

Figure A.4-47: Tank 24 Am-241 Release to the Saturated Zone for Case E

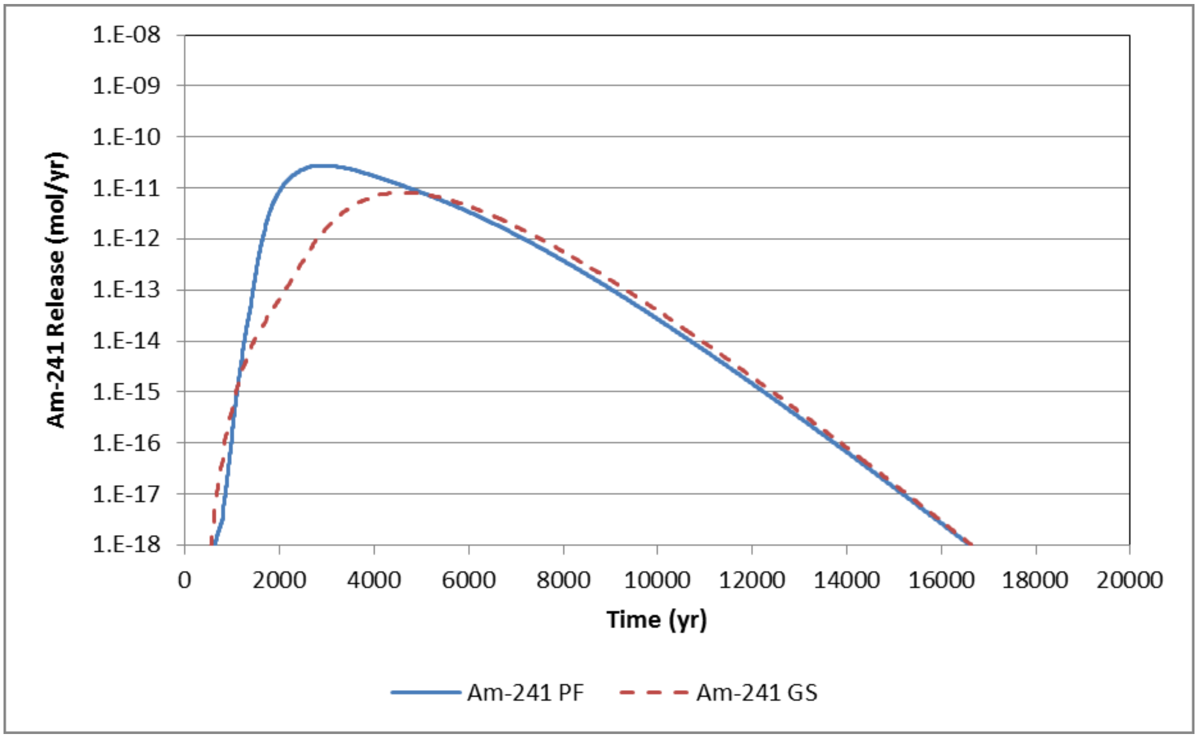

Figure A.4-48: Tank 24 Np-237 Release to the Saturated Zone for Case E

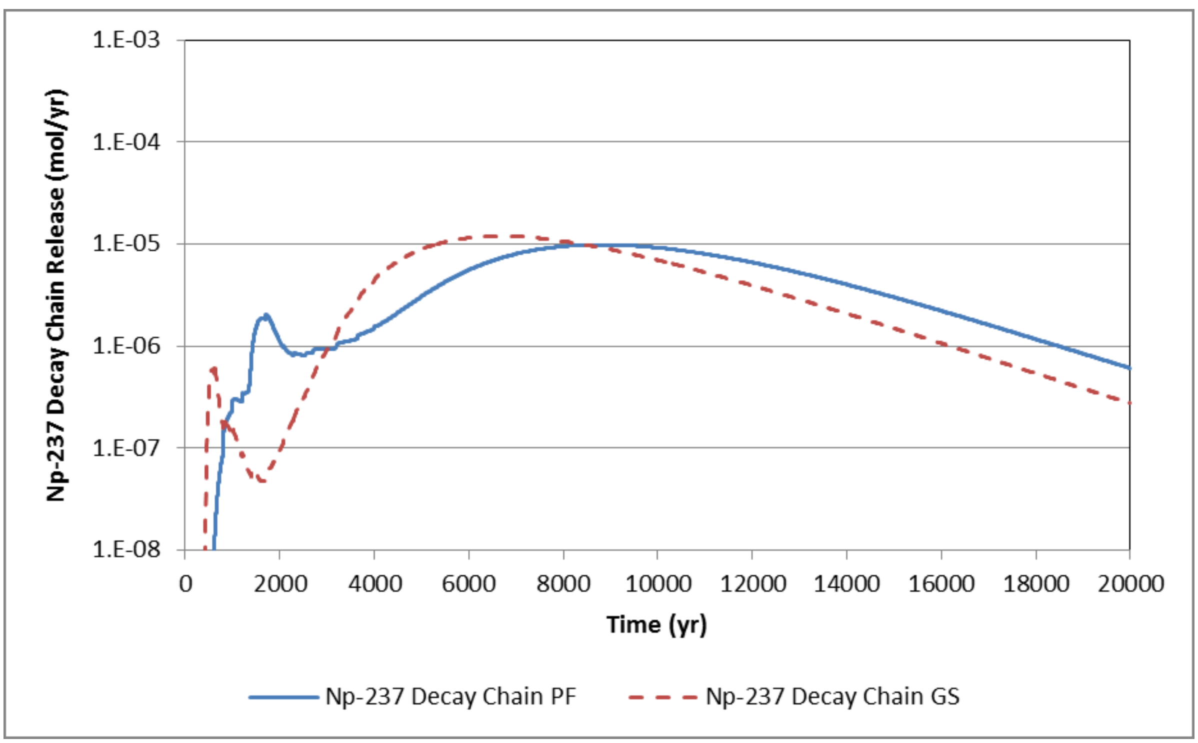

A.4.7 Type III Tank (Tank 31) for Case E

For the Case E configuration, a comparison of the PORFLOW HTF Model and the GoldSim model mass releases of I-129, Tc-99, Am-243, Pu-239, U-234, Ra-226, Am-241, and Np-237, as presented in Figure A.4-49 through Figure A.4-56, indicate that the GoldSim model successfully captures the radionuclide release patterns seen in Tank 31 results generated by the PORFLOW model.

Table A.4-7 summarizes the peak values for these releases showing that when comparing the two models Tc-99, Ra-226, and Np-237 have similar peak releases in the two models. For the other radionuclides, the Case E GoldSim Model has a tendency to conservatively overestimate the peaks of the release breakthrough curves.

Table A.4-7: Case E GoldSim and PORFLOW Model Peak Releases from the UZ to the SZ Comparisons for Tank 31 within 20,000 years

Radionuclide	PORFLOW Peak Release (mol/yr)	PORFLOW Time of Peak Release (yr)	GoldSim Peak Release (mol/yr)	GoldSim Time of Peak Release (yr)	Peak Release Percent Difference GoldSim vs PORFLOW
I-129	3.4E-03	2,080	9.8E-03	2,080	188%
Tc-99	1.5E-08	2,104	1.5E-08	2,100	0%
Am-243	5.3E-08	3,100	2.5E-06	3,100	4617%
Pu-239	1.4E-06	16,140	3.9E-06	3,100	179%
U-234	9.3E-04	2,527	3.9E-03	2,520	319%
Ra-226	2.4E-07	8,349	2.3E-07	2,140	-4%
Am-241	8.3E-07	3,100	1.5E-06	3,100	81%
Np-237	1.8E-01	2,111	1.9E-01	2,110	6%

Figure A.4-49: Tank 31 I-129 Release to the Saturated Zone for Case E

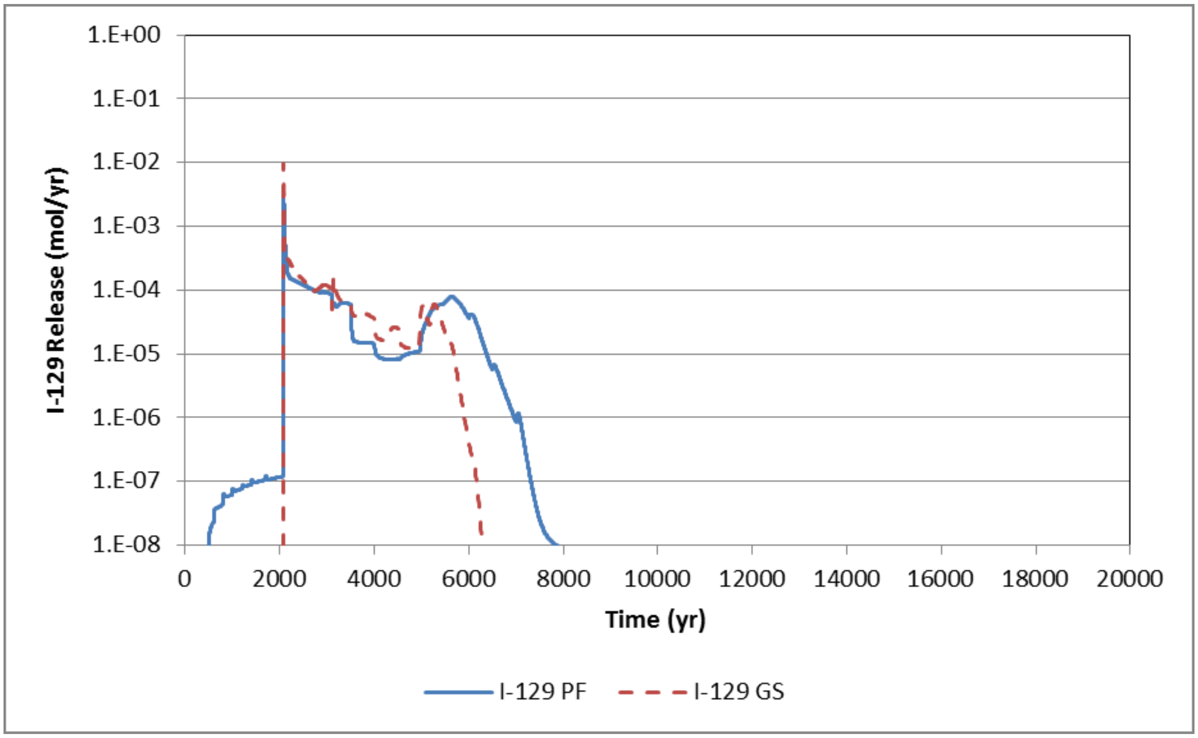

Figure A.4-50: Tank 31 Tc-99 Release to the Saturated Zone for Case E

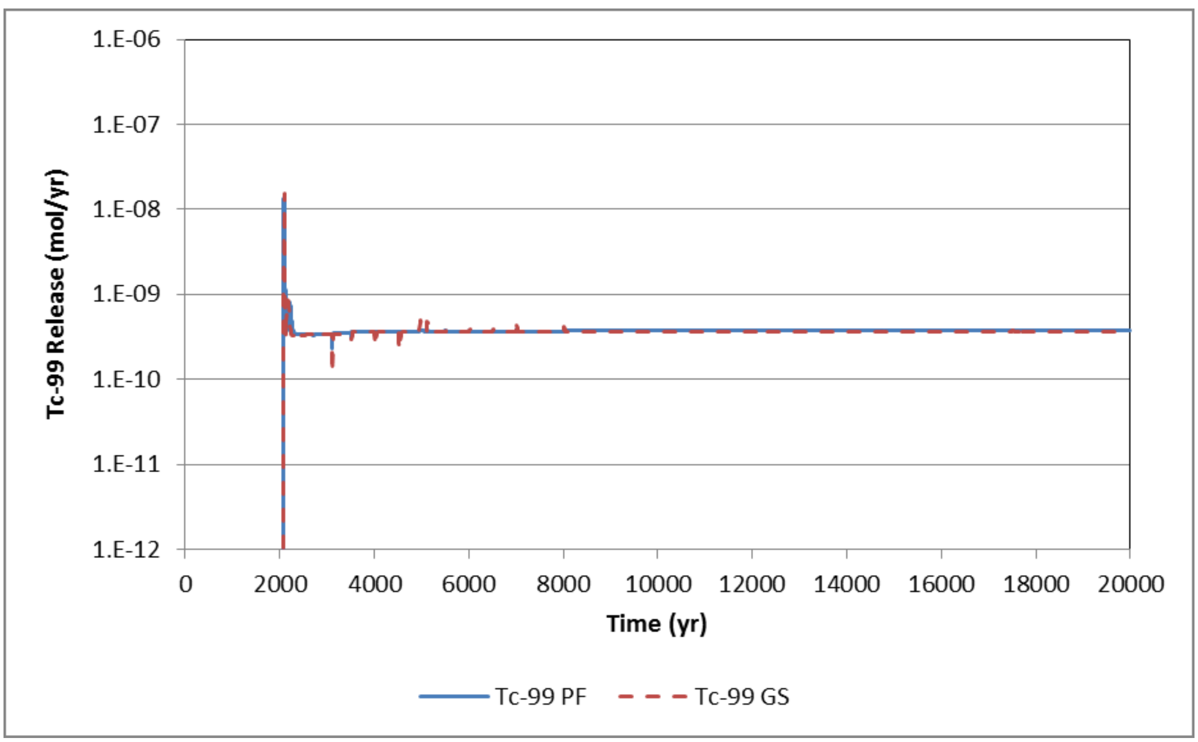

Figure A.4-51: Tank 31 Am-243 Release to the Saturated Zone for Case E

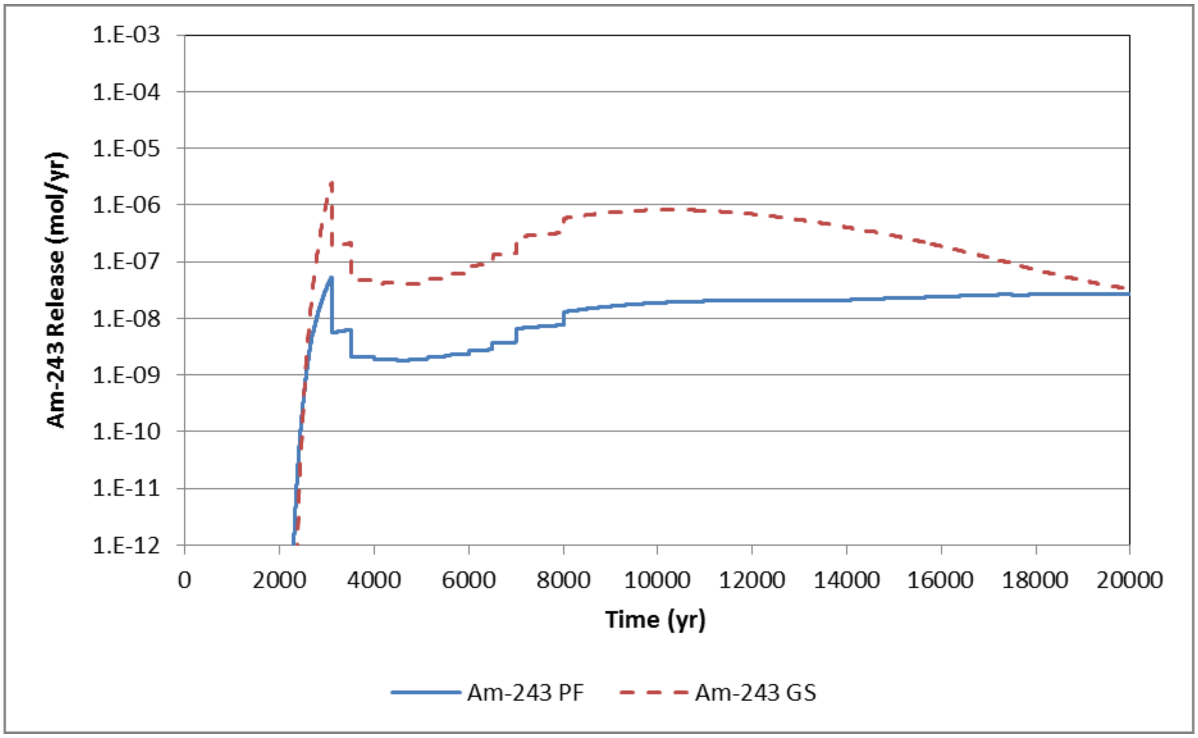

Figure A.4-52: Tank 31 Pu-239 Release to the Saturated Zone for Case E

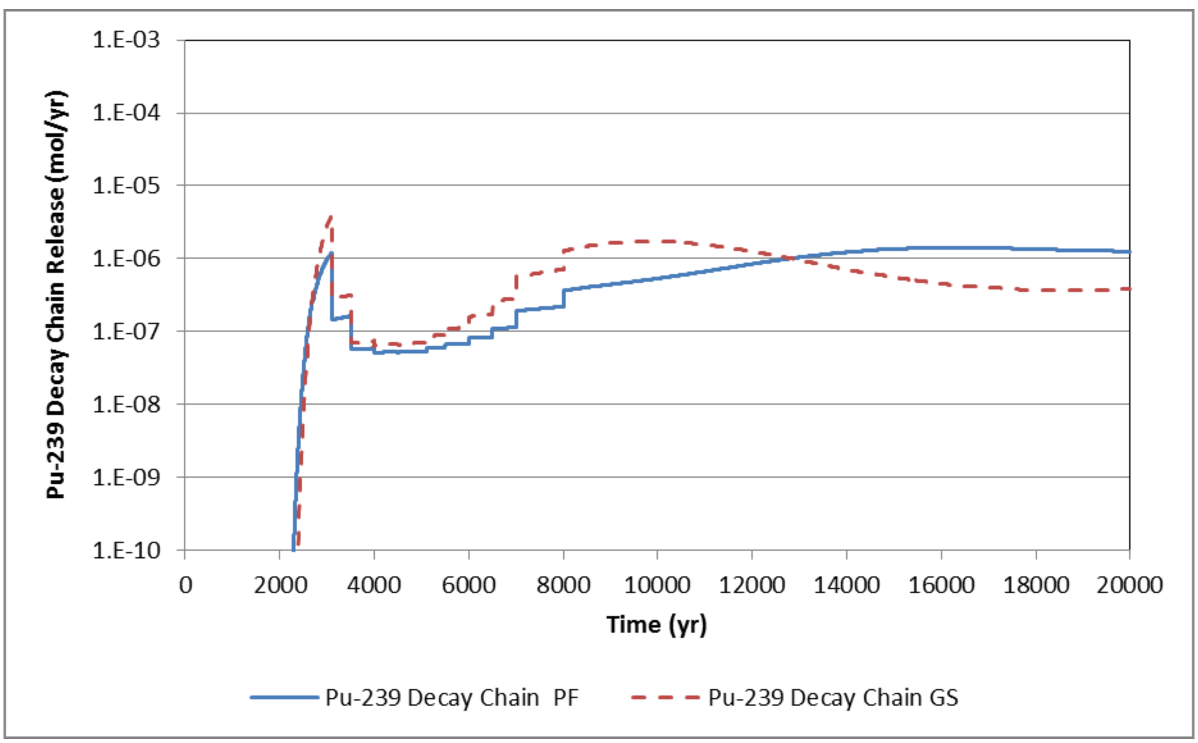

Figure A.4-53: Tank 31 U-234 Release to the Saturated Zone for Case E

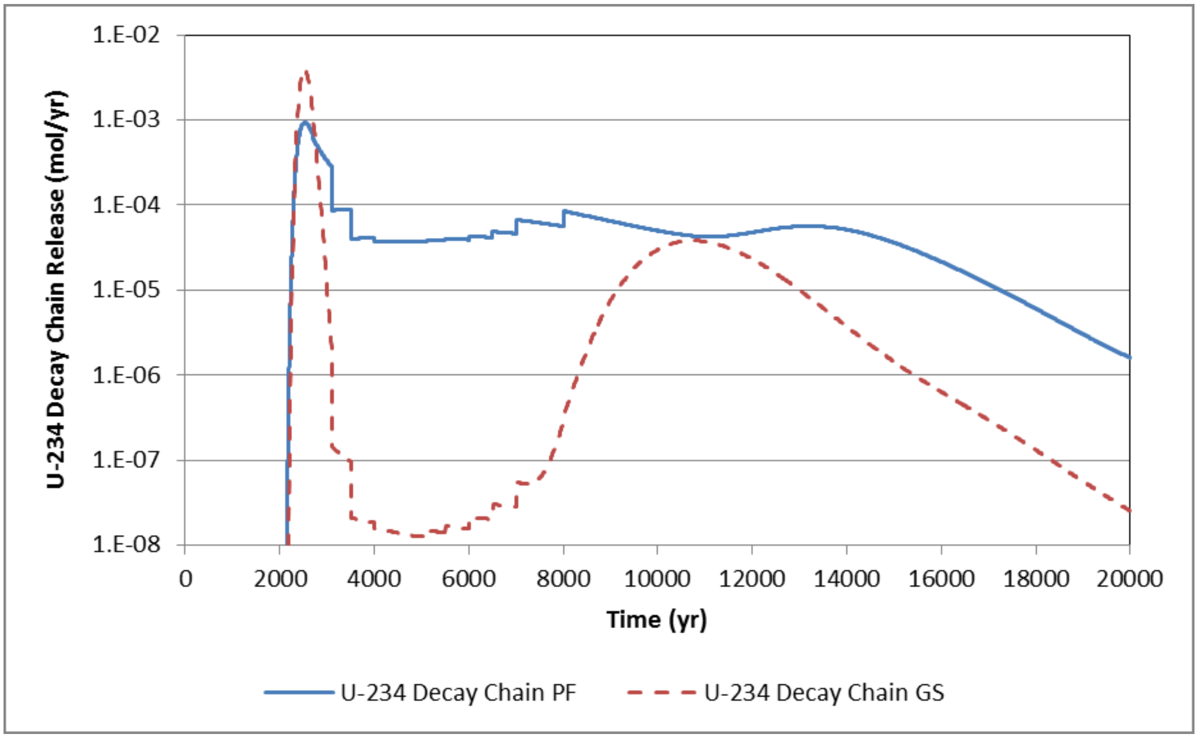

Figure A.4-54: Tank 31 Ra-226 Release to the Saturated Zone for Case E

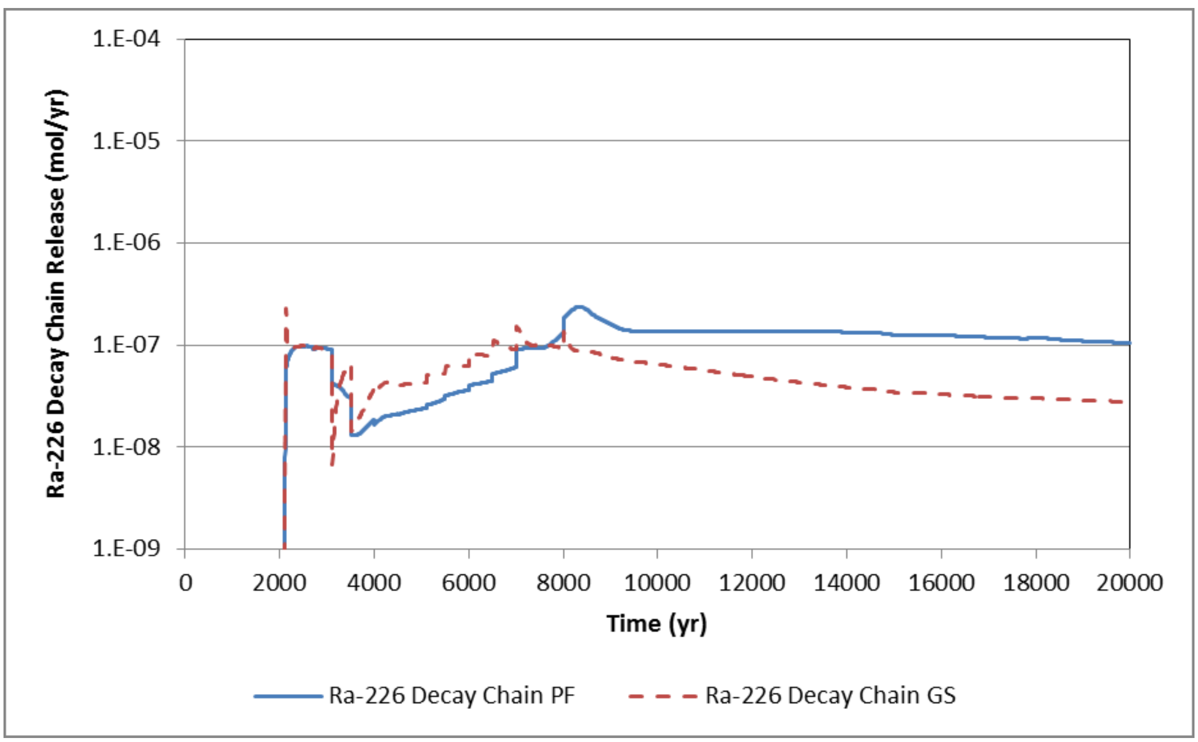

Figure A.4-55: Tank 31 Am-241 Release to the Saturated Zone for Case E

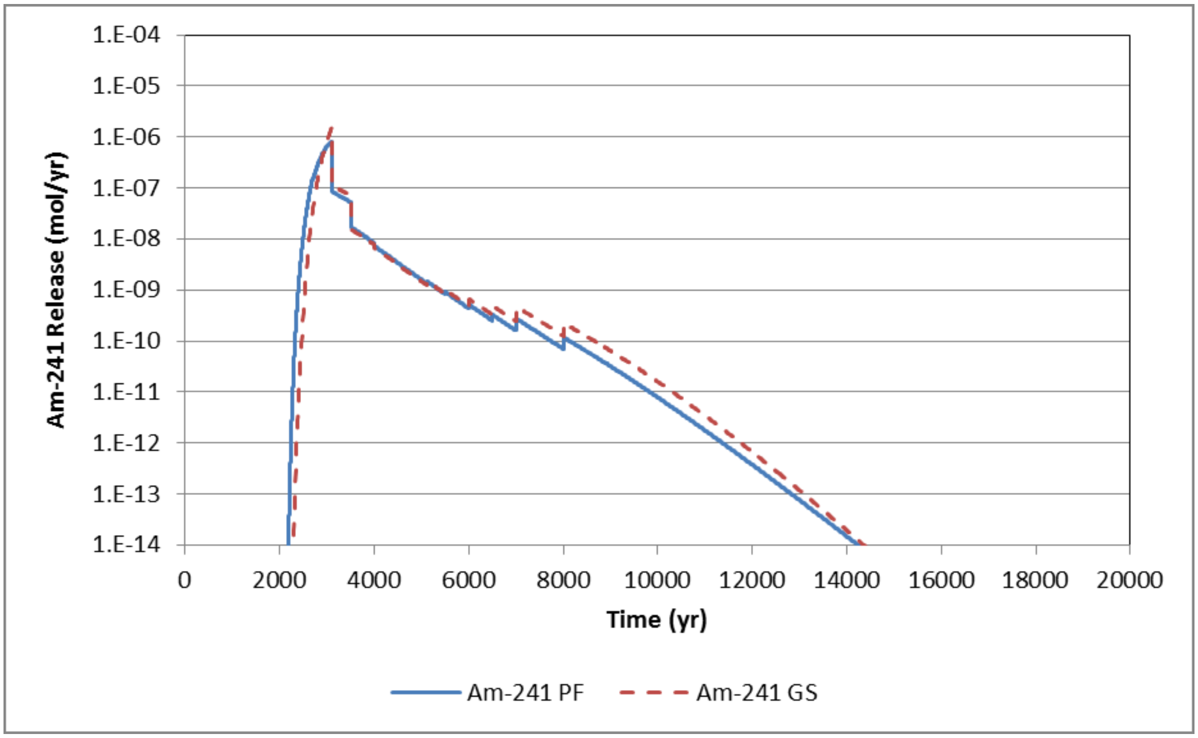

Figure A.4-56: Tank 31 Np-237 Release to the Saturated Zone for Case E